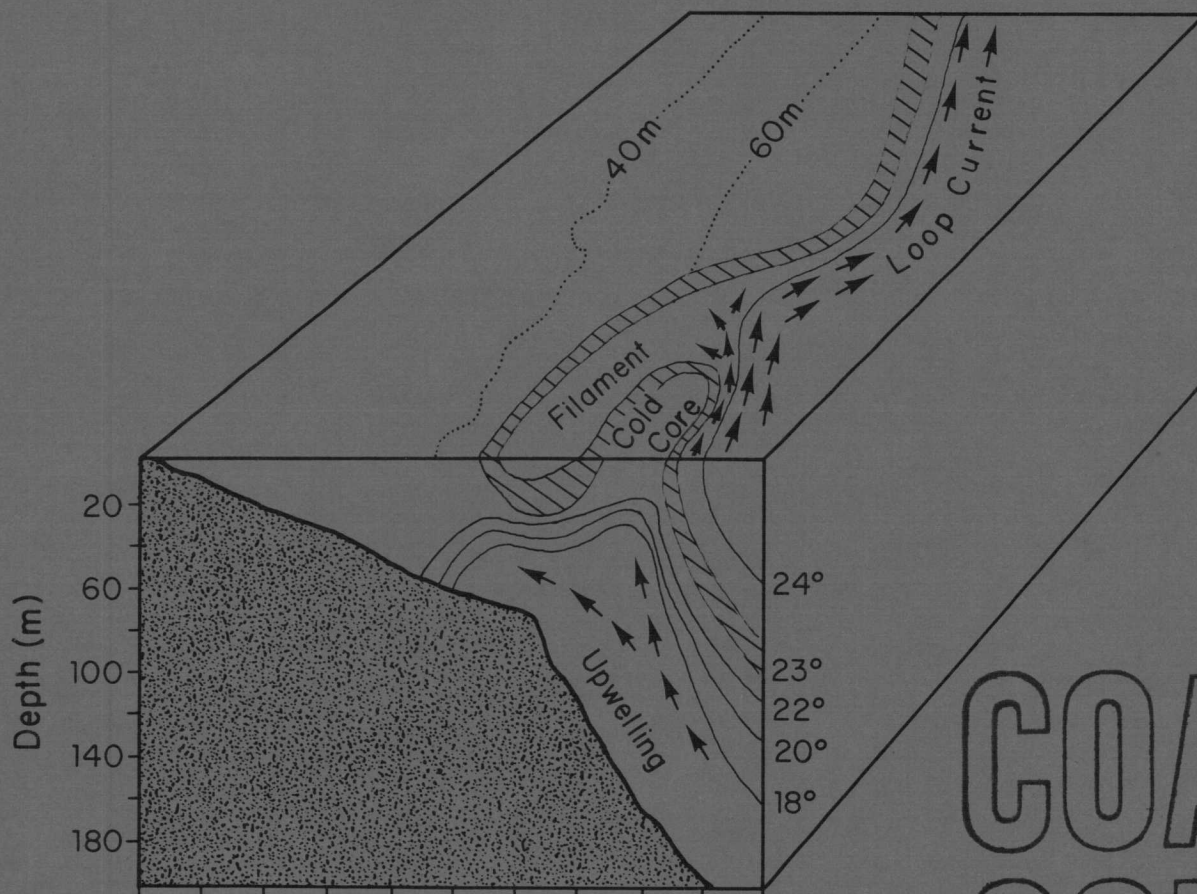GULF OF MEXICO
OUTER CONTINENTAL
SHELF REGIONAL OFFICE

Southwest Florida Shelf Ecosystem Study Year 2 Modification
(Contract No. 14-12-0001-29144)
Final Report

July 1, 1983

U.S. DEPARTMENT OF THE INTERIOR / MINERALS MANAGEMENT SERVICE

Final Report

Southwest Florida Shelf Ecosystems Study - Year 2

HYDROGRAPHY AND PRIMARY PRODUCTIVITY

Woodward-Clyde Consultants

Skidaway Institute of Oceanography

60834A

CONTENTS

Volume I

FIGURES

TABLES

Results of this third phase of the Southwest Florida Shelf Ecosystem Study demonstrated the importance of Loop Current frontal eddies to the primary production of the outer continental shelf off western Florida. This mechanism is analogous to the role of Gulf Stream eddies studied off the southeastern continental shelf of the U.S. (Lee et al., 1981 and Yoder et al., 1981) and may control the observed variability in primary production of the outer southwest Florida shelf. Further, the characteristics and effectiveness of these eddies will play an important part in determining recovery rates in case of accidental contamination by lease oil and gas development activities or the successful simulation of shelf processes in future fates and effects modelling.

As depicted in the cover figure, the general Gulf of Mexico Loop Current eddy system consists of a relatively warm filament of Loop Current Water extending off the main body of the Loop Current front enclosing a cooler tongue of Continental Edge Water. Upwelling generally occurs beneath the cooler water. The surface length scale of this phenomenon is on the order of 200 km; the subsurface extent is at least 100 km. Closely associated with these upwelled waters are the subsurface nutrients which are transported from 10 to 30 m inside the euphotic zone where primary production can occur. Waters affected by these eddies exhibit primary production values of about six times higher than uneffected waters.

The best surface definition of the frontal eddy was achieved during the spring cruise (April 1-7, 1982) with the incorporation of NOAA-7 AVHRR infrared imagery. Spatial errors were only on the order of ± 15 km with thermal

discrepancies of only ±1°C when referenced to onboard hydrographic measurements.

During the summer data collection cruise when lack of sufficient surface thermal contrast precluded effective use of satellite infrared imagery, the mode of shelf water interaction with the Loop Current occurred in a slightly different fashion. Between September 13 and 18, 1982, a 28 km eastward movement of the Loop Current was detected. Concurrent with this toward-shelf movement, mid-depth salinities increased to a subsurface maximum (36.6°/oo); the thermocline dissipated over the outer slope; the volume of near-bottom colder temperatures decreased; an upslope movement of low oxygen, high nutrient water associated with the 26.5 isopycnal was observed; and a progressive doming of isopycnals and isotherms relative to their initial alignments was evident. Moreover, a low-salinity, high chlorophyll a (Chl a) content lens of water about 10 to 30 m thick was measured near the surface. This lens dominated the productivity measurements and is believed to have originated in the northern part of the Gulf. About 70% of the observed variability in primary production during the summer cruise could be explained on the basis of euphotic zone Chl a content and incident irradiance.

Optical oceanographic measurements taken during the spring cruise yielded qualitatively and quantitatively similar distributions to the hydrographic and productivity data collected along the occupied transects. Vertical water mass properties in the study area could be characterized in three optically-derived categories; a) a homogeneous surface layer of low Chl a and suspended matter concentrations, 2) a transition zone of limited vertical extent where Chl a and suspended matter gradients increased, and, 3) an underlying layer

extending downward from about the lower extremity of the euphotic zone where the concentration of Chl $\underline{a}$ and suspended matter gradually decreased.

The color of the surface water mass, depth of the euphotic zone, and Secchi disc depth of visibility varied only slightly over the sampled shelf break study area.

Simultaneous surface chlorophyll concentration mapping using NASA's Ocean Color Scanner during the first two days of the spring cruise further supported the general oligotrophic nature (chlorophyll concentrations of 0.1 to 0.2 $mg \cdot m^{-3}$) of the upper 10 m.

The study phase is concluded with a series of project recommendations for further study. In particular, since the frontal eddy mechanism brings a source of new nutrients to the shelf environment, future study should be directed at tracing the relative importance of nitrogen-bearing compounds as they are used by the phytoplankton and macroalgae of the ecosystem community. Studies of this nature should be able to establish the balance of nutrient resources from which the effects of man-made perturbations may be judged more conclusively.

1.0 INTRODUCTION

HONG CHIN*
WOODWARD-CLYDE CONSULTANTS

Under the authority derived from the 1953 Outer Continental Shelf Lands Act (43 U.S.C. 1331-1343), as amended by the 1978 Outer Continental Shelf Lands Act Amendments, and the National Environmental Policy Act of 1969, the Department of the Interior, Minerals Management Service (MMS), presently administers, manages, and regulates all outer continental shelf activities pertaining to oil and gas leasing, exploration, development, and production in waters beyond the three league limit of coastal states. In 1980, concomitant with this responsibility and in recognition of three important factors;

1. the accelerated five-year leasing plan which included three lease sales in the eastern Gulf of Mexico,

2. recognition of the great importance of Florida's coastal environment as an economic resource, and

3. the generally low level of our present understanding of physical chemical, geological, and biological processes occurring on the southwest outer continental shelf region of Florida; the MMS Environmental Studies Program initiated and sponsored the Southwest Florida Shelf Ecosystems Study.

---

* Present affiliation: Oceanology Associates, San Diego, CA 92120.

1.1 Project Background

The Southwest Florida Shelf Ecosystems Study was a three-year, inter-disciplinary study of the biogeochemical processes and seasonal distributions occurring in the shelf region bounded roughly by 24 to 27°N latitude and 82 to 85°W longitude. The generalized bathymetry of the study area is shown in Figure 1-1. Sea floor slopes in the 20 to 100 m depth range gently incline to the west at about 0.02 to 0.1°; bottom slopes in the 100 to 200 m range average 0.2° with local maxima to 1°.

The study was completed in three phases. Phases (or Years) I and II began in July, 1980 and June, 1981, respectively, and concentrated on mapping the general distribution of substrate types and benthic communities in the 20 to 200 m depth range. Geophysical surveys (side scan sonar, fathometer, and subbottom profiler), underwater television and still camera photography, benthic biological sampling (triangular dredges, otter trawls, and box cores), and water column sampling (temperature, salinity, transmissivity, chlorophyll, and nutrients) were the primary measurements for both phases. The first phase mapped distributions in the spring and fall; the second phase concentrated on summer and winter. A four-volume draft final report and marine habitat atlas covering the results of the first phase and much of the second has been submitted to the MMS (Woodward-Clyde Consultants/Continental Shelf Associates (WCC/CSA); 1982). A second interpretative report which will incorporate the remainder of the second phase results is presently in preparation.
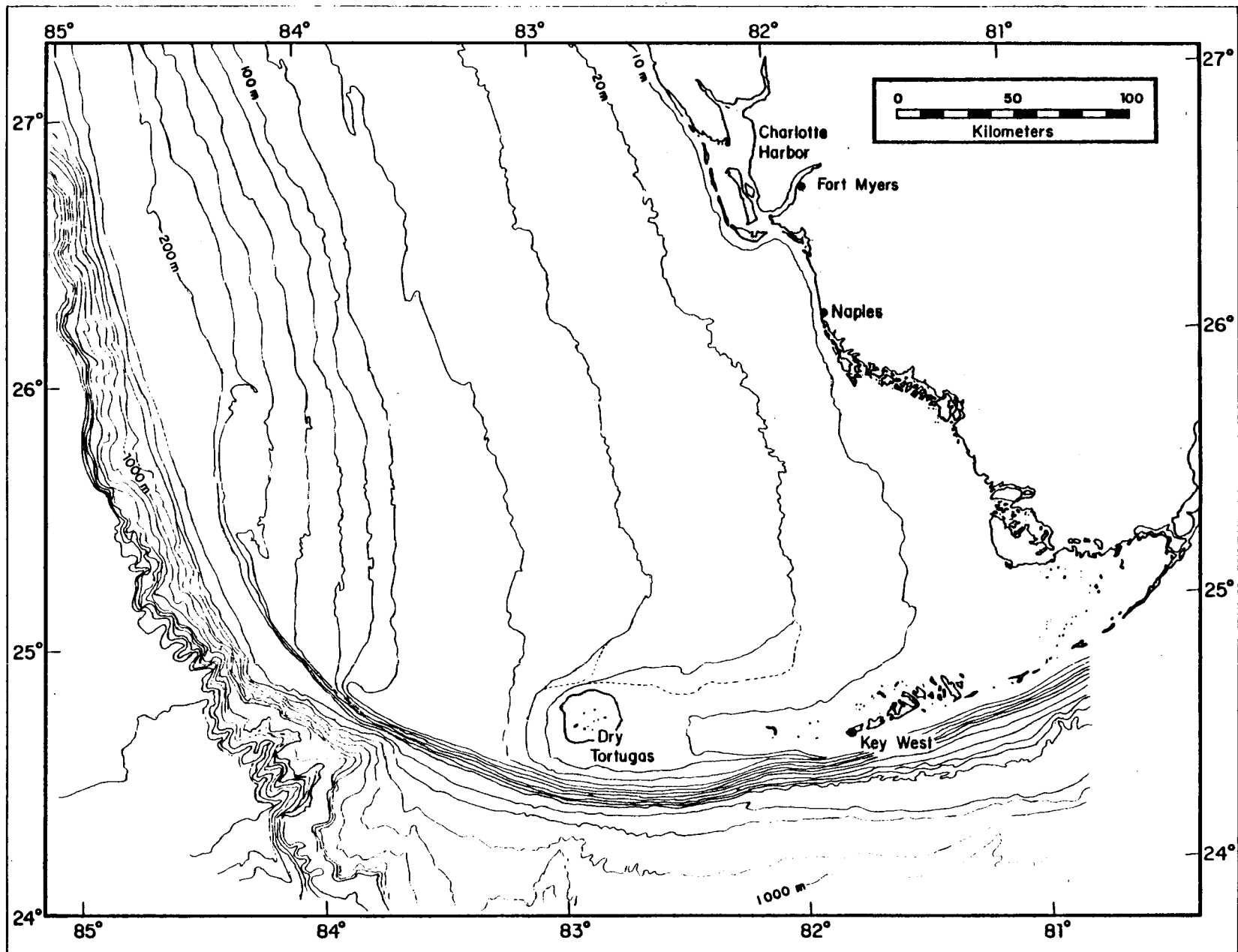
Figure 1-1. Generalized bathymetry of the southwest Florida continental shelf.

The third study phase differed from the first two in that study emphasis was changed from measurement of distributions within the shelf ecosystem to the delineation of a potential driving mechanism for the ecosystem. In a practical sense, this shift in emphasis constituted the first steps taken by the project to address questions relating to factors such as recovery rates in the event of area contamination or specification of appropriate boundary conditions for future Fates and Effects modeling.

From the results of a number of earlier studies, it was known that some form of offshore water intrusion or upwelling occurred near the west Florida shelf break and caused it to be an important commercial and sport fishing ground (Bogdanov, et al., 1968; Austin, 1971; Jones, et al., 1973). Hsueh and O'Brien (1971) showed that a large scale oceanic current, such as the Loop Current, could induce steady upwelling of continental shelf waters and identified the west Florida shelf as a likely candidate for the occurrence of such a process. Hill and Johnson (1974) presented a simple barotropic shelf break/slope model to explain conditions required in the shear layer for upwelling at the shelf break to occur. These conditions are quite typical of the Gulf region in question. Niiler (1976) found evidence of waves moving northward against the Loop Current in current meter data at 150 m near 26°N on the southwest Florida shelf. He proposed Loop Current eddies imbedded in a long meander to be a kinematic explanation for these waves. Maul (1977) detected two "eddies" on the west Florida shelf in Landsat data. He concluded that these eddies were similar to the "spin-off" eddies described by Lee (1975) in the Florida Current. Vukovich et al., (1979) observed large meanders in the cross-shelf direction along the west Florida shelf using satellite data during periods of Loop Current breakdown. Meanders were found

4

in all months when satellite data were available. Huh et al., (1981) documented the intrusion of modified Loop Current water near Pensacola, Florida, and the resulting in-situ modification of approximately half of the intruded waters.

Off the southeastern continental shelf of Georgia and north Florida, a series of studies in 1979 (Lee et al., 1981 and Lee and Atkinson, 1983) showed that finger-like eddies shed from the cyclonic Gulf Stream front were able to exchange significant amounts of heat, momentum, and nutrients in the vicinity of the shelf break. Further, Yoder et al., (1981) showed that upwelling associated with these eddies could cause surface chlorophyll levels to increase by one to two orders of magnitude in localized areas.

A basic objective of this third study phase, therefore, is to demonstrate that a similar upwelling mechanism is active off the west Florida shelf and offers the potential for being a major driving force for the shelf ecosystem. Once the data demonstrate the existence of the upwelling mechanism from several independent points of view, similarities and differences between the Loop Current and Gulf Stream versions are discussed with respect to

    o   probable origins of water masses on the shelf,

    o   modes of interaction or mixing between resident shelf waters, slope water, and Loop Current water,

o   primary productivity rates and areas of maxima and minima, and

o   nutrient distributions in the shelf break region during intrusions.

1.2 Project Scope

The third study phase started in March 1982 with a planning/coordination
meeting for the first of two data collection cruises. During the first
cruise, data were collected simultaneously from several sources. Using
NOAA/NESS satellite imagery to define the surface Loop Current front, Texas
A&M University's R/V GYRE departed St. Petersberg on April 1, 1982 and
followed a cruise track that intersected the front on five separate
cross-shelf transects; two of these sections crossed finger-like eddies
propagating south along the front. A total of 110 stations were sampled over
a seven-day period for different combinations of temperature, salinity,
dissolved oxygen, light transmission, scattering, and irradiance, in-situ
fluorescence, spectral depth of visibility, phytoplankton and suspended
sediment content, primary production, solar transmittance, and water
parameters. Samples returned to the laboratory were analyzed for salinity
calibrations, Chlorophyll a + Phaeopigment a (Chl a + Ph a), nutrients
(nitrate, phosphate, and silicate), Carbon-14 primary productivity, phyto-
plankton identification and enumeration, and suspended sediment load. Con-
current with the shipboard sampling on April 1 and 2, NASA's Ocean Color
Scanner (OCS) mapped the surface chlorophyll concentration in the approxi-
mate 25 to 27°N, 83 to 85°W area from a U-2 aircraft.

In order to examine the seasonal variation of intrusions under more stratified shelf conditions, a second cruise was completed between September 12 and 19 from the Florida Institute for Oceanography's (FIO) R/V SUNCOASTER. Lack of sufficient thermal contrast precluded use of satellite infrared imagery for frontal definition. Ninety-five stations were occupied along four repeated transects. In total, 36 Conductivity, Temperature, Depth (CTD) casts, 57 Expendable Bathythermograph (XBT) profiles, and 15 bottle casts were made; 314 samples were collected for nutrient and oxygen analyses, 366 for chlorophyll, 90 for salinity calibrations, 84 for productivity, and 39 for cell counts (WCC/SIO, 1982b). Light scattering, quantum irradiance, and Secchi disk depths were not measured on this cruise. Likewise, no OCS overflight was scheduled.

On November 16, 1982, a workshop was held at the University of South Florida to discuss, review and critique the results of the study phase with respect to the objectives of the overall study and the current state of knowledge of Gulf of Mexico hydrography and primary productivity. A panel of four recognized specialists in these fields developed both written and verbal comments from their review of the project findings. Additionally, a series of recommendations for further study were formulated.

Copies of all project data were forwarded to the National Oceanographic Data Center (NODC) and designated Principal Investigators.

1.3 Final Report Organization

This final report is divided into two volumes. A separate data appendix volume has been used to facilitate presentation.

The following report section (2.0) presents a general introduction to the physical concepts used in the study and the seasonal variability of water column parameters in the on-shelf (20 to 200 m) portion of the study area. Cross shelf distributions of seven parameters are presented as a "hydrographic atlas" for four seasons along five transects.

Each of the immediately succeeding sections presents discussions and analyses of the study results from a different disciplinary point of view. Section 3.0 deals with the hydrographic, or physical oceanographic, aspects of the Loop Current intrusion/upwelling phenomenon while Section 4.0 extends these analyses through a discussion of the mixing processes associated with the frontal dynamics. Section 5.0 presents a series of analyses from a biological oceanography, or primary production, point of view and is supported by optical oceanographic analyses in Section 6.0. The results of the April 1 and 2 OCS chlorophyll mapping overflights are discussed in Section 7.0. Section 8.0 summarizes the results and conclusions of the study and incorporates the comments of the workshop review panel as well as the recommendations for further study and supporting justification.

Following the report format of EG&G (1980), each section contains a separate bibliography.

1.4 References

Austin, H.M. 1971. The characteristics and relationships between the calculated geostrophic current component and selected indicator organisms in the Gulf of Mexico Loop Current System. Ph.D. Dissertation, Dept. of Oceanography, Florida State University, 369 pp.

Bogdanov, D.V., V.A. Sokolov, and N.S. Khromov 1968. Regions of high biological and commercial productivity in the Gulf of Mexico and Caribbean Sea. Oceanology (Academy of Sciences of the USSR) 9(3): 371-381.

EG&G 1980. New England outer continental shelf physical oceanography program. Appendices D and F of thirteenth quarterly progress report, BLM Contract No. AA551-CT8-46.

Hill, R.B. and J.A. Johnson 1974. A theory of upwelling over the shelf break. J. Phys. Oceanogr. 4(1): 19-26.

Hseuh, Y. and J.J. O'Brien 1971. Steady coastal upwelling induced by an alongshore current. J. Phys. Oceanogr. 1(3): 180-186.

Huh, O.K., W.J. Wiseman, Jr. and L.J. Rouse, Jr. 1981. Intrusion of Loop Current waters onto the west Florida continental shelf. J. Geophys. Res. 86(C5): 4186-4192.

Jones, J.I. et al. 1973. Physical oceanography of the northeast Gulf of
Mexico and Florida continental shelf area, in A summary of knowledge of
the eastern Gulf of Mexico, coordinated by the State University System of
Florida Institute of Oceanography: 69 pp.

Lee, T.N. 1975. Florida current spin-off eddies. Deep-Sea Res. 22: 753-765.

Lee, T.N., L.P. Atkinson, and R. Legeckis 1981. Observations of a Gulf
Stream frontal eddy on the Georgia continental shelf. Deep-Sea Res.
28A(4): 347-378.

Lee, T.N. and L.P. Atkinson 1983. Low frequency current and temperature
variability from Gulf Stream frontal eddies and atmospheric forcing along
the southeast U.S. outer continental shelf. J. Geophys. Res., in press.

Maul, G.A. 1977. The annual cycle of the Gulf Loop Current, Part I.
Observations during a one-year time series. J. Mar. Res. 35: 29-47.

Niiler, P.P. 1976. Observations of low-frequency currents on the west
Florida shelf, in Mem. Soc. Roy. des Sei. de Liege, 10, Seventh Liege
Colloquium on Ocean Hydrodynamics continental Shelf Dynamics, J.C.J.
Nihoul, ed.: 331-358.

Vukovich, F.M., B.W. Crissman, M. Bushnell, and W.J. King 1979. Some aspects
of the oceanography of the Gulf of Mexico using satellite and in-situ
data. J. Geophys. Res 84(C12): 7749-7768.

Woodward–Clyde Consultants/Continental Shelf Associates 1982. Southwest

Florida shelf ecosystems study – Year 1. 4 vols. plus marine habitat

atlas, prepared under BLM Contract No. AA851-CTO-50, in revision.

Woodward–Clyde Consultants/Skidaway Institute of Oceanography 1982a.

Southwest Florida shelf ecosystems study – Year 2, Cruise I summary

cruise report, prepared under BLM Contract No. AA851-CT1-45.

Woodward–Clyde Consultants/Skidaway Institute of Oceanography 1982b.

Southwest Florida shelf ecosystems study – Year 2, Cruise II summary

cruise report, prepared under MMS Contract AA851-CT1-45.

Yoder, J.A., L.P. Atkinson, T.N. Lee, H.H. Kim, and C.R. McClain 1981. Role

of Gulf Stream frontal eddies in forming phytoplankton patches on the

outer southeastern shelf. Limnol. Oceanogr. 26(6): 1103-1110.

2.0 SEASONAL VARIABILITY ON THE SOUTHWEST FLORIDA SHELF - A HYDROGRAPHIC ATLAS

HONG CHIN*
WOODWARD-CLYDE CONSULTANTS

2.1 Introduction

As an introduction to the elementary physical concepts and terminology to be
employed, consider the general Gulf circulation pattern, the water masses
involved, and the seasonal distribution of water column parameters on the
southwest Florida shelf as determined through the first two phases of this
study. This "hydrographic atlas" provides an opportunity to form a background
for the study results in terms of general concepts and salient shelf
distribution features. For brevity, only the shelf factors relating directly
to the study results are discussed.

2.2 General Circulation and Water Masses

Circulation in the Gulf of Mexico is largely under the influence of the upper
layer transport system of the western North Atlantic (Jones et al., 1973).
The Atlantic northeast trade winds drive the Caribbean Current which flows
westward after being formed from the juncture of the Equatorial Current and
the Guiana Current. The Caribbean Current crosses the Caribbean Sea and
continues through the Yucatan Channel into the Gulf with meanders on its way
to form the eastern Gulf Loop Current. Moving clockwise, the Loop Current
dominates the circulation in the eastern Gulf. According to Leipper (1970),
the flow is well represented year-round by the topographies of the 22°C
isothermal surfaces. Additionally, he reported significant variability in the
seasonal and annual areal extent of the current. The maximum northward

* Present affiliation: Oceanology Associates, San Diego, CA 92120

penetration of the Loop Current generally occurs in the summer months, and the minimum penetration occurs in the winter months (Vukovich, et al., 1979). Subsequently, the Loop Current progresses into the Straits of Florida to form a segment of the Gulf Stream.

In 1971, a Ph.D. dissertation by H.M. Austin at the Florida State University formed one of the first attempts to illustrate the modifying effects of the Loop Current on surrounding Gulf waters. His now well-used depiction of water masses in the eastern Gulf (reproduced as Figure 2-1) developed from EGMEX-I (Eastern Gulf of Mexico program) data for May 1970 shows Central Loop water with the same temperature and salinity characteristics as the Subtropical Underwater as defined by Wüst (1964), with temperatures of 18 to 25°C and salinities of 36.5 to 36.8°/oo. The Loop transition water has temperatures between 25 and 27°C with a steep slope to the isotherms. The surface temperatures of the Loop transition range between 23 and 27°C, and the water is a mixture between eastern Gulf water and Central Loop water with salinities ranging between 36.0 and 36.5°/oo. Note the meandering outer limits of the transition zone and the indications of upwelling within the zone.

An important point to consider in this context is that water on the west Florida shelf is affected by its boundaries. The boundaries in this case are the Florida Panhandle to the north, the west coast of Florida to the east, the Florida Keys to the south, the Gulf of Mexico and frequently the Loop Current to the west, and the air-sea interface above (Molinari et al., 1976). The effect of the Loop Current at the western edge of these water mass distributions is one of the main subjects of this report.
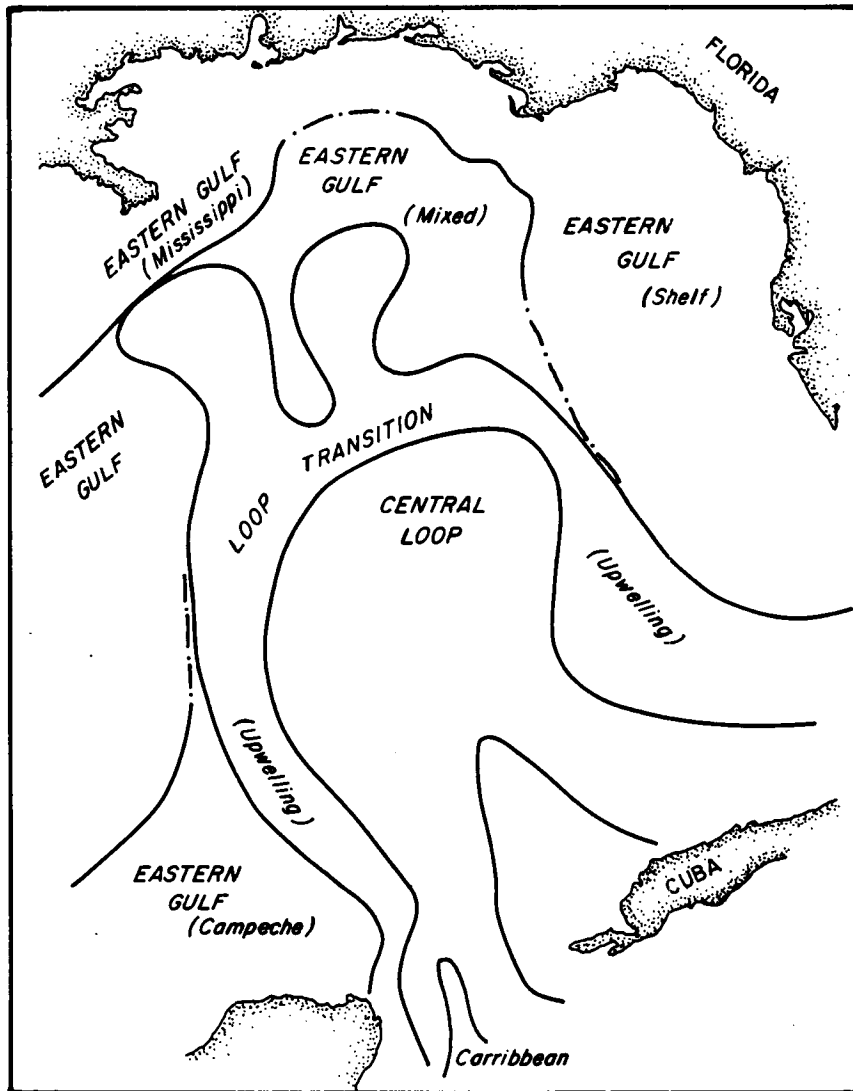
Figure 2-1. Water masses in eastern Gulf of Mexico
during May 1970 (from Austin, 1971).

2.3 Seasonal Shelf Distributions

Seasonal distributions of seven water column parameters in the 20 to 100 m (spring and fall) and 20 to 200 m (summer and winter) depth ranges were mapped along five east-west transects during the first two study phases (years). Collection techniques and analysis methods have been presented earlier in WCC/CSA (1982). As shown in Figure 2-2, the northernmost transect (A) is located near Charlotte Harbor. The southernmost transect (E) is situated just north of the Dry Tortugas. Transect separation is about 50 km. A total of 30 stations were profiled on all transects during each season. Sampling times during each season were as follows:

Season	Sampling Dates
Summer	July 16 to August 15, 1981
Fall	October 25 to November 23, 1980
Winter	January 28 to February 15, 1982
Spring	April 22 to May 5, 1981

Although the sampling periods are not quite synoptic*, the analyses of these data do provide a seasonal overview for the shelf break mechanism discussed below. Discussions of temporal changes along repeated transects in the following section will clarify the necessary degree of approximation in these seasonal composites.

---

* General term derived from meteorology connotating overall view or simultaneity in data collection. Ideally, a synoptic data collection would occur within the time scale of change of the parameter being measured.
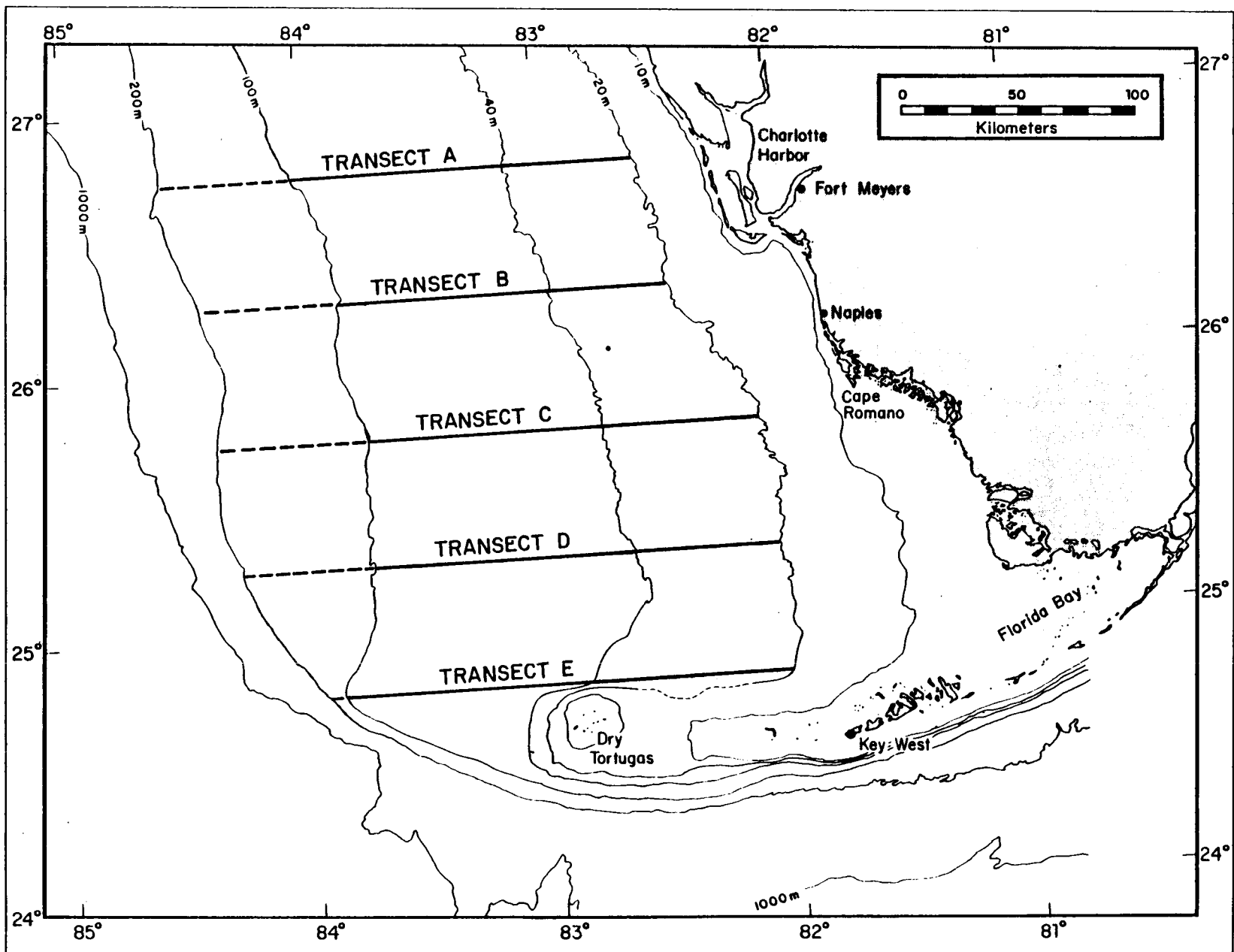
Figure 2-2. Sampling transect locations during Phases (Years) I and II.

2.3.1 Temperature

The average solar radiation reaching the study area ranges from about 350 to 600 langleys* $\cdot$ day^{-1} between January and July, respectively (Sellers, 1965). Heating and mixing from the surface layers causes the summer distributions to be relatively well mixed in shallow depths (at $\sim 30°C$) with a well defined thermal stratification across most of the shelf.

As the fall transition approaches, atmospheric cold fronts begin to penetrate into south Florida and the water column undergoes a surface cooling and wind-induced mixing. The remnant summer thermocline is mixed out to deeper depths as the winter environment begins to intrude onto the shelf. Figures 2-3 through 2-7 show that the surface mixed layer generally extends to a depth of 40 to 60 m in fall along all transects. Temperatures in the mixed layer show a gradual 1.5 to 2.0°C decrease in a southerly direction from Transect A to Transect E. The thermocline is mixed or has retreated to the 40 to 60 m depth contours. Temperatures below the thermocline show a gradual warming from Transect A to Transect E.

Winter distributions show coldest surface temperatures ($\sim 20°C$) in the shallowest waters with slightly warmer temperatures seaward. Thermal stratification is weak with variations generally less than 4°C in the upper 80 to 100 m.

During the spring restratification, a decrease in turbulent forces becomes evident and a gradual warming of surface waters begins to mix into the water column. Spring isotherms tend to align horizontally across the transects and

---

* 1 langley = 1 gm-cal $\cdot$ cm^{-2}.

13
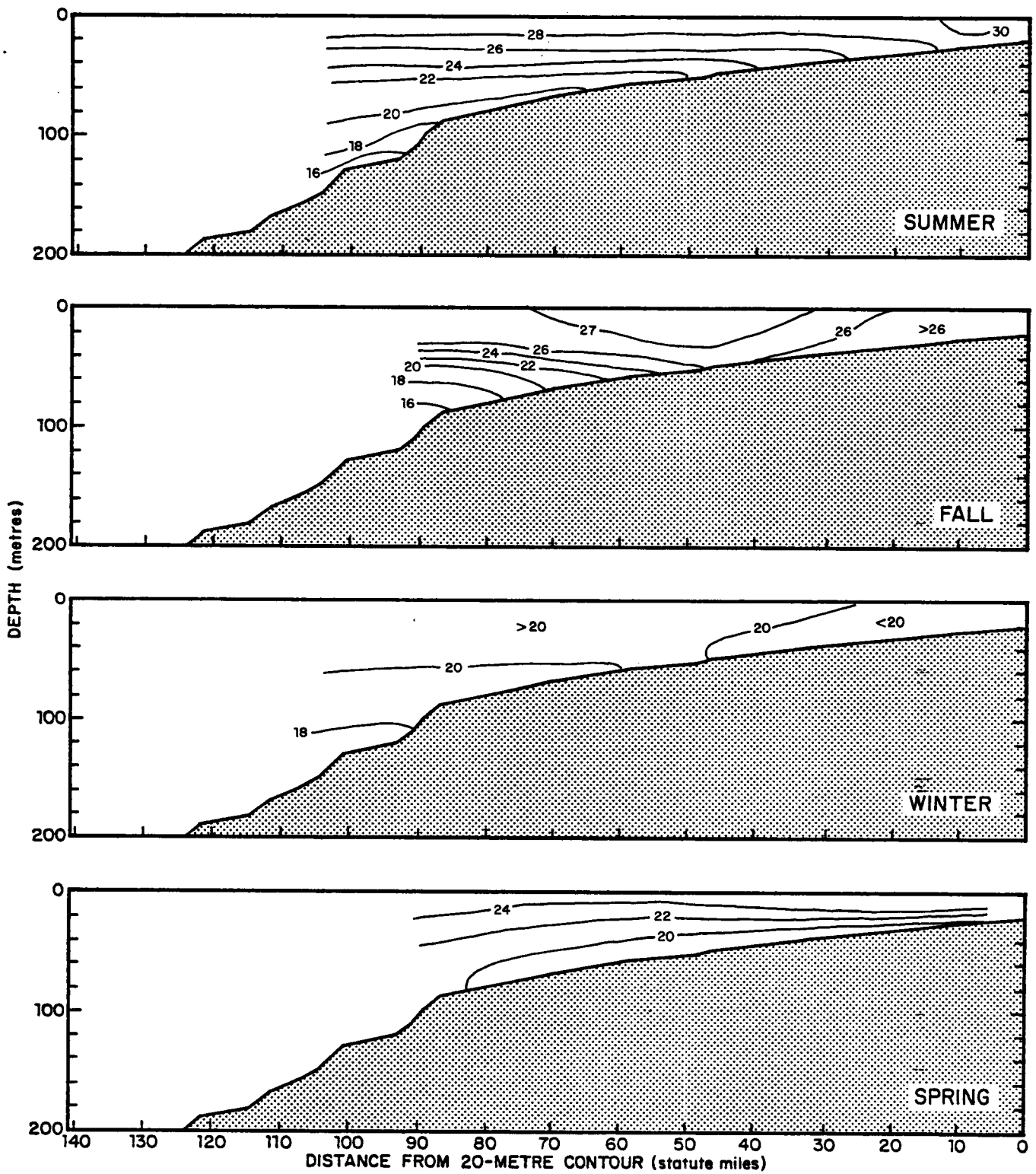
Figure 2-3. Seasonal temperature distributions on Transect A.
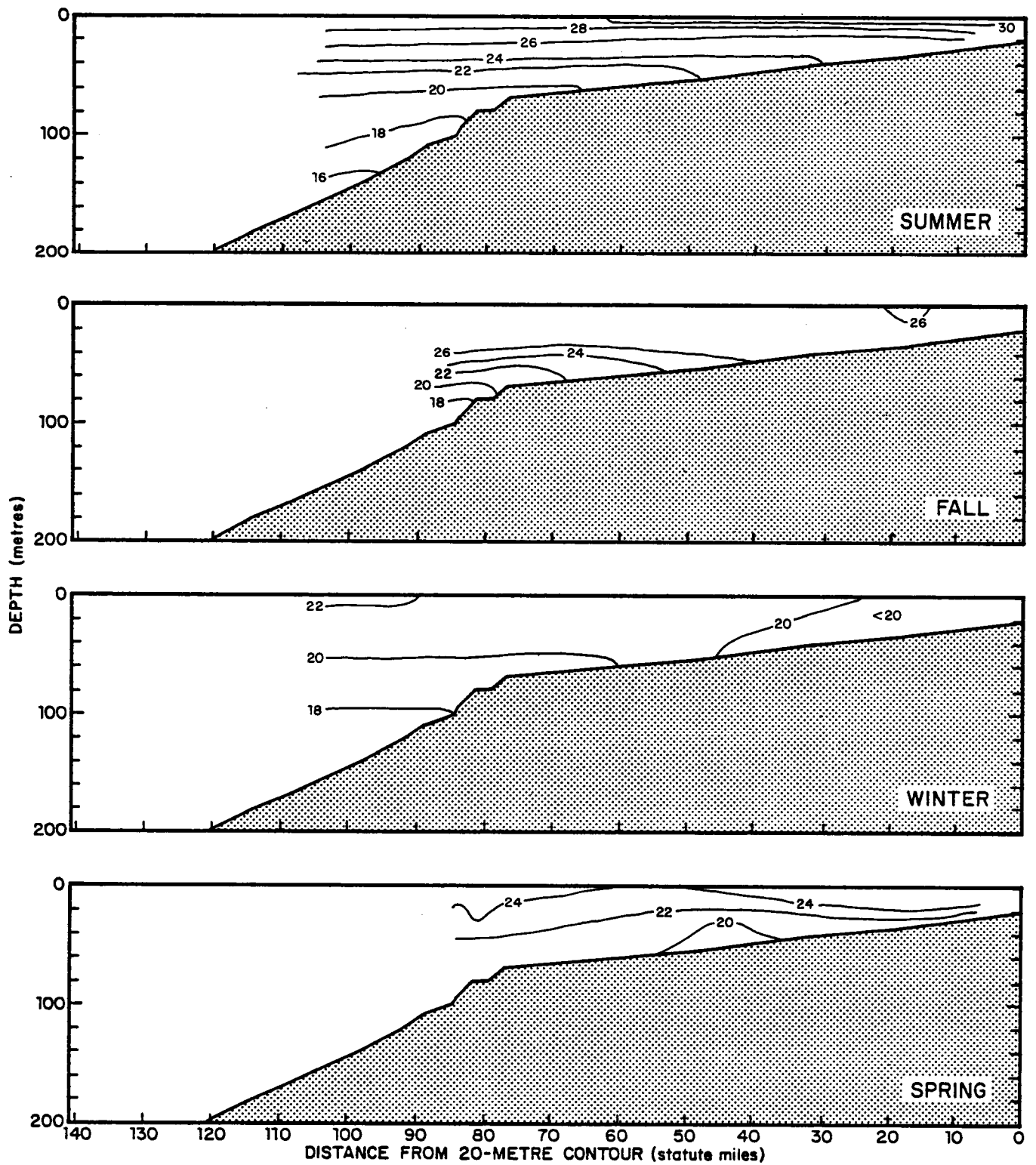
Figure 2-4.   Seasonal temperature distributions on Transect B.
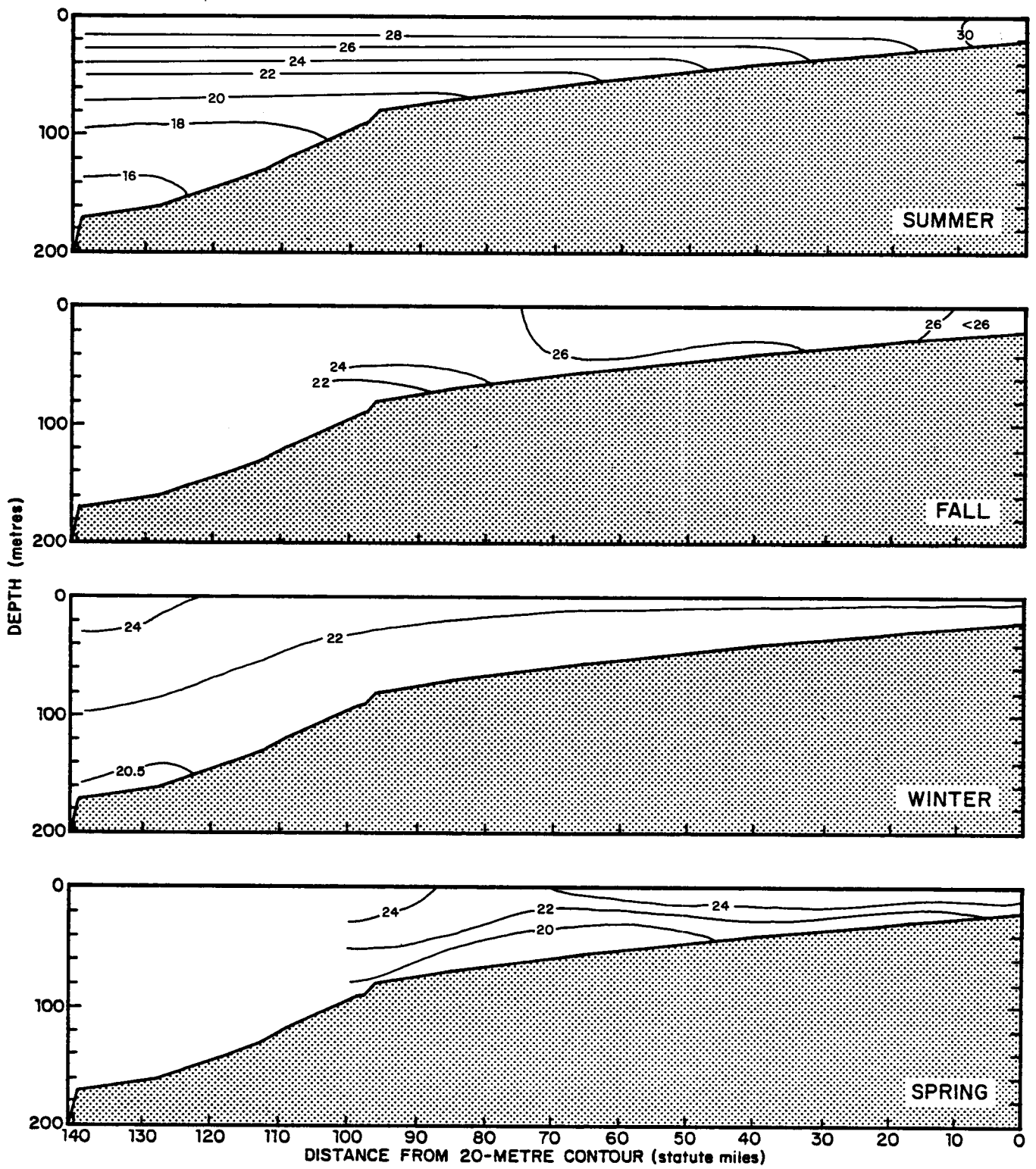
Figure 2-5.   Seasonal temperature distributions on Transect C.

21
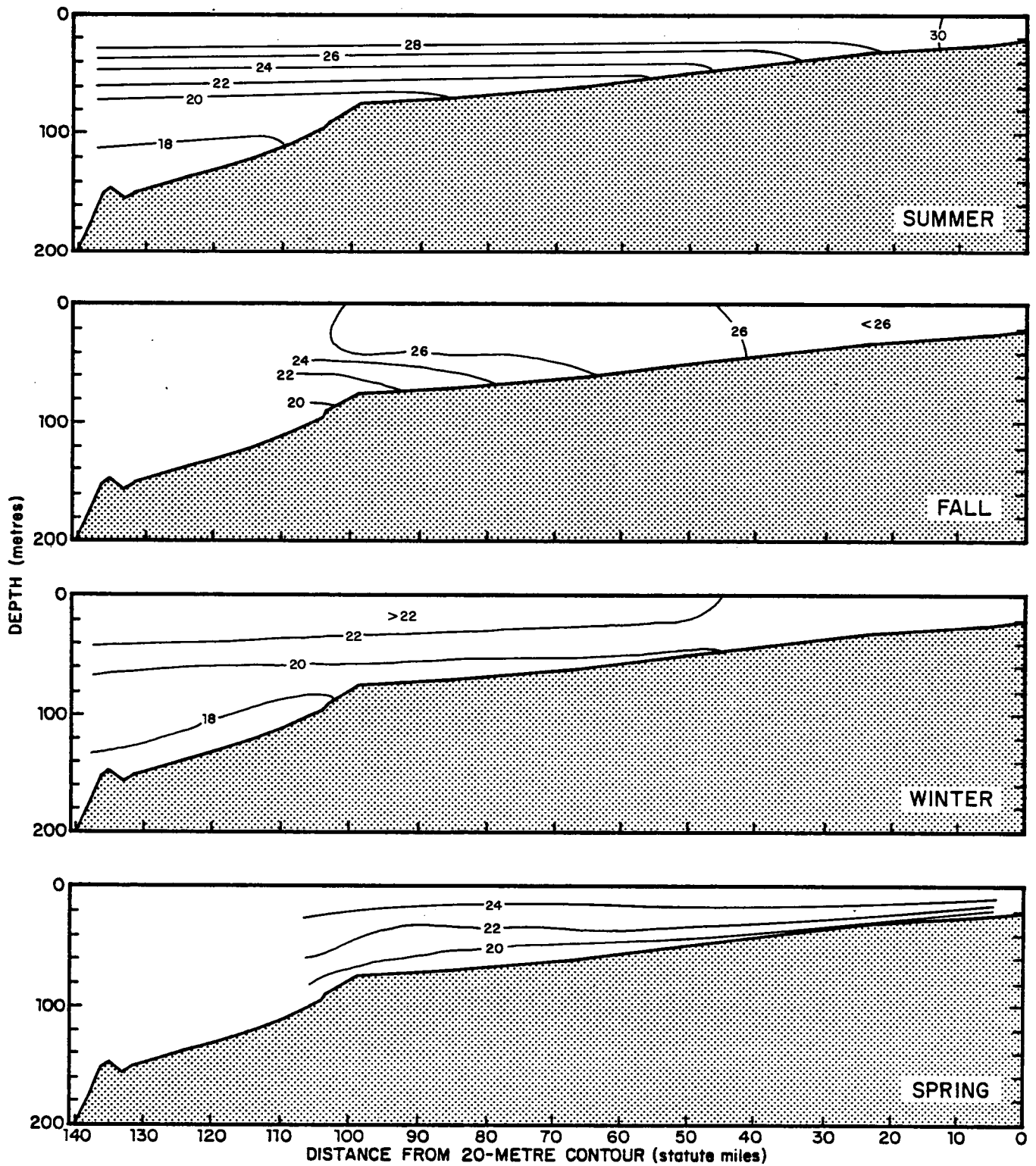
Figure 2-6.   Seasonal temperature distributions on Transect D.

22
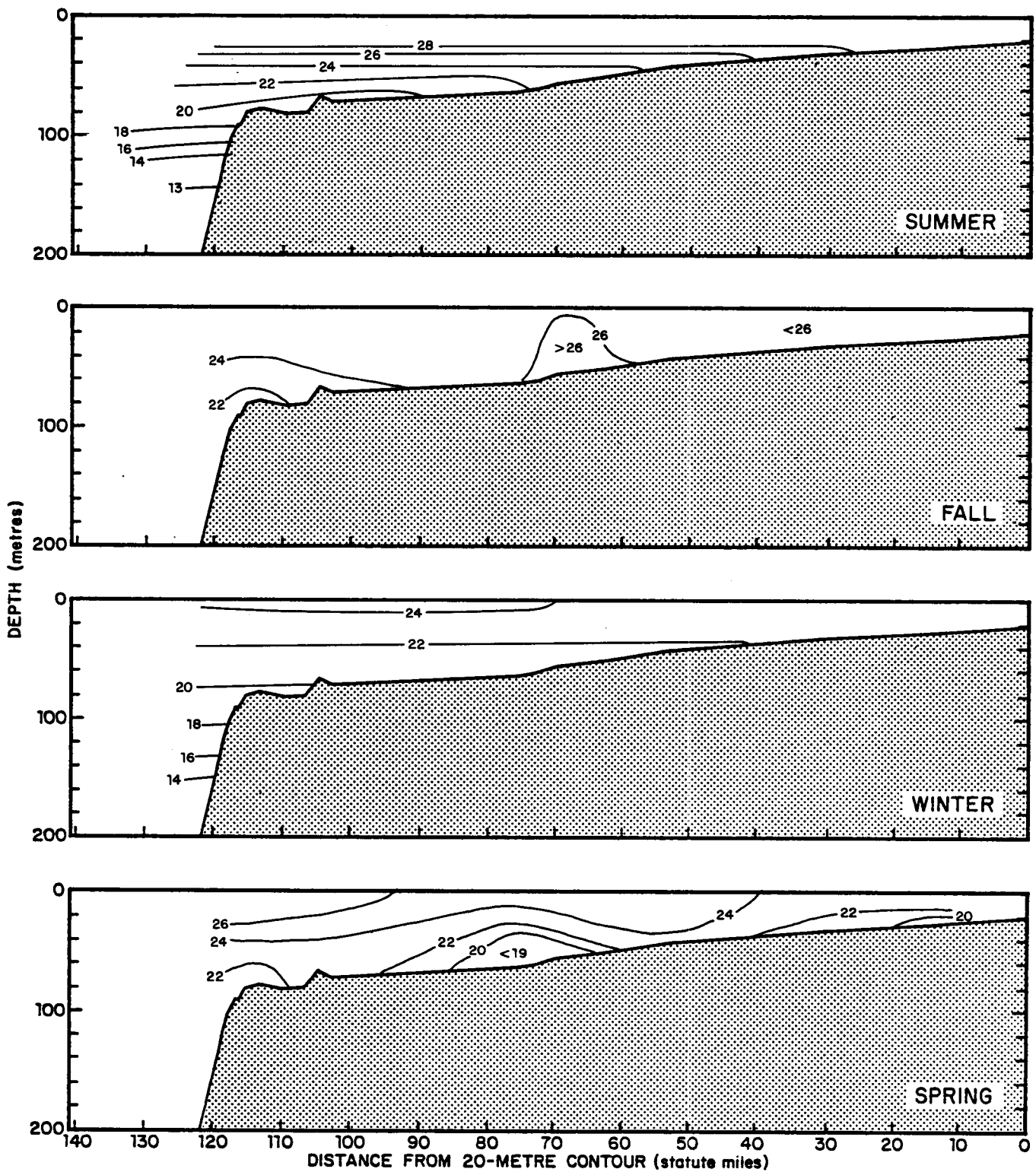
Figure 2-7.   Seasonal temperature distributions on Transect E.

become more compacted, forming a true thermocline only in the near-shore regions. One consequence of this near-shore warming is the appearance of near-bottom, mid-shelf minima (see Figures 2-4, 2-5, and 2-7).

2.3.2 Salinity

Owing to the chemical complexity of sea water, it is generally not practical to determine the total quantity of dissolved solids in a sea water sample by chemical analysis each time. Since the relative composition of sea water is virtually constant, an "artificial" definition of the salinity was introduced in physical oceanography by Forch, Knudsen, and Sorensen in 1902. They defined the salinity of a sea water sample to be the total amount of solid materials in grams contained in one kilogram of sea water, when all the carbonate was thought to be converted to oxide, the bromine and iodine replaced by chlorine, and all organic matter completely oxidized (Pierson and Neumann, 1966). In practice, this definition is applied by measuring conductivity and correcting for temperature and depth through an approximation for the equation of state.

Density, ρ, is defined as mass per unit volume ($gm \cdot cm^{-3}$). In oceanography, specific gravity is used instead of density. Specific gravity is the ratio of two densities and is therefore dimensionless. If, by definition, distilled water at a temperature of 4°C has a density $\rho_m = 1$, then the specific gravity of a substance with density ρ is ρ/ρ_m and is numerically equal to the value of the substance density.

Density, or the specific gravity, of sea water depends on temperature t, salinity s, and, because of the slight compressibility of water, on sea pressure p. Since numerical values of density usually start with 1.0 with the exception of high temperatures and of very low salinities of 5°/oo or less), it has become customary to abbreviate these values as:

$$\sigma_{s,t,p} = (\rho_{s,t,p} - 1) \cdot 10^3 \qquad (2/1)$$

where $\rho_{s,t,p}$ is the density as a function of salinity, temperature, and sea pressure.

If the density of a water sample is determined at atmospheric pressure (that is, at sea pressure p = 0), this is expressed as

$$\sigma_t = (\rho_{s,t,o} - 1) \cdot 10^3 \qquad (2/2)$$

and is called a sigma-t value. Thus, a sigma-t value of 24.78 is equivalent to a specific gravity of 1.02478. As shown in the following discussions, this parameter is very useful in describing mixing surfaces.

Another useful oceanographic tool is the TS diagram. This is simply a temperature - salinity graph showing the relationship between the two variables as observed together at various depths. Although there is no functional physical relationship between temperature and salinity, it has been found that the vertical stratification in different oceanic regions does show a preference for certain TS associations which can be followed over large

25

geographic areas. A particular water mass, water type, or mixture of water masses can be distinguished by its relative location on the diagram.

The shelf salinity distributions in Figures 2-8 through 2-12 show variability patterns within $\pm 1°/oo$ of $36°/oo$. Within this $2°/oo$ band, the association of salinity changes with the corresponding temperature distribution illustrates mesoscale boundary effects which form the shelf distribution. Of particular interest to this study are the anomalously high salinity signatures associated with temperatures in the 18 to 25°C range which may be indicative of Subtropical Underwater intrusions. These features appear in the winter data on Transect C (Figures 2-5 and 2-10) on February 7, 1982 and in the spring data, also on Transect C, near the bottom on April 29, 1981 (also see Figures 2-5 and 2-10). In both cases, back-up satellite imagery appear to confirm the impingement of the Loop Current onto the shelf.

In general, a number of similarites can be seen between the salinity and temperature distributions, i.e., the halocline usually corresponds to the thermocline and mixed-layer salinities are partitioned in a cross-shelf direction; summers show more variability with depth than winter; and fall and spring appear as transitional distributions between winter and summer.

2.3.3 <u>Transmissivity</u>

Before defining transmissivity, or more precisely beam transmittance, first consider a number of the terms used in optical oceanography. Besides leading to a convenient definition, this approach will also serve as an introduction to the concepts used in Section 6.0.

SUMMER

36.0 35.8 35.6
36.2
36.4
36.2
36.0

FALL

35.6
35.8
36.0
36.2

WINTER

36.4
36.4
36.2

SPRING

36.2 36.0 <36.0
36.4

DEPTH (metres)

DISTANCE FROM 20-METRE CONTOUR (statute miles)

Figure 2-8.   Seasonal salinity distributions on Transect A.

Figure 2-9.   Seasonal salinity distributions on Transect B.

28
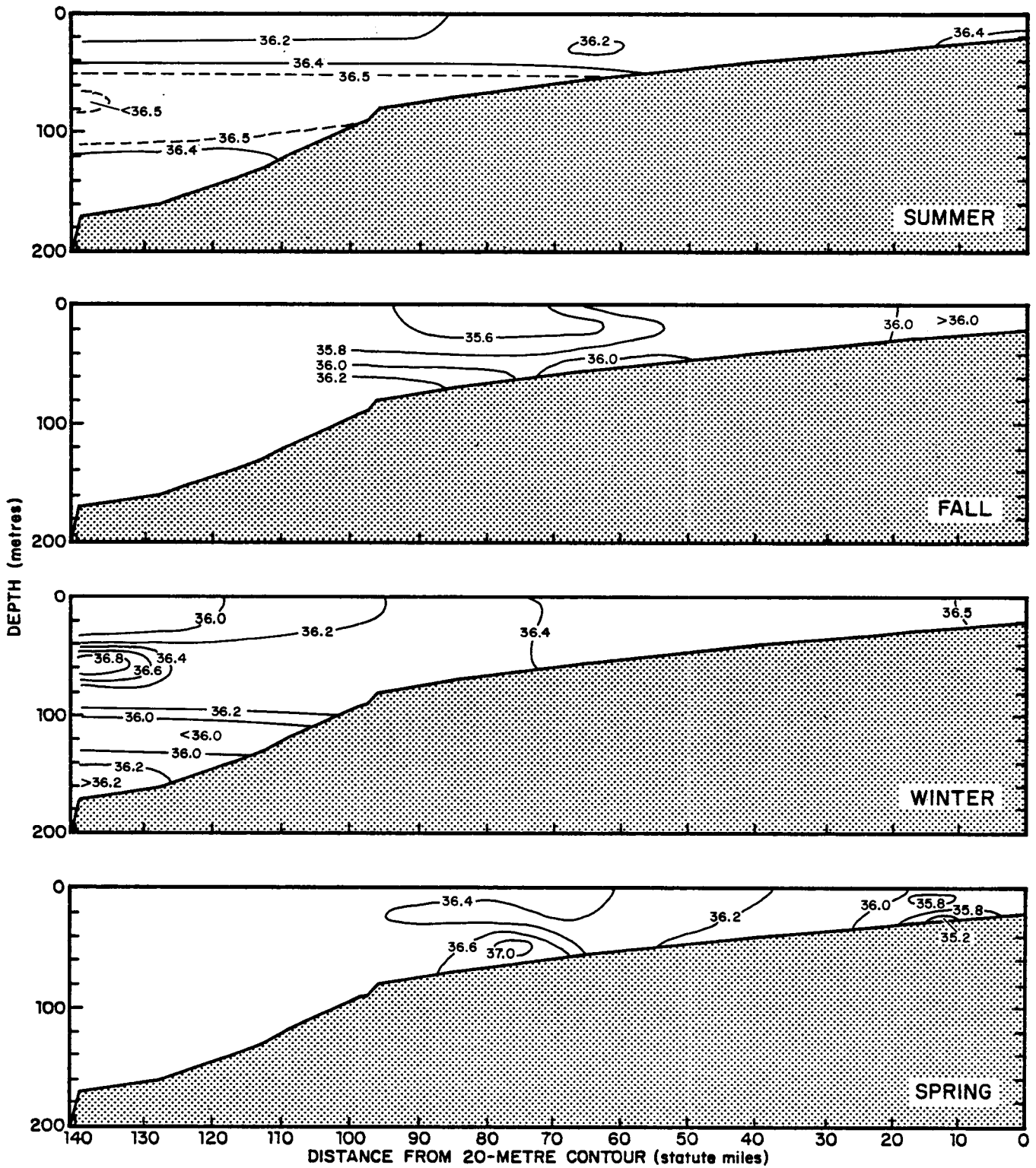
Figure 2-10. Seasonal salinity distributions on Transect C.

29
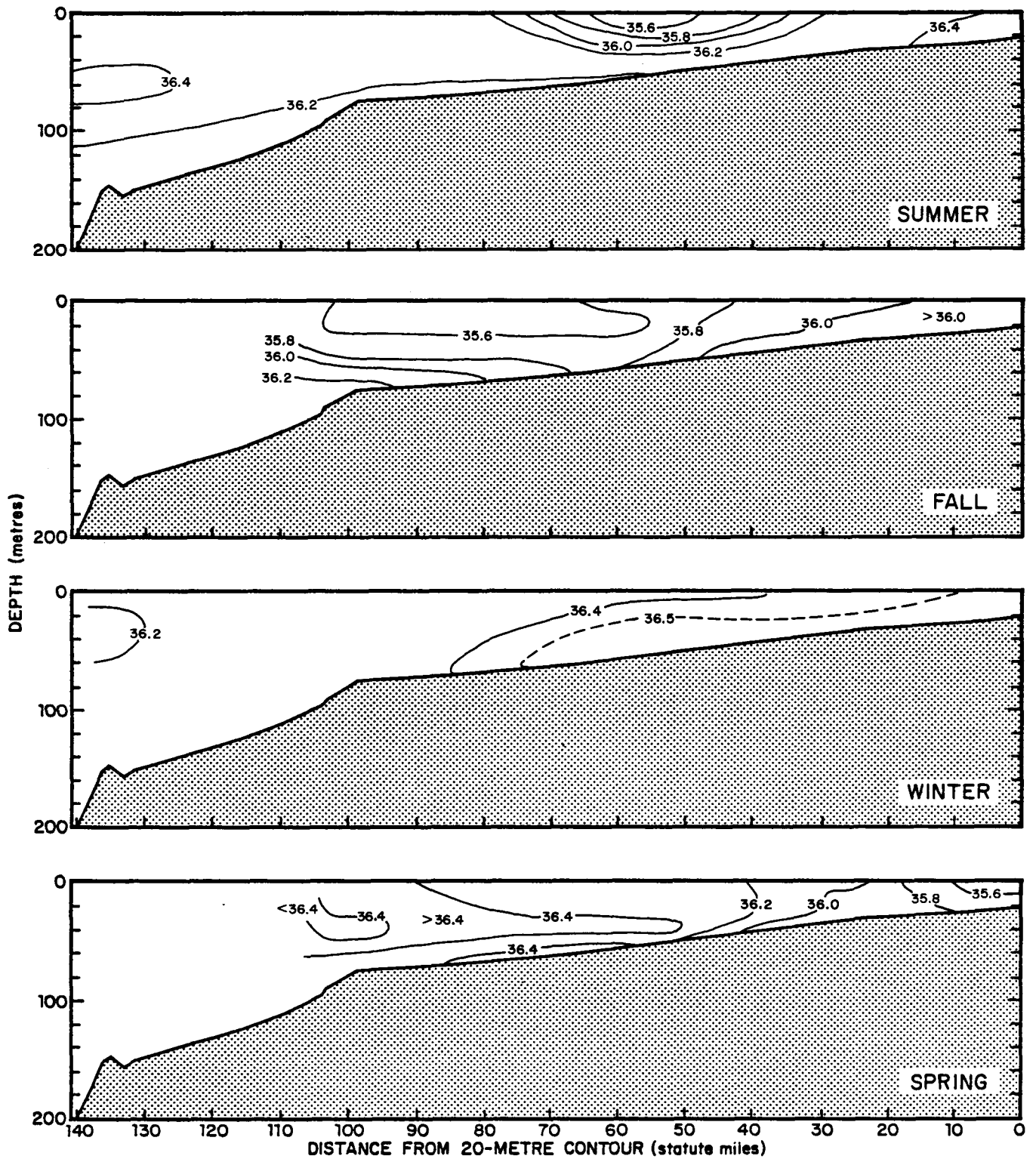
Figure 2-11.   Seasonal salinity distributions on Transect D.

30
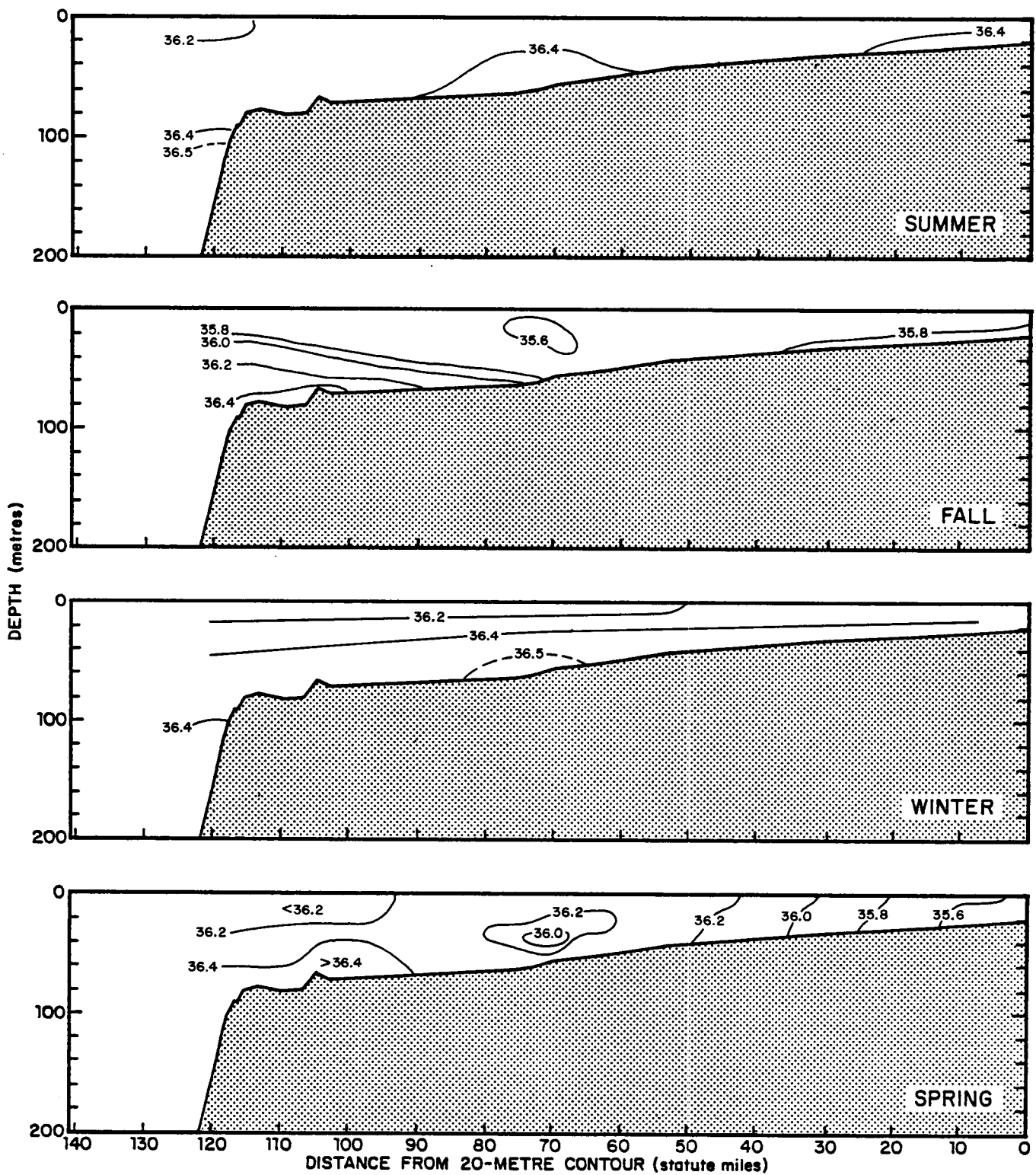
Figure 2-12. Seasonal salinity distributions on Transect E.

31

Consider the differential amount of radiant energy $dQ(\lambda)d\lambda$ in a specified wavelength interval $(\lambda, \lambda + \Delta\lambda)$ which is transported across a small element of area dA in directions confined to an element of solid angle $d\omega$ during a time interval dt. This energy can be expressed in terms of radiance, $L(\lambda)$, as

$$dQ(\lambda)d\lambda = L(\lambda)\cos\Theta \, d\lambda \, dA \, d\omega \, dt \qquad (2/3)$$

where θ is the angle between the direction under consideration and the outward directed normal to dA. Radiance, L, is actually a function of horizontal position, depth, orientation, and time as well as wavelength but normally varies so slowly that it is often assumed to be independent of horizontal position (i.e., x and y).

Radiant flux, F′ is the time rate of flow of Q and can be expressed simply as

$$dF' = \frac{dQ}{dt} = L\cos\Theta \, dAd\omega \qquad (2/4)$$

Intensity, I is defined as

$$dI = \frac{dF'}{d\omega} = L\cos\Theta \, dA \qquad (2/5)$$

Irradiance is the radiant flux per area, or

$$\frac{dF'}{dA} = L\cos\Theta \, d\omega, \qquad (2/6)$$

and is usually considered in five quantities. The two most common are the upward irradiance, E_u,

$$E_u = \int_{-2\pi} L \mid \cos \Theta \mid d\omega \qquad (2/7)$$

in which the integration is completed over all solid angles in the lower hemisphere, and the downward irradiance, E_d,

$$E_d = \int_{+2\pi} L \mid \cos \Theta \mid d\omega \qquad (2/8)$$

in which the integration is completed over all solid angles in the upper hemisphere. Two other irradiances are the vector irradiance, $\underline{E}$,

$$\underline{E} = \int_{4\pi} L \cos \theta \, d\omega \, , \text{ and} \qquad (2/9)$$

the scalar irradiance, E_o,

$$E_o = \int_{4\pi} L \, d\omega \qquad (2/10)$$

where the integration is completed over all solid angles.

Downward quanta irradiance q, in the visible part of the spectrum (350 to 700 nanometers (nm)) can be related to the downward irradiance as

$$q \ (350-700 \ nm) = \int_{350}^{700} E_d(\lambda) \cdot \lambda \cdot h^{-1} \cdot s^{-1} \, d\lambda \qquad (2/11)$$

where h = 6.626 x 10^{-34} joule sec is Planck's constant and S = 3 x 10^8 m sec^{-1} is the speed of light <u>in vacuo</u>. This is a measure of available light energy for photosynthesis.

Optical properties can be divided into two classes --- the inherent and apparent properties. An inherent property is independent of changes in the radiance distribution; an apparent property is dependent. Inherent properties of interest in this context are the absorption coefficient $a(x,y,z,t)$, the scattering coefficient $b(x,y,z,t)$, and the attenuation coefficient $c(x,y,z,t)$ = a + b. All have units of reciprocal length. The light scattering function $\beta(\theta)$, is defined through the equation

$$dI = \beta(\theta) \cdot E \cdot dV \qquad (2/12)$$

where E is the irradiance in the scattering volume dV. $\beta(\theta)$ is related to the scattering coefficient since

$$b = \int_{4\Pi} \beta(\theta) \, d\omega. \qquad (2/13)$$

Apparent properties include the vertical attenuation coefficients for irradiances, such as

$$K_d = -\frac{1}{E_d} \frac{\partial E_d}{\partial Z} \qquad \text{for the downward irradiance} \qquad (2/14)$$

$$K_u = -\frac{1}{E_u} \frac{\partial E_u}{\partial Z} \qquad \text{for the upward irradiance} \qquad (2/15)$$

$$K_E = -\frac{1}{E} \frac{\partial E}{\partial Z} \qquad \text{for the vector irradiance, and} \qquad (2/16)$$

$$K_o = -\frac{1}{E_o} \frac{\partial E_o}{\partial Z} \qquad \text{for the scalar irradiance, and} \qquad (2/17)$$

In practice, the K-functions are calculated as

$$K = \frac{1}{Z_2 - Z_1} \ln \frac{E(Z_1)}{E(Z_2)} \qquad (2/18)$$

Again, all the attenuation coefficients have units of reciprocal length. It might be noted, however, that all the K-functions are apparent properties and, as such, are subject to variability with solar elevation, cloud cover, and state of the sea.

35

Beam transmittance can now be defined easily by considering the ratio of an initial flux, F'_o, travelling in a narrow beam over a distance r to a position where it is measured as F'_t. Thus

$$\ln (F'_t/F'_o) = - cr \qquad\qquad (2/19)$$

defines the (total) attenuation coefficient, c. The distance r for all transmissivity measurements in this study was 1.0 m.

A rough idea of how high the transmissivity of the waters profiled on the southwest Florida shelf appear can be obtained by comparing the contoured magnitudes in Figures 2-13 through 2-17 to the transmittance values listed in Table 2-1 for pure water. Except for the 750 to 760 nm absorption band in the listed visible wavelengths, transmittance values per metre for pure water are generally in excess of 90%. The values contoured in the seasonal cross-sections are of the same magnitude and imply little attenuation over a one-metre path length. Although little seasonal variability is evident over the major part of the shelf, the landward sides of the spring and fall distributions appear to be more turbid than the corresponding summer and winter distributions. Similarly, progressively more structure or variability is evident as the transects are located further south closer to the Dry Tortugas.

On a speculative basis, the large areas of relatively high bottom transmission may be indicative of a lack of significant near-bottom shelf currents to resuspend sediments. Localized areas of lower bottom transmission, on the
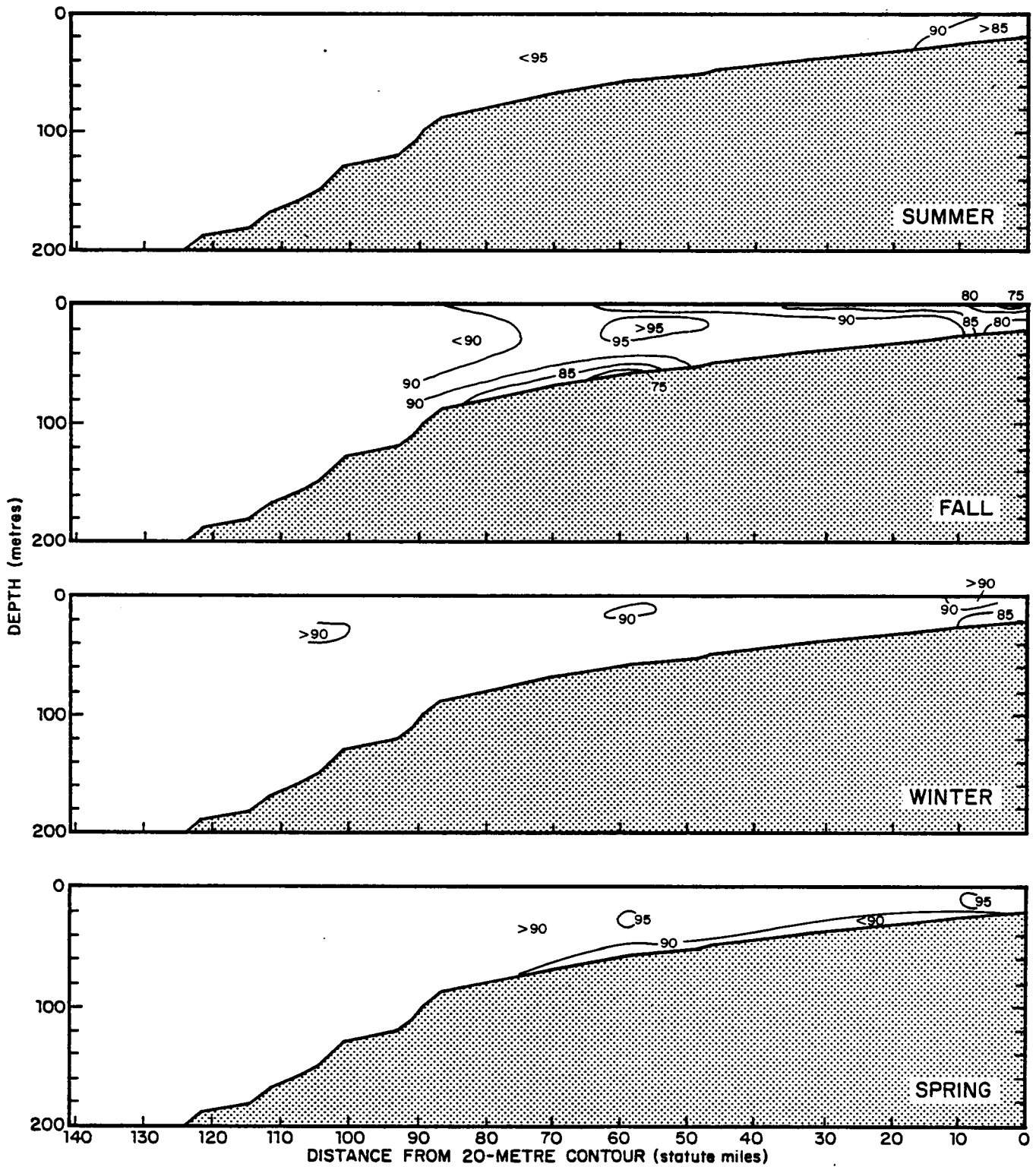
Figure 2-13. Seasonal transmissivity distributions on Transect A.
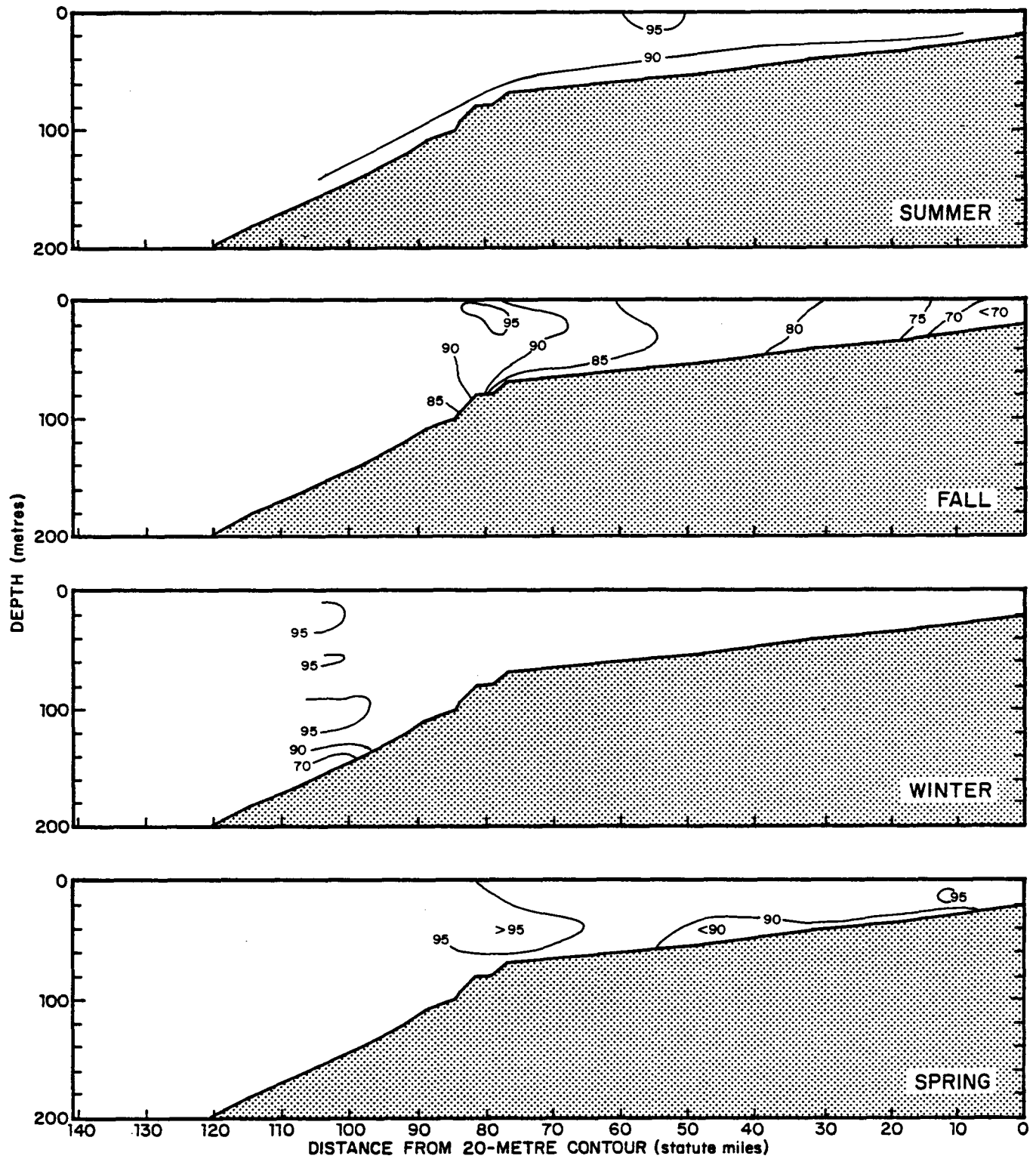
Figure 2-14. Seasonal transmissivity distributions on Transect B.

38
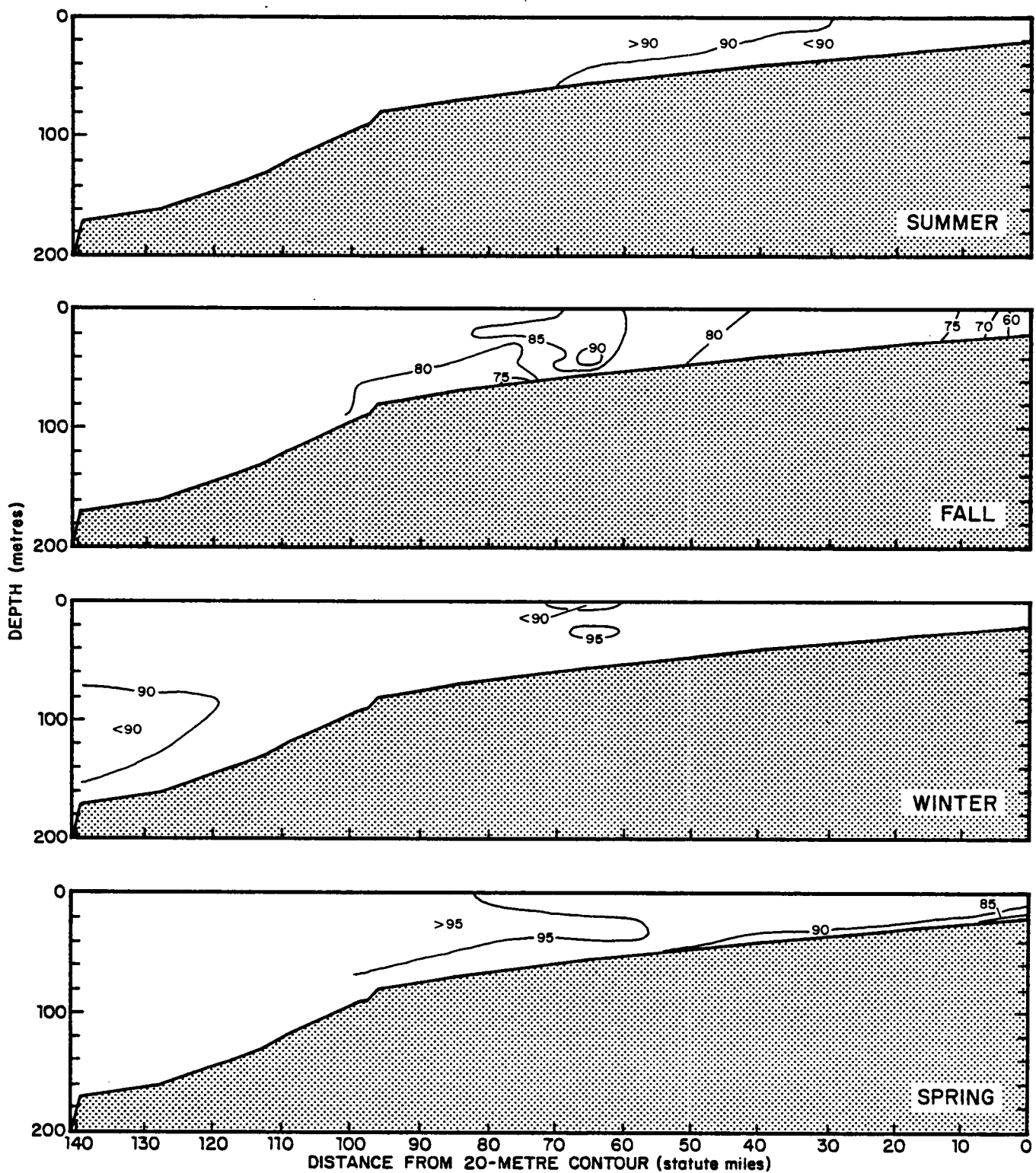
Figure 2-15. Seasonal transmissivity distributions on Transect C.

39
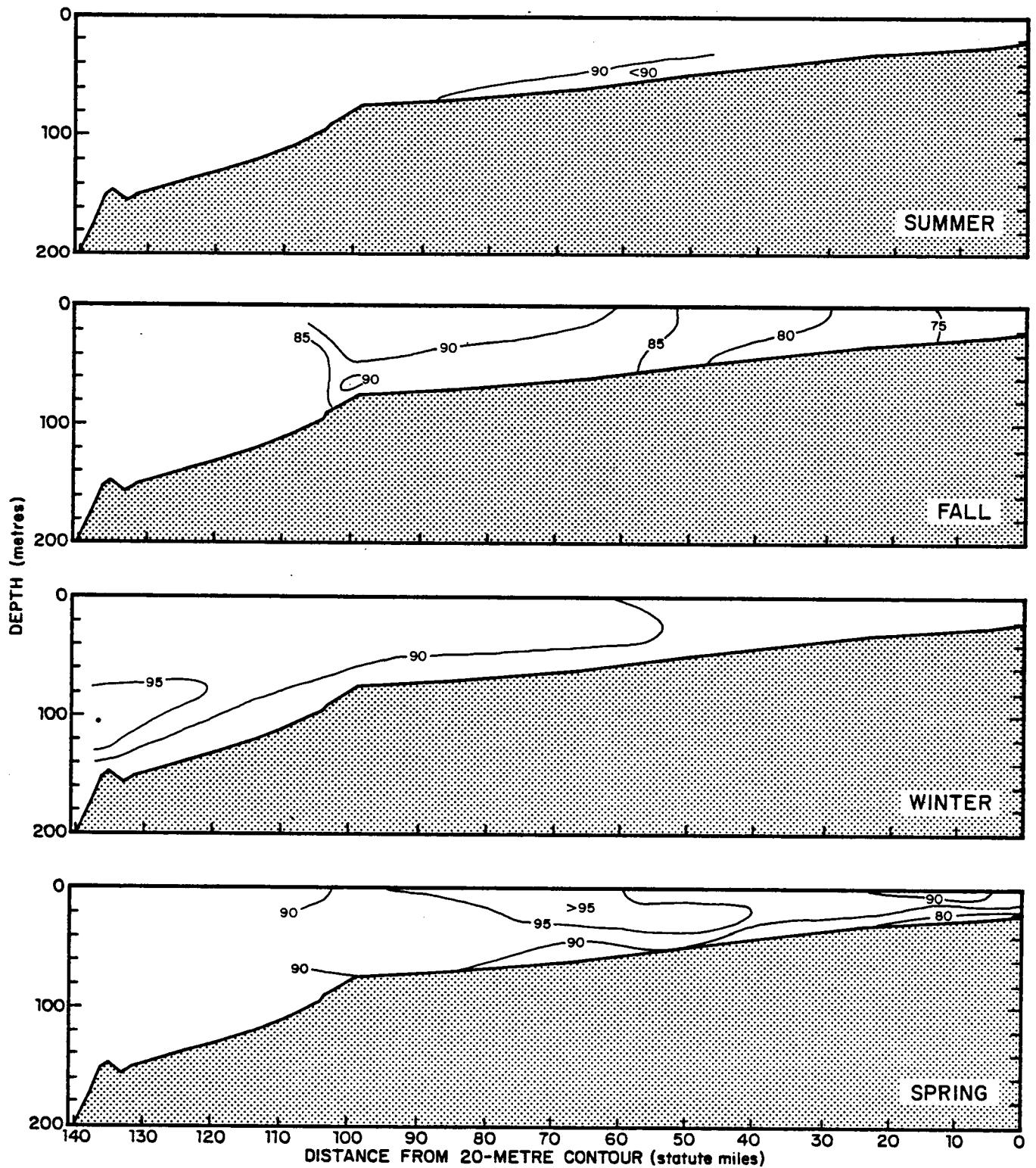
Figure 2-16. Seasonal transmissivity distributions on Transect D.
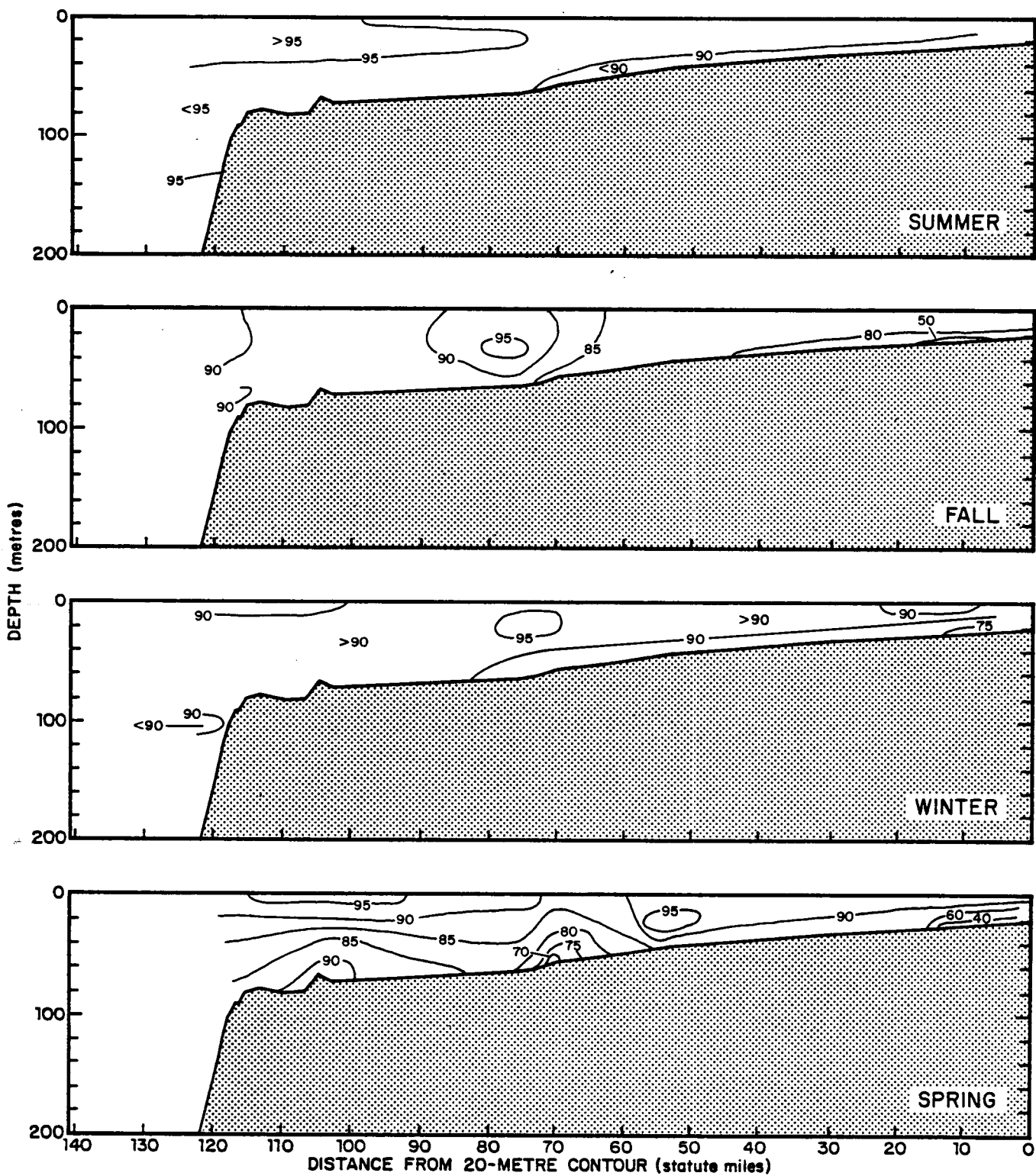
Figure 2-17. Seasonal transmissivity distributions on Transect E.

41

Table 2-1. Observed transmittance and attenuation
coefficient for pure water (modified
from Jerlov, 1968).

Wavelength (nm)	Transmittance (%/m)	Attenuation Coefficient c (m⁻¹)
375	95.6	0.045
400	95.8	0.043
425	96.8	0.033
450	98.1	0.019
475	98.2	0.018
500	96.5	0.036
525	96.0	0.041
550	93.3	0.069
575	91.3	0.091
600	83.3	0.186
625	79.6	0.228
650	75.0	0.288
675	69.3	0.367
700	60.7	0.500
725	29.0	1.240
750	9.0	2.400
775	9.0	2.400
800	18.0	2.050

other hand, may suggest a sediment resuspension or plankton activity. Near-bottom current meter data are needed to clarify these points.

2.3.4 Chlorophyll

The amount of chlorophyll that can be extracted from a unit volume of sea water depends upon the number of plant cells contained in the sample. Three chlorophylls are commonly found in planktonic algae, chlorophylls a, b, and c. The methods used in all phases of this study have yielded estimates for Chlorophyll a (Chl a).

Chlorophyll-containing plants make use of light energy and inorganic constituents of sea water such as water, carbon dioxide, and nutrients to (photo)synthesize complex organic molecules. The chief products are the three major categories of food materials, namely carbohydrates, proteins, and fats. This process is termed "Gross Primary Production" (Tait and De Santo, 1975).

Production rates are usually expressed as the weight of carbon fixed in organic compounds beneath a unit area of sea surface in unit time (e.g., $gC \cdot m^{-2} \cdot day^{-1}$). By far, the greatest part of primary production in the sea is performed by phytoplankton. The consumption of plants by herbivorous animals leads to the formation of animal tissue and so on through the different trophic levels or links in the "food chain".

The chlorophyll distributions in Figures 2-18 through 2-22 indicate several significant features of importance to this study.
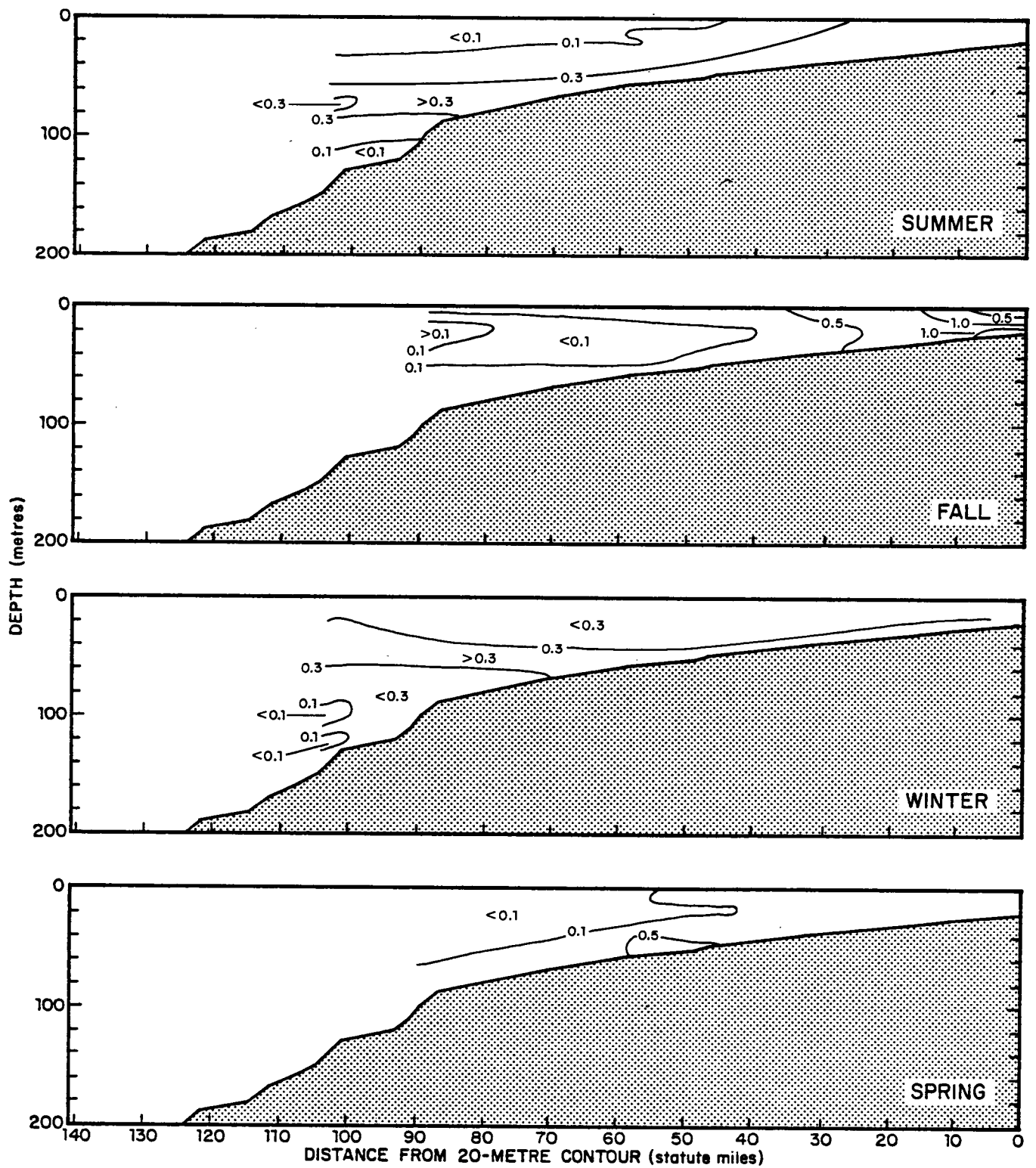
Figure 2-18. Seasonal chlorophyll a distributions on Transect A.

44
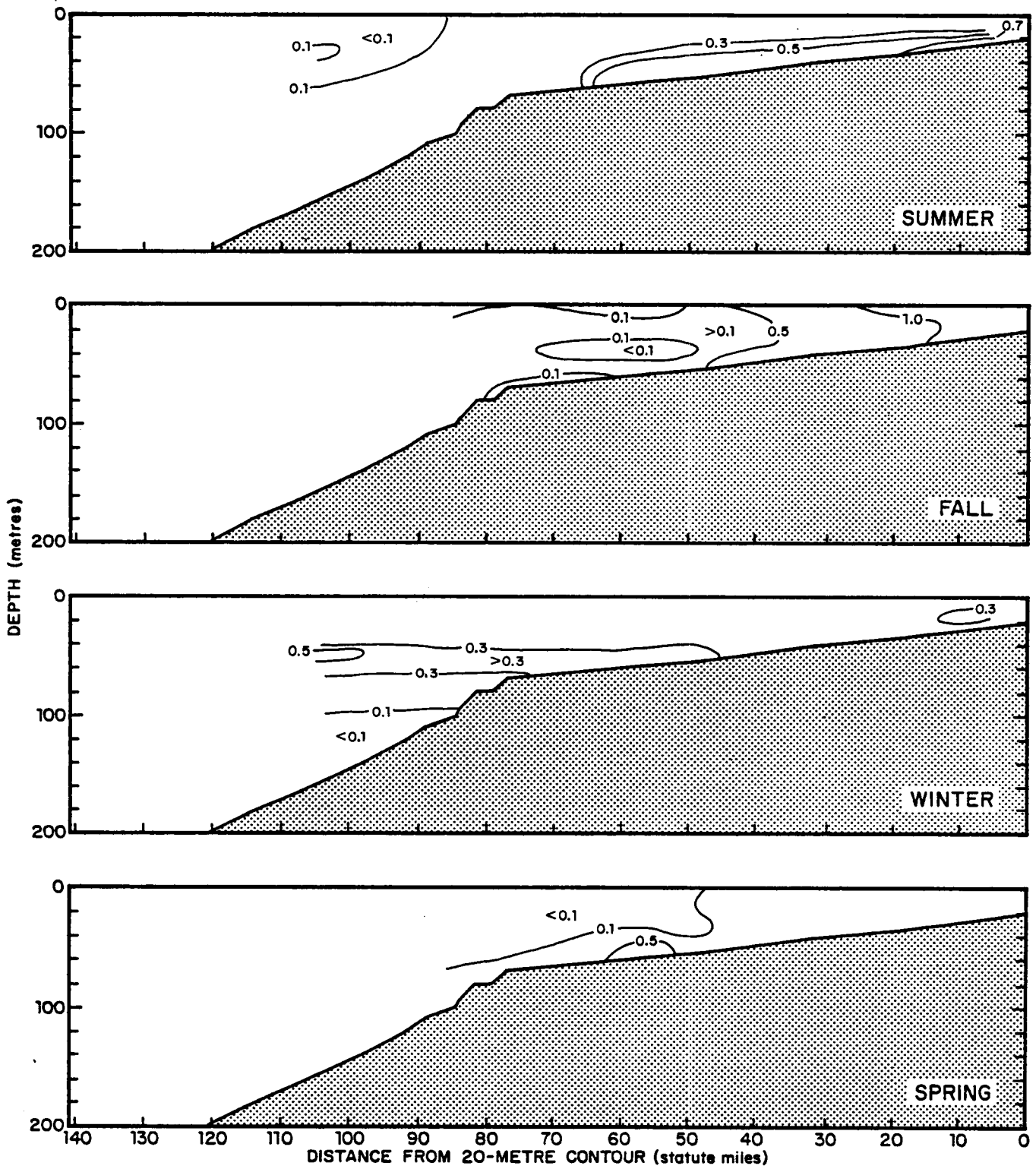
Figure 2-19. Seasonal chlorophyll _a_ distributions on Transect B.

45
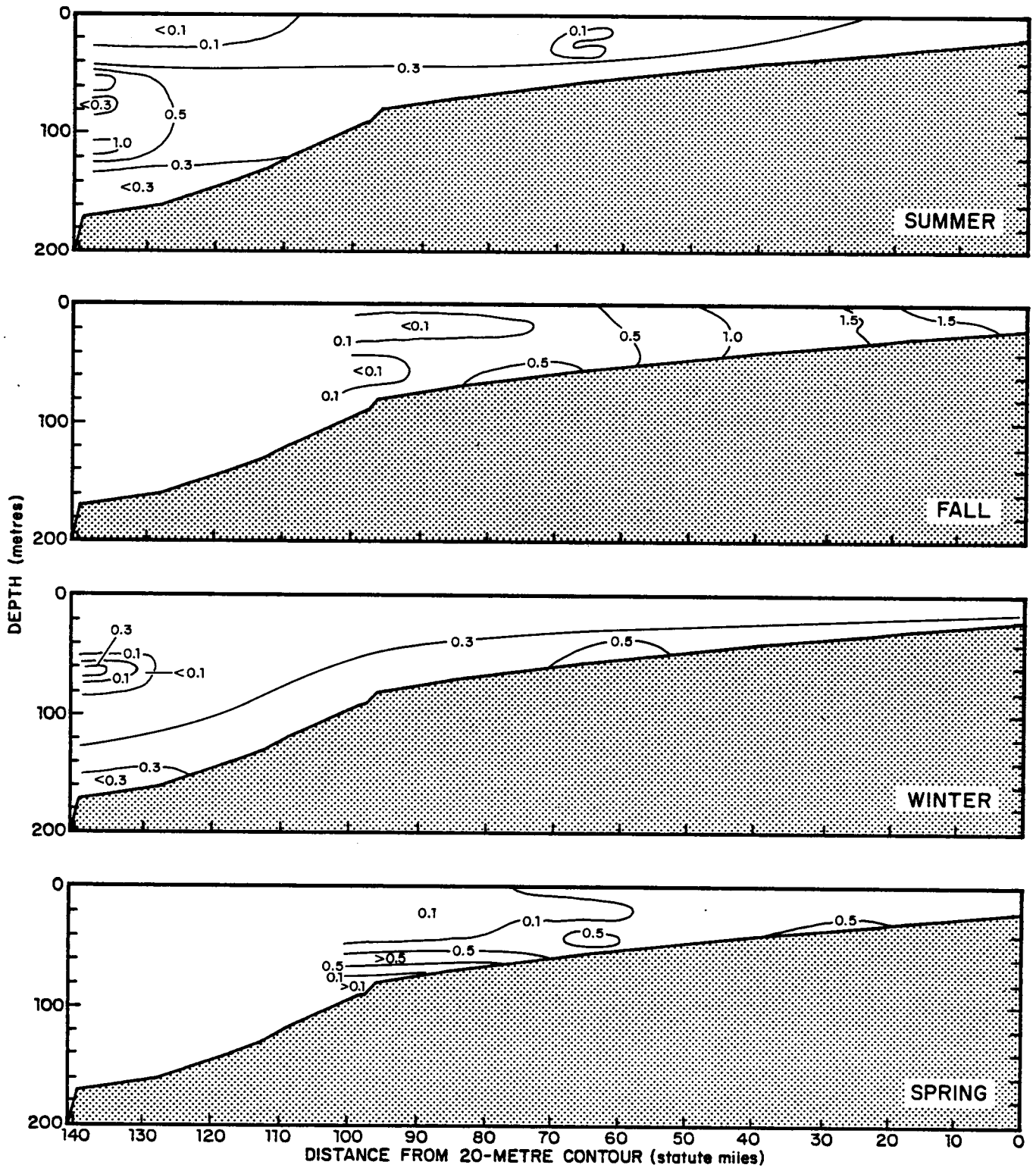
Figure 2-20.   Seasonal chlorophyll _a_ distributions on Transect C.

46
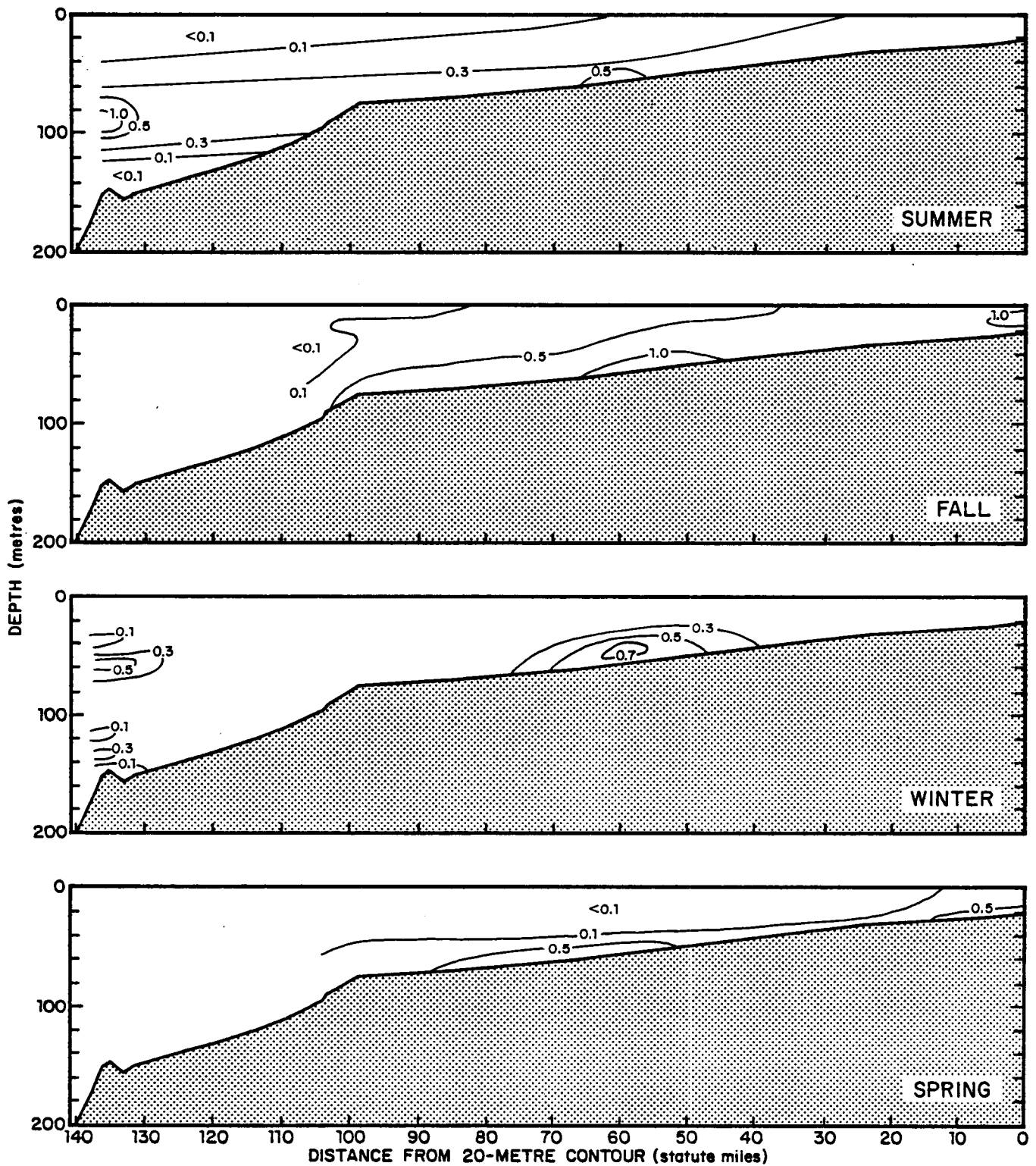
Figure 2-21. Seasonal chlorophyll _a_ distributions on Transect D.

47
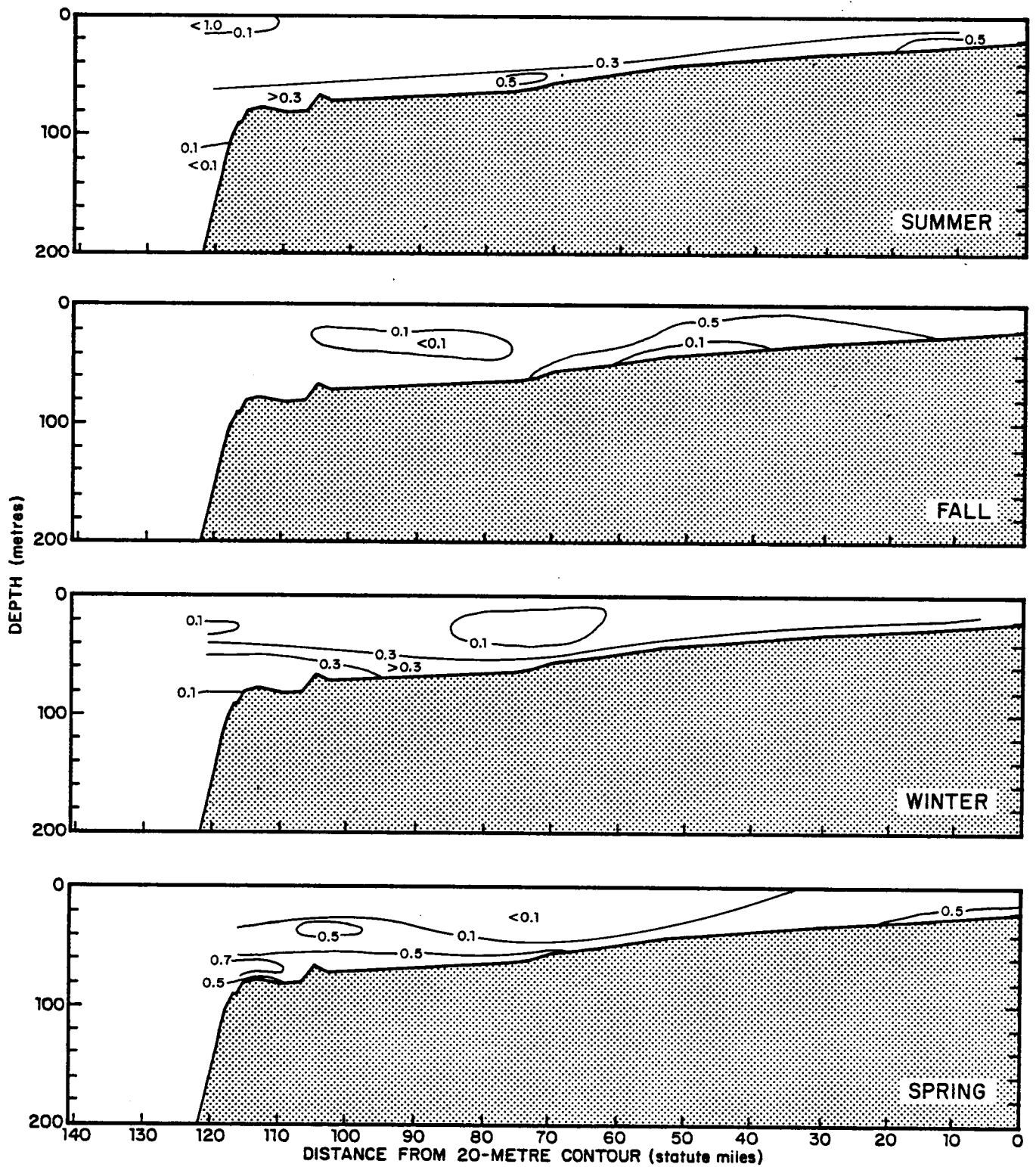
Figure 2-22. Seasonal chlorophyll <u>a</u> distributions on Transect E.

48

1. General chlorophyll levels are low (oligotrophic) across the major part of the shelf and agree with the levels reported by El-Sayed et al. (1972) of 0.20 ± 0.23 mg.m^{-3} (i.e., mean $\pm$ one standard deviation) based on 435 observations for the Gulf of Mexico. As a contrast, fertile coastal waters may exhibit levels from 10 to 40 mg.m^{-3} Chl $\underline{a}$ (Riley and Chester, 1971). Gordon et al. (1980) used Nimbus-7 Coastal Zone Color Scanner (CZCS) satellite imagery to map the surface distribution and concentration of Chl $\underline{a}$ on the Florida continental shelf in November 14, 1978. Their results showed concentrations of Chl $\underline{a}$ and Ph $\underline{a}$ to range from about 0.20 to 2.20 mg.m^{-3}. Haddad (1980) was able to show that some of the higher values in this range were attributable to a red tide bloom in the area at the time of the measurements.

2. Chl $\underline{a}$ maxima across the shelf region shown in the figures are not surface bound (Steidinger, 1973).

3. Subsurface maxima within the distributions generally appear on the extreme east (landward) or west (seaward) sides of the transects. The late fall maxima indicated on the landward side of all transects except E (Figure 2-22) may be indicative of near-shore shelf coupling (Turner et al., 1979; Weinstein, 1981) whereas the maxima indicated on the left-hand (seaward) side of the Transect C winter and spring (Figure 2-20) distributions are probably associated with a Loop Current intrusion as mentioned earlier in Section 2.3.2.

4. Secondary Chl $\underline{a}$ maxima appear to coincide with the depth of the pycnocline (Hobson and Lorenzen, 1972). Since density is mainly a function of temperature and salinity, as also discussed in Section 2.3.2, an example of this can be seen by comparing the fall, Transect A, Chl $\underline{a}$ distribution near the 100 m isobath (in Figure 2-18) with the corresponding transect distributions in Figures 2-3 and 2-8.

2.3.5 Nutrients

Two factors limit productivity: the availability of light and nutrients. The region from the surface to a depth where light has attenuated to one percent of its intensity at the surface is conventionally called the euphotic zone. During the first two study phases, the concentrations of three dissolved micronutrients were examined, phosphate (PO_4-P), nitrite and nitrate (NO_2-NO_3-N), and dissolved silica (SiO_2). Nitrite values were generally so low that separation of nitrite and nitrate was beyond the accuracy limit of the analysis method (WCC/CSA, 1982). Silicon occurs in the sea as silica and probably in true solution as silicate ion (Raymont, 1963). Seasonal shelf distributions of these nutrients are presented as a three-parameter set in Figures 2-23 through 2-27 for the nitrogenous compounds, 2-28 through 2-32 for phosphate, and 2-33 through 2-37 for silica.

The general distributions of PO_4-P and NO_2-NO_3-N are similar in all seasons with minimal values in the surface mixed layer and gradually increasing concentrations below the pycnocline. Also noticeable are the similarities between these distributions and the corresponding temperature sections in Figures 2-3 through 2-7. This similarity suggests a possible
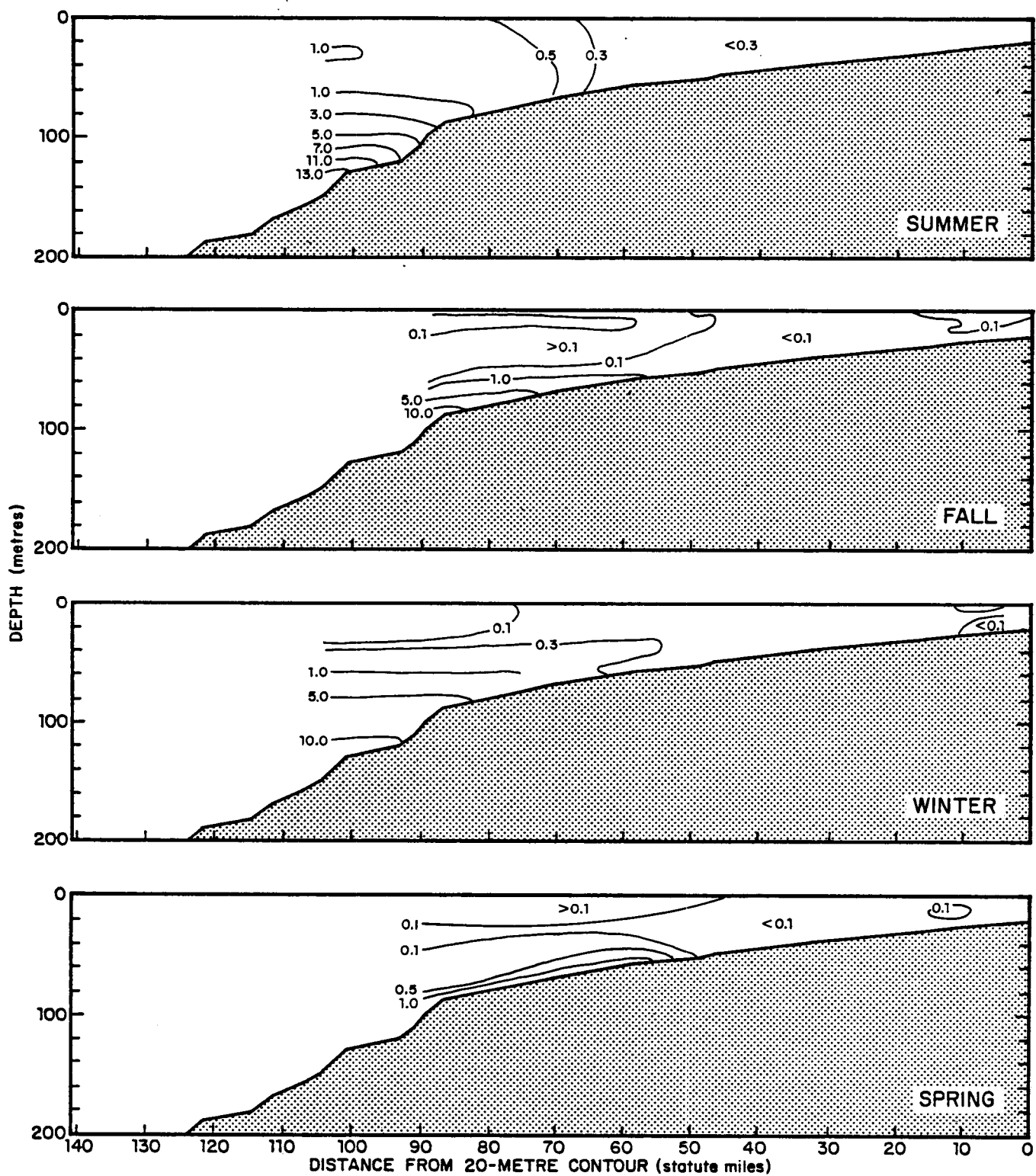
Figure 2-23. Seasonal nitrite + nitrate distributions on Transect A.
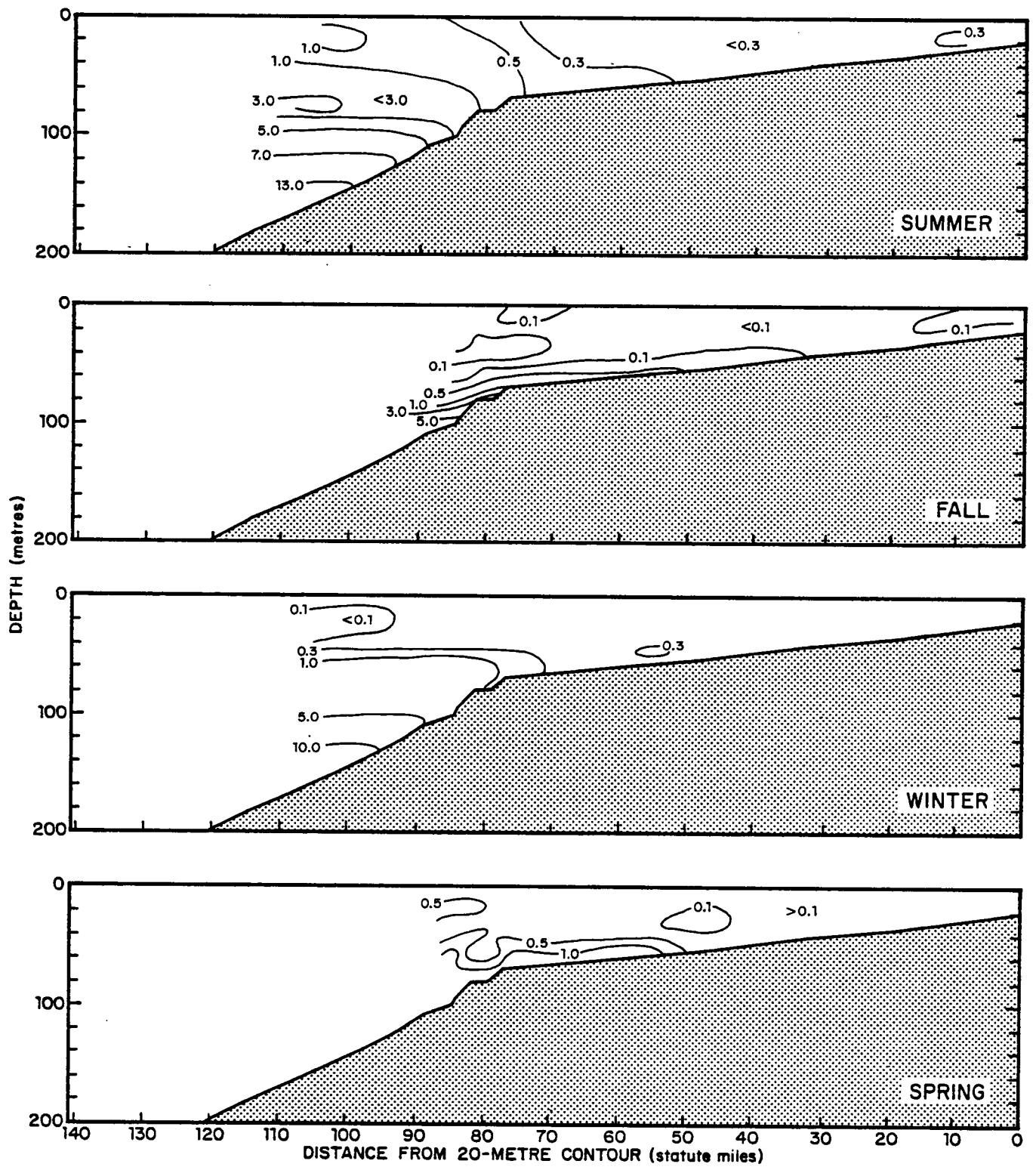
Figure 2-24. Seasonal nitrite + nitrate distributions on Transect B.
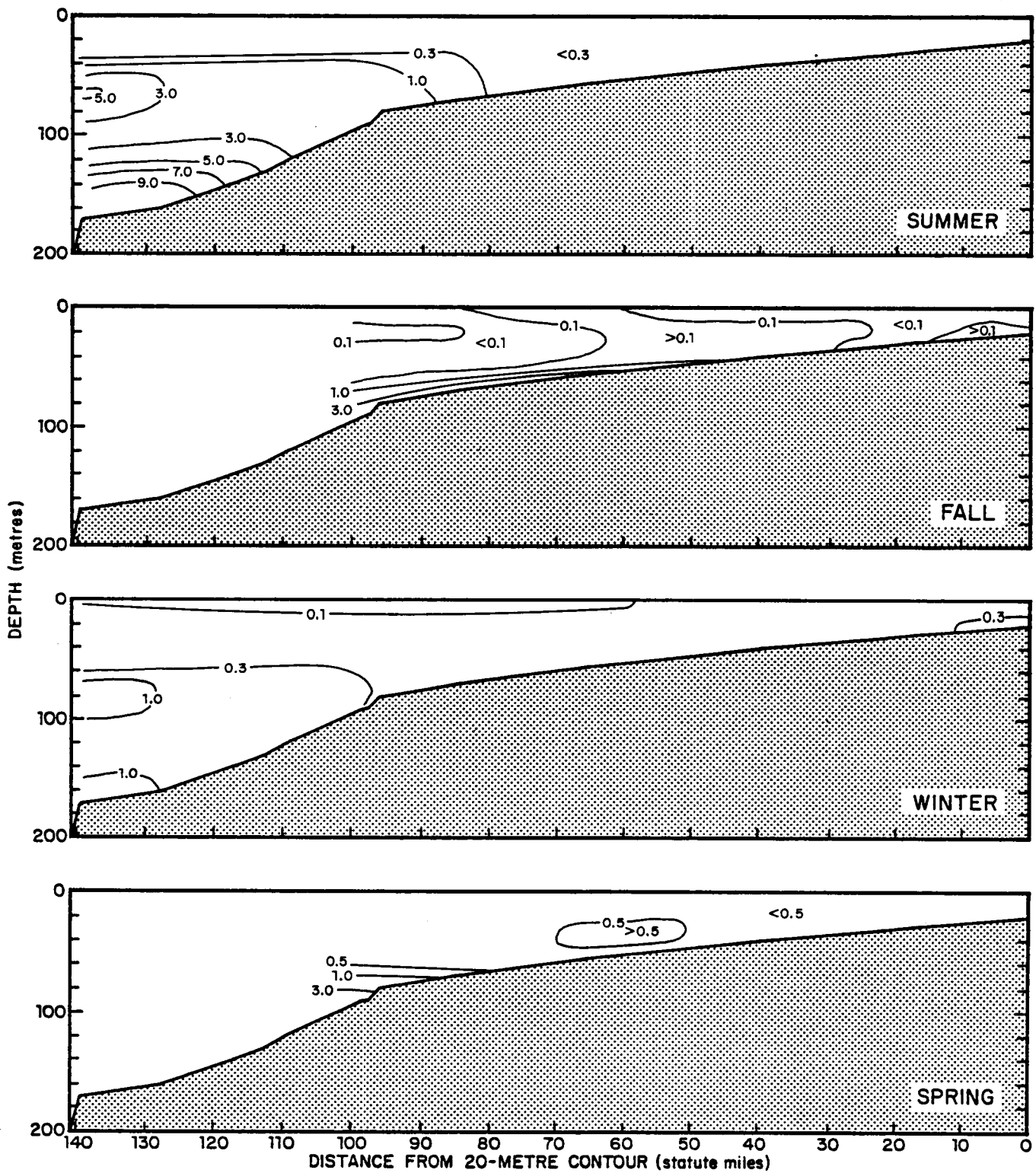
Figure 2-25. Seasonal nitrite + nitrate distributions on Transect C.

53
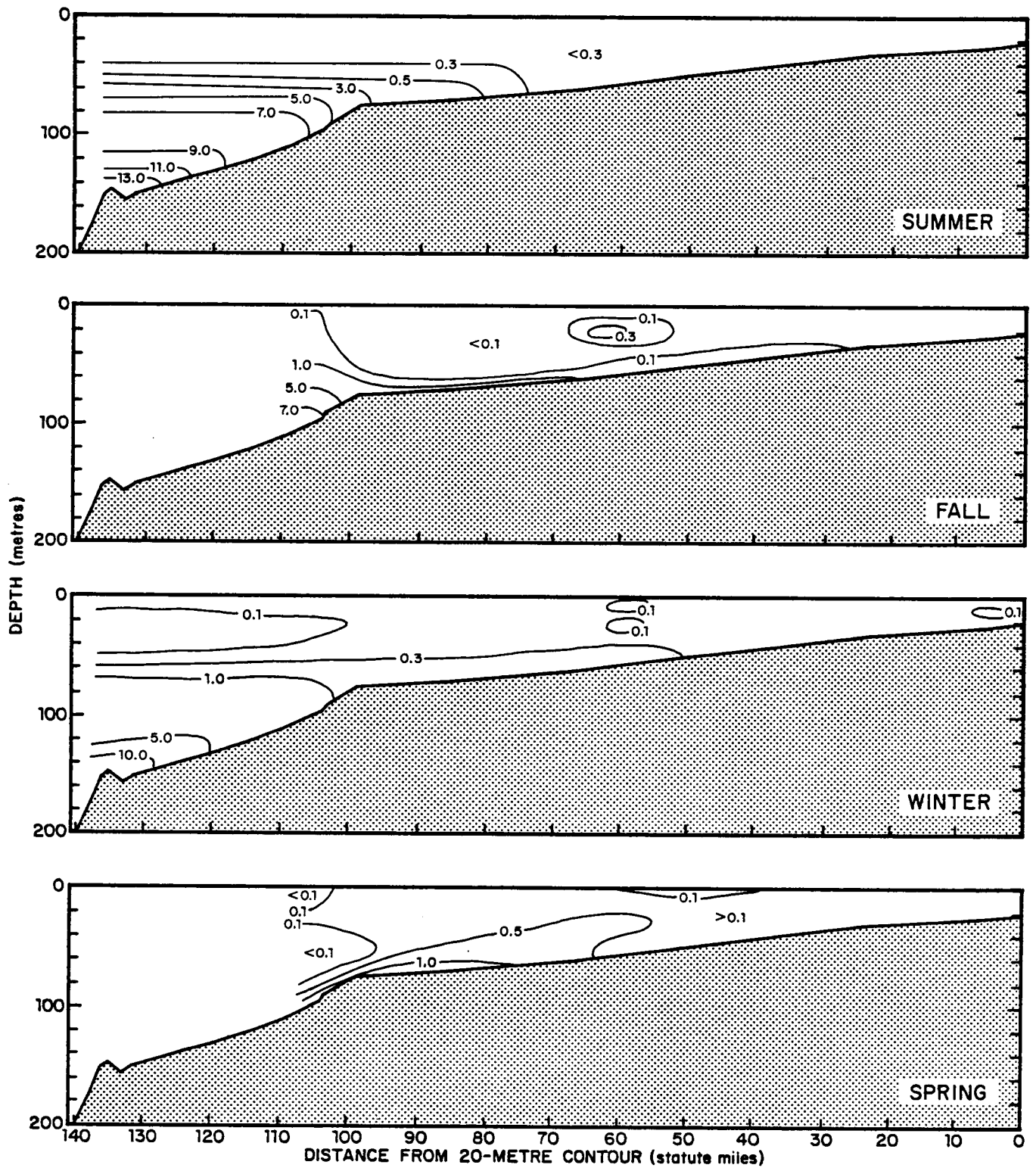
Figure 2-26. Seasonal nitrite + nitrate distributions on Transect D.

54
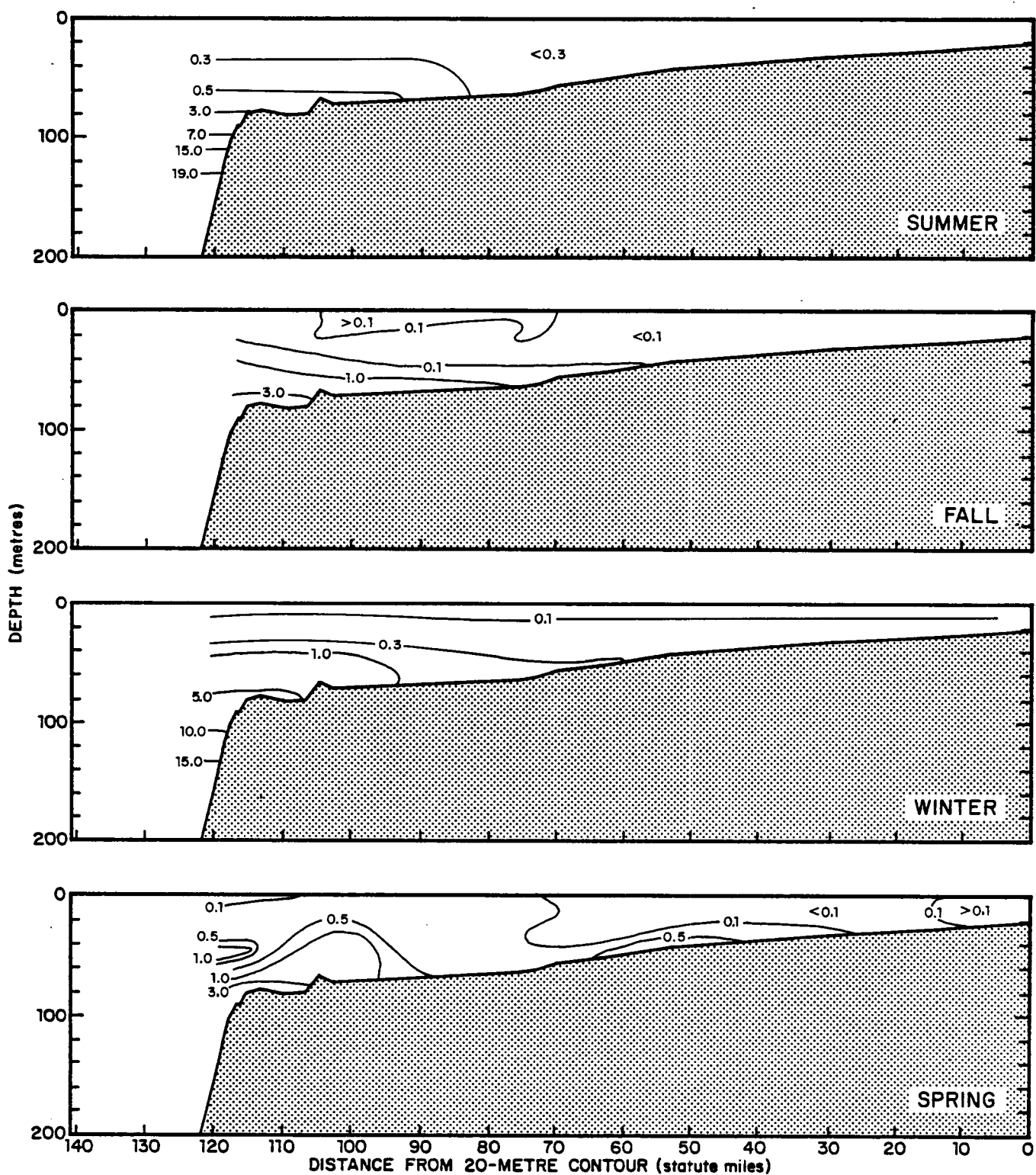
Figure 2-27. Seasonal nitrite + nitrate distributions on Transect E.

55
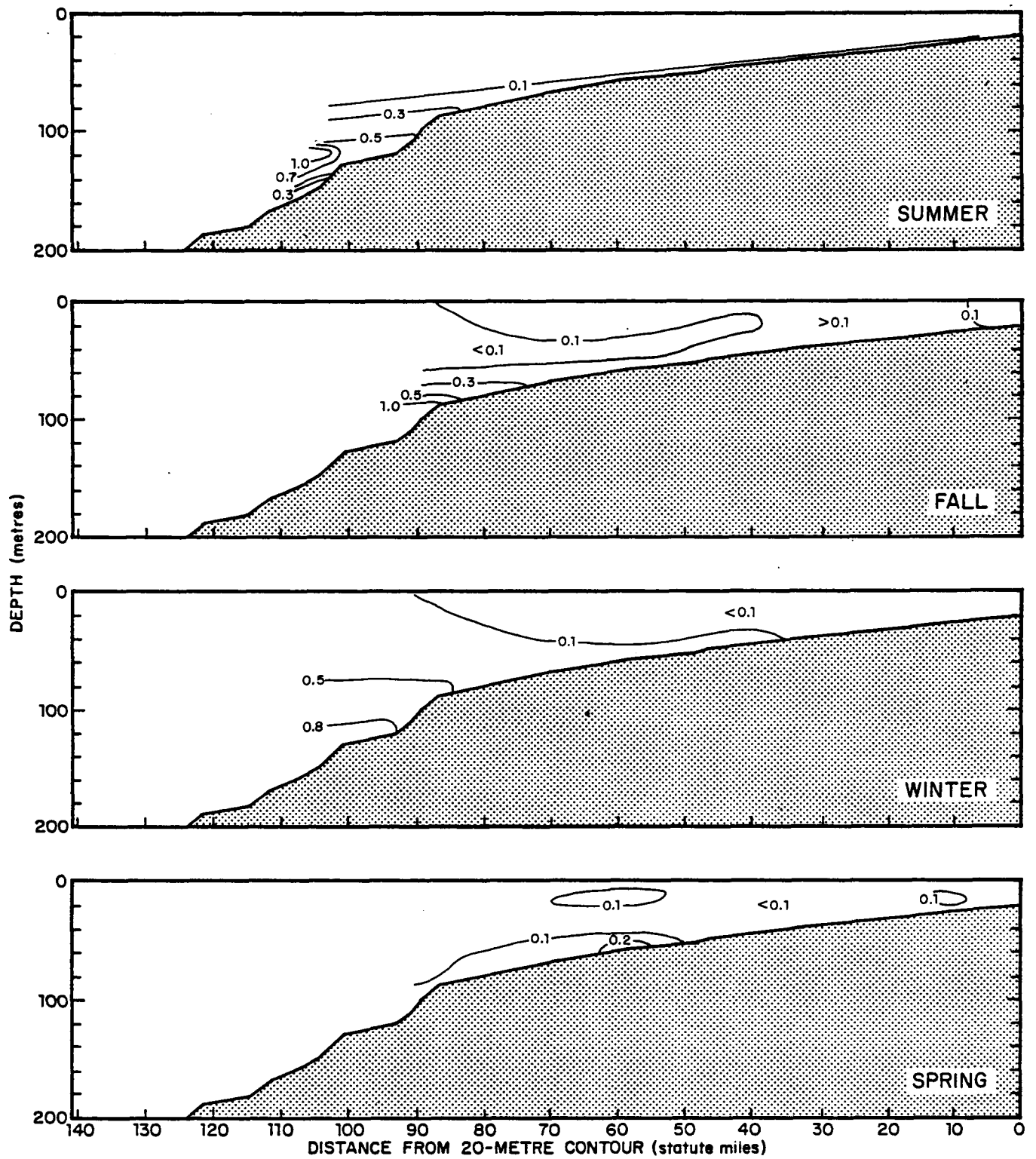
Figure 2-28. Seasonal phosphate distributions on Transect A.

56
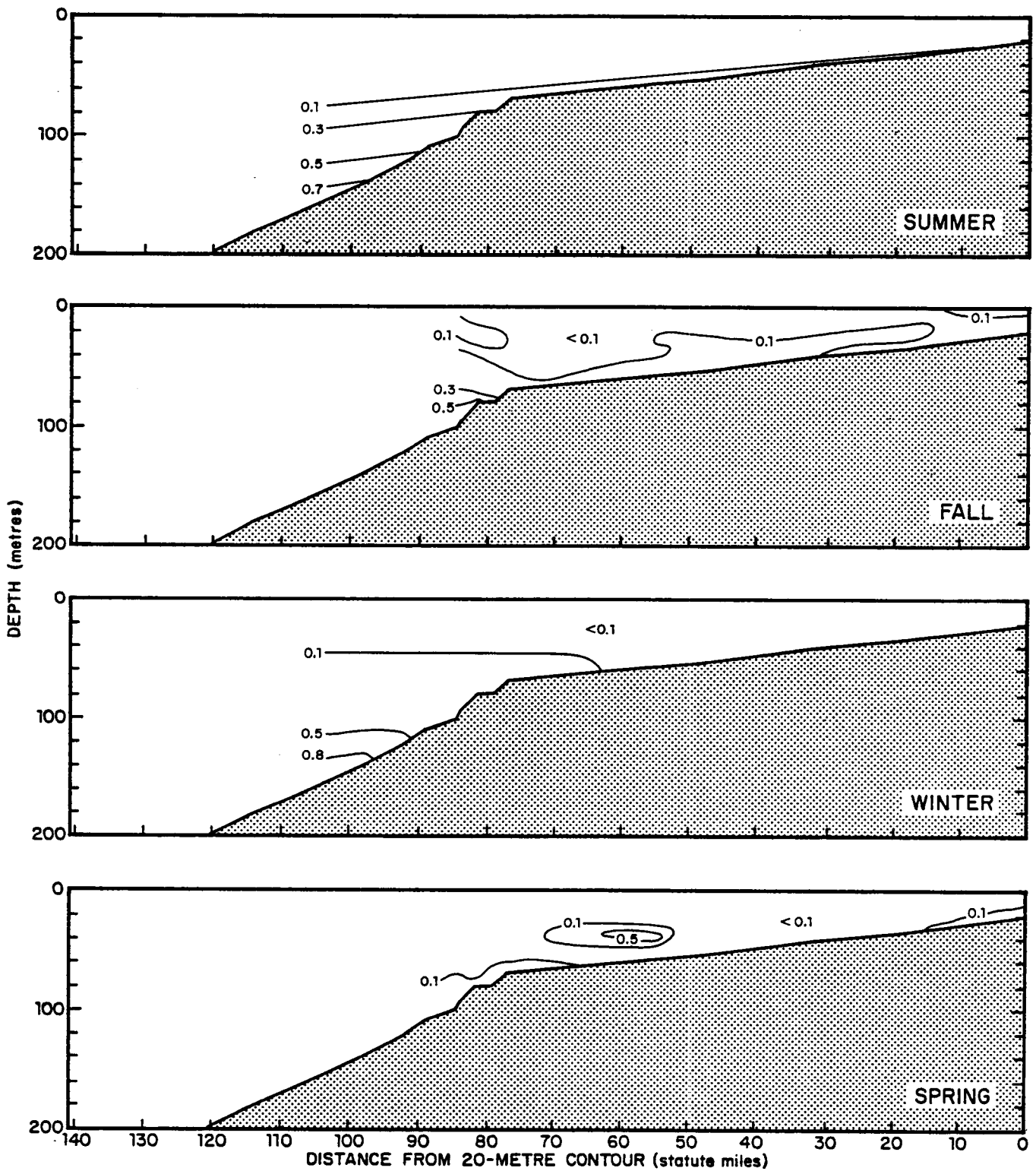
Figure 2-29. Seasonal phosphate distributions on Transect B.
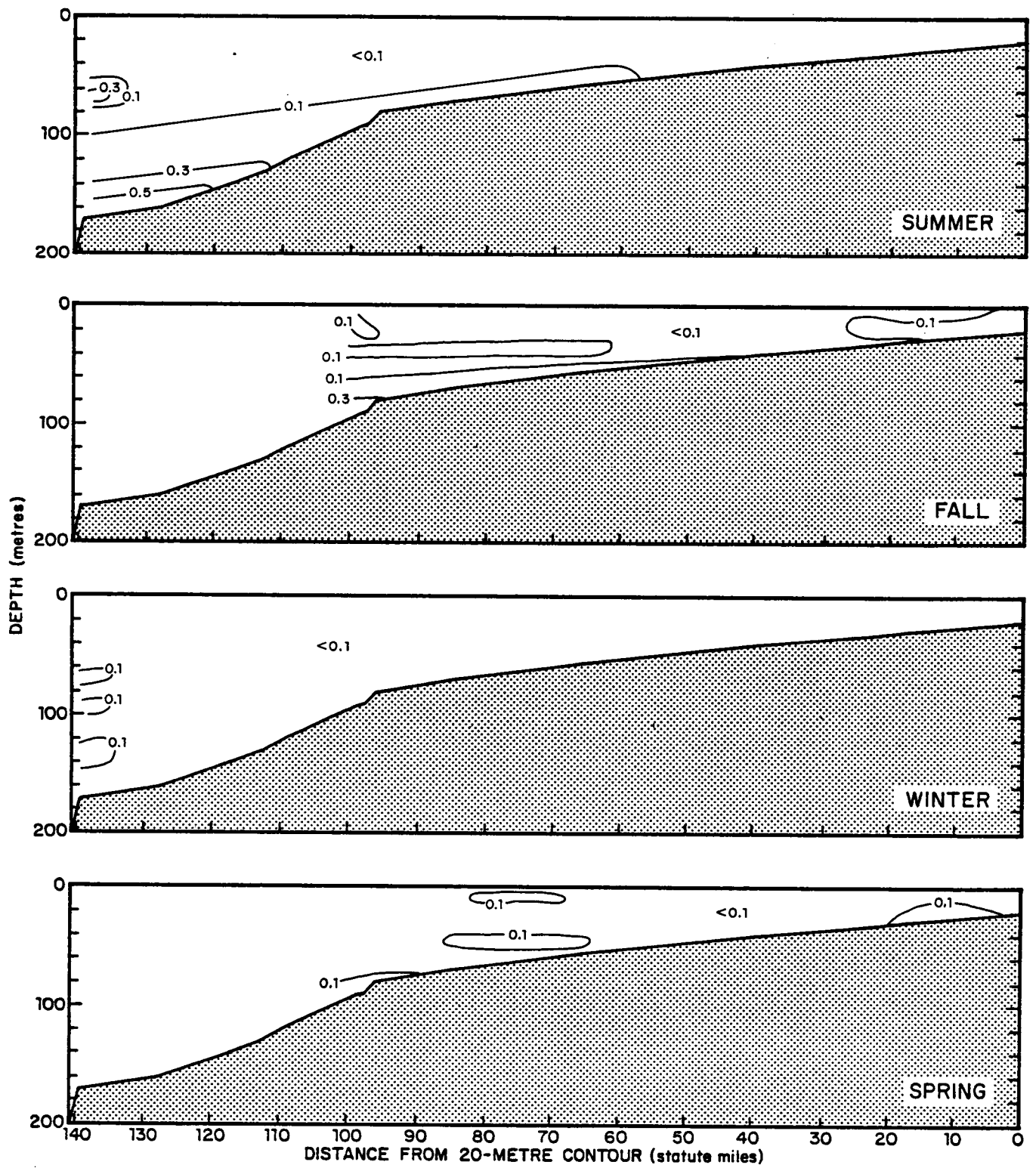
Figure 2-30.   Seasonal phosphate distributions on Transect C.

58
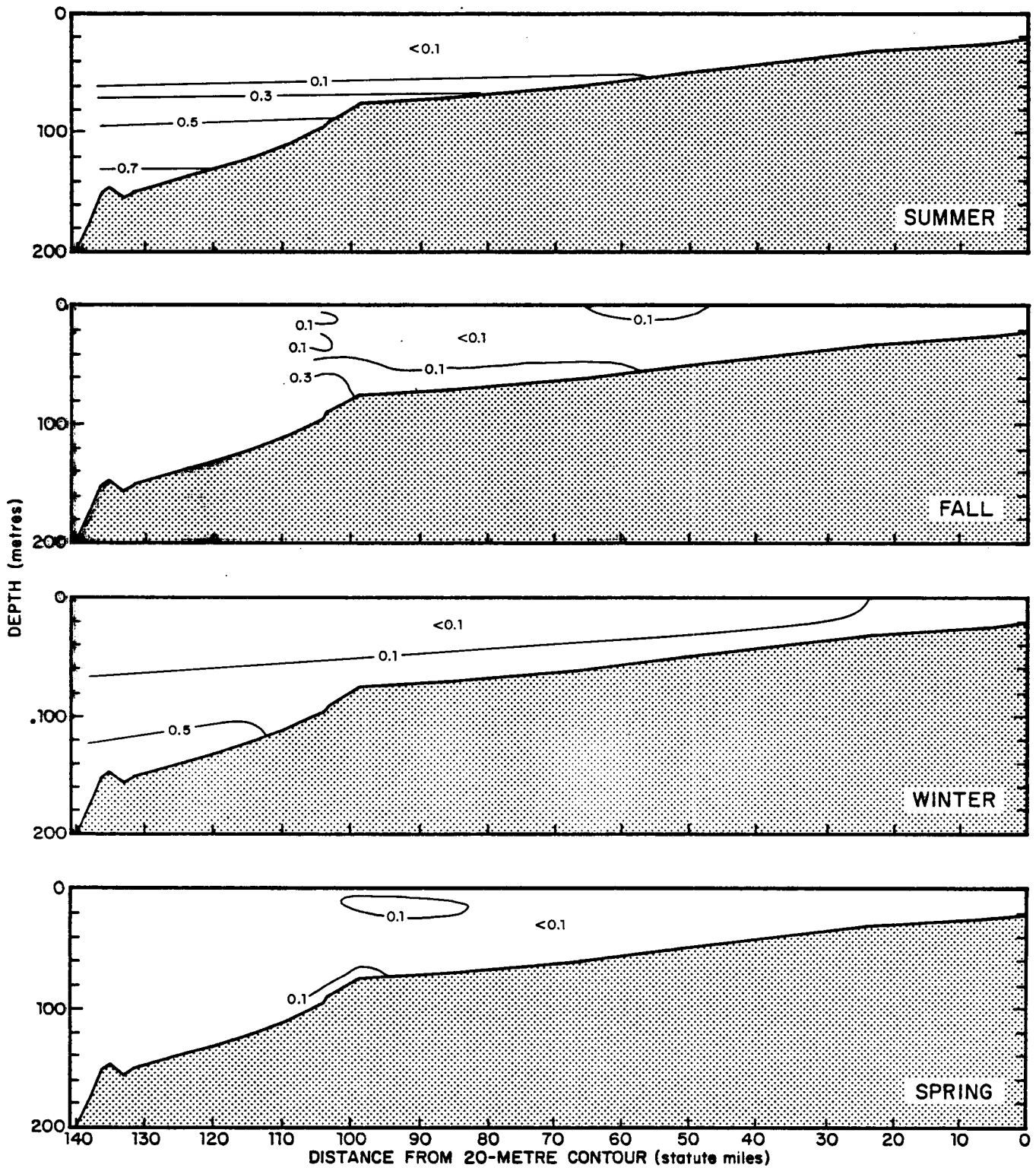
Figure 2-31. Seasonal phosphate distributions on Transect D.

59
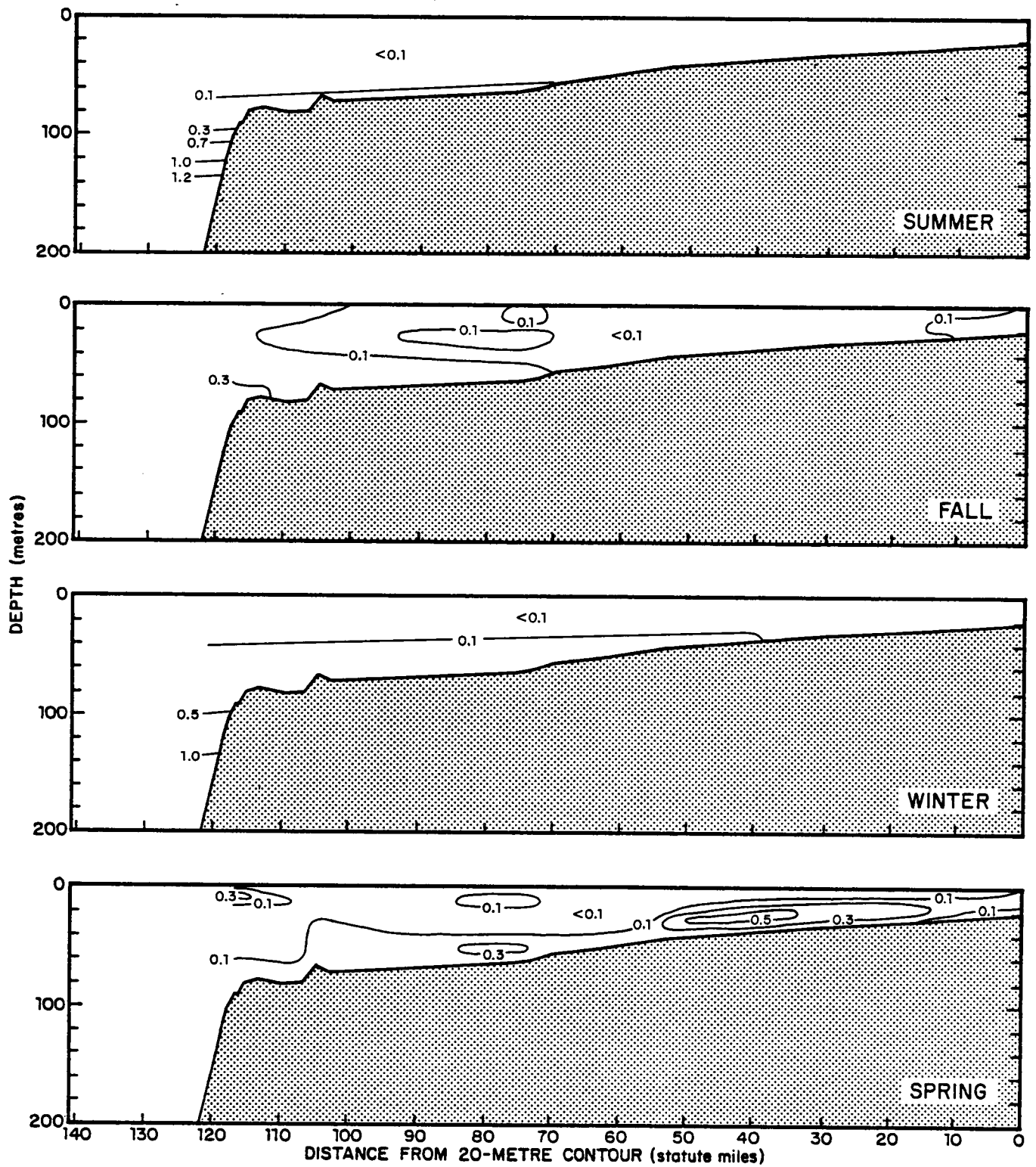
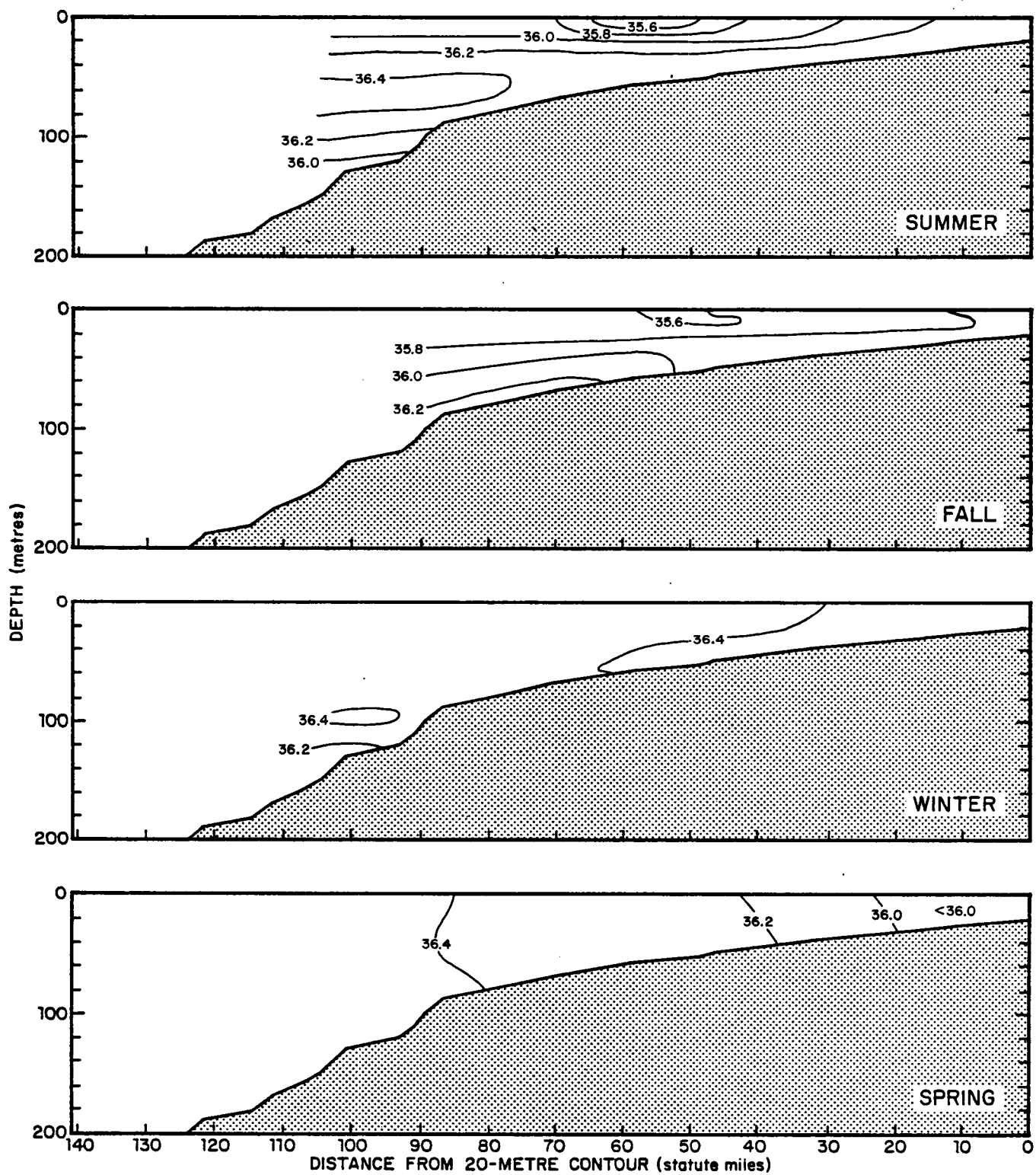Figure 2-32. Seasonal phosphate distributions on Transect E.
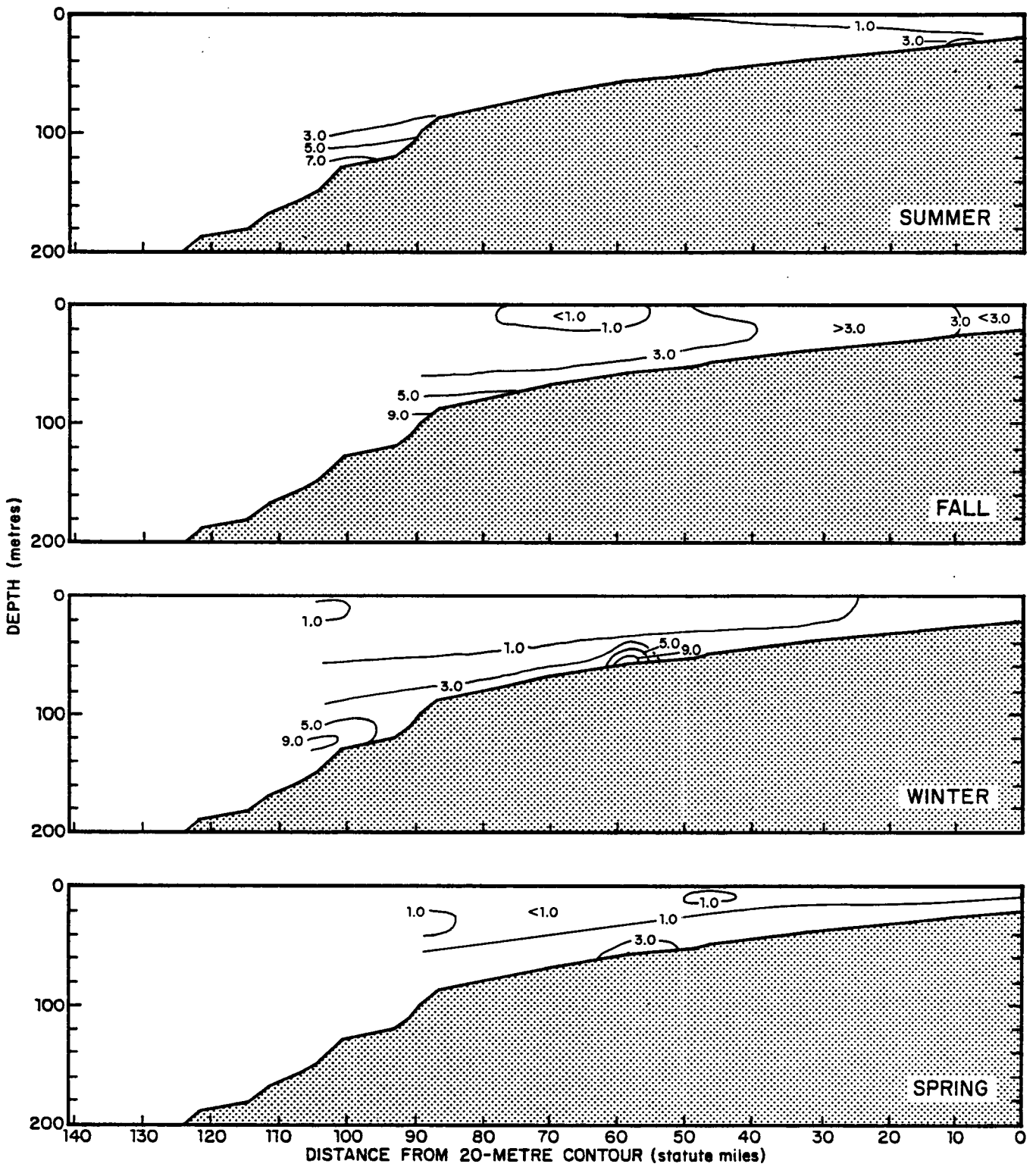
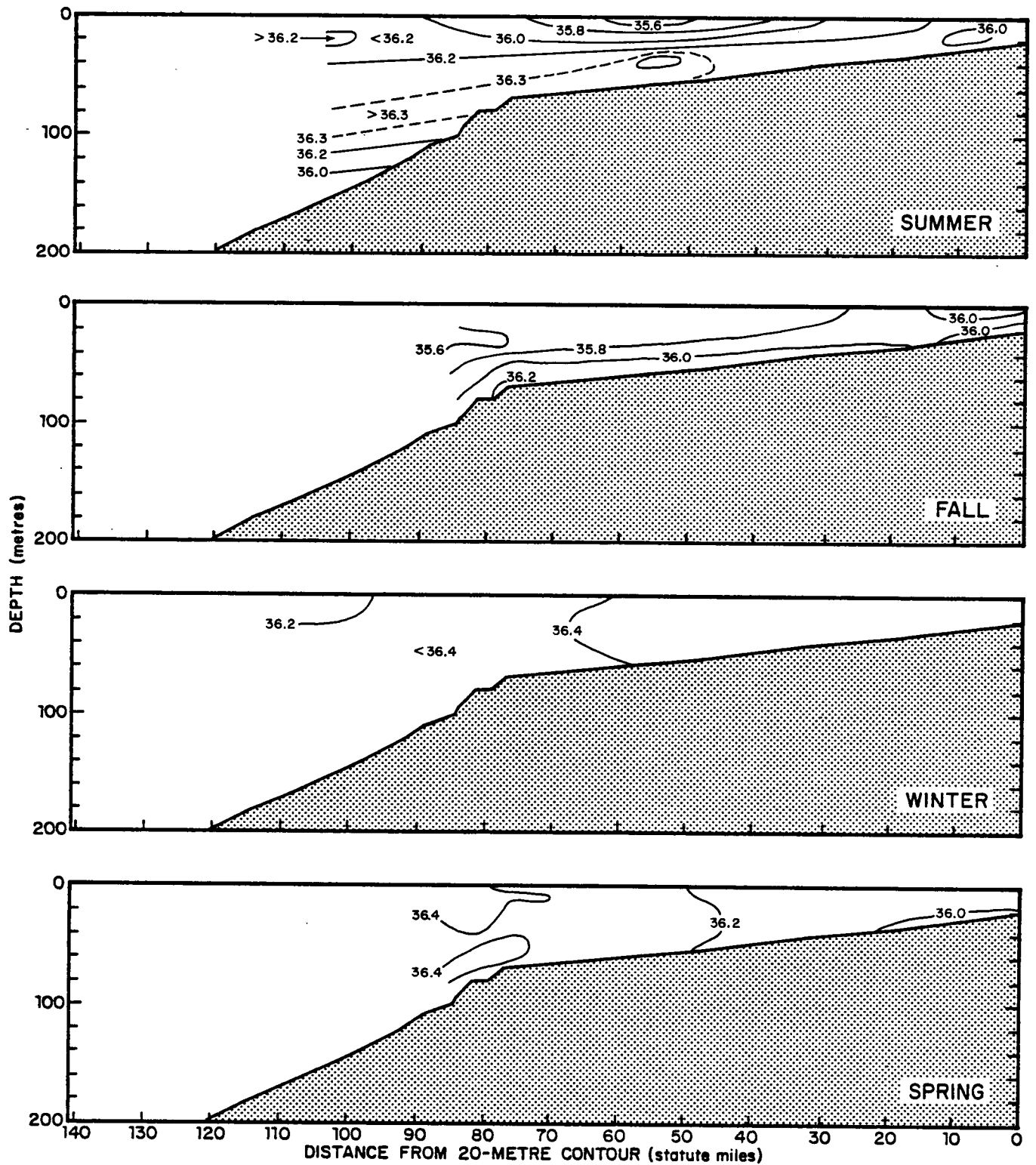Figure 2-33. Seasonal silicate distributions on Transect A.

61
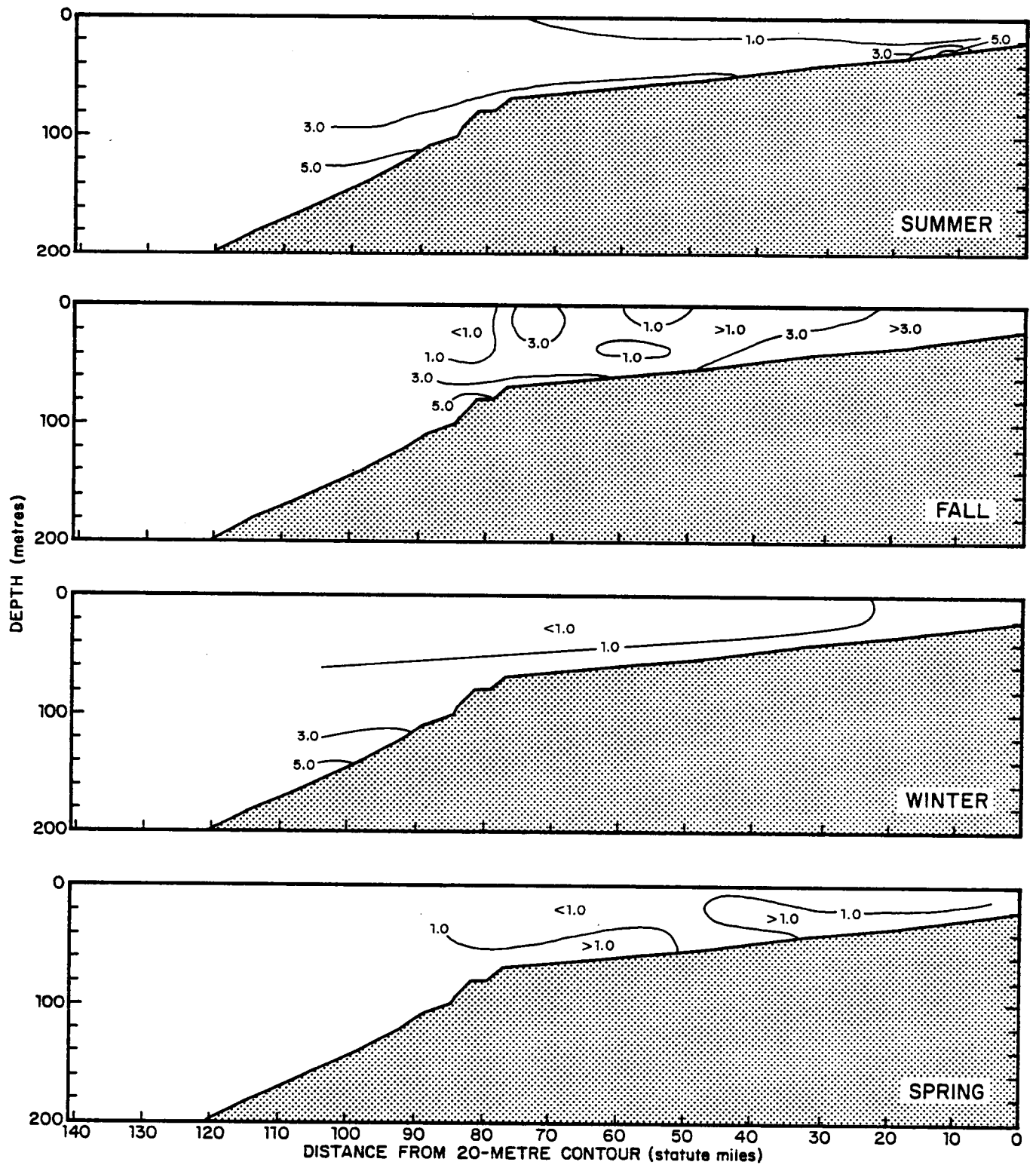
Figure 2-34.   Seasonal silicate distributions on Transect B.
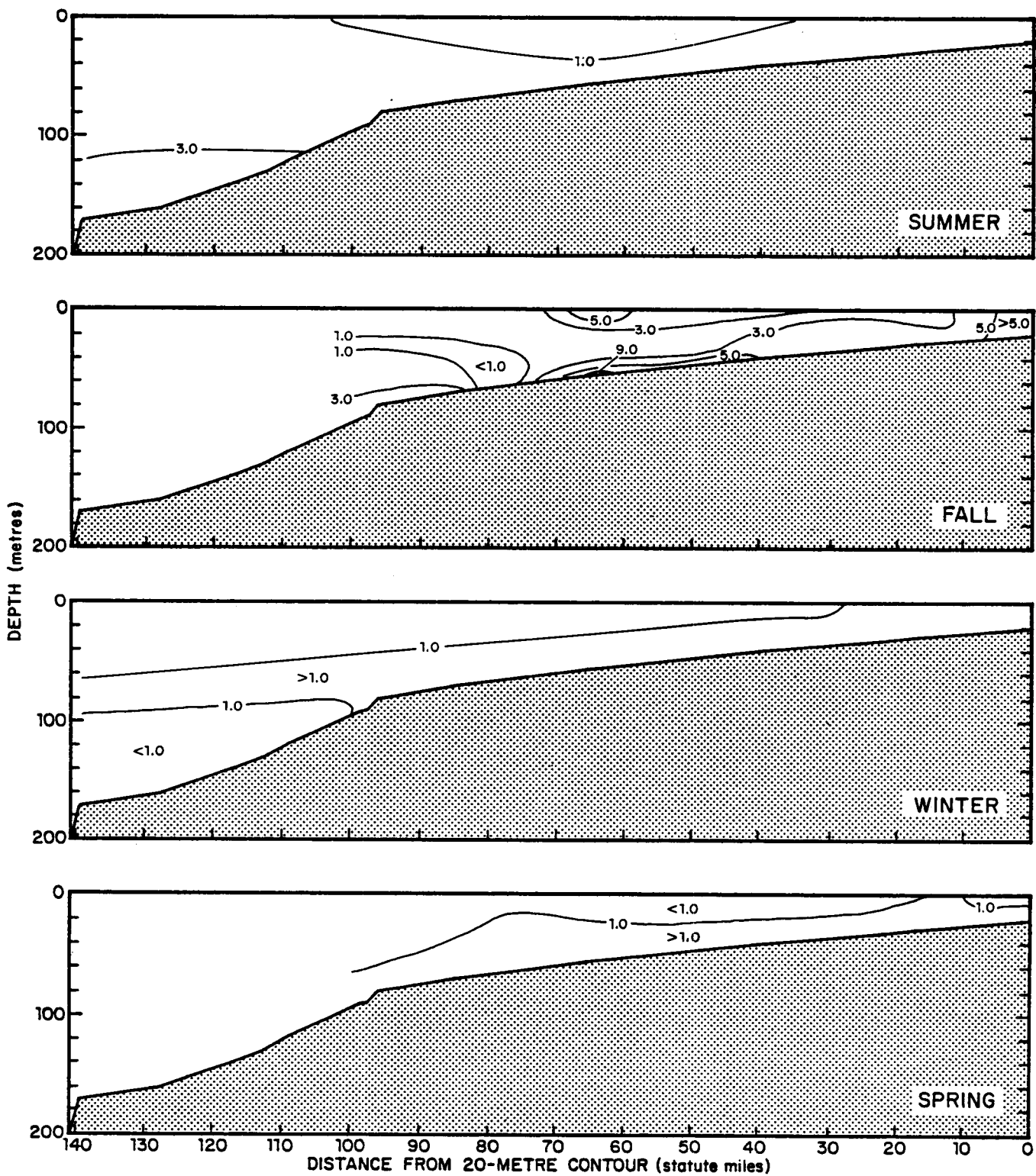
Figure 2-35. Seasonal silicate distributions on Transect C.

63
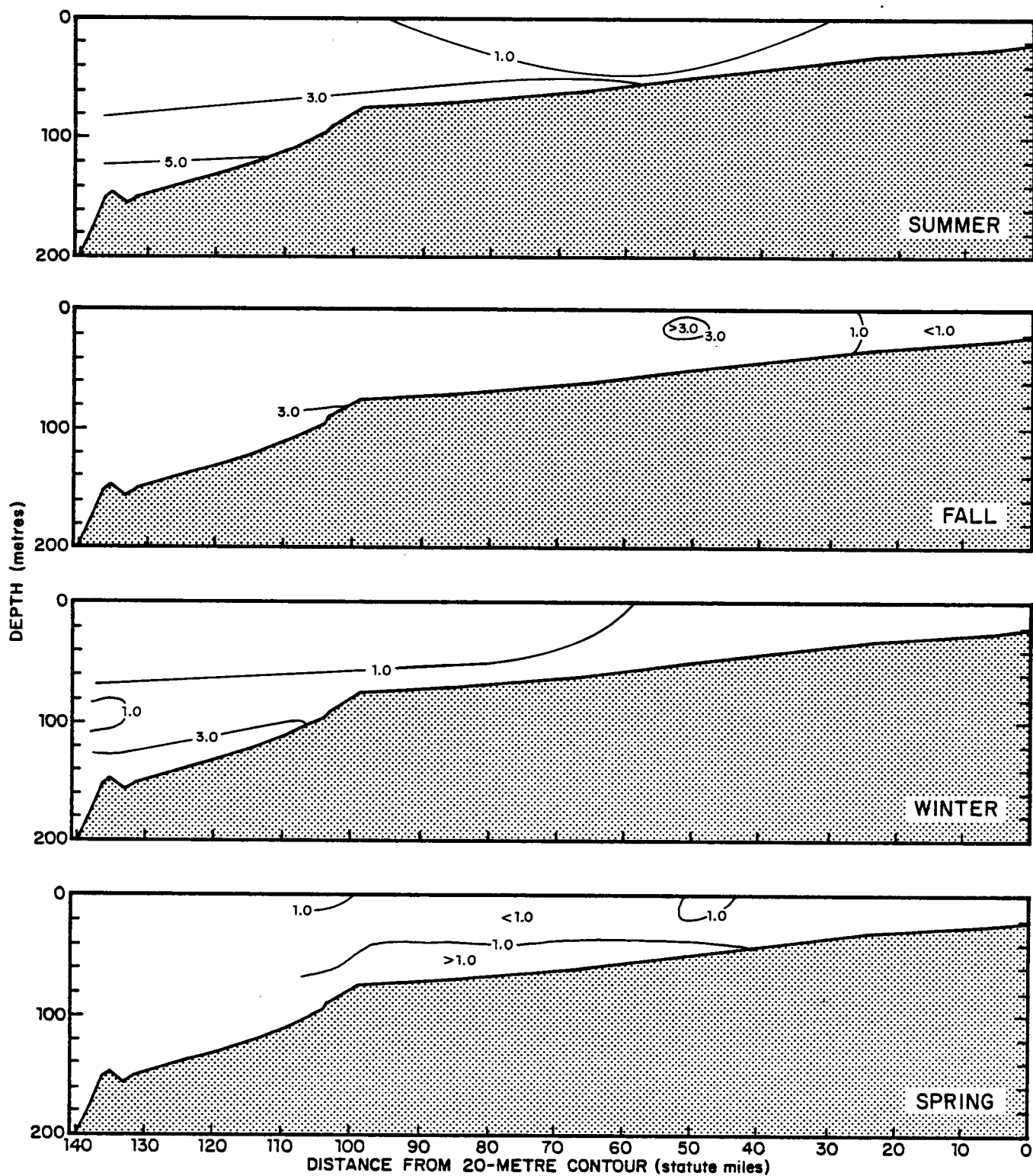
Figure 2-36. Seasonal silicate distributions on Transect D.

64
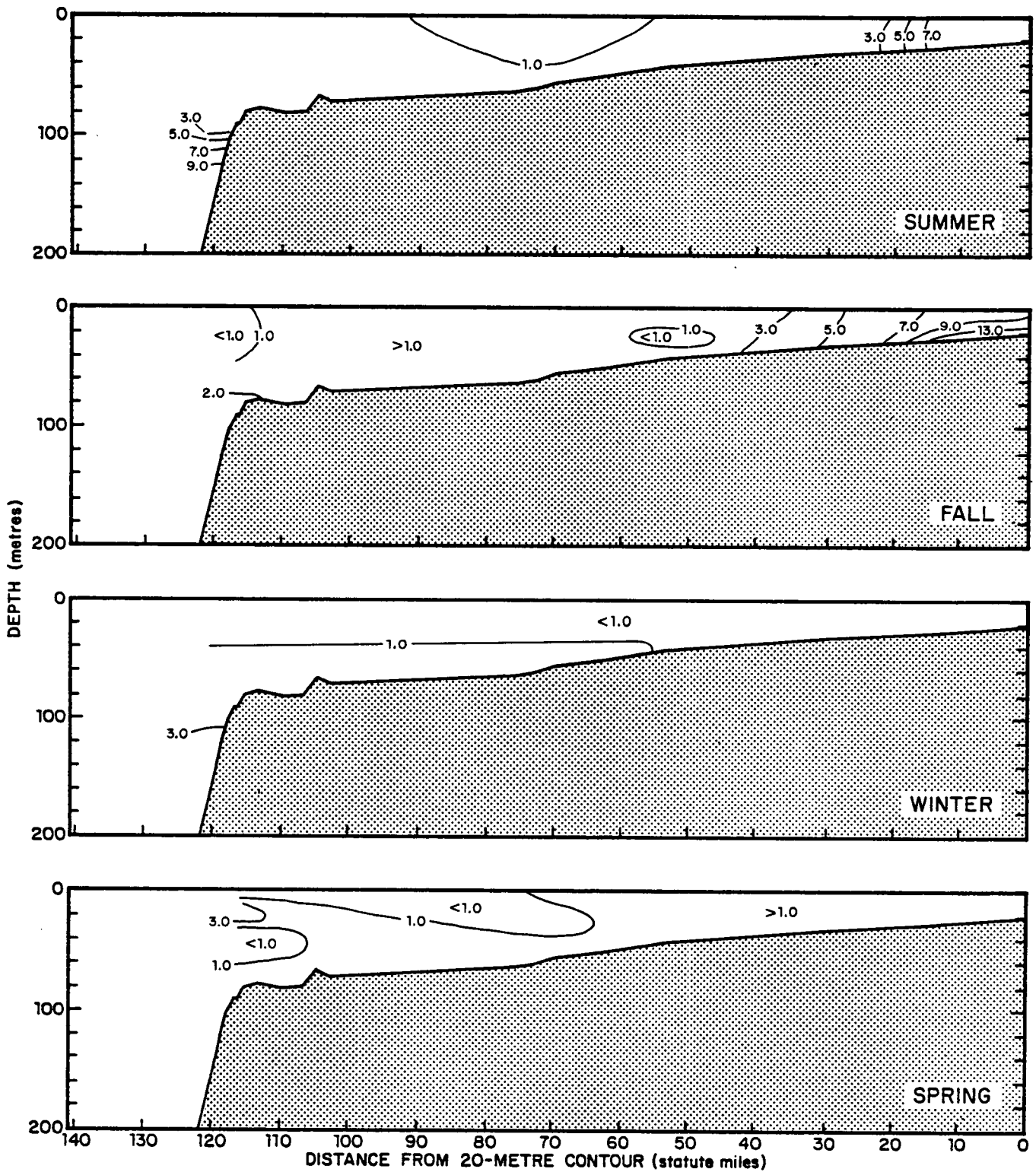
Figure 2-37. Seasonal silicate distributions on Transect E.

upwelling transport or mixing of nutrients along σ_t surfaces near the shelf break.

El Sayed's (1972) phosphate concentration data taken over the entire Gulf show no discernible seasonal fluctuations at the surface and a slight preponderance in the fall season values when integrated to 200 m. The shelf phosphate data indicate a surface concentration on the order of 0.1 μ M in all sections and only a very minor extremum in fall season data integrated to 100 m.

The concentration of nitrite in sea water can be estimated accurately, and the results in general confirm that in almost all parts of the world the amount of nitrite tends to be small; very much smaller than nitrate and usually considerably smaller than ammonium (Raymont, 1963). The nitrite + nitrate contour values presented in Figures 2-23 through 2-27 can therefore be interpreted as seasonal background values for the upwelling nitrate concentrations to be discussed in later sections of this report.

Silica concentrations in the oceans tend to be more variable than other nutrients (such as phosphate) and purportedly reach maximum levels in winter (El-Sayed, 1972). Much of this variability is connected with the more rapid regeneration of silica than other nutrients. The winter on-shelf distributions in Figures 2-33 through 2-37 do not agree with a winter maximum. In fact, the highest values appear on the fall distributions generally near the eastern and western extremes. Whether the maxima in the Transect E, fall cross-section (Figure 2-37) is caused by land runoff or not is presently open to speculation.

2.4 Time Scales and Sampling Strategies

Seasonal distributions developed during the first two study phases and presented in this "hydrographic atlas" represent "averaged" distributions covering periods from 13 to 29 days, depending upon the length of time required to complete each data collection cruise. The purpose of these data was to provide a general, on-shelf representation of water column parameters over a period commensurate with their collection period.

During the third study phase when emphasis was shifted to an examination of a potential off-shelf driving mechanism, not only was the study area moved to the western end of the shelf near the break but a series of shorter sampling and analysis time scales was considered. From a number of earlier area studies (e.g., Vukovich et al. 1979), it was, of course, known that Loop Current motions responded on time scales significantly shorter than about 13 days or two weeks.

The point to note in this context is that mere superposition of the parametric distributions resulting from all three study phases simply produces a mix of processes working on different time scales or averages which can be very mis-leading if applied to the real world. A more logical approach toward incorpor-ating these data sets might be to average the third phase distributions (when-ever possible) over their collection period and then attempt to superimpose them on the closest corresponding shelf distribution. In this case, one would only have to attempt to resolve the discrepancies in different seasonal and spatial effects.

In either case, no such data mixing was attempted in this report because the results would have required too many speculations and assumptions to be useful and would not have assisted in further meeting the present study objectives. If, as requested by MMS reviewers, a study of this nature is required, then it is recommended as an interpretative task that is more appropriate for reporting in the upcoming second phase report for this same study.

2.5 <u>References</u>

Austin, H.M. 1971. The characteristics and relationships between the
calculated geostrophic current component and selected indicator organisms
in the Gulf of Mexico Loop Current system. Ph.D. dissertation, Department
of Oceanography, Florida State University: 369 pp.

El-Sayed, S.Z., W.M. Sackett, L.M. Jeffrey, A.D. Fredericks, R.P. Saunders,
P.S. Conger, G.A. Fryxell, K.A. Steidinger, and S.A. Earle 1972. Serial
atlas of the marine environment, Folio 22, Chemistry, primary
productivity, and benthic algae of the Gulf of Mexico. Am. Geogr. Soc.:
29 pp.

Gordon, H.G., D.K. Clark, J.L. Mueller, and W.A. Hovis 1980. Plankton
pigments from Nimbus-7 Coastal Zone Color Scanner: comparison with
surface measurements. Sci. 210: 63-66.

Haddad, K.D. 1980. Present use of the CZCS in red tide research in the
eastern Gulf of Mexico, p. 37, Abstract. In: Proc. of CZCS workshop.
NOAA Tech. Mem. NMFS-SEFC-9.

Hobson, L.A. and C.J. Lorenzen 1972. Relationships of chlorophyll maxima
to density structure in the Atlantic Ocean and Gulf of Mexico, Deep-Sea
Res. 19: 297-306.

Jerlov, N.G. 1968. Optical Oceanography. Elsevier Publishing Co., 194 pp.

Jones, J.I. et al., 1973. Physical oceanography of the northeast Gulf of
Mexico and Florida continental shelf area. In: A summary of knowledge of
the eastern Gulf of Mexico, coordinated by the State University System of
Florida Institute of Oceanography: 69 pp.

Leipper, D.F. 1970. A sequence of current patterns in the Gulf of Mexico.
J. Geophys. Res. 75(3): 637-657.

Molinari, R.L., D.W. Behringer, and J.F. Festa 1976. A numerical modeling
and observational effort to develop the capability to predict the currents
in the Gulf of Mexico for use in pollutant trajectory computation: Model
studies of the circulation in the Gulf of Mexico. Final report, BLM IA
08550-IA5-26: 244 pp.

Pierson, Jr., W.J. and G. Neumann. 1966. Principles of physical
oceanography. Prentice-Hall, Inc., Englewood Cliffs, N.J., 545 pp.

Raymont, J.E.G. 1963. Plankton and productivity in the oceans. Pergamon
Press: 660 pp.

Riley, J.P. and R. Chester 1971. Introduction to marine chemistry.
Academic Press, London.

Sellers, W.D. 1965. Physical climatology. The University of Chicago
Press, Chicago and London: 272 pp.

Steidinger, K.A. 1973. Phytoplankton. In: A summary of knowledge of the eastern Gulf of Mexico, coordinated by the State University System of Florida Institute of Oceanography: 18 pp.

Tait, R.V. and R.S. De Santo 1975. Elements of marine ecology, Spring Verlag, New York and Heidelberg: 327 pp.

Turner, R.E., S.W. Woo, H.R. Jitts. 1979. Estuarine influences on a continental shelf plankton community, Sci. 206(4415): 218-220.

Vukovich, F.M., B.W. Crissman, M. Bushnell, and W.J. King 1979. Some aspects of the oceanography of the Gulf of Mexico using satellite and in-situ data. J. Geophys. Res. 84(C12): 7749-7768.

Weinstein, M.P. 1981. Plankton productivity and the distribution of fishes on the southeastern U.S. continental shelf. Sci. 214: 351-352.

Woodward-Clyde Consultants/Continental Shelf Associates 1982. Southwest Florida shelf ecosystems study - Year 1. 4 vols. plus marine habitat atlas, prepared under BLM Contract No. AA851-CTO-50, in revision.

Wüst, G. 1964. Stratification and circulation in the Antilles-Caribbean basins. Columbia Univ. Press, New York: 201 pp.

3.0 ANALYSES OF LOOP CURRENT SHELF BREAK UPWELLING

THERESA PALUSZKIEWICZ and LARRY P. ATKINSON
SKIDAWAY INSTITUTE OF OCEANOGRAPHY, UNIVERSITY SYSTEM OF GEORIGA

3.1 Introduction

The objective of this portion of the Southwest Florida Shelf Ecosystems Study was to describe the effect of Loop Current intrusions on the hydrographic regime of the shelf environment. Based on the results of a number of earlier experiments off the Georgia and northern Florida coast, it is now known that Gulf Stream intrusions on the southeastern continental shelf can result in significant exchanges of heat, momentum, and nutrients (Stefansson, Atkinson, and Bumpus, 1971; Lee, Atkinson, and Legeckis, 1981; and Lee and Atkinson, 1983) as well as localized areas of higher production through associated upwelling (Yoder, Atkinson, Lee, Kim, and McClain, 1981).

In 1982, two data collection cruises in the vicinity of the southwest Florida shelf break region demonstrated conclusively that similar water mass interactions and intrusions also occur along the Loop Current front. The purpose of this section is to describe the hydrographic features of these intrusions as they are illustrated in the two cruise data set. Discussion of mixing, productivity, optical, and surface chlorophyll features are presented in the following sections. The two data collection periods were scheduled so that the major analysis effort would occur when sufficient surface thermal contrast was available to permit definition of the Loop Current front from satellite thermal imagery. The second cruise was completed under more stratified summer conditions when intrusions stayed mainly beneath the thermocline and surface contrasts were minimal.

3.2 Seasonal Characteristics

As a means of highlighting the seasonal characteristics of the cruise data in much the same sense as the "hydrographic atlas" of the preceding section, the results of each cruise are discussed separately.

3.2.1 Spring Cruise Data

3.2.1.1 Observational Methods

Prior to the cruise, surface temperature charts (i.e., composite infrared charts from NOAA-NESS, Miami) were examined to determine the present position and most likely propagation path of Loop Current frontal events. Based on these observations, a cruise track was planned in the offshore region bounded by 25 to 27°N and 83 to 85°W. The first data collection cruise ran from April 1 to April 7, 1982. Coincident with the shipboard sampling on April 1 and 2, a NASA U-2 aircraft carrying an Ocean Color Scanner (OCS) mapped the surface chlorophyll distribution in the same general area (Section 7.0). Eight sections consisting of alternating CTD/water sample/optical and XBT stations, spaced at approximate 10 km (5 to 6 nmi) intervals, were run cross-shelf and along the 1,000 m isobath as shown schematically in Figure 3-1. The location of each station (as measured by LORAN-C), time of occupation, and water depth are listed in Appendix A.1.　　　A division of these stations by transects is presented in Table 3-1. Salinity and temperature were determined at CTD stations with a Plessy Model 9400 CTD interfaced to a Hewlett Packard 9825 desktop computer. Water samples were collected at discrete depths with Niskin bottles mounted on a rosette sampler coupled to the CTD as shown in
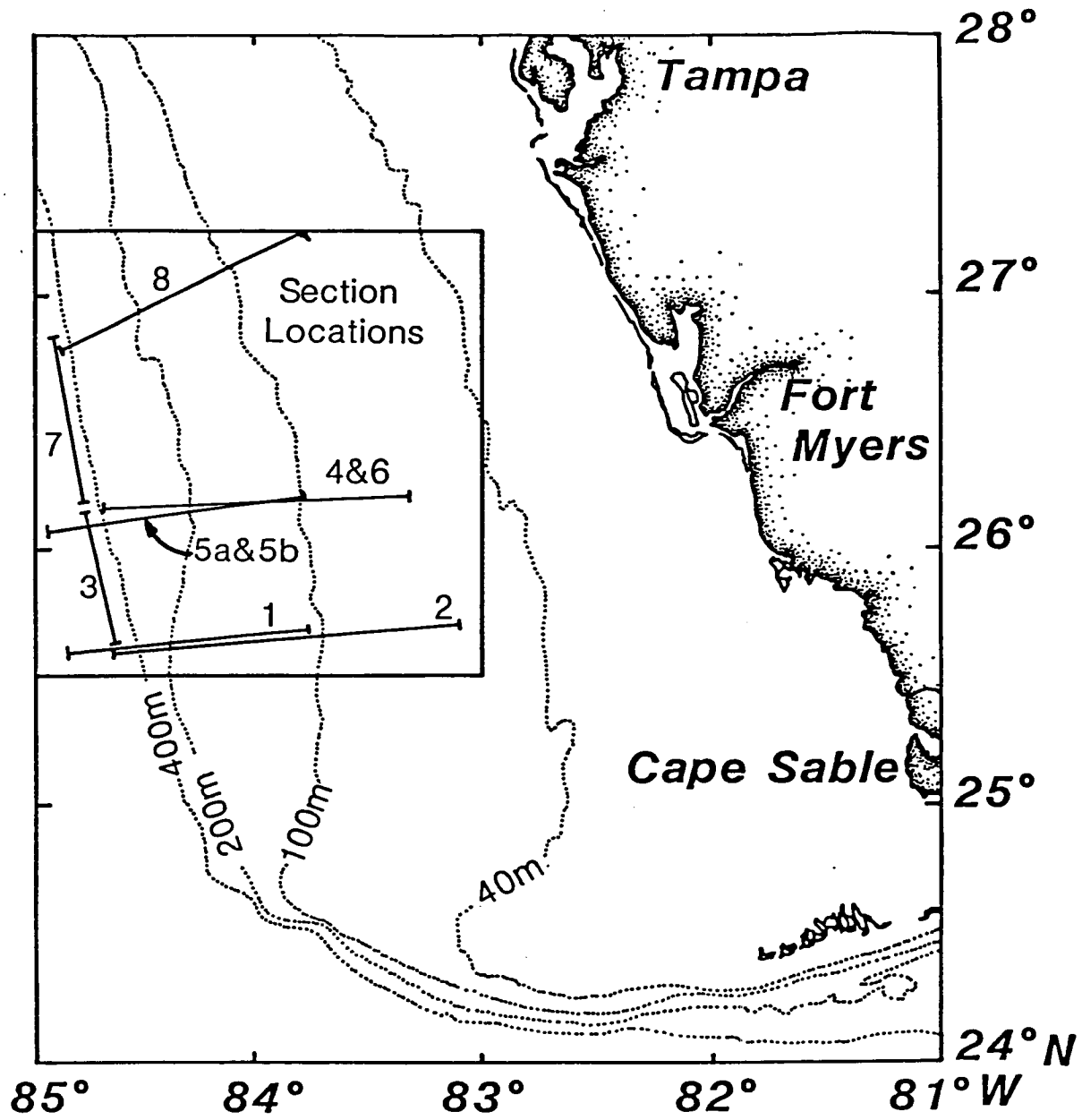
Figure 3-1.   Spring cruise transect locations.

Table 3-1. Assignment of stations to transects during spring cruise

(X = XBT, C = CTD)

Section	Date (1982)	Station Numbers
1	2 April	1C, 2X, 3C, 4X, 5C, 6X, 7C, 8X, 9X, 10C, 11X, 12C
1	3 April	13-23 mapping run
2	3-4 April	24C, 25X, 26C, 27X, 28C, 29X, 30C, 31X, 32C, 33X, 34C, 35X, 36C, 37X, 38C
3	4 April	39X, 40X, 41X, 42X, 43X, 44X, 45X, 46X
4	4 April	47X, 48X, 49X, 50X, 51X, 52X, 53X, 54X, 55X, 56X
5a	4-5 April	57C, 58C, 59C, 60C, 61C, 62C
5b	5 April	63X, 64X, 65X, 66X, 67X, 68X, 69X, 70X, 71X, 72X, 73X, 74X, 75X, 76X
6	5-6 April	77C, 78X, 79C, 80X, 81C, 82X, 83C, 84X, 85C, 86X, 87C, 88X, 89C
7	6 April	90X, 91X, 92X, 93X, 94X, 95X, 96X, 97X, 98X, 99X
8	6-7 April	100C, 101X, 102C, 103X, 104C, 105X, 106C, 107X, 108X, 109X, 110C

Figure 3-2. Sampling depths were selected on the downcast to permit sampling of special features. Specifications for the Plessey Model 9400 are as follows:

	Conductivity	Temperature	Depth
Accuracy	$+0.03$ mmho·cm^{-1}	$+0.02°C$	$+1.5$ m
Resolution	0.0002 mmho·cm^{-1}	0.0001°C	0.0012m
Time Constant	0.1 sec.	0.35 sec.	0.1 sec.

The CTD system is calibrated against water samples from rosette bottles tripped in mixed layers to ensure that the sensors and bottles are both sampling the same water. Chandler et al. (1978) give a complete description of the system, operating procedures, processing programs, and error analyses. The XBTs were Sippican Model T-10 probes with a nominal accuracy of $\pm0.2°C$. Surface temperature, salinity, and relative surface chlorophyll fluorescence were recorded along transects using the CTD and a Turner Designs Model 10 Fluorometer in-line with a flow of surface water. The Model 10 is specified at an accuracy level of about 100 ppb. Phosphate, silicate, and nitrate were analyzed with a Technicon Auto Analyzer II according to the methods of Glibert and Loder (1977). The standard error of the mean for phosphate, nitrate, and silicate are ±0.0008, ±0.11, and $\pm0.02\mu M$, respectively. Dissolved oxygen concentrations were determined according to the methods of Strickland and Parsons (1965).

Sea surface temperatures (SST) were derived from infrared data from the Advanced Very High Resolution Radiometer (AVHRR) onboard the NOAA-7 polar orbiting satellite. These data were calibrated by NASA using a two-channel algorithm (McClain, 1980). The images were then rectified for geometric

WINCH

4 SLIP RINGS

SEACABLE

4 CONDUCTOR ELECTRO MECHANICAL WIRE

4 KEARNEY CLAMPS

SHACKLE

SCOTCHCAST
(waterproof splice)

ROSETTE

GROUND AND SAFETY WIRE

10 ft.

2 pin *

2 pin **

C T D

MIXER

3 pin

9 pin   1 pin

* only one conductor used

** Envirocon Underwater Connectors
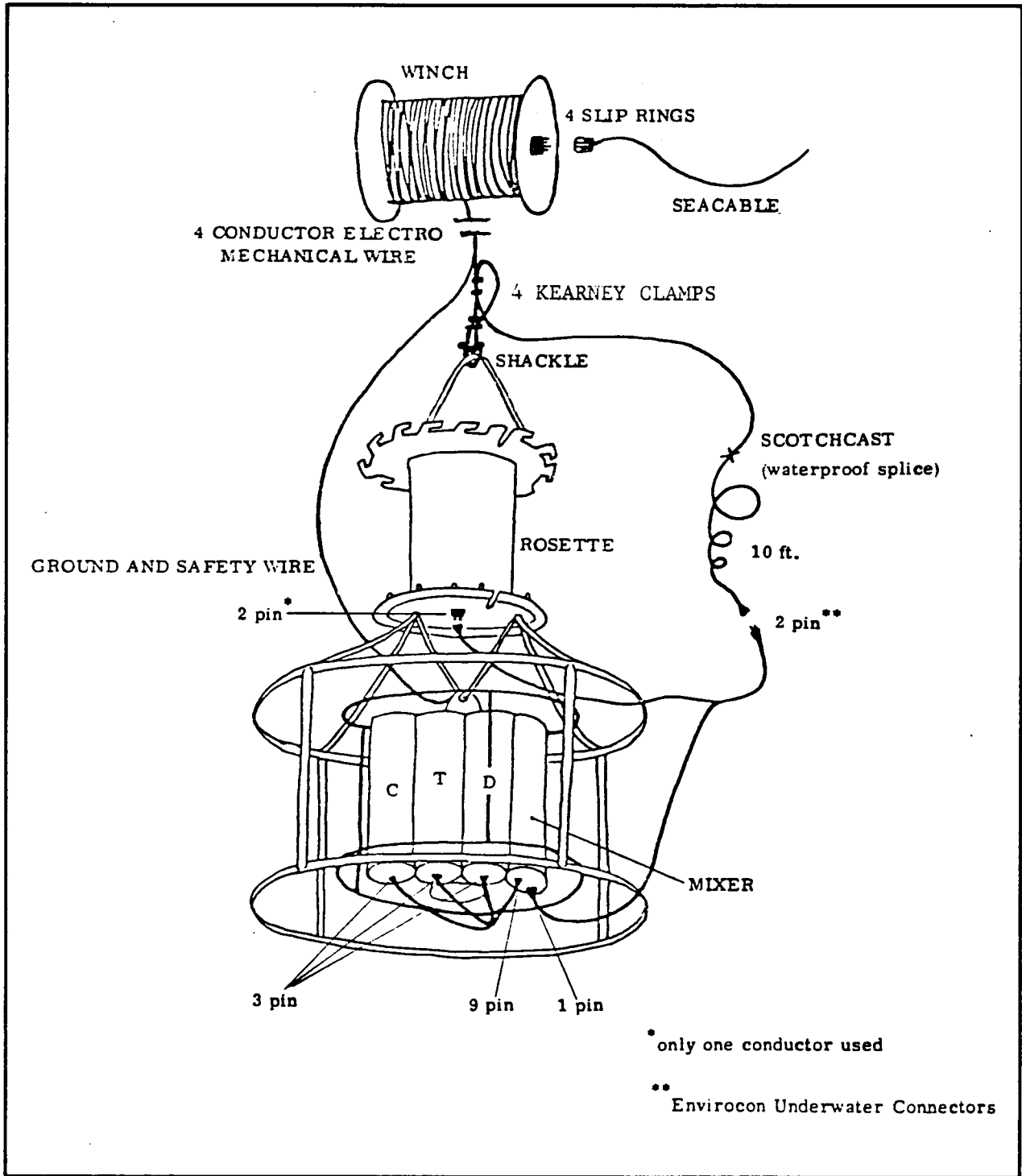
Figure 3-2.   CTD/rosette sampling configuration.

distortion and enhanced to clarify temperature gradients. The spatial error of the imagery was ±15 km; the thermal error was ±1°C. These errors were determined by comparison to hydrographic data and sea surface temperatures derived from the imagery. Thermosalinograph results collected during this cruise were essentially the same as the surface CTD results since the same sensor was used in both cases. Whenever possible, thermosalinograph results were incorporated into the transect plots.

3.2.1.2 Propagation of the Frontal Event

Figure 3-3 presents a composite of the available temperature imagery for the eastern Gulf during the cruise period. The Loop Current, noticeable as a lighter shade indicating warmer temperatures intruded into the Gulf of Mexico northward to 27°30'N, turned south, and exited the Gulf through the Straits of Florida. The filament which is the subject of this section is in the northeast part of the Loop Current. The filament was warm and the area between the filament and Loop Current, was cool. The length of the filament was 220 km from the junction at the Loop Current to the northern tip. This image shows a distribution of surface temperatures on the shelf where cooler water was close to the north Florida coast extending southward to Tampa Bay; warmer water was found off southwest Florida. A cyclonic curl of cooler water originated near the coast and was observed in the middle shelf section, due west of Tampa Bay. A band of cooler (darker shade) water was in the outer slope region between 26 and 28°N.

It is convenient at this time to introduce the term "frontal eddy" to describe the filament of the Loop Current, the core between the filament and the Loop
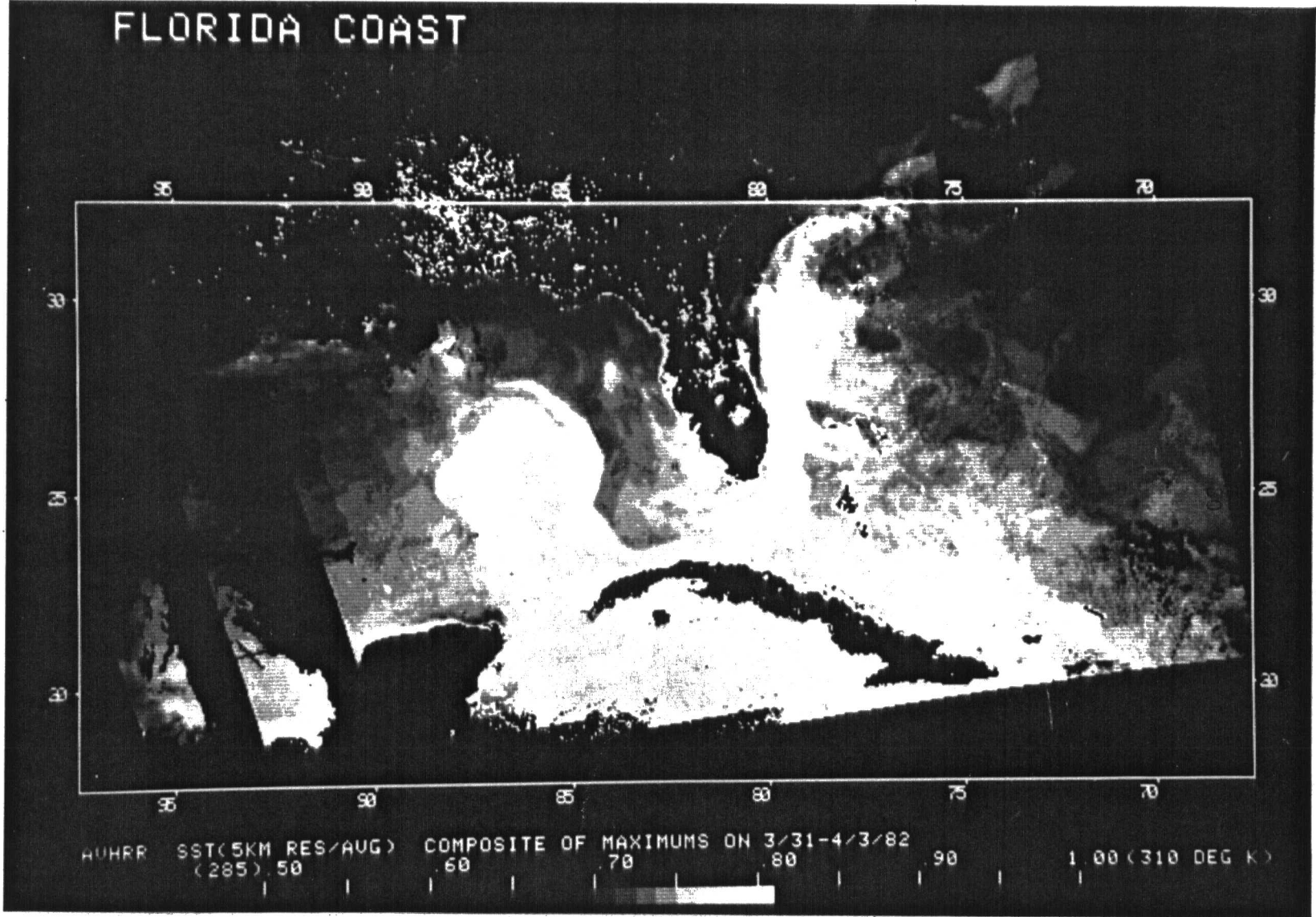
Figure 3-3. NOAA-7 AVHRR infrared composite of Gulf of Mexico from March 31 to April 4, 1982.

Current, and the front associated with the gradient between the Loop Current filament and shelf waters. Figure 3-4 shows the changes of the frontal eddy between April 1 and 4. The contour used to define the Loop Current/Shelf water front is the approximate 24°C isotherm. Because of cloud cover over the northern part of the figure, the northern extent of the filament may be slightly larger than that depicted. The frontal edge and the cold core propagated southeastward a distance of 95 km as measured at the tip of the cold core. Besides moving southward, the frontal eddy also moved eastward 56 km between April 1 and 4, placing the cold core 15 km west of the shelf break at the 200 m isobath. The vector-computed speed was 30 cm.sec^{-1}. The filament became thinner and the width changed from 62 km on April 1 to 35 km on April 4, and warmed (as indicated by the infrared imagery). The width of the cold core increased in the southern portion to 50 km.

Satellite imagery on the following three days was not clear enough to distinguish surface features. Continued tracking of the frontal eddy propagation via satellite was not possible. However, hydrographic data, which will be discussed later, obtained on April 5 through 7 allowed an estimate of the position of the onshore and offshore front associated with the warm filament. Figure 3-5 shows the last position of the cold core on April 4 and the position on April 5 through 7 derived from the hydrographic data.

3.2.1.3 Hydrographic Observations of the Frontal Eddy

The hydrographic data collected during five cross-shelf CTD transects and additional XBT transects cannot be considered synoptic because the time-scale (five days) was long compared to the time scale of the frontal dynamics.
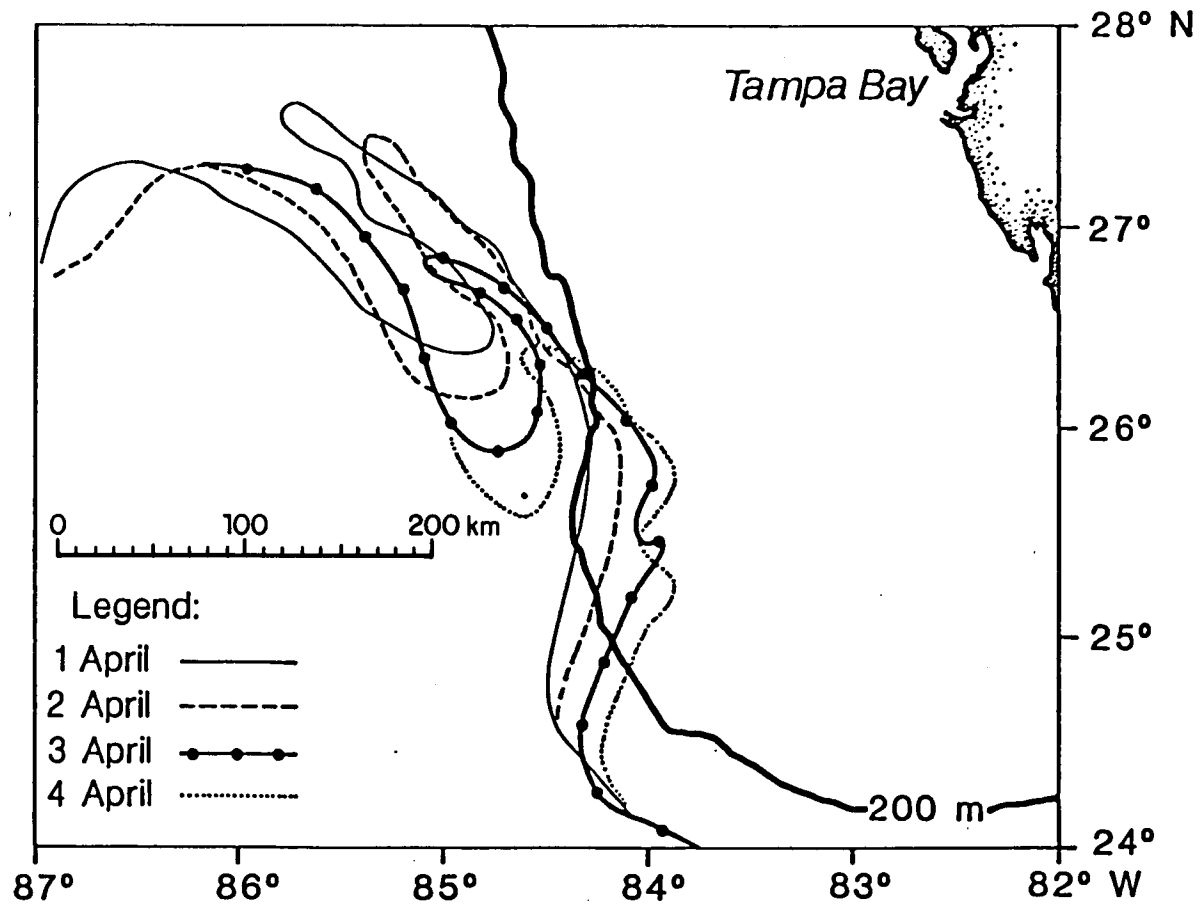
Figure 3-4.   AVHRR time series (April 1 to 4, 1982) of SST
(approximately 24°C) depicting Loop/Current shelf
water front and filament.
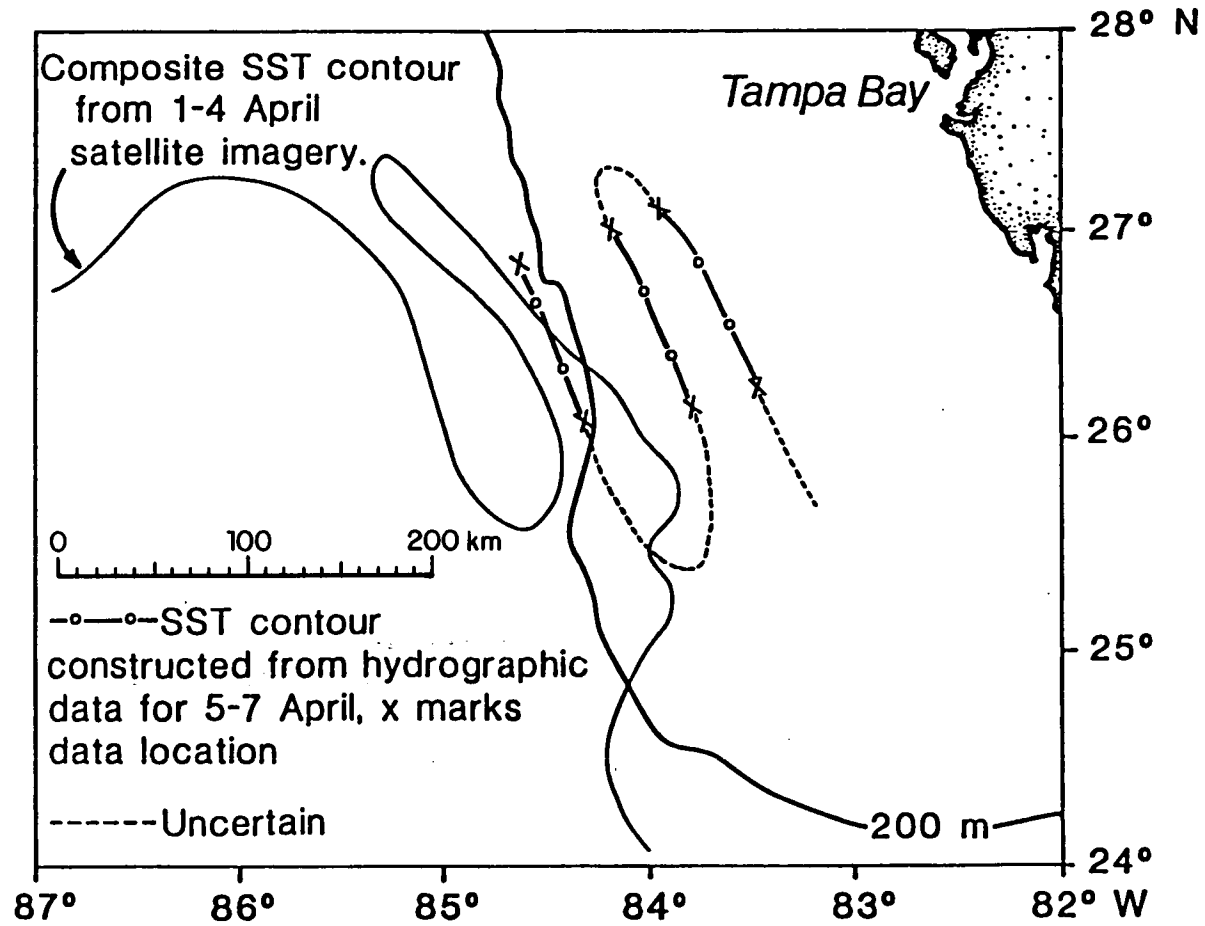
Figure 3-5. Frontal position from April 4 through 7, 1982.

However, several of the hydrographic sections coincide with infrared imagery and provide a three-dimensional view of the frontal eddy as well as providing insight into the interaction of the Loop Current and shelf waters.

Each cross-shelf section is approximated as longitudinal even though it varies from about 3 to 30° off the east-west axis. This minor distortion does not alter the physical interpretation of the data under discussion.

Transect (or Section) 1 (Figure 3-6), occupied on April 2, crossed an area on the shelf (Figure 3-7) where the front had intruded shoreward of the 200 m isobath. A front was indicated on the temperature section (Figure 3-6) near 25°38'N, 84°15'W (Stations 4 through 6*) with a gradient of approximately 2°C over 15 km. This front coincided within about 7 km of the front indicated on the infrared imagery at 25°04', 84°11'W, also with a similar gradient.

Fronts on the images coincided within an acceptable error of the front on the hydrographic data. Consequently, the imagery appears to give accurate spatial representation of the situation. The front occurred over the 160 m isobath; seaward, the inclination of the isotherms indicated the wall of the Loop Current and a southward flow. The intersection of the 22°C isotherm at 100 m defines the cyclonic edge of the Loop Current (Leipper, 1970, Maul, 1977; Behringer et al., 1977; Price, 1976). In this case, the intersection occurred near Station 11 coinciding with the steepest slope of the isotherms, and indicated the proximity of the southward flowing Loop Current. A salinity maximum (>36.6°/oo), characteristic of Loop Current waters, was also observed (Figure 3-8). Sigma-t surfaces sloped upward towards the east with

*The station numbers are listed across the top of each section.
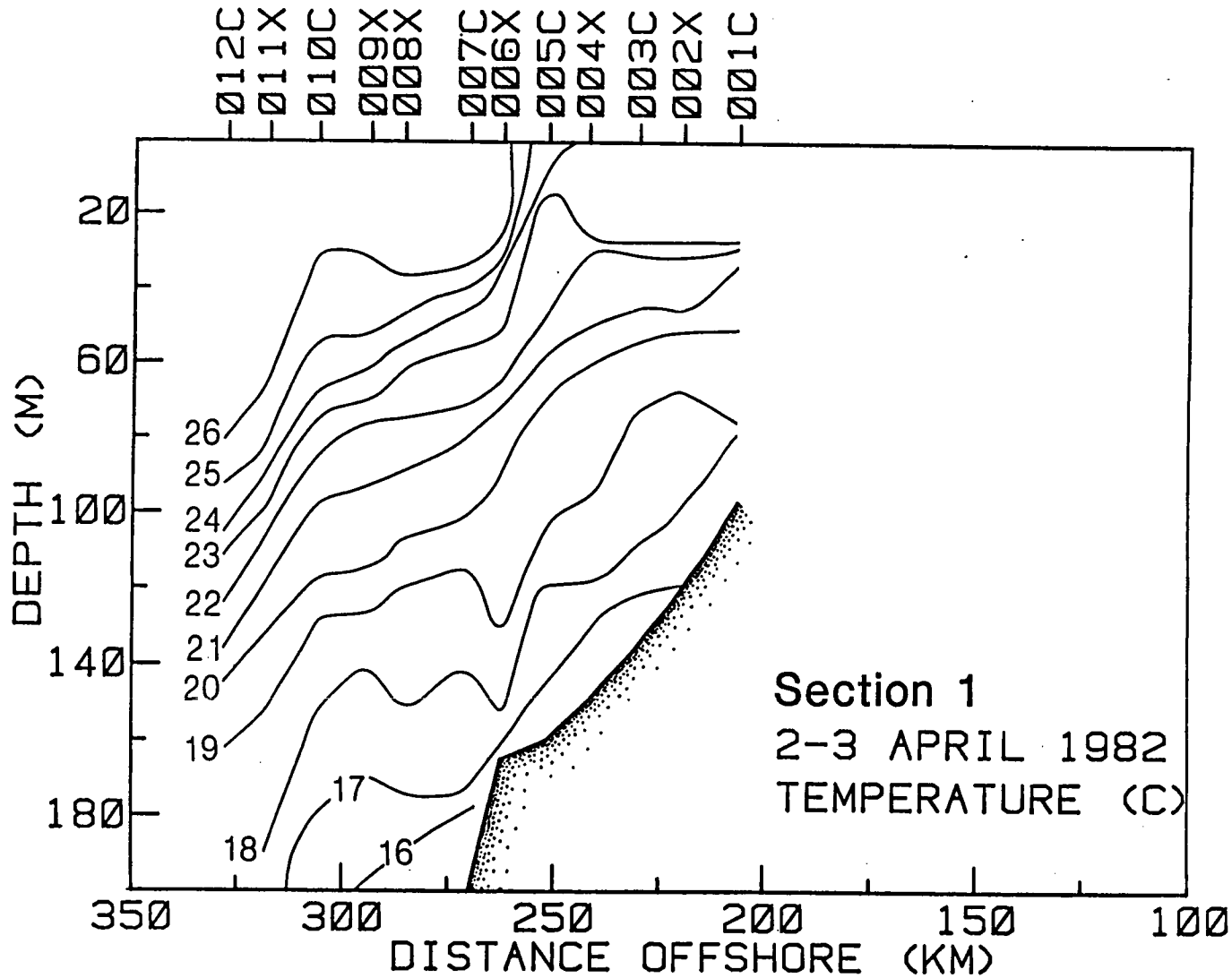
Figure 3-6.   Spring cruise, transect 1 temperature section.

85

Tampa Bay

Section 1 (2-3 April)

0   100   200 km

----- SST contour
from satellite image (2 April)

200 m
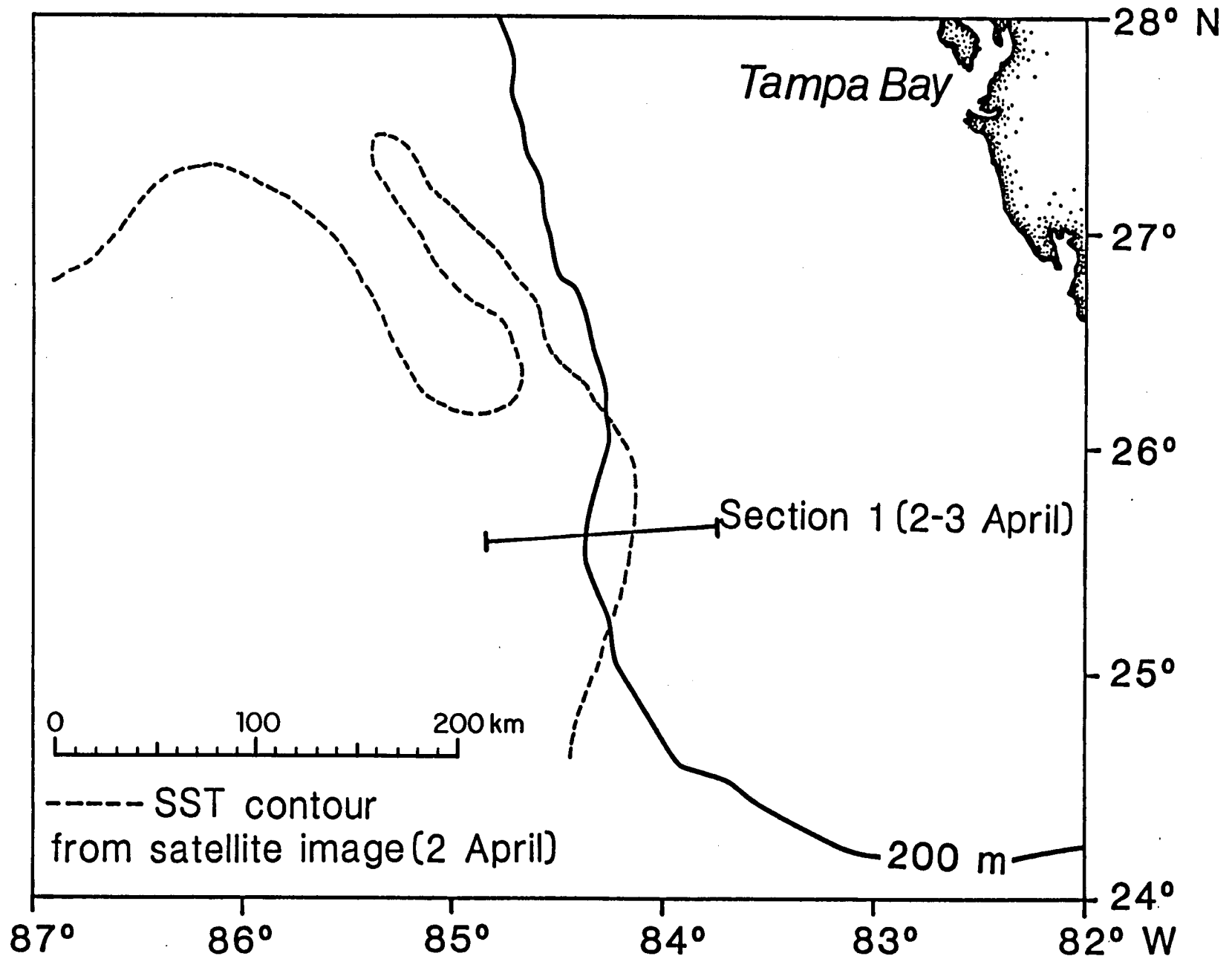
Figure 3-7.   Transect 1 location with respect to front.
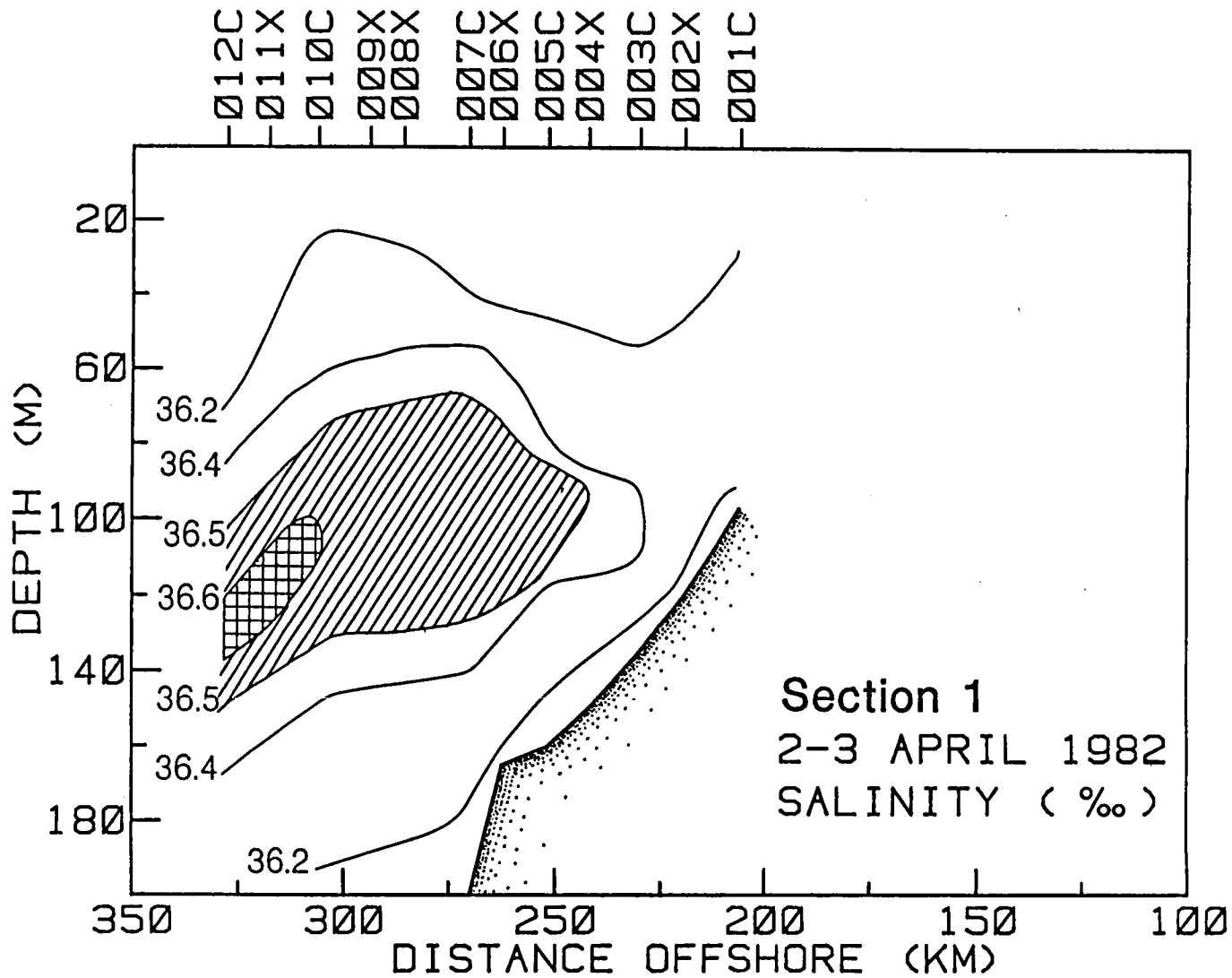
Figure 3-8. Spring cruise, transect 1 salinity section.

σ_t = 24.0, 24.5 reaching the surface between Stations 4 and 7 (Figure 3-9). Oxygen values generally decreased with depth (Figure 3-10). The nitrate section (Figure 3-11) reflected the features of the temperature section and showed that higher nitrate concentrations could be found as shallow as 100 m.

This same area was reoccupied about 36 hours later. By that time, noticeably large changes had occurred in the water characteristics and structure of the water column. The isotherms in the upper water column (< 100 m) were nearly level (Figure 3-12); those deeper had a trough-like depression between Stations 33 and 37. This depression was also apparent in the salinity (Figure 3-13) and nitrate sections (Figure 3-14). Overall, the isotherms were elevated an average of 20 to 30 m from the previous section and the salinity maximum was no longer as intense (36.4°/oo). Corresponding sigma-t surfaces had risen 40 to 60 m (Figure 3-15) while mixed layer oxygen values remained about the same (Figure 3-16). It is possible that further offshore a more intense salinity maximum would have been encountered but judging from the slope of the isotherms, it does not seem probable that the intersection of the 22°C isotherm near 100 m would have been encountered at the same location as in the previous section. The satellite image coinciding with this transect (Figure 3-17) shows that the frontal edge intruded further onto the shelf with a pronounced wave-like shape. The frontal location measured on the image (25°39'N, 84°05'W) was within 15 km of the frontal location indicated in the hydrographic data (25°40'N, 83°52'W; Station 31). The front was located over the 120 m isobath, 15 km shoreward of its previous position. It is not likely that the changes in elevation of the isotherms resulted from tidal displacement (which is usually less than 1 m) or internal tides which even with intensification at the shelf break are only 5 m in amplitude (Koblinsky,
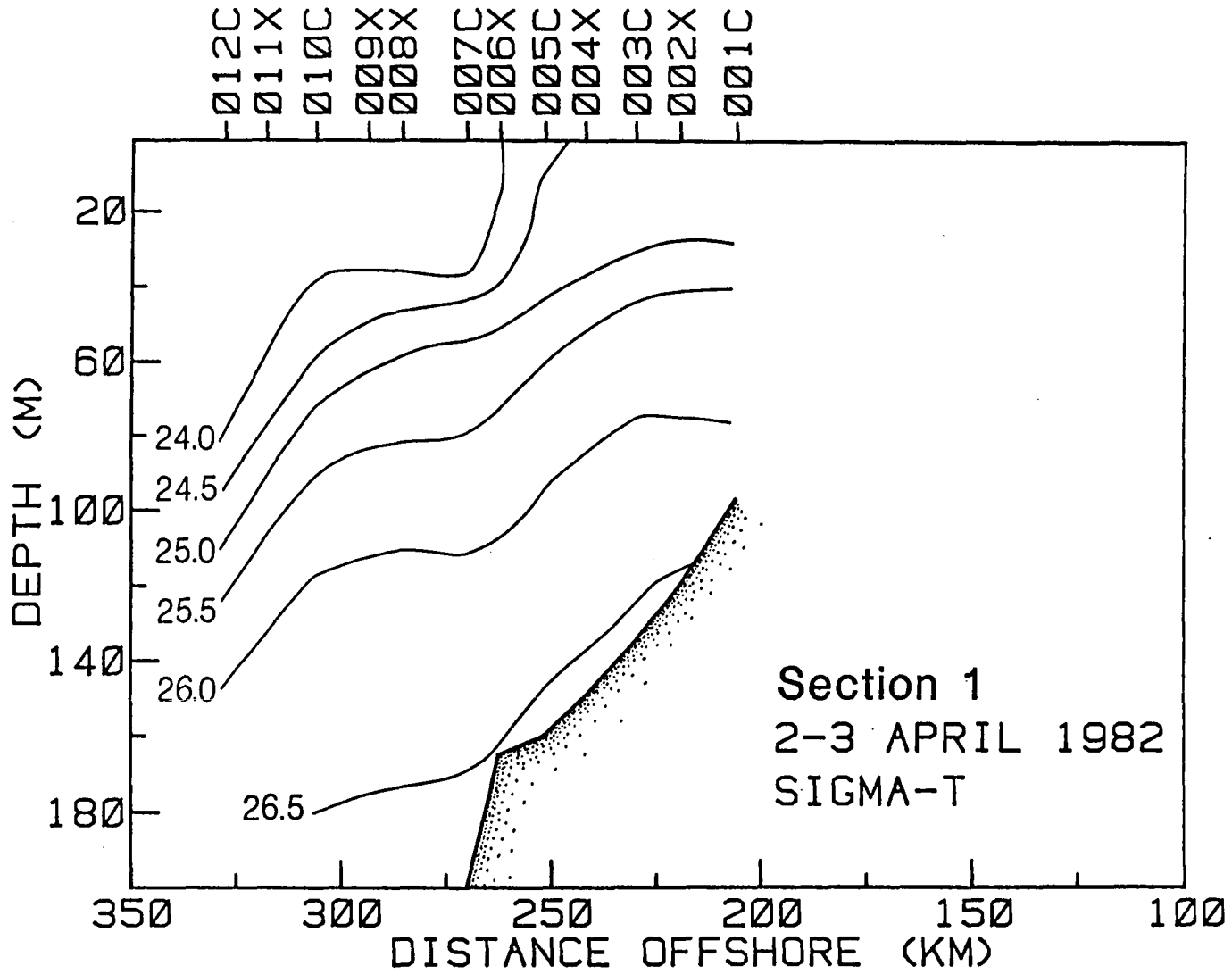
Figure 3-9.   Spring cruise, transect 1 sigma-t section.
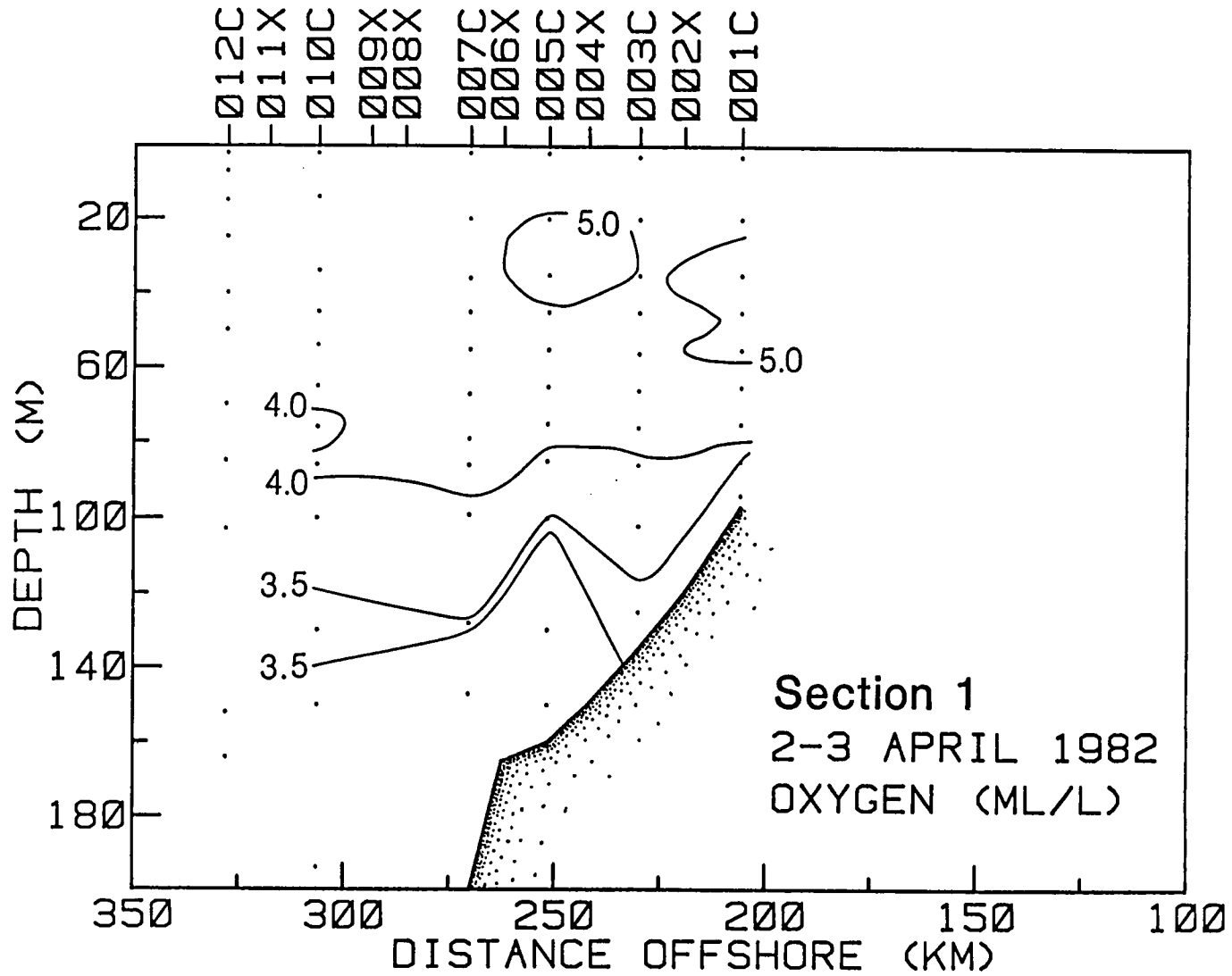
Figure 3-10. Spring cruise, transect 1 oxygen section.
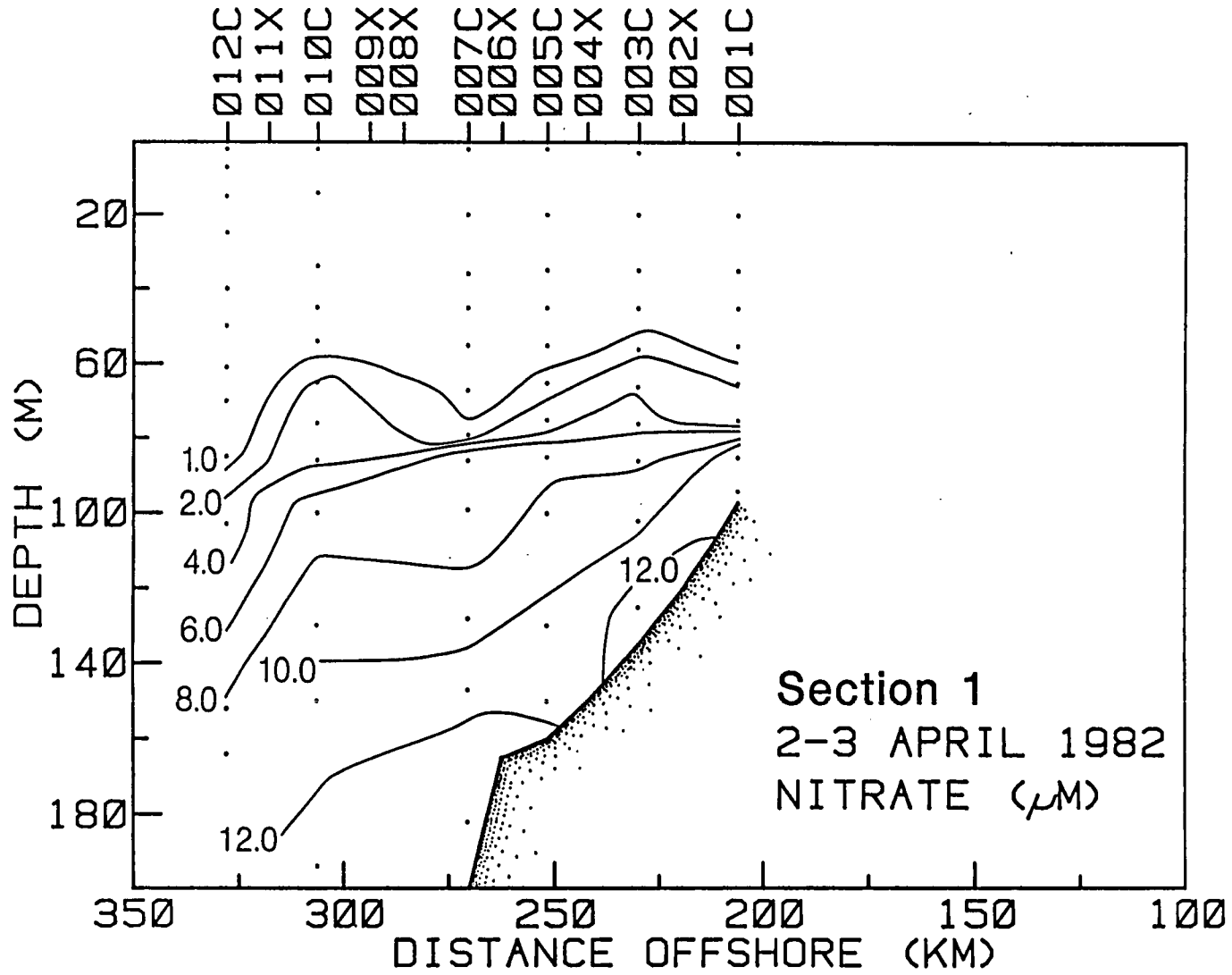
Figure 3-11.   Spring cruise, transect 1 nitrate section.
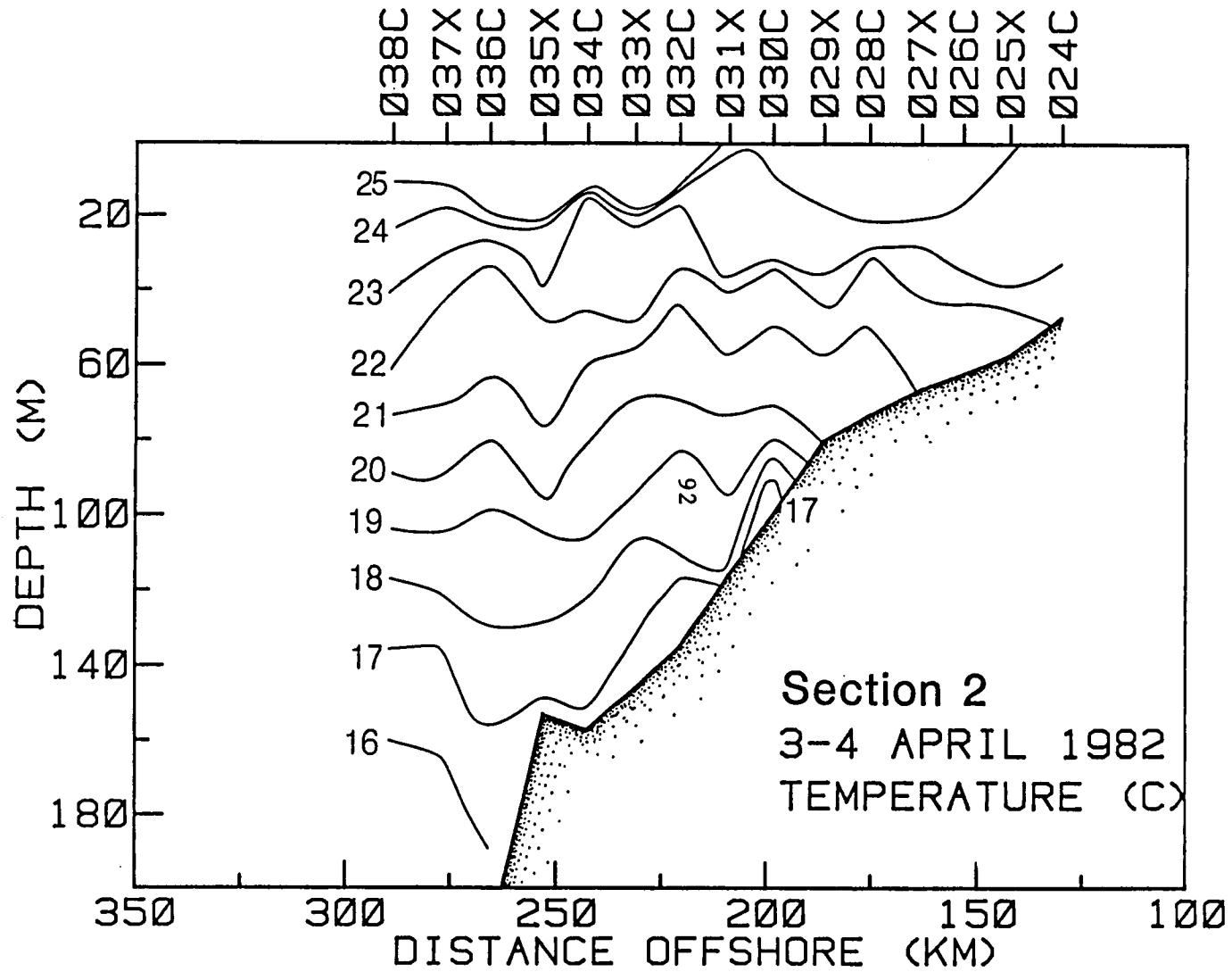
Figure 3-12.   Spring cruise, transect 2 temperature section.
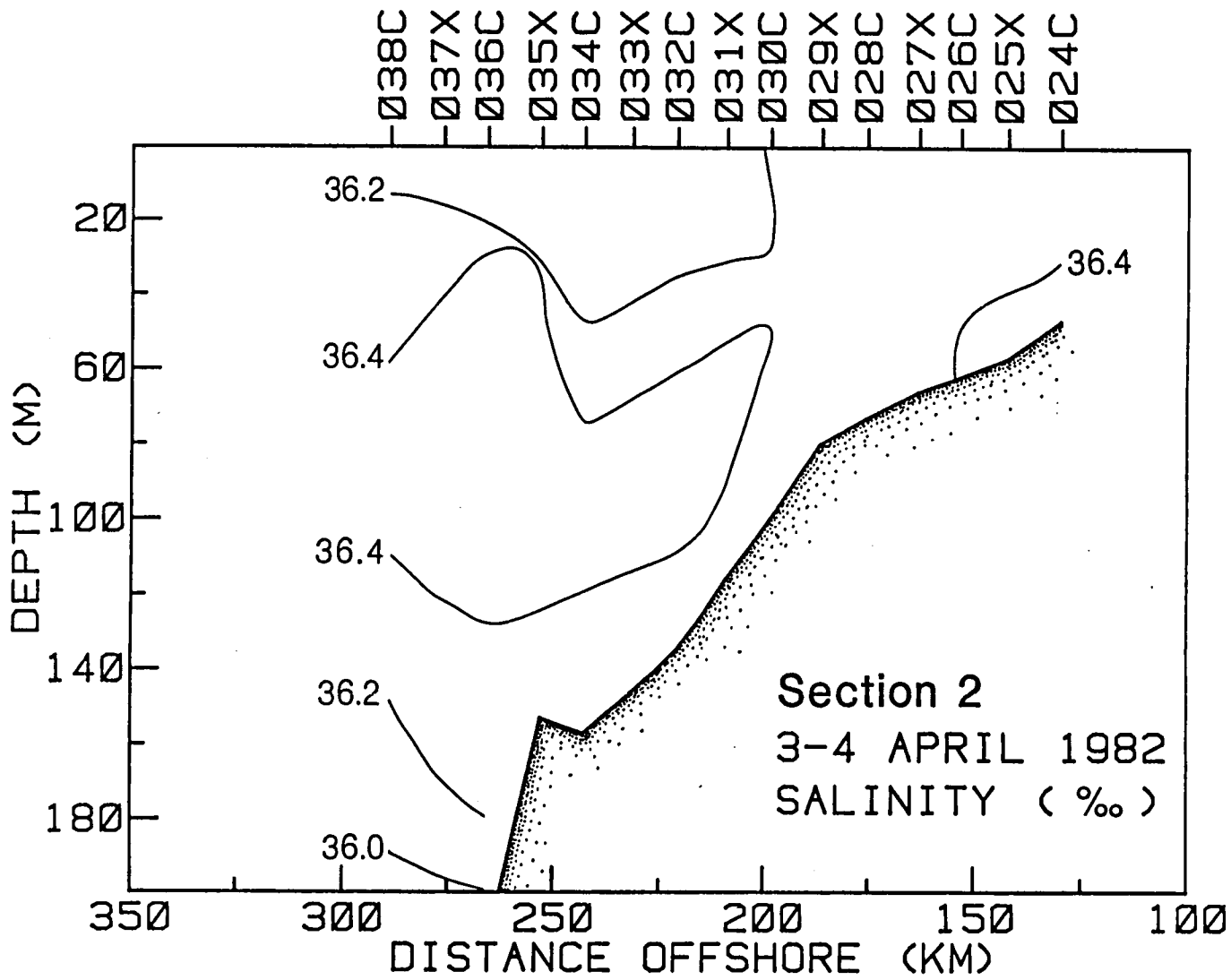
Figure 3-13. Spring cruise, transect 2 salinity section.
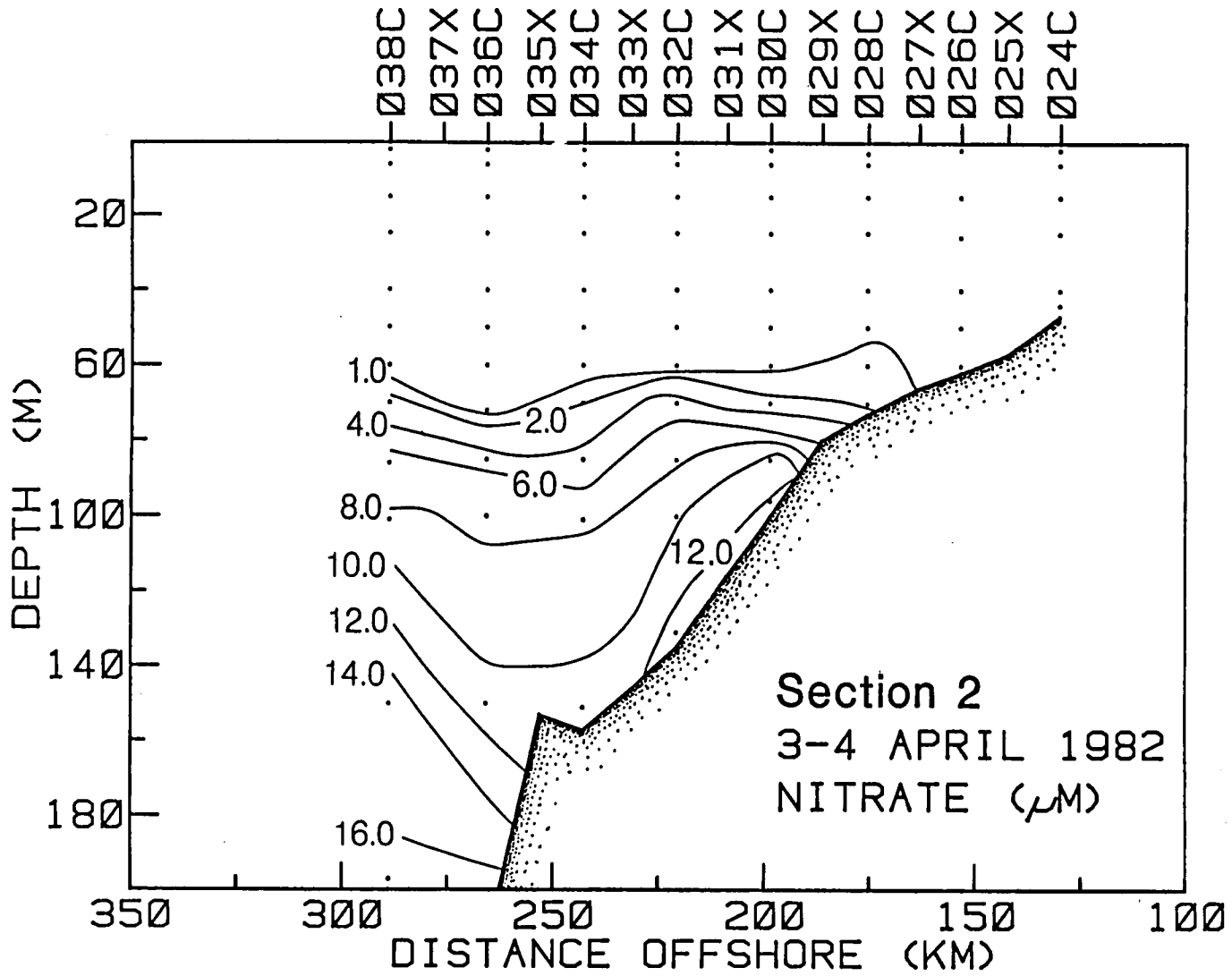
Figure 3-14. Spring cruise, transect 2 nitrate section.

94
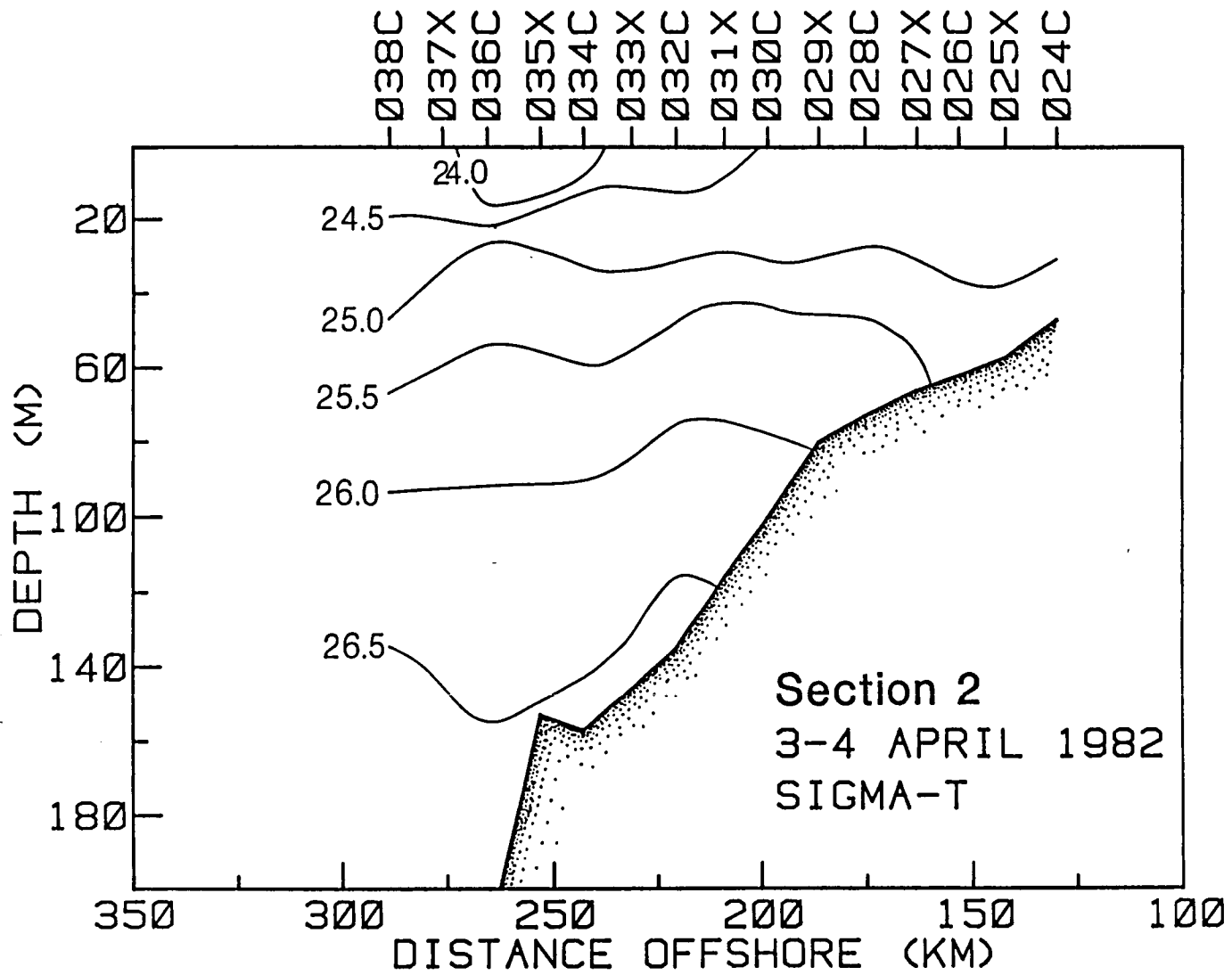
Figure 3-15. Spring cruise, transect 2 sigma-t section.
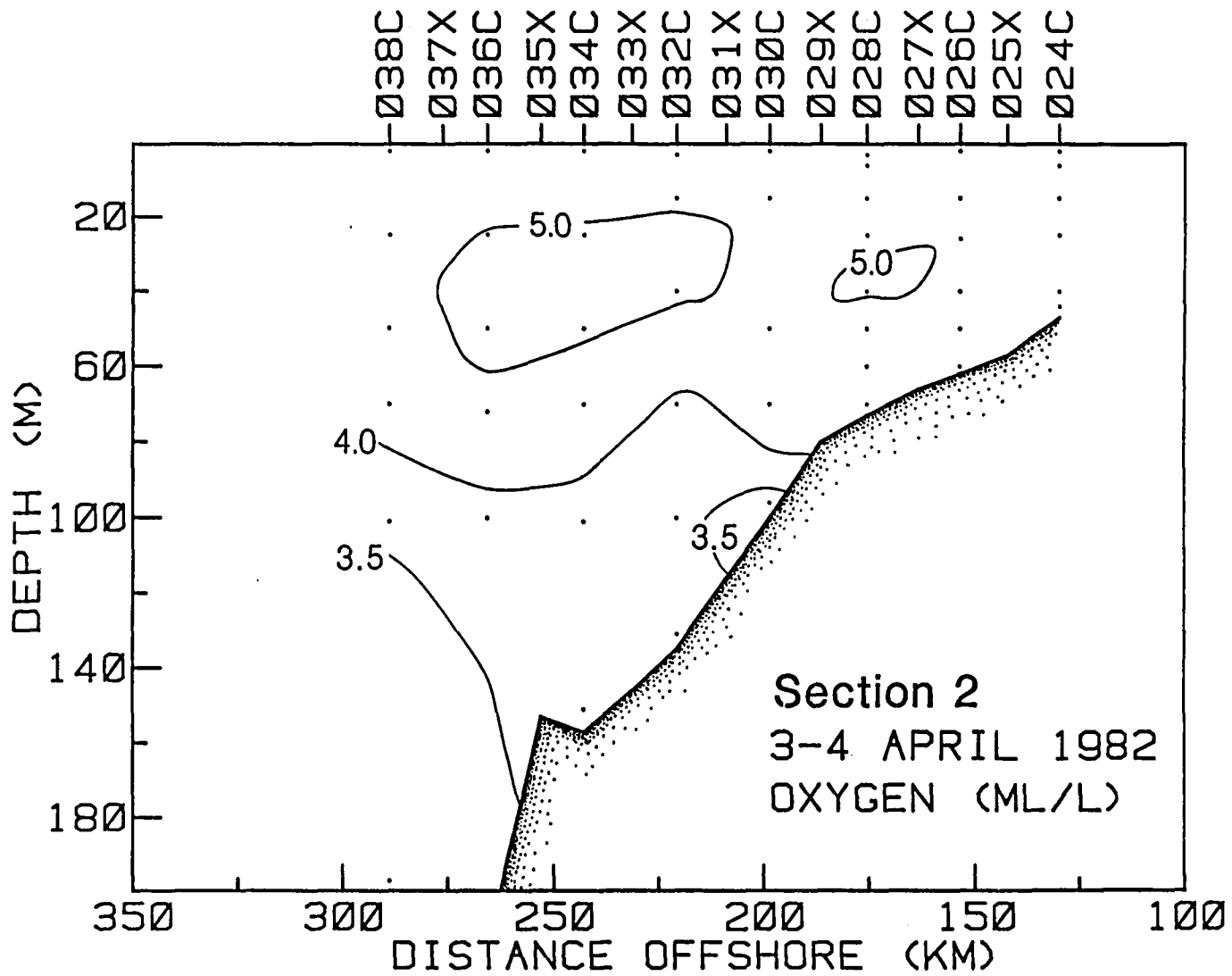
Figure 3-16. Spring cruise, transect 2 oxygen section.
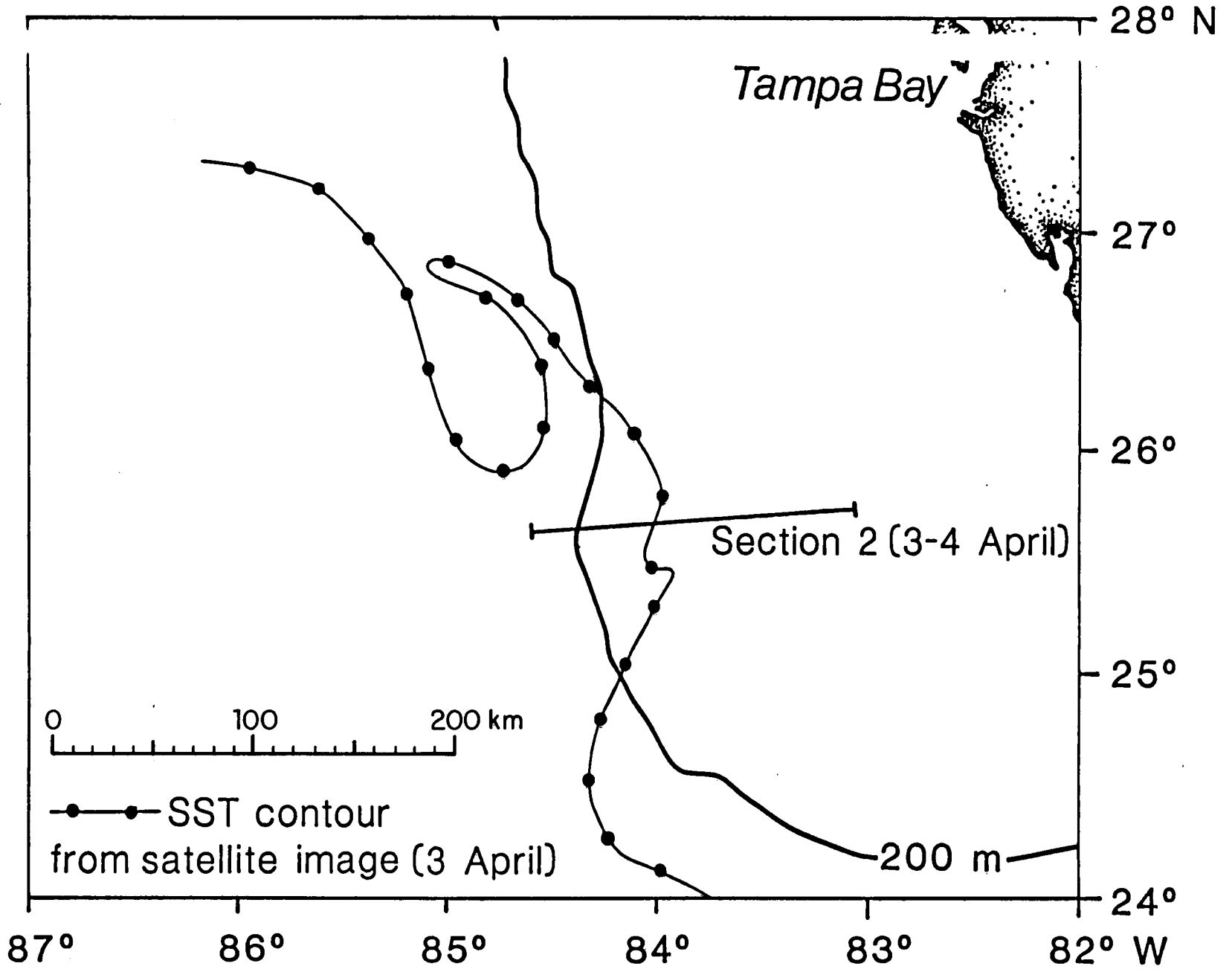
Figure 3-17. Transect 2 location with respect to front.

1979). It seems most likely that the elevation of the isotherms was related to the propagation of the frontal event.

After Transect 2, a northward XBT transect (Section 3) was occupied across the cold core of the frontal eddy. The isotherms in Transect 3 were domed, indicating upwelling (Figure 3-18). The most intense doming occurred at depth and became less noticeable in the upper 50 m. A small temperature difference of 0.5°C was observed over the edges of the cold core. The thermal fronts observed in this transect agreed with those derived from the imagery within 5 km. At this time, the shoreward edge of the cold core was approximately 15 km from the 200 m contour (Figure 3-19).

At the end of this transect, a shoreward XBT transect, Section 4 (Figure 3-20), was occupied. The warm filament was evident in Section 4 (Figure 3-21) by the depression of the isotherms between Stations 46 and 51. The width of the filament measured from the image (~35 km) agreed well with the width indicated by the surface isotherms (40 km). The subsurface extent of the filament was approximately 20 m. The front between the filament and shelf waters was well pronounced; the temperature difference was on the order of 1°C. The location of the front derived from the imagery (26°11'N, 84°09'W) was within 8 km of the location of the front seen in the hydrography (26°10.6'N, 84°03.4'W). The cold core was immediately west of this transect. The structure in the water column, that is, upwelling in the cold core and depression of isotherms across the filament, strengthens the assumption of cyclonic flow in the frontal eddy.
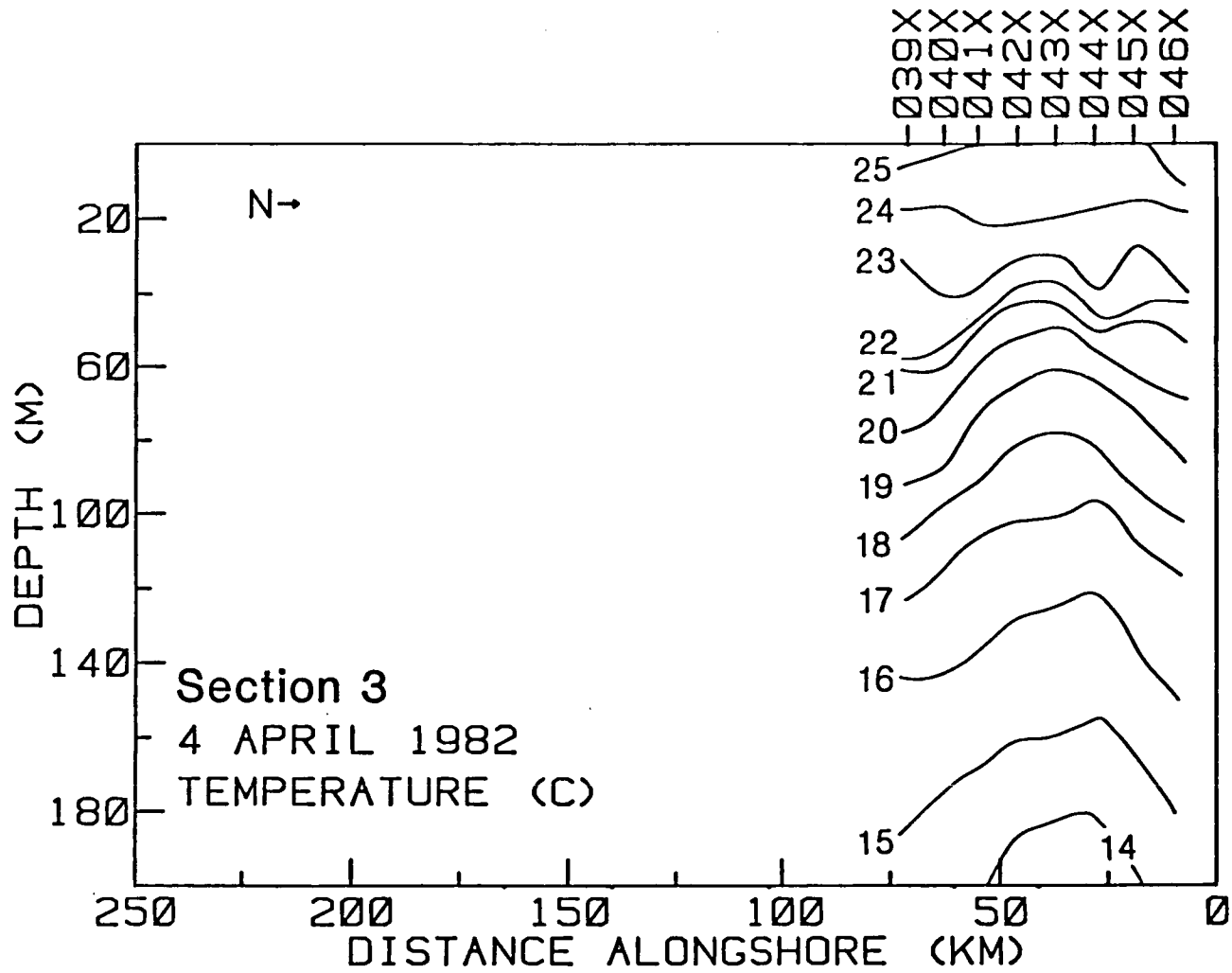
Figure 3-18. Spring cruise, transect 3 temperature section.
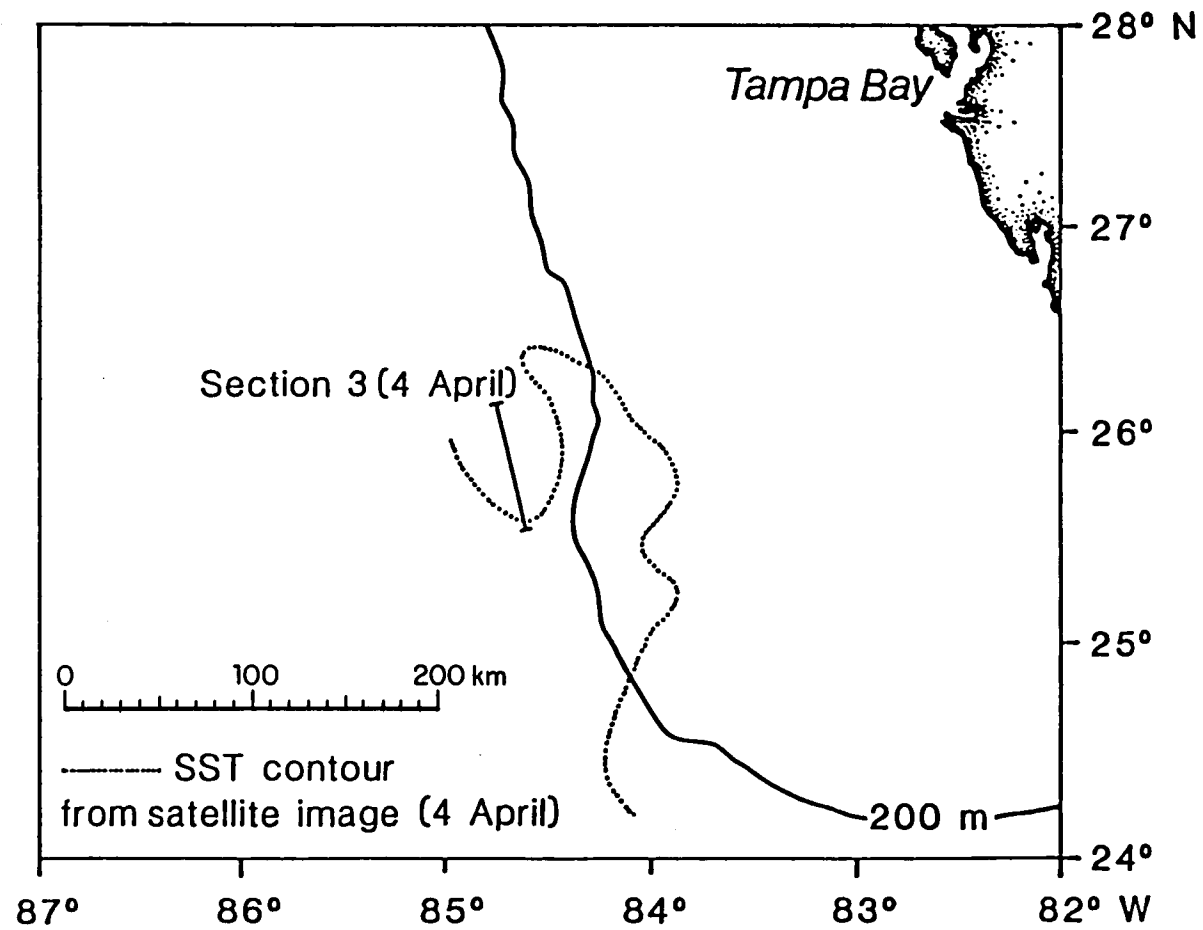
Figure 3-19. Transect 3 location with respect to front.
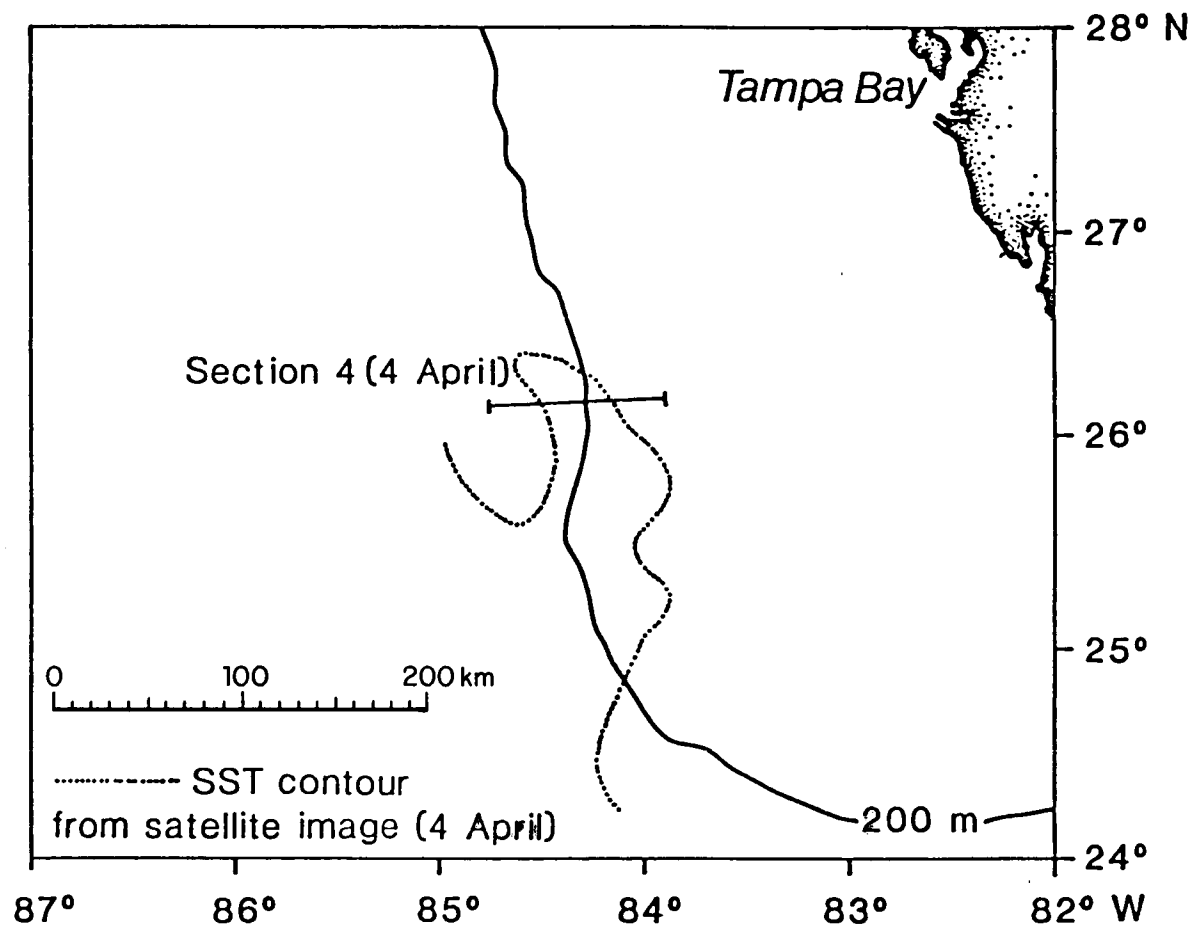
Figure 3-20. Transect 4 location with respect to front.

Figure 3-21. Spring cruise, transect 4 temperature section.

In the following days, transects were repeated in the area of onshore motion. The sections showed a progressive deepening of the isotherms to the west and east, and a more pronounced doming as the cold core intruded onto the shelf. For comparison purposes, the sequence of temperature, salinity, sigma-t, oxygen, and nitrate concentration for Section 5a are presented as Figures 3-22 through 3-26, respectively. Comparison sections for the same parameters for Transect 6 on April 6 are shown in Figures 3-27 through 3-31. Figure 3-32 illustrates the relative position of Transect 6 with respect to the frontal eddy. The location of Transect 5a with respect to Transect 6 is shown in Figure 3-1. Points to note in this comparison are:

- the gradual deepening of the upwelling dome between Figures 3-22 and 3-27 over a period of about one day,

- the lateral reach of the doming structure (Figure 3-27) to as far shoreward as the 60 m isobath, suggesting a marked effect on shelf water distributions,

- indications of the filament by the depression of the 24°C isotherm between Stations 78 and 81 just east of the cold core (Figure 3-27),

- the most intense upwelling occurring between Stations 57 and 59 in Transect 5 (Figure 3-22) and Stations 81 to 85 in Transect 6 (Figure 3-27), both about 200 km offshore,
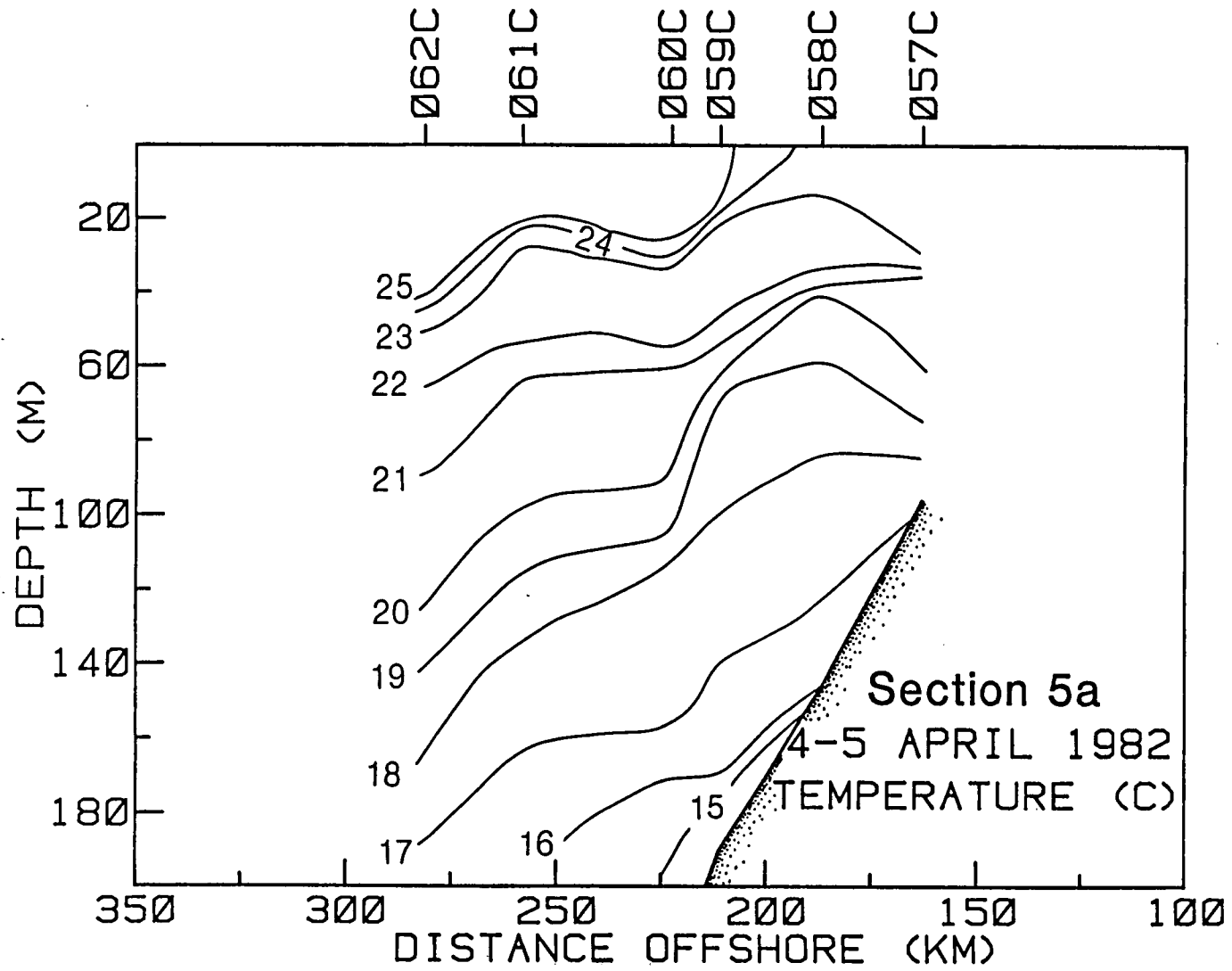
Figure 3-22. Spring cruise, transect 5a temperature section.
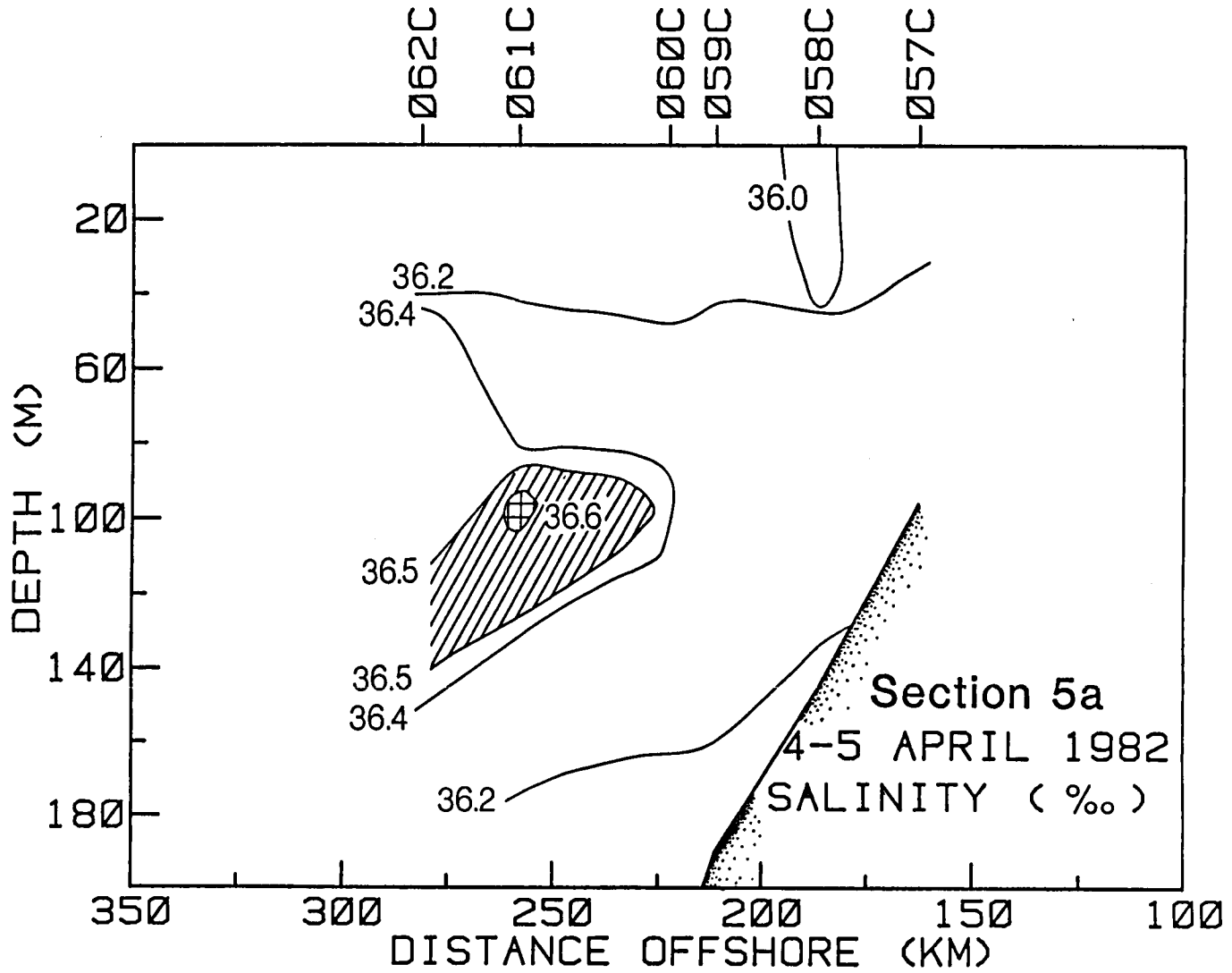
Figure 3-23.   Spring cruise, transect 5a salinity section.
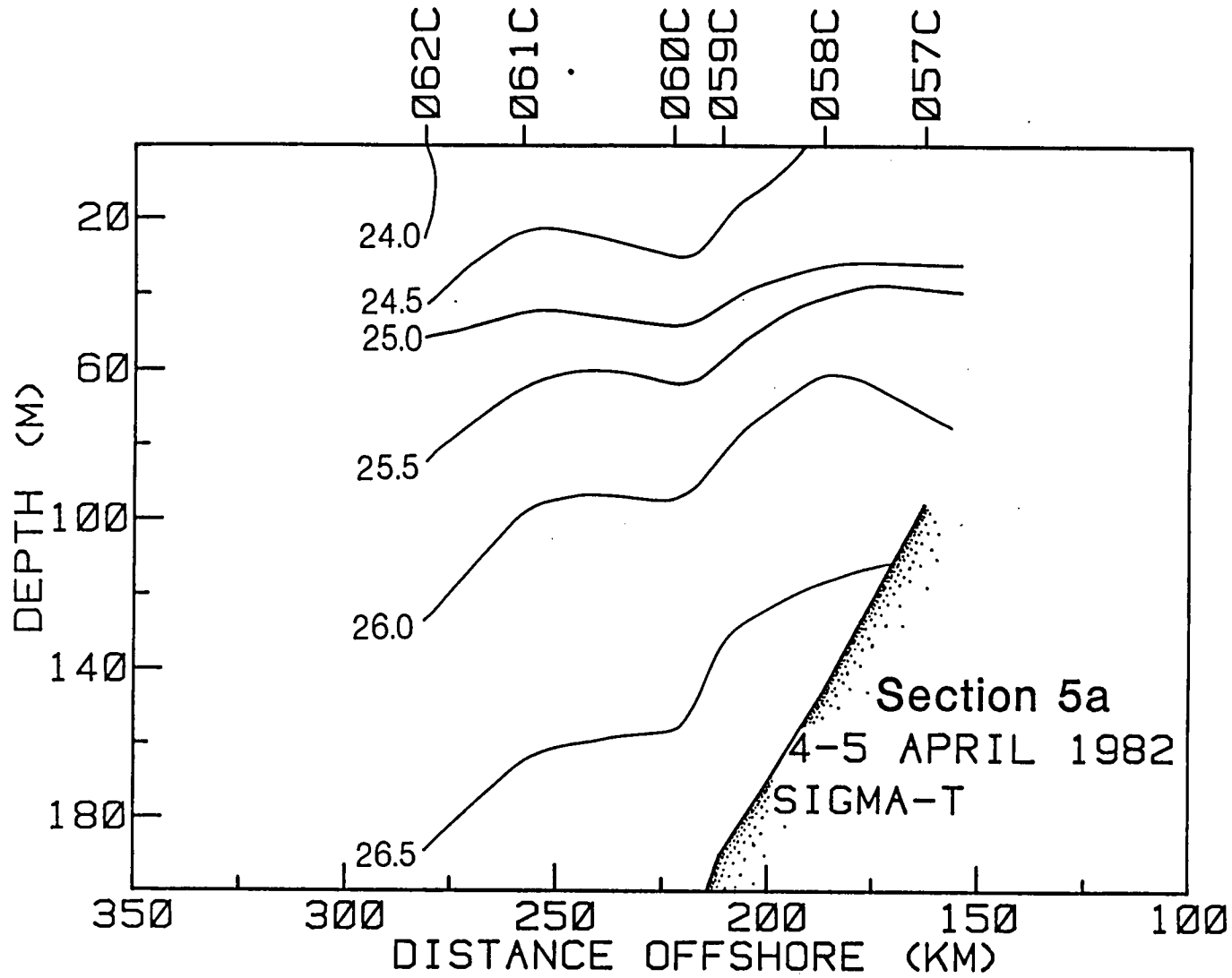
Figure 3-24. Spring cruise, transect 5a sigma-t section.
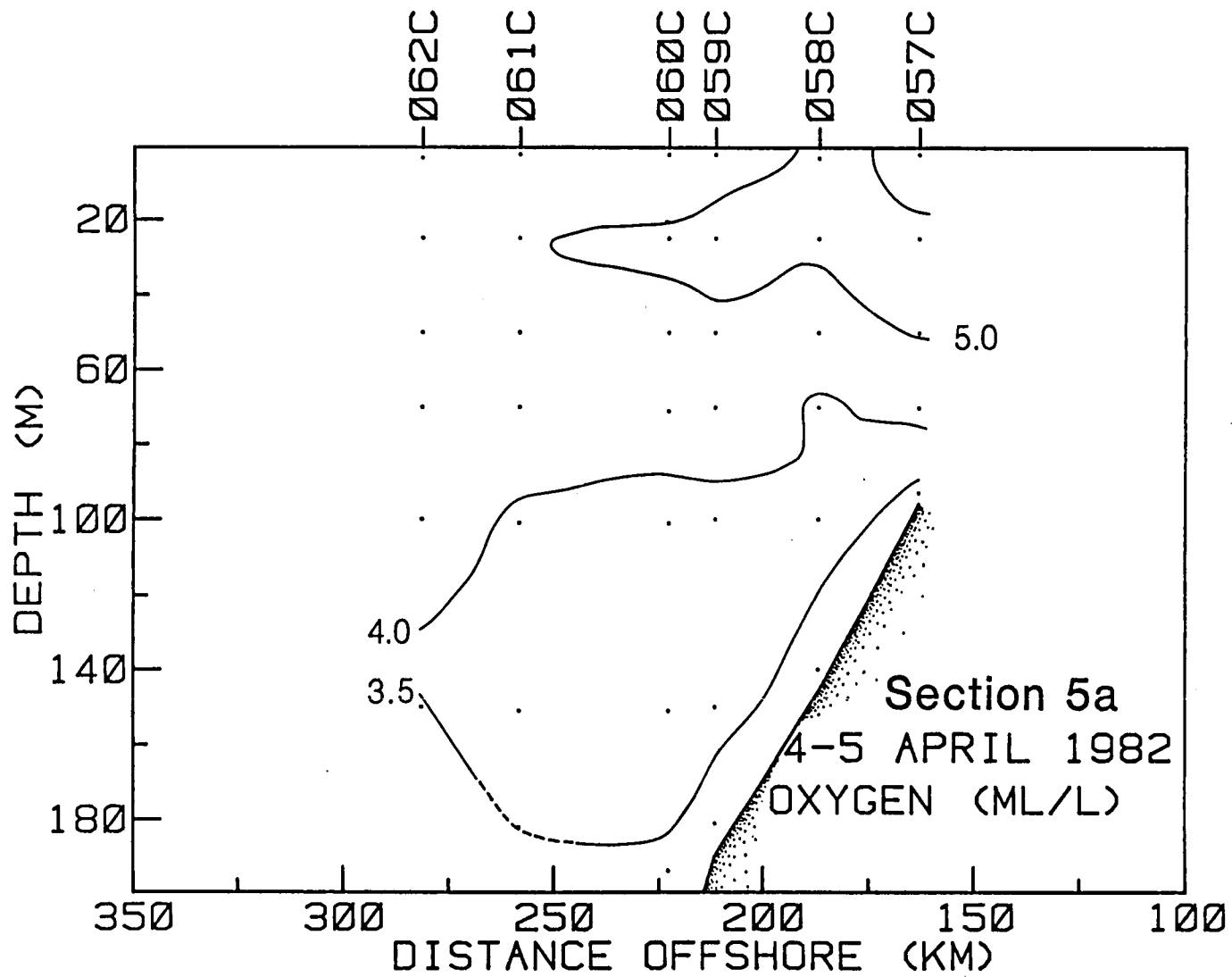
Figure 3-25. Spring cruise, transect 5a oxygen section.
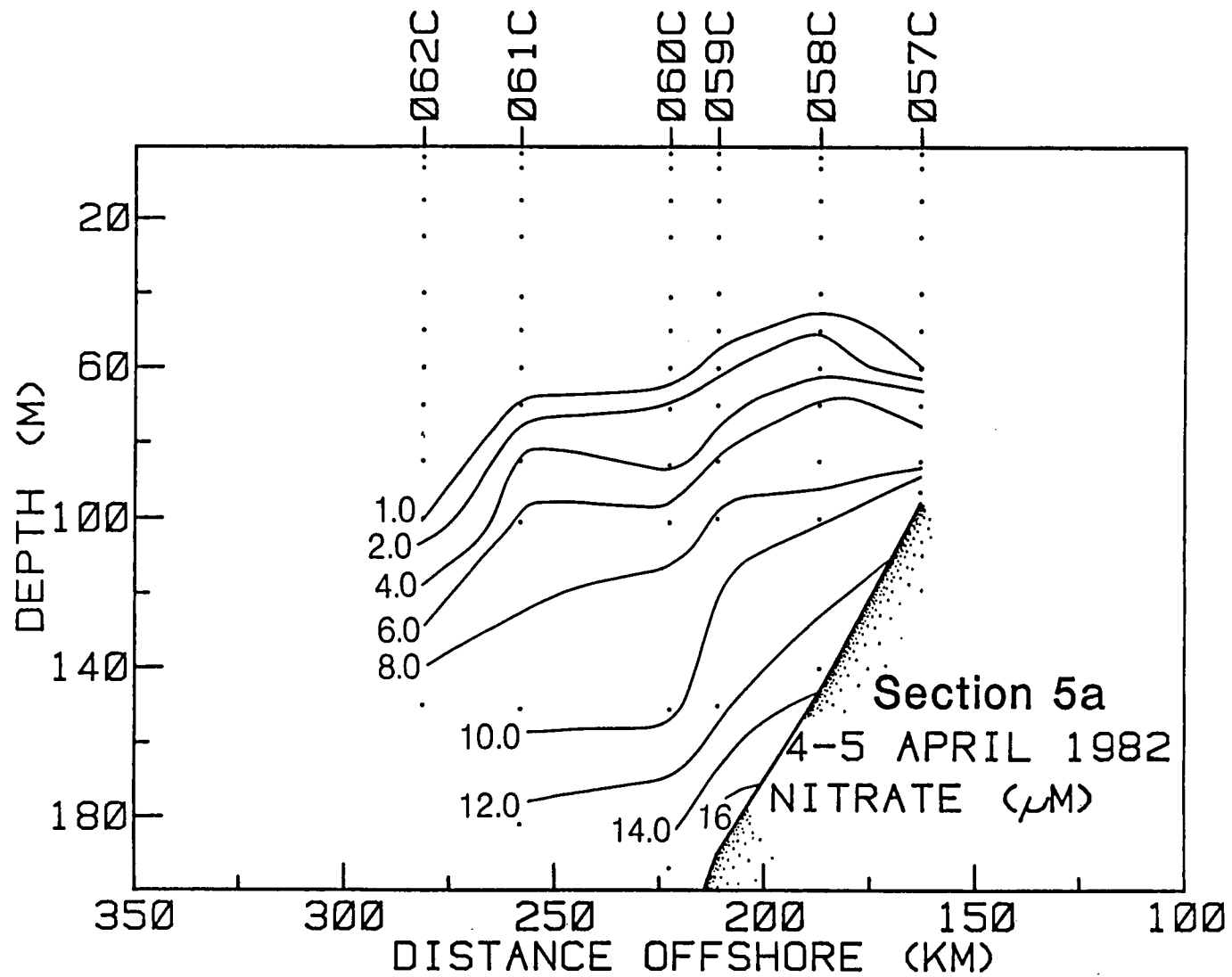
Figure 3-26.   Spring cruise, transect 5a nitrate section.
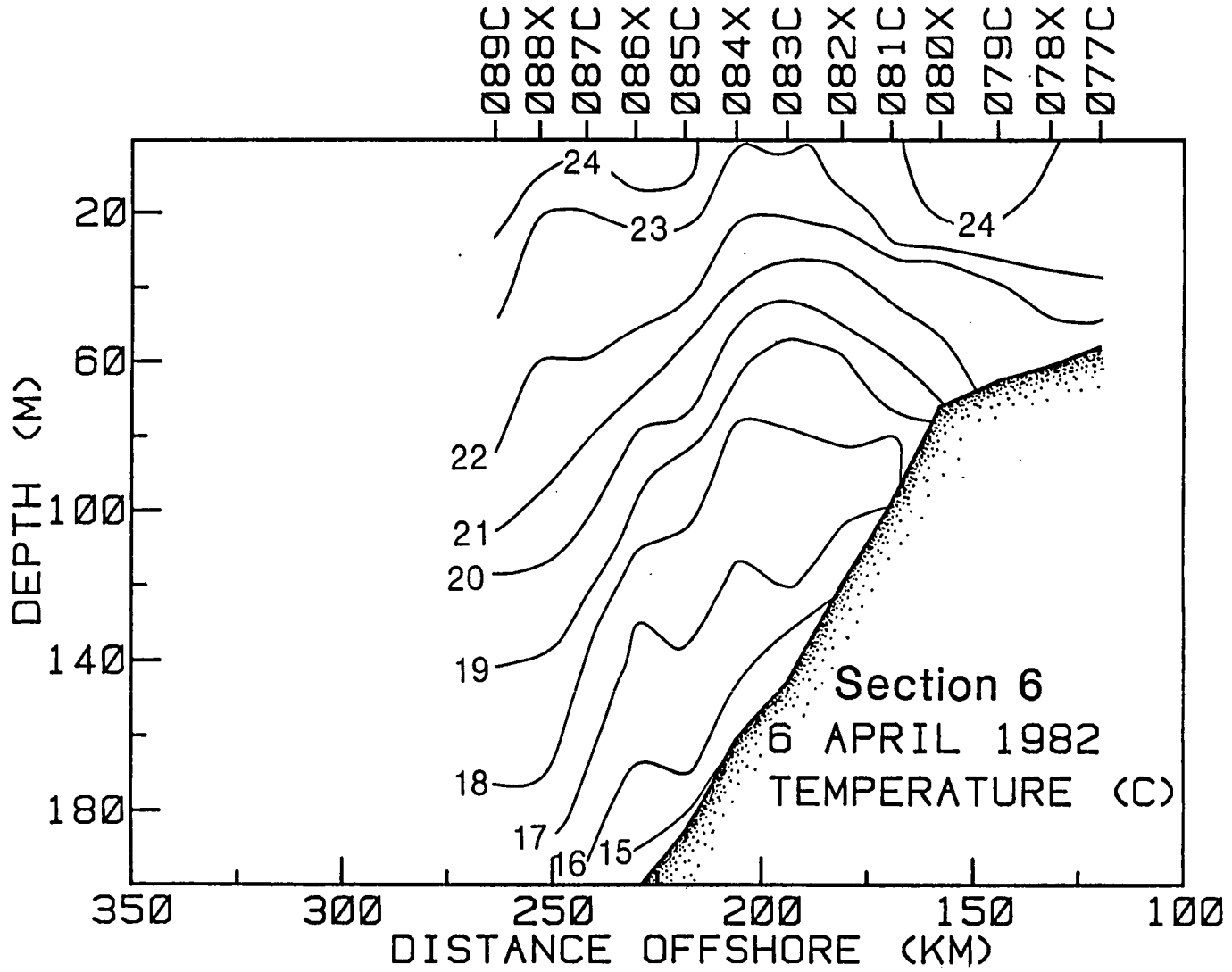
Figure 3-27.   Spring cruise, transect 6 temperature section.

109
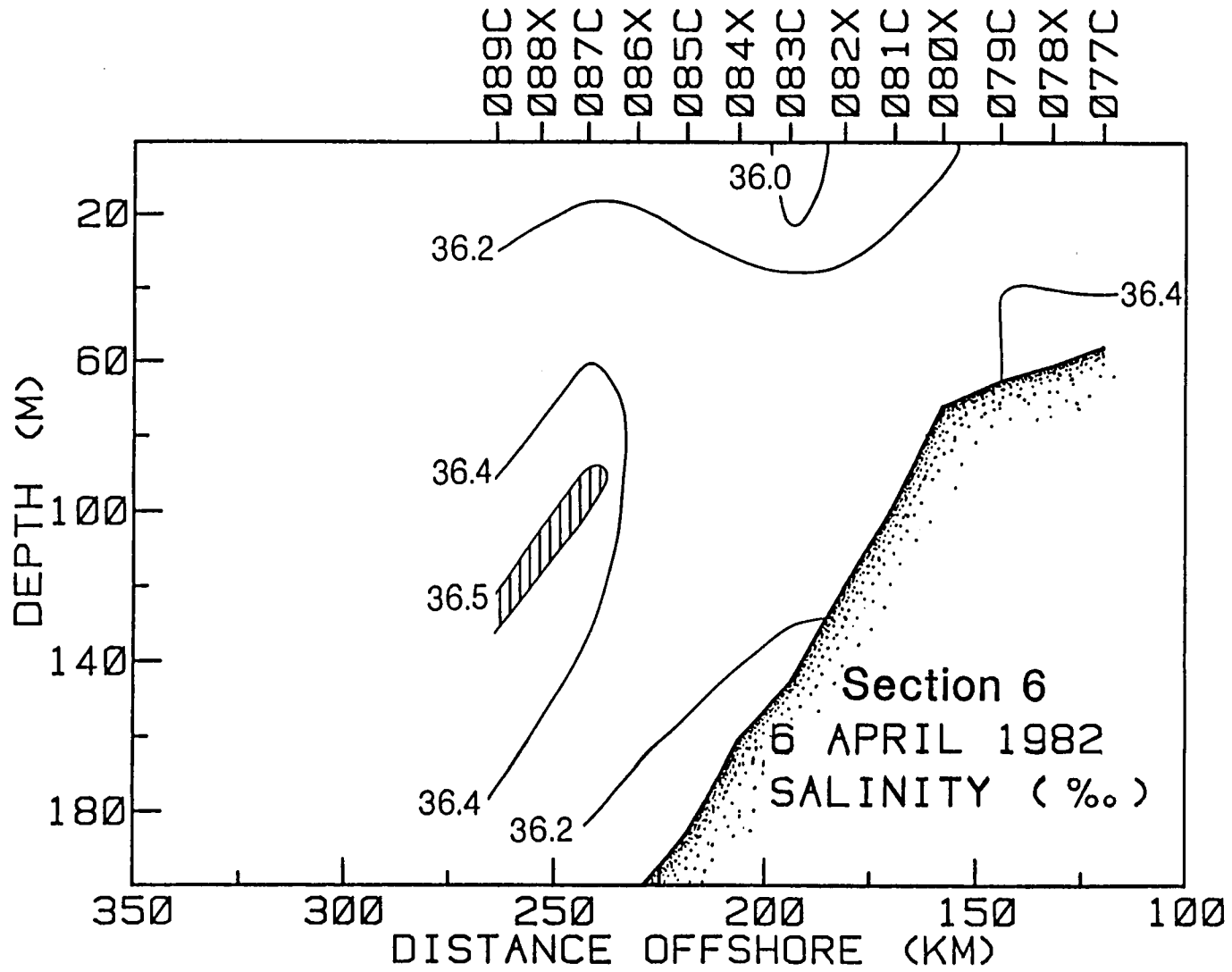
Figure 3-28.   Spring cruise, transect 6 salinity section.
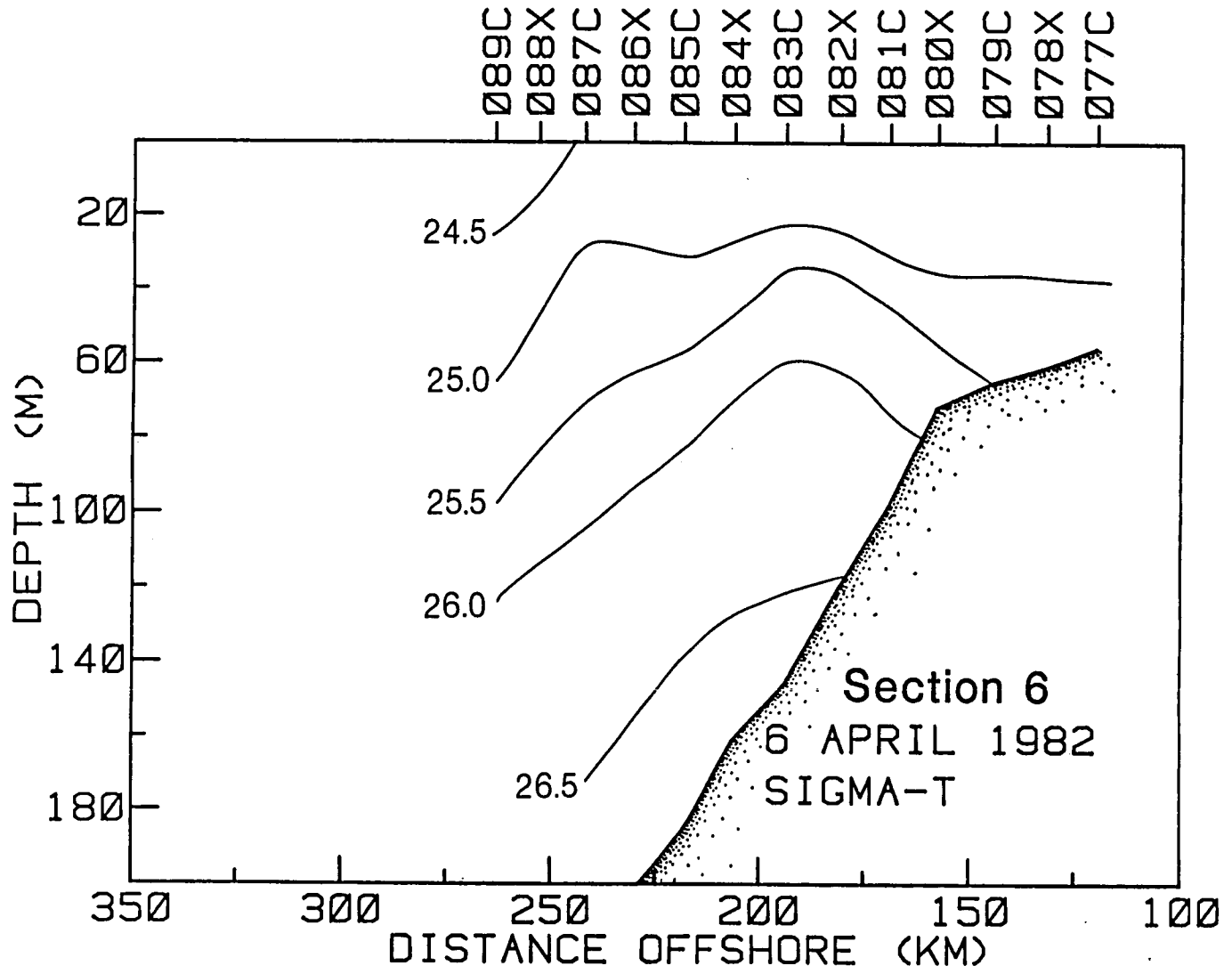
Figure 3-29. Spring cruise, transect 6 sigma-t section.
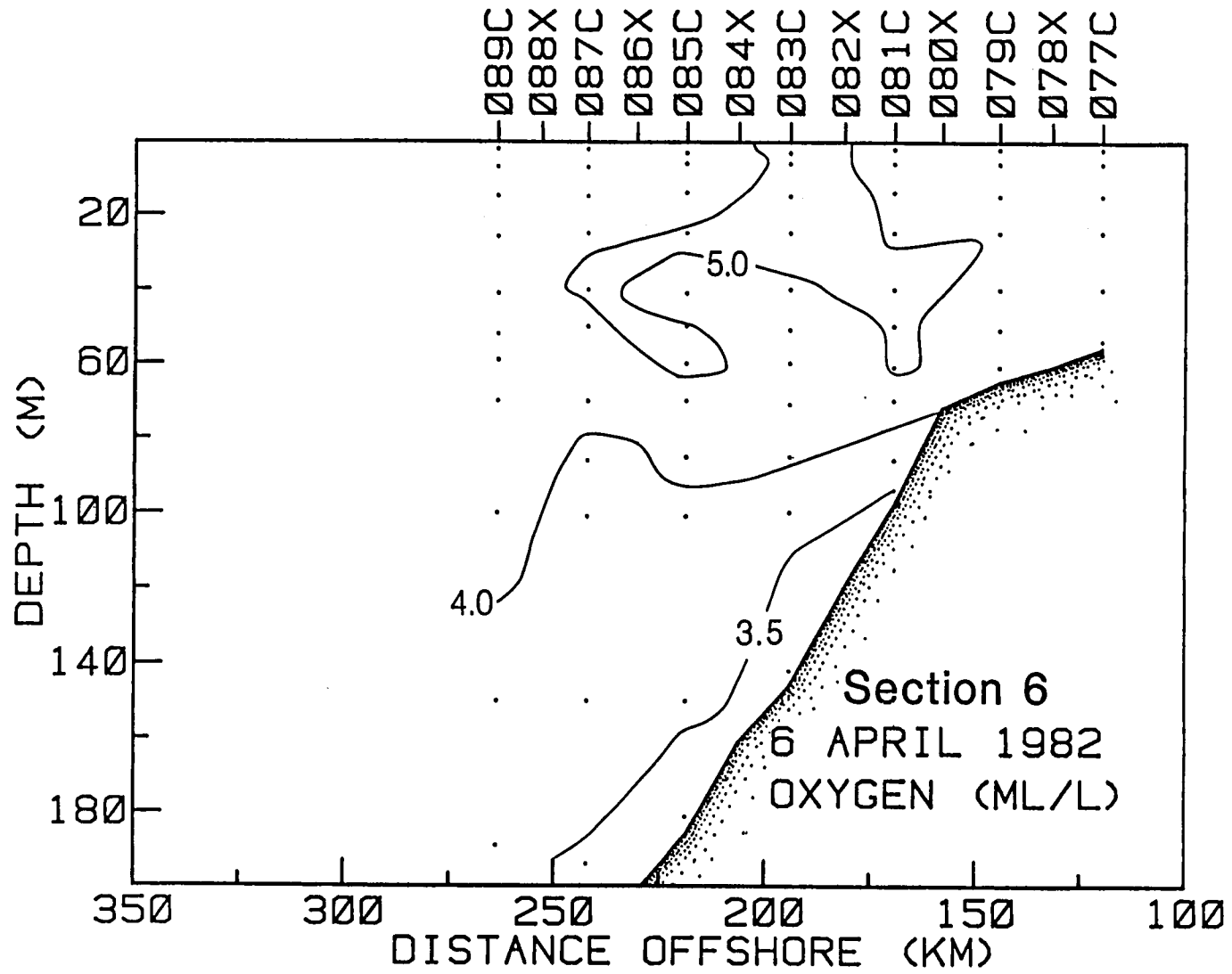
Figure 3-30. Spring cruise, transect 6 oxygen section.
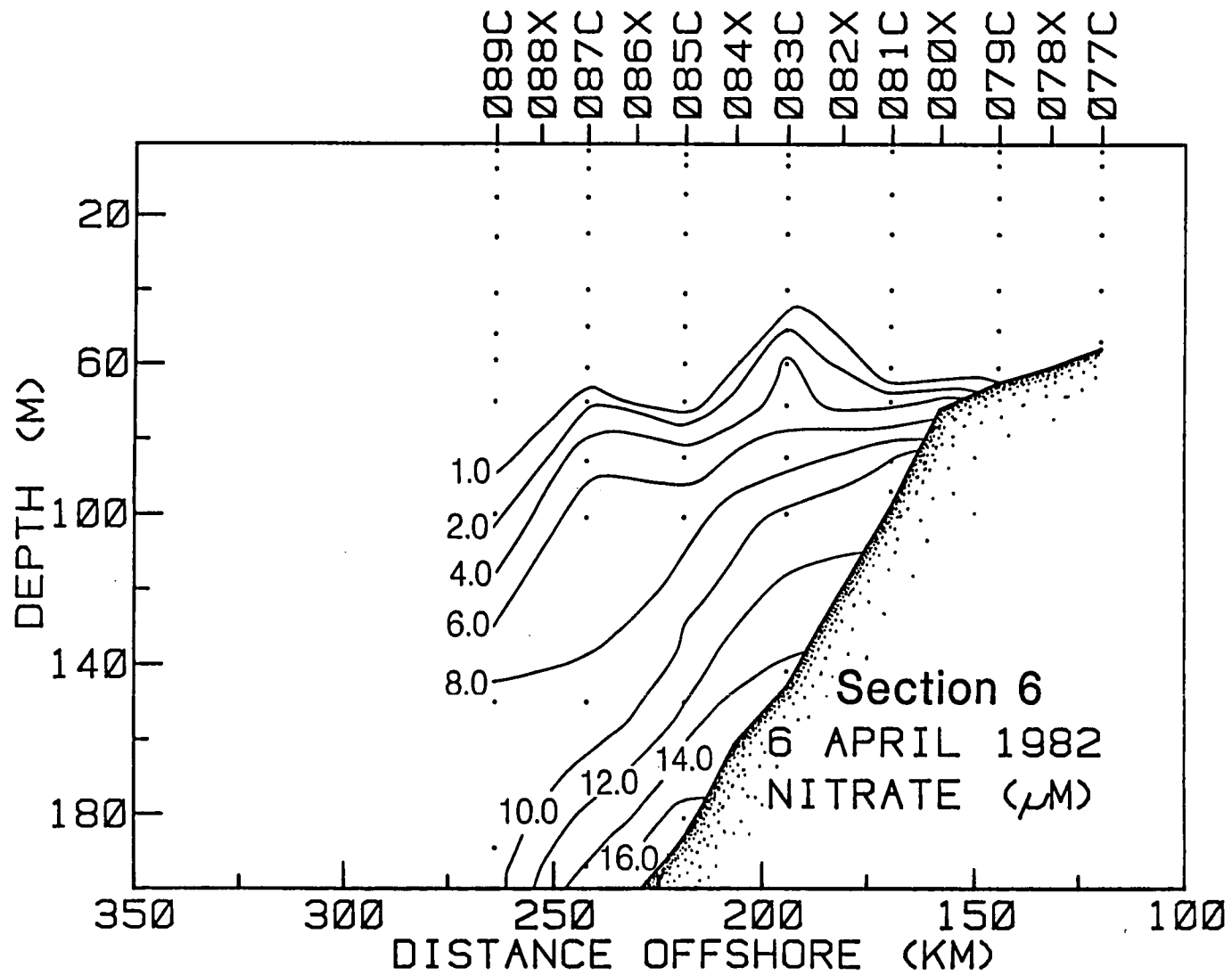
Figure 3-31.   Spring cruise, transect 6 nitrate section.

113
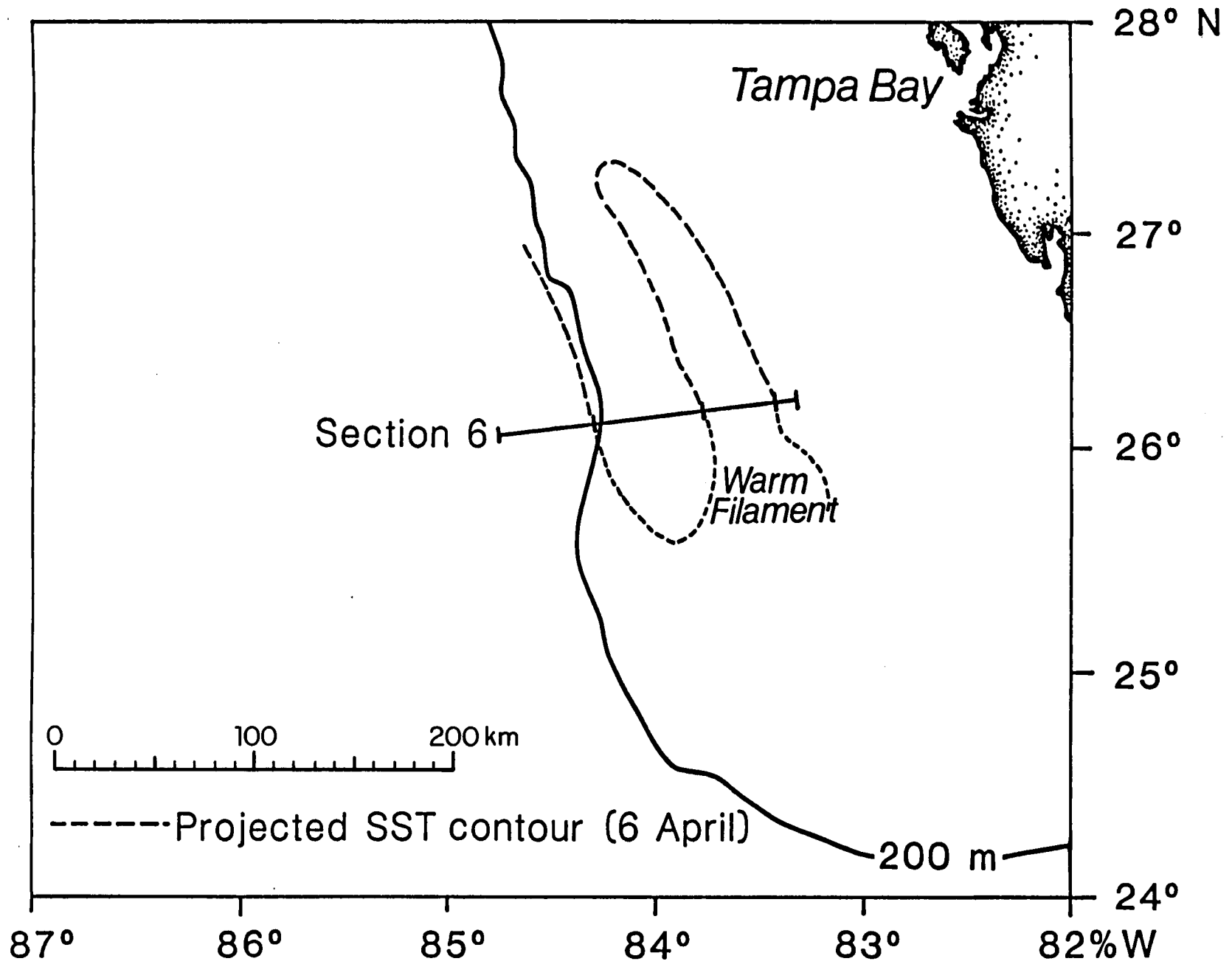
Figure 3-32. Transect 6 location with respect to front.

- the sequential doming of the sigma-t surfaces (Figures 3-24 and 3-29) with a following of the progression by the nitrate (Figures 3-26 and 3-31) and oxygen (Figures 3-25 and 3-30) concentrations, and

- in Figure 3-27, the near intersection of the 22°C isotherm with the 100 m contour which would have indicated the eastern wall of the Loop Current.

On April 7, Transect 8 (Figure 3-33) was occupied about 70 km further north. The corresponding temperature, salinity, sigma-t, oxygen, and nitrate sections (Figures 3-34 through 3-38, respectively) show

- a doming of isotherms (Figure 3-34) and sigma-t (Figure 3-36) values on the shelf followed (in the vicinity of Station 107) by the depression of the 23°C isotherm indicating upwelling in the filament structure,

- intersection of the 22°C isotherm at 100 m indicating the eastern wall of the Loop Current (Figure 3-34), and

- the highest nitrate levels remaining below the mixed layer (Figure 3-38) where oxygen levels were about 5 ml/l.

The occurrence of the cold core on the shelf in Transect 8 with respect to its presence in Transect 6 suggests that the horizontal subsurface length scale of this feature is at least 100 km. As noted above, the surface expression is on the order of 200 km.

115
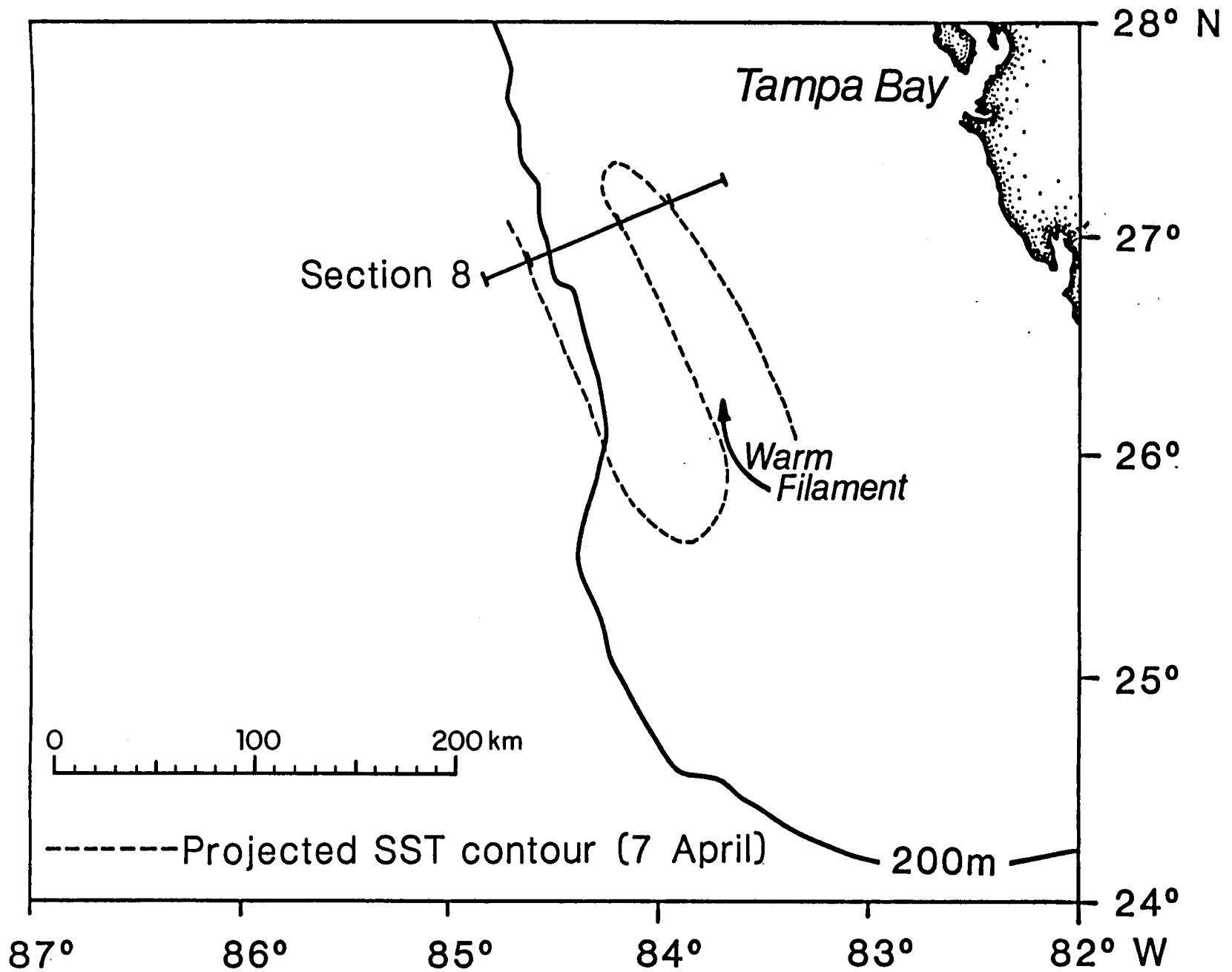
Figure 3-33. Transect 8 location with respect to front.
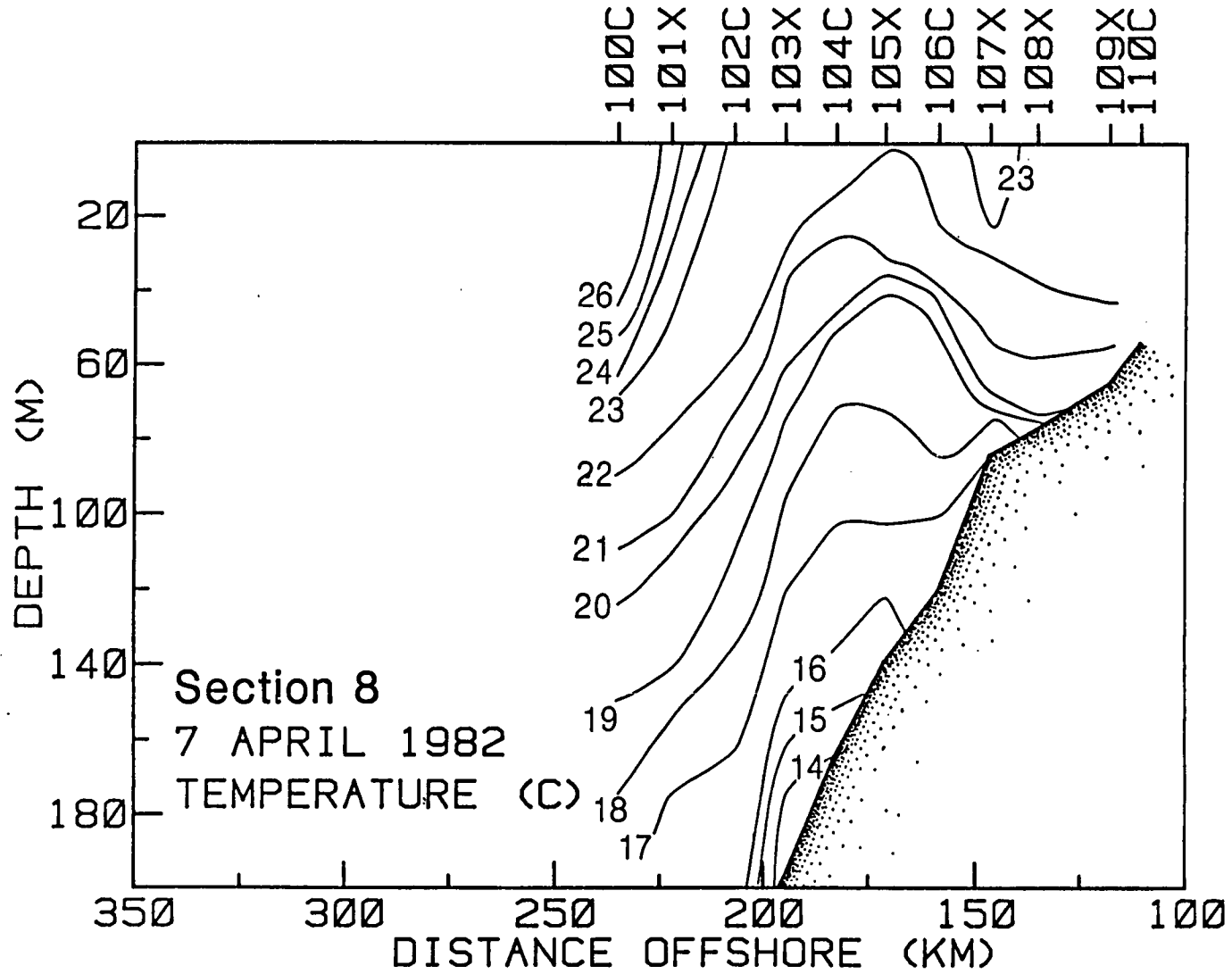
Figure 3-34. Spring cruise, transect 8 temperature section.
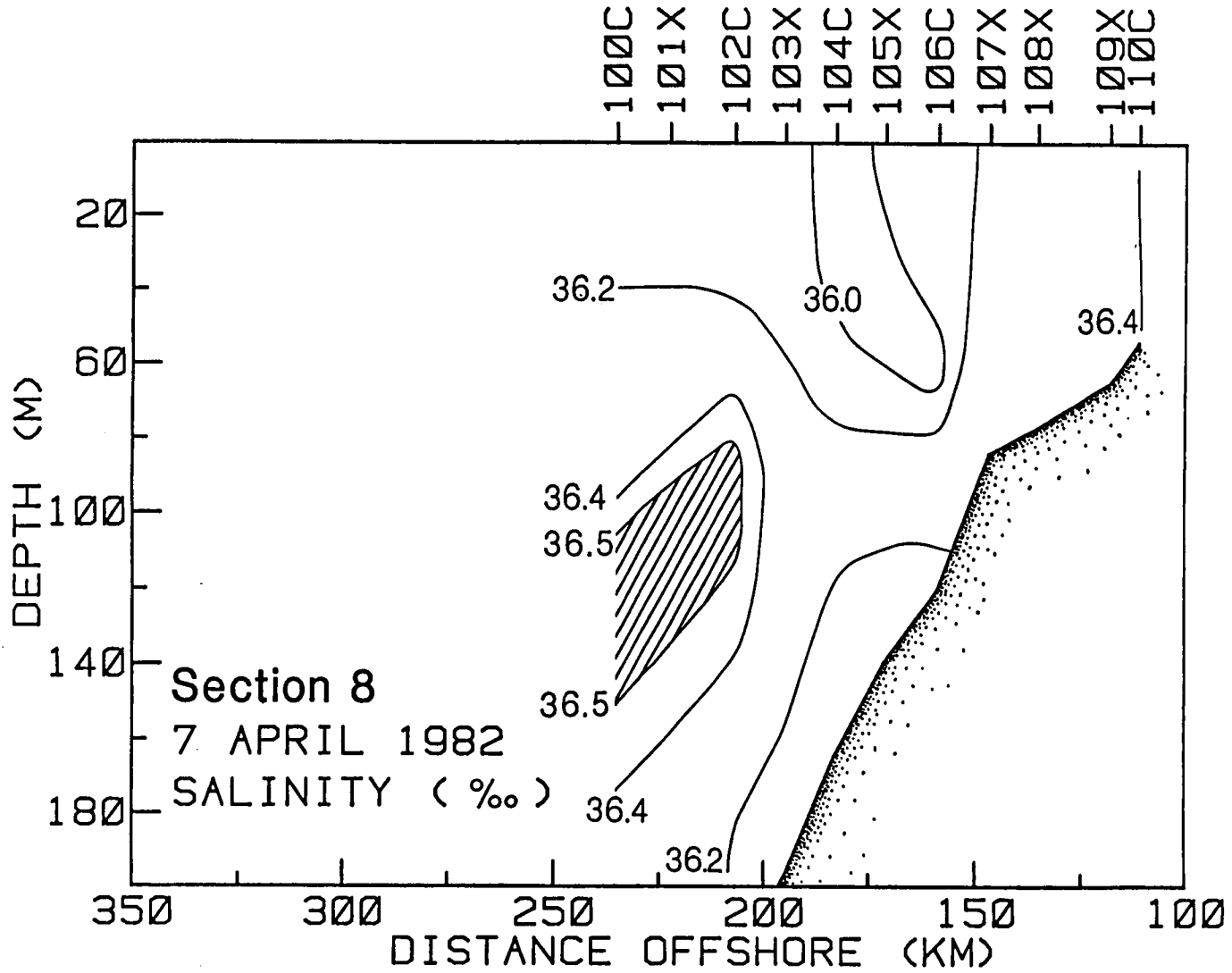
Figure 3-35.   Spring cruise, transect 8 salinity section.
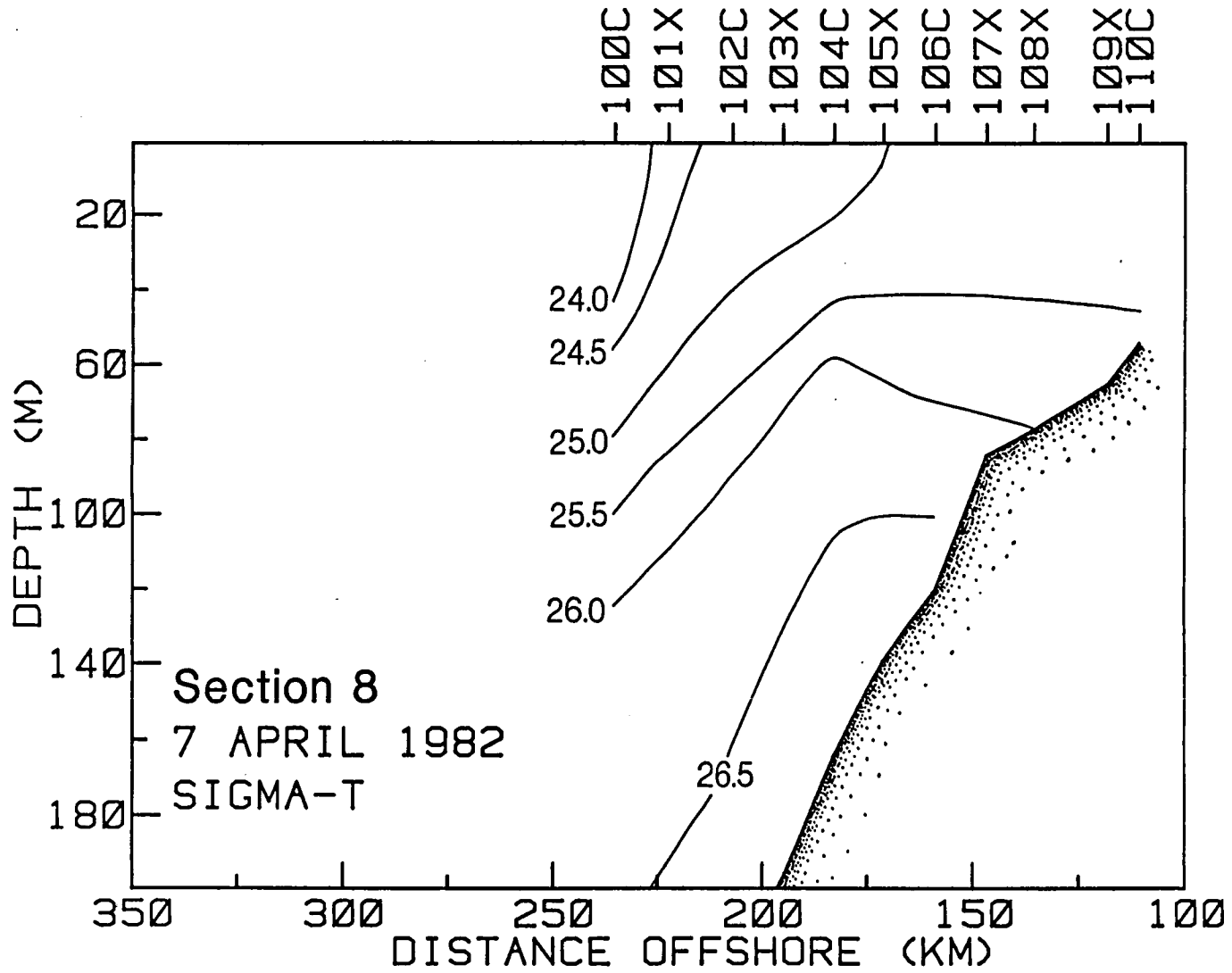
Figure 3-36. Spring cruise, transect 8 sigma-t section.
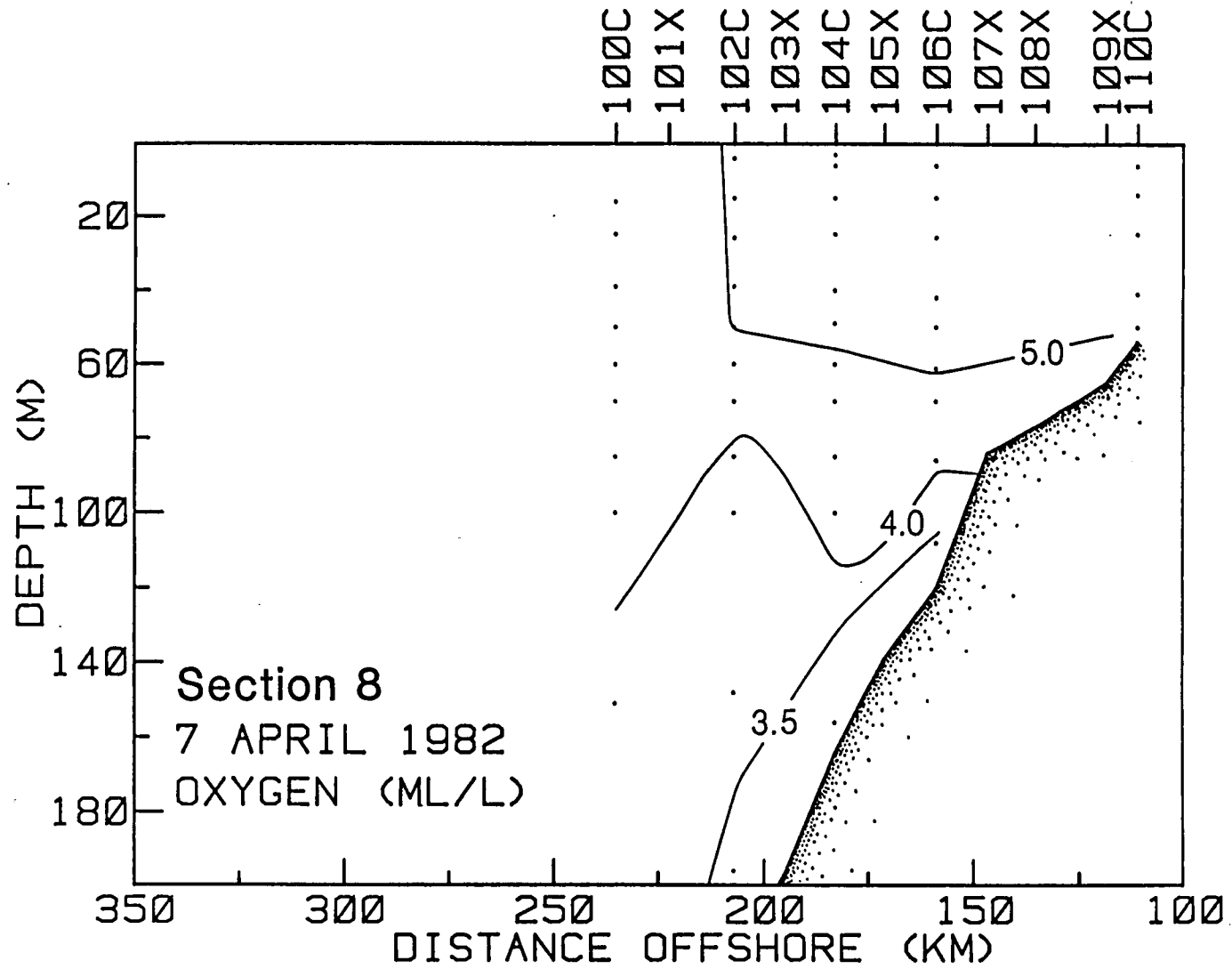
Figure 3-37. Spring cruise, transect 8 oxygen section.
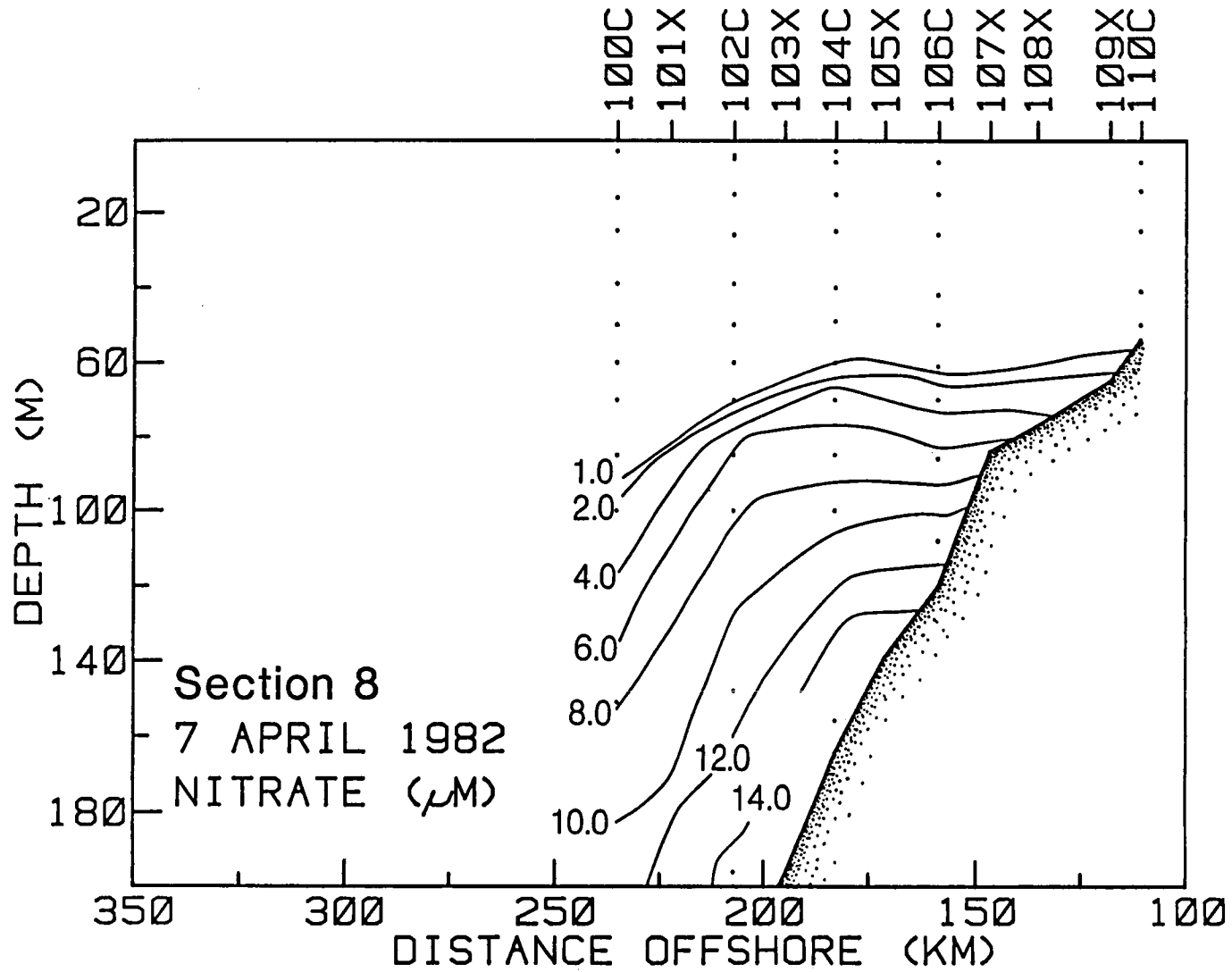
Figure 3-38. Spring cruise, transect 8 nitrate section.

In summary, both satellite and hydrographic data indicated that a frontal eddy, consisting of a cold core and warm filament, propagated southward intruding into upper slope and outer shelf waters; at the same time, the Loop Current moved offshore. Significant changes in hydrographic structure over periods of days were observed over the shelf break region and onto the shelf itself. Nitrate redistribution along sigma-t surfaces is but one of the consequences of the intrusion process.

3.2.1.4 Water Masses

Another consequence of the intrusion of the Loop Current frontal eddy is the associated local interaction of water masses. In this regard, the southwest Florida shelf can be thought of as a transition region. In the offshelf region, the TS characteristics display a salinity maximum (36.6 to 36.8°/oo) near 22.5°C in the upper 200 m. Waters with this characteristic have been called Yucatan Water by Wennekens (1959), Eastern Gulf Loop Water by Nowlin and McLellan (1976), Righthand Water by Leipper (1977), and Loop Current Water by Price (1976). The salinity maximum is characteristic of Subtropical Underwater described by Wüst (1964). In general, the water in the upper layer (0-200 m) of the Loop Current is due to an influx of Caribbean Water which is a mixture of waters with a North Atlantic origin and South Atlantic waters. For simplicity, the waters with the subsurface salinity maximum will be called Loop Current Water (LCW).

Waters with fresher, colder TS characteristics are also found in this region. Wennekens (1959) calls these waters Continental Edge Water (CEW) and notes that the TS characteristics are intermediate between Yucatan and Western Gulf

Water. Continental Edge Water is found along the continental edge of the current. Nowlin and McLellan (1967) and Morrison and Nowlin (1977) also described low salinity values in water bounding the Loop Current. Waters with these characteristics and regional position will be called CEW.

A first step towards understanding these interactions was to characterize the TS features. Figure 3-39 shows the characteristic profiles found throughout the study period. The numbers next to each of the jagged graphs denote station numbers; the skewed lines (24, 26, 28) indicate sigma-t values. Station 12 showed characteristics of LCW. Water in the Loop Current is easily identified by its subsurface salinity maximum, oxygen minimum and higher nutrient concentrations. The salinity maximum occasionally exceeded 36.6°/oo and occurred in the western part of the transects coincident with the steeply sloping isotherms indicating the Loop Current eastern wall. Station 79 is also LCW and was measured in the filament. Comparison of the density profiles at Stations 12 and 79 indicated that they are offset by approximately 80 m in depth. This relationship suggests that, at some point in time, the LCW filament was contiguous with 80 m deeper main LCW. The significance of this is discussed further in Section 4.4 of this report. Station 104 showed characteristics of CEW. Station 34 showed lateral interleaving structures indicative of mixing processes which occurred during the intrusion. Note that the filament and Loop Current front had characteristics of LCW and that the region between had characteristics of CEW. The upwelling occurred under the CEW region.

Figure 3-40 shows the horizontal distribution on the sigma-t = 25.25 surface. The contours in the figure are (salinity - 36) x 100, or ±0.1°/oo (10 units)

123
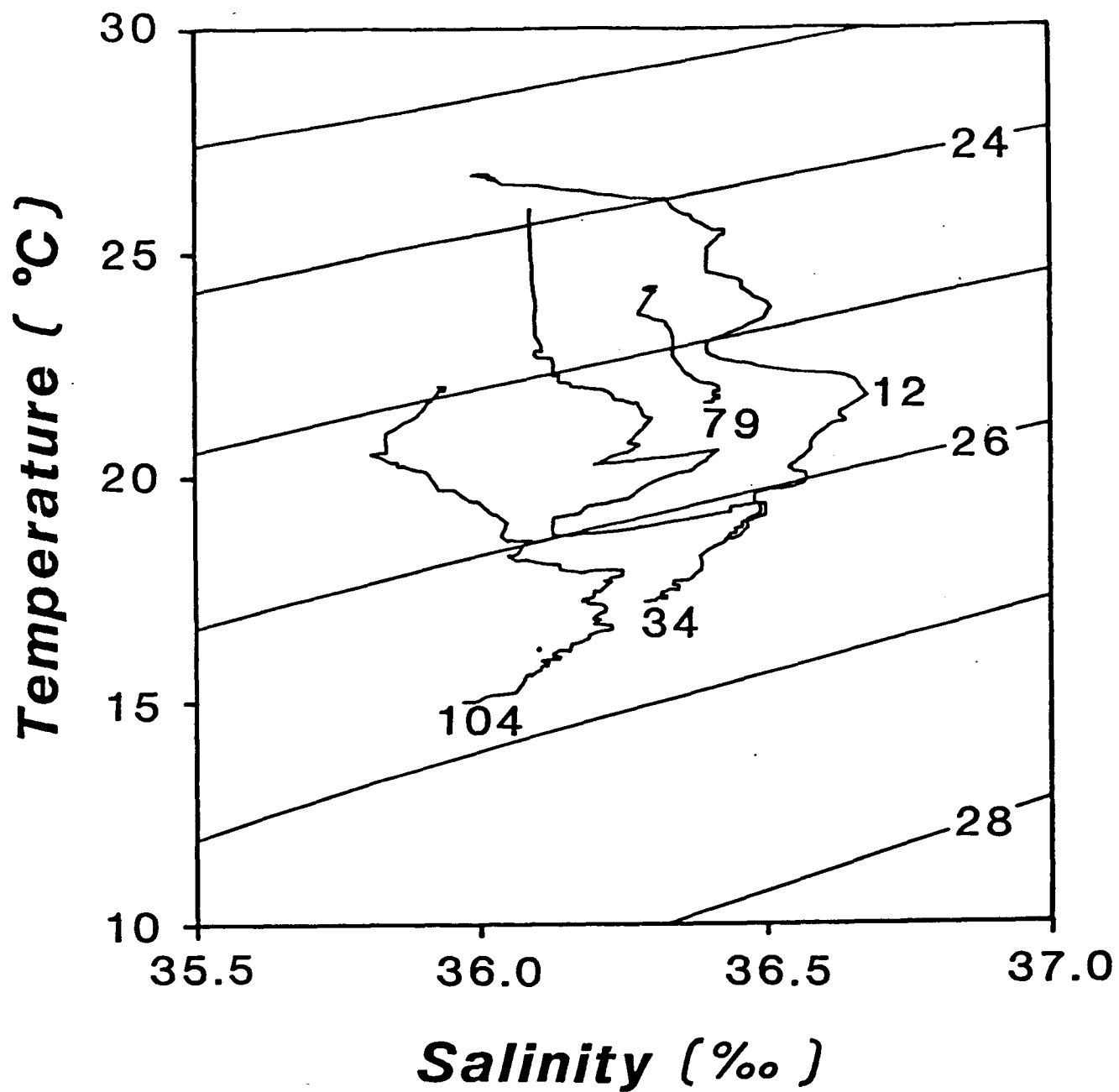
Figure 3-39. TS diagram for stations 12, 34, 79, and 104.

(S-36) x 100 on Sigma-t=25.25
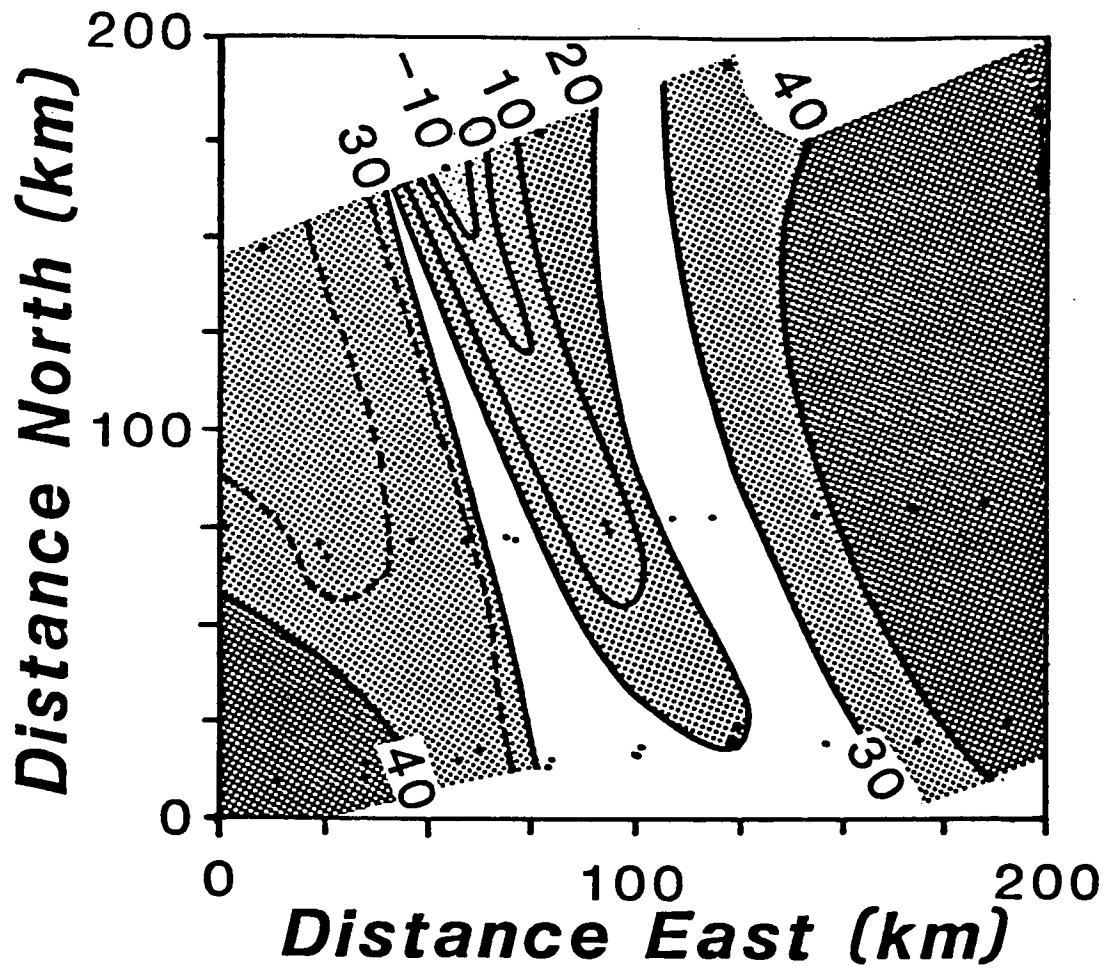
Figure 3-40. Salinity anomaly diagram on sigma-t = 25.25.

relative to 36.0°/oo. This is a convenient notation which will be used more extensively in Section 4.2. The resemblance of this distribution to the patterns of the SST contours (in Figures 3-4 and 3-5) is quite apparent. The relationship of the salinities to the propagation of the event is as follows. Upper layer salinities were greater than 36.0°/oo in Transects 1 and 2 which were downstream from the frontal event. However, lower salinities were observed at sections traversing the cold region of CEW. In Transect 5, during which the frontal eddy intruded, a 40 m thick surface layer with salinities less than 36.0°/oo was observed just east of the Loop Current front (Stations 57-59). A similar low salinity surface layer was observed in Transect 6. Another low salinity surface layer was observed in Transect 8 at the northern edge of the frontal eddy. The low salinity surface water appeared to be associated with the cold region of CEW between the LCW filament and LCW front. The largest volume was found in the northern section. Wennekens (1959) indicates that the shallow low salinity layer in the CEW is a result of land drainage discharge. One would expect the volume to be largest in the northern end of the study area; the data corroborate this.

Oxygen concentrations in the upper layers of the Loop Current are characteristically low (Wennekens, 1959). In the presented transects, the low oxygen concentrations were found in the first section coincident with high salinities and LCW as indicated by the oxygen-density plot (Figure 3-41). With time, oxygen concentrations decreased in the near-bottom layer which was about 20 to 30 m thick. Lowest oxygen concentrations (3.16 ml/l) were found in the lower layer in Transects 5, 6, and 8 (Figures 3-25, 3-30, and 3-37, respectively) which were nearest the upwelling associated with the intrusion of the cold core. Nitrate concentrations increased in the near-bottom layer
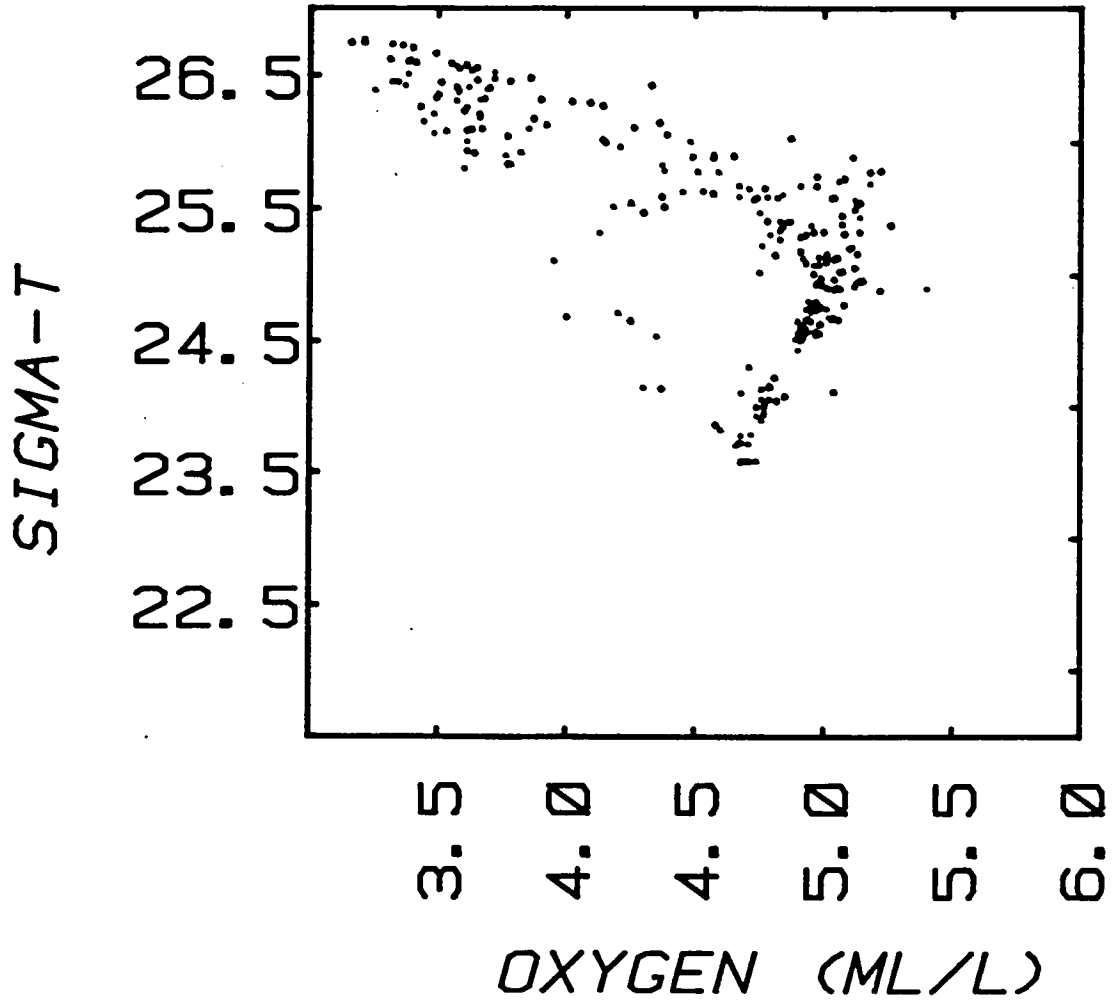
Figure 3-41. Oxygen-density plot for spring cruise data.

also and highest concentrations (16 µM) were found in the lower layer under the region of strongest upwelling (see Figures 3-26, 3-31, and 3-38). Silicate and phosphate concentration (see Appendix A.2) followed the same trends as nitrate with concentrations highest in the lower layer near the cold core. The nitrate-temperature relationship (Figure 3-42) also indicates that the higher nutrient concentrations were associated with the upwelling of colder deeper LCW. These results support the frontal analysis showing the offshore Loop Current movement and propagation of a frontal eddy and also indicate upslope movement of nutrient-rich, oxygen-poor deep LCW water beneath the upwelling core.

In summary, the water masses in the frontal eddy consisted of the LCW front and filament with a region of CEW between. Oxygen and nutrient values indicated that the doming occurring under the region of CEW was due to upwelling of deeper LCW (Nowlin and McLellan, 1967; Morrison and Nowlin, 1977; Morrison, 1977; Wennekens, 1959).

3.2.1.5 Chlorophyll Distributions

Chlorophyll a + Pheopigment a (Chl a + Ph a) sections for cross-shelf transects 1, 2, 5, 6 and 8 are depicted in Figures 3-43 through 3-47, respectively. The most apparent feature of all the transects is the very low (less than 0.25 mg·m^{-3}) surface mixed layer concentrations of Chl a and the presence of a subsurface Chl a maxima at depths of about 40 to 80 m. In all cases, the depth of the Chl a subsurface maxima coincided with the depth where nitrate concentrations first began to increase (i.e., the top of the nitracline). For example, Transect 6 (Stations 77 to 89 in Figure 3-46)

128
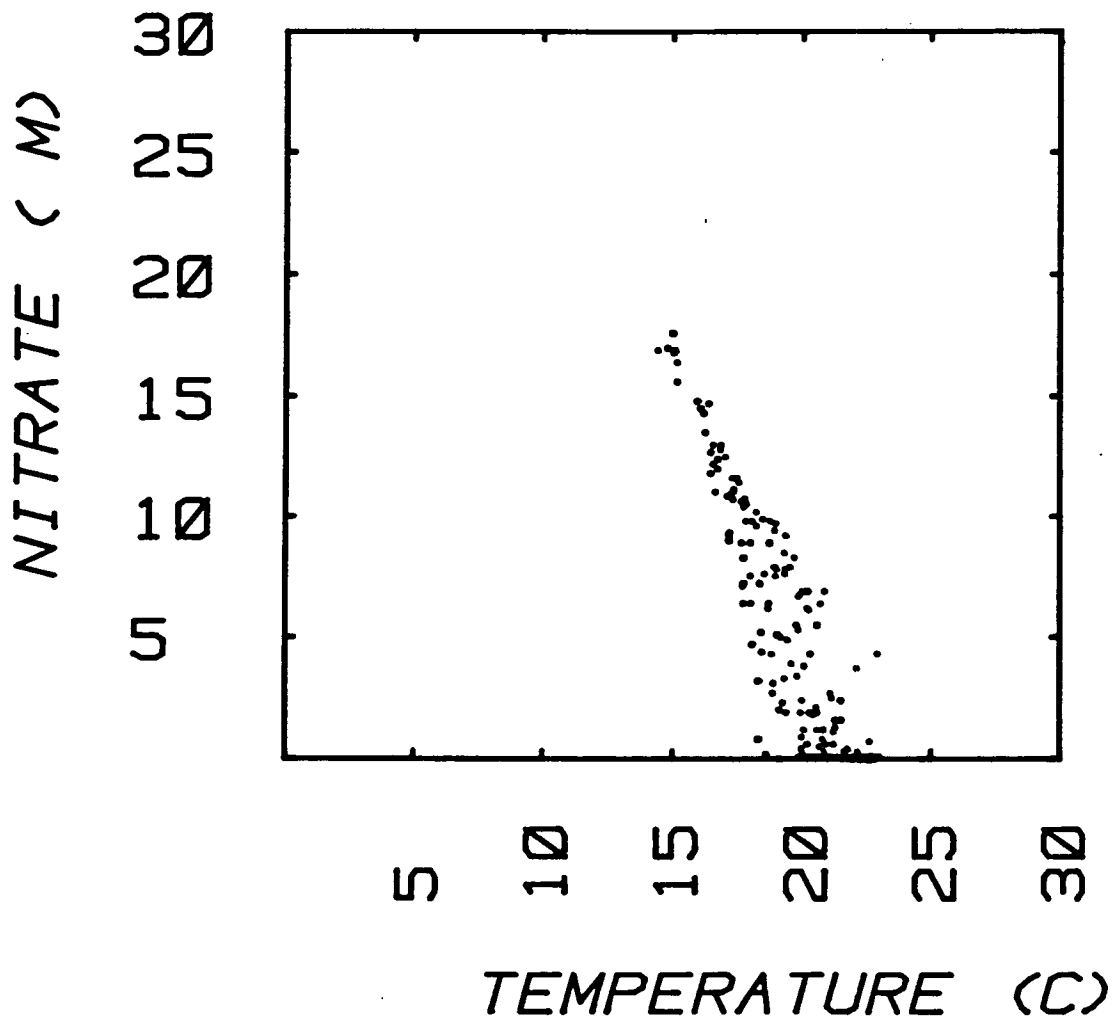
Figure 3-42.   Nitrate-temperature plot for spring cruise data.
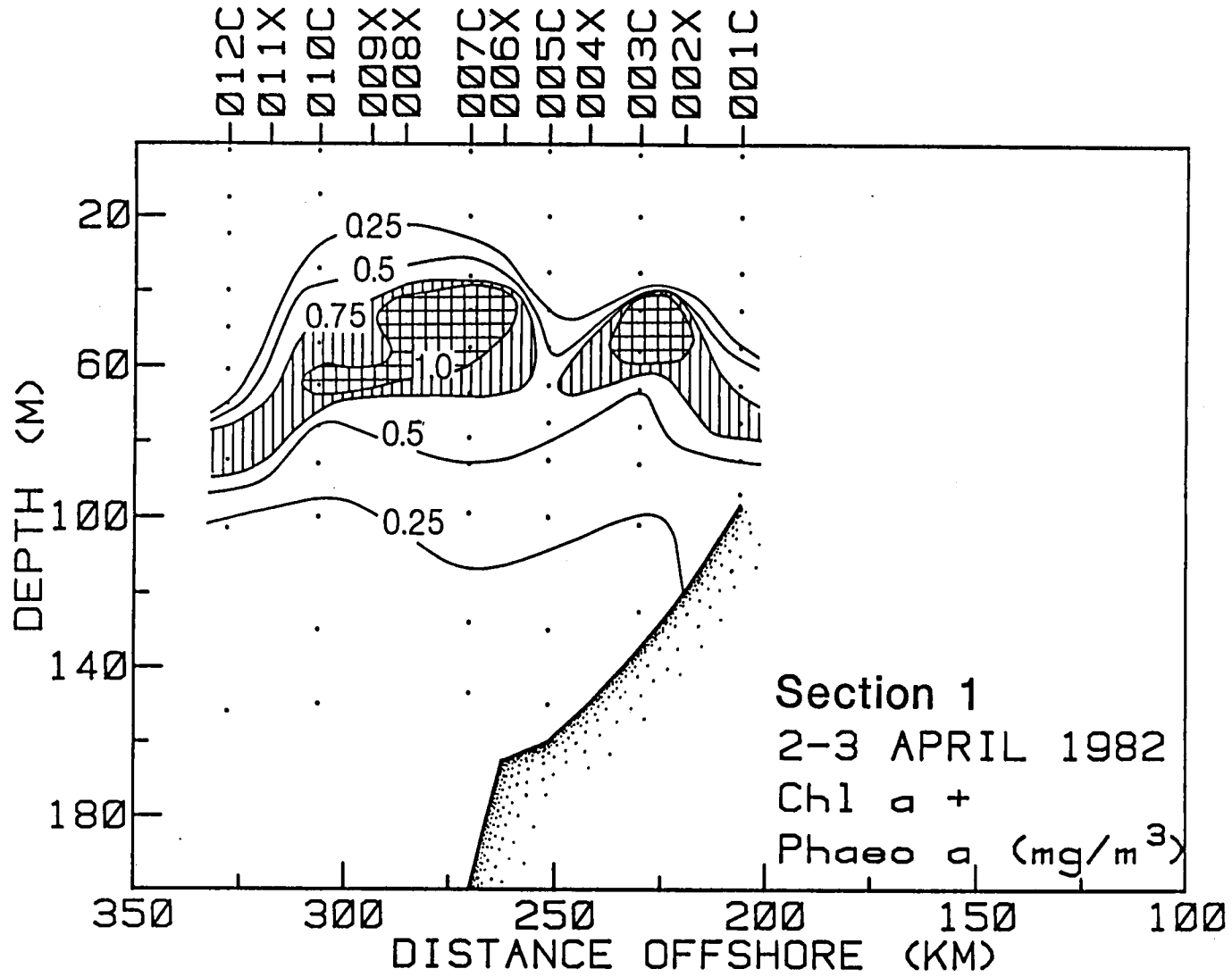
Figure 3-43. Spring cruise, transect 1 Chl _a_ + Ph _a_ section.
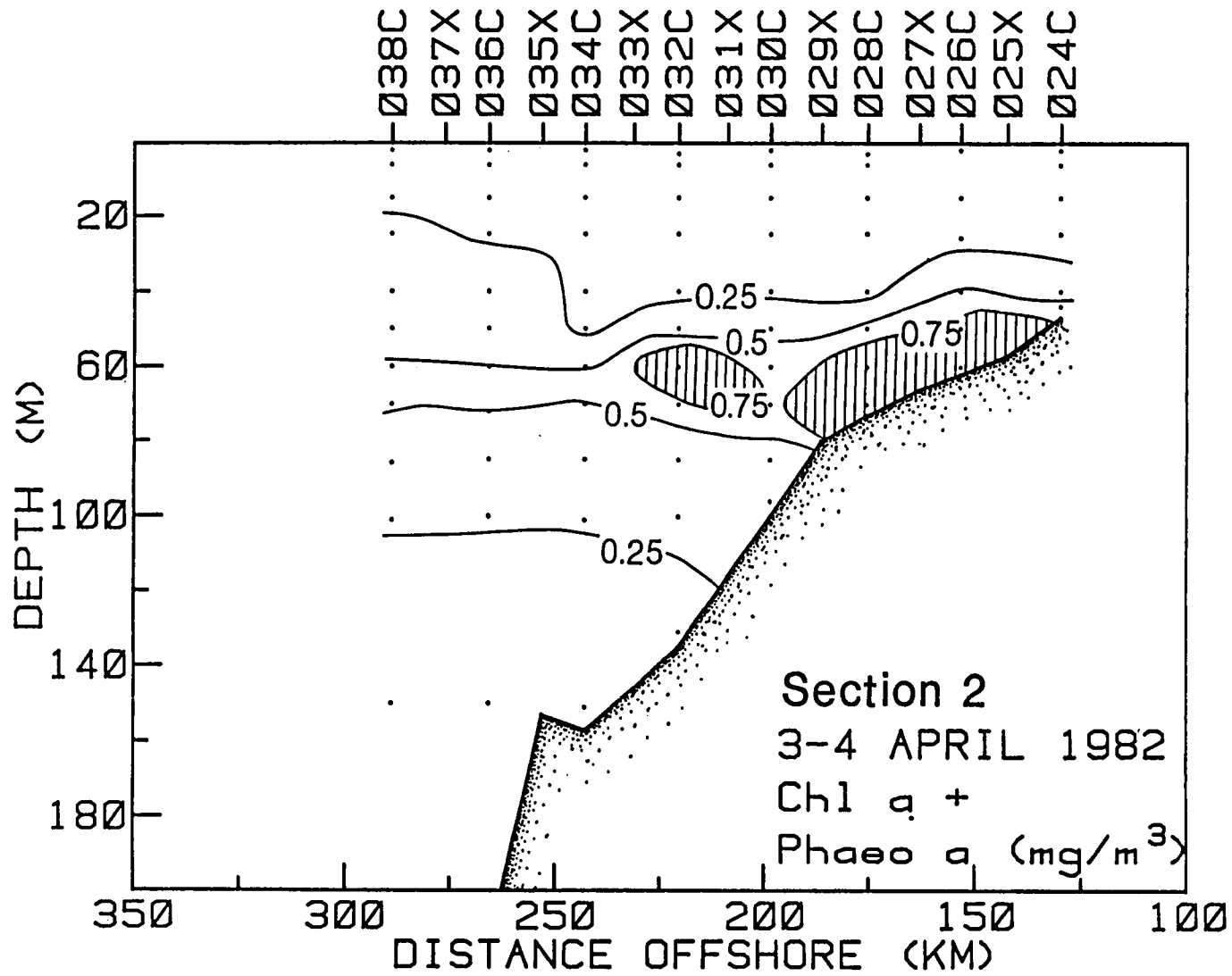
Figure 3-44. Spring cruise, transect 2 Chl a + Ph a section.
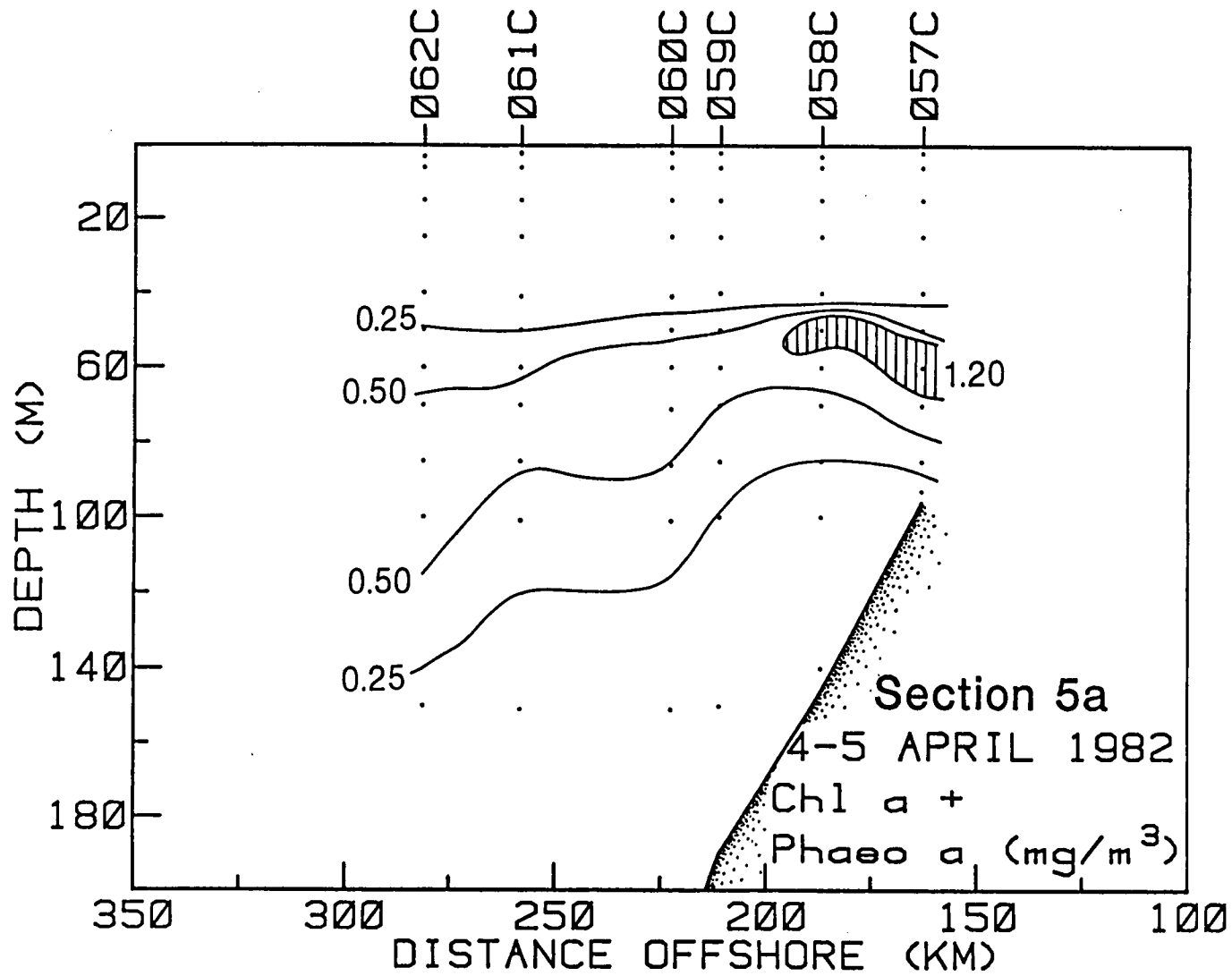
Figure 3-45. Spring cruise, transect 5a Chl _a_ + Ph _a_ section.
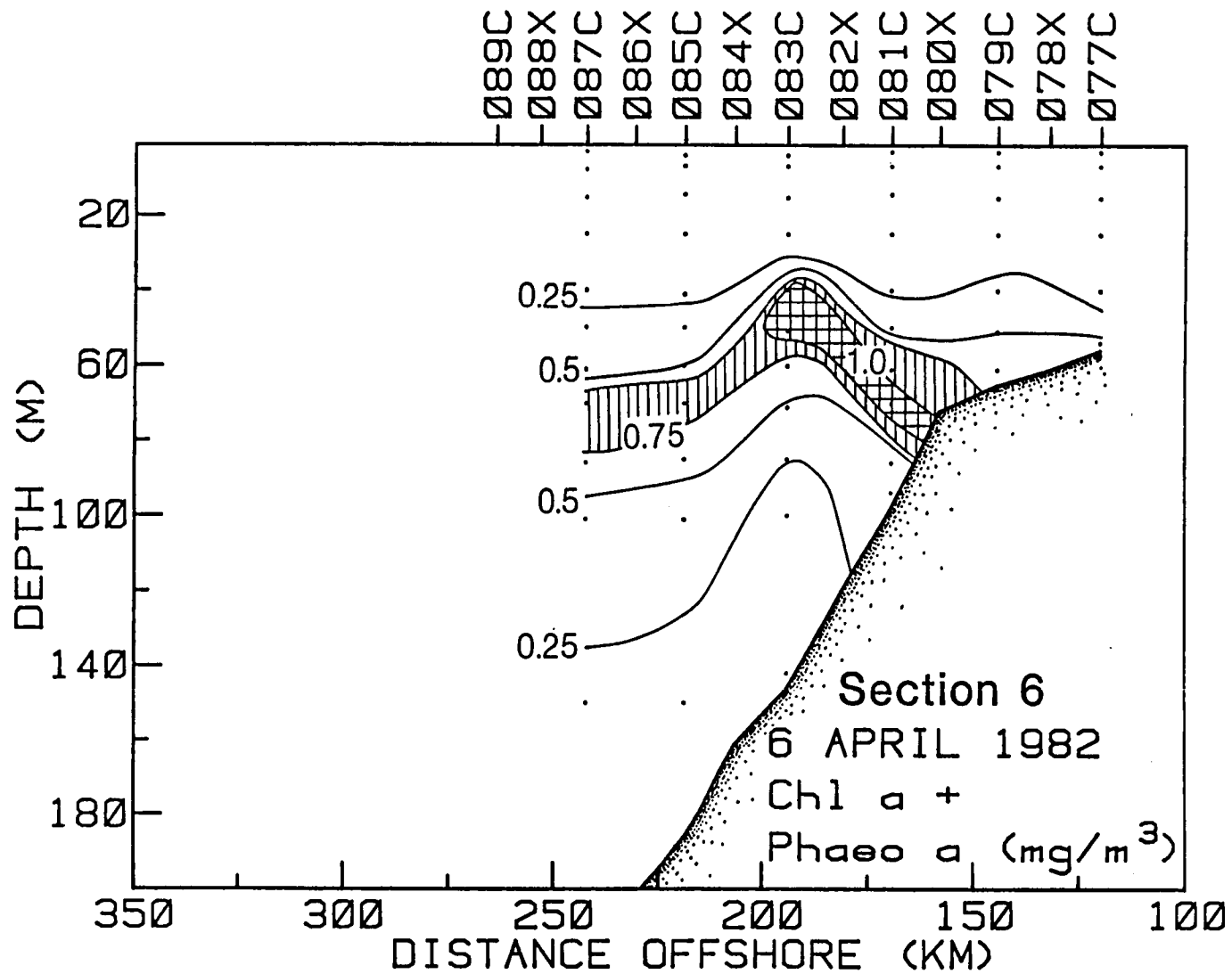
Figure 3-46. Spring cruise, transect 6 Chl _a_ + Ph _a_ section.

133
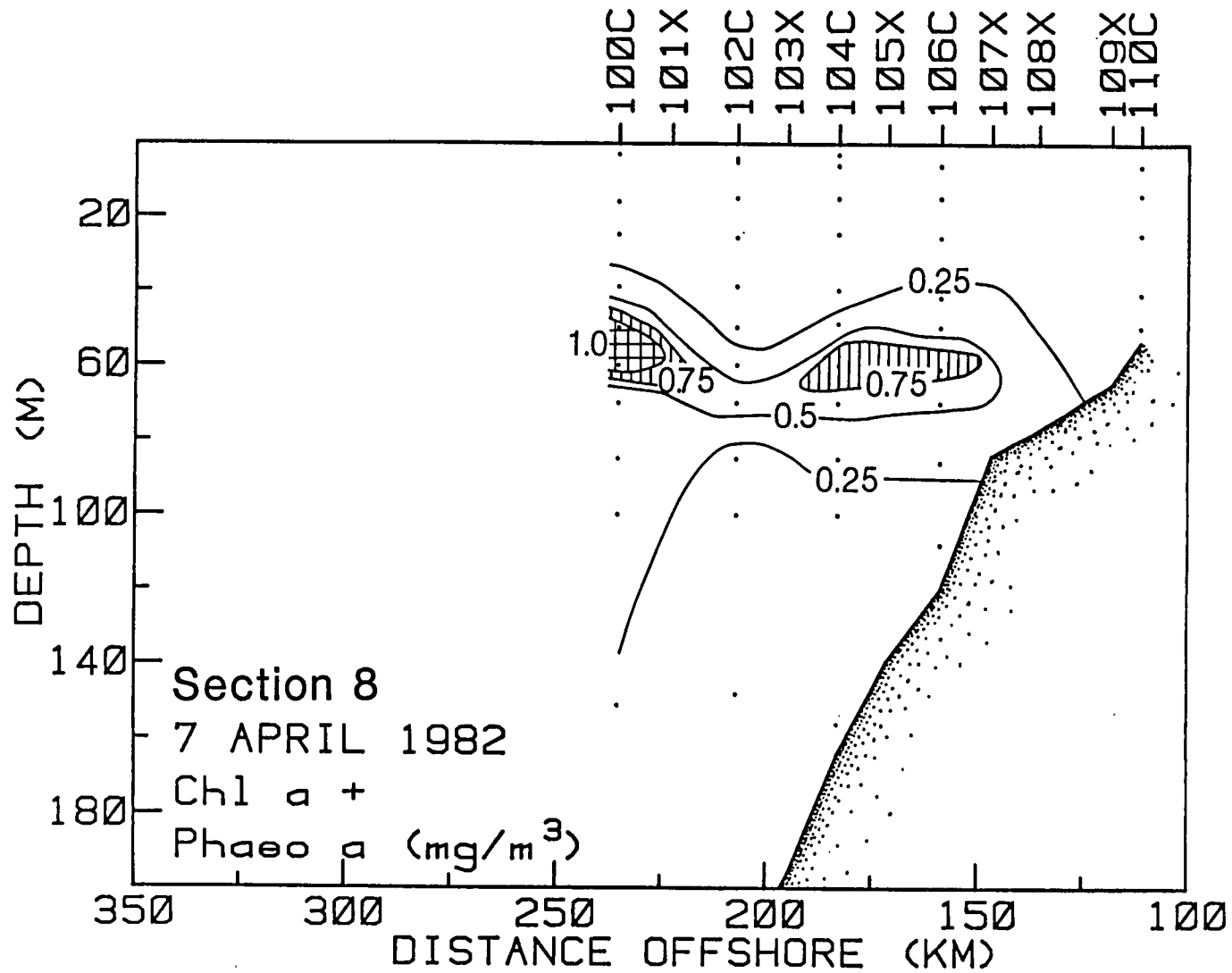
Figure 3-47. Spring cruise, transect 8 Chl <u>a</u> + Ph <u>a</u> section.

crossed the domed density and nutrient isopleths which formed the upwelled core of the eddy. Subsurface maxima of both Chl _a_ and Chl _a_ + Ph _a_ also formed a dome along this section with highest concentrations on the shoreward side of the dome. An analysis of all station data showed that the depth of the subsurface maxima, Chl _a_ was about 0.55 mg·m^{-3} and the population of phytoplankton consisted of a high proportion of physiologically-active cells.

A second important feature apparent in the chlorophyll sections is the speed at which conditions change. For example, Transect 1 (Stations 1 through 12 in Figure 3-43) and Transect 2 (Stations 24 through 38 in Figure 3-44) crossed the same location on the outer shelf approximately 24 hours apart. However, the major subsurface feature present on the outer shelf during Transect 1 (i.e., between Stations 5 and 12) was not found during Transect 2 (i.e., between Stations 32 and 38).

3.2.1.6 Comparison With Previous Studies of Loop Current Meanders

Leipper (1970), Maul (1977), Vukovich et al. (1979) and Molinari et al. (1976) have studied the annual and seasonal variance of the northern extent of the Loop Current and the meanders or filaments which form on the eastern boundary of the current. Vukovich et al. (1977) describe the frequency of appearance, size, and approximate speed of these filaments. Huh et al. (1981) studied the intrusion and interaction of LCW in DeSoto Canyon in the northern Gulf of Mexico. The propagation speed (30 cm·sec^{-1} or 26 km·day^{-1}) calculated from the west Florida shelf imagery is slightly less than the speed (28 km·day^{-1}) that Vukovich et al. (1979) computed and slightly greater than the speed (20 cm·sec^{-1}) that Huh et al. (1981) computed for the

progression of Loop Current filaments. All these propagation speeds are of the same magnitude. It is not clear whether a phase speed is appropriate in this case. Although the Loop Current front has a small wave-like perturbation on April 3 and 4 and, overall, the front is wave-like, it is not nearly as pronounced as Gulf Stream perturbations. On a large scale, the frontal eddy appears to be part of a 200 km wavelength frontal perturbation, with an approximate phase speed of 28.5 $km \cdot day^{-1}$. This is similar to the speed computed from the satellite images (26 $km \cdot day^{-1}$).

The length of the filament (approximately 220 km) in this study compares favorably with the range of lengths (between 140 and 220 km with an average at 210 km) found by Vukovich et al. (1979). The southwest Florida shelf filament occurred during a time of relatively deep (northward) penetration by the Loop Current (27.5°N) as did the large filaments described by Vukovich et al. (1979). Overall, the Loop Current filament of this study is similar in general characteristics to those discussed by Vukovich et al. (1979).

Evidence that a similar intrusion occurred on the west Florida shelf is found in Price and Mooers (1974). Figure 3-48 is a reproduction of their data. The similarities between this figure and Figures 3-34 through 3-36 are the domed isotherms over the shelf and the warm trough further on the shelf. In the salinity section, there is evidence of higher salinities (>36.6°/oo) along the westward edge of what appears to be a cold core, indicating the proximity of the Loop Current, as does the intersection of the 22°C isotherm at 100 m. The trough-like depression over the shelf is in a similar configuration as that in Figure 3-34 which shows the cold core and the filament. This section was taken along 26°N, the same locale where the April intrusion occurred and is
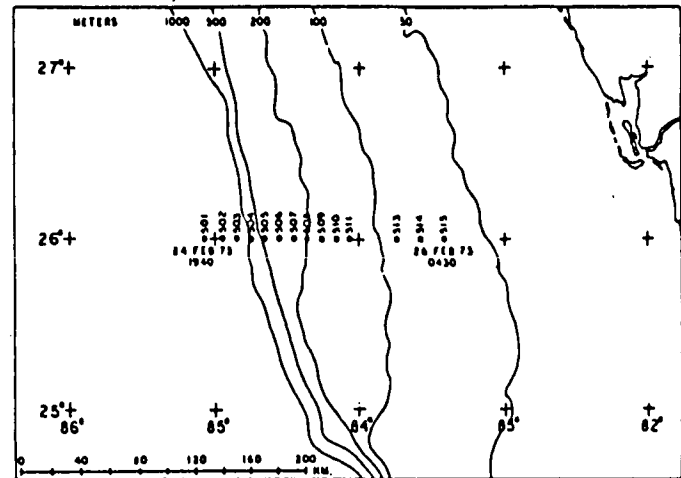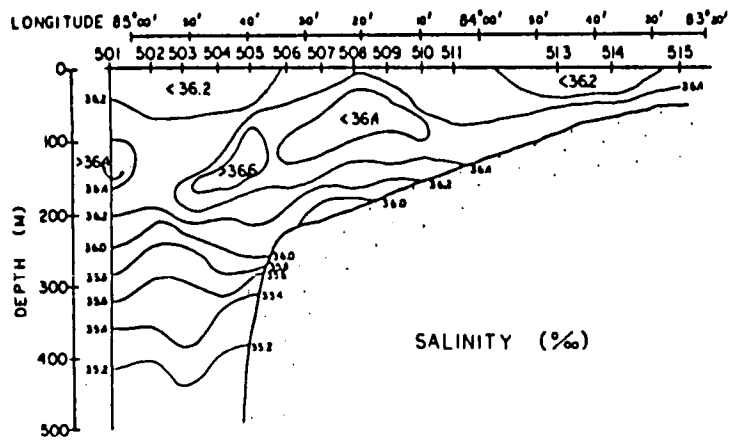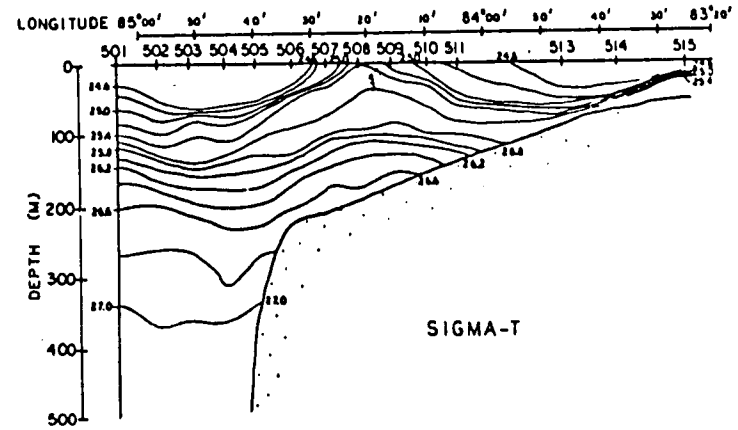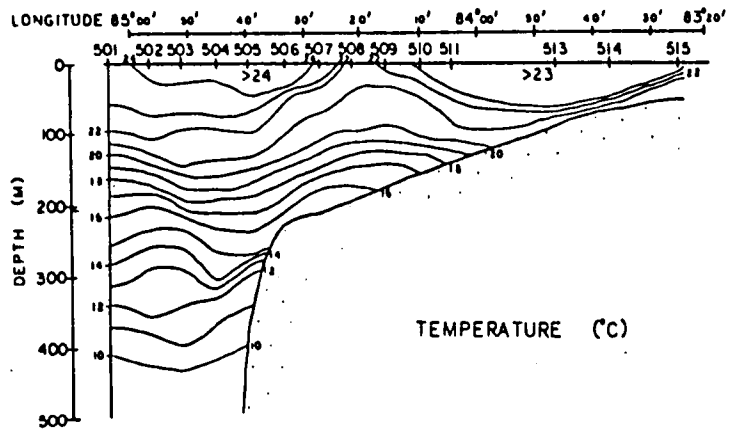
Figure 3-48. Temperature, sigma-t, salinity and station locations from Continental Shelf Dynamics program (from Price and Mooers, 1974).

evidence that intrusions of Loop Current eddies may occur occasionally (more than this one time), if not frequently. The frequency of these intrusions cannot be considered to be known at this time.

Huh et al. (1981) recorded the intrusion of modified Loop Current water onto the shelf near Pensacola, Florida. While this intrusion may have the same consequence, the appearance and dynamics of the intrusion appear to differ. The intrusion described by Huh et al. (1981) occurred when a warm plume of modified LCW followed the trend of DeSoto Canyon and affected the shelf waters to within 8 km of the beach. A major difference is that the intruded waters near Pensacola are highly modified—with a salinity of 35.9°/oo, whereas the intruded waters in the April 1982 intrusion occurred when a LCW filament impinged on the shelf and these waters were less modified. The dynamics implied from the hydrographic data, i.e., upwelling under the cold region, are not implied in the plume and the consequent effects may be missing. The Pensacola intrusion did affect much shallower shelf waters and resulted in a modification of the ambient shelf waters. The April 1982 intrusion also caused a modification of outer shelf waters but did not reach as close to shore.

3.2.1.7 Comparison of West Florida Shelf Frontal Eddies to Gulf Stream Frontal Eddies

The intrusion of the Loop Current frontal eddy onto the southwest Florida shelf is evidence of a boundary current interaction with the shelf. Similarly, the intrusion of Gulf Stream frontal eddies are examples of the interaction of the Gulf Stream (also a boundary current) with a shelf (Lee et

al., 1981, and Lee and Atkinson, 1982). In general, the major features of both frontal eddies are basically the same; they both consist of a counter-flowing warm filament or streamer of the main current which extends 15 to 20 m deep and have filaments which are separated from the main current by a region of cooler water. In both cases, upwelling occurs under this cold region.

Further, the filaments are of the same length scale; 100 to 200 km for Gulf Stream filaments; 200 km for the Loop Current Water filament. Gulf Stream frontal eddies move faster (approximately 40 cm·sec^{-1}) then the Loop Current frontal eddy (30 cm·sec^{-1}). This difference in propagation speed could indicate different consequences when the frontal eddies finally intrude onto the shelves. During the intrusion of the Gulf Stream frontal eddy described by Lee et al. (1981), there were large drops in temperature accompanying the intrusion. These "before and after" effects in the Loop Current frontal eddy intrusion were not observed in this data set but the presence of finestructure suggests that changes in the water column properties may evolve more slowly. There was no evidence for the finestructure presented by Lee et al. (1981) for the case of the Gulf Stream frontal eddy intrusion.

Lee et al. (1981) and Lee and Atkinson (1982) indicate that the Gulf Stream frontal eddies form from amplified waves of the Gulf Stream front. It is not clear whether the Loop Current frontal eddy is formed in a similar manner. The data of Maul (1979) and Vukovich et al. (1979) suggest wave-like perturbations of the Loop Current as does the time series presented in Figure 3-4. On a small scale, wave-like perturbations are apparent along the front and along the edge of the filament; however, without further evidence it can

only be suggested that the Loop Current frontal eddies develop from a wave-like perturbation of the Loop Current front.

The density profiles from the southwest Florida shelf filament indicate that at some point in time it was contiguous with the main body of LCW which was 80 m deeper at that time. Leipper (1977) has attributed differences in depth (150 to 300 m) of a representative point on the TS curve between righthand and lefthand water to the uplifting of lefthand water as it passes across the shallower Yucatan bank when entering the Gulf. Processes similar to this may account for the observed 80 m depth difference between TS points in the main body of LCW and the filament of LCW. There are indications (e.g., Vukovich et al., 1979; Maul, 1977; GOES imagery examined prior to this cruise) of these filaments along the Yucatan bank and all along the western and northern boundaries of the Loop Current. The uplifting may occur at any time along the boundary between the shelf edge and the Loop Current, or as the frontal eddy intrudes onto the southwest Florida shelf. This relationship between filament TS characteristics and deeper main current waters has still not been established for Gulf Stream eddies.

Similar to Gulf Stream frontal eddies, upwelling under the cold region transported deep waters with high nutrient concentrations onto the shelf. In the Gulf Stream case, the upwelling brought nitrate concentrations of 10 µM to the 30 m depth (Lee et al., 1981). Nitrate concentrations of 10 µM were found between 80 and 100 m in the southwest Florida case. Generally, the concentrations of nutrients in the upper 50 m were not as high during the intrusion of the southwest Florida shelf frontal eddy. It appears that southwest Florida shelf upwelling is less intense than similar processes off

Florida's east coast. Two possible explanations are offered; both involve the relative bottom topographies; (1) if the 200 m isobath is used as the shelf break and a Loop Current frontal eddy is to affect waters less than 100 m deep, it must move at least 50 km horizontally across the southwest Florida shelf. On the other hand, Gulf Stream frontal eddies need only move 15 to 25 km to reach the 70 m isobath from the mean Gulf Stream position given by Bane and Brooks (1979). Thus, the additional shelf area that the Loop Current frontal eddy crosses means that there is more friction and turbulent mixing which could play a role in altering the energy of this process and thus eroding the pressure gradient that maintains the upwelling; (2) Hill and Johnson (1974) show that the upwelling velocity at the shelf break is directly proportional to the average east-west slope from the abyssal plain up to the shelf. The overall slopes in the area off Amelia Island where the Gulf Stream studies were conducted are significantly steeper than those in the southwest Florida study area.

The impact of the Gulf Stream frontal eddies on productivity off the Georgia and northeast Florida shelf were assessed by Lee et al. (1981) and Yoder et al. (1981). The former estimated that the eddy-induced nitrate flux could be 55,000 tons N per year which would result in a carbon production of 32 to 64 $gC \cdot m^{-2} yr^{-1}$. The latter showed that the upwelling associated with eddies resulted in patches of high near-surface production and plant biomass. While the results of the upwelling on production of the southwest Florida shelf are not yet fully understood, these initial observations do indicate chlorophyll maxima within the domed areas of upwelling along the 1 μM nitrocline. Chlorophyll $\underline{a}$ maxima were also coincident with finestructure in areas of LCW/CEW interaction.

In an overall sense, the gross features and circulation patterns in both Gulf Stream and Loop Current eddy events appear to be quite similar. The differences which will ultimately affect their contribution to an area's produtivity lies in their mode of formation, frequency of intrusion, distance over-shelf traveled to shallow water, and the intensity of upwelling. The Loop Current frontal eddy must propagate over a greater distance of shelf, hence undergo more frictional influence and more energy dissipation. This may affect the depth to which high nutrient concentrations are elevated. With less energy and a greater distance to travel, the high nutrient concentrations do not reach as extensively into the euphotic zone as in the Gulf Stream case.

3.2.1.8 Conclusions

Hydrographic and enhanced infrared satellite data showed an intrusion of a Loop Current frontal eddy onto the southwest Florida shelf between April 1 and 7, 1982. TS characteristics showed that the filament was of LCW and that it had at some time earlier been uplifted 80 m from deeper main LCW. A region of cool surface water between the filament of LCW and the main body of LCW was identified as CEW by its cooler, fresher TS characteristics. Sections through this region prior to and during the intrusion showed the upwelling occurred beneath this region. Nutrient and oxygen concentrations indicated that the upwelled water was deeper LCW water.

In terms of length scale and speed, the Loop Current frontal eddy was similar to the Gulf Stream frontal eddies described by Lee et al. (1981). Upwelling on the southwest Florida shelf was less intense than upwelling associated with Gulf Stream frontal eddies and may decrease the impact of the intrusion on

productivity. This may be due to a less energetic current or less   energy due to topographic effects.

Further studies are needed to address how these frontal eddies are formed, the frequency with which they intrude upon the shelf and the overall impact on the productivity of shelf waters. It would also be enlightening to develop evidence of these events along other current/shelf boundaries and then identify the common process by which they are related and their impact on shelf nutrient supply in general.

3.2.2   Summer Cruise Data

3.2.2.1   Introduction

Descriptions of the currents on the outer shelf by Niiler (1976) and an examination of the data from Price and Mooers (1974) indicate that the position of the Loop Current along the west Florida shelf is variable and consequently results in low frequency variability of currents and hydrographic properties in the outer shelf region. In order to evaluate the effects of this seasonal variability on the ecology of the region, an understanding of changes in the hydrographic regime over time with respect to Loop Current position was sought.

Hydrographic data from a time series of sections occupied near 25°30'N during September 13 through 18, 1982 showed a toward-shelf movement of the Loop Current. An increase in the subsurface salinity maximum, an increase in bottom temperatures, and a doming of isopycnals were observed in association

with this toward-shelf movement. An upslope movement of the oxygen minimum and higher nutrient concentrations were also observed. A layer of low surface salinities was seen throughout the sampling and was believed to originate in the northern Gulf as a result of land drainage. A decrease in volume of the low salinity layer could have been related to the toward-shelf movement of the current as well as variations in the alongshelf currents.

3.2.2.2 Observational Methods

Owing to the lack of sufficient surface thermal contrast in the summer, infrared imagery was not useful in planning the cruise sampling strategy. Instead, an alongshelf XBT transect following the 70 m isobath was occupied to determine any areas of anomalously warm or cold bottom temperatures. Based on this information, a section line was selected near 25°30'N (Figure 3-49) perpendicular to the shelf. Similar to the April cruise, hydrographic sections consisting of alternating CTD and XBT stations were run every 10 km (5 to 6 nmi) across the shelf along each selected transect. Position (using LORAN-C) data for the 95 sampled stations are listed in Appendix A.1. Table 3-2 lists the division of these stations into transect sections. Each section was extended offshelf until the signature of the Loop Current was encountered. This signature helped establish the position of the edge of the Current with respect to conditions on the shelf. As a means of providing a time lapse between consecutive sections, a small transect alongshelf to the north was occupied. This information was helpful in verifying the position of the Loop Current. The ship then returned to the location of the time series transect and continued sampling. The time series was interrupted between 1900 hrs, September 15 to 0400 hrs, September 17 (WCC/SIO, 1982b).

144
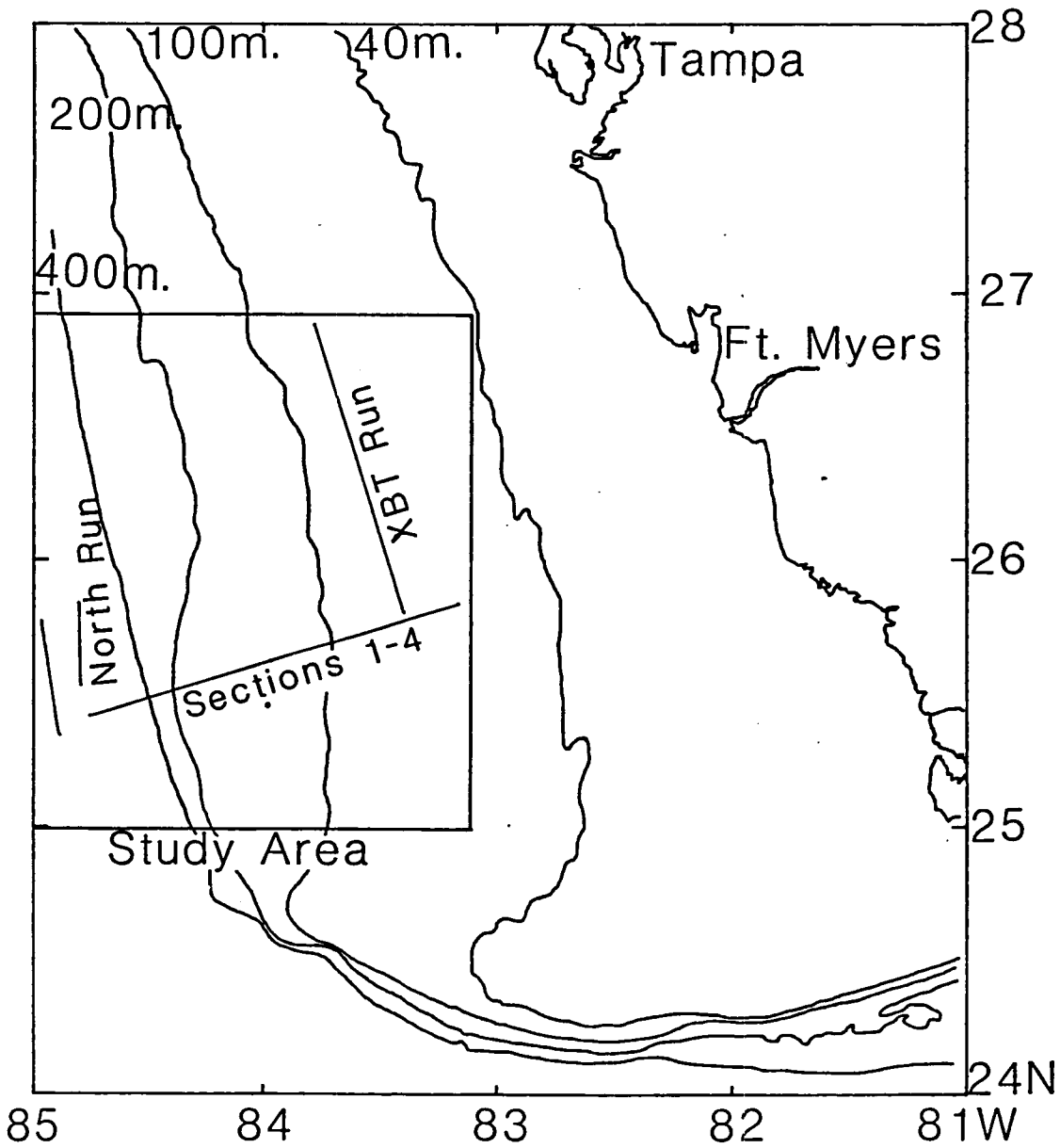
Figure 3-49. Summer cruise transect locations.

Table 3-2. Assignment of stations to transects during summer cruise.

(X = XBT, C = CTD, B = bottle cast)

Section	Date (1982)	Stations	Types
Test	13 Sept.	1X to 9X	X
1	13-14 Sept.	10B to 27C	XCB
North Run	14 Sept.	27C to 30C	XC
Deep Run	14 Sept.	30C to 33C	C
South Run	14 Sept.	33C to 36C	C
2	14-15 Sept.	36C to 56C	XCB
3	17 Sept.	57C to 75C	XC
4	18 Sept.	77C to 95C	XC

As a means of ensuring continuity with the April data, the same data collection techniques were used for this cruise. That is, salinities and temperatures were determined at CTDstations with the same Plessey Model 9400 CTD interfaced to a Hewlett Packard 9825 desktop computer, and water samples, including nutrients, oxygen, bottom salinities and temperatures were taken at discrete depths with Niskin bottles mounted on a rosette sampler coupled to the CTD. Sample depths were chosen during the downcast to enable sampling of special features and to select the best locations for calibration data. Bottom and surface salinities and temperatures were used to calibrate the CTD data and to establish any depth effect on CTD and bottle salinities. There were no such effects in this data set. Meaurements of surface temperature and chlorophyll fluorescence were taken every 10 km (5 nmi). Nitrate, phosphate and silicate concentrations were again determined with a Technicon Auto Analyzer II according to the methods of Glibert and Loder (1977). Likewise, dissolved oxygen concentrations were again determined by the Strickland and Parsons (1965) method.

3.2.2.3 Temporal Variability of Hydrographic Parameters

The hydrographic transects extended from the 60 m isobath past the shelf break at the 200 m isobath to the wall of the Loop Current. The time series of transects showed that the Loop Current wall (as defined by the intersection of the 22°C isotherm at 100 m and subsurface salinity maximum) moved shoreward a total distance of 28 km over a period of four days. Most of this movement (25 km) occurred between consecutive Transects 2 and 3.

For brevity's sake, the time series cross-sections are presented as a four-parameter set for each section. That is, Figures 3-50 through 3-53 present the temperature, salinity, sigma-t, and oxygen cross-sections for Transect 1, respectively; Figures 3-54 through 3-57 present the corresponding data in the same order for Transect 2; Figures 3-58 through 3-61 for Transect 3; and Figures 3-62 through 3-65 for Transect 4.

In the Transect 1 temperature distribution (Figure 3-50), there is a well defined thermocline with a homogeneous upper layer of approximately 20 m in thickness with no pronounced surface gradients. In the following temperature sections for Transects 2 (Figure 3-54), 3 (Figure 3-58), and 4 (Figure 3-62), the thermocline has dissipated over the upper slope and was found only from the 60 m to over the 100 m isobaths in the final cross-section (Figure 3-62). It appears that this "breakdown" of the thermocline intensity was related to the toward-shelf movement of the Loop Current. The lowest temperatures (<14°C) were found as shallow as 180 m between Stations 23 and 27 of Section 1 (Figure 3-50). These low temperatures were found at the time when the Loop Current was most distant from the shelf break. Through the remainder of the time series, a bottom layer of 15°C was found at 130 m or deeper. The volume of the 15°C bottom layer decreased with toward-shelf movement of the Loop Current, and the 16°C isotherm was found at progressively deeper depths in the time series. The indications are that the toward-shelf movement of the Loop Current forced warmer water onto the bottom layer. Coldest temperatures were found when the current was farthest from the shelf break. Similar results have been found by Lee et al. (1981) and Webster (1961) in their studies of the Gulf Stream.
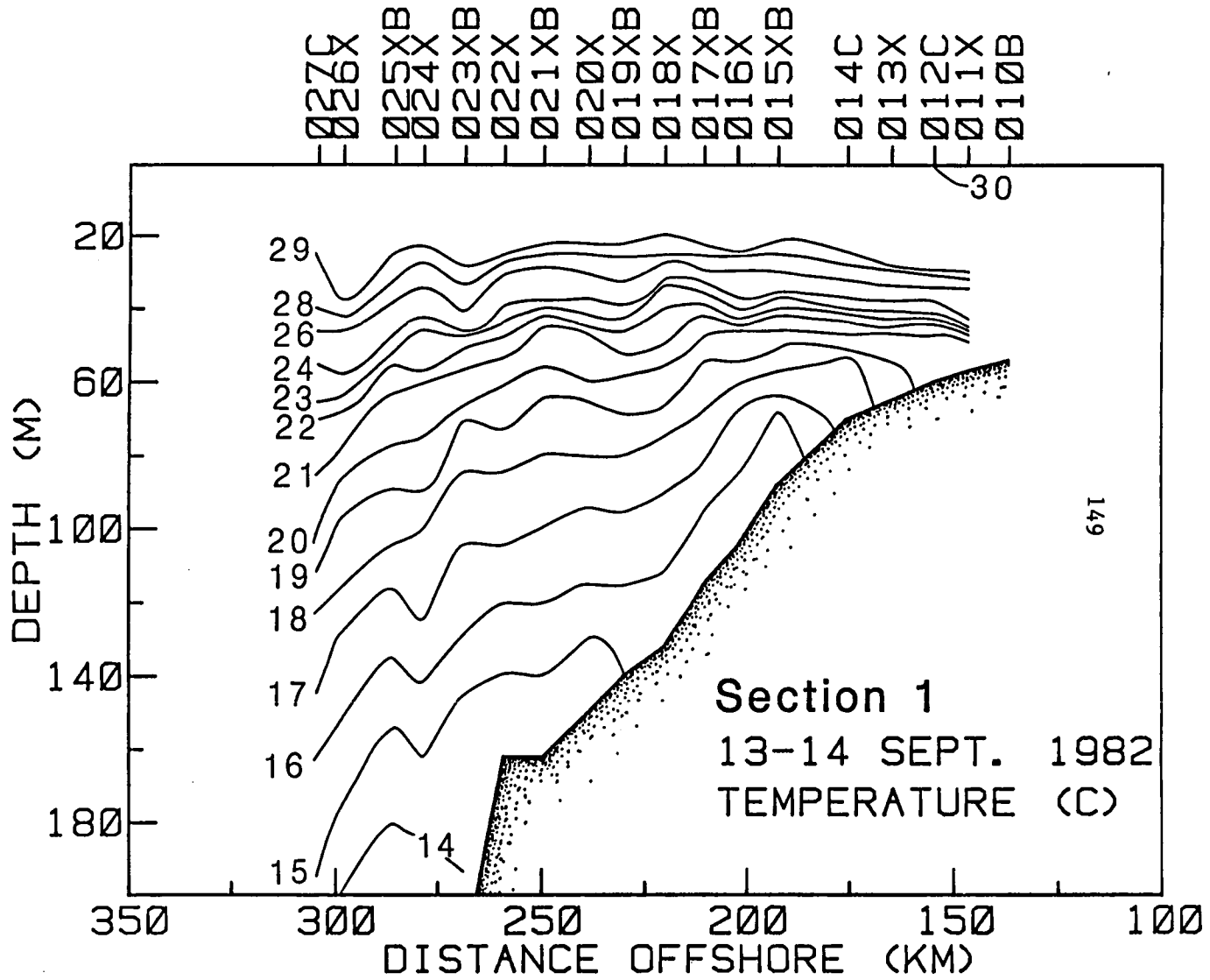
Figure 3-50. Summer cruise, transect 1 temperature section.
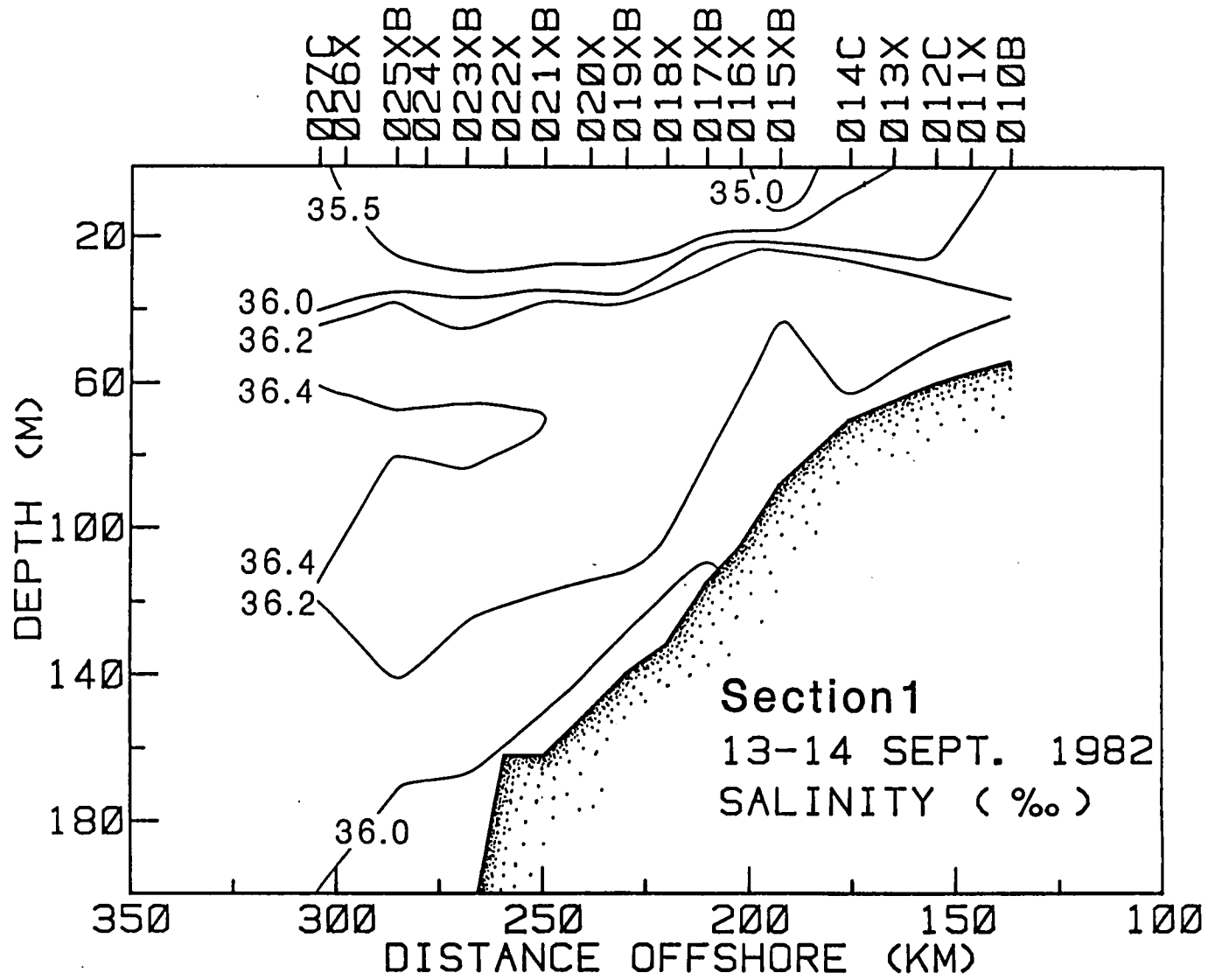
Figure 3-51. Summer cruise, transect 1 salinity section.
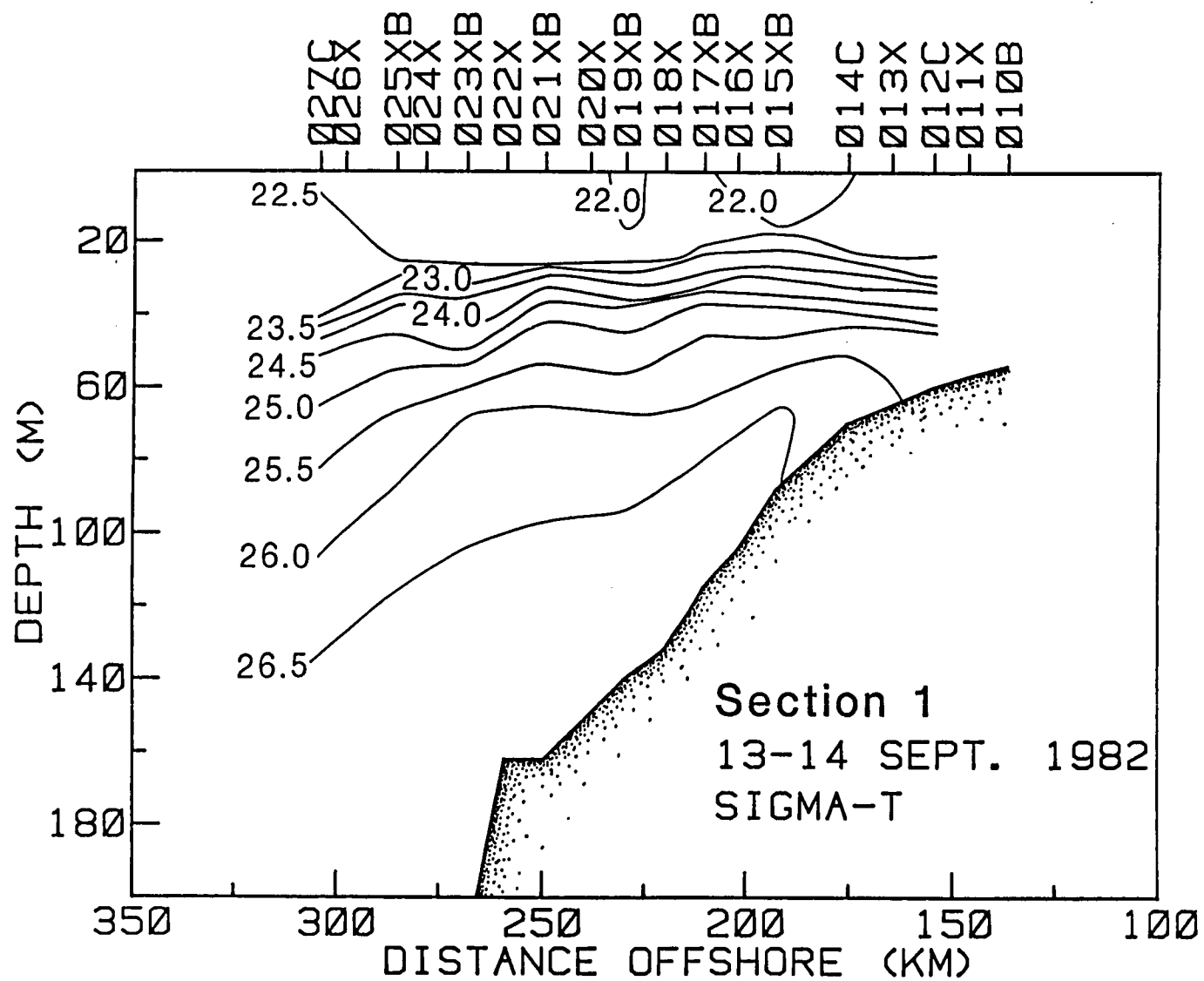
Figure 3-52. Summer cruise, transect 1 sigma-t section.

151
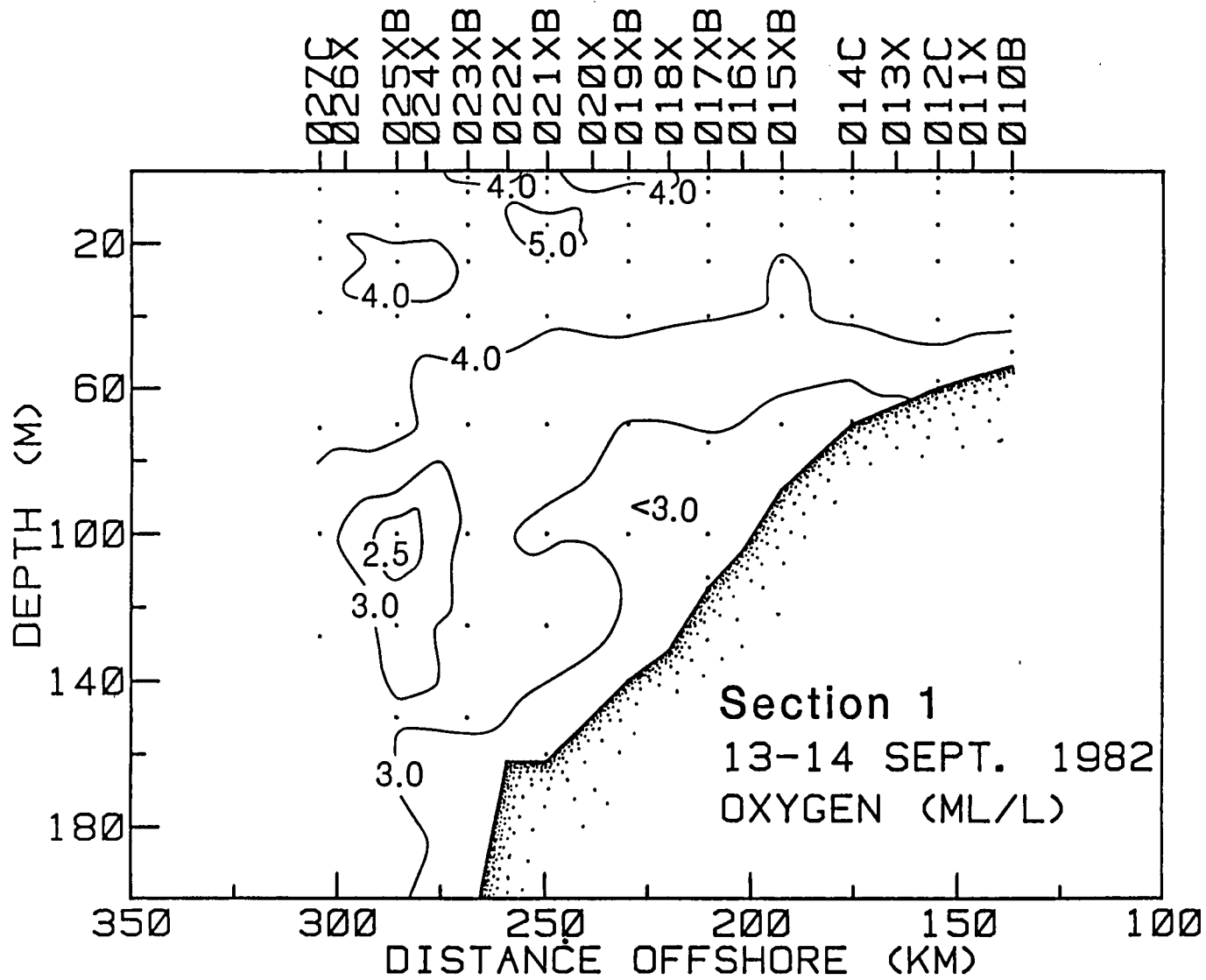
Figure 3-53. Summer cruise, transect 1 oxygen section.
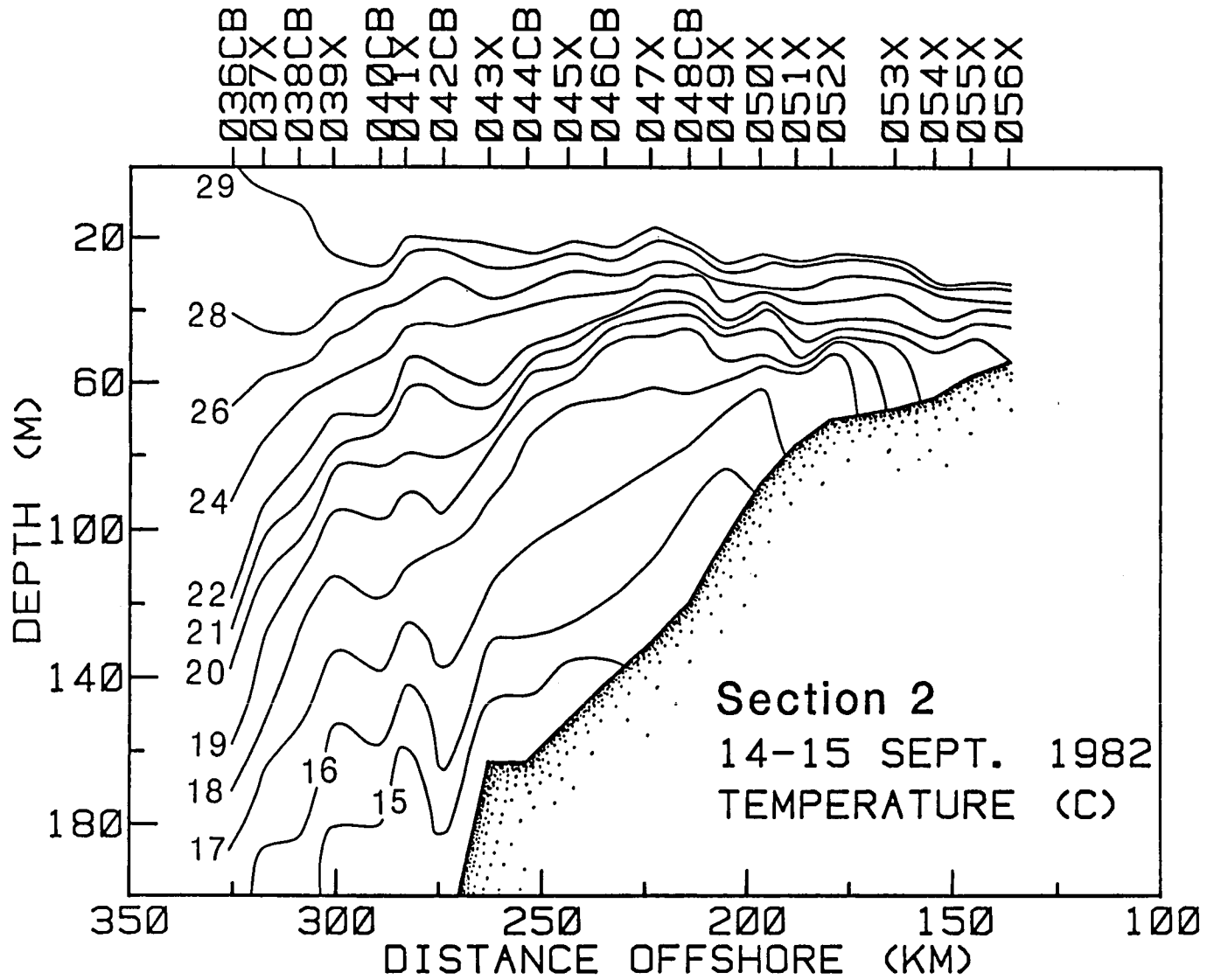
Figure 3-54. Summer cruise, transect 2 temperature section.

153
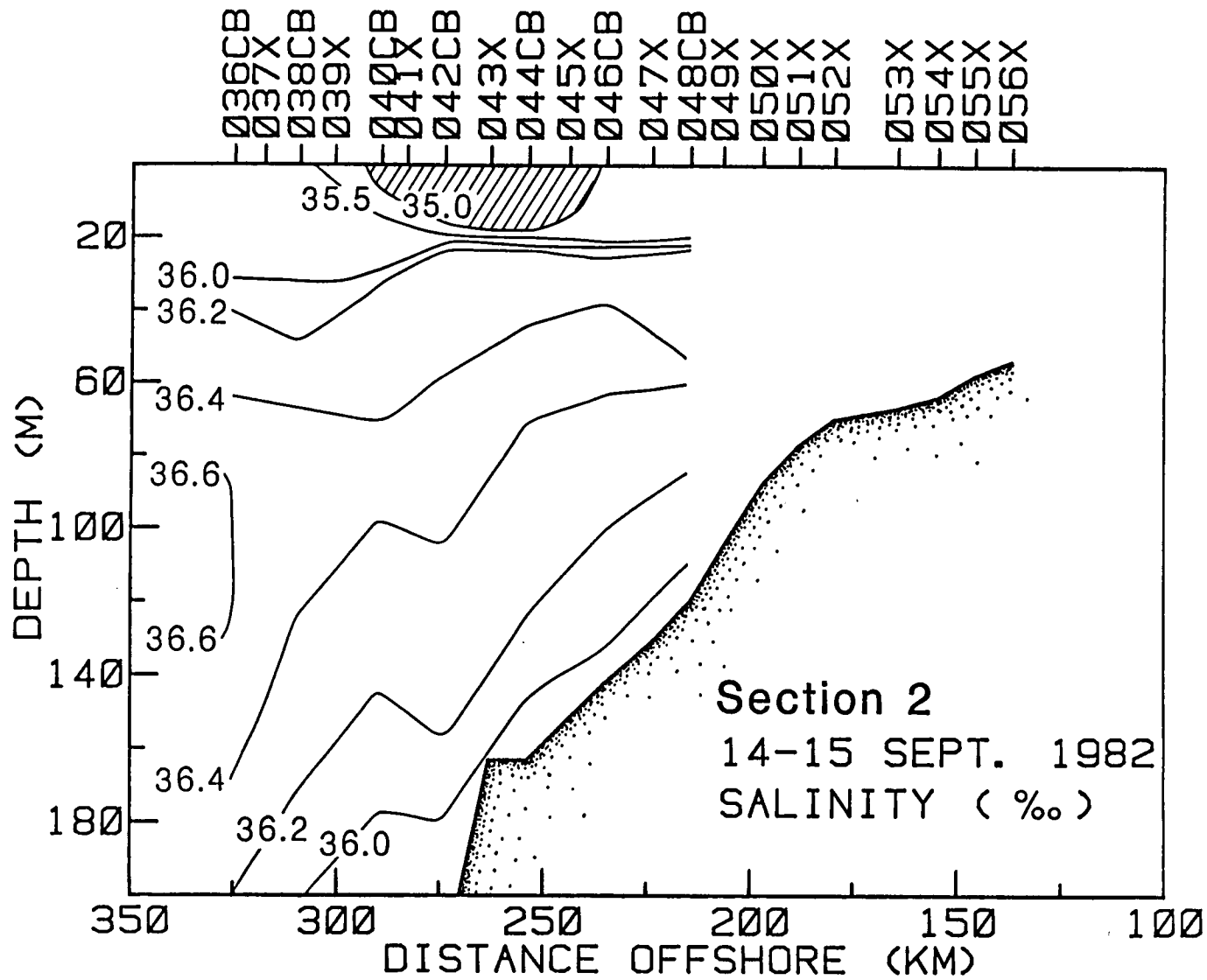
Figure 3-55. Summer cruise, transect 2 salinity section.
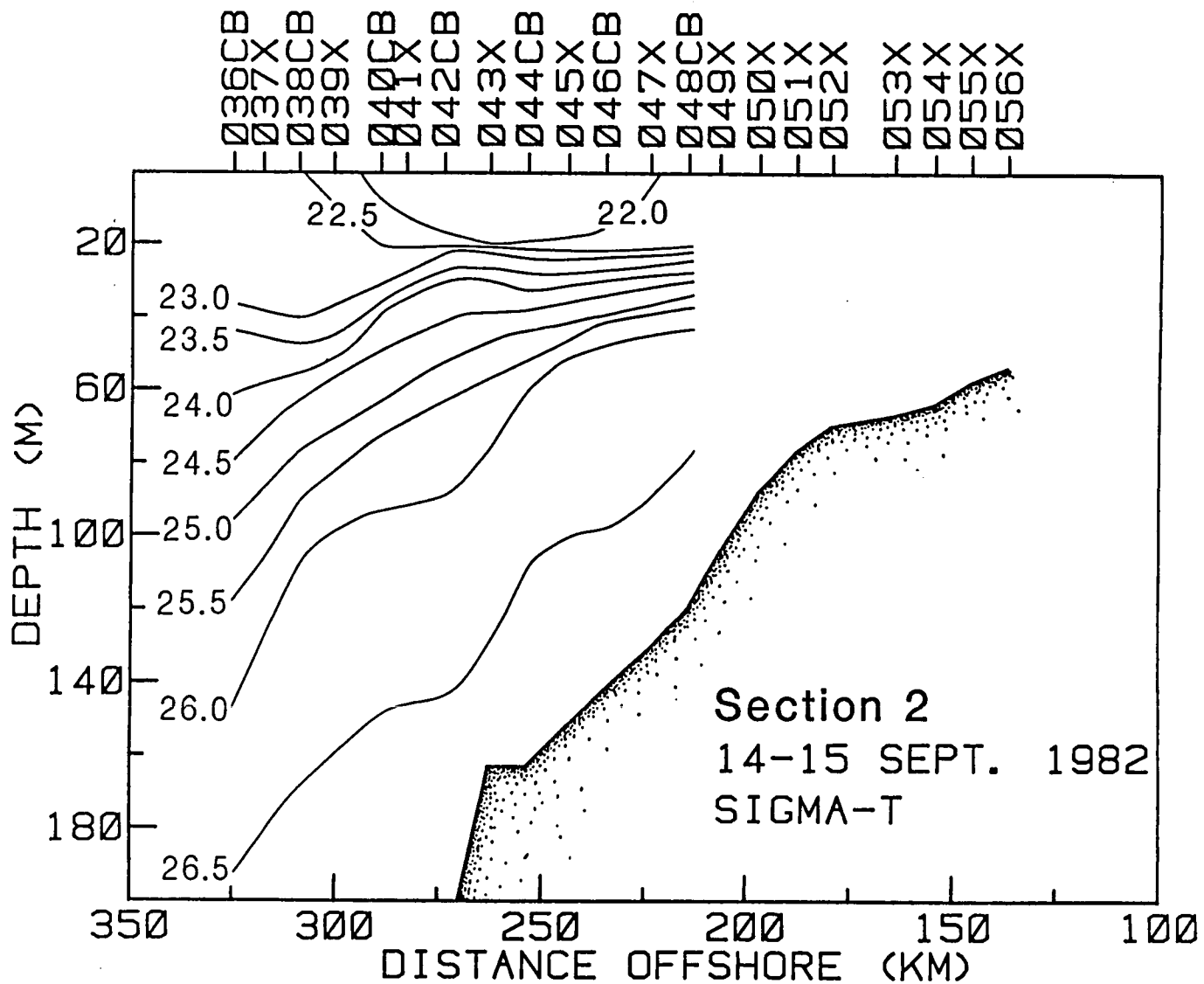
Figure 3-56.   Summer cruise, transect 2 sigma-t section.

155
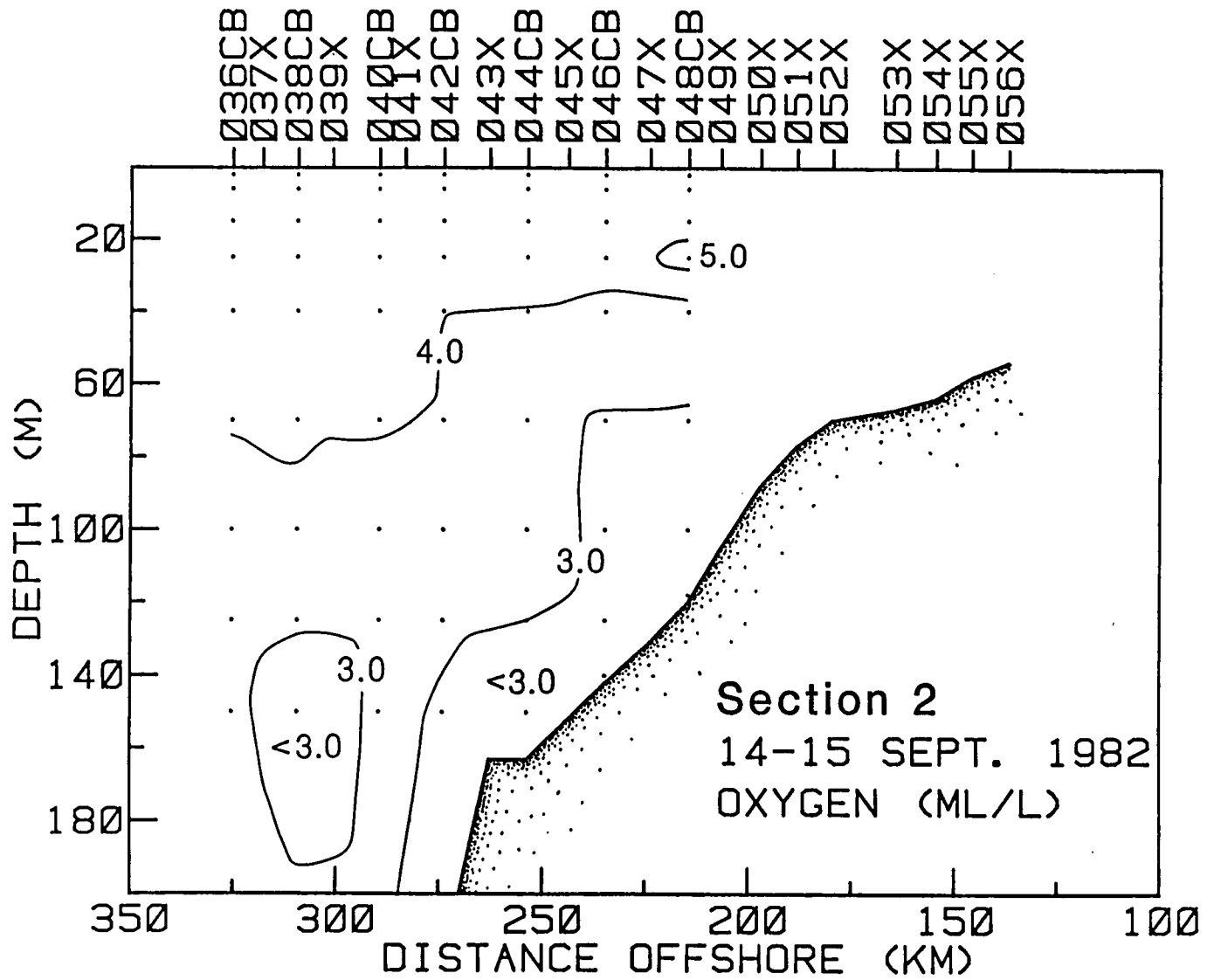
Figure 3-57. Summer cruise, transect 2 oxygen section.
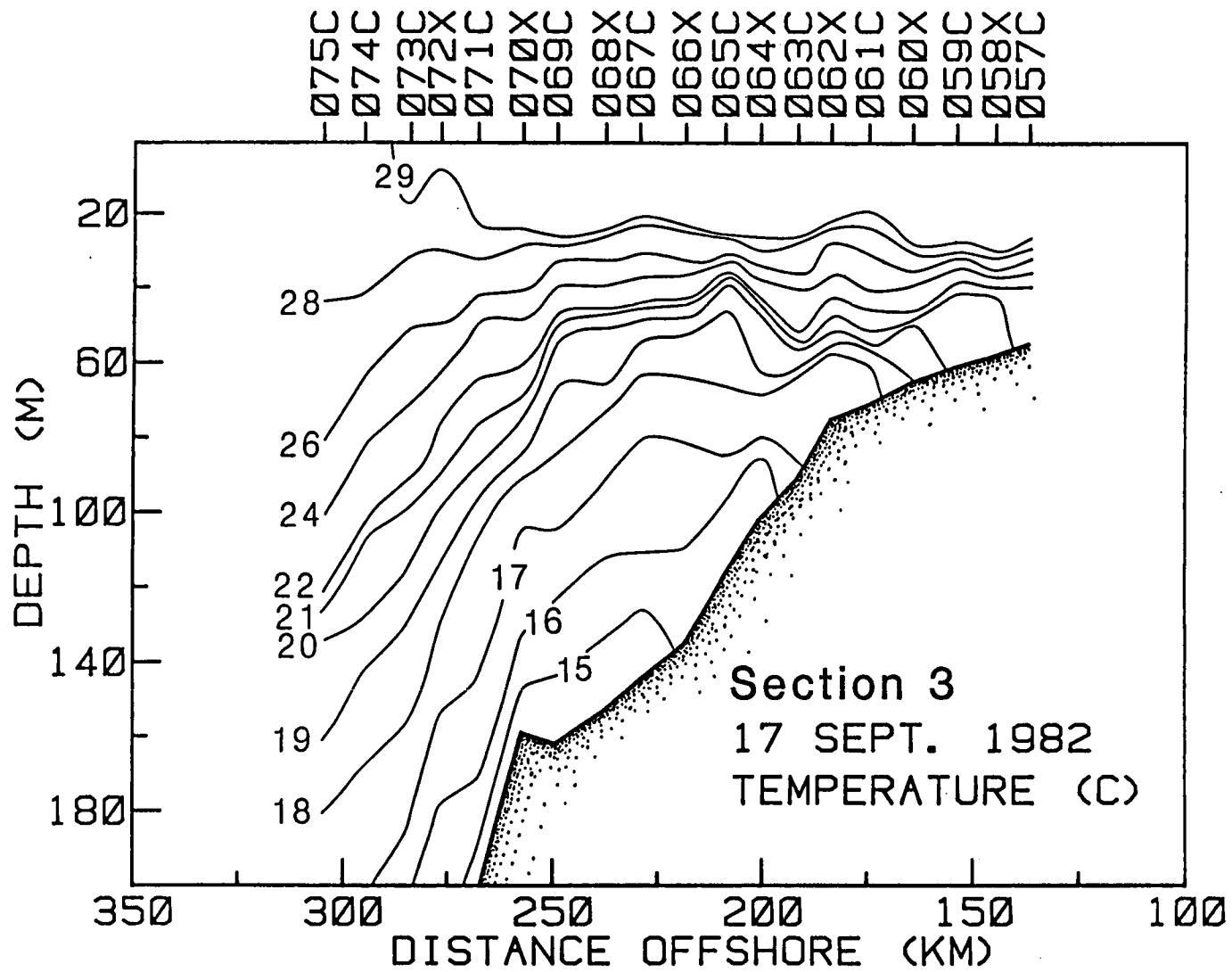
Figure 3-58.   Summer cruise, transect 3 temperature section.
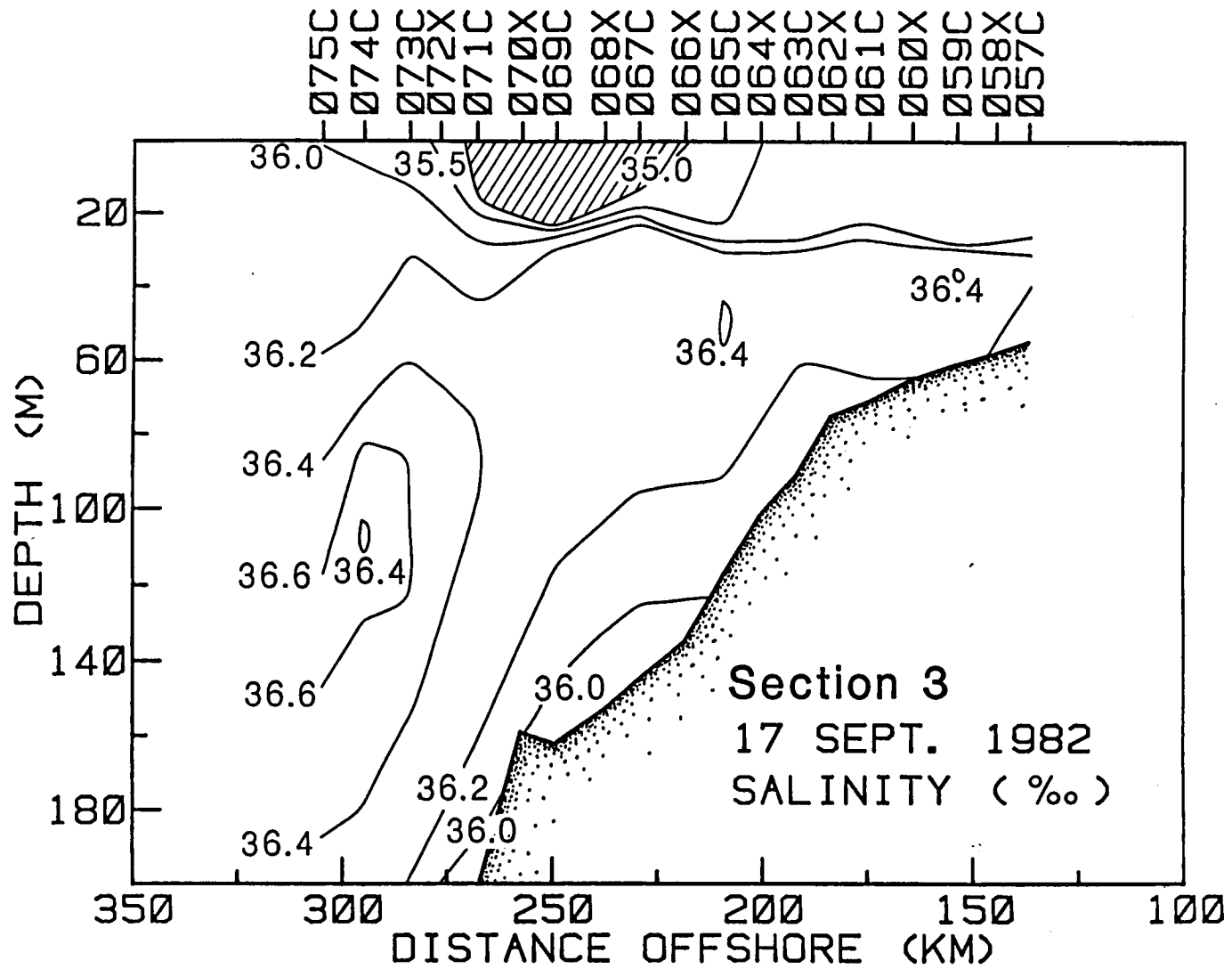
Figure 3-59. Summer cruise, transect 3 salinity section.
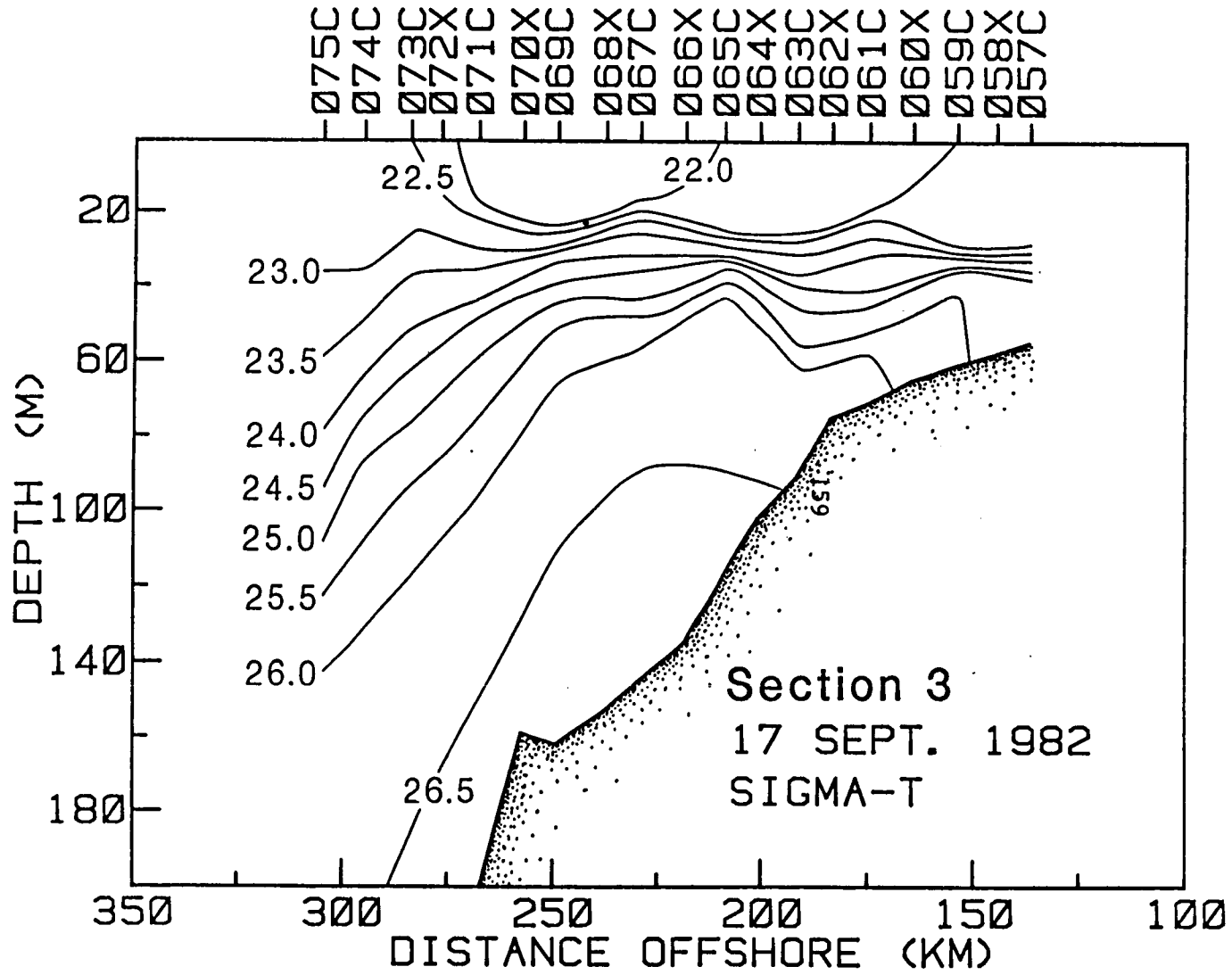
Figure 3-60. Summer cruise, transect 3 sigma-t section.
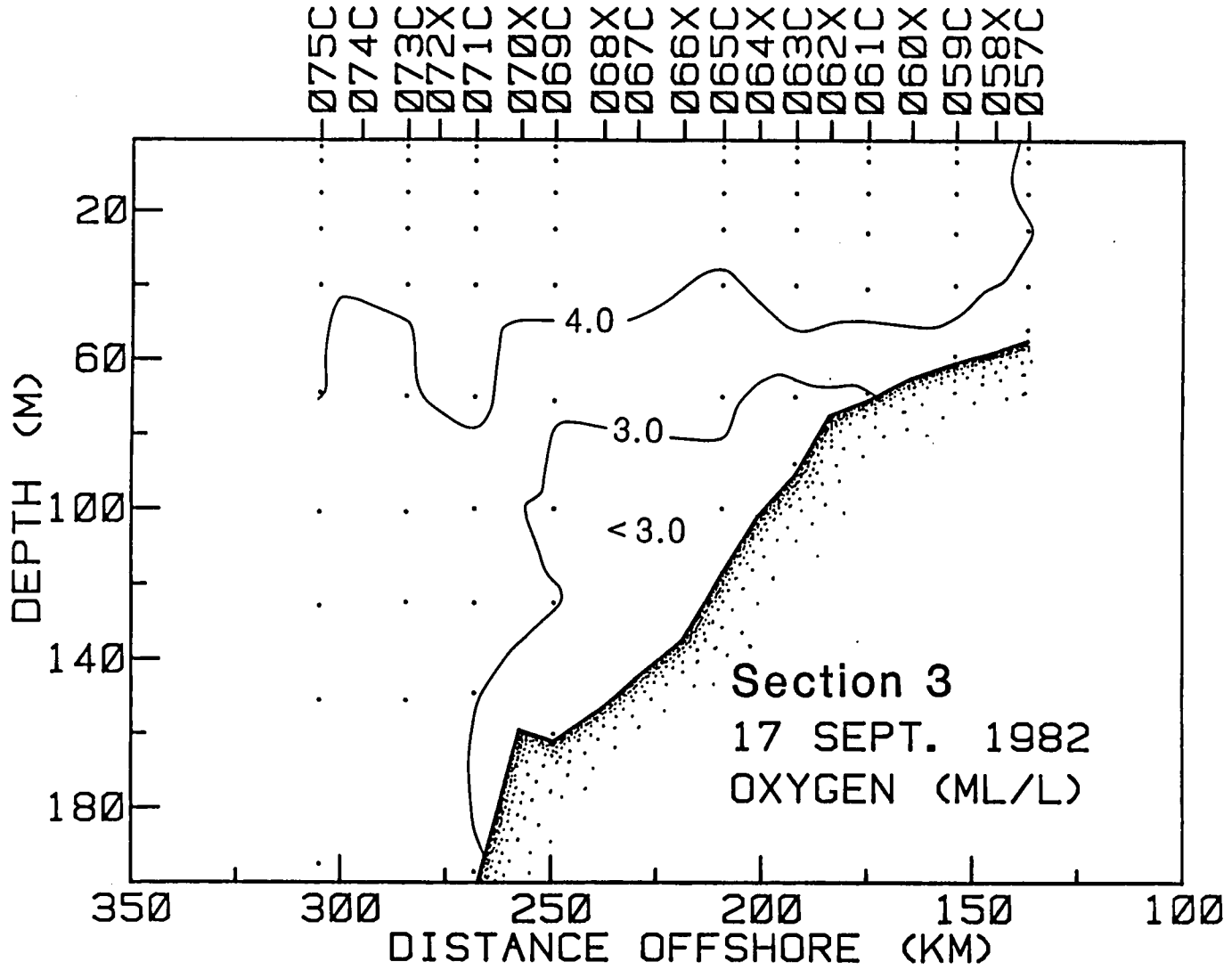
Figure 3-61. Summer cruise, transect 3 oxygen section.
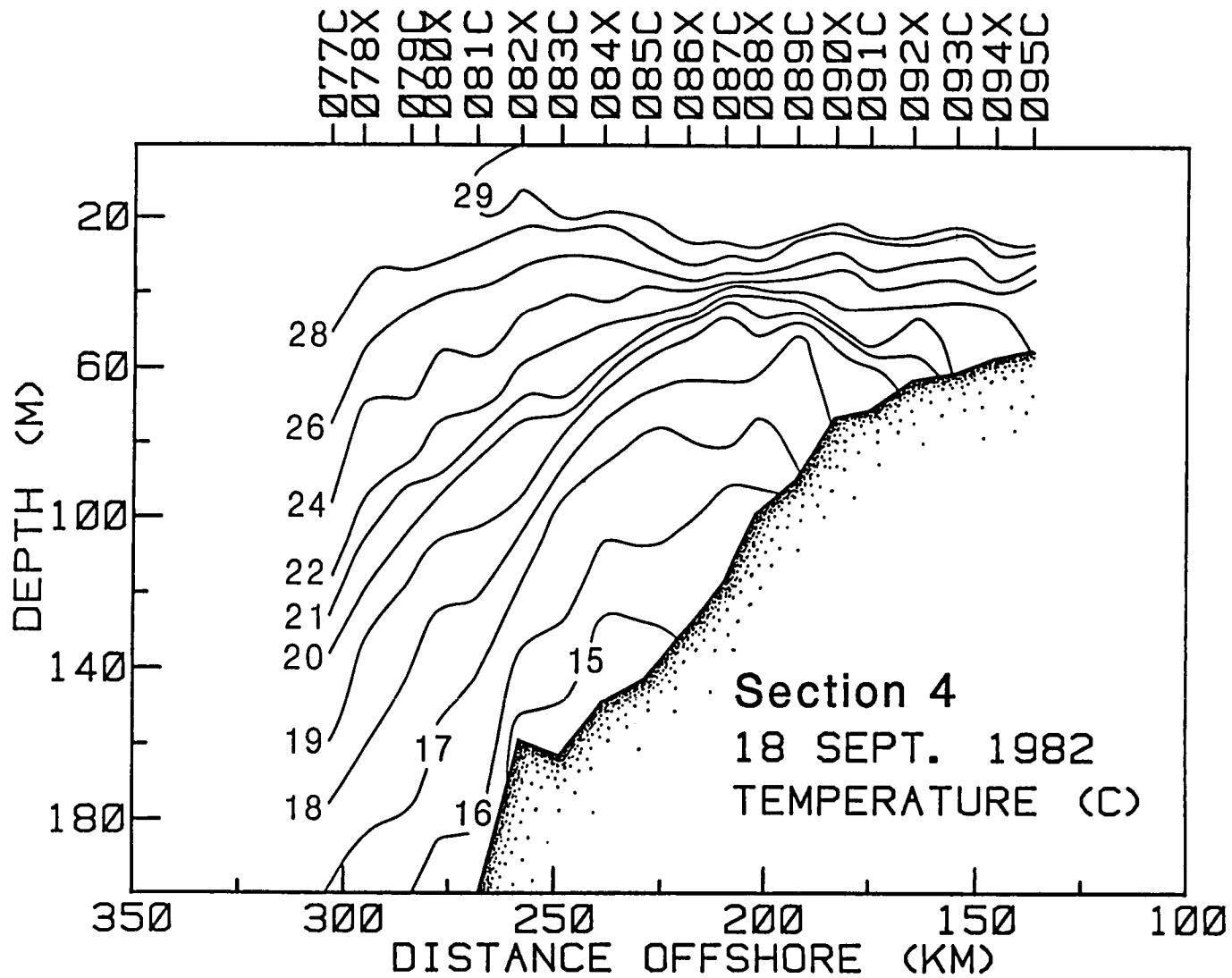
Figure 3-62.   Summer cruise, transect 4 temperature section.
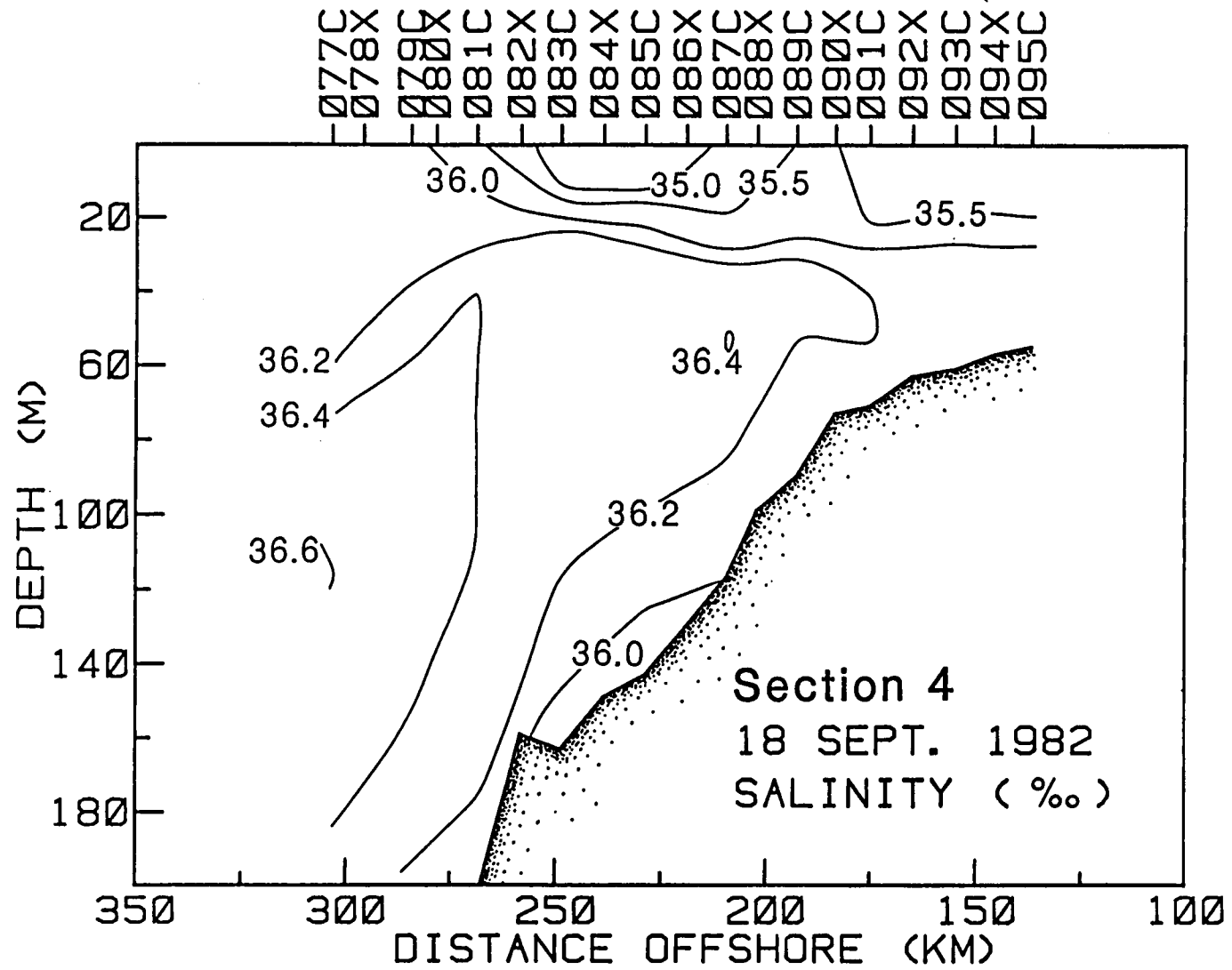
Figure 3-63. Summer cruise, transect 4 salinity section.
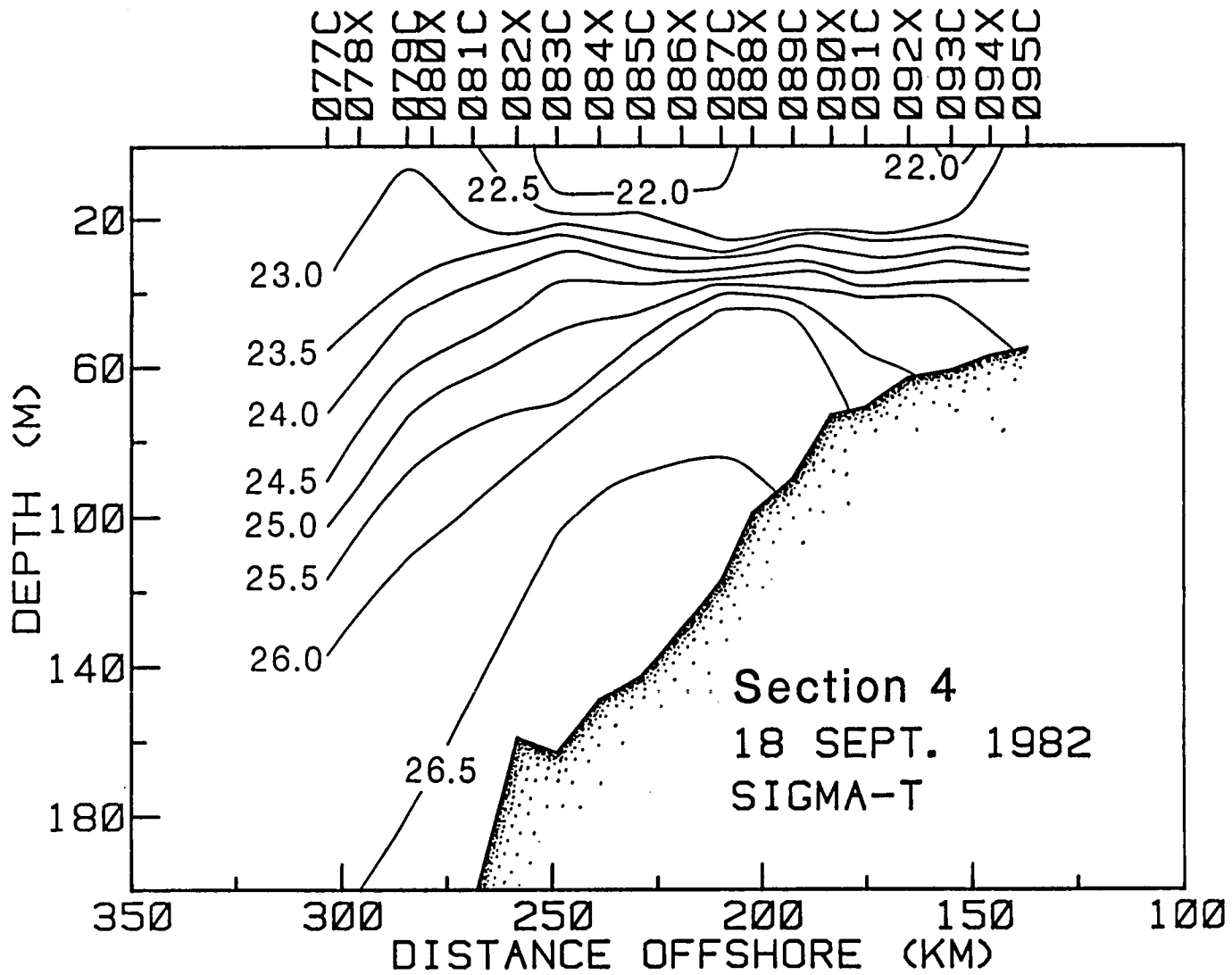
Figure 3-64.   Summer cruise, transect 4 sigma-t section.

163
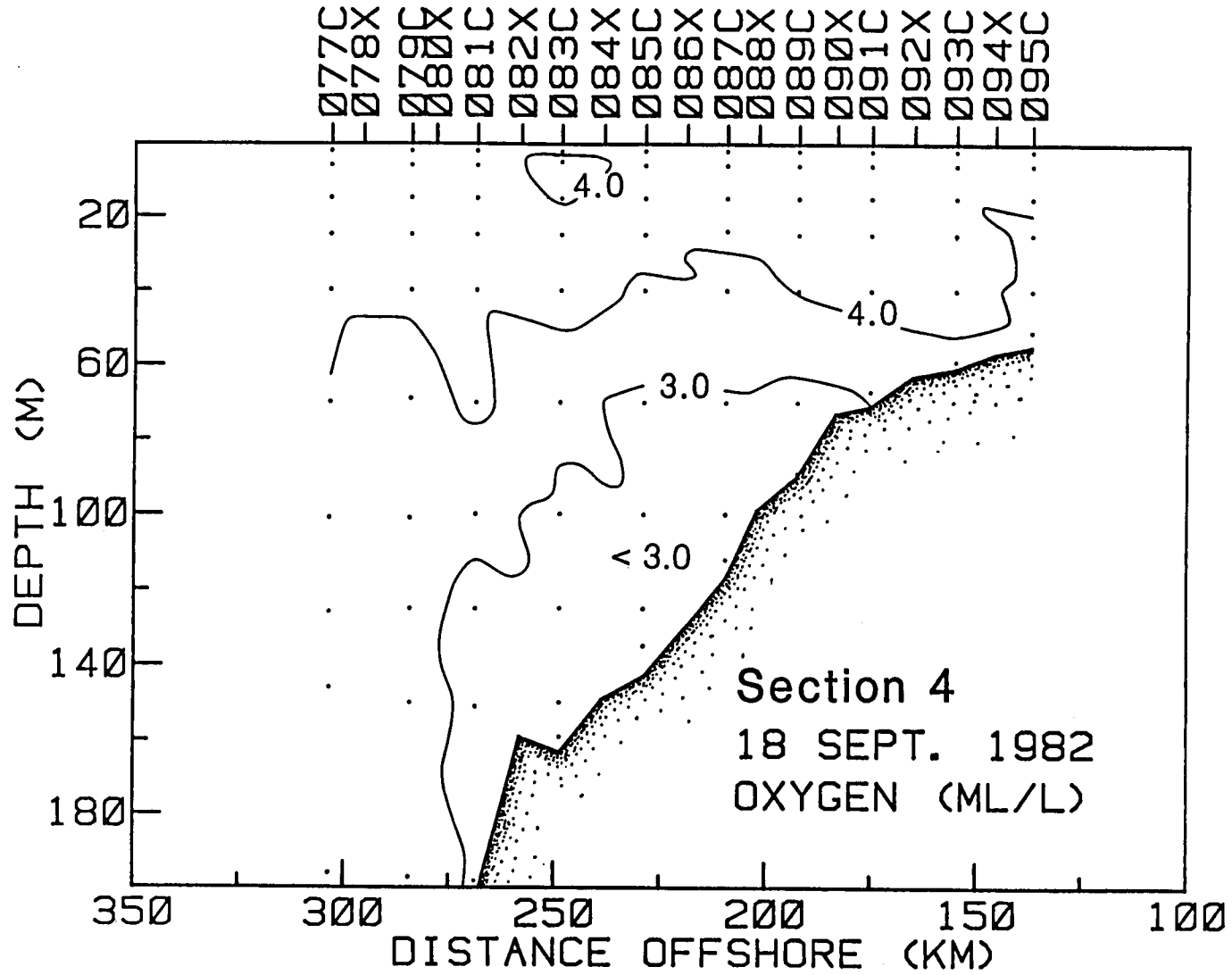
Figure 3-65. Summer cruise, transect 4 oxygen section.

164

A word of caution should be interjected at this time. Although the hydrographic interpretation given above is probably the most reasonable with the information at hand, the temporal and spatial variations in the region must also be a function of alongshelf currents. In a recent study by Molinari and Mayer (1982), they showed that most of the low frequency energy appeared along the isobaths. Thus, a simultaneous current meter/hydrographic study in this area under similar conditions may prove to be quite valuable in further establishing the relationships between hydrographic variability and changes in Loop Current location, and cross-shelf and alongshelf flow.

The salinity and density of the upper water column (<50 m) were influenced by a shallow layer of fresher water (Figures 3-51 and 3-52 for Transect 1; Figures 3-55 and 3-56 for Transect 2; Figures 3-59 and 3-60 for Transect 3; and Figures 3-63 and 3-64 for Transect 4). The area of fresher water (<36.0°/oo) extended as far offshore as 325 km and shoreward to the limit of the sections at the 60 m isobath. Minimum salinities (less than 35°/oo) were found in all transects with the largest areas in Transects 2 (Figure 3-55) and 3 (Figure 3-59). The layer of fresher water with salinities less than 36.0°/oo was deepest (40 m) and largest in Transect 1 (Figure 3-51). Consequently, the halocline rose and the volume of low salinity water decreased as the Loop Current moved closer to the shelf. Shelfward movement of the current could have induced turbulent mixing of the layer but it is more likely that the volume changes of the lower salinity water were related to changes in alongshore currents.

The source of this low salinity water is believed to be from land drainage, most likely from the Mississippi delta. Atkinson and Wallace (1975) showed

that salinities as low as 34.5°/oo were found along the Gulf Stream near the southeastern U.S. coast. They suggested that the Mississippi River was the most likely source. In addition, certain planktonic species (discussed further in Section 5.3.2.2) were found within this layer and are commonly found near the Mississippi drainage. It is likely that southward transport of fresh water in this region is enhanced via entrainment by the southward flowing branch of the Loop Current. The entrainment of fresher coastal waters along the outer shelf regime is a shelf-current interaction process which may play a significant role in the hydrographic regime of this region.

The largest volume of high salinity water (>36.6°/oo) within 50 km of the shelf break was found on Transect 3 (Figure 3-59) and was much greater than that found in either Transects 2 or 4. Transect 1 (Figure 3-51) had no high salinities (>36.4°/oo). The large volume in Transect 3 appears to reflect the strong onshore movement of the current. The relatively small volume (within 50 km of the shelf break) in Transect 4 (Figure 3-63) could reflect the diffusion of the high salinity area by mixing.

The slope of the isopycnals increased with time from relatively level isopycnals in Transect 1 (Figure 3-52) to steeper sloping doming isopycnals in Transects 2, 3 and 4 (Figures 3-56, 3-60, and 3-64, respectively). The doming beneath the pycnocline became more pronounced with onshore movement of the Loop Current edge. This doming was indicative of enhanced vertical velocities or possibly some weak counter flow on the shelf. Along with the elevation of the isopycnals was the upward movement of lower oxygen isopleths and higher nutrients associated with water of that density.

3.2.2.4 Oxygen Distributions

Oxygen concentrations of less than 3.0 ml/l but greater than 2.5 ml/l were found along the bottom and reached as shallow as 70 m in all sections (Figures 3-53, 3-57, 3-61 and 3-65). Nowlin and McLellan (1967) and Morrison and Nowlin (1977) present values of 2.5 to 2.7 ml/l for the oxygen-minimum core. They report that the oxygen-minimum core usually occurs much deeper (700 m) in the center of the Eastern Gulf Loop and in the main Yucatan inflow but also occurs at lesser depths (approximately 200 m) at stations to the left of the inflow and outflow because of the mass adjustment associated with the circulation. The present oxygen distributions reflect a further elevation of this oxygen minimum layer associated with lateral movement of the Loop Current. The minimum oxygen concentrations corresponded to a sigma-t range of 26.0 to 26.5 as shown in Figure 3-66. Data from Morrison and Nowlin (1977) (their Figure 4) shows the 26.5 isopycnal at a depth of 200 m near the shelf break. The present data show that isopycnals can also be elevated from 200 m to approximately 80 m at the shallowest point.

3.2.2.5 Nutrient Distribution

Nitrate distributions were similar to temperature distributions (Figures 3-67 through 3-70). Highest concentrations of nitrate coincided with the coldest waters. Concentrations as high as 18 μM were found on the shelf throughout the first three transects. The progressive doming of the isopleths brought the higher concentrations to shallower depths. In Transects 3 (Figure 3-69) and 4 (Figure 3-70), concentrations as high as 12
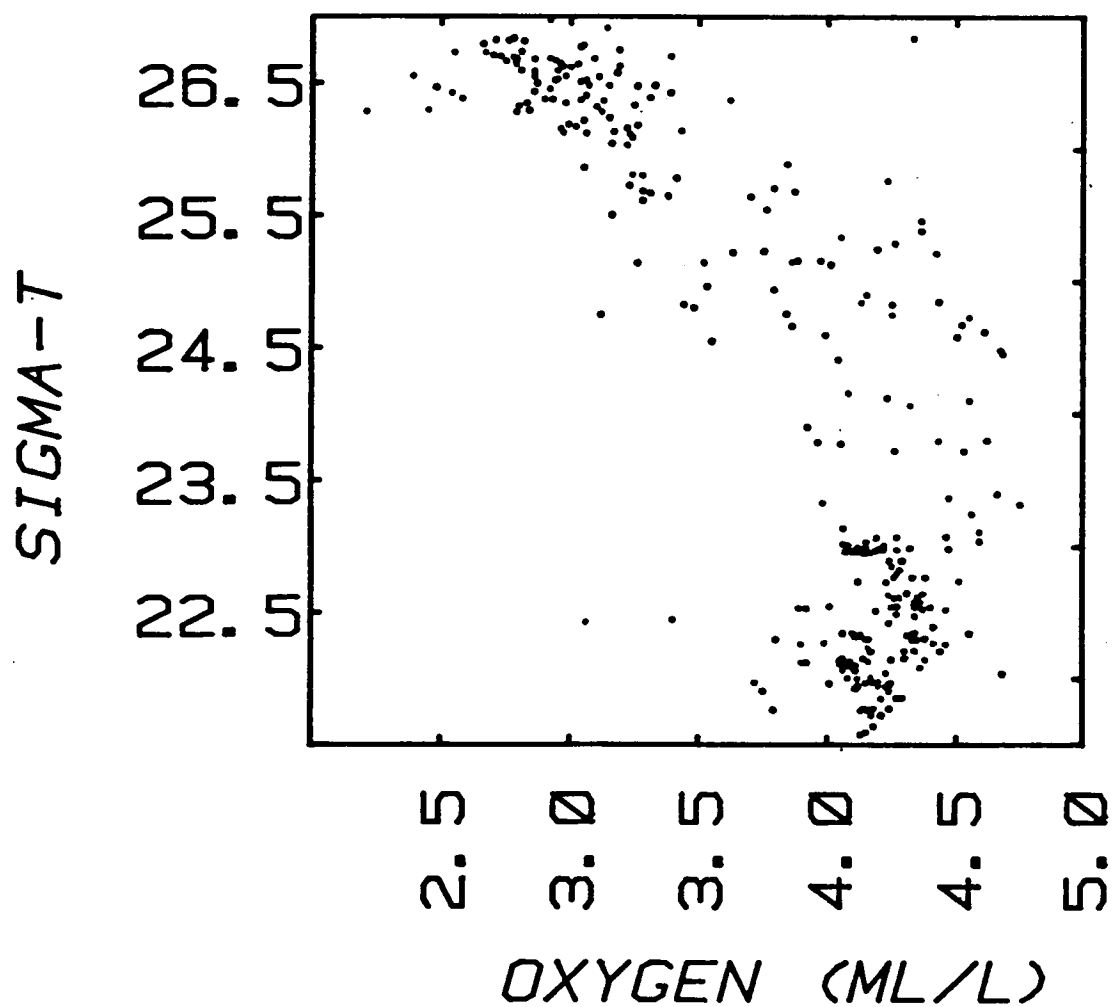
Figure 3-66. Oxygen-density plot for summer cruise data.

168
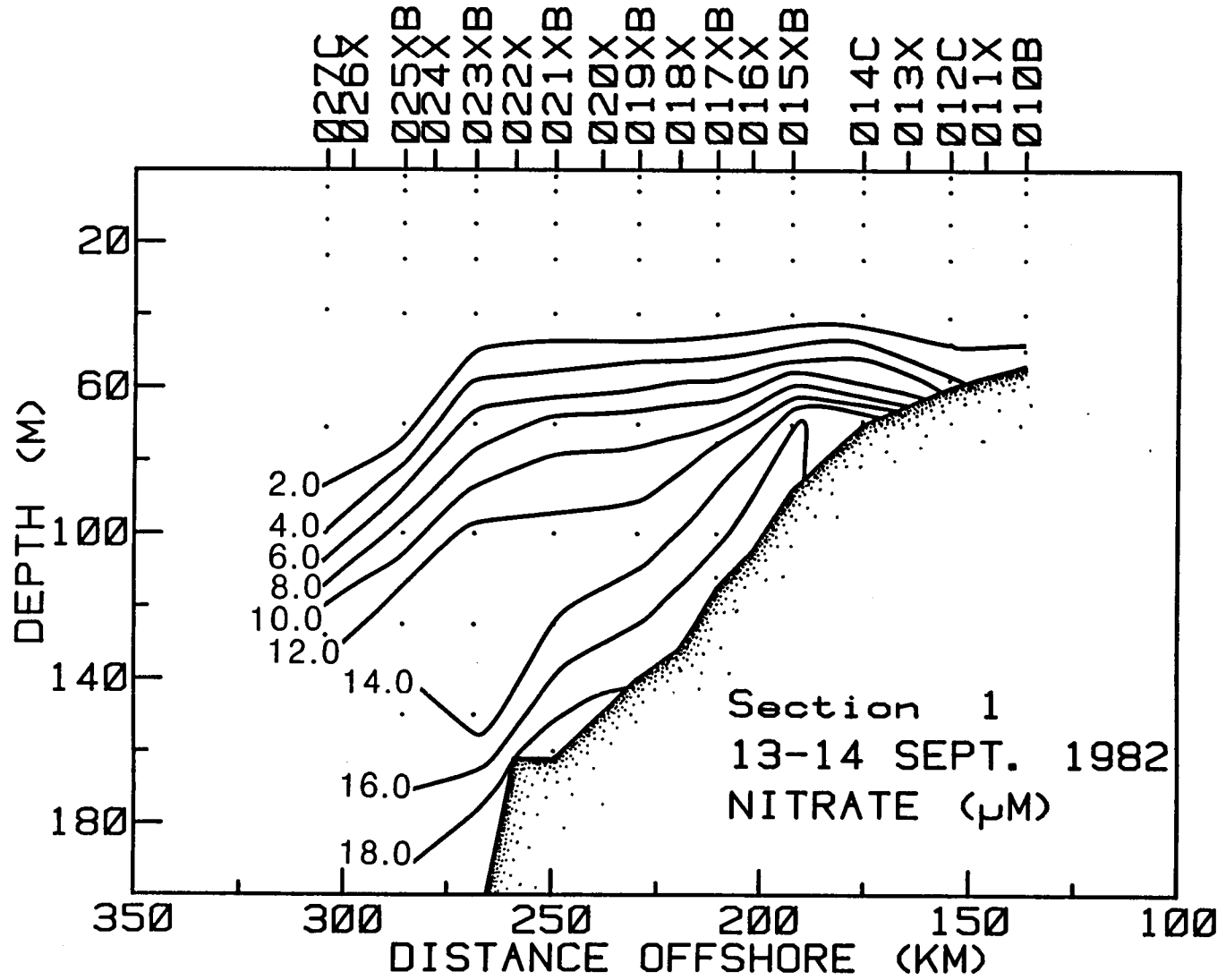
Figure 3-67.   Summer cruise, transect 1 nitrate section.
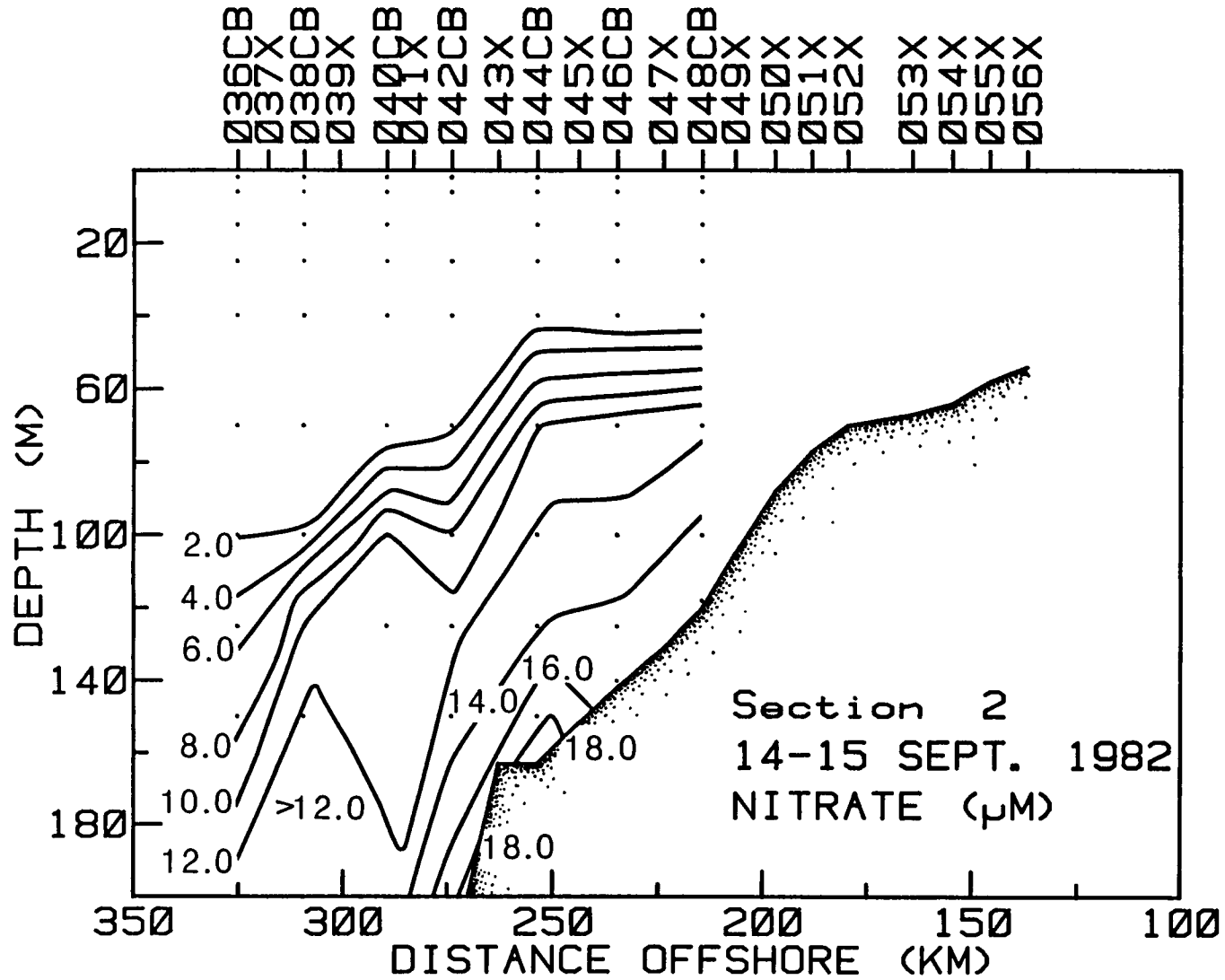
Figure 3-68. Summer cruise, transect 2 nitrate section.
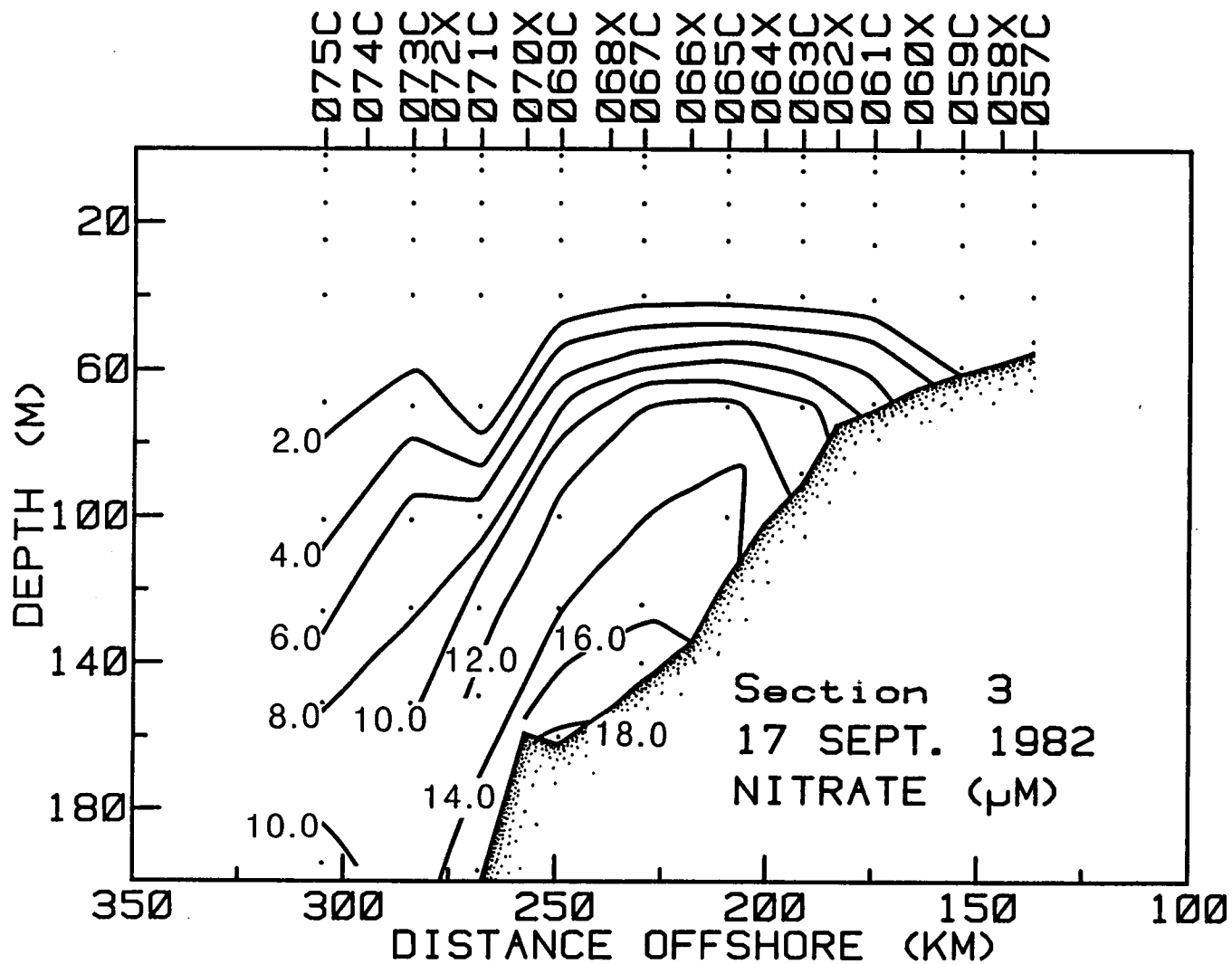
Figure 3-69. Summer cruise, transect 3 nitrate section.
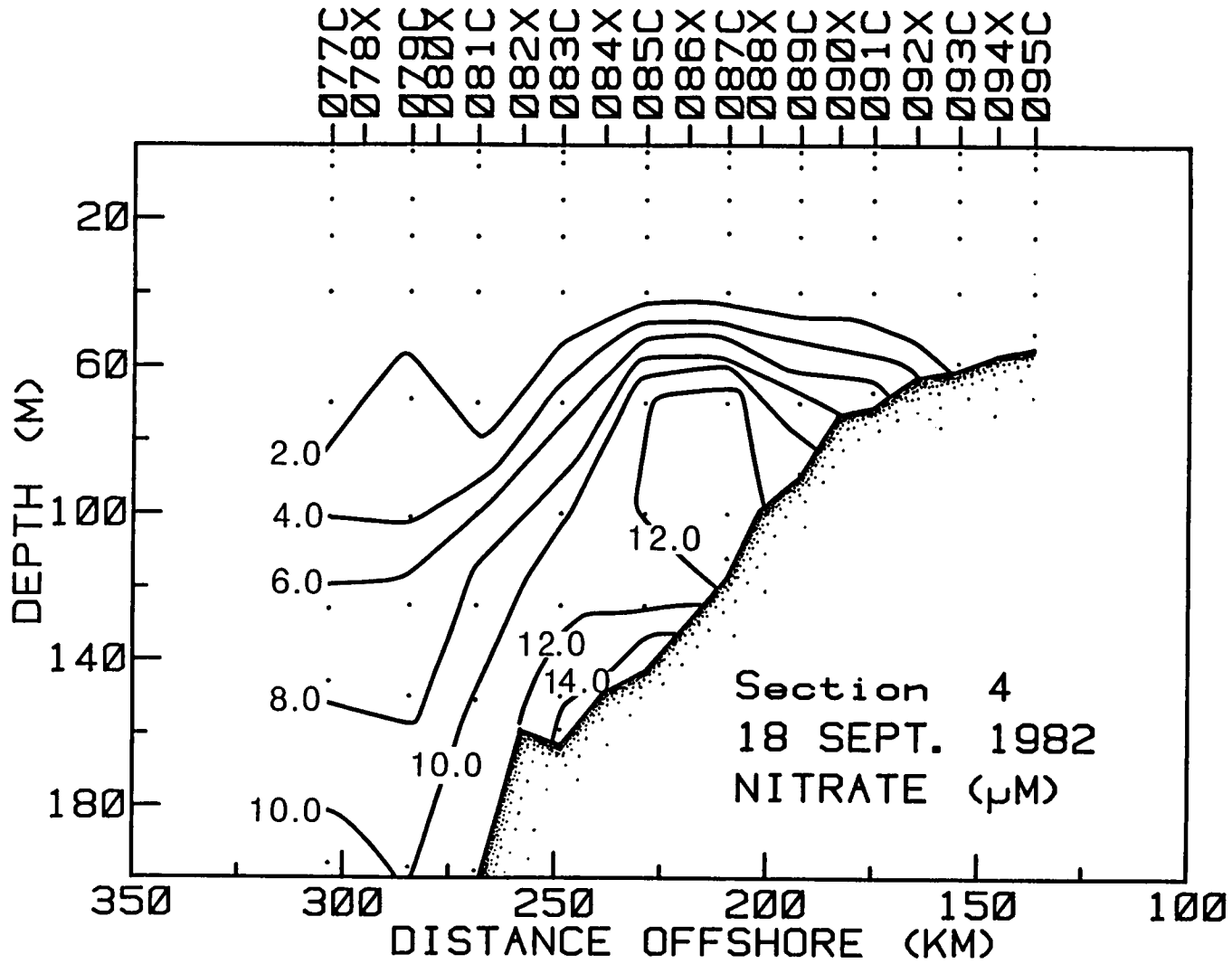
Figure 3-70. Summer cruise, transect 4 nitrate section.

μM were found as shallow as 70 m. The presence of the high concentrations in the water column appeared to be associated with the shelfward movement of the Loop Current edge.

Throughout the cruise, a sharp nitrocline was found over the shelf at approximately 60 m. The nitrocline was deeper than the thermocline and the low salinity layer, but decreased in intensity over time, as did the thermocline and halocline.

Silicate and phosphate (see Appendix A-3) showed distributions similar to nitrate. Higher concentrtions were associated with cooler water and low oxygen. The progressive doming was also observed in the silicate and phosphate contours. The higher nutrient concentrations were associated with deeper Loop Current water brought on the shelf during the shelfward movement of the edge of the current.

3.2.2.6 Chlorophyll Distributions

As a means of maintaining continuity in presentation, the time series cross-sections for Chl a (Figures 3-71 through 3-74) and Chl a +Ph a (Figures 3-75 through 3-78) for Transects 1 through 4, respectively, are presented at this time. The sections show the presence of subsurface maxima (about 0.25 mg.m^{-3} for Chl a + Ph a) on the outer shelf near the depth of the top of the nitracline.

More detailed discussions of these distributions are deferred to Section 5.3.2.1.
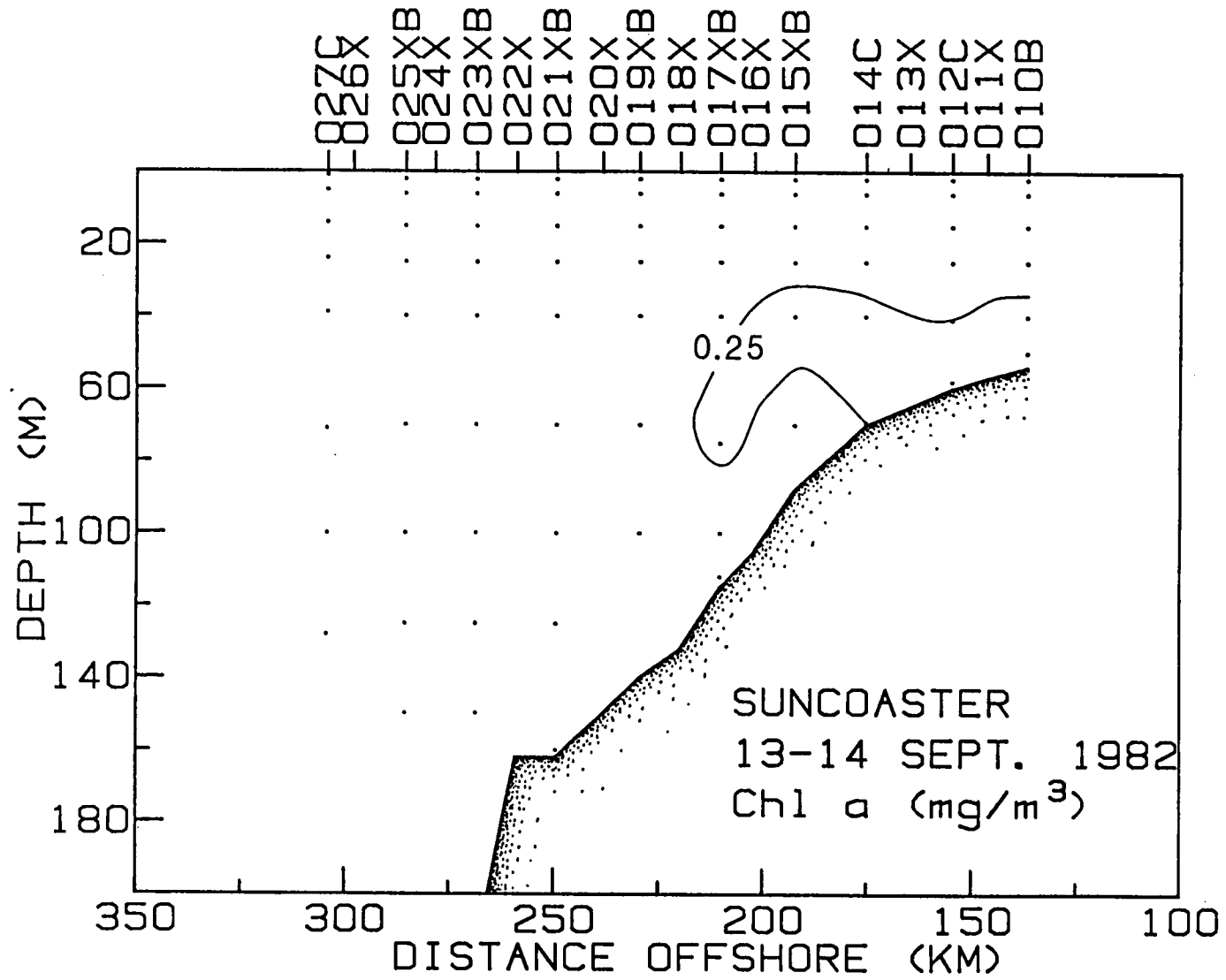
Figure 3-71. Summer cruise, transect 1 Chl _a_ section.

174
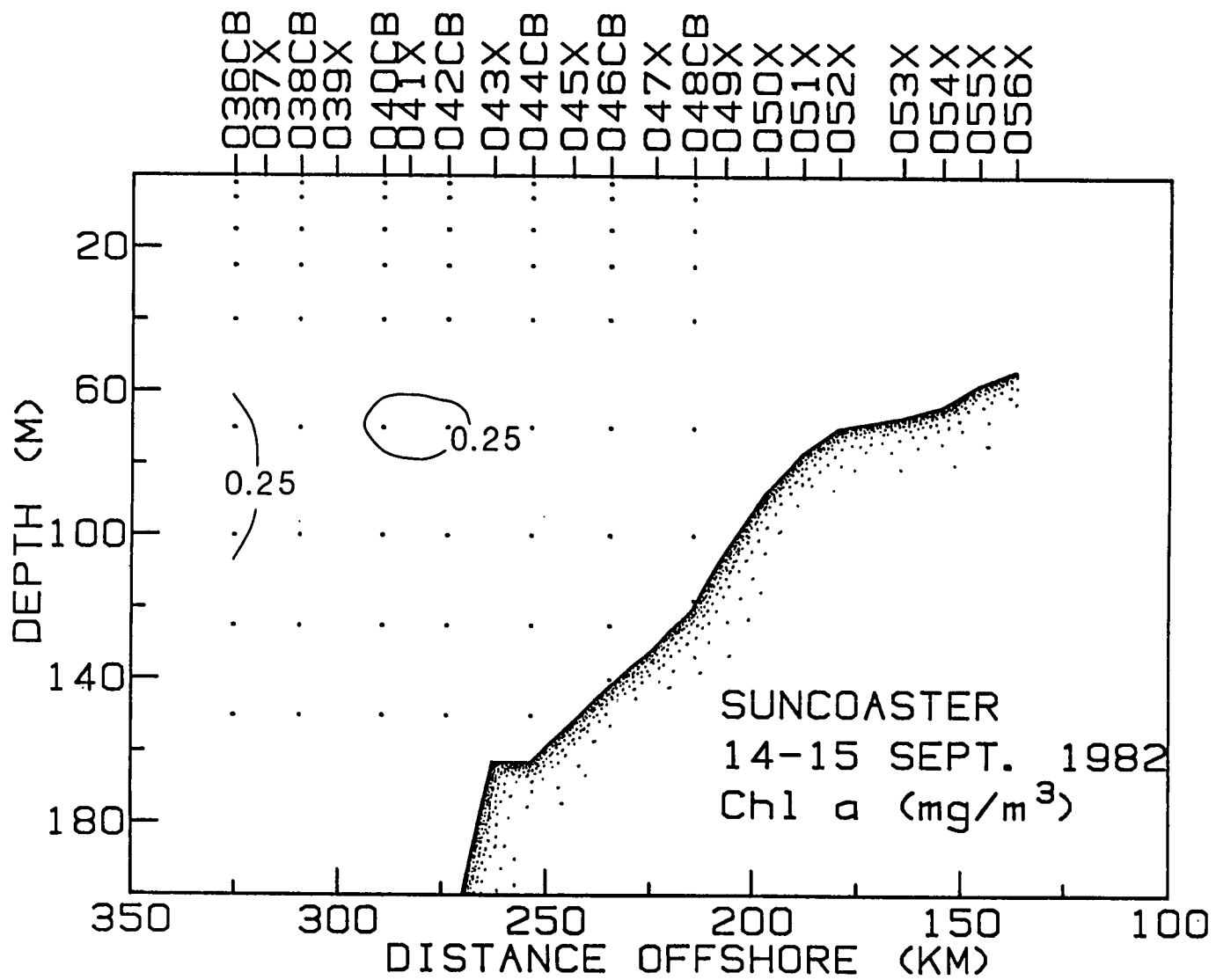
Figure 3-72.   Summer cruise, transect 2 Chl _a_ section.
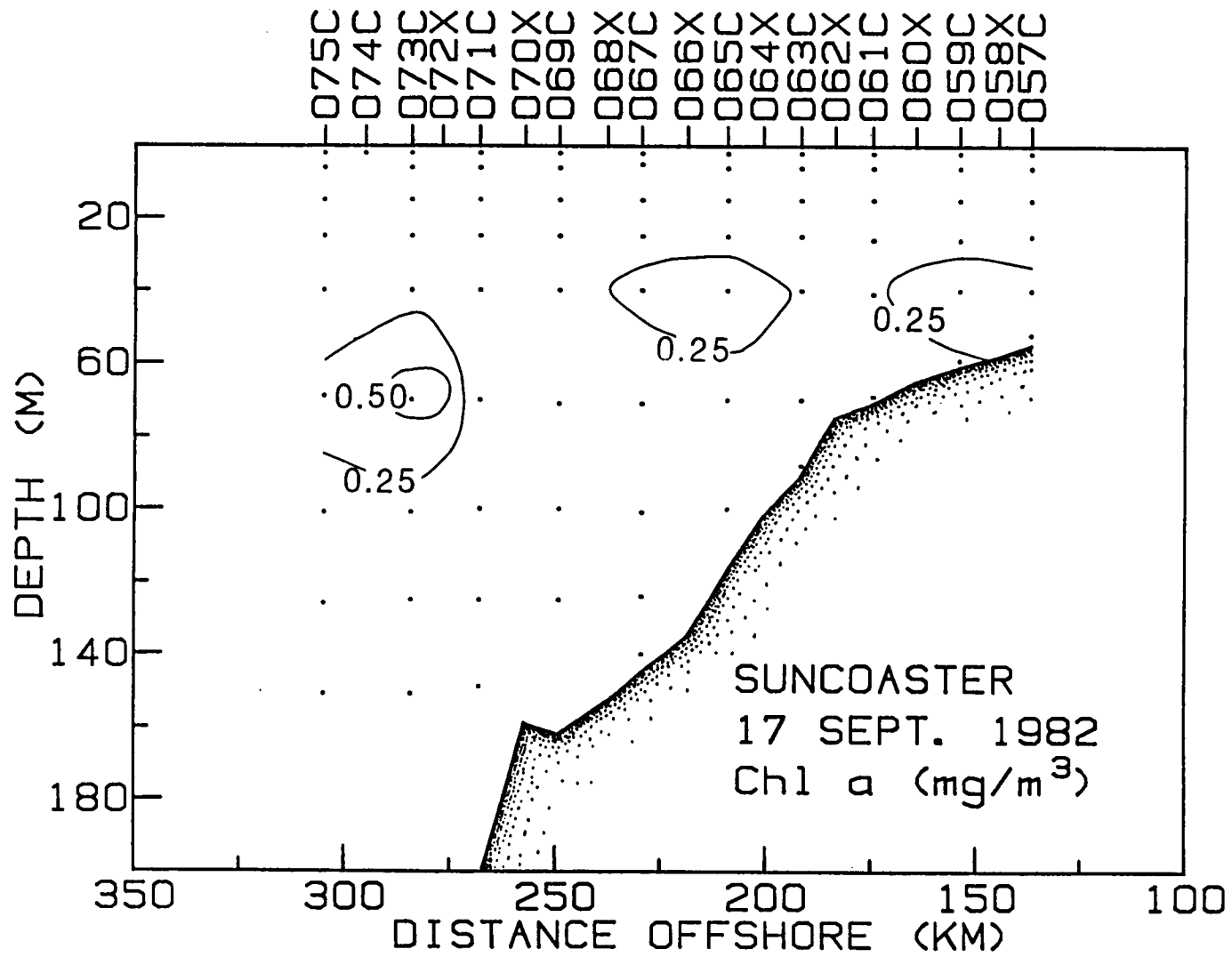
Figure 3-73. Summer cruise, transect 3 Chl _a_ section.
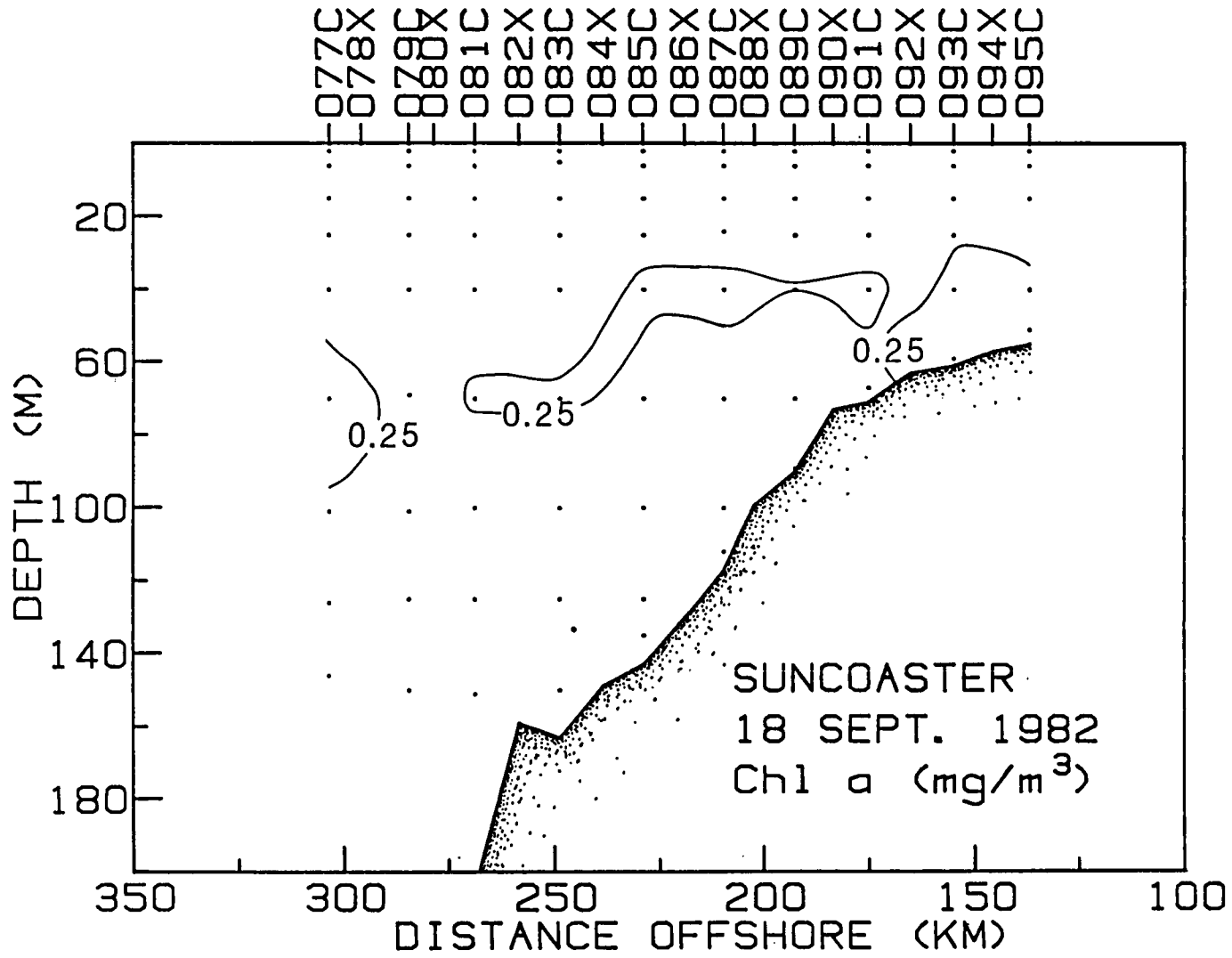
Figure 3-74. Summer cruise, transect 4 Chl a section.

177
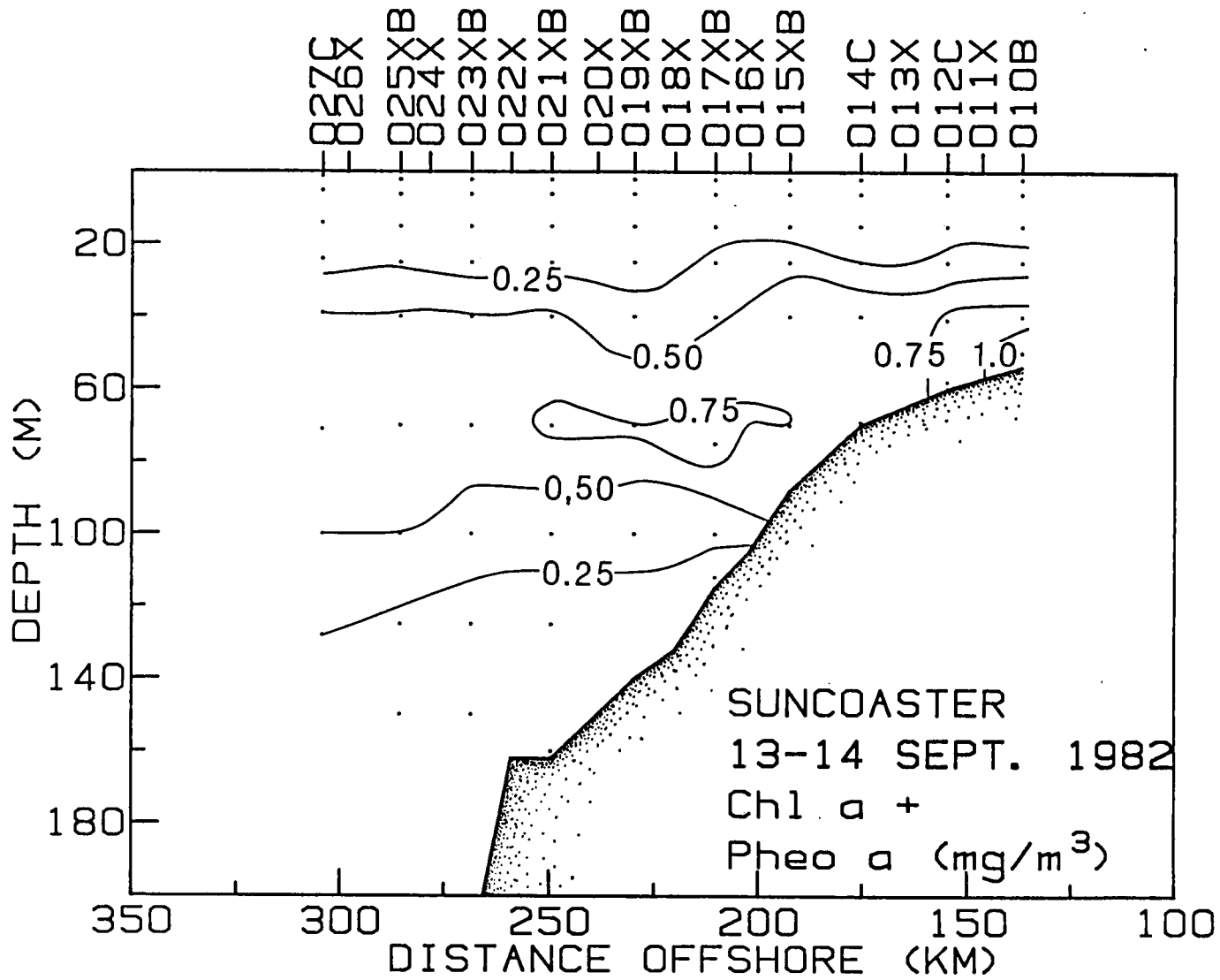
Figure 3-75. Summer cruise, transect 1 Chl a + Ph a section.
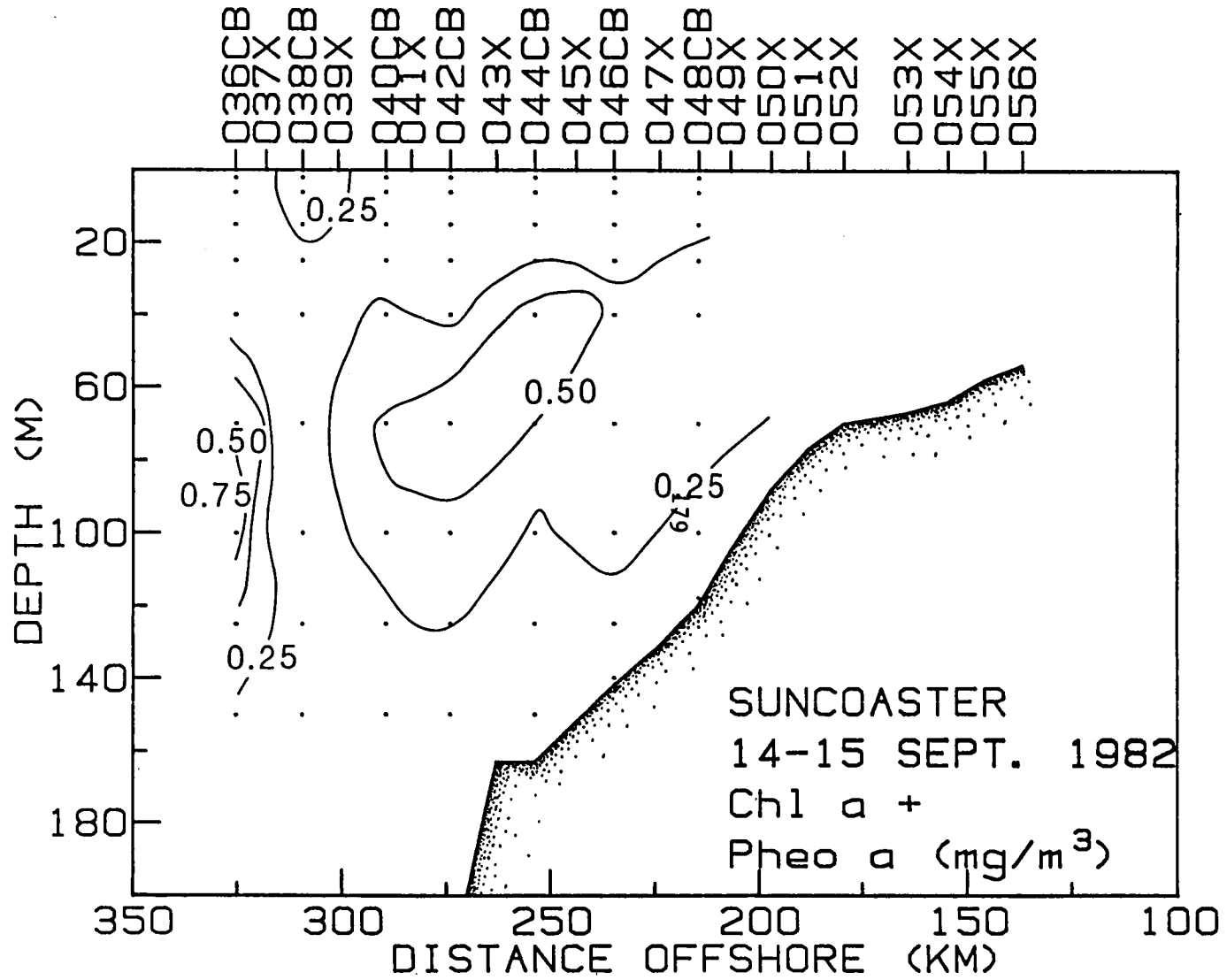
Figure 3-76.   Summer cruise, transect 2 Chl a + Ph a section.
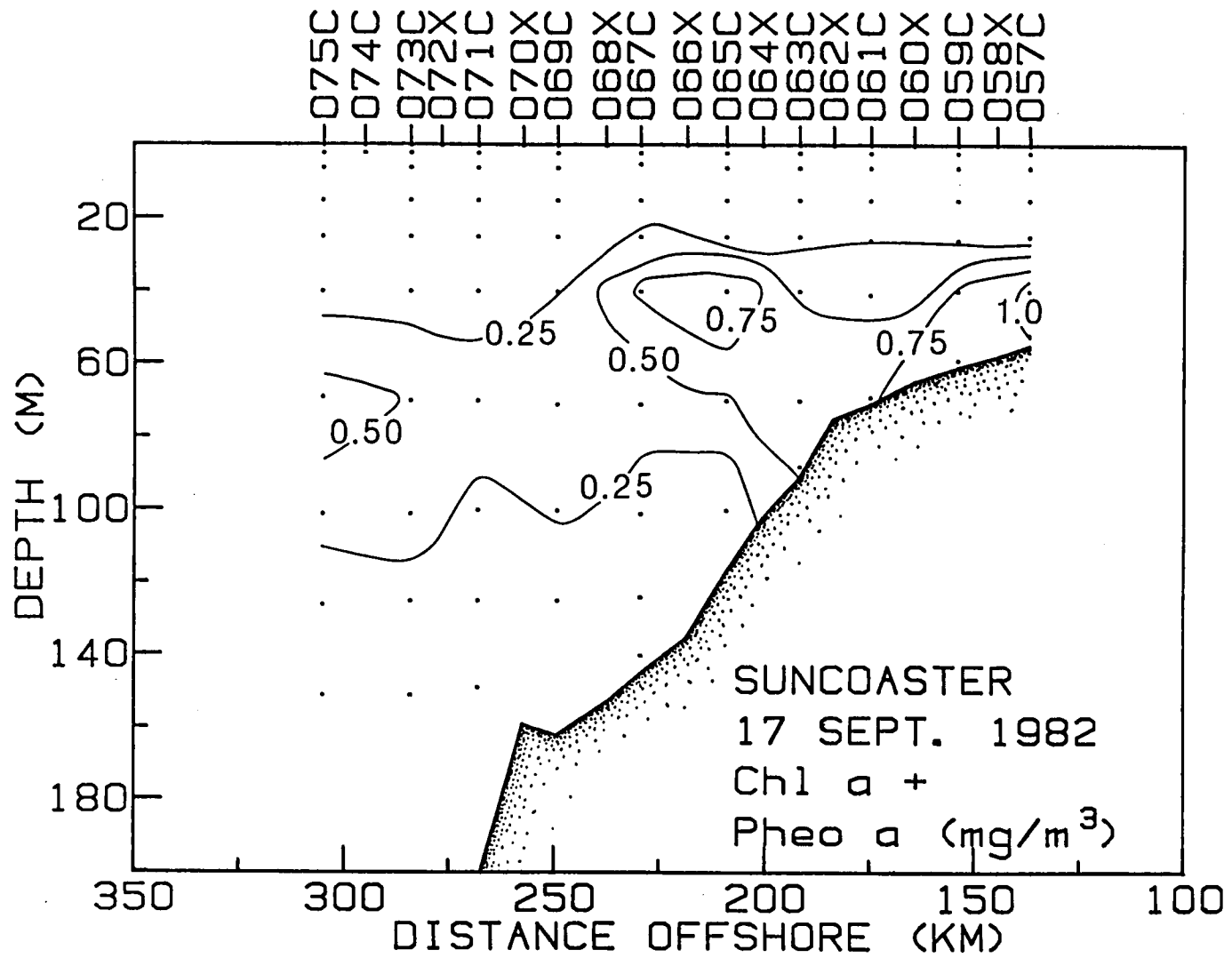
Figure 3-77.   Summer cruise, transect 3 Chl _a_ + Ph _a_ section.
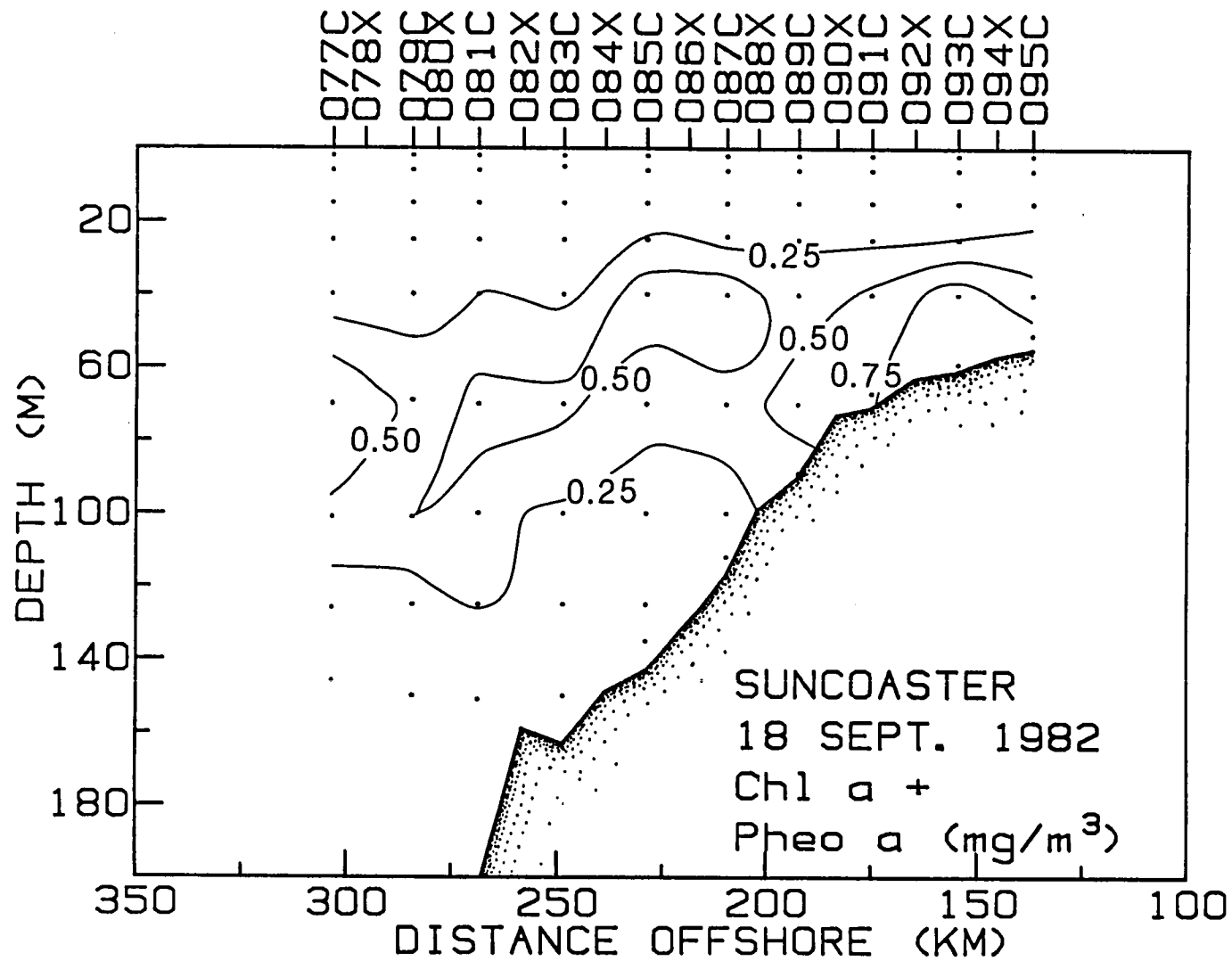
Figure 3-78. Summer cruise, transect 4 Chl _a_ + Ph _a_ section.

3.2.2.7 Water Masses

The TS plot of all stations (Figure 3-79) shows two general envelopes, one is characterized by a high subsurface salinity maximum; the other has a lower salinity at mid-depths. Using Wüst's (1964) characateristic Subtropical Underwater core (>36.6°/oo at approximately 22.5°C) as a criterion for separation, the plots were separated to show the distinction between the two TS envelopes. Figure 3-80 illustrates the TS envelope with the characteristics of Subtropical Underwater, the subsurface salinity maximum greater than 36.6°/oo and presence of fresher water (35.5 to 36.0°/oo) in the surface waters. Stations 30 through 36, and 73 through 79 fell within this envelope and consequently were influenced by Loop Current Water (LCW) which is characterized by the Subtropical Underwater core. These stations are found at the westward edges of Transects 2, 3 and 4. The TS characteristics confirm the presence of the LCW indicated in the hydrographic data. Figure 3-81 presents the second envelope which is characterized by a less intense subsurface salinity maximum (36.4°/oo) and a larger envelope of lower salinities (<35.0°/oo). The characteristics seen in this envelope are similar to those described by Morrison and Nowlin (1977) for Gulf-type water which corresponds to Wennekens' (1959) Continental Edge Water (CEW). This water mass has been found to the left (when facing in the direction of flow) of the current and along the continental margin. These data indicate its presence shoreward of the Loop Current and over the outer shelf.

A final method for illustrating the toward-shelf progression of the Loop Current in terms of water masses is through a TS time series plot at
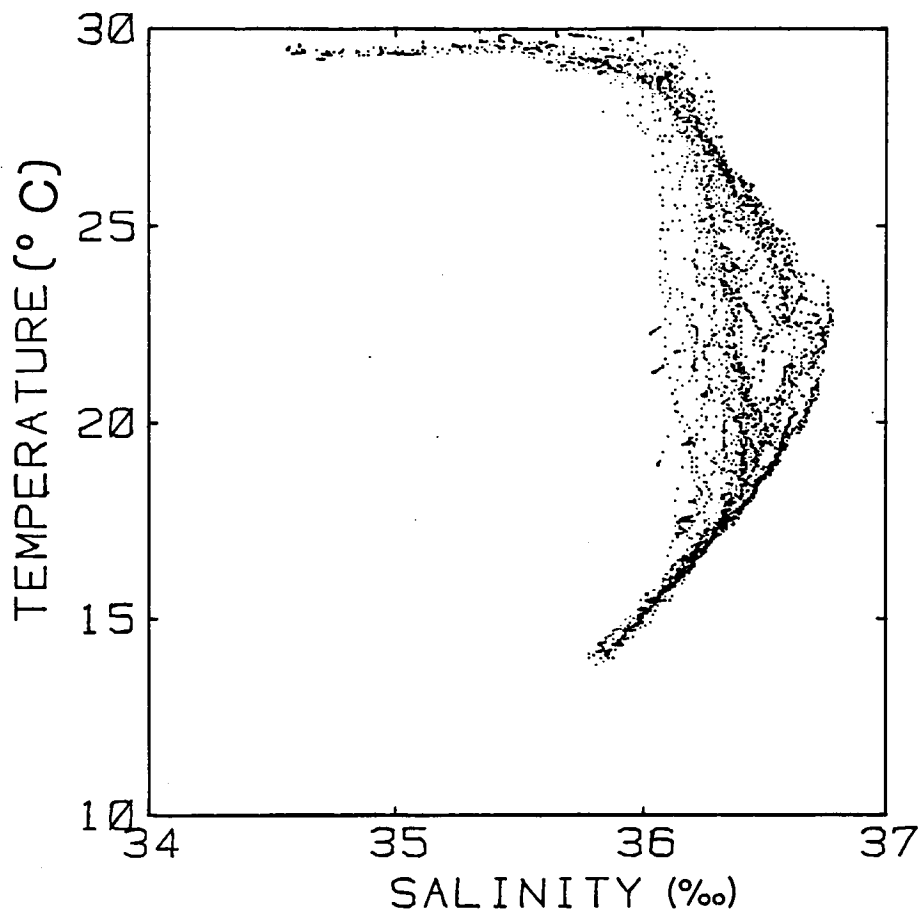
Figure 3-79. TS diagram for all summer station data.
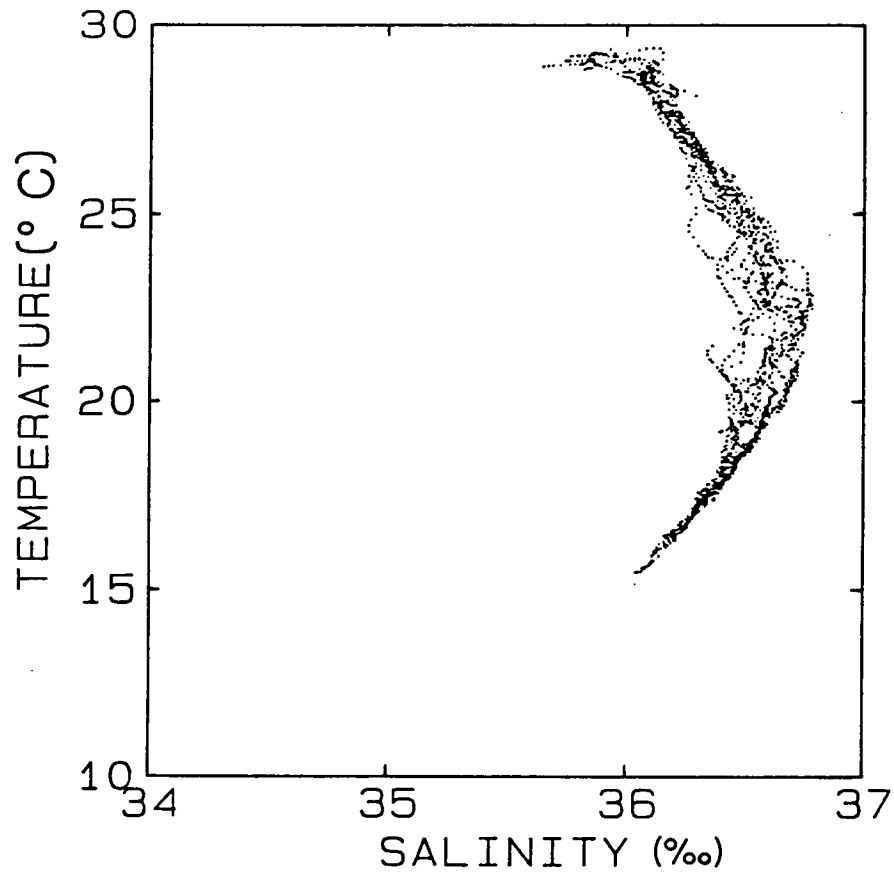
Figure 3-80.   Subdivided TS diagram emphasizing Subtropical
                Underwater characteristics.
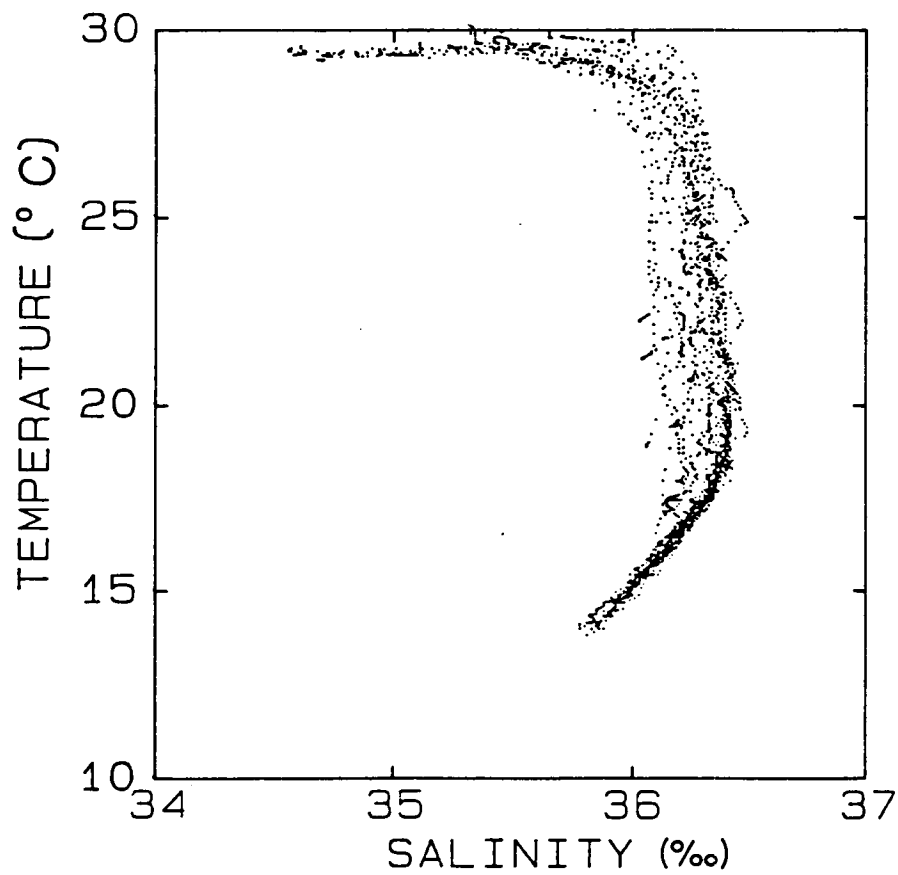
Figure 3-81. Subdivided TS diagram emphasizing Continental
Edge Water characteristics.

selected station depths. For example, Figure 3-82 presents a series of station plots at the extreme western ends of the sections in 1,980 m of water. Note how the subsurface salinity maximum at 22°C is present during Transects 3 (Station 75) and 4 (Station 77). Closer to the shelf break in 1,260 m of water, Figure 3-83 shows the time series TS maximum to be present in Transect 3 (Station 73) but not in Transect 4 (Station 79). Still closer to the shelf break at a depth of 215 m, Figure 3-84 shows no maxima at all. Thus the same intrusion discussed earlier in the hydrographic data can also be seen from a water mass point of view.

All plots seaward of the shelf break also showed small scale finestructure (i.e., the jagged lines). This finestructure is indicative of mixing which occurred as a result of the intrusion.

3.2.2.8 Summary

The summer cruise data show an approximate 28 km eastward shift of the Loop Current between September 13 and 18, 1982. The doming of isopycnals, an increase in subsurface salinity, warmer subthermocline temperatures and a decrease in the volume of the fresher upper layer appeared to be associated with the toward-shelf movement. Alongshore currents probably affected these hydrographic distributions in some fashion that could not be directly assessed because of lack of current data. Low oxygen values and high nutrient concentrations along the bottom layer of the shelf indicated upslope movement of the oxygen minimum and high nutrients which are characteristic of Loop Current waters. TS characteristics show that LCW was situated within 50 km of the shelf break concurrent with the toward-shelf

186
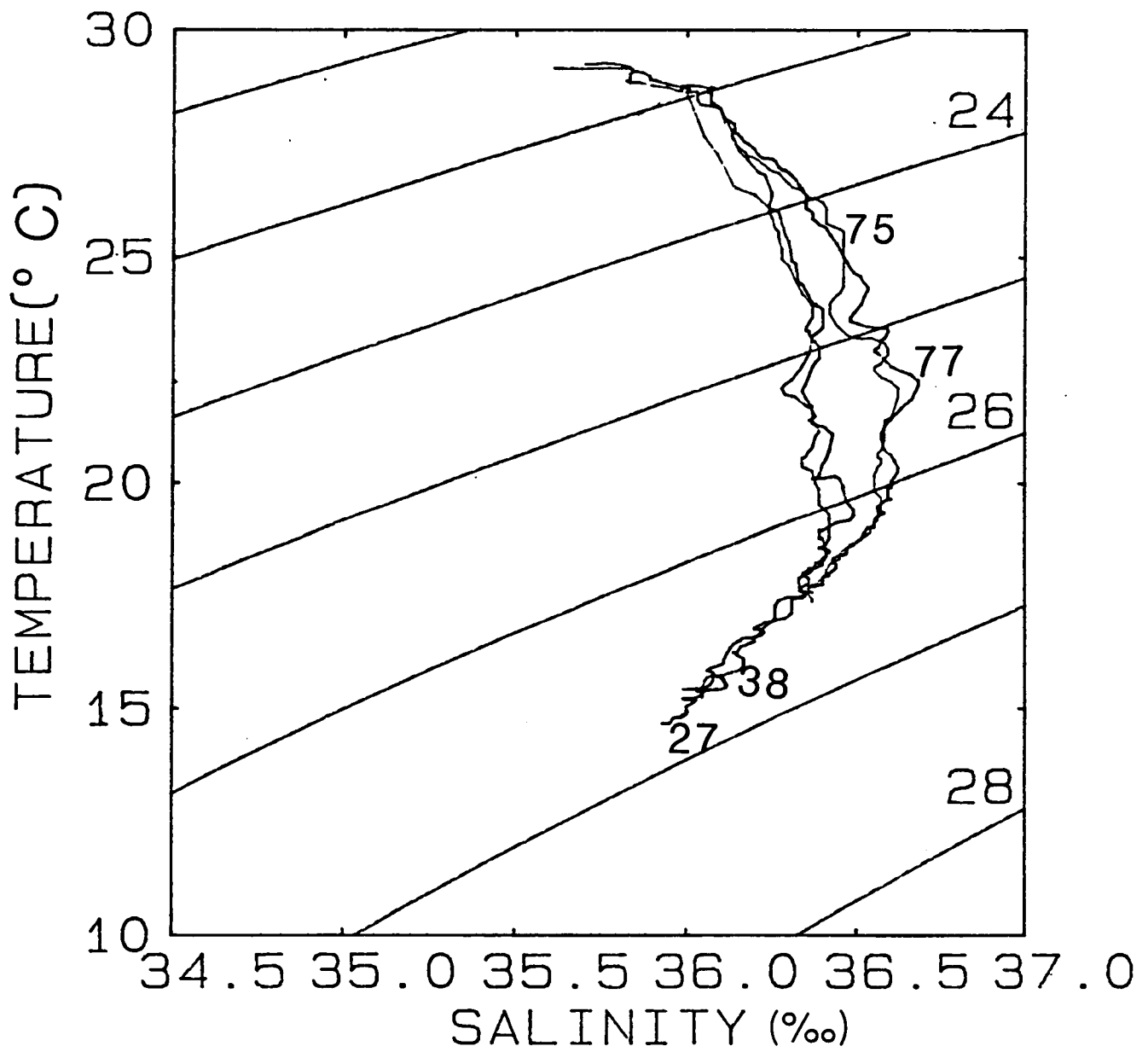
Figure 3-82. TS time series plot for stations at 1,980 m water depth.
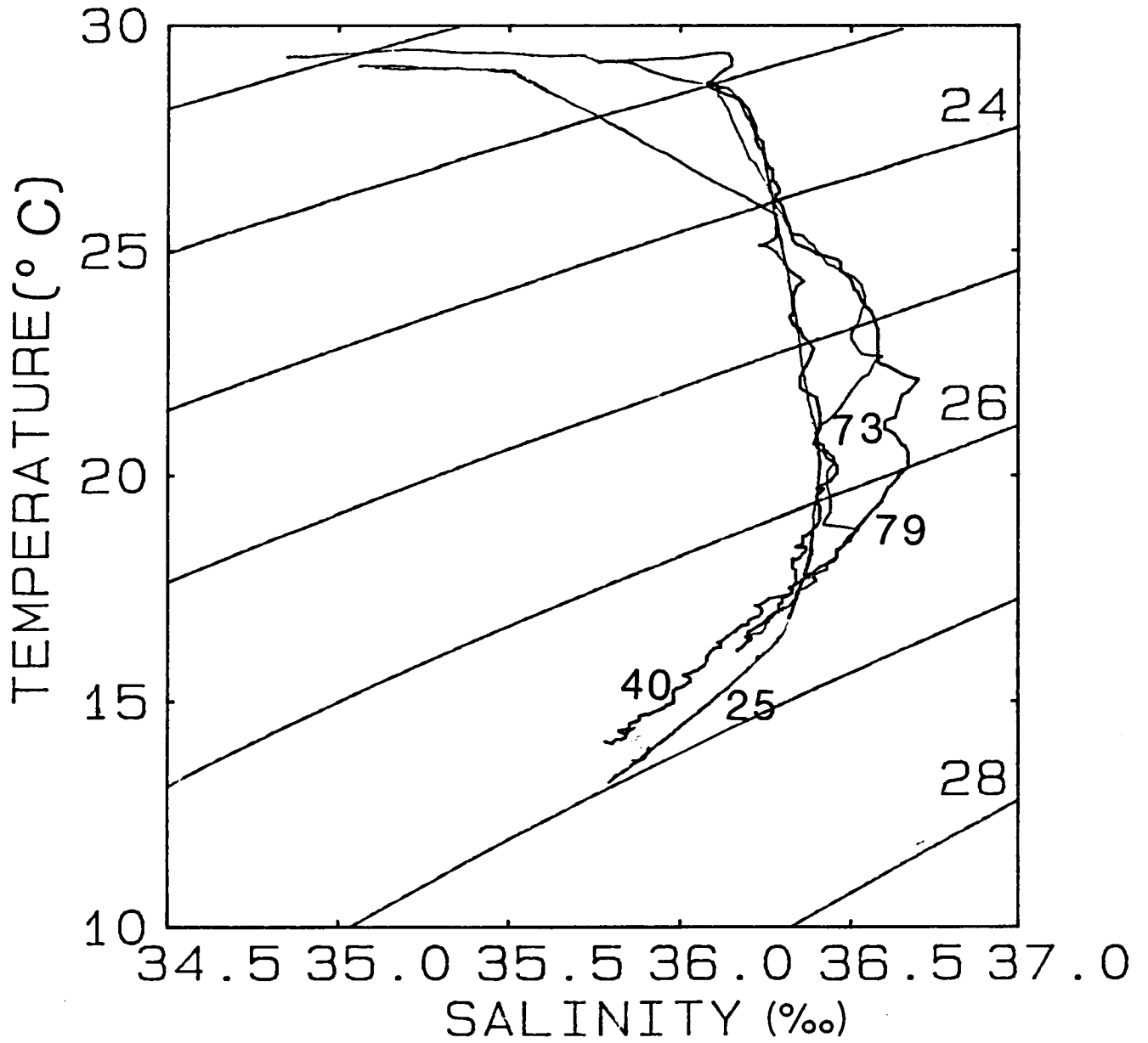
Figure 3-83.   TS time series plot for stations at 1,260 m water depth.
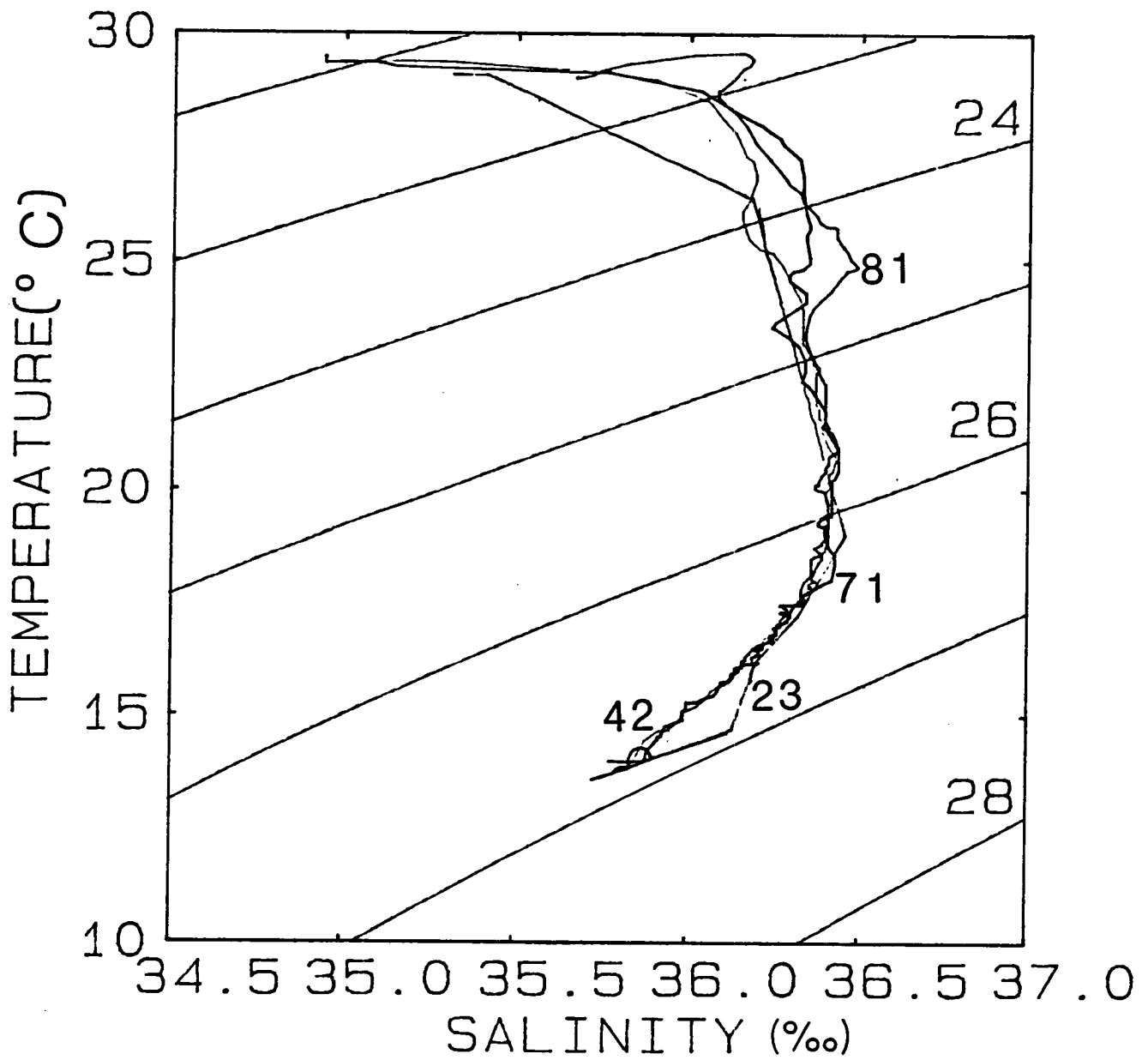
Figure 3-84. TS time series plot for stations at 215 m water depth.

movement of the Loop Current. Stations in this region showed small scale finestructure indicating mixing. The remaining stations were of CEW and showed little finestructure.

3.2.2.9 Conclusions

Hydrographic data from the southwest Florida shelf during September 13 through 18, 1982 were used to study temporal variations of hydrographic distributions. These variations appeared to be related to a toward-shelf movement of the Loop Current.

Analysis of four repeated transects constituting a time series showed that coldest bottom temperatures and lowest salinities were present at the onset of the sampling period. Concurrent with toward-shelf movement of the Loop Current, mid-depth salinities increased to a subsurface salinity maximum (36.6°/oo) which is characteristic of LCW. The thermocline dissipated over the outer slope and the volume of near-bottom, cold temperatures decreased. Upslope movement of low oxygen, high nutrient water associated with the 26.5 isopycnal was observed during the toward-shelf movement of the Loop Current. A progressive doming of isopycnals and isotherms relative to the initially level isolines was observed during the toward-shelf movement of the current. The low salinity layer at the surface is believed to originate in the northern Gulf, possibly from the Mississipi delta. The changes in volume of the low salinity layer were probably related to alongshelf currents, although there are indications that the volume decreased with the toward-shelf movement of the current. The water masses found during this study were: LCW at the outer stations of the transects occupied during the toward-shelf movement of the

current and CEW at the remainder of the stations. Finestructure was present at those stations on the western end of the sampling cross-sections and indicated diffusive mixing at the water mass boundaries.

The data show a large degree of hydrographic variability over short time scales (4 to 5 days) at the outer shelf. These variations appear to be related to the position of the Loop Current along the shelf break and to cross-shelf and alongshelf currents. Some of the changes that appear to correlate with shoreward movements of the Loop Current have been described; however, it is obvious that joint current meter/hydrographic studies are now required to understand shelf break processes, Loop Current interactions, and resulting variability in the outer shelf domain to a sufficient degree that reasonable Fates and Effects modelling of the shelf environment will be possible in the near future.

3.3 References

Atkinson, L.P. and D. Wallace 1975. The source of unusually low surface salinities in the Gulf Stream off Georgia, Deep-Sea Res., 23: 913-916.

Bane, J.M., Jr. and D.A. Brooks 1979. Gulf Stream meanders along the continental margin from the Florida Straits to Cape Hatteras, Geophys. Res. Lett., 6(4): 280-282.

Behringer, D.W., R.L. Molinari, and J.F. Festa 1977. The variability of anticyclonic current patterns in the Gulf of Mexico, J. Geophys. Res., 82(14): 5469-5476.

Chandler, W.S., L.P. Atkinson, J.J. Singer, P.G. O'Malley, and C.V. Baker
1978. A CTD system: Description, operation, data acquisition and
processing. Georgia Mar. Sci. Center, Univ. Syst. of Georgia, Tech. Rept.
Ser. No. 78-7: 84 pp.

Glibert, P.M. and T.C. Loder 1977. Automated analysis of nutrients in
seawater: a manual of techniques, Woods Hole Oceanographic Institution
Technical Report, WHOIO-77-47, unpublished manuscript: 46 pp.

Hill, R.B. and J.A. Johnson 1974. A theory of upwelling over the shelf
break, J. Phys. Ocean., 4(1): 19-26.

Hsueh, Y. and J.J. O'Brien 1971. Steady coastal upwelling induced by an
alongshore current, J. Phys. Oceanogr., 1: 180-186.

Huh, O.K., W.J. Wiseman, Jr. and L.J. Rouse, Jr. 1981. Intrusion of Loop
Current waters onto the West Florida continental shelf, J. Geophys. Res.,
86(C5): 4186-4192.

Koblinsky, C.J. 1979. Tides on the west Florida shelf, Ph.D. Dissertation,
Oregon State University: 110 pp.

Lee, T.N. 1975. Florida current spin-off eddies, Deep Sea Res. 22:
753-765.

Lee, T.N. and L.P. Atkinson 1983. Low frequency current and tempe   ture
     variability from Gulf Stream frontal eddies and atmospheric   :cing along
     the southeast U.S. outer continental shelf, J. Geophys. Res   in press,
     April.

Lee, T.N., L.P. Atkinson, and R. Legeckis 1981. Observations of a ulf
     Stream frontal eddy on the Georgia continental shelf, April 1 7, Deep Sea
     Res., 28A(4): 347-378.

Leipper, D.F. 1970. A sequence of current patterns in the Gulf of exico,
     J. Geophys. Res., 75(3): 637-657.

Maul, G.A. 1977. The annual cycle of the Gulf Loop Current. Part   .
     Observations during a one-year time series, J. Mar. Res., 35:   9-47.

McClain, C.P. 1980. Multiple atmosphe. -window techniques for s: llite-
     derived sea surface temperatures, in Oceanography From Sp   . COSPAR/
     SCOR/IUCM Symposium, May 26-30, 1980, Venice, Italy.

Molinari, R.L., D.W. Behringer, and J.F. Festa 1976. A numerical   deling
     and observational effort to develop the capability to predict he currents
     in the Gulf of Mexico for use in pollutant trajectory comput ion: Model
     studies of the circulation in the Gulf of Mexico. Final r   )rt, BLM IA
     08550-IA5-26: 244 pp.

Molinari, R.L. and D.A. Mayer 1982. Current meter observations on the continental slope at two sites in the eastern Gulf of Mexico J. Phys. Ocean. 12(12): 1480-1492.

Morrison, J.M. 1977. Water mass properties used as flow indicators within the Eastern Caribbean Sea during the winter of 1972 and fall of 1973, Ph.D. Dissertation, Texas A&M University: 75 pp.

Morrison, J.M. nd W.D. Nowlin 1977. Repeated nutrient, oxygen and density sections through the Loop Current, J. Mar. Res., 35: 105-108.

Niiler, P.P. 1976. Observations of low-frequency currents on the West Florida shelf, in Memoires Societe Royale des Sciences de Liege, Vol. 10, Seventh Liege Colloquium on Ocean Hydrodynamics Continental Shelf Dynamics, J.C.J. Nihoul, ed: 331-358.

Nowlin, W.D., Jr. and H.J. McLellan 1967. A characterization of the Gulf of Mexico waters in winter, J. Mar. Res., 25: 29-59.

Posmentier, E.S. and C.B. Hibbard 1982. The role of tilt in double diffusive interleaving, J. Geophys. Res. 87(C1): 518-524.

Price, J.F. and C.N.K. Mooers 1974. Hydrographic data report from the winter 1973 NSF Continental Shelf Dynamics program. Sci. Rept. UMRSMAS 74006, U. Miami, Miami, FL: 61 pp.

Price, J.F. 1976. Several aspects of the response of shelf waters to a cold front passage, in Seventh Liege Colloquium on Ocean Hydrodynamics Continental Shelf Dynamics, J.C.J. Nihoul, ed.: 201-208.

Stefansson, U., L.P. Atkinson, and D.F. Bumpus 1971. Hydrographic properties and circulation of the North Carolina shelf and slope waters, Deep Sea Res., 18: 383-420.

Strickland, J.D.H. and T.R. Parsons 1965. A manual for sea water analysis, Bulletin Fisheries Res. Bd. Can., Vol. 125: 185 pp.

Vukovich, F.M., B.W. Crissman, M. Bushnell, and W.J. King 1979. Some aspects of the oceanography of the Gulf of Mexico using satellite and in situ data, J. Geophys. Res., 84(C12): 7749-7768.

Webster, R. 1961. The effect of meanders on the kinetic energy balance of the Gulf Stream, Tellus, 13: 392-401.

Wennekens, M.P. 1959. Water mass properties of the Straits of Florida and related waters, Bull. Mar. Sci. Gulf Carib., 9(1): 1-52.

Woodward-Clyde Consultants/Skidaway Institute of Oceanography 1982a. Southwest Florida shelf ecosystems study - Year 2, Cruise I summary cruise report, prepared under BLM Contract No. AA851-CT1-45.

Woodward-Clyde Consultants/Skidaway Institute of Oceanography 1982b.
Southwest Florida shelf ecosystems study - Year 2, Cruise II summary
cruise report, prepared under MMS Contract AA851-CT1-45.

Wüst, G. 1964. Stratification and circulation ion the Antillean-Caribbean
basins, Part 1, Columbia University Press, New York: 201 pp.

Yoder, J.A., L.P. Atkinson, T.N. Lee, H.H. Kim., and C.R. McClain 1981.
Role of Gulf Stream frontal eddies in forming phytoplankton patches on the
outer southeastern shelf, Limnol. Oceanogr., 26(6): 1103-1110.

4.0 MIXING PROCESSES

ERIC POSMENTIER
SOUTHAMPTON COLLEGE OF LONG ISLAND UNIVERSITY

4.1 Introduction

East/west movements of the Loop Current and the passage of frontal events such as eddies all impact upper slope and shelf water masses by advection or mixing on a localized scale. The frontal analyses and hydrographic data demonstrated the large scale advection that occurred during the passage of the frontal eddy, and the TS plots (e.g., Figure 3-39, Station 34) indicated the occurrence of a finer scale mixing. The characteristics of this mesoscale mixing will, to a large extent, determine the environment experienced by the regional ecosystem.

The objective of this section, therefore, is to analyze portions of the previously discussed (in Section 3.0) hydrographic data from a mixing processes point of view in order to characterize the observations in terms of numerical diffusivity rates. Estimates for diffusivity coefficients are, of course, the types of tools that future Fates and Effects modellers will need to simulate these types of processes.

Three steps are taken to develop an understanding of the cross-shelf mixing process. First, salinity anomaly diagrams for five of the spring cruise sections are developed and discussed with respect to salient mixing features. Second, length scales are evaluated along east-west, sigma-t sections to quantify some of these features. A consideration of the

kinetics* involved in the processes provides the third ingredient for the parameterization estimates.

4.2 Hydrography

Consider a slightly modified version of the standard salinity cross-section plots presented in the previous section (3.0). Instead of contouring the values in x-z (longitude-depth) space, replace the ordinate with σ_t and contour around a mean salinity of 36.0°/oo. That is, develop isopleths of

$$(salinity - 36.0) \times 100$$

in $x - \sigma_t$ space. This is the same nomenclature used in Section 3.2.1.4 for the salinity anomaly diagram presented in Figure 3-40. Deviations from a mean salinity at a particular density value give a spatial representation of mixing between water masses since density generally increases with pressure or depth. The advantage of such a representation is its graphical ability to show coherent inter-station features directly. This is a result of the fact that many oceanic processes such as mixing, interleaving, or even many aspects of upwelling tend to be quasi-lateral in nature and align with isopycnals more readily than isobars.

Figures 4-1 through 4-5 present $x - \sigma_t$ cross sections for the salinity data taken during the spring cruise on Sections 1, 2, 5a, 6, and 8, respectively. The contour interval has been chosen as 10 units, or 0.1°/oo. The uppermost heavy line is the surface; the lowermost stipled line is the bottom. These sections are analogous to Figures 3-8, 3-13, 3-23, 3-28, and 3-35, respectively. In each of these sections, note how the isohalines appear to elongate in the lateral direction; this is an indication of

---

* Kinetics is a branch of dynamics that deals with the effects of forces in causing or changing the motion of objects (Neumann and Pierson, 1966).

198
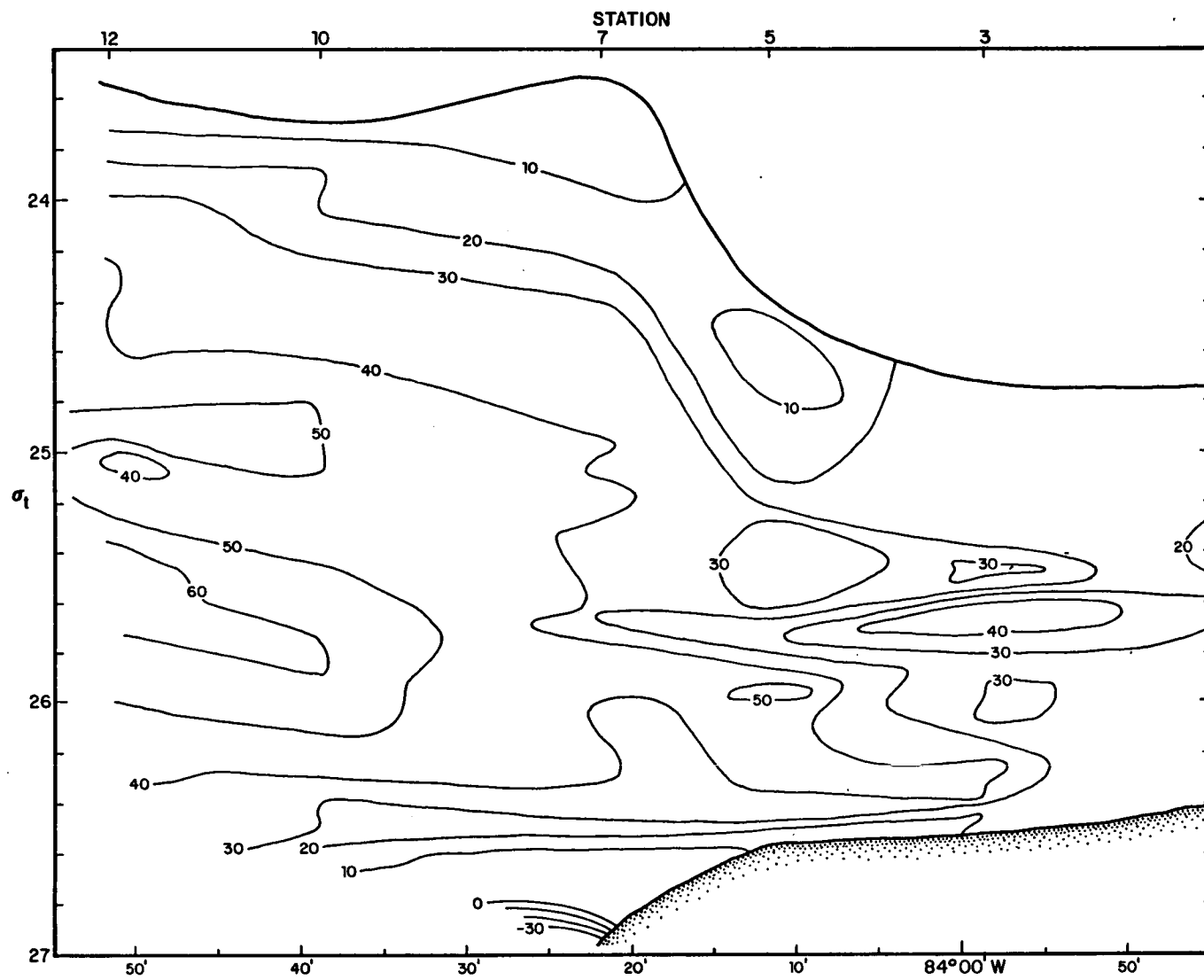
Figure 4-1.   Spring cruise, transect 1 salinity anomaly section in x − σ_t space.

199

Figure 4-2.   Spring cruise, transect 2 salinity anomaly section in x - σ_t space.

Figure 4-3.   Spring cruise, transect 5a salinity anomaly section in $x - \sigma_t$ space.
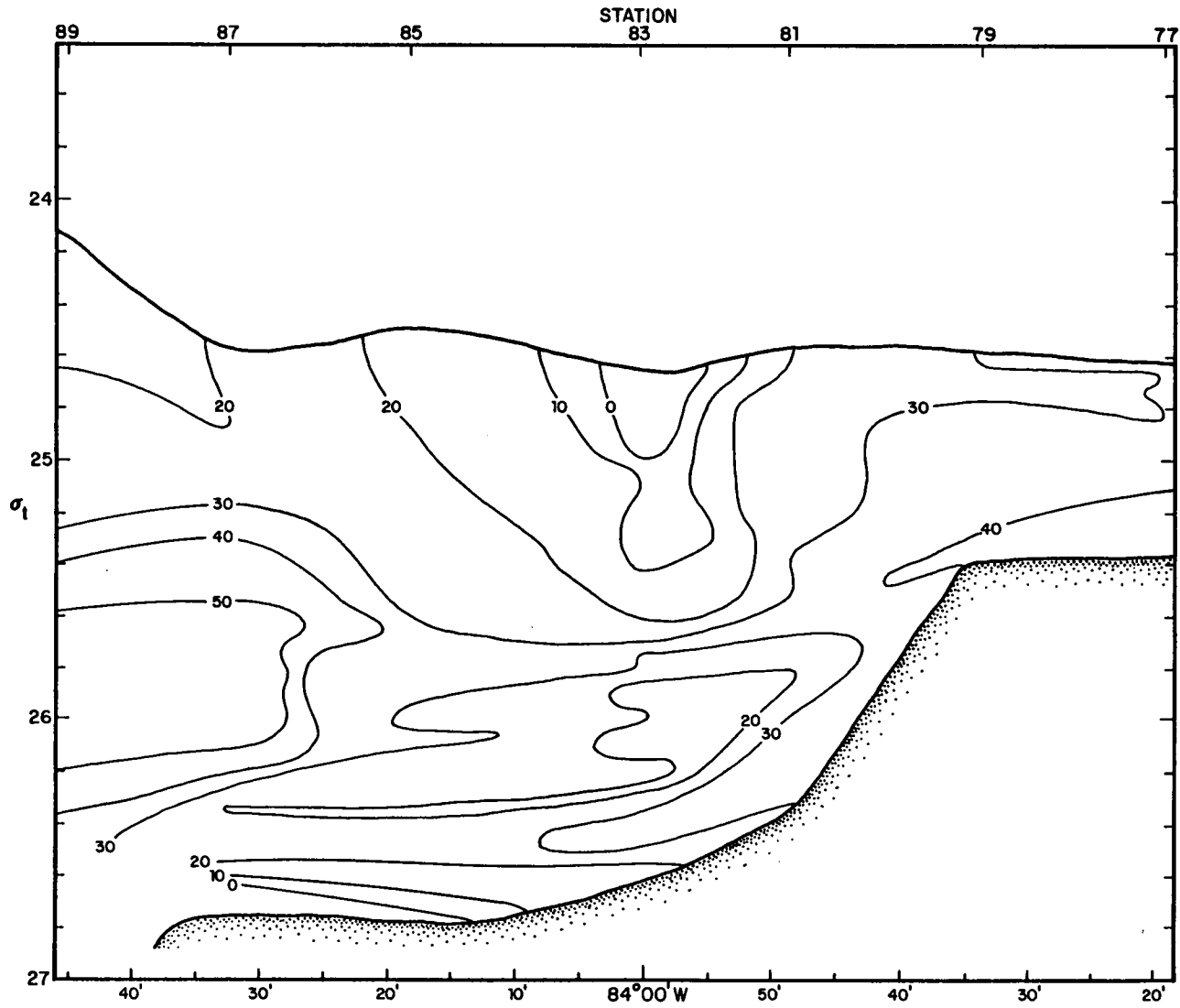
Figure 4-4. Spring cruise, transect 6 salinity anomaly section in x - σ_t space.
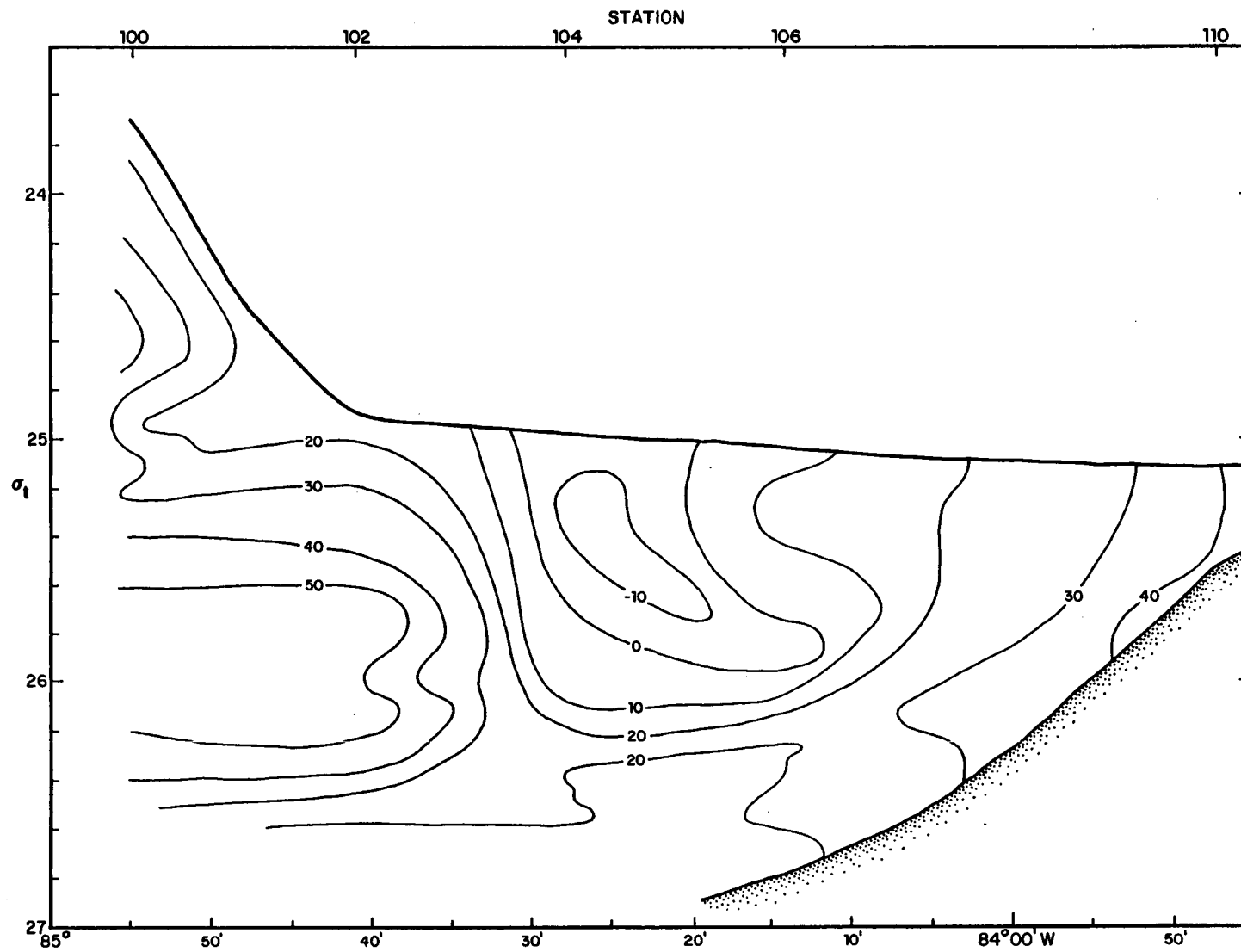
Figure 4-5.   Spring cruise, transect 8 salinity anomaly section in x − σ_t space.

interleaving or mixing along σ_t surfaces. The interleaving was most pronounced between Stations 83 and 87 (in Figure 4-4) which coincided with the location of the front between Loop Current Water (LCW) and Continental Edge Water (CEW). It was also prominent between Stations 81 and 83 which coincided with the surface front between the cold CEW region and the LCW filament. The interleaving was coherent over several stations and strongest where isotherms and isohalines slope steeply but isopycnals were nearly horizontal. Interleaving along water mass boundaries was evident in all sections; its presence implies mixing and exchange of heat and salt as a result of the frontal eddy intrusion. Other features worth noting in these figures are:

- the salinity maxima of 36.5 to 36.6°/oo (50 and 60 isopleth, respectively) near $\sigma_t = 26$ in Figures 4-1, 4-3, 4-4 and 4-5 at the western end of the transects; these regions are indicative of LCW, and

- the salinity minima (temperature minima) near Station 58 in Transect 5 (Figure 4-3), Station 85 in Section 6 (Figure 4-4), and Station 104 in Transect 8 (Figure 4-5); these minima were strongest near the surface and penetrated into the water column. These features were the tongue of CEW between the main body of LCW and the filament.

At the shallower, eastern end of the transects, the salinity (and temperature) rose again as the LCW was reentered in the filament which separated from the main body. This separation was most apparent in the northernmost section (Figure 4-5).

204

Another way of looking at this concept of mixing between two water masses is to contour the observed salinities on a particular σ_t surface similar to that presented in Figure 3-40. For convenience, Figure 3-40 is reproduced as Figure 4-6 with selected labelling of sections and stations. Again, the lower left-hand corner is situated at 25°30'N, 85°00'W; the contour intervals are the same as in Figures 4-1 through 4-5; and the surface is σ_t = 25.25. The strongest manifestation of CEW is at the upper left-hand side of the diagram progressing down (southward) the center and toward the right (east) in a tongue-like fashion. Warmer, saltier LCW lies on both sides of the CEW tongue--to the west is the main body; the filament lies to the east. The southward weakening of the tongue suggests a possible connection between the main body and the filament to the south (beyond the southward extent of the diagram).

This interpretation is further supported by plotting representative station data on a TS diagram. Figure 4-7 presents such a plot for all data less than 25°C for Stations 12 (solid graph), 24 (dashed), 34 (dotted), and 104 (also solid). The relative positions of these stations are shown in Figure 4-6. Stations 12 and 24 are both the highest salinities found at any density, but are at the western and eastern ends, respectively, of their transects. Their relative positions in the TS diagram, however, confirms the contention that the filament and the main body of LCW are of the same water type. Station 104 is representative of the low salinity stations in the tongue of CEW. It is clearly a distinct water type, not produced by mixing different parts of LCW or by local cooling.
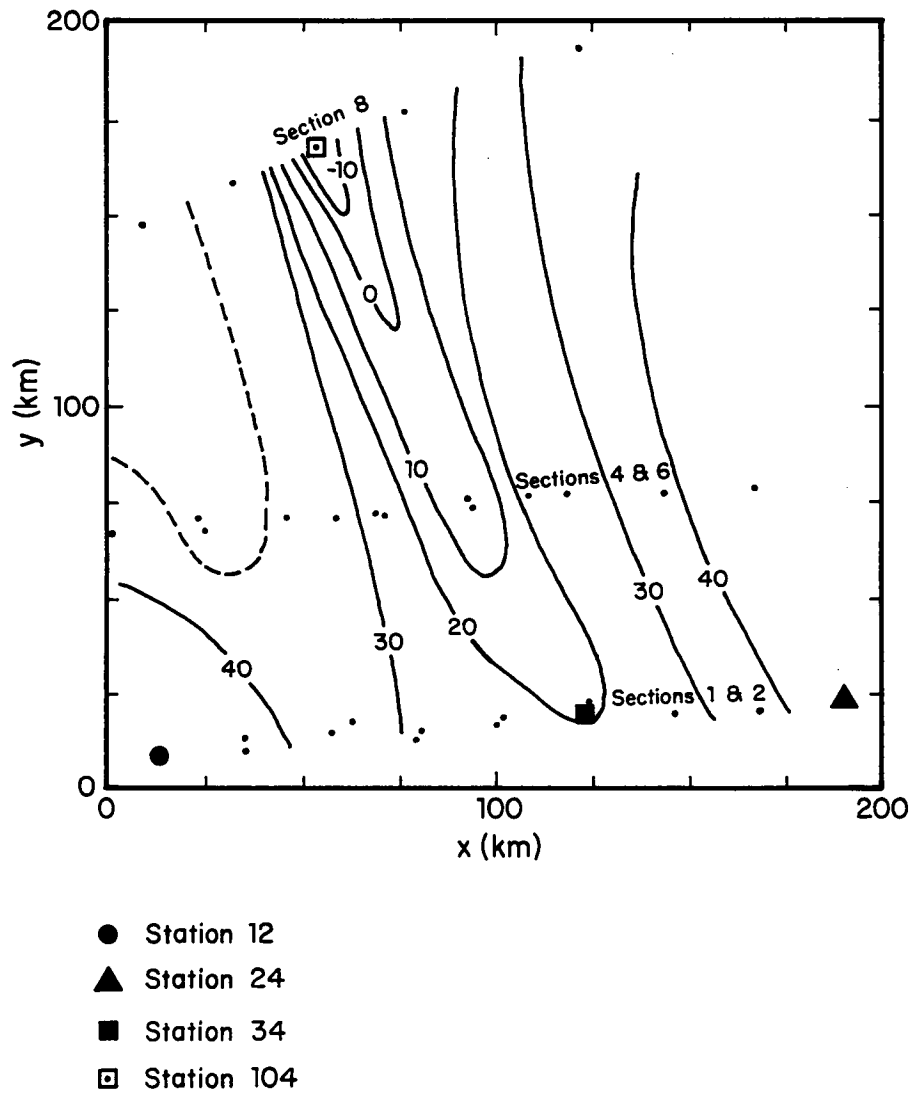
Figure 4-6.   Salinity anomaly diagram on sigma-t = 25.25
(after Figure 3-40) with annotated transect
and station locations.

206
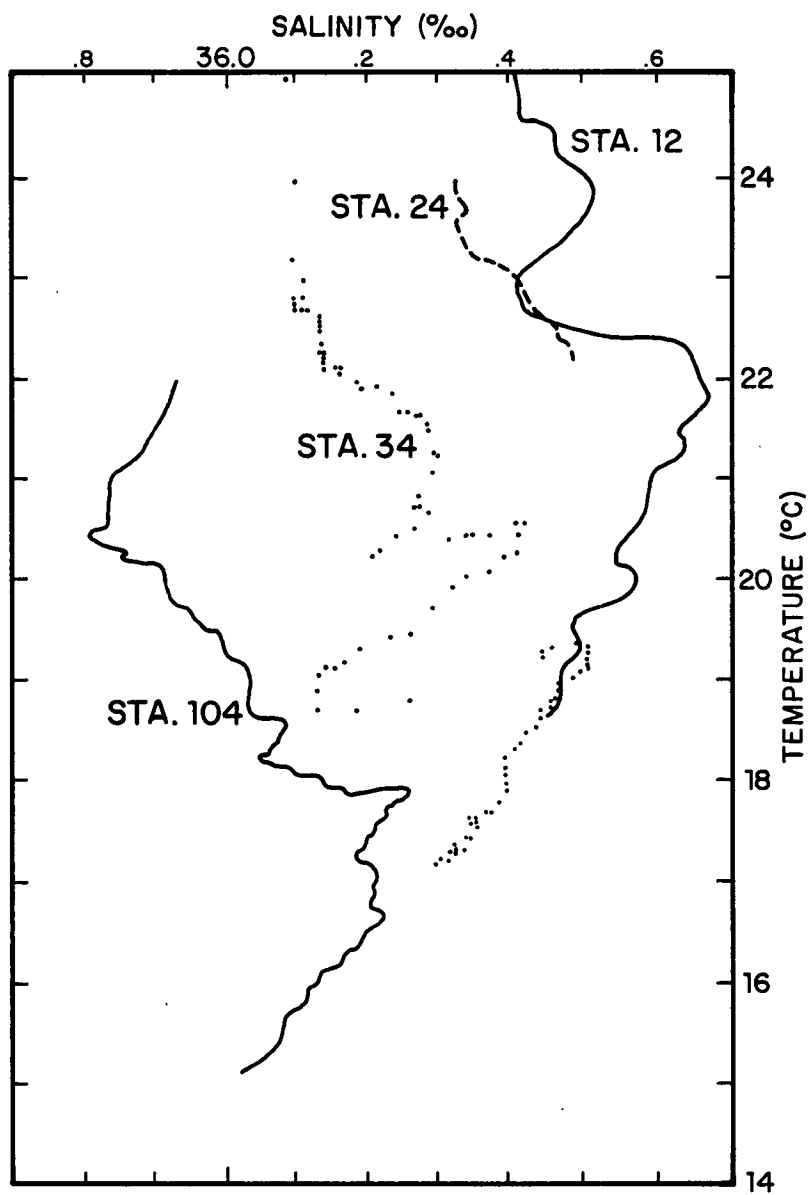
Figure 4-7.   TS diagram for stations 12, 24, 34, and 104.

The data at Station 34 are indicative of stations in the frontal zone between LCW and CEW. They exhibit pronounced interleaving which may be caused by double diffusion as discussed by Posmentier and Hibbard (1982). Further, interleaving almost certainly caused double diffusion in both the salt fingering and temperature diffusion regimes since several high gradient interfaces between interleaving layers exhibited nearly compensating vertical gradients of temperature and salinity.

4.3 Correlation Analysis

A correlation analysis was performed on the hydrographic data following a procedure similar to that used by Halliwell and Mooers (1979) and by EG&G (1980). Two modifications were made in the technique. First, the correlation was performed among salinity data on several isopycnal surfaces, rather than on horizontal surfaces. The advantages of this method are the same as those of plotting sections in $x - \sigma_t$ planes, rather than $x - z$ planes, as discussed above. The second modification was to calculate correlations using all pairs of stations where both of each pair are on the same approximately east-west transect line (but different pairs from different transect lines were combined) and where the eastward component of separation between each pair was between $x \pm 12.5$ km. Thus, the correlation function R was a function only of x, for each value of σ_t. The northward separation was not used as a second independent variable because of the small number of CTD transect lines and because they were roughly equally-spaced.

The actual function, R, incorporating the above modifications, is written below. The program used to calculate the function appears in Appendix A.4.

$$R(x) = U/V$$

where

$$U = \sum_{1}^{N} A_i B_j$$

and

$$V^2 = (\sum_{1}^{N} A_i^2)(\sum_{1}^{N} B_j^2).$$

In the above expressions, A_i and B_j are salinities at density σ_t at CTD stations i and j, decremented by the mean salinity over all stations i and j. Stations i and j are both on the same transect line; their eastward separation is $x \pm 12.5$ km. N is the number of such pairs.

The results of the correlation analysis for the spring cruise data are shown in Figure 4-8. The graphs show the correlation values R for (eastward separation) for every 6 km from 0-120 km, at σ_t = 24.75, 25.25, and 25.75. The solid dots represent R values based on at least 5.7 pairs of stations; the open circles are based on fewer than six. The solid dots obviously have greater statistical significance. The main inference which may be drawn from these results is that the correlation falls off on a spatial scale of roughly 30 km, indicating that the cross-shelf scale of salinity variability on isopycnal surfaces is roughly 30 km. This agrees with the widths of the "filaments" discussed in Section 3.2.1.2, and is consistent with one-fourth the scale of the full width across the low salinity anomaly in Figure 4-6.
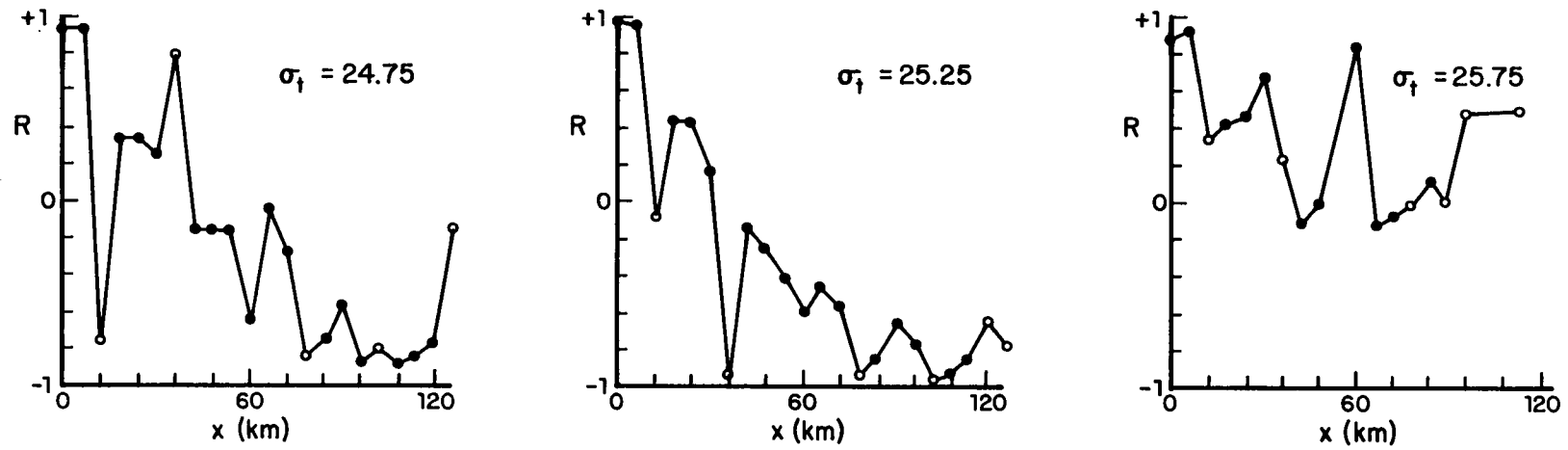
Figure 4-8. Spring cruise correlation analysis results on sigma-t surfaces.

In extending the correlation analysis to investigate seasonal differences, the salinities recorded along Transects 2, 3, and 4 on the 23.00, 24.25, and 25.50 sigma-t isopycnals in the summer cruise data set were used. The mean salinities on each isopycnal were computed for each section. One of these nine means was subtracted from each salinity. Since the same transect was run as a time series during this cruise, the correlation analysis used pairs of salinities from both the same section and combined pairs from all three sections (Figure 4-9). At the two shallower levels (of sigma-t at 23.00 and 24.25), the correlations drop rapidly to zero and remain small; this is because the scales are mostly separated by one station interval or less (about 16 km). This feature is especially evident on the 23.00 isopycnal where salinities deviated from the transect means by only about $\pm 0.1°/oo$.

On the other hand, the deepest isopycnal showed a correlation that dropped to a minimum at a 37.5 km lag and increased at greater lags. At this depth, all sections exhibit a maximum of 36.58 to 36.70°/oo at the deepest station in LCW. A salinity minimum is evident in the middle of the sections. The correlation at 25.50 thus reflects the presence of a low salinity region with a scale of roughly 75 km. This scale is similar to the lower salinity region present during the spring cruise.

4.4 Kinetics

It is of interest to examine the consistency of a few hydrodynamic quantities with the circulation inferred from hydrographic considerations. The first quantity is the baroclinicity in the region of the front between the main body of LCW and the tongue of CEW. For this purpose the densities at

211
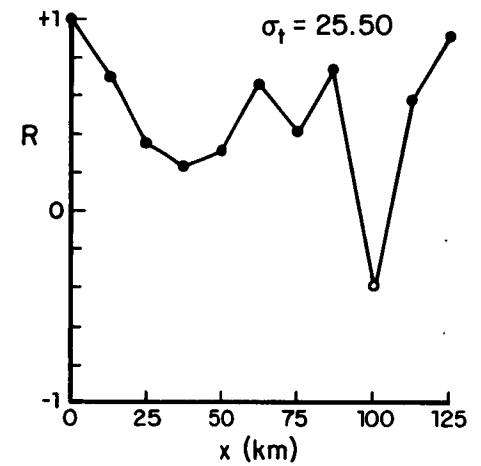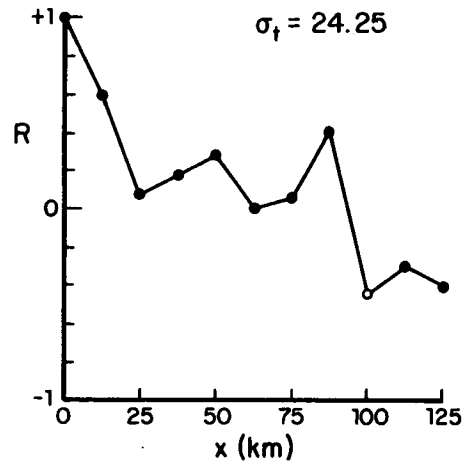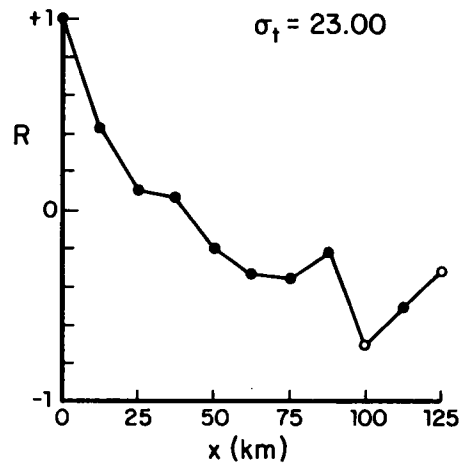
Figure 4-9.   Summer cruise correlation analysis results on sigma-t surfaces.

Stations 100 and 102 were used to estimate the geostrophic shear between the surface and 80 m. (The significance of this depth is discussed below.) The result is a speed of 51 $cm \cdot sec^{-1}$ northward at 80 m relative to the surface. There is order of magnitude agreement between this result and the region's dynamic topography according to Nowlin and McLellan (1967).

The second quantity is the potential energy associated with the upwelling. The density profiles of stations typical of the main body of LCW and of the filament of LCW (for example, Stations 12 and 24, in Figure 4-10) are offset by about 80 m in depth. The same depth difference occurs between corresponding points in their coinciding TS relationships (Figure 4-7). It may therefore be inferred that the filament of LCW on the shallow shelf was contiguous with 80 m deeper LCW in the main body of LCW to the west. The density differences between the deep and shallow stations average roughly 1.4 $x \ 10^{-3} \ g \cdot cm^{-3}$. The increase of potential energy which would occur during 80 m of elevation during which the density anomaly increases gradually from 0 to 1.4 $x \ 10^{-3} \ g \cdot cm^{-3}$, is equivalent to the kinetic energy of the geostrophic velocity discussed above is almost the correct magnitude to provide the necessary potential energy for the communication between the main body of LCW and the shallower LCW filaments.

The third calculation concerns the vorticity differences between the LCW main body and the filament. Consider a scenario in which a current extending from the surface to 160 m and leaving no relative vorticity is funneled into 80 m where its combined planetary and relative vorticities are the same as the original planetary vorticity. The resulting relative vorticity is 3.2 $x \ 10^{-5} \ sec^{-1}$, which is equal to 64 $cm \cdot sec^{-1}$ per 20 km, a velocity and
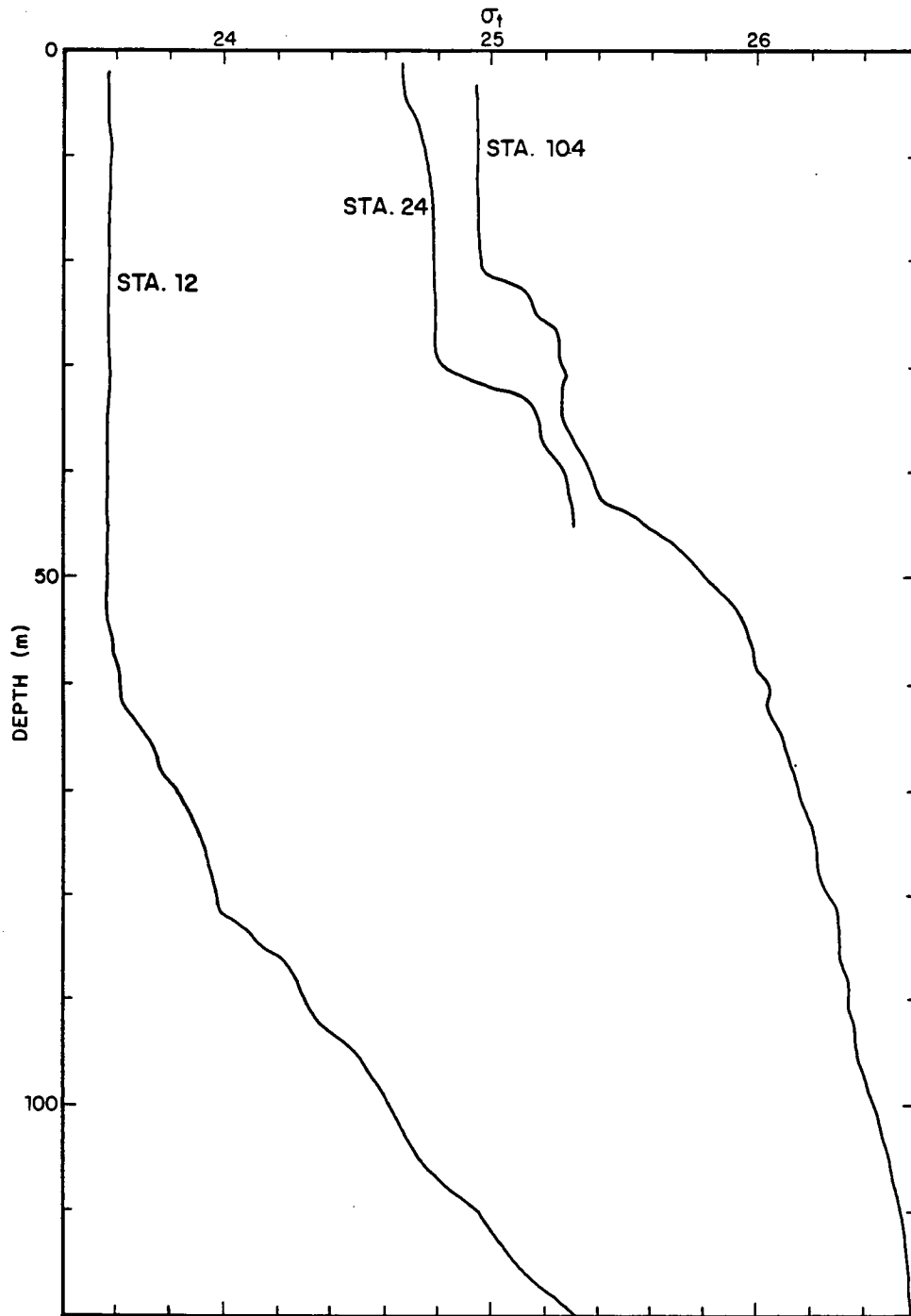
Figure 4-10. Density profiles for spring cruise stations 12, 24, and 104.

distance in good agreement with the geostrophic and upwelling energy speeds, and with the filament half-widths, respectively. This agreement shows that the topographic effect of moving 160 m of LCW onto an 80 m deep shelf would cause an anticyclonic vorticity on the shelf comparable in magnitude to the observed vorticities.

4.5 Cross-Shelf Mixing

There are several crude but useful approaches to obtaining order-of-magnitude estimates for an effective lateral diffusion coefficient (K_H) of the processes under discussion. Taking the cross-shelf displacements of the filaments from their main bodies as 100 km, and an event frequency of once per month, results in $K_H = 4 \times 10^7$ $cm^2 \cdot sec^{-1}$. From a different point of view, if six layers of interleaving, each 10 m thick, are displaced 10 km cross-shelf every day, and if their effect on cross front exchanges is distributed over a 100 m depth, this corresponds to

$$K_H = (10 \text{ km})^2 \cdot (6 \text{ layers}) \cdot (10 \text{ m})/100 \text{ m } /1 \text{ day} = 0.7 \times 10^7 cm^2 \cdot sec^{-1}.$$

Yet another estimate may be obtained by scaling down the K_H for heat for double diffusive intrusions derived by Posmentier and Hibbard (1982). Their theoretical value was $K_H = 3.7 \times 10^7$ $cm^2 \cdot sec^{-1}$ for a normalized interleaving factor of 1°/oo. In this case, the amplitude of interleaving is 0.2°/oo so that K_H is reduced by a factor of $(0.2°/oo/1°/oo)^2$. The result is $K_H = 0.15 \times 10^7$ $cm^2 \cdot sec^{-1}$. The range of these three estimates is not disturbingly large considering the degree of approximation. Their trend of decreasing K_H with decreasing spatial scale of corresponding

phenomenon, however, is consistent with the fact that these hydrographic features are not completely dissipated by the next smaller scale process before the next event occurs.

4.6 Conclusions

As a consequence of LCW filament and front intrusion on the shelf, interleaving of isohalines occurred along both boundaries of the CEW region. This interleaving was indicative of mixing between the two water masses.

The filament of LCW which separated from the main body encompassed a tongue of CEW and gradually caused a mixing of water masses. Correlation analyses across the shelf during the intrusion showed length scales to be on the order of 30 to 40 km. Order-of-magnitudes estimates for the effective lateral diffusion coefficient yielded estimates on the order of $0.15 - 4.00 \times 10^7$ $cm^2 \cdot sec^{-1}$.

4.7 References

EG&G 1980. New England OCS physical oceanography program. Appendix F of thirteenth quarterly progress report, BLM Contract No. AA551-CT8-46.

Halliwell, G.R. and C.N.K. Mooers 1979. The space time structure and variability of the shelf water - slope water and Gulf Stream surface temperature fronts and associated warm core eddies. J. Geophys. Res., 84(C12): 7707-7725.

Nowlin, W.D. and H.J. McLellan 1967. A characterization of the Gulf of

    Mexico waters in winter. J. Mar. Res. 25: 29-59.

Posmentier, E.S. and C.B. Hibbard 1982. The role of tilt in double

    diffusive interleaving. J. Geophys. Res. 87(C1): 518:524.

5.0 PRIMARY PRODUCTION IN LOOP CURRENT UPWELLING

JAMES A. YODER

SKIDAWAY INSTITUTE OF OCEANOGRAPHY, UNIVERSITY SYSTEM OF GEORGIA

ALBERT MAHOOD

SAN RAFAEL, CA.

5.1 Introduction

The objective of this portion of the Southwest Florida Shelf Ecosystems Study was to determine whether upwelling induced by Loop Current eddies and meanders resulted in enhanced primary production on the outer southwest Florida shelf. Up until this study, this question had not been adequately addressed for this region. Recent studies off the southeastern continental shelf between Cape Canaveral, Florida and Cape Hatteras, North Carolina were used as a model to plan the study for the southwest Florida shelf. Both locations are subtropical and both have strong western boundary currents that flow along the shelf break.

The cyclonic side of the Gulf Stream front is generally located near the 200 m isobath along the southeastern shelf. The front is "disturbed" by meanders and eddies that propogate northward with a frequency of one every five to 14 days (Vukovich et al. 1979; Lee et al., 1981). In response to these "disturbances", nutrient-rich waters upwell at the shelf break and intrude onto the shelf (Lee et al., 1981). The distance that intrusions of upwelled waters penetrate across the shelf depends on the shelf topography and meteorological and oceanographic conditions, including wind direction-velocity and the degree of water column stratification (Blanton et al. 1981). In general, nutrient-rich upwelled waters reach the outer shelf (40 to 200 m isobaths) during all seasons of the year, reach the middle shelf (20 to 40 m isobaths) during warmer months of the year when the shelf is

stratified, and reach the inner shelf (0 to 20 m isobaths) only south of Jacksonville, Florida during warmer months of the year.

Relatively high concentrations of phytoplankton and zooplankton develop within upwelled waters on the southeastern shelf (Dunstan and Atkinson, 1976; Atkinson et al., 1978; Bishop et al., 1980; Yoder et al., 1981a; Yoder et al., in press). On the outer shelf where upwelling occurs throughout the year, primary and "new" production are relatively high at about 300 to 400 $gC \cdot m^{-2} \cdot yr^{-1}$ with about 50% new production (Yoder et al., in press). When upwelled waters reach the middle shelf, primary production is about $2 \ gC \cdot m^{-2} \cdot day^{-1}$ (Yoder et al., in press). Yoder et al., (1981b) concluded that upwelling and intrusion of offshore nutrients are the principal processes controlling biological productivity of the outer southeastern shelf.

The analyses presented in this section represent the first primary productivity studies of this nature for the Gulf of Mexico Loop Current near the shelf break of southwest Florida.

5.1 Methodology

All water samples for chlorophyll, primary production, and cell count measurements were obtained from Niskin bottles attached to the rosette of the CTD. These procedures have been described earlier in Section 3.2.1.1

Immediately after sample collection, replicate 50 ml water samples were filtered through 25 mm diameter, 0.45 μm pore diameter glass fiber filters. Filters were frozen and then analyzed for Chlorophyll a (Chl a) and

Pheopigment a (Ph a) in the laboratory after the cruise. The acid ratio, fluorescence method of Yentsch and Menzel (1963) as described by Strickland and Parsons (1972) was used to determine Chl a and Ph a. The fluorometer was calibrated with pure Chl a obtained from Sigma Chemical Company using extinction coefficients measured with a Shimadzu spectrophotometer.

Primary production was determined with the ^{14}C method first described by Steemann-Nielsen (1952). For each productivity station, water samples were collected from depths representing 100, 50, 25, 10, 5, and 1% of incident irradiance. Five μ-Curies of ^{14}C-sodium bicarbonate (pH = 8) were added to water samples dispensed into 125 ml glass bottles. The bottles were sealed and placed within sacks constructed of neutral density plastic screen. The sacks were then placed in one of two plexiglass tanks located on the deck of the ship. The temperature of each of the two tanks was independently regulated by cooling/heating baths so that the incubation bottles were kept within about 3°C of the in-situ water temperature at the depth from which each sample was collected. After 24 hours, the bottles were removed from the tanks, and three 8 ml aliquots from each bottle were placed in liquid scientillation vials and treated by the acid bubbling method described by Schindler et al. (1972), with the modifications described by Wessels and Birnbaum (1979). For each experiment, the acid-bubbling method was also used to determine six replicate "zero-time" blanks. Radioactivity of each vial was determined by liquid scintillation counting. Standard procedures were followed to determine quench and to calibrate the ^{14}C-sodium bicarbonate stock solution. Counts of the zero-time blanks were subtracted from the mean count of each sample. Results were then expressed in $mgC \cdot m^{-3} \cdot hr^{-1}$.

Integral production was determined by linearly integrating production with depth and expressed as $gC \cdot m^{-2} \cdot day^{-1}$.

Cell count samples (300 ml) were preserved with hexamine-buffered formalin following a procedure recommended by Dr. Greta Fryxell of Texas A&M University. One hundred to 400 ml aliquot samples were settled and examined under high magnification. An Olympus IM inverted microscope, equipped with Nomarski interference contrast, phase contrast, and brightfield illumination was used for identification and counting.

During the spring cruise, surface water was continuously pumped through the hull of the ship, through a Turner Designs Model 10 fluorometer, and then past the sensors of the CTD (see Section 3.2.1.1). The fluorometer was equipped with appropriate filters to determine in vivo Chlorophyll a fluorescence (Strickland and Parsons, 1972). At periodic intervals (0.5 to 1.0 hrs), surface water samples were collected with a bucket and the Chlorophyll a and Pheopigment a concentrations were determined as described above. These samples were used to calibrate the in vivo fluorescence readings. The coefficient of variability for the factor relating Chl a to in vivo fluorescence was 17% (n = 60) and 38% (n = 60) for the factor relating in vivo fluorescence to Chl a + Ph a.

The depths of the required isolumes were provided by the onboard optical oceanography group during the spring cruise (see Section 6.0). During the summer cruise, a spherical quantum sensor (LI-COR, Inc., Model #LI-193) was used to determine underwater irradiance (400 to 700 nm) between the surface and to depths of 30 to 35 m. These readings were used to determine the mean

attenuation coefficient which was used to estimate the depths of various isolumes. A listing of the determined attenuation coefficients for five selected summer cruise stations is presented in Appendix A.8.

5.3 Seasonal Characteristics

5.3.1 Spring Cruise Data

5.3.1.1 Primary Production

As discussed in Section 3.2.1.3, most of the stations occupied during the spring cruise were along transects that crossed through "domed" nutrient and density isopleths --- i.e., the defined structure of an eddy. Also, highest Chl $\underline{a}$ concentrations occurred near the top of the nitracline (below the surface mixed layer) which occurred at depths of 40 to 50 m within the core of the eddy (Figures 3-43 through 3-47). Surface mixed layer Chl $\underline{a}$ concentrations were always less than 0.25 mg·m^{-3} and generally less than 0.10 mg·m^{-3}.

Table 5-1 presents a list of the integrated euphotic zone Chl $\underline{a}$ and primary production results for the 15 spring cruise productivity stations. Table 5-2 summarizes these values according to three depth ranges. Productivity of the two stations shoreward of the 100 m isobath were not directly affected by nutrients upwelled by the eddy, since nitrate was very low (less than 1.0 μM) throughout the water column. The nine stations occupied between the 100 to 200 m isobaths were in the region most affected by eddy-induced upwelling. Three of the four stations offshore of the 200 m isobath were also affected

Table 5-1. Euphotic zone Chl a and daily primary production for spring cruise stations.

Station Number	Chl a $(mg \cdot m^{-2})$	Primary Production $(gC \cdot m^{-2} \cdot day^{-1})$
1	15.0	0.6
5	13.0	0.2
12	5.0	0.1
24	5.0	0.4
30	8.0	0.5
34	7.0	0.5
38	10.0	0.7
57	9.0	0.6
59	6.0	0.5
61	10.0	0.5
77	2.5	0.5
81	11.0	0.6
85	10.0	0.4
100	9.0	0.7
104	9.0	0.7

Table 5-2 Summary of euphotic zone Chl $\underline{a}$ and primary production by depth
ranges for spring cruise.

Chl $\underline{a}$ $(mg \cdot m^{-2})$

Isobath (m)	Number of Stations	Range	Mean (S.D.)
< 100	2	2.5 - 5	4 (0)
$\sim 100 - 200$	9	6 - 15	10 (3)
> 200	4	5 - 10	9 (2)

Primary Production $(gC \cdot m^{-2} \cdot day^{-1})$

Isobath (m)	Number of Stations	Range	Mean (S.D.)
< 100	2	0.4 - 0.6	0.45 (0)
$\sim 100 - 200$	9	0.2 - 0.8	0.5 (0.2)
> 200	4	5. - 10.	0.5 (0.3)

by upwelling associated with the eddy, whereas the station (i.e., Station 12) having the lowest productivity (0.1 $gC \cdot m^{-2} \cdot day^{-1}$) was within the Loop Current (See Figure 3-43). As illustrated in Table 5-2, average Chl $\underline{a}$ for the two shelf stations shoreward of the 100 m isobath was only about half that of the average for the other two isobath ranges (ca. 4 versus 9 to 10 $mg \cdot m^{-2}$). However, the mean rate of primary production was essentially the same (approximately 0.5 $gC \cdot m^{-2} \cdot day^{-1}$) for all three depth ranges.

Figures 5-1 to 5-4 show the relation between the major hydrographic features observed during the spring cruise and the vertical distribution of Chl $\underline{a}$ and primary production. Similar profile sets for all spring cruise productivity stations are presented in Appendix A.5. The nomenclature in all of these profile sets is the same; that is, sigma-t in the left-most graph is the dashed line, temperature (°C) is the solid line; Chl $\underline{a}$ ($mg \cdot m^{-3}$) in the center graph is the dashed line, nitrate (μM) is the solid line; primary productivity ($mgC \cdot m^{-3} \cdot day^{-1}$) in the right-most graph is the solid line. Station 12 (Figure 5-1) was the only productivity station occupied within the Loop Current (and thus seaward of upwelled density and nutrient isopleths). At this station, the top of the nitracline was below 80 m (and below the 1% light level), and primary production was the lowest observed during the spring study (0.1 $gC \cdot m^{-2} \cdot day^{-1}$). Mixed layer Chl $\underline{a}$ and production were relatively low (less than 0.1 $mg \cdot m^{-3}$ and less than 5 $mgC \cdot m^{-3} \cdot hr^{-1}$, respectively). A subsurface Chl $\underline{a}$ maximum (about 0.4 $mg \cdot m^{-3}$) was present near 80 m, but primary production in this layer was not determined because it was below the 1% level.

SIGMA T

CHL A (mg·m⁻³)

| 23 | 24 | 25 | 26 |

| 0.0 | 0.5 | 1.0 |

PRIMARY

TEMP (°C)

NITRATE (μM)
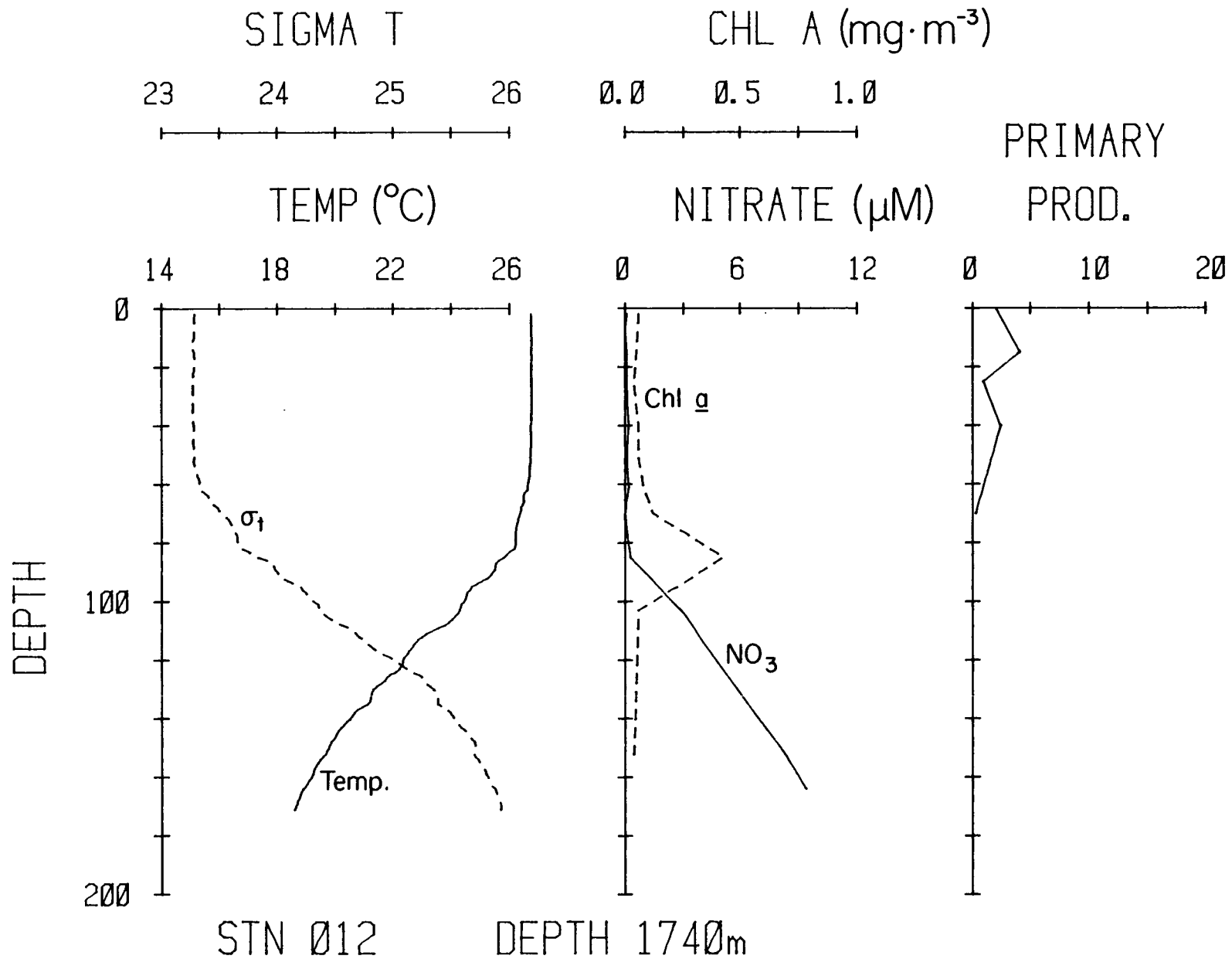
PROD.

Figure 5-1.   Vertical profiles for spring cruise station 12.
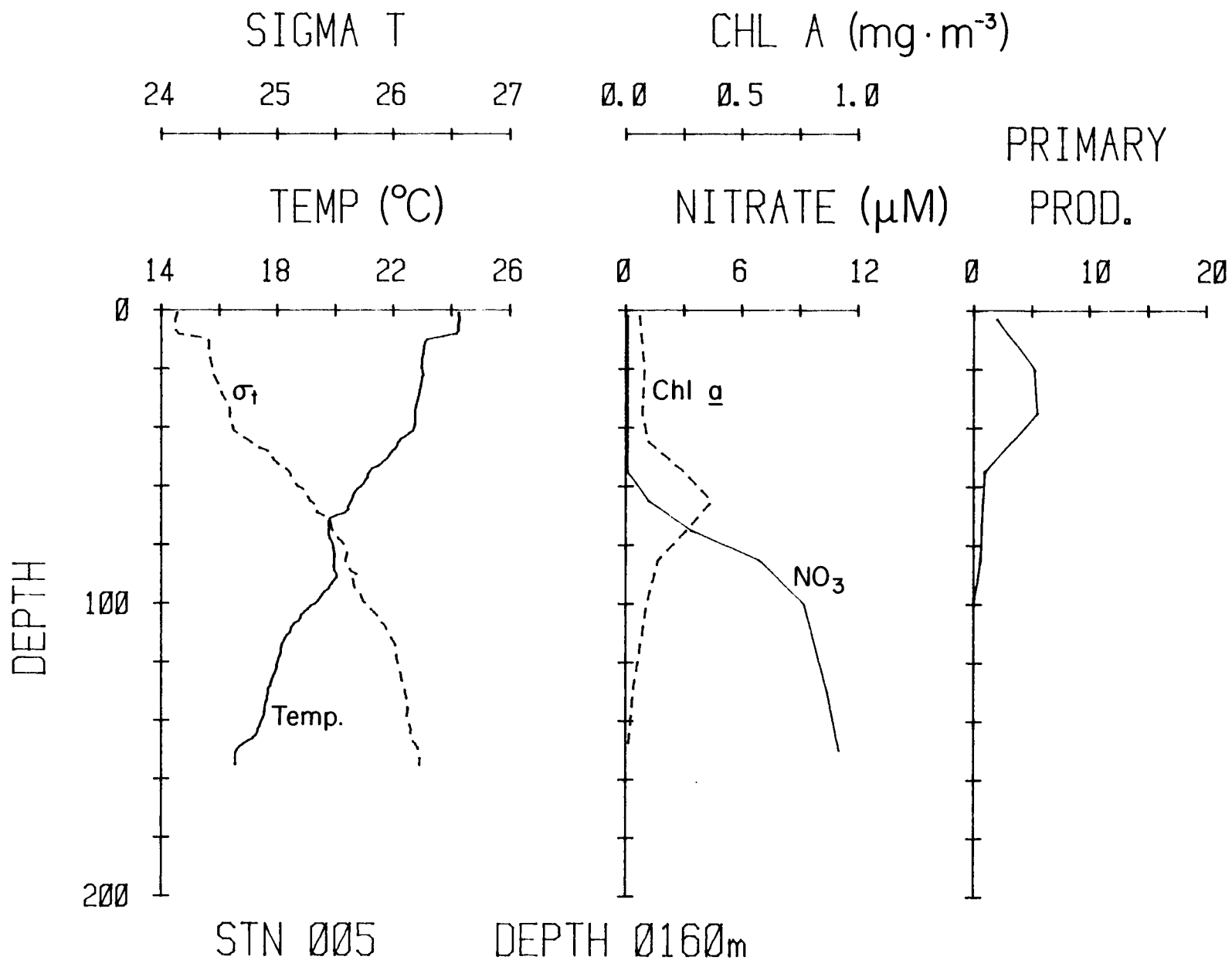
Figure 5-2.   Vertical profiles for spring cruise station 5.

228

SIGMA T

CHL A (mg·m⁻³)

TEMP (°C)

NITRATE (μM)

PRIMARY PROD.

STN 034   DEPTH 0157m
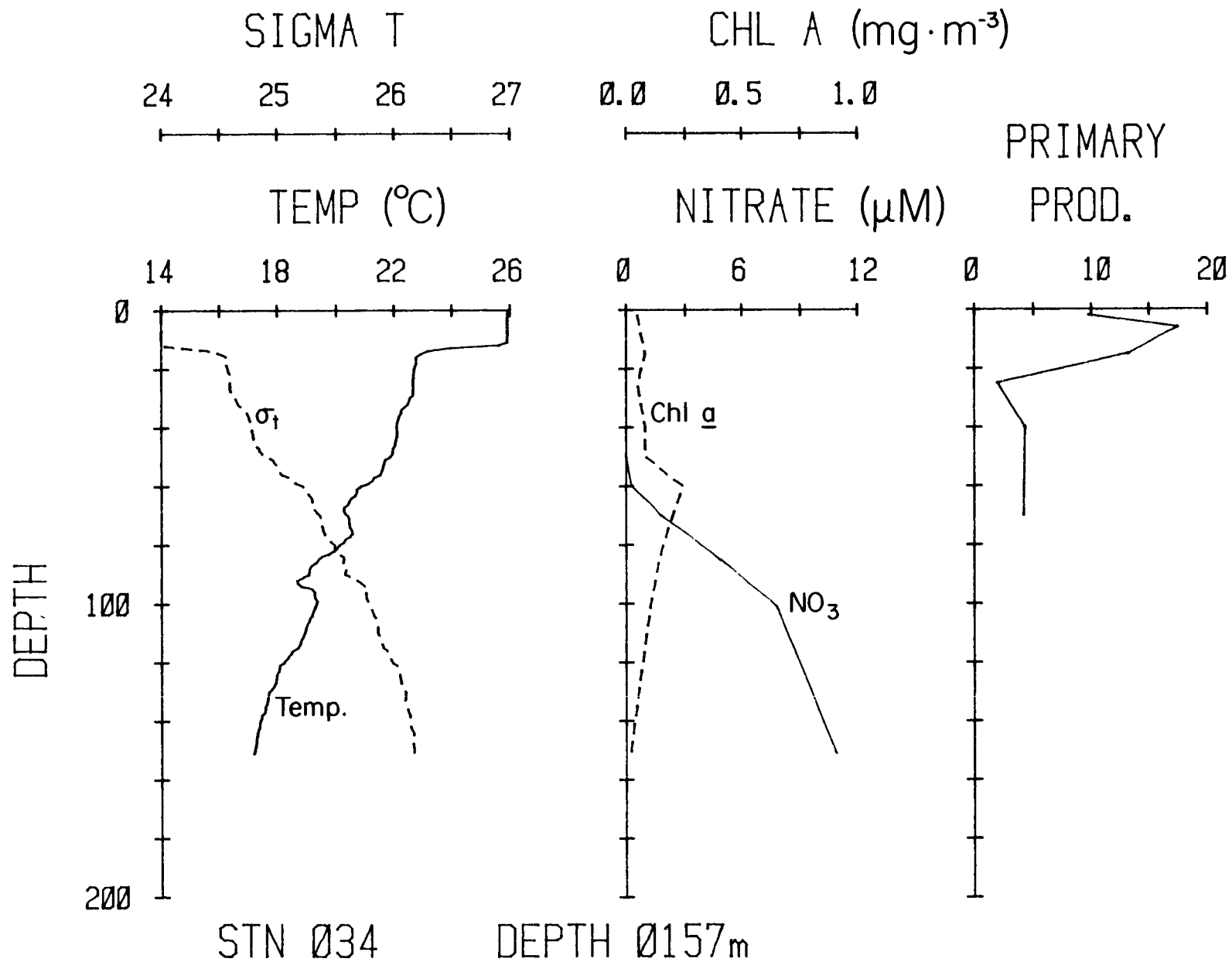
Figure 5-3.   Vertical profiles for spring cruise station 34.

SIGMA T

CHL A (mg·m⁻³)

23   24   25   26

0.0   0.5   1.0

PRIMARY
PROD.

TEMP (°C)

NITRATE (μM)

14   18   22   26

0   6   12

0   10   20

DEPTH

0

σₜ

Chl a

100

NO₃

Temp.

200

STN 100   DEPTH 1020m
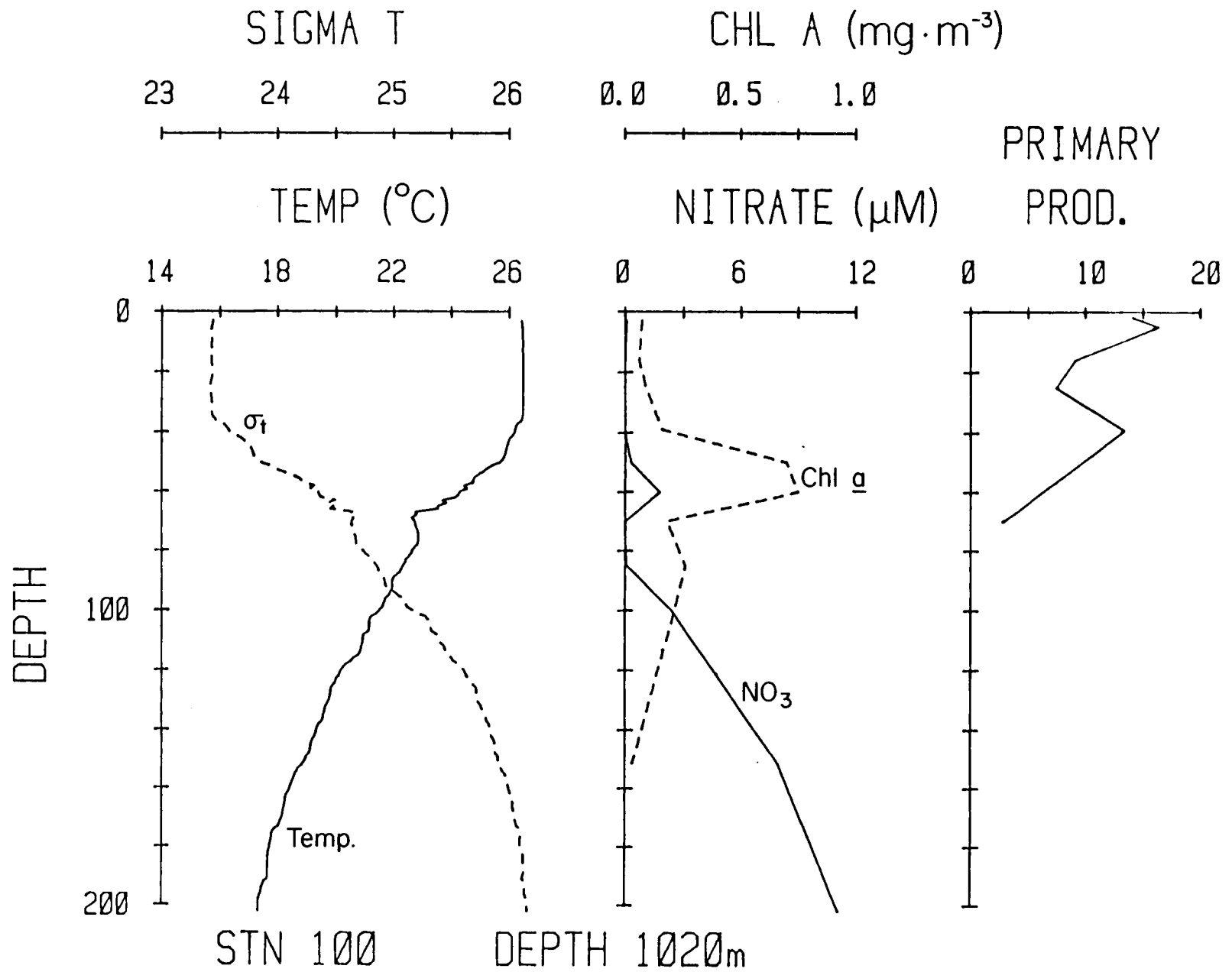
Figure 5-4.   Vertical profiles for spring cruise station 100.

230

Productivity at Station 5 (Figure 5-2) was also low (0.2 $gC \cdot m^{-2} \cdot day^{-1}$).
The top of the nitracline was near 55 m, and a subsurface Chl a maximum layer
was present. However, the subsurface Chl a layer contributed little to water
column productivity. In contrast to Station 5, the subsurface Chl a maximum
layer at Stations 34 and 100 (Figures 5-3 and 5-4, respectively) contributed
significantly to water column primary production. At both stations, the
nitracline was located between 40 and 60 m. At Station 100, the vertical
distribution of primary production was bimodal, with both near-surface (6 m)
and subsurface (40 m) peaks greater than 10 $mgC \cdot m^{-3} \cdot hr^{-1}$ (Figure 5-4).
The large subsurface peak at 40 m resulted from the relatively high
concentrations of Chl a (about 0.75 $mg \cdot m^{-3}$) within the subsurface layer.

Table 5-3 lists total numbers of diatoms, dinoflagellates, and
coccolithophores observed near the surface and at the depth of the subsurface
Chl a maximum at the eight stations where samples were collected. Complete
enumeration results are presented in Appendix A-6. At two of the four
stations (i.e., Stations 5 and 85) where phytoplankton samples were collected
from the subsurface Chl a maximum, numbers of coccolithophore were about two
times higher in the subsurface layer than near the surface, whereas diatoms
were several times higher. The dominant coccolithophore species within the
subsurface Chl a maximum was Coccolithus huxleyi (Lohman) Kamptner. No
single diatom species accounted for more than about 25% of the total, and
thus the subsurface assemblage was relatively diverse. These results are
discussed further in Section 5.3.1.3.

231

Table 5-3. Phytoplankton cell counts at depth of chlorophyll maxima during spring cruise.

(Dashed line indicates either the absence of a subsurface chlorophyll maximum or it was not sampled).

Station	Depth of Chl Max. (m)	No. of Cells ($\times\ 10^3 \cdot \text{liter}^{-1}$)		
		Diatoms	Dinos	Coccolith
1	3	44	12	154
	-	-	-	-
5	2	223	11	151
	55	16	16	302
24	2	18	8	41
	-	-	-	-
77	2	51	12	42
	-	-	-	-
81	2	8	8	73
	70	77	12	136
85	2	78	8	88
	70	18	13	239
100	2	126	12	104
	-	-	-	-
104	3	14	7	157
	70	74	13	184

5.3.1.2 Effects of Loop Current Intrusion

As illustrated earlier in Table 5-2, mean productivity for the three depth ranges (i.e., less than 100 m, 100 to 200 m, and greater than 200 m) was roughly the same at about 0.5 gC $\cdot$ m^{-2} $\cdot$ day^{-1}. Eddy-induced upwelling primarily affected the portion of the outer shelf seaward of the 70 to 100 m depth range. The obvious question then is: What is the effect, if any, of the eddy on primary production?

Of the four productivity stations located seaward of the 200 m isobath, three (i.e., Stations 38, 61, and 100) were in areas where nutrient and density isopleths had been uplifted by the eddy (see Section 3.2.1.3). At these three stations, the top of the nitracline was above 60 m and thus at least 10 m above the 1% light level. The range in primary production at these three stations was 0.5 to 0.7 (average = 0.6) gC $\cdot$ m^{-1} $\cdot$ day^{-1}. Only one of the four stations (Station 12) was within the Loop Current, seaward and south of the region principally affected by the eddy. In contrast to the other three stations, primary production at Station 12 was only 0.1 gC $\cdot$ m^{-2} $\cdot$ day^{-1}. This suggests that primary production seaward of the 200 m isobath may be enhanced by as much as six times in areas affected by eddy-induced upwelling (vis-a-vis, those unaffected by upwelling).

The two stations (Stations 24 and 77) located shoreward of the direct effect of the eddy (i.e., where nitrate concentrations were less than 1.0 μM throughout the euphotic zone) had about the same mean rate of primary production as those stations located near or within the upwelled core of the eddy (i.e., those stations between the 100 and 200 m isobaths). One

possibility for the relatively high production at Stations 24 and 77 is that the shelf shoreward of about the 100 m isobath has a source of "new" nitrogen (in sensu Dugdale and Goering, 1967) other than upwelling and intrusion of offshore waters. However, a second possibility is that phytoplankton at Stations 24 and 77 were using recycled nitrogen (e.g., ammonia or urea) that originated as nitrate and was transported shoreward of the 100 m isobath by an earlier upwelling event(s). Further studies are required to distinguish between these two possibilities.

As noted earlier, frontal eddies propagating along the cyclonic Gulf Stream front between Cape Canaveral, Florida and Cape Hatteras, North Carolina also cause upwelling and intrusions of nutrient-rich waters onto the outer southeastern continental shelf (Lee et al., 1981). During these events, surface mixed layer Chl $\underline{a}$ attains concentrations as high as 5 $mg \cdot m^{-3}$ or more, and primary production exceeds 5 $gC \cdot m^{-2} \cdot day^{-1}$. (Yoder et al., 1981a). Average production during upwelling events is about 1.8 $gC \cdot m^{-2} \cdot day^{-1}$. During winter and spring, upwelling is the most important process controlling primary production on the outer southeastern shelf (Yoder et al., in press). The results of the spring Loop Current cruise suggest that the effect of eddy-induced upwelling on primary production of the outer southwest Florida shelf is comparatively not as dramatic as on the outer southeastern shelf. Average outer shelf productivity at about 100 to 200 m depths during the cruise was about 0.5 $gC \cdot m^{-2} \cdot day^{-1}$, which is only about 25% of that observed during similar events on the southeastern shelf. The most likely explanation for the difference between the two areas is the intensity of upwelling as evidenced by the depth of the top of the nitracline and the arguments in Section 3.2.1.7. During eddy-induced upwelling on the

outer southeastern shelf, the top of the nitracline can come within 10 to 15 m of the surface. Typically, the nitracline is within 20 to 25 m of the surface during these events. In contrast, the top of the nitracline in the core of the Loop Current eddy during the spring cruise was only within 40 to 50 m of the surface. Thus, most of the euphotic zone was not affected by nutrients upwelled by the eddy.

5.3.1.3 Phytoplankton Variability

Another perspective on the intrusion process can be gained by closer examination of the phytoplankton species and counts collected during the two cruises. During the spring cruise, these data were collected between April 2 and 7, 1982. Figure 5-5 shows the locations of stations where phytoplankton samples were taken. Samples from Station 1 and 5 were collected on a transect made between April 2 and 3. The 24 to 26°C isotherms had formed a noticeable surface upwelling region about 250 km from shore between Stations 4 and 6 (Figure 3-6).

Station 1 samples (at depths of 3, 20, 55, 85, and 94 m) were taken inshore of the upwelling peak. Any upwelling effect at this sampling station may therefore be overshadowed by the influence of the shelf diatoms; it may also account for the reverse in diatom to coccolithophore ratio with depth (Figure 5-6)*.

---

* Enumeration results for coccolithophores, dinoflagellates, and diatoms are presented as cumulative bar graphs with proportional divisions for each major species as a function of sample depth. Euphotic zone Chl a, primary productivity, and depth of Chl a maximum are annotated in the upper right-hand corner of each figure.
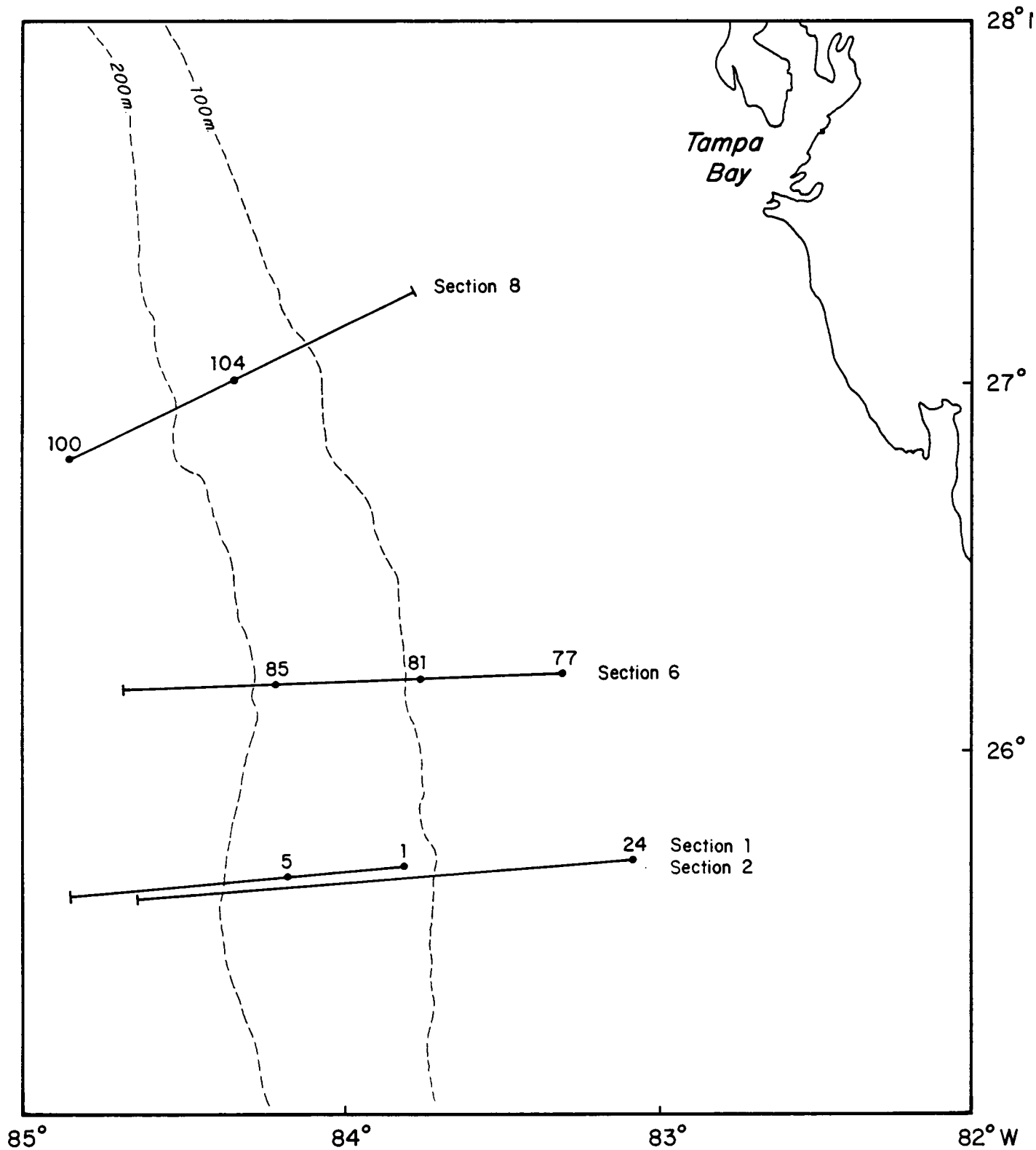
Figure 5-5.   Spring cruise phytoplankton collection station locations.
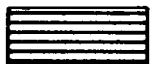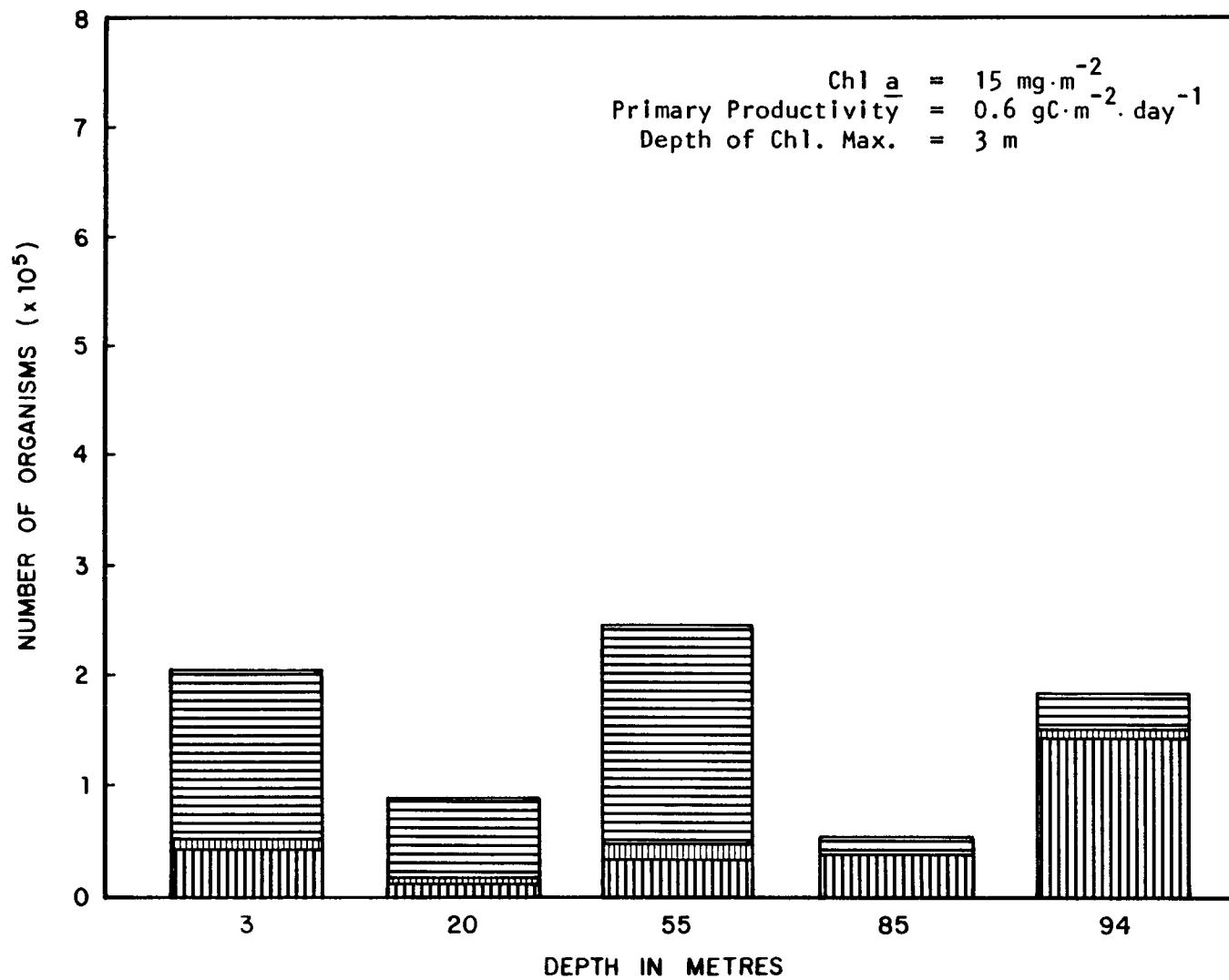
Figure 5-6.   Phytoplankton enumeration results for spring cruise station 1.

Station 5 results (sample depths of 2, 20, 55, 85, and 100 m) shows a greater response to the upwelling. Samples at the three middle depths were dominated by coccolithophore with their maxima corresponding closely to the 23°C isotherm position at about 20 m (Figure 5-7).

One way to examine the species variability associated with the upwelling process is to compare pairs of stations for common species in the three major groupings. Table 5-4 presents such a comparison for four pairs of stations for the spring cruise. For Stations 1 and 5, the percentage of common species in each group were about the same.

On April 3, a single set of samples was taken. Station 24 samples (at depths of 2, 6, 15, 26, and 45 m) show a small number of organisms at each depth with a more or less homogeneous distribution with depth (Figure 5-8). A secondary cell number maximum near the surface appears to correspond to the chlorophyll maximum depth.

On April 6, three stations were sampled for phytoplankton content; two to the east of the subsurface temperature dome (Stations 77 and 81) and one to the west (Station 85). Probably because of their proximity to shore on the shelf, Station 77 results (Figure 5-9) are quite similar to Station 24 results as far as species composition (see Table 5-4). The cell maximum at 15 m is located within the LCW filament.

Around the upwelling dome, Station 81 results at 2, 6, 25, 40, and 70 m (Figure 5-10) show a dominance of coccolithophore at all depths with the depth of the cell number maximum corresponding to the chlorophyll maximum.

238
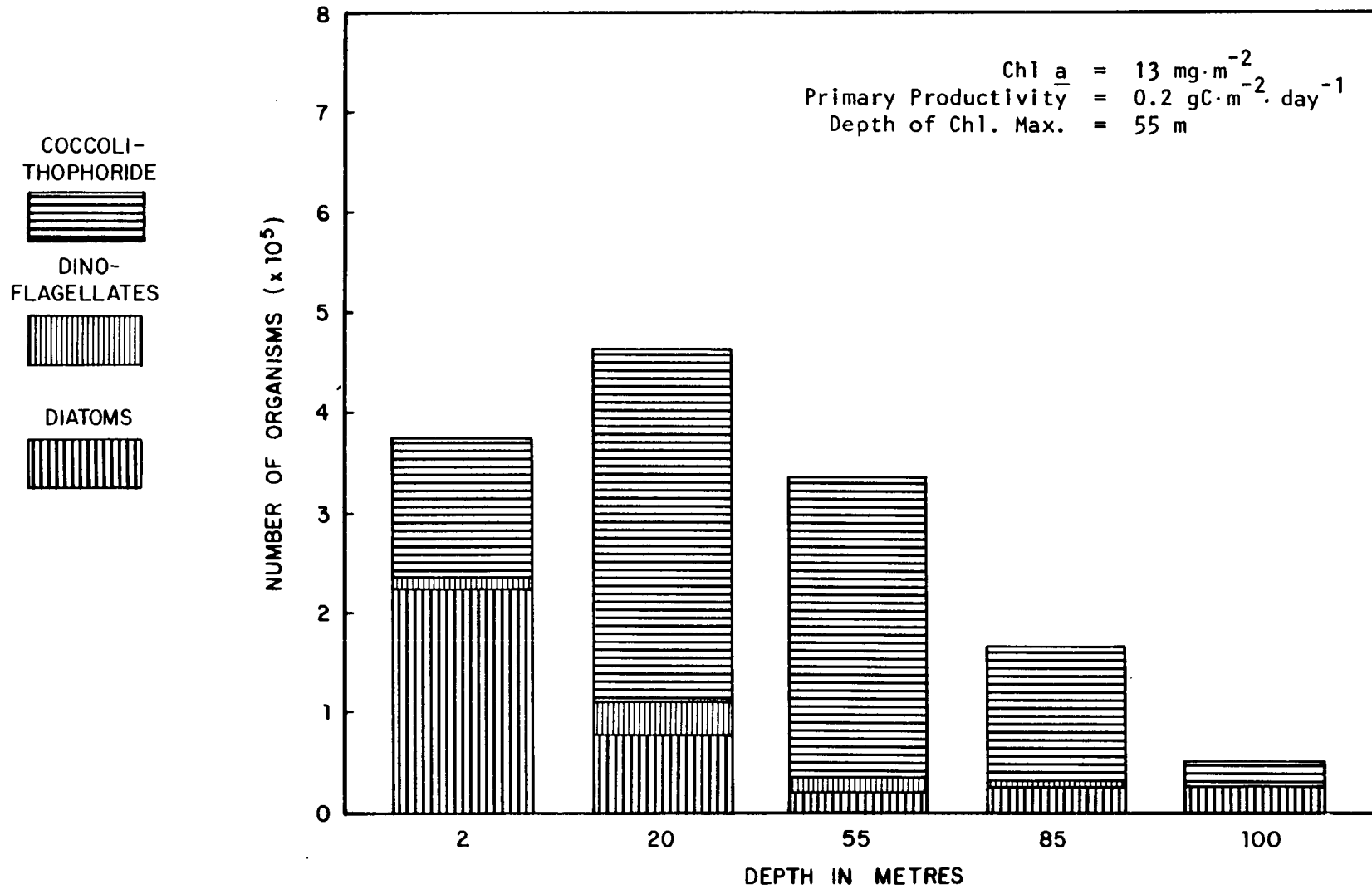
Figure 5-7.   Phytoplankton enumeration results for spring cruise station 5.

Table 5-4. Phytoplankton species common at paired stations during spring
cruise

Stations	Group	Number of Species	Common Species	Percent in Common
1 and 5	Diatoms	29	13	44.9
	Dinoflagellates	13	4	30.7
	Coccolithophores	23	10	43.5
100 and 104	Diatoms	30	14	46.7
	Dinoflagellates	21	10	47.6
	Coccolithophores	15	12	80.0
81 and 85	Diatoms	29	18	62.0
	Dinoflagellates	20	11	55.0
	Coccolithophores	19	12	63.2
24 and 77	Diatoms	25	18	72.0
	Dinoflagellates	31	14	55.0
	Coccolithophores	18	12	66.7
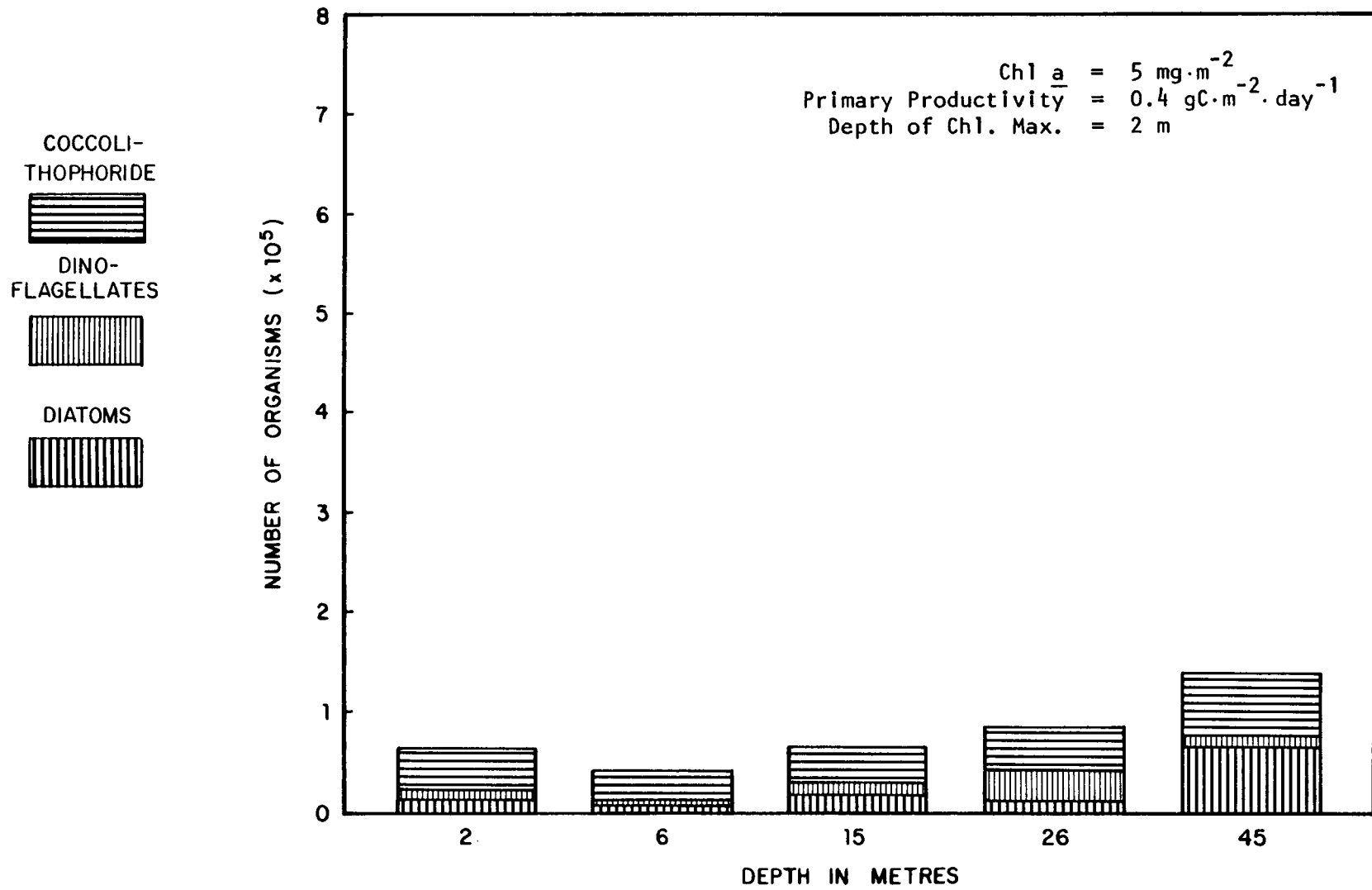
Figure 5-8.   Phytoplankton enumeration results for spring cruise station 24.

241

Figure 5-9.   Phytoplankton enumeration results for spring cruise station 77.
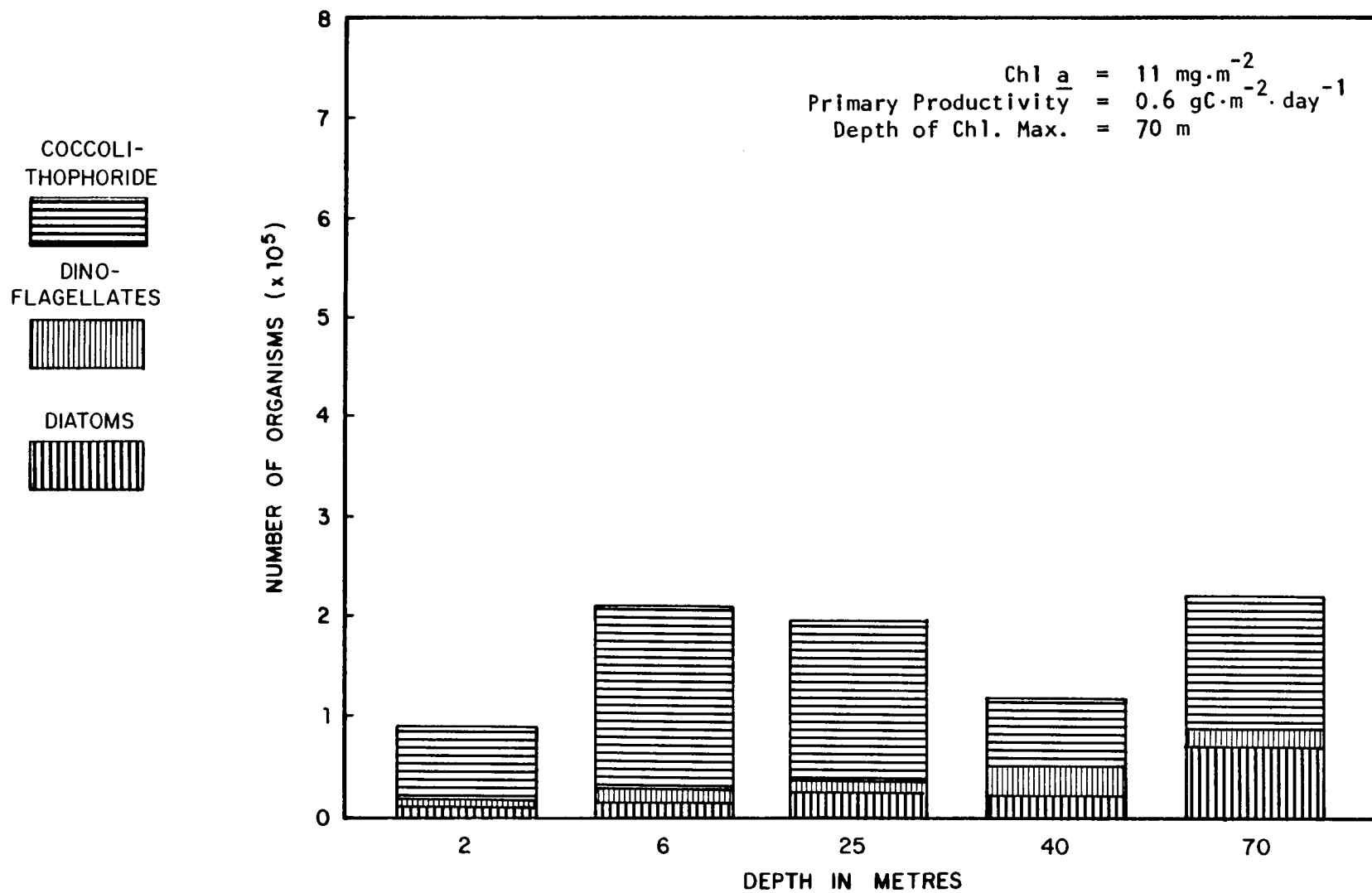
Figure 5-10.   Phytoplankton enumeration results for spring cruise station 81.

The presence of <u>Navicula</u> Sp. and <u>Nitzchia</u> Sp. indicate a potential shelf influence.

Samples from 2, 6, 25, 41, and 70 m at Station 85 (Figure 5-11) show generally higher cell counts with more organisms in the upper 25 m and near the depth of maximum chlorophyll at 70 m. The diatoms present at the lower levels lack the diversity of the common planktonic forms such as <u>Ceratulina</u>, <u>Chaetoceros</u>, and <u>Hemiaulas</u>, which are evident in the 2 and 6 m samples.

On April 6 and 7, Stations 100 (Figure 5-12) and 104 (Figure 5-24) were sampled. Within the approximate 50 km separating the two stations, the numbers of organisms changed quite markedly but not the integrated chlorophyll or primary productivity values. At three Station 100 sampling depths (2, 25, and 39 m), temperate pelagic diatoms dominated the community (Hendey, 1964; Cupp, 1943) and even included a few <u>Oscillatoria</u> Sp. These samples were all in the 23 to 26°C temperature range.

Phytoplankton samples taken at Station 104 (depths of 3, 6, 15, 40, and 70 m) were in the upwelling dome along Section 8. The dominance of coccolithophore (Figure 5-13) and lower number of diatoms are indicative of the upwelling process. The chlorophyll and cell maxima (at 70 m) appear to be closely related. The total cell count at 40 m was composed of a wider variety of diatoms than the upper levels and may be showing some influence from the shelf. Although Stations 100 and 104 differ in diatom to coccolithophore ratio, they are composed of similar diatoms species and compare favorably with Stations 1 and 5.

Figure 5-11. Phytoplankton enumeration results for spring cruise station 85.

COCCOLI-
THOPHORIDE

DINO-
FLAGELLATES

DIATOMS

246

NUMBER OF ORGANISMS ($\times 10^5$)

8

7

6

5

4

3

2

1

0

Chl $\underline{a}$ = 9 mg·m^{-2}
Primary Productivity = 0.7 gC·m^{-2}·day^{-1}
Depth of Chl. Max. = 2 m

2   16   25   39   70

DEPTH IN METRES

Figure 5-12.   Phytoplankton enumeration results for spring cruise station 100.

Figure 5-13.   Phytoplankton enumeration results for spring cruise station 104.

At the present time, the question as to whether coccolithophore distributions and specific temperatures or depths are correlated is still a moot point. The dominant species Coccolithus luxleyi (Lohmann) May and Mahler (Emiliania husleyi) is a widely reported species. Gaarder and Hasle (1971) report C. huxleyi (E. huxleyi) from 0 to 100 m ; Haq and Baesma (1970) report findings from 0 to 50 m; Okado and McIntyre (1979) from 20 m. Throndsen (1972) reports a maximum concentration of coccolithophore between 50 and 70 m; Norris (1965) reports Ceratolithus cristatus Kamptner at 72 to 94 m. As noted earlier in Section 5.3.1.1., C. huxleyi was the dominant species in most samples regardless of temperature or depth.

The appearance of higher cell numbers with specific upwelling temperatures in these data may also be more of a reflection of the sigma-t dependence on temperature in the upwelling process rather than a direct correlation between coccolithophore distributions and temperature.

In considering the values in Table 5-4, it appears that something on the order of 40% of the species in each major group are common within each of the four station pairs. Stations on either side (east and west) of the Section 6 upwelling dome (i.e., Stations 81 and 85) and the shallowest stations (i.e., Stations 24 and 77) show the highest percentages of common species. At the shallow stations, the cell counts were generally low with little depth variation; around the upwelling dome, both cell numbers and variation with depth increased.

5.3.2 Summer Cruise Data

5.3.2.1 Primary Production

During the summer cruise, a subsurface intrusion of offshore water containing relatively high nutrient concentrations covered the region from the outer shelf break (200 m) to within the 100 m isobath. These data provided an opportunity to assess the effect of subsurface intrusions on the rate of phytoplankton production under different seasonal conditions. Table 5-5 presents a list of Chl a and primary production euphotic integrals (surface to 1% light level) for stations occupied during the summer cruise. Table 5-6 summarizes these values according to depth ranges in the same sense as Tables 5-1 and 5-2. These results show that highest mean euphotic zone Chl a and daily rates of primary production occurred between the 100 to 200 m isobaths (average = 0.8 $gC \cdot m^{-2} \cdot day^{-1}$; n = 6) and were about double that of the stations located shoreward of the 100 m isobath (average = 0.4 $gC \cdot m^{-2} \cdot day^{-1}$; n = 3). They were also about double that of the stations located seaward of the 200 m isobath (average = 0.3 $gC \cdot m^{-2} \cdot day^{-1}$; n = 5). Mean euphotic zone Chl a was also highest for stations located between the 100 and 200 m isobaths. Highest primary production (1.2 $gC \cdot m^{-2} \cdot day^{-1}$) and highest euphotic zone Chl a (34 $mg \cdot m^{-2}$) were observed at Station 48 where the water depth was 120 m.

Figures 5-14 through 5-16 illustrate the relation between the major hydrographic observations during the summer cruise (Section 3.2.2.3) and the vertical distribution of Chl a and primary production. Similar profile sets for all summer cruise productivity stations are presented in Appendix A.7.

Table 5-5. Euphotic zone Chl a and daily primary production for summer criuse stations.

Station Number	Chl a ($mg \cdot m^{-2}$)	Primary Production ($gC \cdot m^{-2} \cdot day^{-1}$)
10	10	0.25
17	16	0.6
23	11	0.4
27	7	0.3
38	5	0.15
42	9	0.4
48	34	1.2
57	12	0.4
65	15	0.8
71	7	0.9
75	8	0.5
81	11	0.6
87	13	0.9
89	11	0.6

Table 5-6. Summary of euphotic zone _a_ and primary production by depth ranges for summer cruise.

Chl _a_ $(mg \cdot m^{-2})$

Isobath (m)	Number of Stations	Range	Mean (S.D.)
< 100	3	10 - 12	11 (1)
~ 100 - 200	6	7 - 34	10 (3)
> 200	5	5 - 11	8 (2)

Primary Production $(gC \cdot m^{-2} \cdot day^{-1})$

Isobath (m)	Number of Stations	Range	Mean (S.D.)
< 100	3	0.25 - 0.60	0.40 (0.20)
~ 100 - 200	6	0.60 - 1.20	0.80 (0.20)
> 200	5	0.25 - 0.50	0.30 (0.10)

SIGMA T

CHL A (mg·m⁻³)

21   23   25   27

0.0   0.2   0.4

TEMP (°C)

NITRATE (μM)

PRIMARY
PROD.

13   19   25   31

0   12   24

0   5   10

σₜ

Chl a

Temp.

NO₃

DEPTH

100

200

STN 038   DEPTH 1980m

252
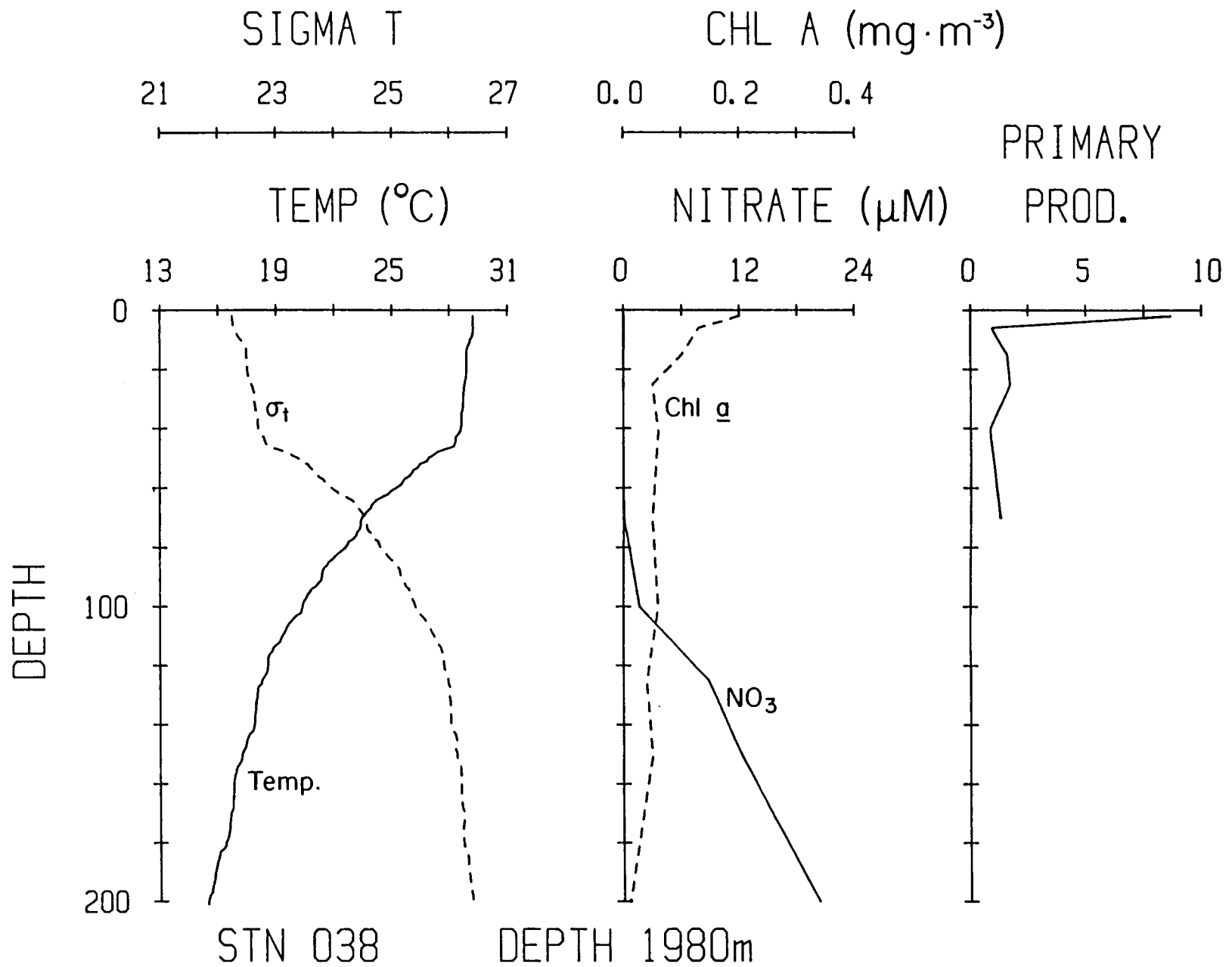
Figure 5-14. Vertical profiles for summer cruise station 38.
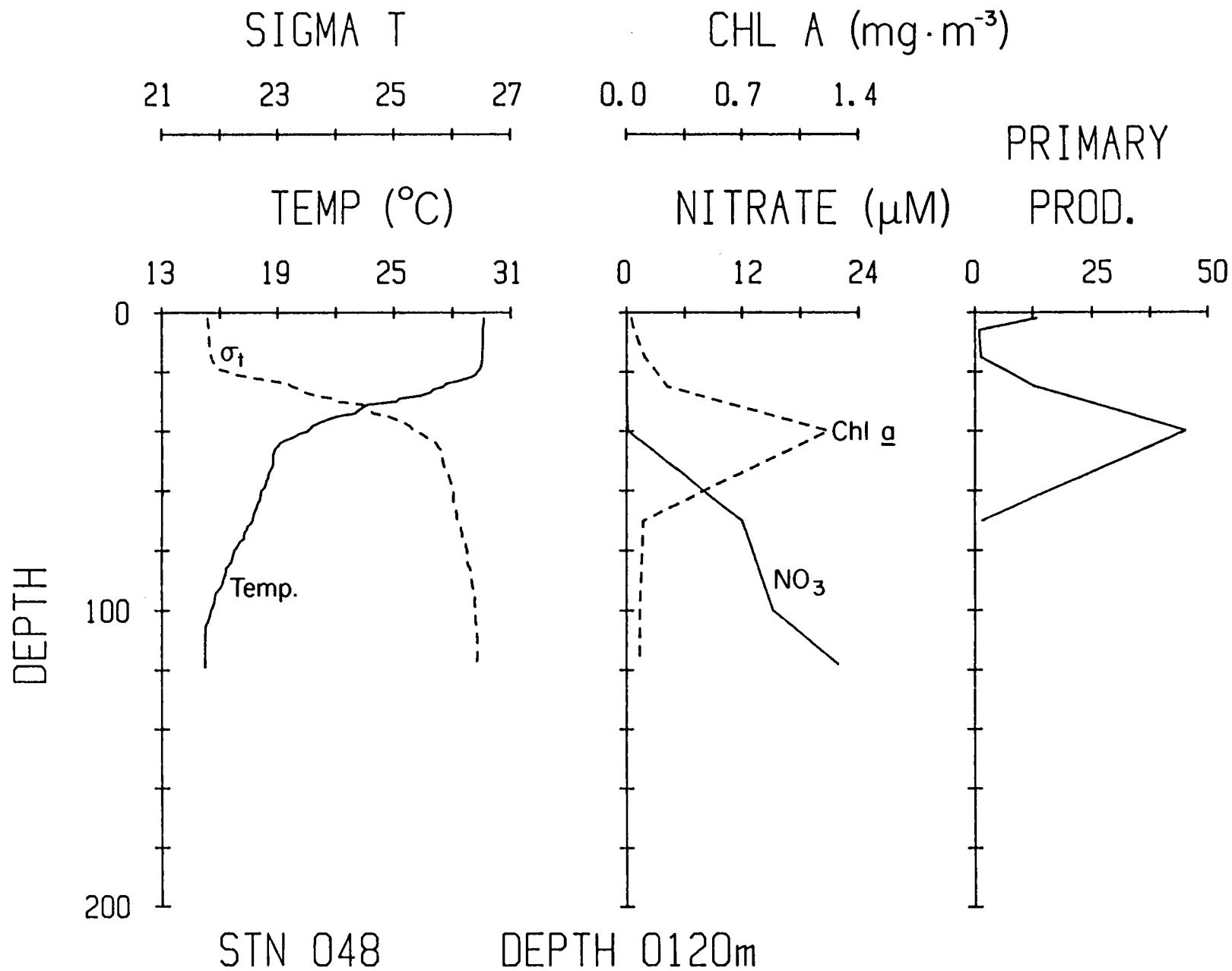
Figure 5-15. Vertical profiles for summer cruise station 48.

SIGMA T

CHL A (mg·m⁻³)

TEMP (°C)

NITRATE (μM)

PRIMARY PROD.

σₜ

Temp.

Chl a

NO₃

DEPTH

STN 087   DEPTH 0117m
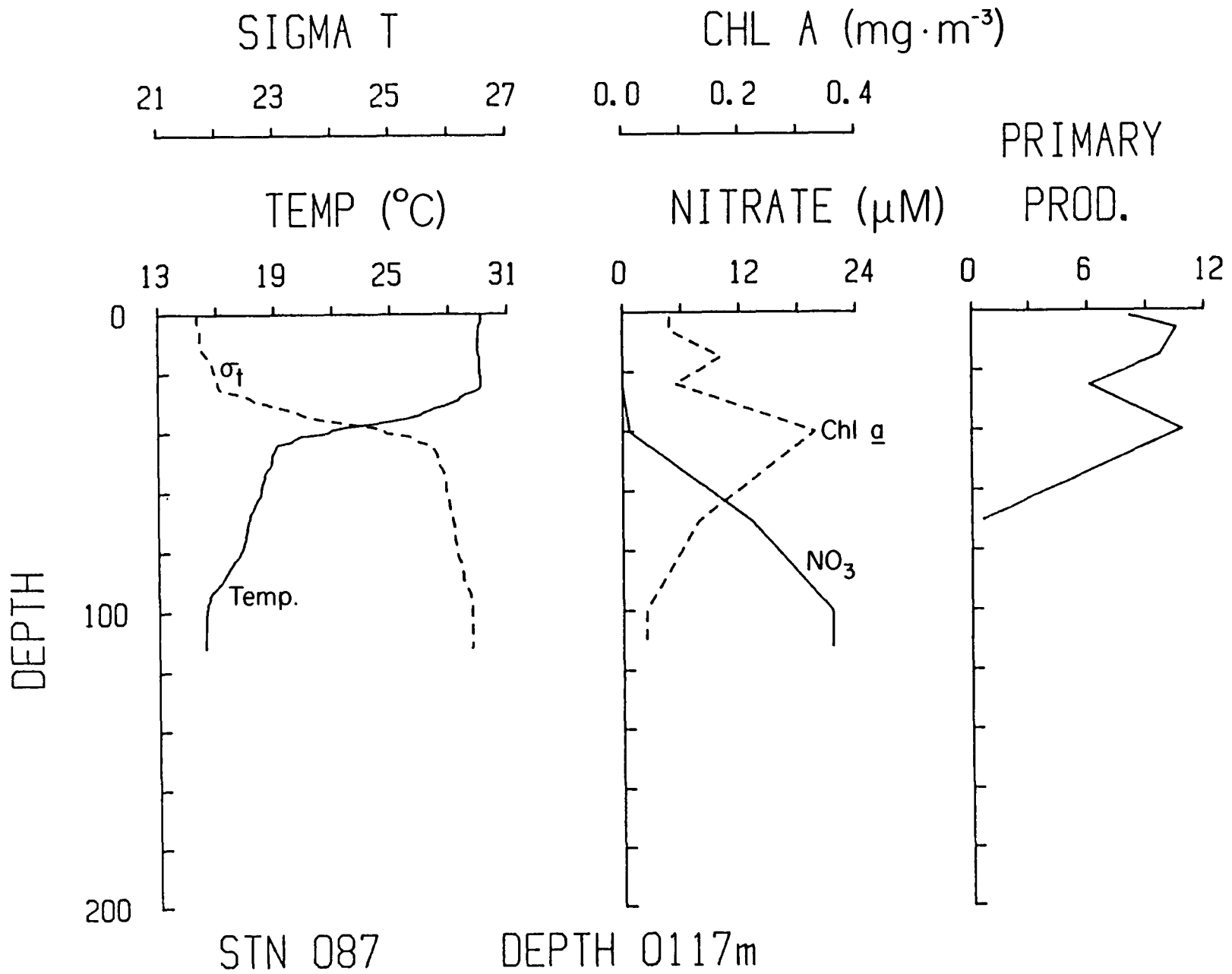
Figure 5-16. Vertical profiles for summer cruise station 87.

254

The nomenclature is the same as that used for the spring cruise. At Station 38 (Figure 5-14), a lens of relatively low salinity water (less than 35.5°/oo) was present between the surface and the top of the nitracline which coincided with the approximate depth of the 1% light level at 70 m. At this station, surface Chl a was relatively high (at about 0.2 mg·m^{-3}) within the lens of low salinity water, and no subsurface Chl a maximum was observed. As a result, primary productivity near the surface was high (about 10 gC·m^{-3}·day^{-1}) and decreased sharply with depth.

Contrary to the measurements at Station 38, surface Chl a at Station 48 (Figure 5-15) was low (at about 0.05 mg·m^{-3}). This station was characterized by a pronounced subsurface Chl a maximum (greater than 1.0 mg·m^{-3}) at the top of the nitracline near 40 m. As a result of this high subsurface Chl a concentration, the peak in primary production occurred at 40 m ($\sim$ 50 gC·m^{-3}·day^{-1}).

The data collected at Station 87 (Figure 5-16) provide an example of a bimodal distribution where Chl a was high near the surface ($\sim$ 0.2 mg·m^{-3}) and at depth ($\sim$ 0.4 mg·m^{-3} at 40 m). As a result, the vertical distribution of primary production was also bimodal with both near-surface and subsurface peaks of approximately 11 gC·m^{-3}·day^{-1}.

To look for general patterns, euphotic zone primary production from each of the 14 stations was scaled by the total incident irradiance received during each of the 14 productivity incubations and regressed against euphotic zone Chl a. The regression yielded a correlation coefficient of 0.84 (n = 14). Thus, about 70% of the observed variability in daily primary production

measured during the summer cruise could be explained solely by the amount of Chl $\underline{a}$ in the euphotic zone and by the incident irradiance.

Table 5-7 summarizes the total numbers of diatoms, dinoflagellates, and coccolithophores observed near the surface and at the depth of the subsurface Chl $\underline{a}$ maximum. Complete summer cruise enumeration results are presented in Appendix A.9. For five of eight stations (i.e., Stations 10, 42, 48, 65, and 87), near-surface total diatoms concentration clearly exceeded 10^5 cells·liter^{-1}. All five of these stations were characterized by low salinity water (less than 35.5°/oo) in the upper 10 to 30 m (see Section 3.2.2.3). A single species, Rhizosolenia alata, comprised more than 80% of total diatom cells within the low salinity water at these five stations.

At five of the eight stations (i.e., Stations 42, 48, 65, 81, and 87), samples for phytoplankton cell counts were obtained within the subsurface Chl $\underline{a}$ maximum which occurred near a depth of either 40 or 70 m. At four of these five stations (i.e., Stations 42, 65, 81 and 87), the concentration of coccolithophore within the subsurface Chl $\underline{a}$ maximum was about four to ten times higher than near the surface. The dominant species was Coccolithus huxleyi (Lohman) Kamptner which accounted for more than 80% of the total number of coccolithophore at each station. At two of five stations (i.e., Stations 48 and 87), diatom concentration within the subsurface Chl $\underline{a}$ maximum exceeded 10^5 cells·liter^{-1}. In contrast with the near-surface samples at these stations, however, the dominant diatom species of the subsurface maximum was not $\underline{R}$. alata, which was either undetectable at this depth or at very low abundance. At Station 48, the subsurface Chl $\underline{a}$ maximum was dominated by several diatom species including Nitzschia sp. and Dactyliosolen

256

Table 5-7. Phytoplankton cell counts at depth of chlorophyll maxima during summer cruise

(Dashed line indicates either the absence of a subsurface chlorophyll maximum or it was not sampled).

Station	Depth of Chl Max (m)	No. of Cells ($\times 10^3$ liter^{-1})		
		Diatoms	Dinos	Coccolith
10	2	96	37	80
	-	-	-	-
27	2	5	6	55
	-	-	-	-
42	2	120	10	48
	70	15	8	191
48	6	245	56	135
	40	200	54	196
65	6	108	16	39
	40	10	15	391
71	6	59	22	46
	-	-	-	
81	6	18	19	51
	70	69	25	337
87	6	280	17	35
	40	101	73	416

antarcticus. $\underline{D}$. antacrticus was also the dominant diatom within the subsurface Chl $\underline{a}$ maximum at Station 87.

5.3.2.2 Effects of Loop Current Intrusion

A somewhat unexpected hydrographic feature observed during the summer cruise was the presence of a relatively shallow lens (about 10 to 30 m deep) of relatively low salinity water (less than $35.5°/oo$) which covered much of the outer shelf. In some instances, the productivity of this layer was a significant component of euphotic zone primary production. Relatively high concentrations ($\sim 10^5$ cells $\cdot$ liter^{-1}) of the diatom, $\underline{R}$. $\underline{alata}$, characterized the low salinity layer. In general, Chl $\underline{a}$ concentrations in excess of 1 mg$\cdot$m^{-3} are expected to be associated with diatom cell concentrations of this order (e.g., Yoder et al., 1981a). However, near-surface Chl $\underline{a}$ concentrations within the low salinity water were only 0.05 to 0.2 mg$\cdot$m^{-3}. This apparent discrepancy between relatively low Chl $\underline{a}$ and relatively high diatom cell numbers within the surface lens of low salinity water may be explained by either: (1) a large proportion of dead cells containing either little or no Chl $\underline{a}$, or (2) living cells containing relatively low amounts of Chl $\underline{a}$ in comparison to carbon, nitrogen, or cell volume. Phytoplankton kept at near-surface levels of irradiance for one day or more adapt to high levels of irradiance by lowering their intracellular content of Chl $\underline{a}$ by a factor of two or more.

Most of the productivity stations were characterized by a subsurface Chl $\underline{a}$ maximum layer located near the top of the nitracline. At eight of 14 stations, the maximum rate of primary production occurred at or near the

depth of the subsurface Chl $\underline{a}$ maximum. Phytoplankton within the maximum were different than those dominating surface waters at the same stations. The subsurface Chl $\underline{a}$ maximum were dominated by either coccolithophore or by diatoms. Given the relatively high proportion of euphotic zone primary production that occurred below the mixed layer, it may be assumed that the productivity of the subsurface Chl $\underline{a}$ maximum is important to higher trophic levels.

The southeastern U.S. continental shelf off the north Florida and Georgia coasts is narrower and shallower than the southwest Florida continental shelf. In both cases, an intense western boundary current flows along the shelf break and influences the exchange of waters between the shelf and the adjacent ocean (see Section 3.2.1.7). As observed on the outer southwest Florida shelf, subsurface intrusions of offshore, nutrient-rich water also move onto the southeastern shelf during summer months. Chl $\underline{a}$ and primary productivity within southeastern shelf intrusions average about 50 to 100 $mg \cdot m^{-2}$ and 2 to 3 $gC \cdot m^{-2} \cdot day^{-1}$, respectively (Dunstan and Atkinson, 1976; Atkinson et al., 1978; Yoder et al., in press; Yoder, unpublished). For comparison, the average Chl $\underline{a}$ and primary production observed during the summer cruise on the outer southwest Florida shelf (in depths of 100 to 200 m) was only 16 $mg \cdot m^{-2}$ and 0.8 $gC \cdot m^{-2} \cdot day^{-1}$, respectively. One of the principal reasons for this lower productivity on the outer southwest Florida shelf (compared to the southeastern shelf) is related to the depth of the top of the nitracline when an intrusion is present. On the southeastern shelf, the top of the nitracline often reaches within 10 to 15 m of the surface (about 30% light level) (Dunstan and Atkinson, 1976; Atkinson et al., 1978; Yoder, et al., in press; Atkinson, personal communication). In

contrast, during the summer cruise on the southwest Florida shelf, the top of the nitracline was generally at 40 m or deeper (10% light level or less). Thus, on the southeastern shelf, nutrients which are essential for phytoplankton production move higher into the euphotic zone than for the outer southwest Florida shelf.

5.3.2.3 Phytoplankton Variability

The September phytoplankton samples were distinctly different from the April samples. By comparison, the summer samples exhibited a limited range of species. Figure 5-17 shows the relative positions of the summer sampling stations along the repeated time series transect. Stations 10 (depths at 2, 6, 15, and 25 m; Figure 5-18) and 27 (depths at 2, 6, 15, 25, and 70 m; Figure 5-19) were sampled on September 13 and 14, and represent the extremes in near- and off-shore collection points, respectively. Samples collected at Station 10 were limited to the (29 to 30°C) generally isothermal mixed layer and did not display the species stratification evident at other stations, e.g., Discospharea tubifera (Murray, Blackm.) Osten. and C. cristatus Kamptner. Samples at Station 27 were dominated by coccolithophore and thus appeared to represent a distinctly different community. Neither of these station distributions appear to show a correlation between population density and depth of the chlorophyll maximum.

Phytoplankton samples collected on September 14 and 15 at Stations 42 (depths of 2, 6, 15, 40, and 70 m) and 48 (depths of 6, 15, 25, 40, and 70 m) appear to show a stratification about the bottom of the surface mixed layer at about 30 m. These results are presented in Figures 5-20 (Station 42) and 5-21
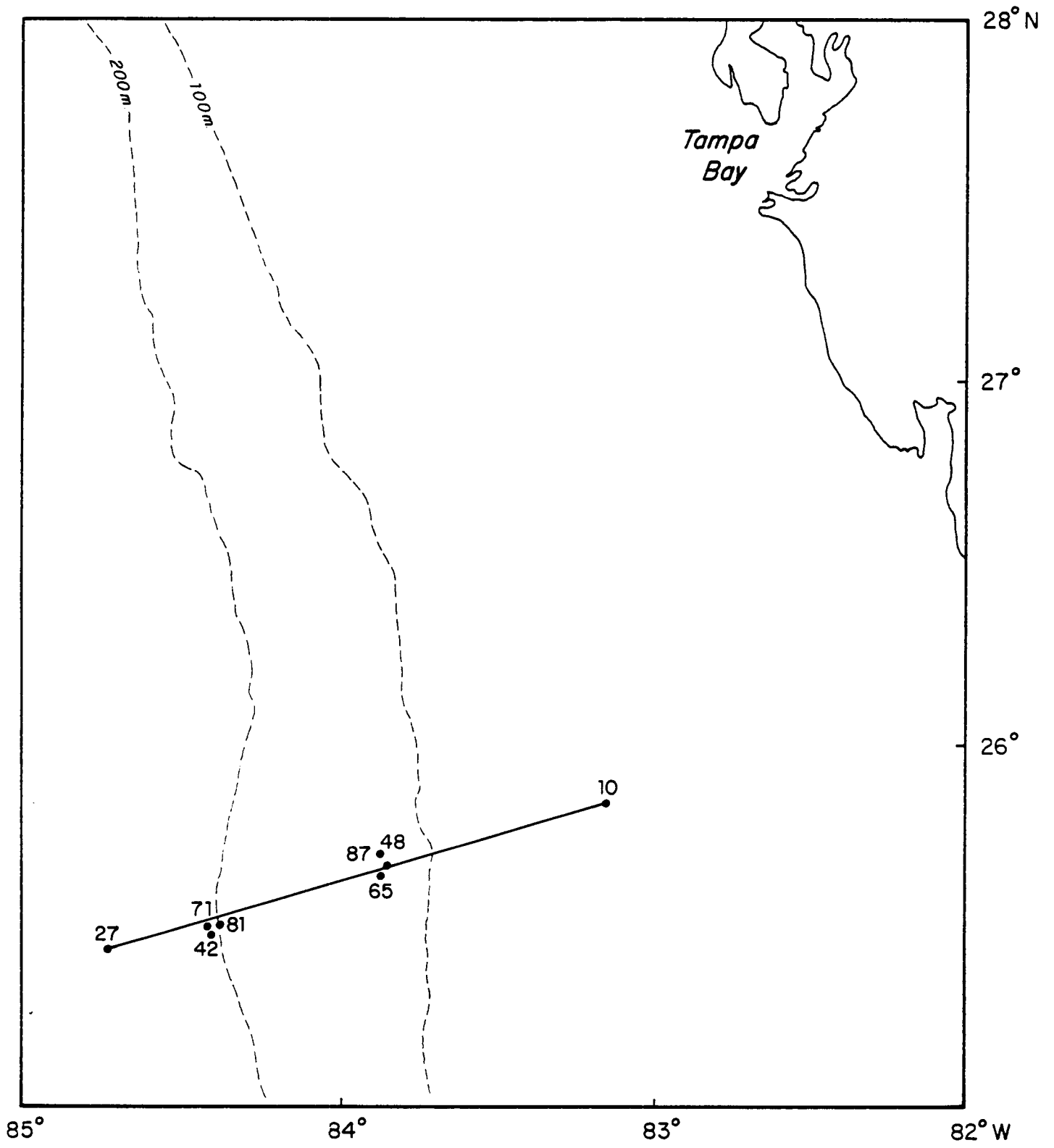
Figure 5-17. Summer cruise phytoplankton collection station locations.
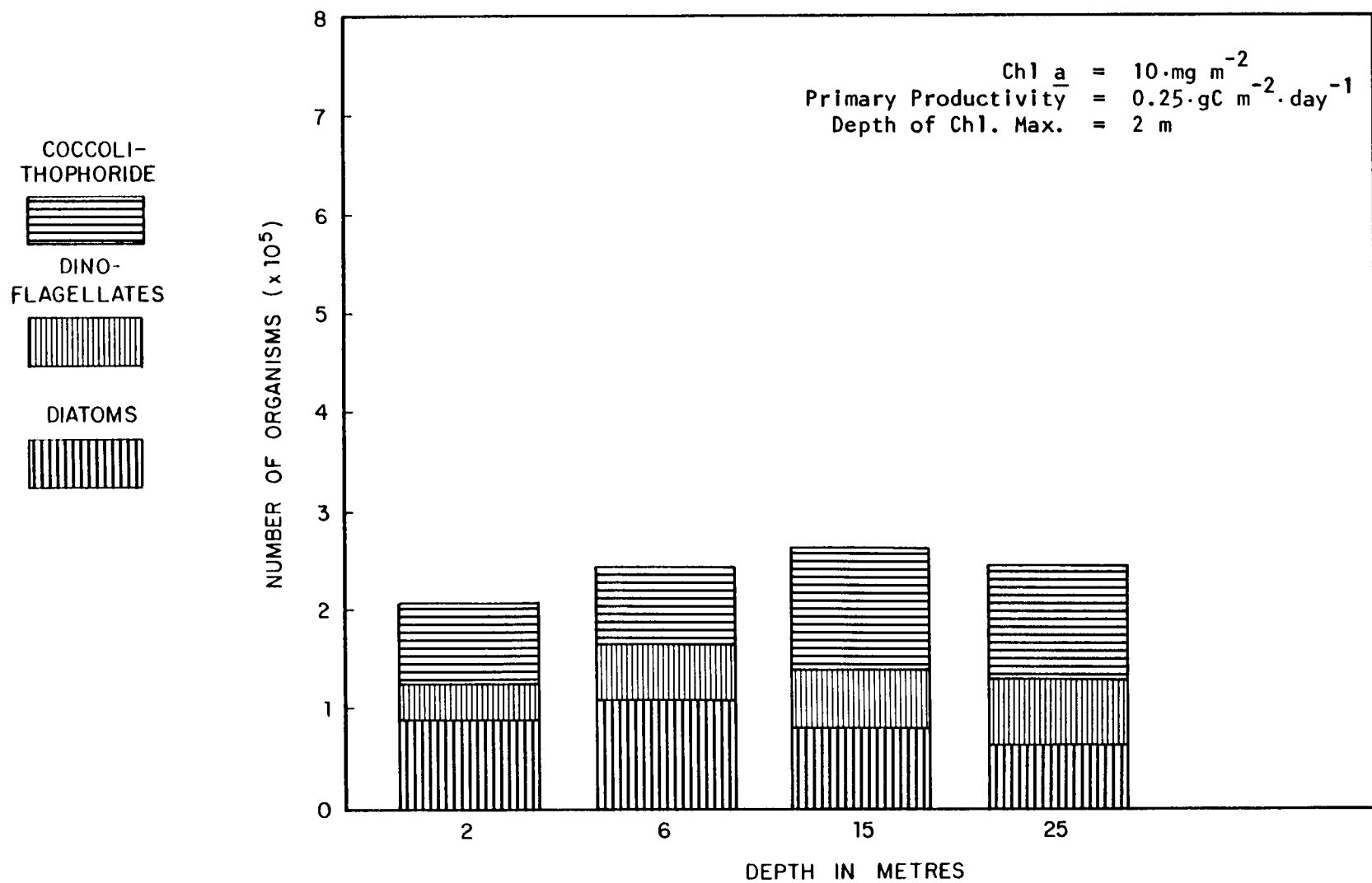
Figure 5-18. Phytoplankton enumeration results for summer cruise station 10.
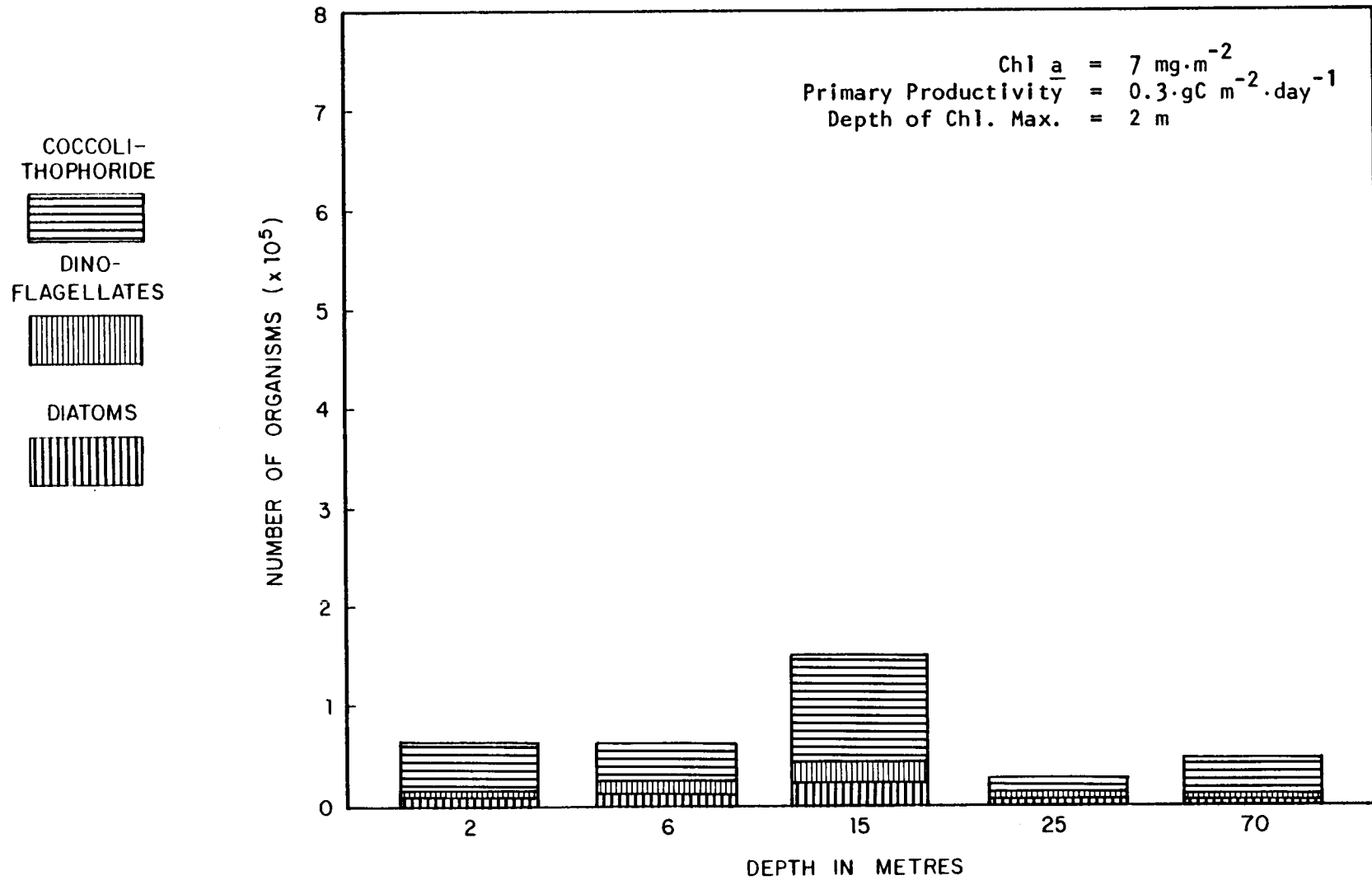
Figure 5-19.   Phytoplankton enumeration results for summer cruise station 27.

263
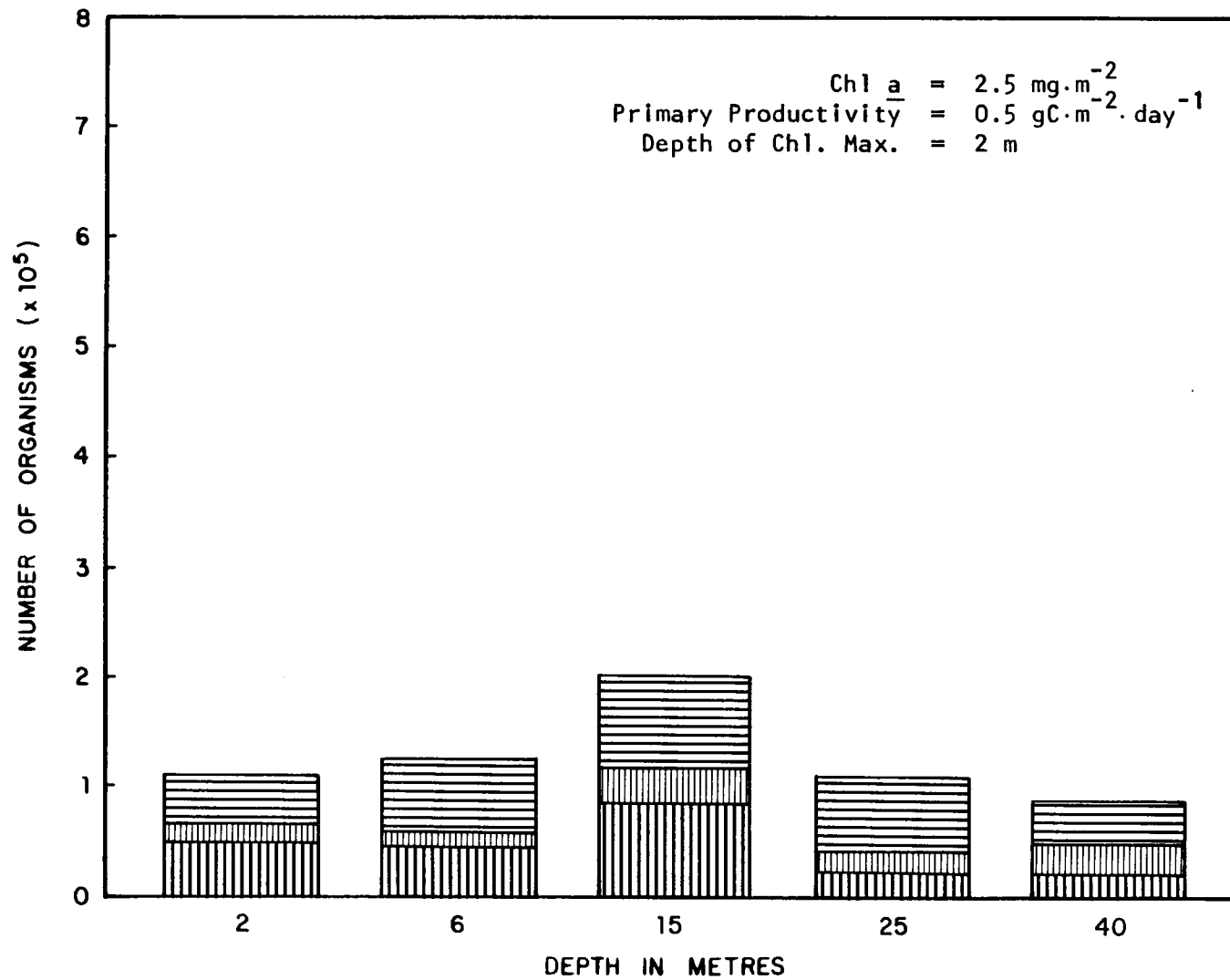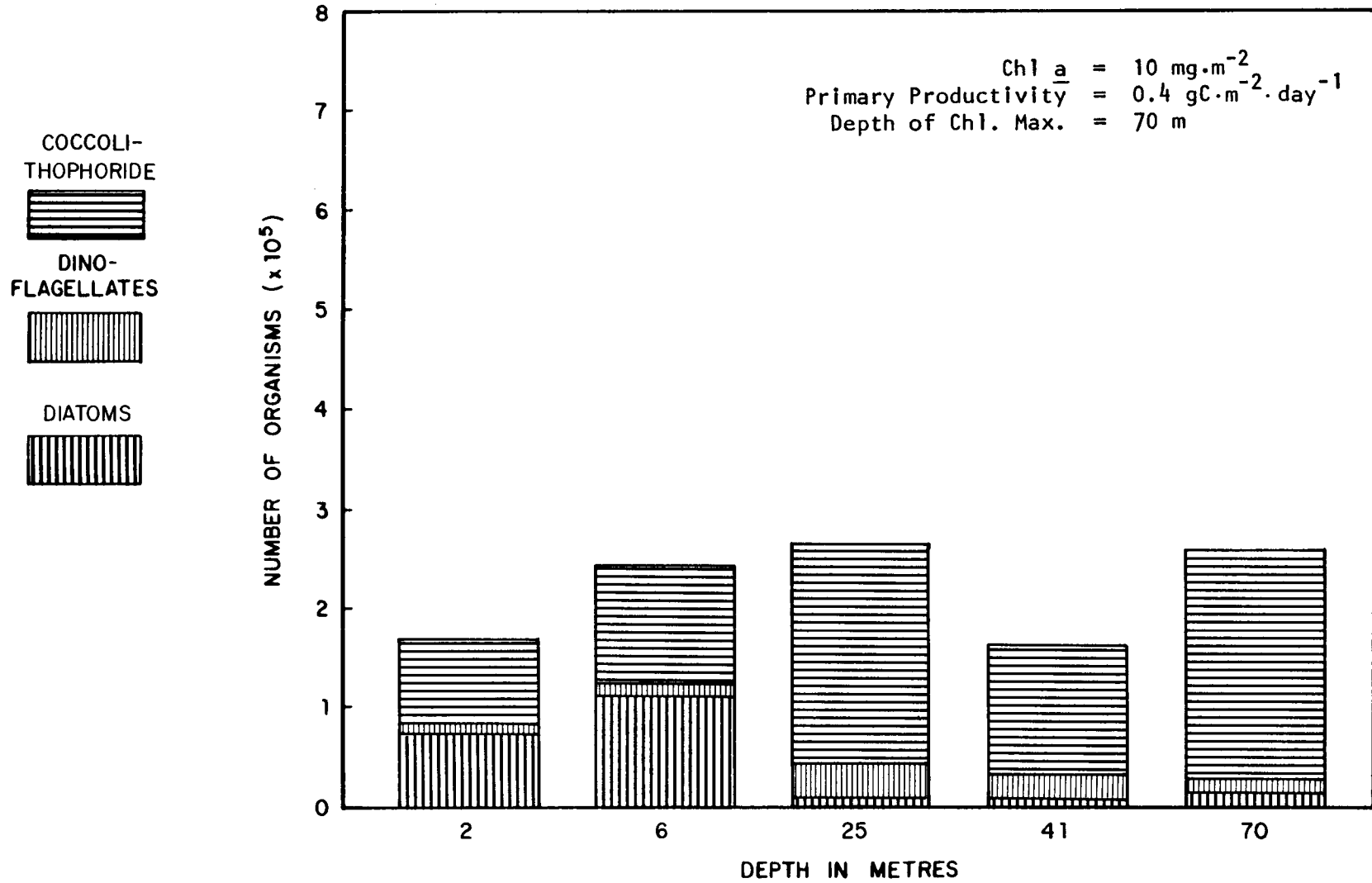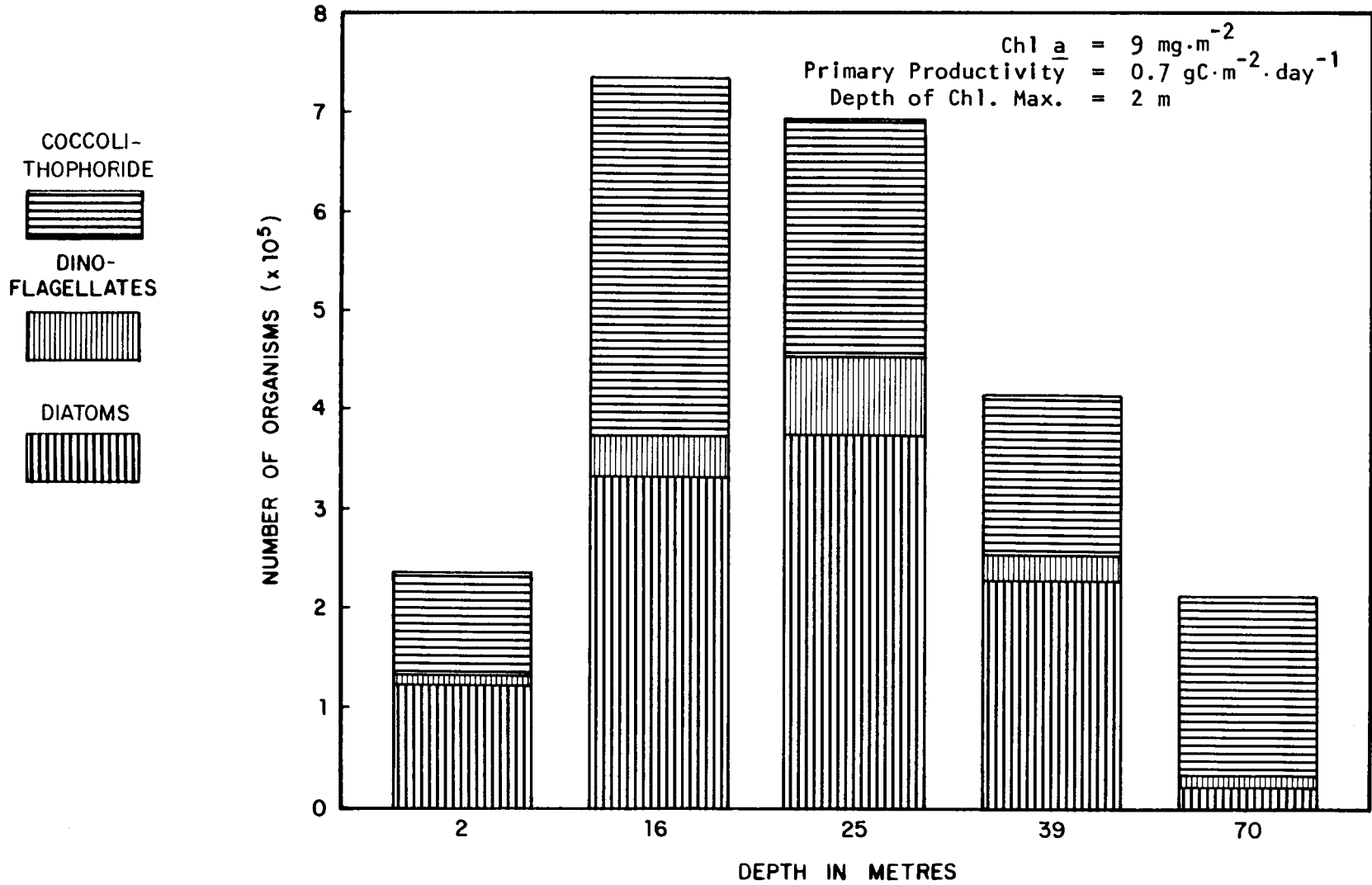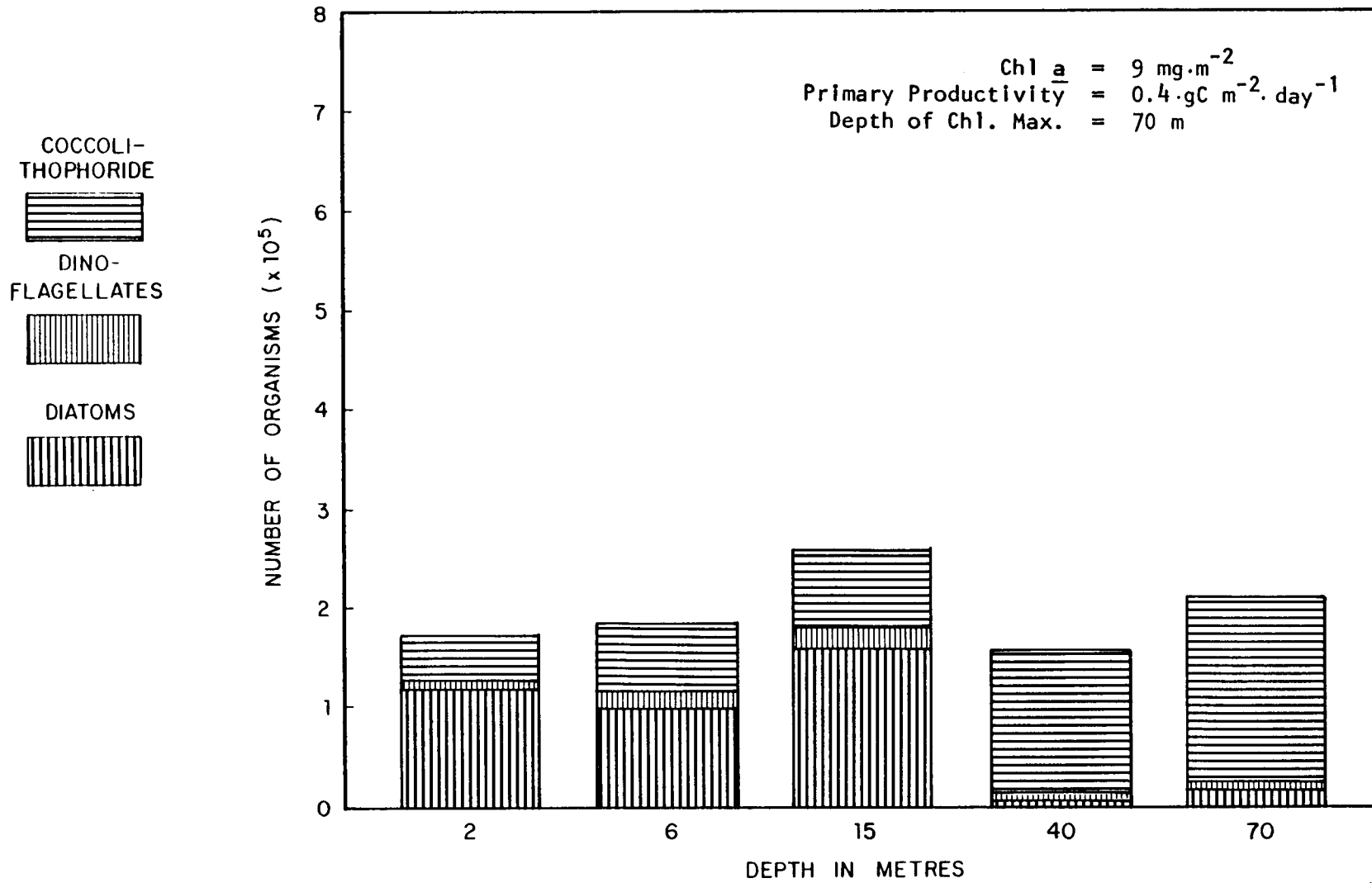
Figure 5-20. Phytoplankton enumeration results for summer cruise station 42.
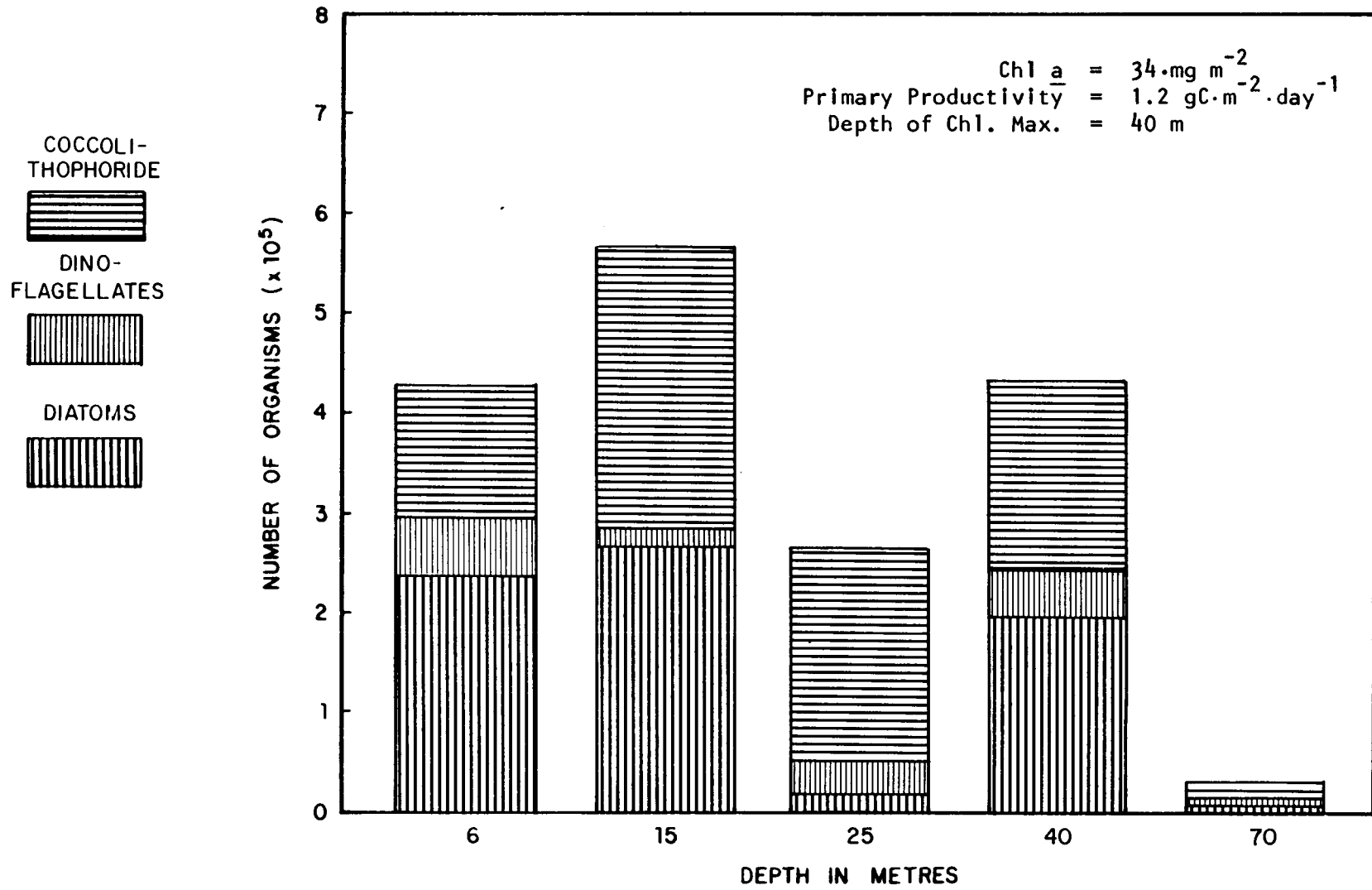
Figure 5-21. Phytoplankton enumeration results for summer cruise station 48.
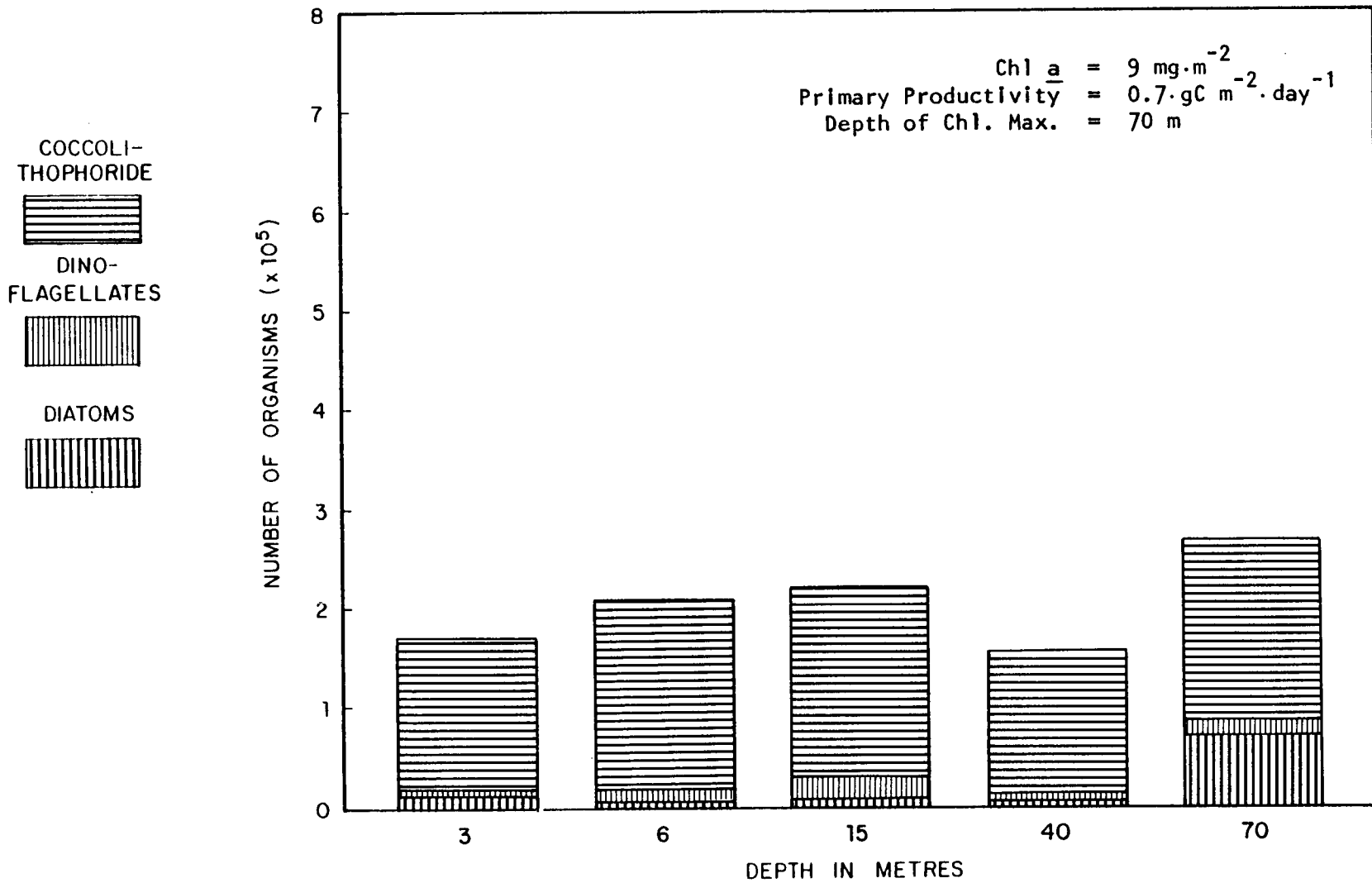
265

(Station 48). This stratification is more easily seen in the coccolithophore species such as Ceratolithus cristatus, and Discosphaera tubifera which are present only in the isothermal layer at both stations. Formation of the chlorophyll maximum at 40 m is well below the population increases at Station 48, but compares favorably with the coccolithophore dominated population increases at Station 42 at a depth of 70 m.

On September 17, samples were collected at Stations 65 (depths of 6, 15, 25, 40, and 70 m in Figure 5-22) and 71 (depths of 6, 15, 25, 40, and 70 m in Figure 5-23) under stratification conditions similar to those samples at the four previous summer stations. When the commonality of species at each station (Table 5-8a) and between pairs of stations (Table 5-8b) is examined, similar to Table 5-4 for the spring cruise, then a large number of coccolithophore species can be seen to be common between Stations 65 and 71. With the exception of the 40 m sample taken at Station 65 (Figure 5-22) which was dominated by C. huxleyi, the coccolithophore were again restricted to the surface isothermal layer which is consistent with the results at the other summer stations. The presence of C. cristatus, Rhizosolenia alata Brightw., and Thalassiothrix frauenfeldii Grunow near the bottom of the surface layer emphasizes the stratification. Although R. alata was also found in the 40 and 70 m samples, they only represented about 3% of the species found above 25 m.

Stations 81 (sampling depths of 6, 15, 25, 40, and 70 m) and 87 (sampling depths of 2, 15, 24, 40, and 70 m) were sampled on September 18. The resulting vertical distributions are presented in Figures 5-24 and 5-25, respectively. Species stratification is still evident in these distributions

266

COCCOLI-
THOPHORIDE

DINO-
FLAGELLATES

DIATOMS

NUMBER OF ORGANISMS ($\times 10^5$)

$$\text{Chl } \underline{a} = 15 \text{ mg} \cdot \text{m}^{-2}$$
$$\text{Primary Productivity} = 0.8 \text{ gC} \cdot \text{m}^{-2} \cdot \text{day}^{-1}$$
$$\text{Depth of Chl. Max.} = 40 \text{ m}$$

DEPTH IN METRES
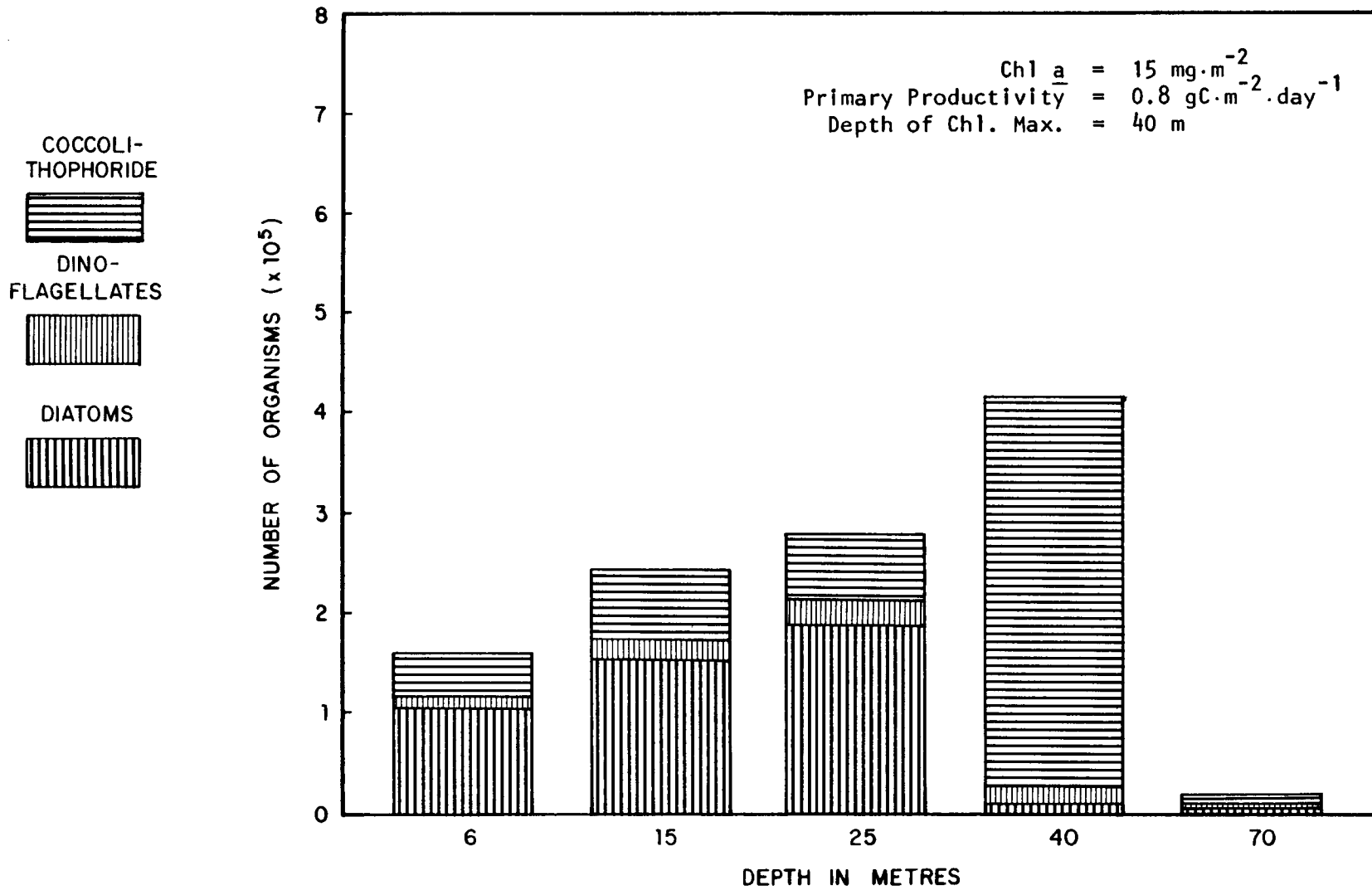
Figure 5-22. Phytoplankton enumeration results for summer cruise station 65.
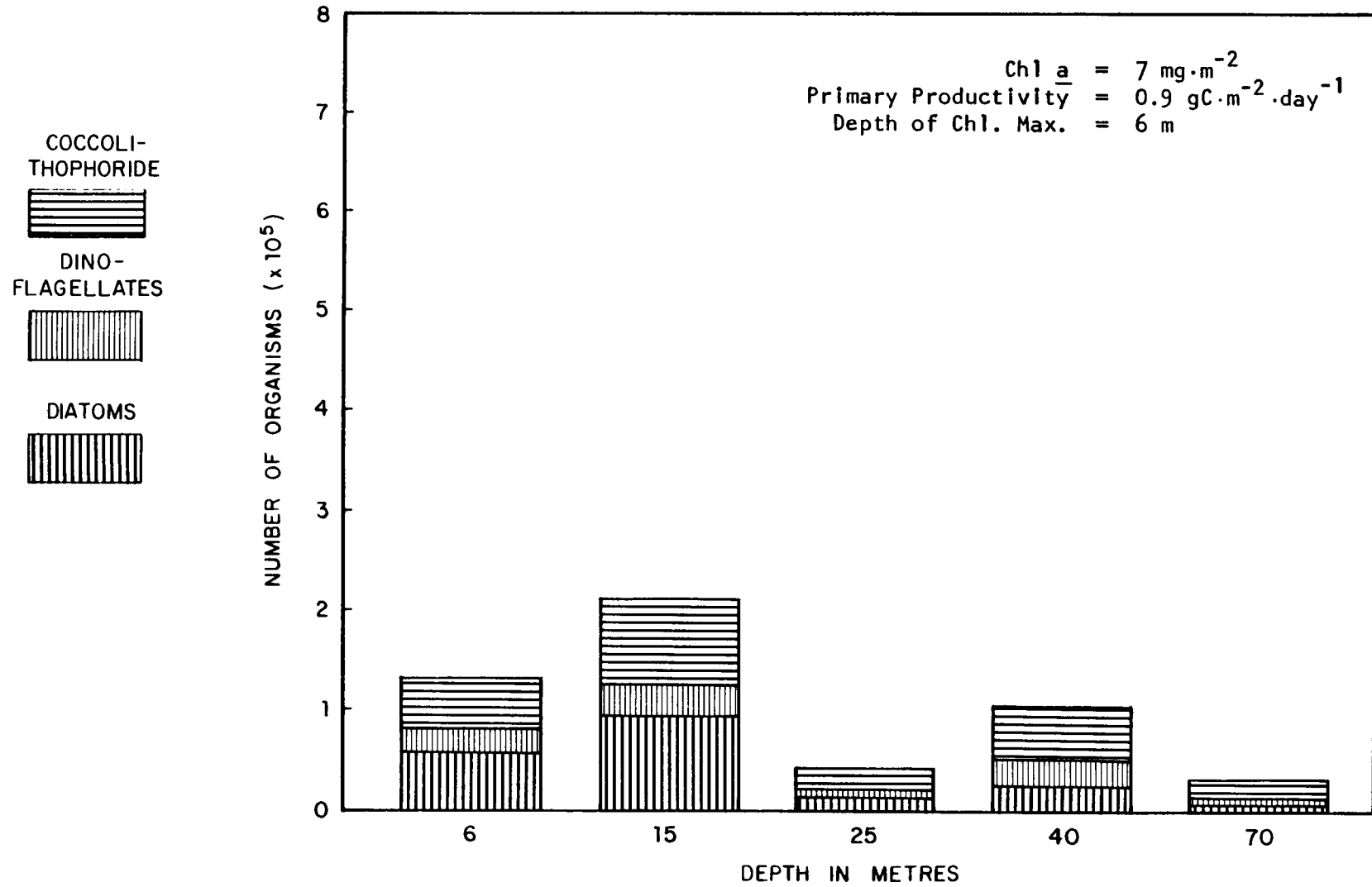
Figure 5-23. Phytoplankton enumeration results for summer cruise station 71.

Table 5-8. Phytoplankton species common at paired stations during summer cruise.

a) Percentage of species common at all depths.

Station #	10	27	42	48	65	71	81	87
Diatoms	35.6	28.0	11.7	19.1	26.7	7.1	25.0	40.0
Dinoflagellates	35.7	27.0	13.3	16.7	18.8	15.3	30.7	8.3
Coccolithophores	64.3	72.7	38.9	43.8	35.3	20.0	64.2	28.6

b) Percentage of species common to paired stations.

Stations	10 & 27	42 & 48	65 & 71	81 & 87
Diatoms	39.3	56.0	52.4	59.3
Dinoflagellates	40.0	50.0	33.3	60.0
Coccolithophores	57.1	52.4	81.3	46.7
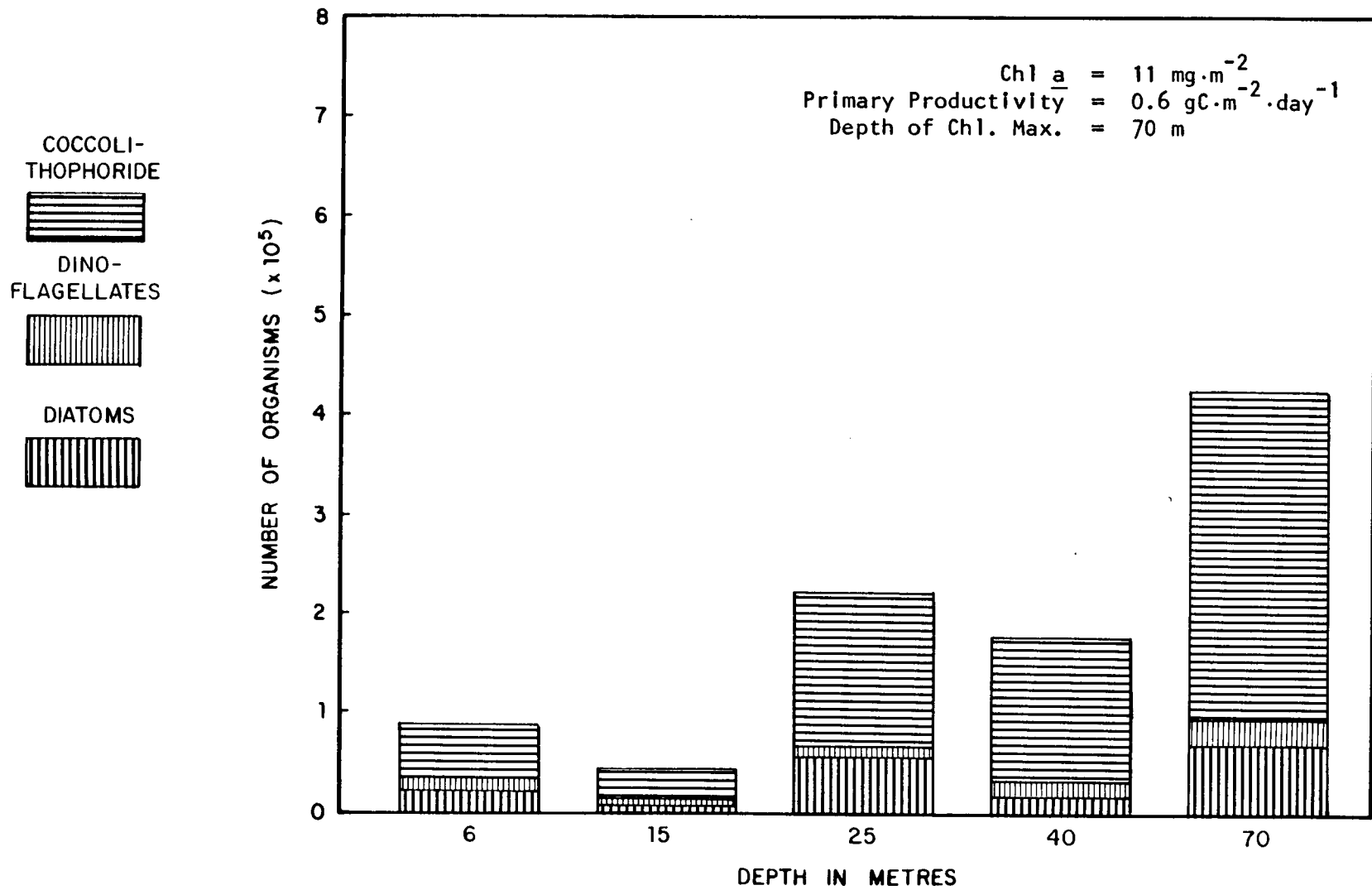
Figure 5-24. Phytoplankton enumeration results for summer cruise station 81.
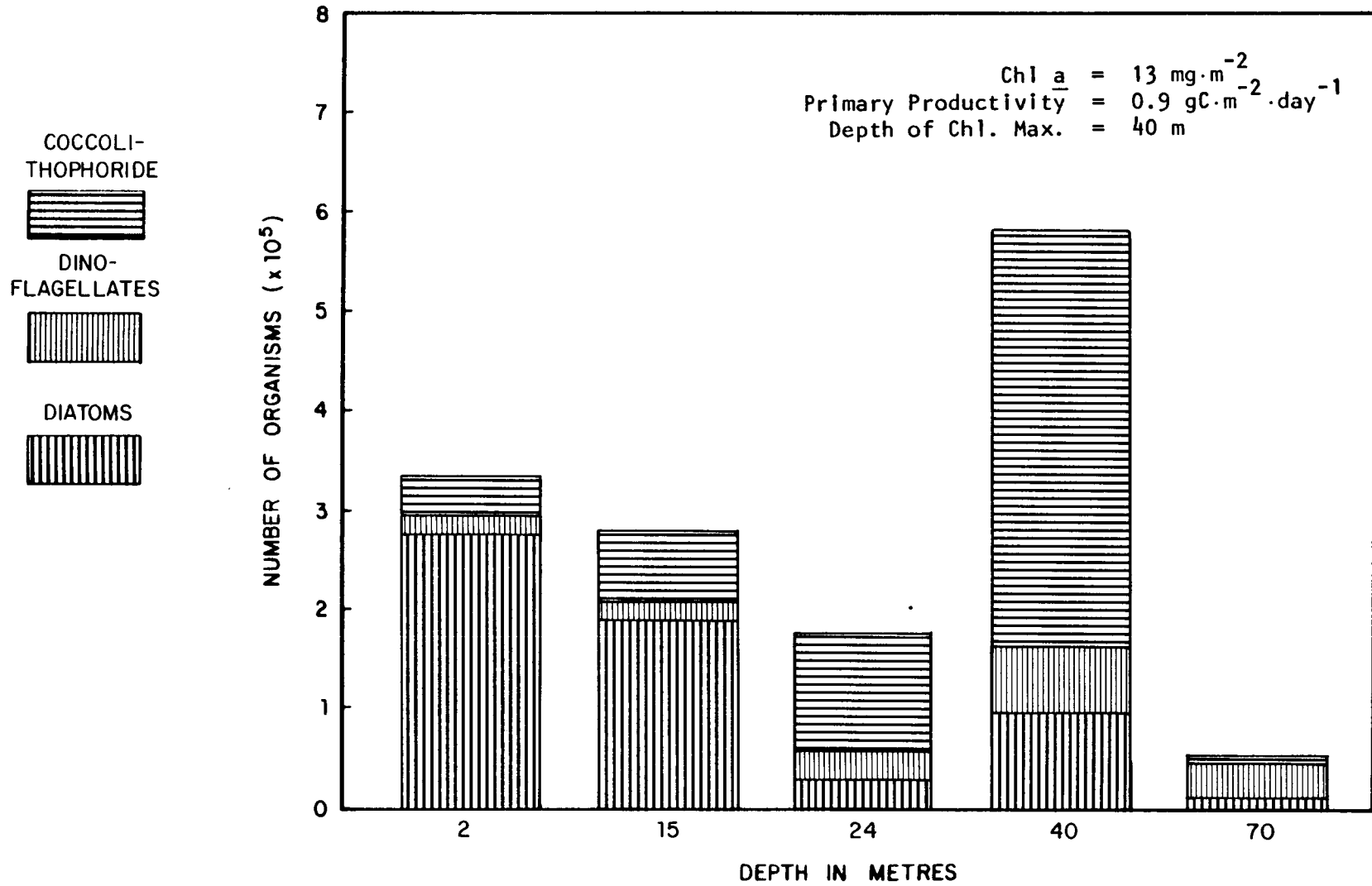
Figure 5-25.   Phytoplankton enumeration results for summer cruise station 87.

with the restriction of C. cristatus and D. tubifera to the upper three depths, greater concentrations of R. alata in the upper three depths, and higher concentrations of C. huxleyi at the lower three depths. In comparing the distributions by station pairs, (Table 5-8b) it appears that about half of the species within each major group are common in all four pairs.

5.4 Conclusions

During both spring and summer cruises, Chl a concentrations in the surface mixed layer were generally very low at about $0.1 \text{ mg} \cdot \text{m}^{-3}$ or less. The exceptions were the summer cruise stations which were characterized by a surface lens (~ 10 to 30 m thick) of relatively low salinity water (less than $35.5°/oo$). At these stations, near-surface Chl a was as high as $0.3 \text{ mg} \cdot \text{m}^{-3}$.

In both cruise data sets, most stations seaward of the 100 m isobath were affected by a subsurface intrusion of nutrient-rich, offshore water. At these stations, the top of the nitracline was generally located at depths of 40 to 60 m. A subsurface Chl a maximum layer was present at or near the depth of the top of the nitracline. Maximum Chl a concentrations associated with the subsurface layer ranged from approximately 0.2 to $1.2 \text{ mg} \cdot \text{m}^{-3}$.

Dominant phytoplankton species of the surface mixed layer were generally different than those dominating the subsurface Chl a maximum layer at the same station. This was particularly dramatic at those stations occupied during the summer cruise that were characterized by relatively low surface salinities. The diatom, Rhizosolenia alata, accounted for more than 80% of total diatom numbers within the low salinity surface layer. Coccolithophores

272

(primarily <u>Coccolithus huxleyi</u>) or diatoms other than <u>R</u>. <u>alata</u> dominated the subsurface Chl <u>a</u> maximum layer.

A closer examination of individual diatom species, e.g., <u>T</u>. <u>frauenfeldi</u> and <u>R</u>. <u>alata</u> and their relation to environmental factors will be necessary to evaluate the role of diatom systemmatics in Loop Current waters. The coccolithophore presently appear to be the best indicators of these relations --- especially individual species that are easily identified such as <u>C</u>. <u>cristatus</u>, <u>D</u>. <u>tubifera</u>, and <u>C</u>. <u>murrayi</u>. The role of dinoflagellates is presently unclear because of the relatively few observed and the lack of knowledge concerning their response to changes in physical factors.

Primary production was enhanced by movement of offshore nutrients onto the outer shelf. This was particularly evident during the summer cruise because mean primary production of stations most directly influenced by intruded waters was double that of stations located either seaward or shoreward of the intrusion. At most of the stations where a subsurface Chl <u>a</u> maximum layer was present, the layer contributed significantly to water column productivity. At more than one-third of the productivity stations occupied during the summer cruise, the rate of primary production of the subsurface Chl <u>a</u> maximum layer was as high, or higher, than the maximum rate observed in the surface mixed layer. Lowest productivity (0.1 $gC \cdot m^{-2} \cdot day^{-1}$) was observed during the spring cruise at a station located off the shelf within the Loop Current.

Highest productivity $(1.2 \ gC \cdot m^{-2} \cdot day^{-1})$ was observed during the summer cruise at the station having the highest concentration of Chl a within the subsurface maximum layer.

On the outer shelf, rates of productivity and euphotic zone Chl a change dramatically in time and space depending on the hydrographic characteristics of the station where measurements are made. The present data suggest that upwelling versus non-upwelling conditions may control most of the variability in outer shelf primary production. Since the mean position of the Loop Current varies with season, this control is probably seasonal in nature with an intensity dependent upon local atmospheric and oceanographic conditions. During periods when upwelling is occurring, this control may be more important than seasonal effects in the same region.

Based on hydrographic, nutrient, Chl a, and primary productivity measurements the dynamics of primary production on the outer southwest Florida continental shelf are markedly similar to those of the outer southeastern shelf between Cape Canaveral and Cape Hatteras. The major difference between the regions is that production rates and phytoplankton biomass are several times higher during upwelling and intrusion events on the outer southeastern shelf than observed during the two data collections on the outer southwest Florida shelf. A probable explanation is that the top of the nitracline reaches higher into the euphotic zone during upwelling on the outer southeastern shelf than on the outer southwest Florida shelf.

During the summer cruise, about 70% of the observed variability in primary production could be explained solely by euphotic zone Chl $\underline{a}$ and by the incident irradiance received during the incubation period. This observation could be useful to those formulating ecological models of the outer southwest Florida shelf.

Color scanners mounted in satellites (e.g., CZCS) will probably not yield reliable estimates of either euphotic zone Chl $\underline{a}$ or of daily primary production (which is based in part on euphotic zone Chl $\underline{a}$). Much of the euphotic zone Chl $\underline{a}$ and primary production is often located beneath the surface mixed layer, and the subsurface values of production and Chl $\underline{a}$ have little or no relation with that of the overlying surface mixed layer.

5.5 References

Atkinson, L.P., G.A Paffenhofer, and W.M. Dunstan 1978. The chemical and biological effect of a Gulf Stream intrusion off St. Augustine, Florida. Bulletin of Marine Science, 18: 667-679.

Bishop, S.S., J.A.Yoder, and G.A. Paffenhofer 1980. Phytoplankton and nutrient variability along a cross-shelf transect off Savannah, Georgia, U.S.A. Estuarine and Coastal Marine Science, 11: 359-368.

Blanton, J.O., L.P. Atkinson, L.J. Pietrafesa, and T.N. Lee 1981. The intrusion of Gulf Stream water across the continental shelf due to topographically-induced upwelling. Deep-Sea Research, 28A: 393-405.

Cupp, E.E. 1943, Marine plankton Diatoms of the west coast of North America. Bull. Scripps Inst. Oceanogr., tech. ser. 5(1): 1-238.

Dugdale, R.C. and J.J. Goering 1967. Uptake of new and regenerated forms of nitrogen in primary productivity. Limnology and Oceanography, 12: 196-206.

Dunstan, W.M. and L.P. Atkinson 1976. Sources of new nitrogen for the South Atlantic Bight. In: Estaurine Processes, Vol. 1, M. Wiley, editor, Academic Press: 69-78.

Gaarder, K.R. and G.R. Hasle 1971. Coccolithophorids of the Gulf of Mexico, Bulletin of Marine Science, 21(2): 519-544.

Haq, B.U. and A. Baesma eds. 1970. Calcareous nannoplankton: Introduction to Marine Micropaleontology, 376.

Hendey, N.I. 1964. An introductory account of the smaller algae of British coastal waters. Part V: Bacillariophyceae. Fishery investigations Series IV. Her Majesty's Stationary Office, London.

Lee, T.N., L.P. Atkinson, and R. Legeckis 1981. Observations of a Gulf Stream frontal eddy on the Georgia continental shelf, April, 1977. Deep-Sea Research, 28A: 347-378.

Norris, R.E. 1965. Living cells of Ceratolithus cristatus (Coccolithophorae). Arch. Protistenk. Bd. 108.5: 19-24.

Okada, H. and A. McIntyre 1979. Seasonal distribution of modern Coccolithophores in the western North Atlantic Ocean. Marine Biology, 54: 319-328.

Schindler, D.W., R.V. Schmidt, and R.A. Reid 1972. Acidification and bubbling as an alternative to filtration in determining phytoplankton production by the ^{14}C method. J. Fish. Res. Bd. Can., 29: 1627-1631.

Steeman-Nielsen, E. 1952. The use of radioactive carbon (C^{14}) for measuring organic production in the sea. J. du Cons. Internat. Explor. Mer., 19: 117-140.

Strickland, J.D.H. and T.R. Parsons 1972. A practical handbook of seawater analysis. Bulletin 167, Fisheries Research Board of Canada, Ottawa.

Throndsen, J. 1972. Coccolithophorids from the Caribbean Sea. Norw. J. Bot. 19: 51-60.

Vukovich, F.M., B.W. Crissman, M. Bushnell, and W.J. King 1979. Gulf Stream boundary eddies off the east coast of Florida. Journal of Physical Oceanography, 9: 1214-1222.

Wessels, C. nd E. Birnbaum 1979. An improved apparatus for use with the ^{14}C acid-bubbling method of measuring primary production. Limnology and Oceanography, 24: 187-188.

Yentsch, C.S. and D.W. Menzel 1963. A method for the determination of phytoplankton chlorophyll and phaeophytin by fluorescence. Deep-Sea Res., 10: 221-231.

Yoder, J.A., L.P. Atkinson, J.O. Blanton, D.R. Deibel, D.W. Menzel, and G.A. Paffenhofer 1981. Plankton productivity and the distribution of fishes on the southeastern U.S. continental shelf. Science, 214: 352-353.

Yoder, J.A., L.P. Atkinson, S.S. Bishop, E.E. Hofmann, T.N. Lee. Effect of upwelling on phytoplankton productivity on the outer southeastern U.S. continental shelf. Continental Shelf Research, in press.

6.0 OPTICAL OCEANOGRAPHIC ANALYSES

NIELS K. HOJERSLEV
INSTITUTE OF PHYSICAL OCEANOGRAPHY, UNIVERSITY OF COPENHAGEN

6.1 Introduction

Although the results of some significant optical oceanographic studies have recently been reported for the Gulf of Mexico (e.g., Austin 1980), the Gulf area still remains one of the least understood oceanic areas in terms of its optical properties. Moreover, the observed dynamic and kinematic relationships represented by selected parameters such as Chl a or suspended matter concentrations still pose a number of presently unanswerable questions mainly because of the dearth of concurrent hydrographic, in-situ and remote sampling, current measurements, marine optics, and biological studies.

As part of its Environmental Studies Program, the Minerals Management Service (Gulf of Mexico Outer Continental Shelf Regional Office) has focused an interest on the study of the southwest Florida shelf ecosystem. Part of this interest stems from the need to evaluate the potential hazards to the marine ecosystem by inadvertent introduction of particulate matter into the water column by presently anticipated offshore minerals development in the eastern Gulf. As part of that study, optical oceanographers from the University of Copenhagen, Institute of Physical Oceanography were invited to participate in a joint biological-optical, remote sensing study of the hydrography and primary production characteristics of the eastern Gulf. The objectives of this combined biological-optical oceanographic segment of this study were four-fold.

1) To measure the joint distribution of temperature, salinity, penetration depth of the photosynthetically active daylight (euphotic) zone, chlorophyll-like pigment concentrations, suspended (seston plus sediments) and dissolved organic matter (yellow substance) concentrations, upward daylight radiances, and irradiances just below the sea surface (color of the sea).

2) To establish possible correlations between dynamical, or kinematic, features derived from the field of mass and pertinent parameters such as suspended matter and Chl $\underline{a}$ concentrations.

3) To check existing color algorithms against concentrations of Chl $\underline{a}$ + Ph $\underline{a}$ and the depth of the euphotic zone.

4) To compare the sea truth data set against remotely measured concentrations such as those derived from the CZCS.

The measurements taken to meet these objectives were collected exclusively during the spring cruise.

6.2 Instrumentation

Seven (7) optical oceanographic sensors were used for the Southwest Florida Shelf Ecosystems Study. These specialized sensors were developed at the University of Copenhagen, Institute of Physical Oceanography for measurement of optical oceanographic parameters in different parts of the world. A review of these sensors has recently been completed by Hojerslev and Larsen (1980).

In terms of their functions and precision, the sensors can be listed as follows.

6.2.1. F – meter

The color index meter measures nadir radiances, L (180°) at 447 and 521 nm just below the sea surface. The half widths in both channels is approximately 15 nm. The ratio between the blue (447 nm) and green (521 nm) signals produces a quantity (defined by Hojerslev and Jerlov; 1977) called the colc index, F. As discussed by Hojerslev (1980), the color index is a very convenient quantity for optical oceanic blue water studies because any color of the sea can be described by a combination of only these two colors. Actually, any color can be described by three primary colors. However, it can be noted that oceans and intercontinental mediterraneans are generally blue to turquoise, marginal seas are turquoise to green, and intracontinental mediterraneans are green to yellow. Rarely are seas redish or brownish in color. Thus, any natural color of the sea can be described by essentially two primary colors rather than three --- specifically blue and green.

Further, the color meter wavelengths are quite close to Channels 1 (443 nm) and 2 (520 nm) of the NIMBUS-7 CZCS which permits an almost direct comparision between measurements taken by both systems.

The color meter is calibrated against an Epply standard of spectral irradiance No. EPI – 1486. Repeated calibrations of this sensor over a period of more than a decade have shown overall variations of less than two percent. In terms of field usage, color index measurements are collected as close to the

water surface as possible to define the ratio at zero depth (just below the surface). If an estimate for the maximum relative error is sought, then

$$\frac{\Delta F}{F} = \frac{L \ (180°, \ 447 \ nm, \ Z=0)}{L \ (180°, \ 521 \ nm, \ Z=0)} \cdot \frac{1}{2} \cdot \frac{e^{-K_L(447) \cdot \Delta Z}}{e^{-K_L(521) \cdot \Delta Z}}$$

where $K_L(447)$ and $K_L(521)$ are the vertical attenuation coefficients for the nadir radiances at 447 and 521 nm, respectively. The uncertainty in depth, ΔZ is the total vertical displacement of the color index meter from the actual sea surface. In this particular investigation,

$K_L(447) \simeq 0.036 \ m^{-1}$, $K_L(521) \simeq 0.054 \ m^{-1}$, and $\Delta Z \leq 0.5$ m. Thus,

$$\frac{\Delta F}{F} \cdot 100 \leqslant 0.5\% \quad \text{and}$$

the overall color index accuracy is within the $\pm$ 2.5%.

Further details pertaining to this instrument have been presented by Jerlov (1974).

6.2.2. E - meter

The twelve (12) channel irradiance meter measures downward irradiance, E_d, at 371, 403, 455, 477, 492, 517, 533, 573, 602, 634, 674, and 687 nm. The half widths in all channels are about 15 nm. When oriented downward, the instrument measures upward irradiance, E_u.

The E – meter is calibrated in the same manner as the F – meter with similar precision results.

Field use of the sensor consists of E_d and E_u measurements in the 371 to 687 nm range in the air, just below the surface ($z = 0$)' and at 1, 5, and 10 m. The vertical attenuation coefficient for downward irradiance (see Section 2.3.3.), K_d and the reflectance ratio $R = E_u/E_d$ are calculated.

An error analysis developed by Hojerslev (unpublished) has shown that the maximum error in E_d can be ± 25% whereas the overall accuracy for R is within ± 4%. These errors arise from changing surface light conditions and uncertainties in depth determinations during measurement.

6.2.3 q – meter

The quantum irradiance meter measures the number of photons incident on a horizontal unit area in a unit time in the 350 to 700 nm spectral range. The q – meter is calibrated to yield a reading that is proportional to the radiant input energy at a given wavelength and the wavelength itself in the 350 to 700 nm range. Detailed discussions of this sensor has been presented by Jerlov and Nygård (1969).

In practice, the relative errors in the vertical attenuation coefficient for downwelling quanta irradiance, K_q must be examined carefully because of the irradiance variability in the euphotic zone, the significant light fluctuations in shallow depths, allowance for integration effects in the

283

visible range, and the wavelength dependence of the cosine collector. As such, the maximum relative error may exceed $\pm$ 25%.

6.2.4. b - meter

The light scattering meter integrates the light scattering function, $\beta(\theta)$ from 3 to 150 degrees at 655 nm. Since $b = \int_{4\pi} \beta(\theta) \, d\omega$ (eqn. 2/13), the sensor provides a measure of the scattering coefficient.

A Lambert emitter, mounted in front of a lamp housing, is configured to produce a cosine emission at grazing angles; this emission minimizes integration errors caused by the dominant forward scattering. Integration of the light scattering function is performed in the interval $3° \leq \theta \leq 150°$. An error analysis for this sensor (Hojerslev, unpublished) utilizing 36 combinations of Junge distribution particles showed that the total light scattering coefficient can be profiled to an accuracy on the order of 5%. Details pertaining to b - meter calibration procedures have been discussed earlier by Jerlov (1961, 1976).

6.2.5 c - meter

This particular light transmission sensor provides a measure of the (total) light attenuation coefficient, c at 631 nm over a fixed path length of 1.0 m. Readings in the water column are normalized to a reading in air. Absolute c-values can only be obtained if the sensor is calibrated in a tank (Hojerslev and Larsen, 1980).

Photodiode output at 631 nm is collimated by a double lens system. In air, the collimated beam has a solid angle of acceptance of 10^{-4} steradians; in sea water, the solid angle of acceptance is 0.56×10^{-4} steradians. Transmission is defined in the same sense as equation (2/19) as the ratio of signal reading in water to air over a one metre path length. Its relations to c is given by

$$\text{Transmission} = ke^{-cr}$$

where k is a calibration constant dependent on geometry, wavelength, acceptance angles, and changes in sensor window reflections.

An error analysis by Hojerslev (unpublished) for this sensor based on Mie scattering theory shows the error in c to be on the order of $\pm$ 10%.

6.2.6 Chl a - meter

Chlorophyll distribution in the water column was profiled with a one-channel fluorescence meter. Excitation wavelengths were located in the blue-green part of the spectrum; emission wavelengths were in the red part. The fluorescence technique is approximate but yields a convenient relative profile for Chl a. The fluorescence yield from Phaeophytin a is generally negligible. During earlier experiments, this sensor was calibrated against various plankton monocultures at different Chl a levels (Hundahl and Holck, 1980). Experience has shown that fluorescence yields from monocultures having the Chl a concentration may differ by a factor of two. For the spring cruise, therefore, the fluorescence meter was "field calibrated" so that 100 mV output

corresponded to 1 mg·m^{-3} Chl <u>a</u>. This concentration is believed to be "average" for worldwide marine plankton populations. The maximum absolute error introduced by this assumption is on the order of ± 30% (Hojerslev, unpublished). The relative error for a specific area such as the southwest Florida shelf where phytoplankton species are less variable during a given season (see Section 5.3.1.3) probably yields a maximum relative error of much less than ± 30%.

6.2.7 <u>Secchi Discs</u>

Standard Secchi discs were used to estimate the attenuation coefficient in the blue, green and red parts of the spectrum and the depth of the euphotic zone. First, a white disc (albedo $\simeq$ 0.80, diameter = 0.3 m) was lowered to its depth of visibility in three color ranges; blue (λ max = 465 nm), green (λ max = 525 nm), and red (λ max = 655 nm). Broad glass filters were used to minimize liminal contrast in the eye of the observer. Following these measurements, the procedure was repeated with a black Secchi disc.

A critical correction for these measurements is the accounting for surface wave height along the suspension wire. Hojerslev and Lundgren (1977) have shown that a one-metre wave height can cause a 40% decrease in Secchi disc depth when referenced to a calm sea. The correction is applied as

$$D_o = D_H \ (1 + 0.4 \ H)$$

where D_o is the Secchi disc depth for a completely calm sea, and D_H is the Secchi disc depth measured in the presence of a wave height H (m). Station

sea state data were transmitted to the NODC as part of the project data submittal. Correction for wave height reduces the error to within ± 10% (Hojerslev, unpublished).

6.3. Results and Discussion

Weather conditions were fair and seas were calm during the April 1 through 7, 1982 combined sampling period. Of the total 110 occupied stations, 32 were selected for optical measurements of Chl a and light scattering during day and night. These stations coincided with CTD casts and are listed across the transect parameter cross-sections presented in this section. The locations of the sampling transects have been presented earlier in Figure 3-1. At daytime optical stations, downward quanta irradiance (350 to 700 nm), downward and upward UV-B irradiances (310 nm), downward and upward spectral irradiance (371 to 687 nm) and water-leaving nadir radiances (447 and 521 nm) were measured routinely whenever surface light conditions were favorable. During the first two cruise days, light transmission at 631 nm and spectral Secchi disc depths were measured as well. Satellite imagery updates were received on board the R/V GYRE on April 2, 5, and 7.

6.3.1. Inter-station Comparisons

One method for illustrating significant features in the data is to simply compare the profiles at pairs of stations. Figure 6-1 shows the relative locations of spring cruise station pairs used in this comparison.
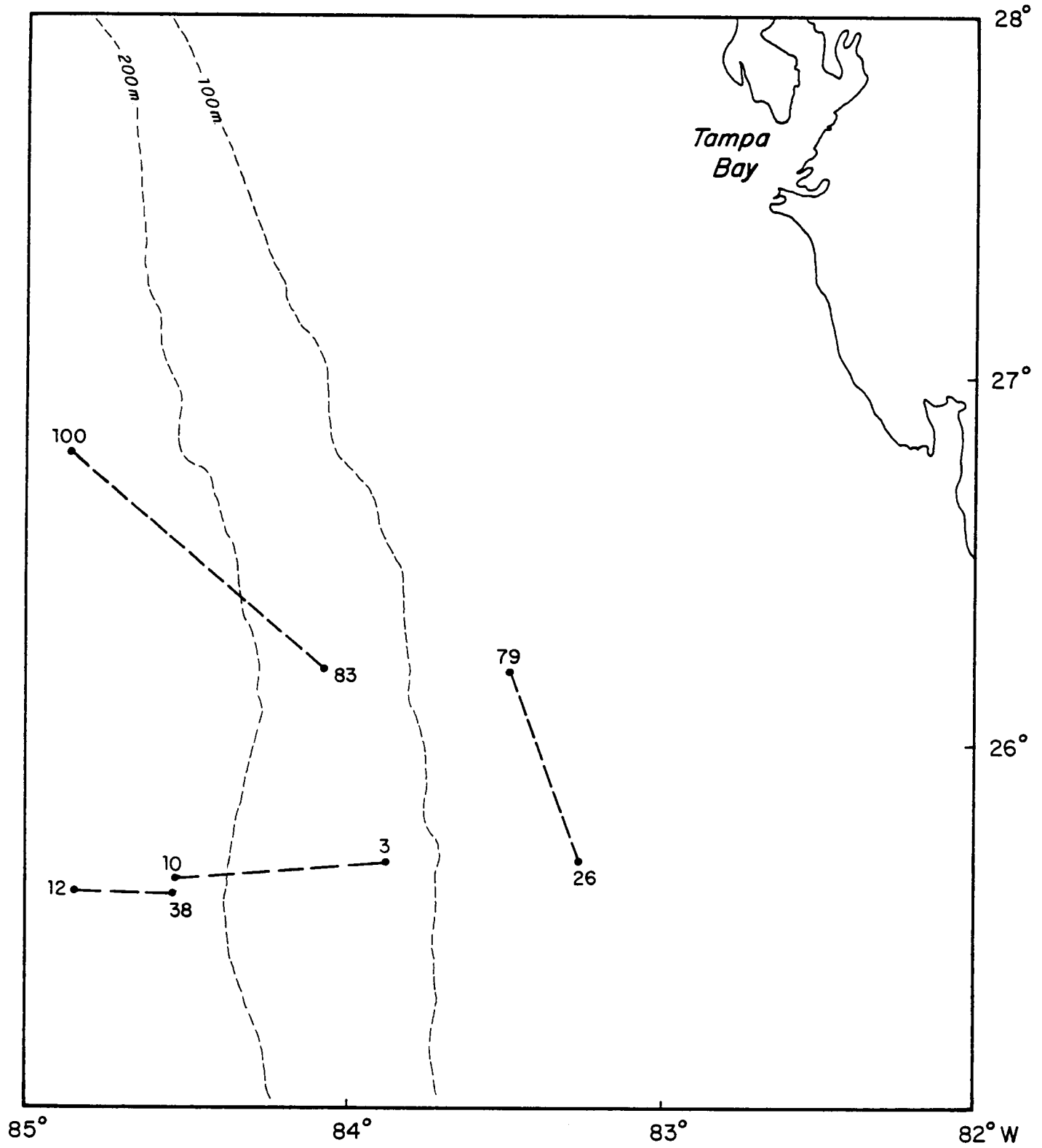
Figure 6-1. Spring cruise station pair locations.

6.3.1.1. Stations 12 and 38

Both of these stations (Figure 6-2) were located west of the shelf break in water depths greater than 200 m. Station 12 (on Transect 1) was profiled about 33 hrs. before Station 38 (on Transect 2). At Station 12, the depth of the mixed layer is around 60 m with no pronounced gradients in either Chl a or light scattering, b. Both σ_t and b values are relatively low. At Station 38, the depth of the mixed layer has risen to about 10 m, scattering values have increased considerably, and vertical gradients of Chl a and b are comparable to Station 12. As discussed in Section 3.2.1.3, these profile differences are attributed to the occurrence of the cyclonic edge of the Loop Current which occurred near Station 11 (25° 36' N, 84° 46' W) between these two stations (i.e., 12 and 38).

Special attention should also be directed at a comparison of the Chl a profiles at these stations (derived from chlorophyll fluorescence) to the center dashed Chl a graphs in Appendix Figures A-21 and A-25 (derived from in-situ sampling). Note the general agreement between results using both techniques.

6.3.1.2 Stations 3 and 10

Both of these stations (Figure 6-3) were situated on Transect (Section) 1 and were profiled about 10 hrs apart. Station 3 was located on the shelf in 135 m; Station 10 was off the shelf in 1046 m. Note the well-defined 10 m mixed layer and pronounced Chl a and b gradients in the vicinity of the pycnocline at Station 3. The Chl a and b maxima below the pycnocline are fairly broad

289
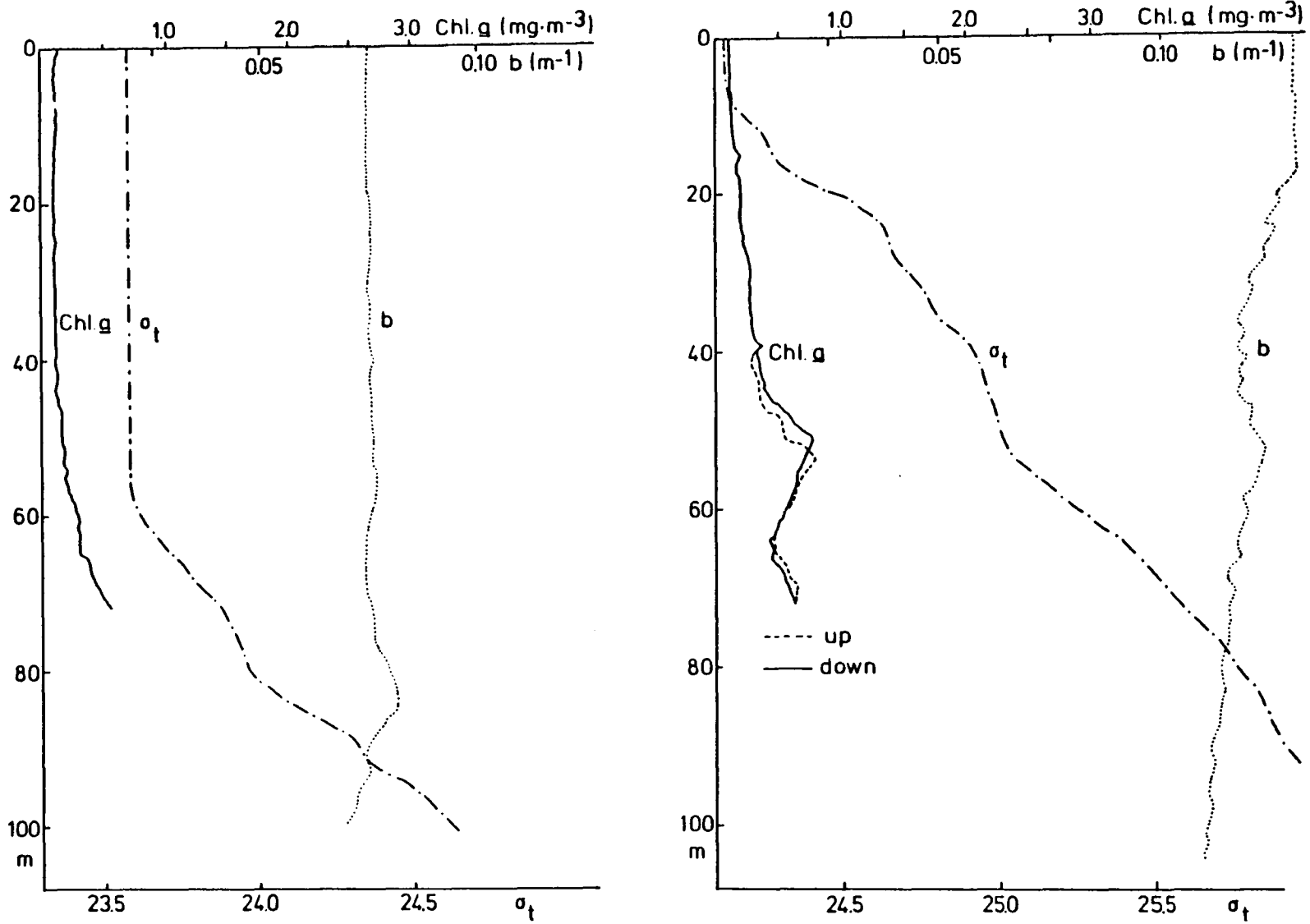
Figure 6-2. Chlorophyll, scattering coefficient, and density profiles at stations 12 (left) and 38 (right).
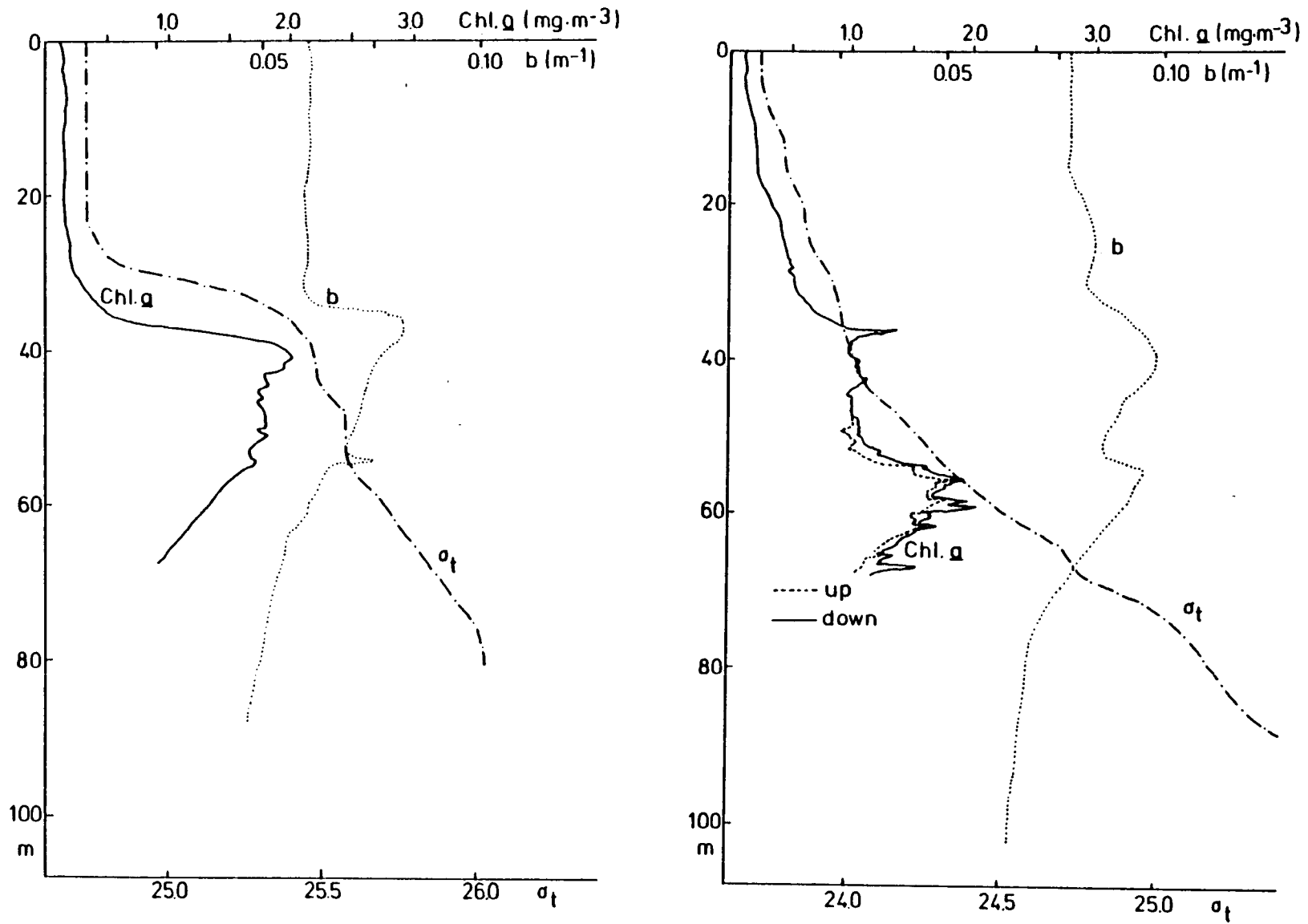
Figure 6-3. Chlorophyll, scattering coefficient, and density profiles at stations 3 (left) and 10 (right).

and agree with the in-situ sampling maximum in Figure 3-43. Closer to the

Loop Current front at Station 10, the mixed layer is missing and the vertical

distribution of both Chl $\underline{a}$ and b display finescale interleaving features.

Comparison features in this case should be cross-referenced to the

corresponding salinity interleaving in Figure 4-1 around σ_t = 24.0; this is

indicative of the mixing processes discussed earlier.

6.3.1.3 Stations 26 and 79

Both of these stations (Figure 6-4) were located on the shallower eastern

sides of their respective transects. At Station 26, the mixed layer is

missing but is present at Station 79 to a depth of about 20 m. The vertical

distributions of Chl $\underline{a}$ appear similar between stations contrary to the

distributions of scattering media. An important feature to note at these

stations is the lack of increase in b-values near the shelf bottom. This

indicates a sandy bottom and/or sluggish bottom currents on the shelf. WCC/CSA

(1982) show this shelf area to be composed of sand and shells.

6.3.1.4 Stations 83 and 100

Station 83 was located on the shelf in 146 m of water while Station 100 was

located well off the shelf in 1020 m (Figure 6-5). The obvious features to

note in this comparison are the pronounced subsurface Chl $\underline{a}$ and b maxima and

fine structure at both stations near the bottom of the mixed layer. Station

83 was situated in an area of most intense upwelling (see Section 3.2.1.3.)

and interleaving (see Section 4.2). Station 100 was situated in an area where

density and nutrient isopleths were uplifted by the Loop Current eddy (see
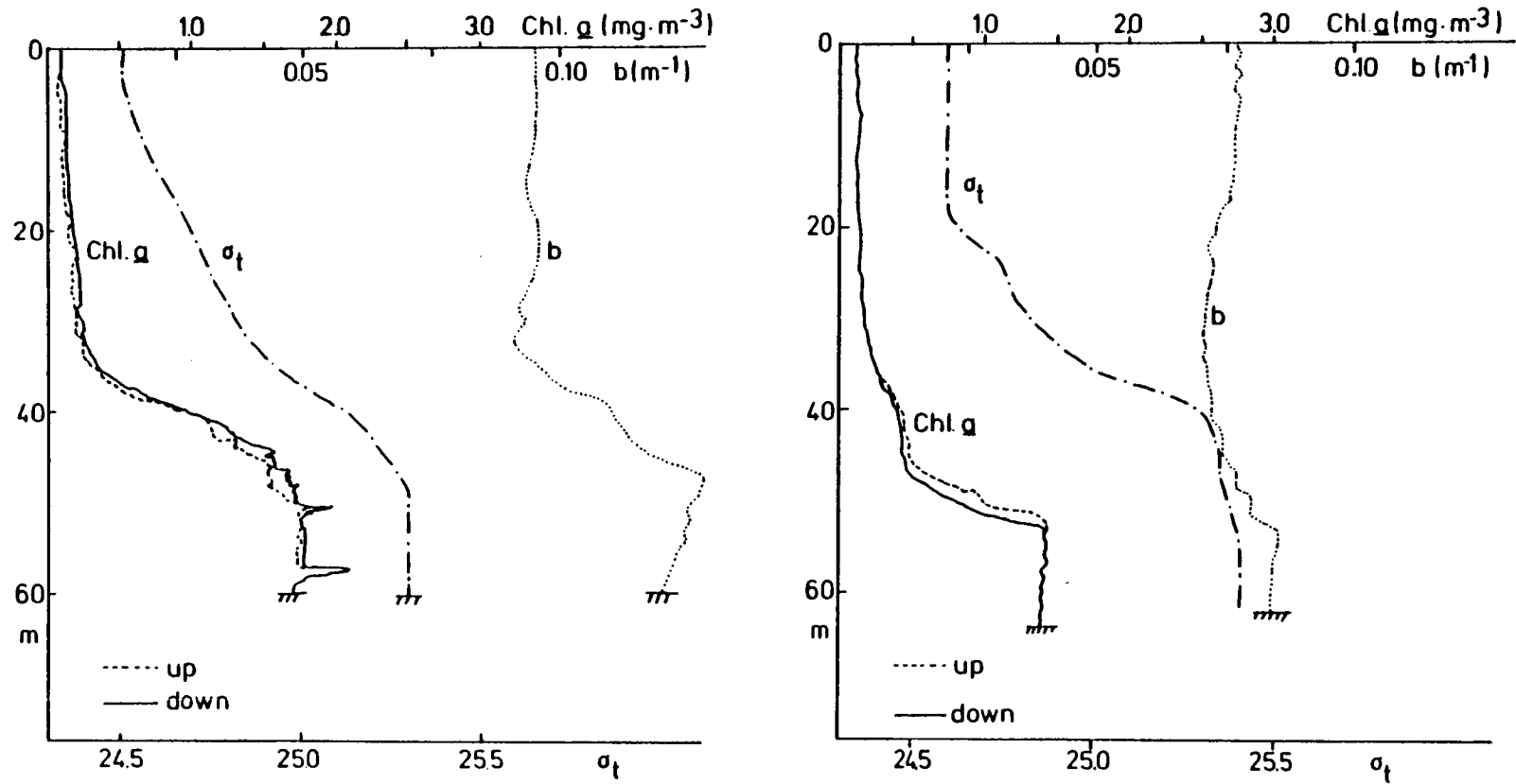
Figure 6-4. Chlorophyll, scattering coefficient, and density profile at stations 26 (left) and 79 (right).
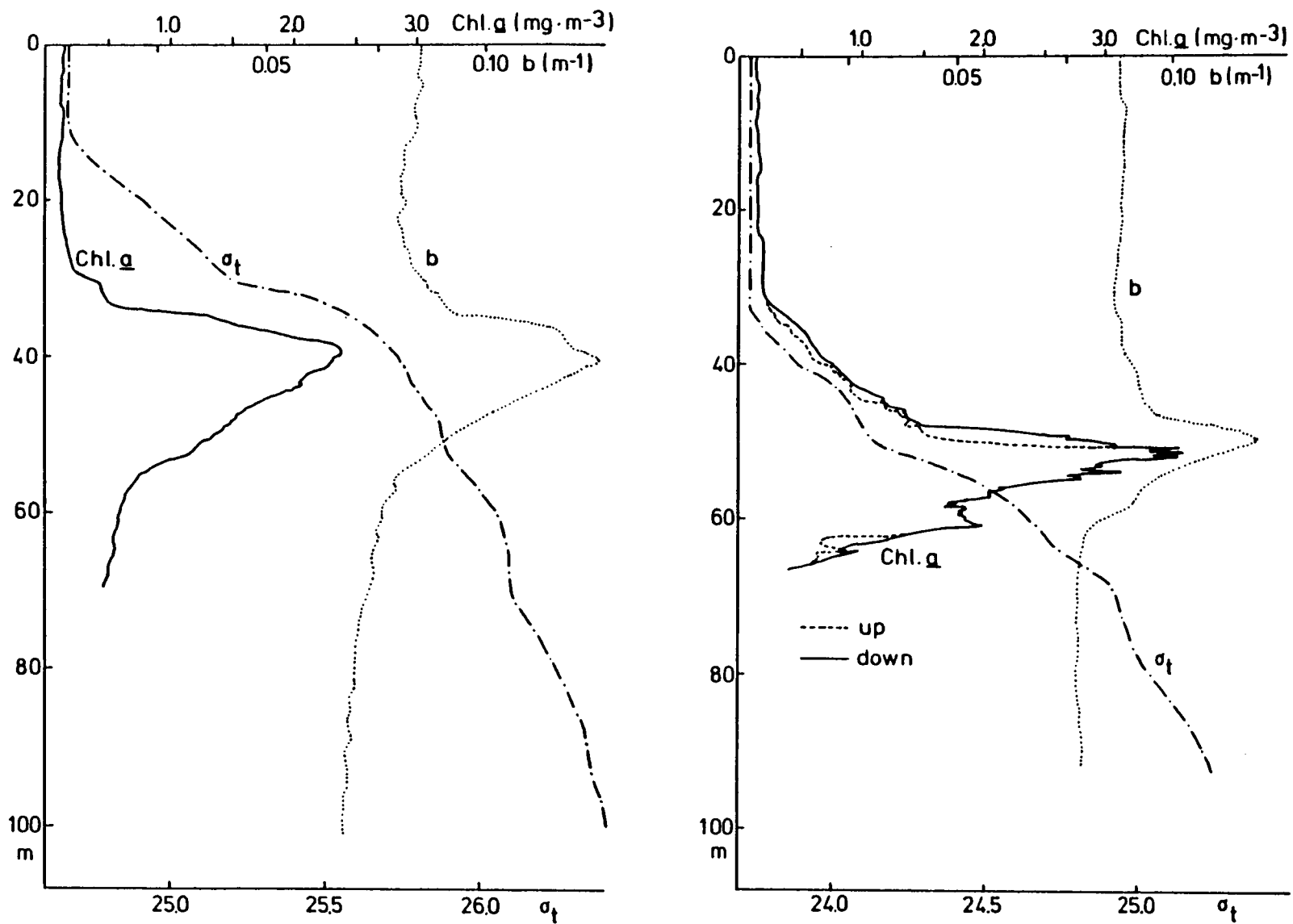
Figure 6-5. Chlorophyll, scattering coefficient, and density profiles at stations 83 (left) and 100 (right).

Section 5.3.1.2). In both cases, the optical data clearly indicate and support the previously discussed hydrographic and biological interpretations.

At Stations 38, 79, and 100, the Chl $\underline{a}$ profiles revealed several small vertical displacements of about one-metre in height. These events are commonly observed in the marine environment and usually indicate the presence of internal waves (Hojerslev, 1977b: Hojerslev and Lundgren, 1977).

6.3.2 Chl $\underline{a}$ Fluorescence

Resultant Chl $\underline{a}$ distributions for all 32 optical stations are summarized in cross-section form for Transects (Sections) 1, 2, 5, 6, and 8 in Figures 6-6 through 6-10, respectively. These figures correspond to in-situ sampling Figures 3-43 through 3-47 in Section 3.2.1.5. The general distributions can be characterized in three layers;

1) a homogenous surface layer with low (oligotrophic) concentrations around 0.1 to 0.2 mg·m^{-3},

2) an intermediate Chl $\underline{a}$ maximum layer around 50 m where a horizontal wave-like variation occurs, and

3) high concentration patches in which the Chl $\underline{a}$ levels reach 2 to 3 mg·m^{-3}.

A daylight effect on Chl $\underline{a}$ fluorescence reported by other investigators (e.g., Kiefer, 1973 a, b; Setser et al. 1982) was not evident in these data.

If it is recognized that cyclonic eddies in the northern hemisphere can produce upwelling of chlorophyll-bearing phytoplankton (as reported by Hojerslev, 1970, 1981a, and Hojerslev and Lundgren, 1977), then upwelling is

SECTION 1
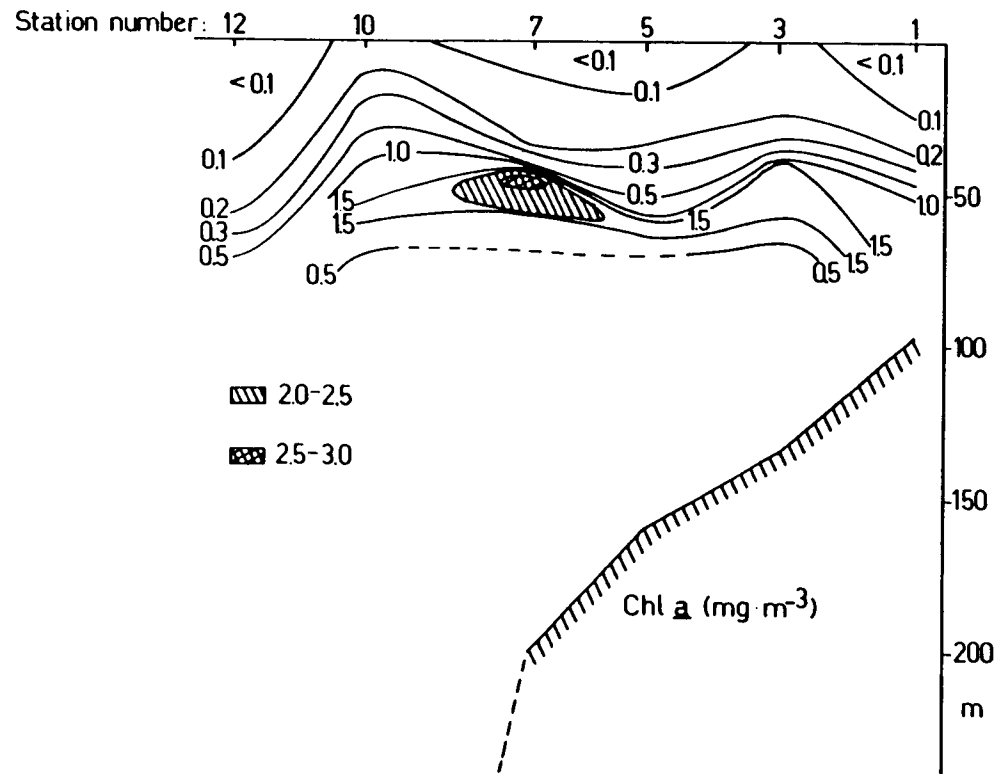
Figure 6-6. Vertical distribution of Chl a along Transect 1, April 2, 1982.
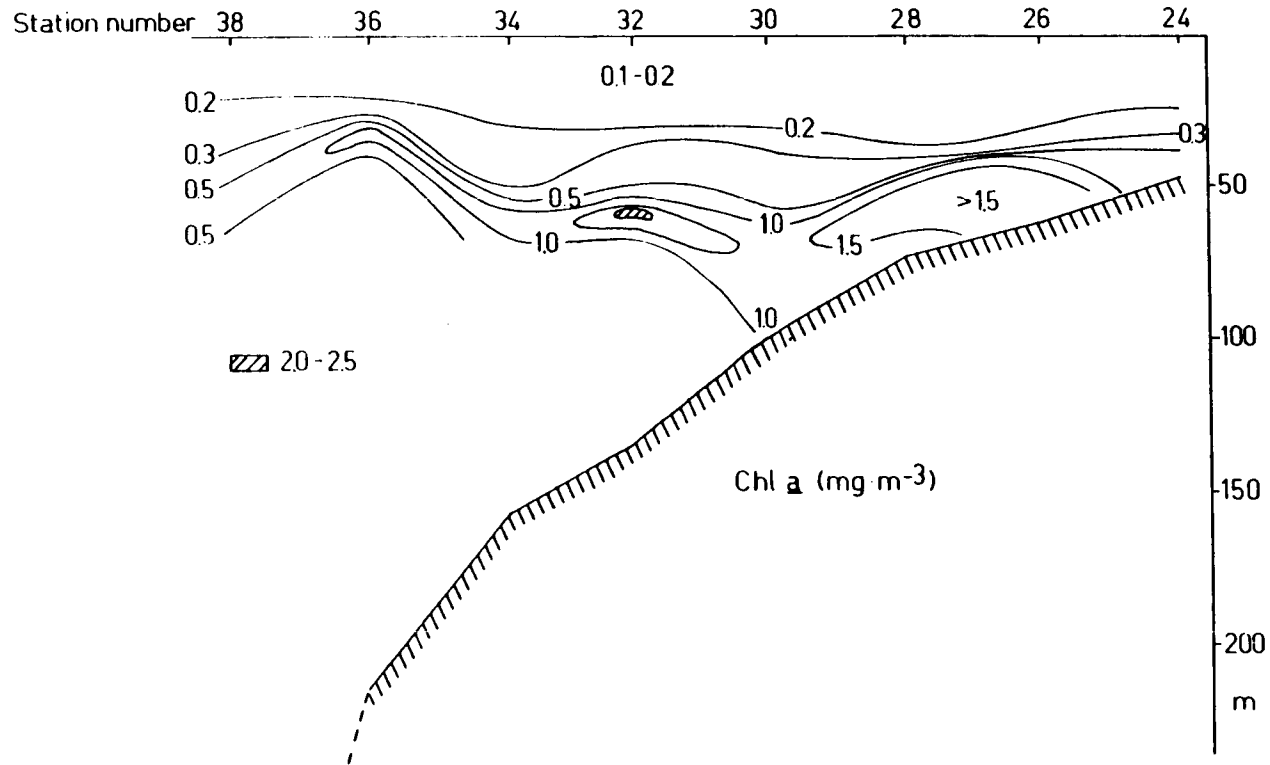
SECTION 2

Figure 6-7. Vertical distribution of Chl a along Transect 2, April 3-4, 1982.
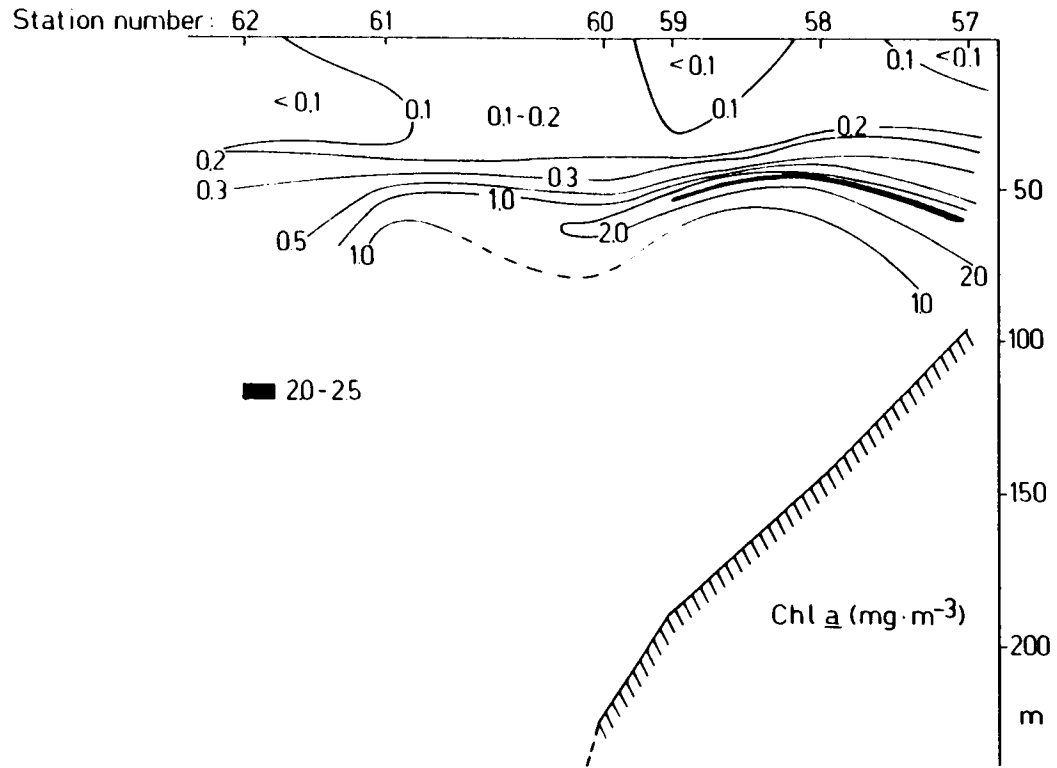
Figure 6-8. Vertical distribution of Chl a along Transect 5, April 4-5, 1982.
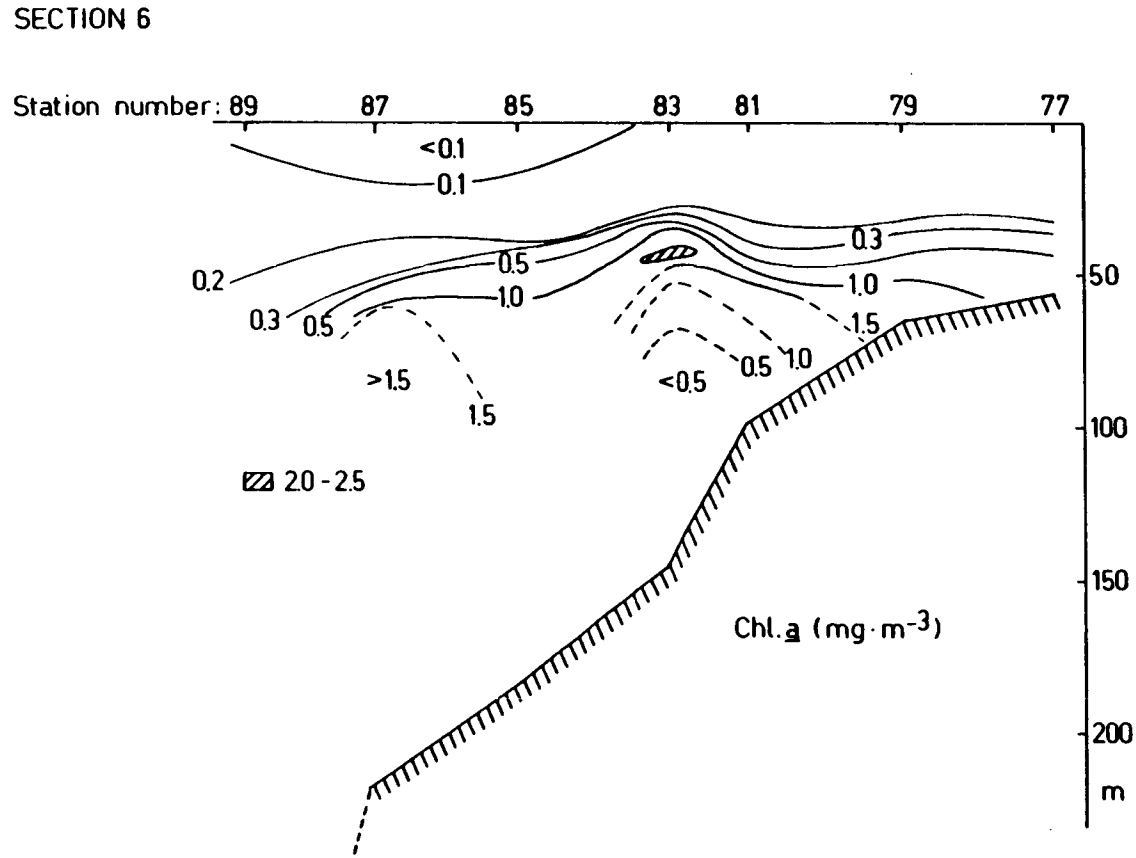
SECTION 6

Figure 6   Vertical distribution of Chl a along Transect 6, April 5-6, 1982.

SECTION 8
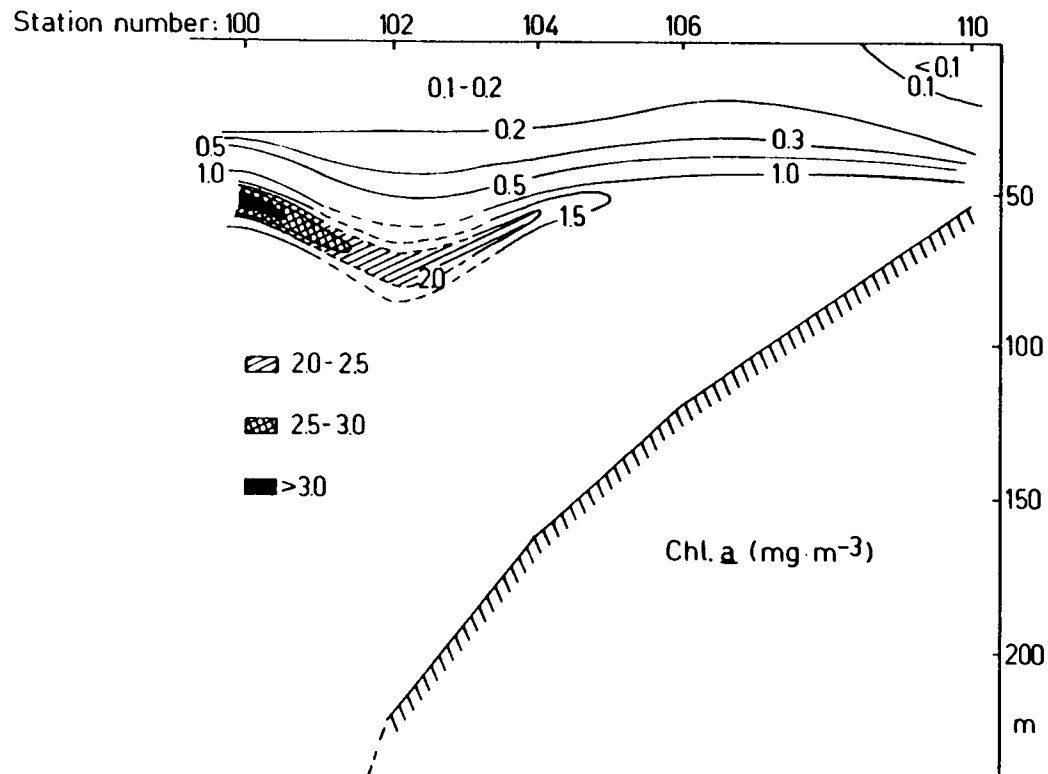
Figure 6-10. Vertical distribution of Chl a along Transect 8, April 6-7, 1982.

indicated in Figures 6-6 through 6-10 at Stations 3, 10, 26, 32, 36, 58, 83, and 100. The location of these stations provides yet another level of physical support for the Loop Current mechanism discussed in hydrographic terms in Section 3.2.1.3.

Comparison of Figures 6-6 through 6-10 to Figures 3-43 through 3-47 for the same sections shows a general agreement in distributions and gradients. At the maxima, however, the fluorescence results appear to exceed the in-situ maxima by about a factor of two.

6.3.3. Scattering Coefficient

Contouring the light scattering coefficient profile data in the same sense as Figures 6-6 through 6-10 for Chl a yields Figures 6-11 through 6-15 for Transects 1, 2, 5, 6, and 8, respectively. On Transects 1 (Figure 6-11), 2 (Figure 6-12), and 6 (Figure 6-14), the clearest waters are generally found in the surface layer on the eastern side of the transects. Transects 5 (Figure 6-13) and 8 (Figure 6-15), on the other hand, show the clearest waters on the western side at depth. In general, the patterns show varying degrees of clarity and turbidity generally associated with the upwelling process. For instance, the dark ($b > 0.14$ m^{-1}) area over the shelf in Transect 5 (Figure 6-13) can be related to the top of the nitracline(in Figure 3-26),the Chl a maximum (in Figures 3-45 and 6-8) and upwelling (in Figure 3-22 and Section 3.2.1.3).

It can also be noted that since chlorophyll-bearing phytoplankton also act to scatter ambient light, the distributions in Figures 6-11 through 6-15 are

SECTION 1
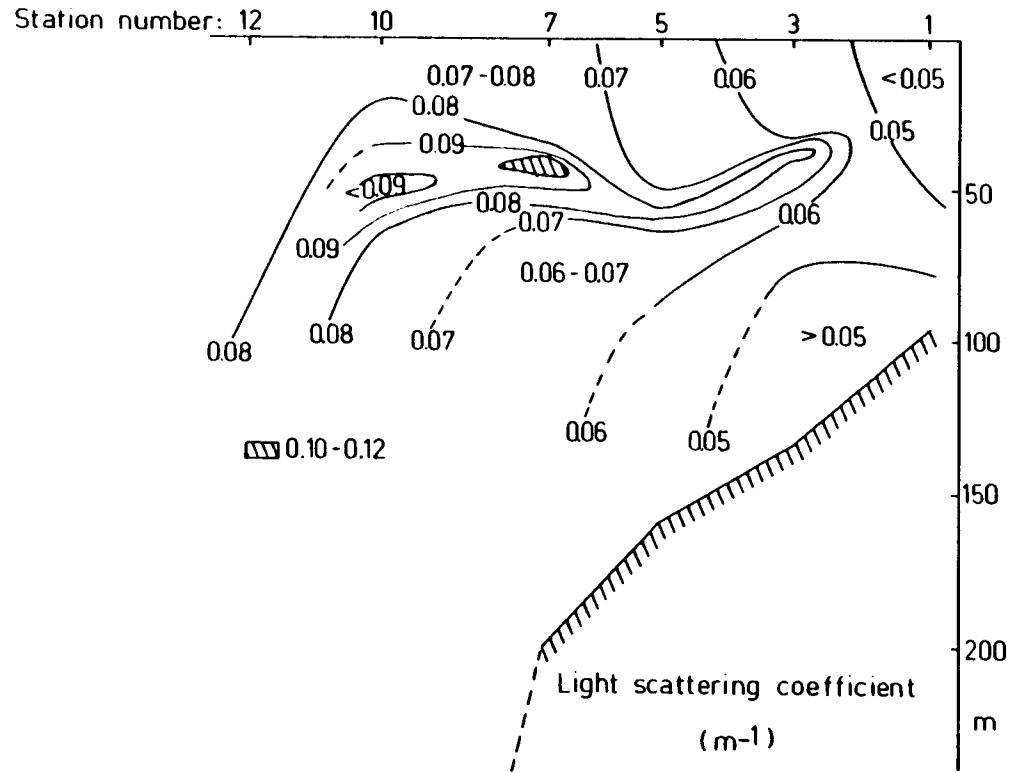
Figure 6-11. Vertical distribution of light scattering coefficient along Transect 1, April 2, 1982.
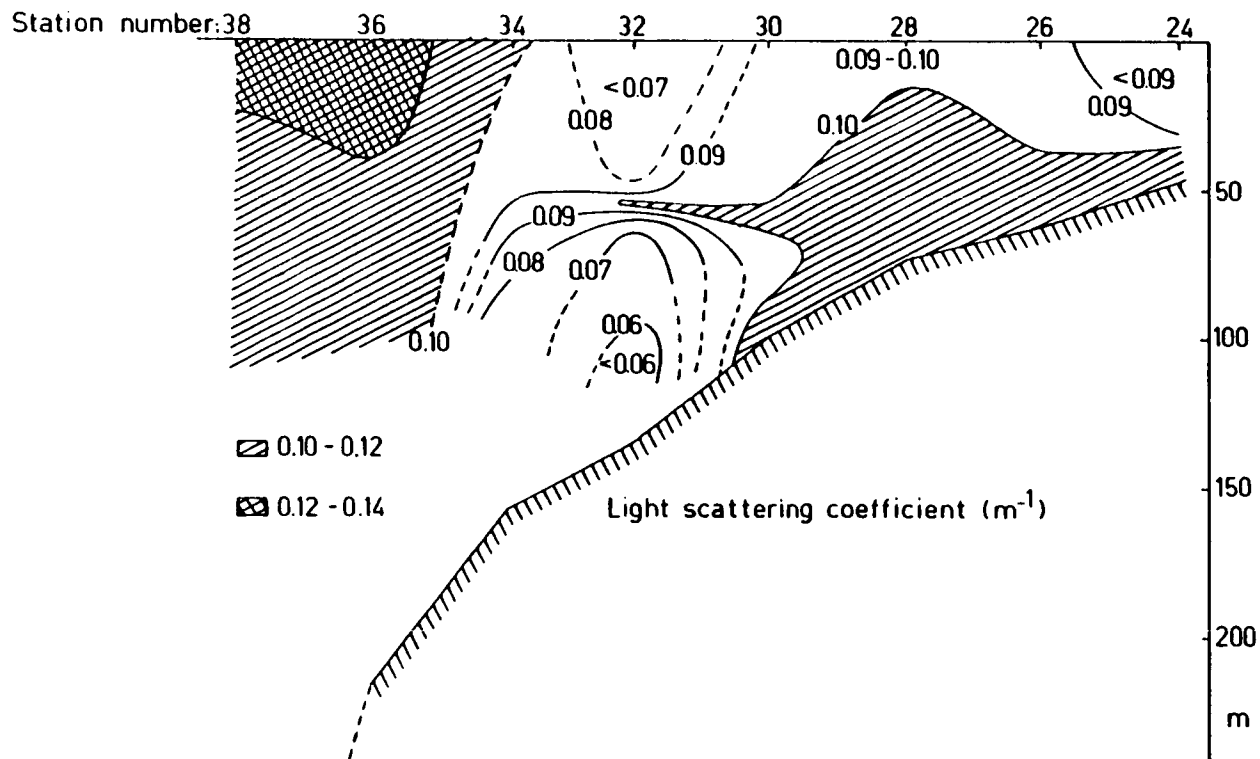
SECTION 2

Figure 6-12. Vertical distribution of light scattering coefficient along Transect 2, April 3-4, 1982.

SECTION 5
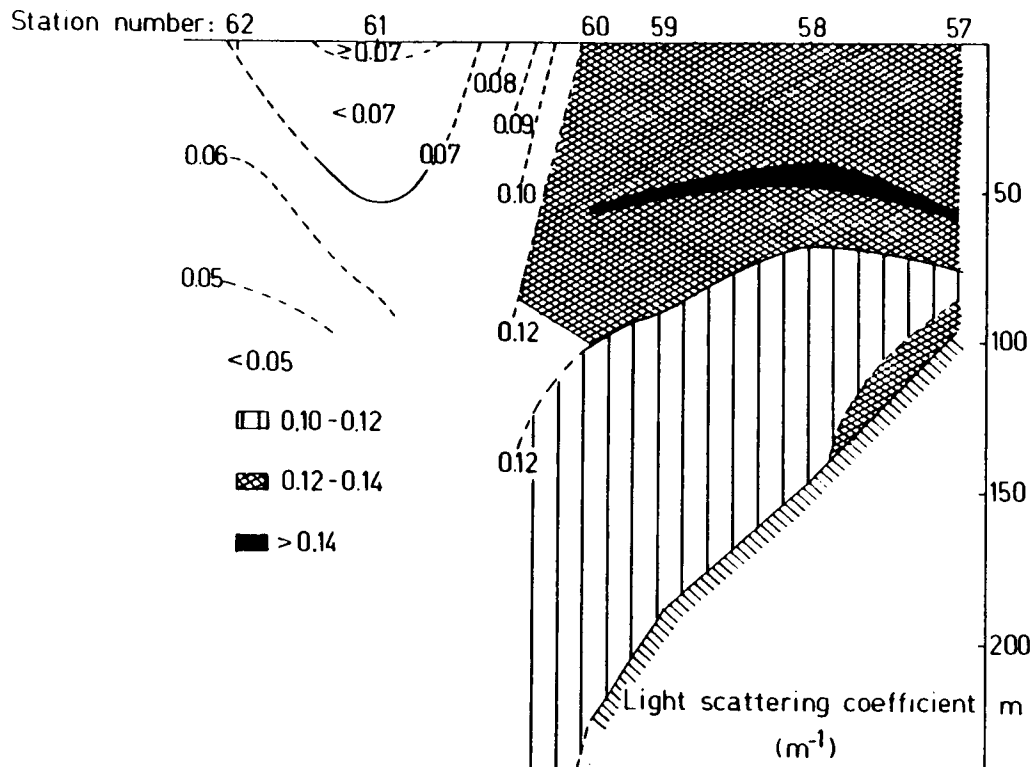
Figure 6-13. Vertical distribution of light scattering coefficient along
Transect 5, April 4-5, 1982.
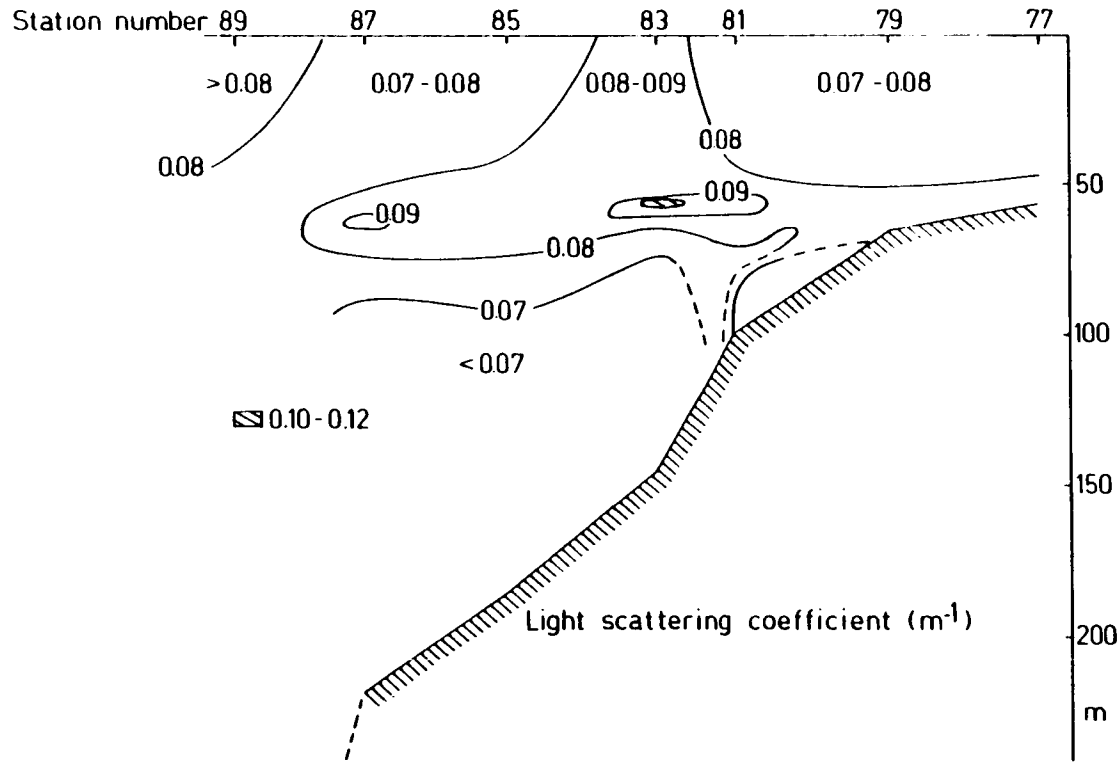
SECTION 6

Figure 6-14. Vertical distribution of light scattering coefficient along Transect 6, April 5-6, 1982.

SECTION 8

Station number: 100   102   104   106   110
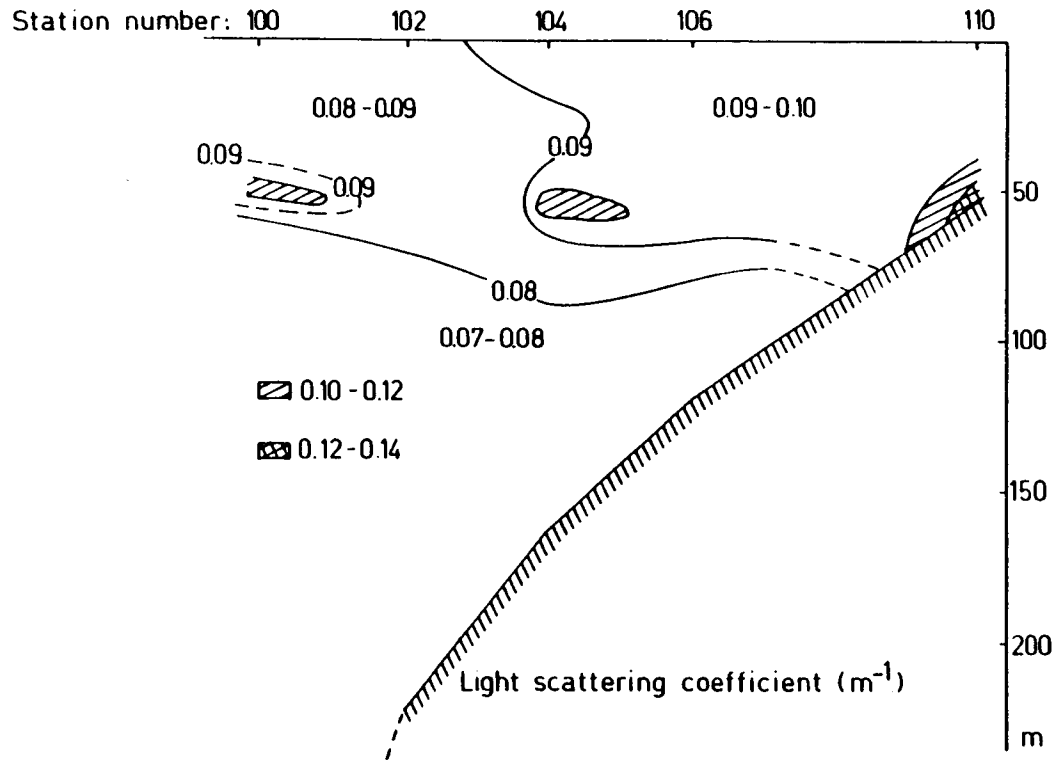
Figure 6-15.   Vertical distribution of light scattering coefficient along
Transect 8, April 6-7, 1982.

similar to Figures 6-6 through 6-10. As such, indications of cyclonic eddies in the scattering cross-sections are found around Stations 10, 28, 32, 58 and to a lesser extent around Stations 83, 100, and 104; these are essentially the same stations identified in Section 6.3.2.

Measurements of suspended matter (i.e., filtered samples dried at 105°C) were taken at selected stations in an attempt to quantify the relation between scattering and suspended (seston plus sediments) matter. These data are listed in Table 6-1 along with the corresponding Chl $\underline{a}$ measurements at the same station sampling depth. Note the relatively low concentrations of suspended matter throughout the study area. For comparison, Strickland and Parsons (1972) indicate that the largest amounts likely to be encountered in most truly marine environments away from excessive mud and sand is 10,000 $mg \cdot m^{-3}$.

The values in Table 6-1 are plotted as a pair of scatter diagrams in Figure 6-16. In both plots, no apparent correlation is evident. No regression fit was therefore attempted.

6.3.4 Irradiances

Downward spectral irradiance, E_d at 10 m and spectral reflectance $R = E_u / E_d$ at the surface in the 310 to 687 nm range measured at four selected stations are listed in Table 6-2. Both E_d (λ) and R (λ) varied only slightly between all stations. Moreover, R (λ) was nearly invariant with depth. The general distributions of E_d (λ) and R (λ) as a function of (visible) wavelength can therefore be represented as shown in Figure 6-17.

Table 6-1. Suspended matter, Chl a and scattering coefficient at selected spring cruise station depths.

Station No.	Depth (m)	Suspended matter ($mg \cdot m^{-3}$)	Chl a ($mg \cdot m^{-3}$)	Light scattering coefficient (m^{-1})
1	10	480	0.075	0.046
3	33	260	0.38	0.060
5	60	180	1.48 - 1.58	0.081
7	50	60	2.50	0.090
10	60	60	1.50 - 1.68	0.089
12	75	-	-	0.075
24	45	740	-	0.107
26	50	410	1.75	0.124
28	60	490	1.48	0.110
30	10	430	0.12	0.096
32	56	60	2.08 - 2.25	0.100 - 0.102
34	60	-	1.33	0.095
36	32	170	1.00 - 1.03	0.130
38	55	2,390	0.63 - 0.70	0.120
57	65	40	-	0.134
58	45	600	1.83 - 2.00	0.161
59	54	200	1.50 - 1.65	0.137
60	60	3,440	1.50	0.141
61	60	470	1.13	0.074
62	60	1,280	-	0.055
77	54	1,560	1.20	0.090
79	55	1,160	1.43	0.084
81	65	910	1.45 - 1.75	0.087

Table 6-1. (Continued)

Station No.	Depth (m)	Suspended matter $(mg \cdot m^{-3})$	Chl a $(mg \cdot m^{-3})$	Light scattering coefficient (m^{-1})
83	40	160	2.38	0.124
85	60	220	1.33 – 1.40	0.088
87	60	3,280	0.68 – 1.18	0.092
89	60	4,170	–	0.080
100	52	4,290	3.57	0.107
102	60	1,490	–	0.086
104	60	1,250	1.38 – 1.55	0.101
106	55	1,250	–	0.100
110	48	820	1.28	0.127
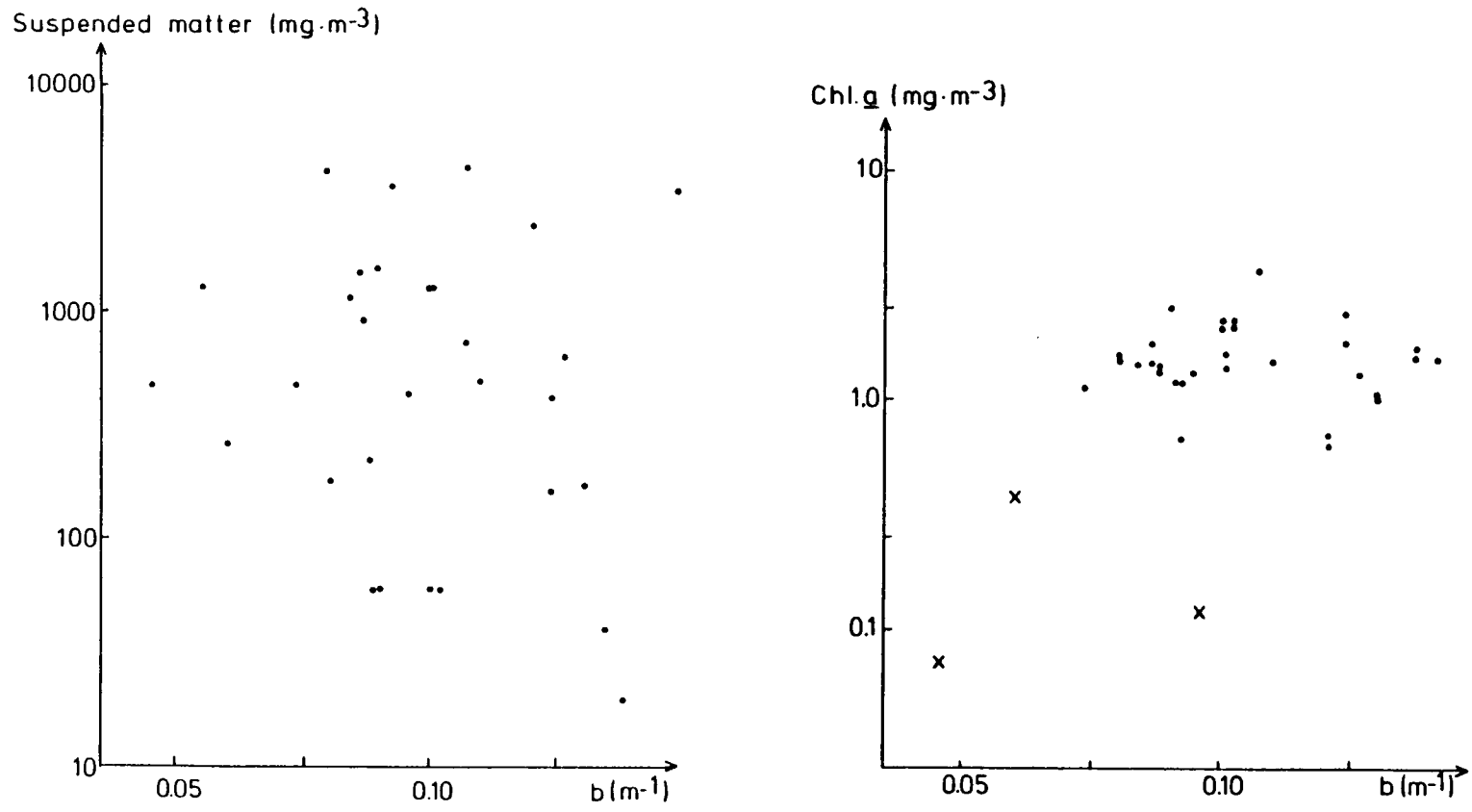
Figure 6-16. Scatter diagrams for suspended matter (left) and Chl a (right) versus scattering coefficient, b.

Table 6-2. Downward irradiance and spectral reflectance at selected spring cruise sampling stations.

Wavelength (nm)	Station number							
	26		50		72		87	
	$E_d(10m)\%$	$R(0m)\%$	$E_d(10m)\%$	$R(0m)\%$	$E_d(10m)\%$	$R(0m)\%$	$E_d(10m)\%$	$R(0m)\%$
310	-	-	-	-	-	-	23.2	1.31
371	42.2	3.10	46.8	3.21	43.1	3.08	47.1	3.25
403	56.0	4.21	59.2	4.59	56.2	4.25	60.5	4.63
455	72.4	5.68	74.1	5.71	72.2	5.70	75.4	5.75
477	70.4	5.02	72.7	4.78	70.3	4.98	73.8	4.80
492	68.0	4.43	69.0	4.14	68.4	4.47	69.4	4.10
517	60.3	3.10	62.9	2.95	61.2	3.10	63.0	2.80
533	55.1	2.29	56.9	2.17	55.7	2.21	57.4	2.00
573	38.8	0.92	39.0	0.91	39.1	0.92	39.1	0.91
602	12.2	0.39	21.2	0.38	12.2	0.39	12.2	0.38
634	3.43	0.12	3.43	0.12	3.43	0.12	3.43	0.12
674	1.30	-	1.30	-	1.30	-	1.30	-
687	0.95	-	0.95	-	0.95	-	0.95	-

311
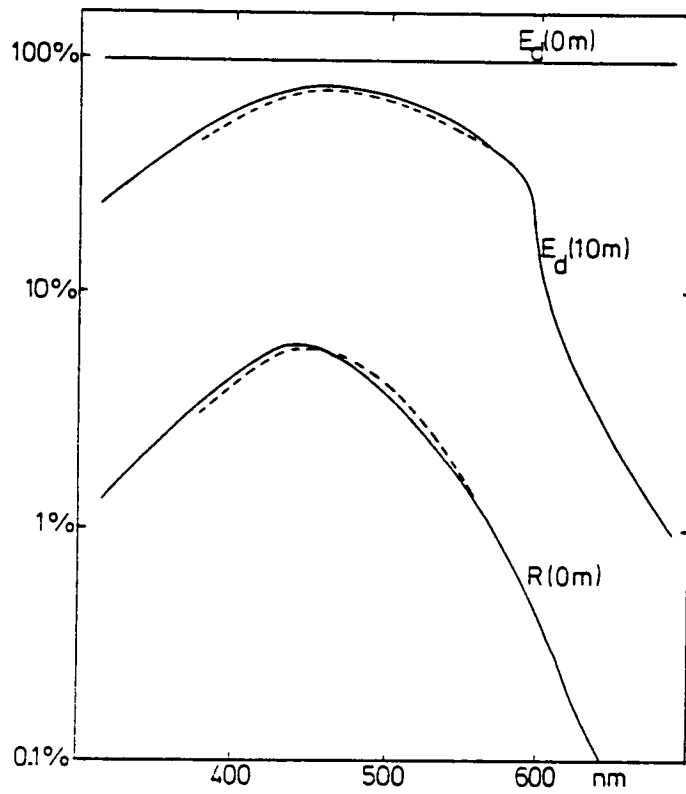
Figure 6-17.   Relative spectral distribution of downward daylight irradiance at 10m depth and the absolute spectral distribution of reflectance just below the surface.

A similar representation for upward and downward irradiance attenuation with depth at 310 nm is shown in Figure 6-18.

Corresponding K_d (310 nm), depth of the euphotic zone, Zq (1%), and absorption coefficient, a (310 nm) for selected stations, are listed in Table 6-3. The magnitude of the K_d (310)-values was very low for the marine environment. A re-calibration and check of the UV-B irradiance meter, however, provided no reason to doubt the validity of these measurements. The depth of the euphotic zone showed little change between stations. Also, as shown by the listed absorption coefficients, the amount of yellow substance was negligible; this agrees with the earlier results of WCC/CSA (1982) and Hojerslev (1982a). A typical depth attenuation curve for q(Z) showing how the euphotic zone depths were determined is shown in Figure 6-19. This particular graph is for Station 26 which was sampled on April 3, 1982 at 21.9 GMT. A possible explanation for the consistency of the depth of the euphotic zone lies in the lack of light absorption and scattering by particulate matter. The vertical attenuation of quantum irradiance, K_q was therefore dominated by the vertical attenuation in water alone K_w.

6.3.5. Color Index

Hojerslev (1980, 1981b, and 1982b) has derived two color index relationships for surface concentration of Chl a + Ph a in $mg \cdot m^{-3}$ and the depth of the euphotic zone, Zq (1%) in metres. These are;
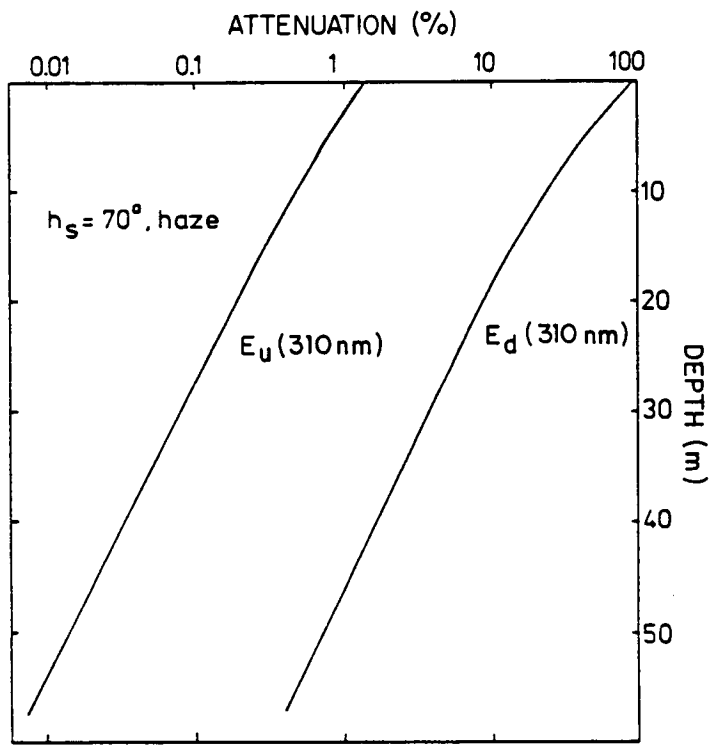
Figure 6-18. Relative upward and downward UV-B irradiance at station 87. Solar elevation is h_s.

Table 6-3. Vertical attenuation of downward irradiance coefficient, depth of euphotic zone, and scattering coefficient for selected spring cruise stations.

Station No.	$K_d(310)$ (m^{-1})	$z_q(1\%)$ (m)	$a(310)$ (m^{-1})
5	0.12	67.5	0.091
7	0.098	67.2	0.074
24	0.11	-	0.084
26	0.10	65.7	0.076
72	0.10	-	0.076
87	0.10	-	0.076
110	0.11	-	0.084
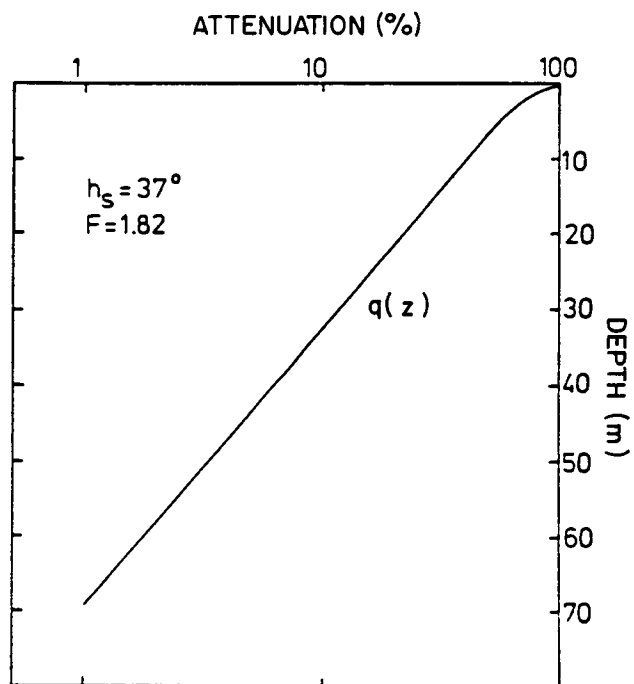
Figure 6-19.   Relative quanta irradiance at station 26.

$$\text{Chl } \underline{a} + \text{Ph } \underline{a} = 54.5 \ (1 + 2.57 \ F)^{-3.40} \ (\text{mg} \cdot \text{m}^{-3})$$

and

$$Zq \ (1\%) = -65.4 + \sqrt{3200 + 7692 \quad F} \quad (\text{m})$$

$$Zq \ (10\%) = -31.7 + \sqrt{769 + 1667 \quad F} \quad (\text{m})$$

where

$$F = \frac{L_u \ (447\text{nm})}{L_u \ (521 \ \text{nm})}$$

In order to test the validity of the Chl $\underline{a}$ + Ph $\underline{a}$ algorithm, a Chl $\underline{a}$/Ph $\underline{a}$ ratio determined by standard laboratory techniques was required. This ratio on a station by station basis was provided through the courtesy of Dr. James A. Yoder of the Skidaway Institute of Oceanography. Dr. Yoder's Chl $\underline{a}$ and Ph $\underline{a}$ values are listed in the second and third columns, respectively, in Table 6-4. The corresponding surface Chl $\underline{a}$ value as measured by the fluorescence meter (see Section 6.2.6) is listed in the fourth column. The fifth column lists the Chl $\underline{a}$ and Ph $\underline{a}$ sum as determined by the fluorescence value and the Chl $\underline{a}$/Ph $\underline{a}$ ratio. The computed Chl $\underline{a}$ + Ph $\underline{a}$ sum given by Hojerslev's algorithm using the color index in the rightmost column is listed in the sixth column. Note the general degree of agreement between the values in the fifth and sixth columns.

A similar comparison for Zq (10%) and Zq (1%) using measured value and Hojerslev's algorithm is presented in Table 6-5.

317

Table 6-4. Measured Chl $\underline{a}$ + Ph $\underline{a}$ versus derived values using the color index.

Station No.	Yoder Chl $\underline{a}$ (mg·m^{-3})	Ph $\underline{a}$ (mg·m^{-3})	Hojerslev Chl $\underline{a}$ (mg·m^{-3})	Chl $\underline{a}$ + Ph $\underline{a}$ (mg·m^{-3})	Derive Chl $\underline{a}$ + Ph $\underline{a}$ (mg·m^{-3})	Color Index F
3	0.07	0.06	0.13	0.24	0.15	1.82
5	0.06	0.04	0.08	0.13	0.14	1.88
7	0.07	0.05	0.08	0.14	0.14	1.87
10	0.05	0.05	0.11	0.22	0.13	1.92
24	0.06	0.05	0.06	0.11	0.14 - 0.17	1.74-1.84
26	0.06	0.04	0.10	0.17	0.14 - 0.16	1.77-1.87
50	-	-	-	-	0.13	1.90
62	0.07	0.05	0.08	0.14	0.15 - 0.16	1.81-1.86
72	-	-	-	-	0.15	1.82
82	-	-	-	-	0.15 - 0.16	1.78-1.80
87	0.07	0.05	0.09	0.15	0.14	1.88
89	-	-	0.10	-	0.13 - 0.15	1.80-1.91
106	0.08	0.05	0.14	0.21	0.21	1.61
110	0.43	0.26	0.09	0.14	0.19	1.67

Table 6-5   Measured attenuation depths versus derived depths using the color index.

Station No.	Measured $Z_q(10\%)$ (m)	Measured $Z_q(1\%)$ (m)	Derived $Z_q(10\%)$ (m)	Derived $Z_q(1\%)$ (m)	Color Index F
5	36.0	71.0	30.8	67.5	1.88
7	33.0	70.0	30.6	67.2	1.87
26	32.5	69.0	30.0	65.7	1.82

Again, the degree of agreement is quite favorable and indicates the general utility of the color index (also see Hojerslev 1980 a, b and 1982b).

Another way of using the color index is to compare its results to data taken by the NIMBUS-7 CZCS. Applying the findings of Austin and Petzold (1980) to the above color index algorithms transforms them to

$$\text{Chl } \underline{a} + \text{Ph } \underline{a} = 54.5 \ (1 + 2.31 \ \text{CI}^{0.742})^{-3.40} \ (\text{mg} \cdot \text{m}^{-3})$$

and

$$Z_q \ (1\%) = - 65.4 + \sqrt{3200 + 6923 \cdot \text{CI}^{0.742}} \qquad (\text{m})$$

where

$$\text{CI} = \frac{L_u \ (443 \ \text{nm})}{L_u \ (550 \ \text{nm})} \ .$$

Now, reflectance values from Table 6-2 can be used to form a reflectance ratio. The ratio of R (440 nm) to R (550 nm) in the rightmost column of Table 6-6 is sufficiently accurate to approximate the nadir radiance ratio, CI (Hojerslev and Jerlov; 1977). Likewise, R (440 nm)/R (520 nm) approximates F.

Table 6-6. Reflectance ratio.

Station No.	R(440 nm)	R(520 nm)	R(550nm)	$\dfrac{R(440\ nm)}{R(520\ nm)}$	$\dfrac{R(440\ nm)}{R(550\ nm)}$
26	5.26	2.95	1.71	1.78	3.08
50	5.38	2.80	1.63	1.92	3.30
72	5.28	2.93	1.66	1.80	3.18
87	5.43	2.65	1.54	2.04	3.52

Using these values in the above algorithm and comparing the results to similar CZCS algorithms derived by Gordon and Clark (1980) and Morel (1980) for Stations 26 and 87 produces the comparison values in Table 6-7.

Table 6-7. Derived Chl $\underline{a}$ + Ph $\underline{a}$ values using color index algorithms.

	Chl a + Ph a (mg·m-3)		
Station No.	Gordon & Clark	Morel	Hojerslev
26	0.12	0.17	0.15
87	0.097	0.14	0.14

For further comparison purposes, the comparable measured values from Table 6-4 are 0.10 and 0.12 mg·m^{-3} in Yoder's data and 0.17 and 0.15 mg·m^{-3} in Hojerslev's data for Stations 26 and 87, respectively. The degree of agreement between measurements and the three simulation algorithms is again quite high.

6.3.6 Secchi Disc

Table 6-8 presents the results of the Secchi disc measurements at Stations 5, 7, 24, 26, and 72. When corrected for wave height (see Section 6.2.7), the Secchi disc depths are as follows:

$$D_o(y_\lambda) \text{ (m)}$$

Station No.	Secchi disc depth
5	36.4
7	32.0
24	29.4
26	32.9
72	41.6

Note the similarities between these depths and the value listed in Table 6-5.

6.4 Conclusions and Recommendations

The chlorophyll measurements and especially the light scattering measurements have demonstrated the necessity for combining optical oceanographic investigations with both hydrographic and primary production measurements to interpret the bio-physical dynamics of the southwest Florida shelf study area properly. The only obvious missing component from this study plan was the lack of direct current measurements.

Satellite thermal maps indicated the surface features of the rapidly changing study area conditions. Because of this ability, satellite imagery should (whenever possible) be incorporated as a navigational aid into sea-truth data

Table 6-8.   Secchi disc measurement results.

Station no.	$D_H(\lambda)$ (m)				$d_H(\lambda)$ (m)				Wave Height H (m)
	y_λ	465 nm	525 nm	655 nm	y_λ	465 nm	525 nm	655 nm	
5	26	22	24.5	8.5	10.5	10	9	3	1.0
7	20	18	17.5	7	7.5	7	5	2.5	1.5
24	21	18.5	19.5	5.5	6.5	5.5	3	1.5	1.0
26	23.5	22.5	20.5	6.5	9	6	6	3	1.0
72	26	24	24	6.0	-	-	-	-	1.5

collection for locating fronts, and as an auxilliary data source for facilitating interpretation of observed phenomena.

The color index algorithms discussed in this section provided a very convenient and satisfactory method for determining surface Chl $\underline{a}$ + Ph $\underline{a}$ concentrations as well as the depth of the euphotic zone. The virtual absence of yellow substance in the study area contributed significantly to their successful applicability. As such, future Fate and Effects modellers may be well advised to consider algorithms of this type for this area.

Finally, it was shown that the depth of the euphotic zone did not vary significantly throughout the study area. To a large extent, this was due to the high transparency and lack of ambient particulate matter for light scattering. In terms of future shelf development, this implies that the waters of the southwest Florida shelf may be able to tolerate fairly large injections of suspended matter before light available for phytoplankton or benthos photosynthesis will be adversely affected.

6.5 References

Austin, R.W. 1980. Gulf of Mexico Ocean - Color Surface - truth measurements.
    J. Bound. Layer Meteor. 18(1): 269-286

Austin, R.W. and Petzold, T. J. 1981. The determination of the diffuse
    attenuation coefficient of the sea water using the Coastal Zone Color
    Scanner. Proc. Oceanogr. from Space, Venice 1980: 239-256.

Gordon, H.R. and Clark, D.K. 1980. Atmospheric effects in the remote

sensing of phytoplankton pigments. J. Bound. Layer Meteor. 18(1): 229-314

Hundahl, H. and Holck, J. 1980. A new *in-situ* fluorometer for detection of

Rhodamine B and Chlorophyll. Rep. Inst. Phys. Oceanogr., Univ. Copenhagen

42: 145-153.

Hojerslev, N.K.1971. Tyndall and fluorescence measurements in Danish and

Norwegian water related to dynamical features. Rep. Inst. Phys.

Oceanogr., Univ. of Copenhagen 16: 46 pp.

Hojerslev, N.K. 1977a. Spectral daylight irradiance and light transmittance

in natural waters measured by means of a Secchi disc only. ICES - C.M.

77, Paper C, 42: 7 pp.

Hojerslev, N.K. 1977b. Inherent and apparent optical properties of the North

Sea, Fladen Ground Experiment - FLEX-75. Rep. Inst. Phys. Oceanogr., Univ.

of Copenhagen 32: 39 pp.

Hojerslev, N.K. and Lundgren, B. 1977. Inherent and apparent optical

properties of Icelandic waters, "Bjarni Saemundsson Overflow 73". Rep.

Inst. Phys. Oceanogr. Univ. of Copenhagen, 33: 63 pp.

Hojerslev, N.K. and Jerlov, N.G. 1977. The use of the Colour Index for

determining quanta irradiance in the sea. Rep. Inst. Phys. Oceanogr.,

Univ. of Copenhagen 35: 12 pp.

Hojerslev, N.K. 1978. Daylight measurements appropriate for photosynthetic
    studies in natural sea water. J. Cons. Int. Explor. Mer, 38: 131-146.

Hojerslev, N.K. and Larsen, K. 1980. On the optical instruments developed at
    the Institute of Physical Oceanography - University of Copenhagen. Rep.
    Inst. Phys. Oceanogr., Univ. Copenhagen, 42: 155-191.

Hojerslev, N.K. 1980. Water color and its relation to primary production.
    J. Bound. Layer Meteor., 18(1): 203-220.

Hojerslev, N.K. 1981a. Optical water mass classification in Skagerrak and the
    Eastern North Sea. In: The Norwegian Coastal Current. Univ. of
    Bergen: 331-339.

Hojerslev, N.K. 1981b. Assessment of some suggested algorithms on sea color
    and surface chlorophyll. Proc. Oceanogr. from Space, Venice (1980:
    347-355.)

Hojerslev, N.K. 1982a. Yellow substance in the sea. In: The Role of Solar
    Ultraviolet Radiation in Marine Ecosystems. Ed. J. Calkins, Plenum
    Press: 263-282.

Hojerslev, N.K. 1982b. Bio-optical properties of the Fladen Ground:
    "Meteor" - FLEX-75 and FLEX-76. J. Cons. int. Explor. Mer., 40: 272-290.

Jerlov, N.G. 1961. Optical measurements in the Eastern North Atlantic. Medd.
    Inst. Oceanogr. Gothenburg, Ser. B., 8: 40 pp.

Jerlov, N.G. and Nygård, K. 1969. A quanta and energy meter for

   photosynthetic studies. Rep. Inst. Phys. Oceanogr., Univ. of Copenhagen

   10: 29 pp.

Jerlov, N.G. 1974. Significant relationships between optical properties of

   the sea. In: Optical Aspects of Oceanogrphy, p. 77-94. Ed. by N.G.

   Jerlov and E. Steemann Nielsen. Academic Press, New York, N.Y., 494 pp.

Jerlov, N.G. 1976. Marine Optics. Elsevier, Amsterdam, 2nd ed: 203 pp.

Kiefer, D.A. 1973a. Flourescence properties of natural phytoplankton

   populations. Mar. Biol. 22: 263-269.

Kiefer, D.A. 1973b. Chlorophyll a fluorescence in marine centric Diatoms:

   Responses of chloroplasts to light and nutrient stress. Mar. Biol. 23:

   39-46.

Morel, A. 1980. In-water and remote measurements of ocean color. J. Bound.

   Layer Meteor., 18(1): 177-202.

Setser, P.J., Guinasso, N.L. and Schink, D.R. 1982. Daily patterns of

   fluorescence in-vivo in the Central Equatorial Pacific. J. Mar. Res.

   40(2): 453-471.

Strickland, J.D.H. and T.R. Parsons 1972. A practical handbook of seawater

   analysis. Bulletin 167. Fisheries Research Board of Canada, Ottawa.

Woodward-Clyde Consultants/Continental Shelf Associates 1982. Southwest

Florida shelf ecosystems study - Year 1. Prepared for Minerals Management

Service under Contract No. AA851-CTO-50 (in review).

7.0 REMOTE SENSING OF CHLOROPHYLL GRADIENTS

HONG CHIN*
WOODWARD-CLYDE CONSULTANTS

HONGSUK H. KIM
NASA - GSFC

7.1 Introduction

On April 1, 1982, the first of a series of two chlorophyll gradient mappings in the approximately 25 to 27°N, 83 to 85°W area was completed from a U-2 aircraft based out of Wallops Island, Virginia. On the next day, the second mapping in this same area was completed along similar flight lines (see Figures 7-1 and 7-2). During both mapping runs, the remote sensing system carried onboard the U-2 aircraft was NASA's Ocean Color Scanner (OCS). Essentially this is the same system described by Kim et al. (1980), Kim, Fraser, Thompson and Bahethi (1980a) and Kim, McClain and Hart (1979). The OCS works on the principle that chlorophyll-a pigment which is present in phytoplankton selectively absorbs in the blue part of the visible spectrum. This absorption causes a slight shift in the overall ocean color to a greenish hue. In turn, this shift acts as an indicator of phytoplankton presence. Thus, the mapping of ocean color (when corrected for atmospheric effects) forms an approximate distribution of chlorophyll in the surface layer of upwelled light.

7.1.1 U-2 Ocean Color Scanner

The U-2/OCS is a 10-channel scanning radiometer having a 90-degree total field-of-view and a 3.5 milliradian(mr) instantaneous field of view (IFOV). The general instrument and platform parameters are listed in Table 7-1. Critical radiometric and spectral characteristics are presented in Table 7-2.

---

* Present affiliation: Oceanology Associates, San Diego, CA 92120
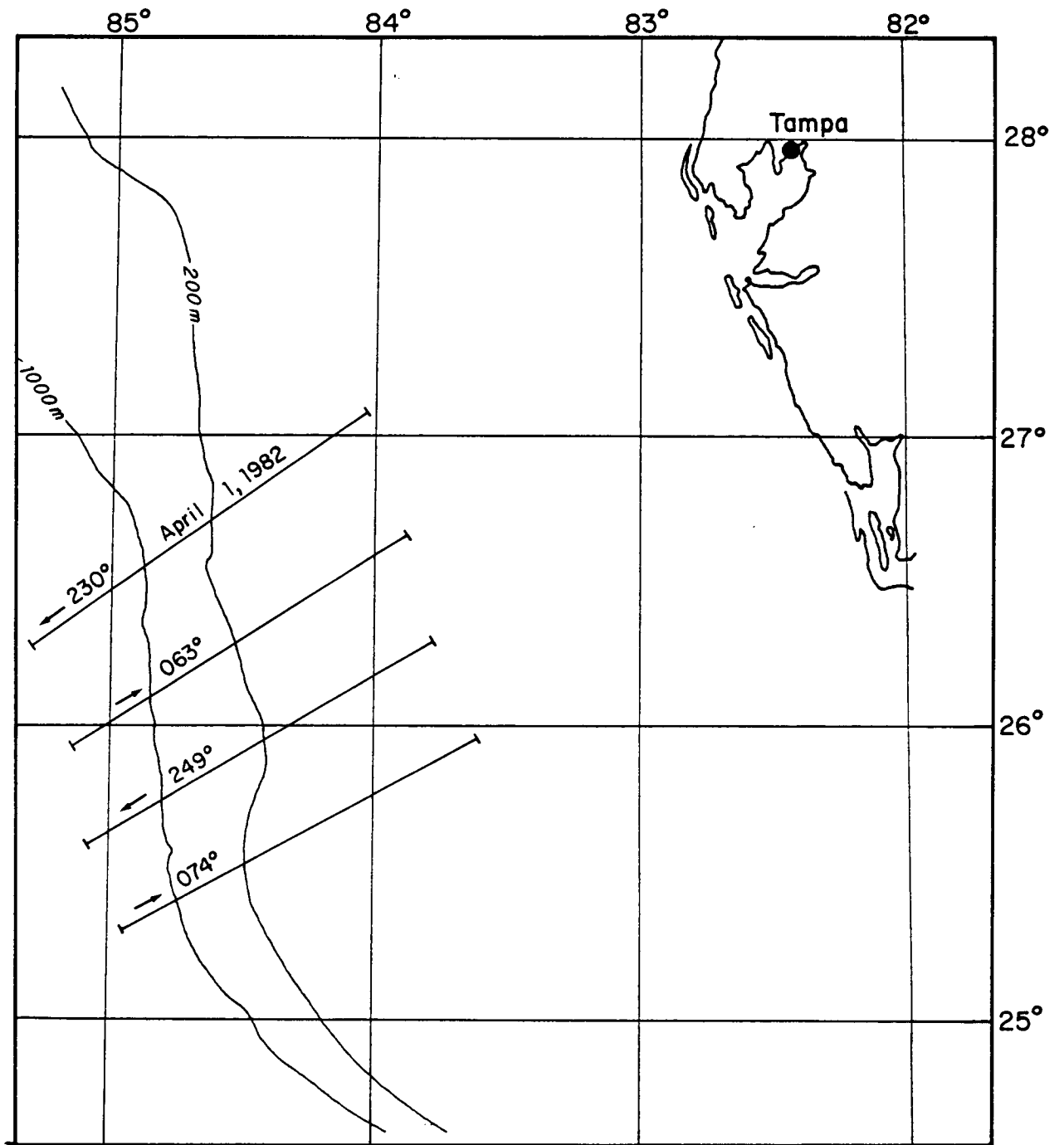
Figure 7-1.   Flight lines for first series of OCS chlorophyll mappings.
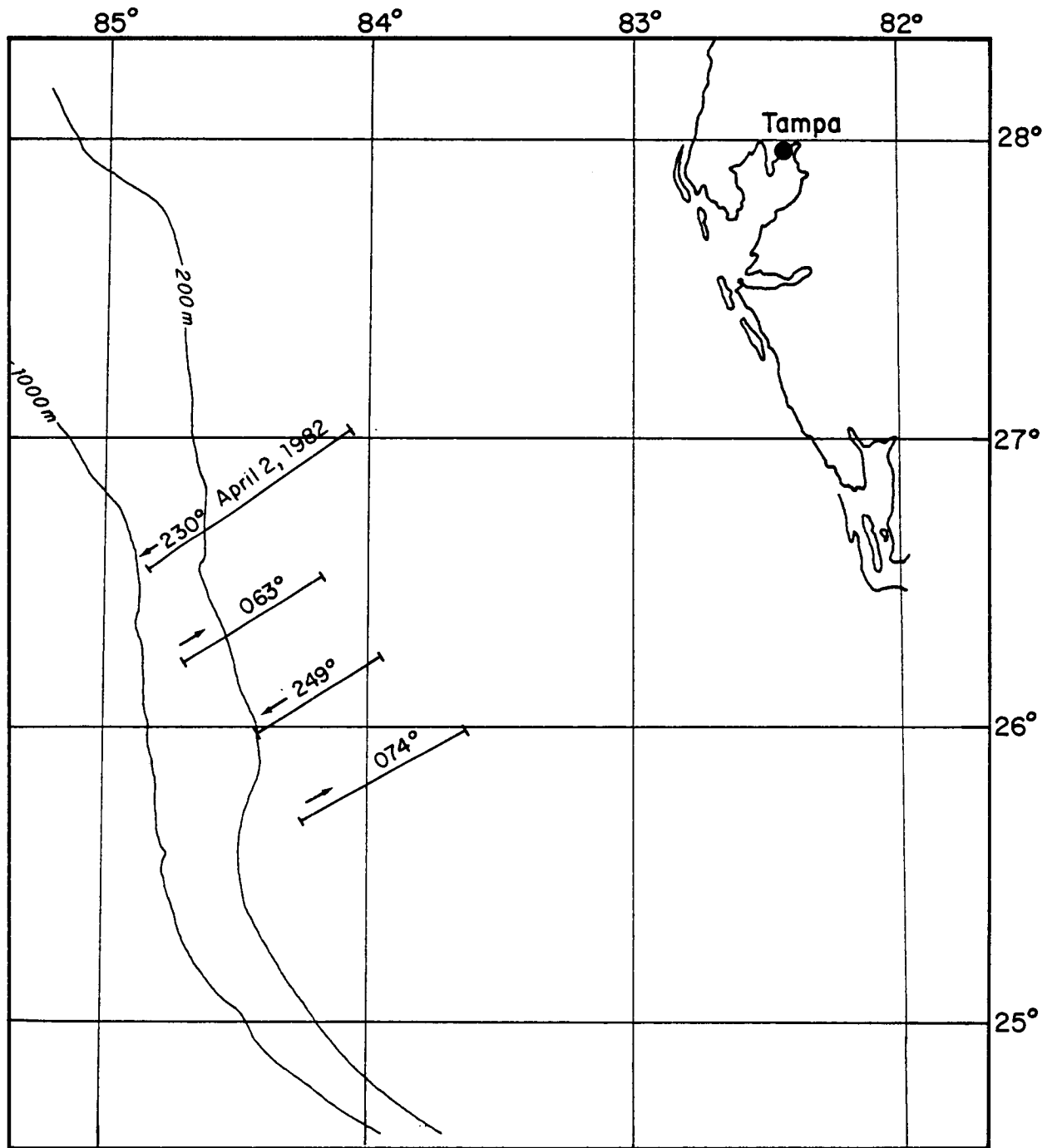
Figure 7-2. Flight lines for second series of OCS chlorophyll mappings.

Table 7-1. U-2 and OCS parameters (from Kim et al., 1980)

Parameter	Value
Aircraft speed	201 m/sec (390 knots nominal)
Air altitude	19.8 km (nominal)
Angular resolution (IFOV)	3.5 mr
Footprint	69.3 x 69.3 m
FOV	$\pm 45°$ from nadir
Scan rate	2.727 rev/sec
Swath width	39.6 km
Output voltage	0 to ± 5 volts
Output bandwidth	0 to 2,500 Hz
Output rms noise and level	8 mV (nominal)

Table 7-2. Optical parameters of the U-2/OCS channels (from Kim et al., 1980)

Channel	Wavelength (nm)	Full Bandwidth at Half Intensity (nm)	Spectral Radiance (Ocean Targets) $(mw\ cm^{-2}sr^{-1}\ m^{-1})$	Calibration Function Slope $(mw\ cm^{-2}\ m^{-1}sr^{-1}v^{-1})$
1	431	24.2	25.54	7.29
2	472	26.0	20.94	5.98
3	506	25.0	13.49	3.85
4	548	26.3	8.27	2.36
5	586	24.1	6.33	1.81
6	625	25.3	5.00	1.43
7	667	24.2	3.88	1.11
8	707	26.0	3.16	0.9
9	738	24.0	40.33	11.52
10	778	26.1	2.14	0.61

When flown on a U-2 aircraft operating at an altitude of 20 km, the OCS swath width is 39.6 km; the footprint, or pixel size, at nadir is approximately $(69 \text{ m})^2$. Approximately 94% of the atmospheric mass is below the aircraft at this altitude.

7.1.2 Calibration and Field Operation

To assure radiometric accuracy, the OCS is returned to the laboratory for testing and calibration checks at approximate six month intervals. The U-2/OCS was calibrated just prior to and immediately following this particular mission. The inspection consists of an examination of each channel with respect to spectral position, half width, shape, and radiometric calibration. Spectral examination is carried out using a 0.5 m Ebert spectrometer and the radiometric phase using a 1.83 m (6-ft) integrating sphere; the sphere is color corrected to approximate the sun's spectral power distribution.

The long-term stability of the large sphere is about 5%. The OCS instruments are maintained within a 2% fluctuation limit to the sphere reading. In addition, the performance of the scanner is also examined by use of sky radiance. To effect such a comparison, the downwelling intensity at ground level is measured by pointing the OCS toward zenith. The resulting measurements are corrected to spectral radiance values and compared to numerically calculated values for the same conditions. Kim et al. (1980) present the results of such a comparison for a given sun angle, ground reflectivity, and aerosol content. The reported results demonstrate the instrument's general reliability as a function of wavelength.

Previous experience* with operation of the U-2/OCS and its two companion systems (one for operation from a Learjet at an altitude of 10 km; the other for operation from a space shuttle at 280 km) has shown that four separate conditions must be present in order to achieve best data results. They are:

1. OCS data should be recorded only over the deep and clear water conditions of the open ocean.

   It has been noted that reflection of light from the ocean floor and scattering by sediment can strongly interfere with the chlorophyll absorption signature. Detailed accounting for these effects would involve the specification of light scattering properties from various phytoplankton and marine sediments with arbitrary size distributions. At present, these radiative transfer processes are still not understood sufficiently to permit such a reliable treatment.

   Present-day analyses, therefore, assume an open ocean color with relatively few impurities under a near Rayleigh sky. For the generally less than 500 $mg \cdot m^{-3}$ suspended sediment loads in the upper 10 m (see Table 6-1), total water depths in excess of 50 m, and the cloudless conditions of the first mapping day, this assumption was quite satisfactory. As cloud cover increased on April 2, the Rayleigh scattering part of the assumption became less tenable (see discussion below).

---

* e.g., Monterey Bay Biological Experiment in 1977, pre-Georgia Bight Experiment (GABEX) off Jacksonville, Florida in 1979, and the Space Shuttle Columbia's second flight in 1981.

2. Second, care be taken to collect overflight data totally free from sea surface sun glint.

    This can be avoided by flying the aircraft directly toward or away from the sun, and, at the same time, maintaining a solar zenith angle within the range of 35 to 60° for optimum conditions.

3. As a means of minimizing atmospheric effects, data should only be collected when the sky is relatively clear and the surface is free of white caps.

4. Last, sea truth support data including vertical chlorophyll profiles and surface temperature and salinity should be taken at a reproducible location within a few hours of the time of the overflight.

All four of these conditions were addressed in the development of the cruise and flight plans. Sea truth data collected from the R/V GYRE in support of the mapping runs included chlorophyll fluorescence, temperature and salinity (thermosalinograph), solar transmission, and weather/sea state data.

7.2 Data Reduction

During each flight day, approximately 90 minutes of high-density magnetic tape were recorded. Of this length, approximately 60 minutes contained the actual mapping data; the remainder were engineering data for calibration and stabilization purposes. All data were processed on NASA's IBM 3081 computer.

In principle, the data reduction algorithms can be described in two parts.

7.2.1 Atmospheric Effects Correction

The upwelled radiance measured at the U-2/OCS altitude can be considered to have two components (Kim et al., 1980):

1. Photons that have not penetrated the sea surface but are returned to the sensor from the atmospheric path and sea surface backscattering; and

2. Photons that have penetrated the sea surface resulting in signatures which are associated with the water and its chlorophyll content. The upwelling intensity in the visible channel $I_{\lambda i}^{total}$ can be expressed as:

$$I_{\lambda i}^{total} = I_{\lambda i}^{atm \& sfc} + I_{\lambda i}^{water}$$

$$(7/1)$$

Now, consider the same relationship in the near-infrared region; ocean water in this region is nearly opaque. Thus, the upwelling intensity in the (infrared) region, $I_{\lambda j}^{total}$, can be written as:

$$I_{\lambda j}^{total} = I_{\lambda j}^{atm \& sfc}$$

$$(7/2)$$

By modeling the upwelling radiances in both the visible and near-infrared regions, one can derive a proportionality factor, $E_{\lambda ij}$. This factor can then be applied to observations on a pixel by pixel basis to correct the atmospheric perturbations imposed upon the visible radiation.

Thus,

$$E_{\lambda ij} = \frac{I_{\lambda i}^{atm \& sfc}}{I_{\lambda j}^{atm \& sfc}},\qquad (7/3)$$

and the true water radiance term at each pixel can be written as

$$I_{\lambda i}^{water} = I_{\lambda i}^{total} - E_{\lambda ij} \cdot I_{\lambda j}^{total} \qquad (7/4)$$

In order to define the proportionality factor and radiance values for evaluation, an adaptation of a radiative transfer model (called Dave code) to an ocean-atmosphere environment is used. The model requires four input parameters:

1. Solar zenith angle

2. Sea surface reflectivity

3. Optical thickness of the atmosphere, and

4. Refractive index and size distribution of aerosols.

Detailed discussions of the different computational steps and ramifications are provided by Kim et al. (1980), Kim et al. (1980a), and more recently by Kim (1982); reiteration of these steps is not attempted here.

338

In 1981, Gordon and Clark (1981) challenged the sea surface boundary condition application as listed (above) for the second input parameter. Kim et al. (1981) responded with a demonstration of the validity of their approach.

Further, as mentioned above, recordings of solar transmission were also attempted during the sea truth data collection; these data were designed to define the actual optical depth (Parameter 3 above) at the time of the overflights. Unfortunately, intermittent cloud cover precluded the successful application of these measurements to the extent that the aerosol loading had to be estimated by a more conventional technique using the Channel 10 (778 nm) output (see Kim et al., 1980 for details). This alternate approach proved to be more than adequate.

7.2.2 Chlorophyll Analysis

The next step in the reduction algorithm is to form the chlorophyll index, R'

$$R' = \frac{I_{472nm}^{water} - I_{548nm}^{water}}{I_{472nm}^{water} + I_{548nm}^{water}} \qquad (7/5)$$

where $I^{water}_{\lambda i}$ is defined by Eq. (7/4) in Channels 2 and 4.

Based on previous OCS experience R' is then related to chlorophyll concentration $C'(\mu g/l)$ as

$$C' = ae^{bR'}$$ (7/6)

where a = 801; b = -20.8.

7.3 Results

Prior to the mission, study of NOAA Miami SFSS Gulf Stream Flow Charts (#2450) for March 24, 26, and 29, 1982 showed two distinct finger-like eddies on the thermally defined Loop Current front. The Loop Current intrusion pattern for March 29 is reproduced as Figure 7-3. The northernmost eddy was centered around 27°N, 86°W off the continental shelf and appeared to remain stationary over the last six days. On March 29, the second (southern) eddy was situated near 25°30'N, 84°30'W in the vicinity of the shelf break and appeared to be propagating southward intact at a speed of about 30 km·day^{-1}*. During a pre-cruise coordination meeting held at the Florida Institute for Oceanography on March 31, it was decided to extrapolate this meander pattern and have the U-2/OCS flight lines intercept the path of the southernmost eddy on the next available flight day (April 1). The resulting flight pattern based on this extrapolation has been presented earlier in Figures 7-1 and 7-2.

---

* Vukovich et al. (1979) indicate an average speed for these small meanders to be 28 km day^{-1} (see Section 3.2.1.6).
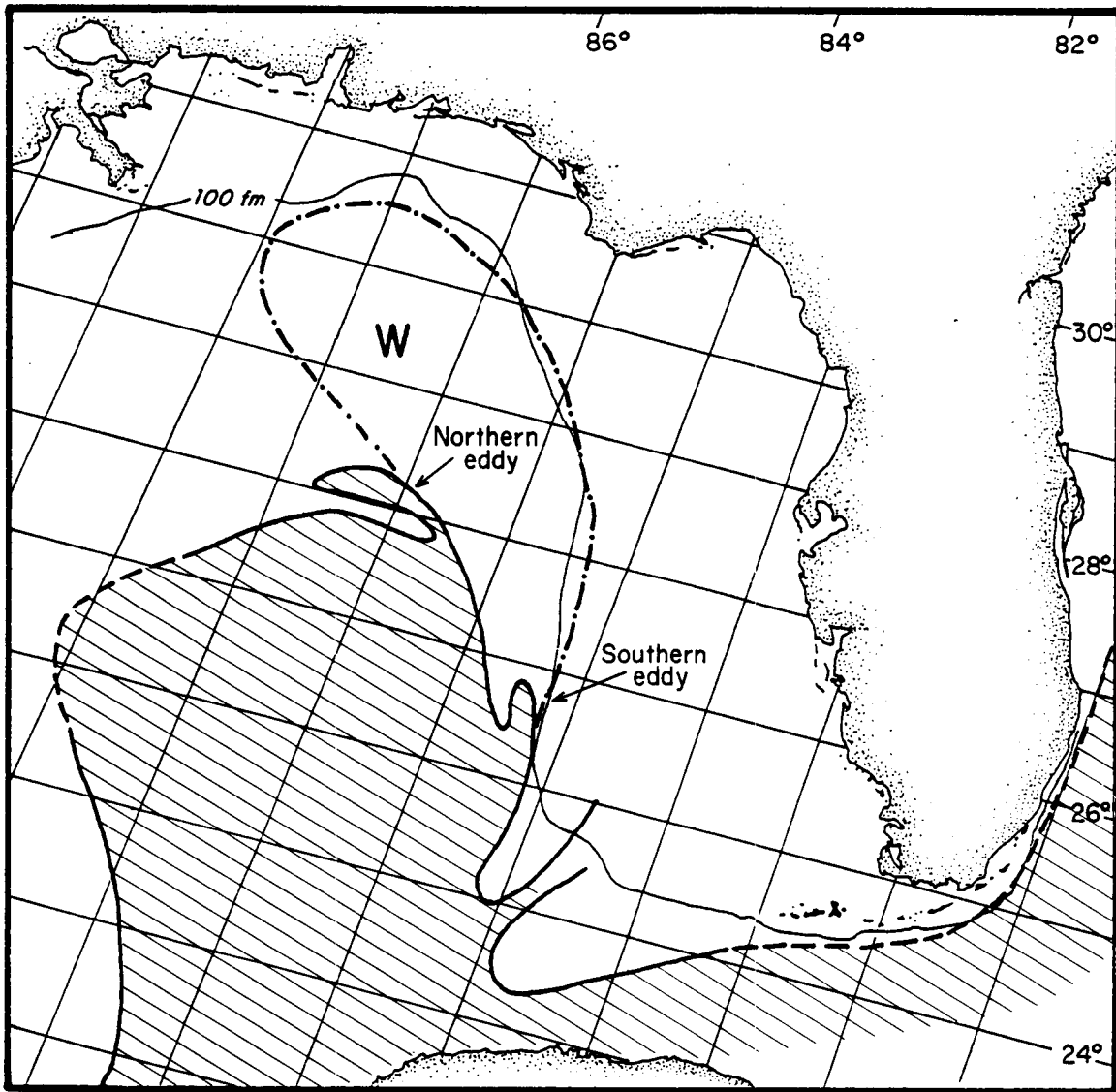
Figure 7-3.   Composite satellite imagery defining Loop Current front
on March 29, 1982.

7.3.1 First Mapping Run (April 1, 1982)

The next NOAA SFSS update on April 2 (Figure 7-4) shows a breakdown in the southern eddy and an unanticipated enlargement and movement of the northern eddy; the latter propagating southeastward along the front at about 30 km·day^{-1}. By the time the U-2 aircraft reached the planned mapping area, the surface manifestations of the target eddy had dissipated to the thermal pattern shown in Figure 7-5. The results of the four OCS mapping runs are shown in Figure 7-6. Surface areal coverage was about 28×10^3 km^2. Note that both the area temperature distribution (Figure 7-5) and OCS chlorophyll results (Figure 7-6) are presented at the same scale for ease of comparison.

7.3.2 Second Mapping Run (April 2, 1982)

During the second day of operations, increasing cloud cover began to obscure the sea surface and cause erroneous results. As indicated by the third condition discussed in Section 7.1.2, cloud cover increases the apparent albedo which effectively increases the backscattered radiance. These increases are indistinguishable from chlorophyll signatures and appear as higher concentration values in the computerized results (Figure 7-7). Noting this apparent cloud cover, only 21×10^3 km^2 (8,106 sq. mi) were mapped during the second day. Essentially the same flight headings were run over abbreviated lengths.
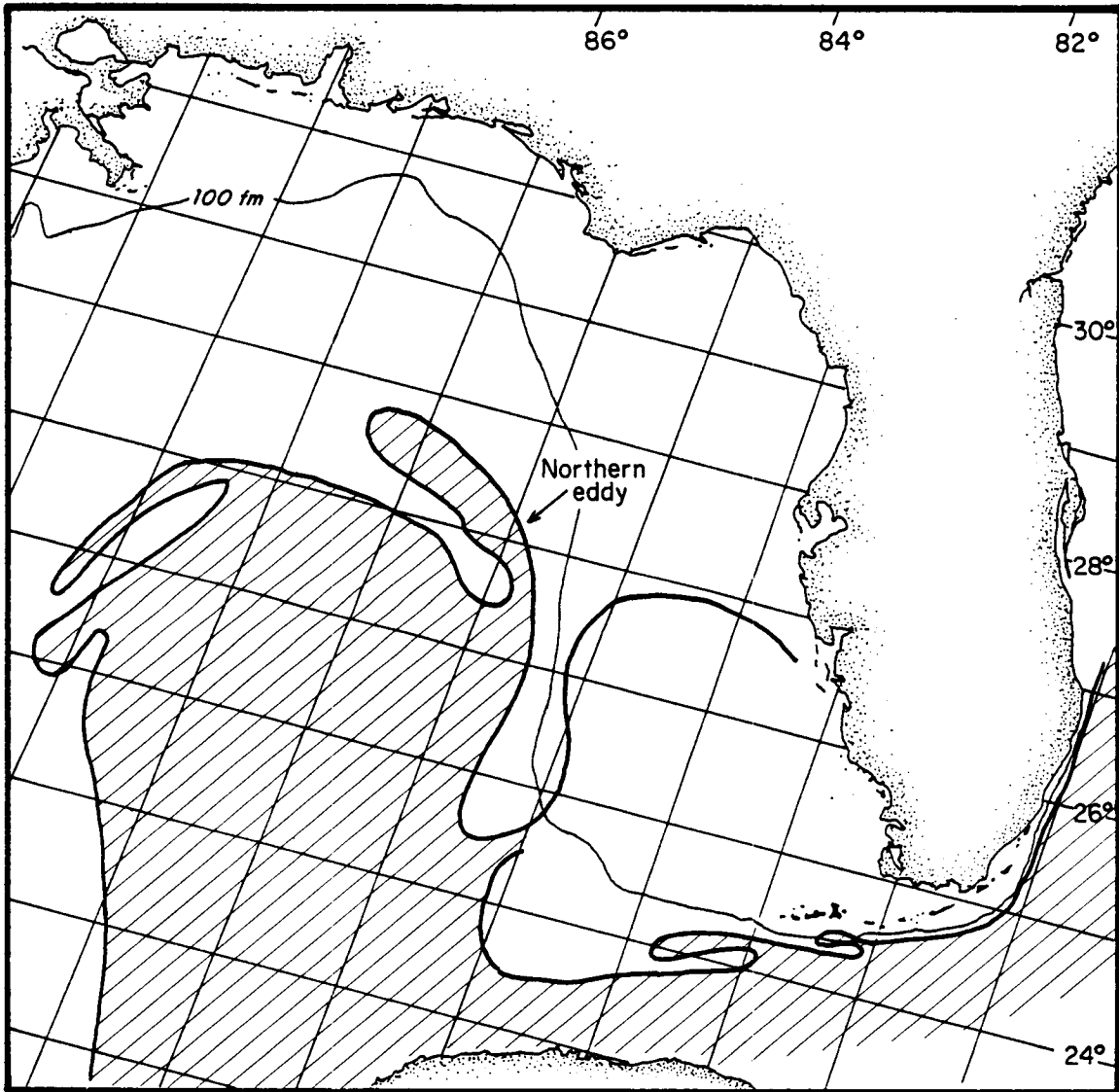
Figure 7-4.   Composite satellite imagery defining Loop Current front
              on April 2, 1982.

343

THIS PAGE IS INTENTIONALLY
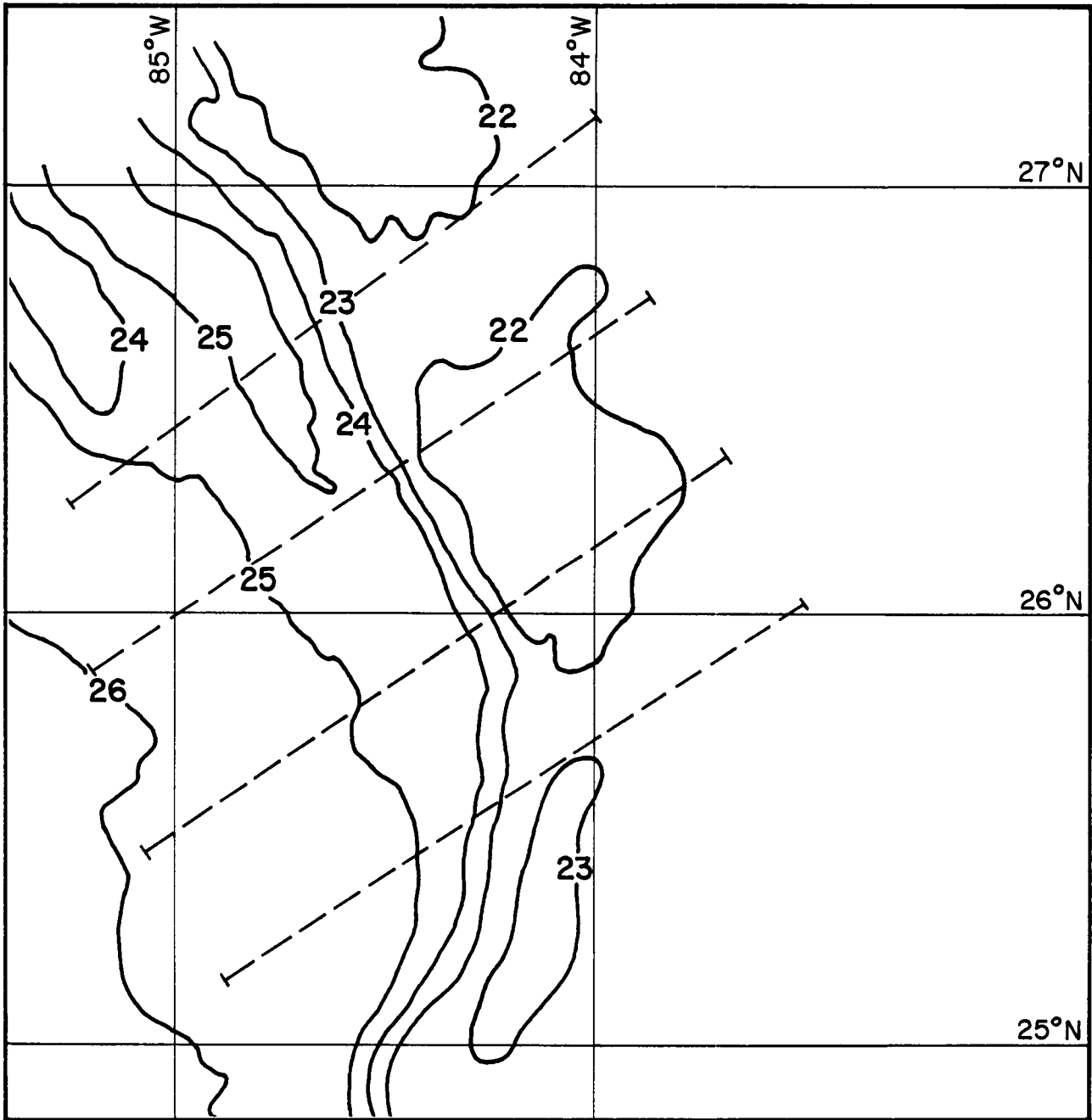
LEFT BLANK

Figure 7-5.   Surface temperature (°C) distribution in chlorophyll mapping area on April 1, 1982.

THIS PAGE IS INTENTIONALLY

LEFT BLANK

CHLOROPHYLL CONC.

■	0.68 mg·m^{-3}
	0.45 mg·m^{-3}
	0.35 mg·m^{-3}
	0.25 mg·m^{-3}
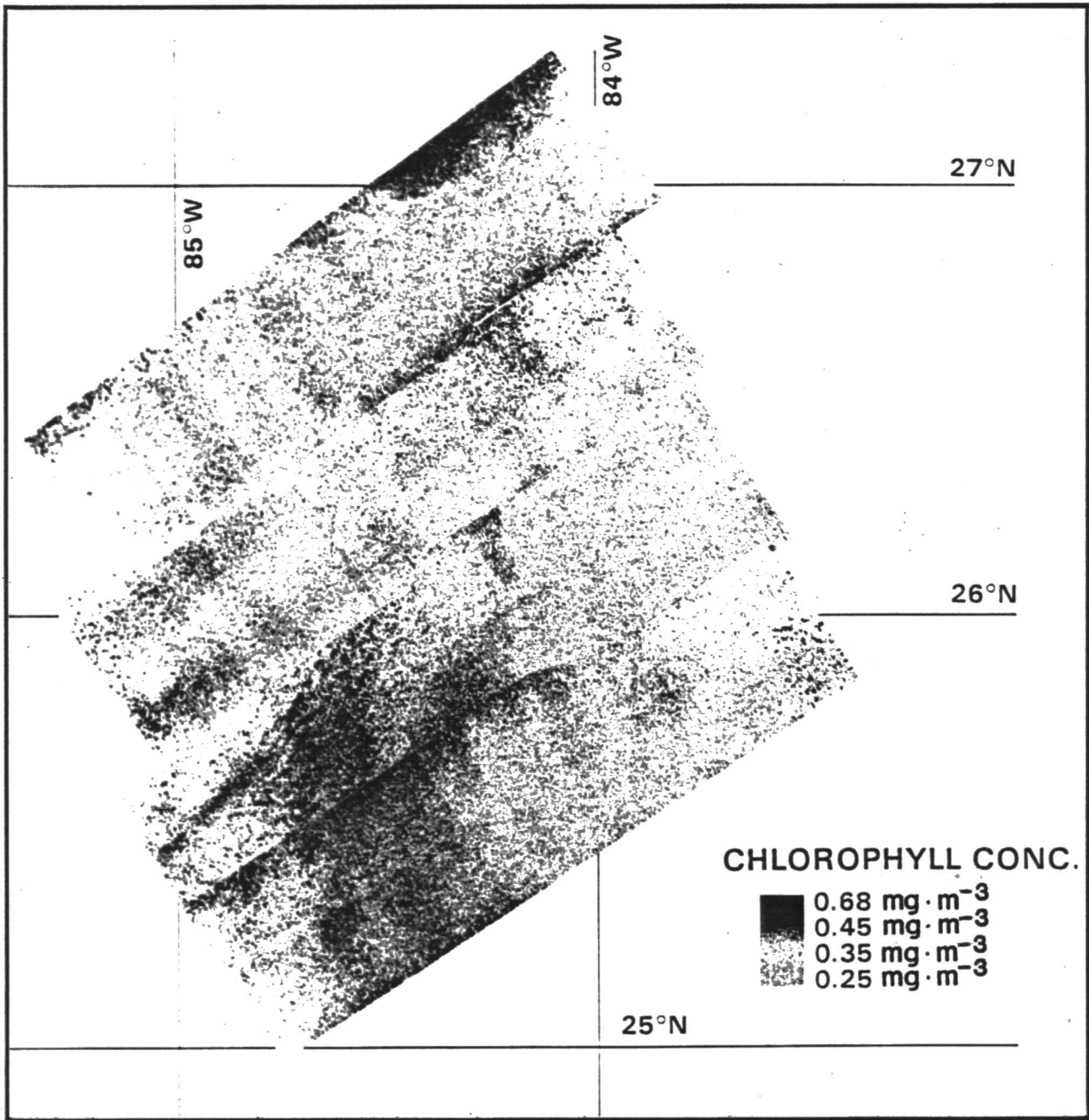
Figure 7-6.   OCS chlorophyll mapping results for April 1, 1982.

THIS PAGE IS INTENTIONALLY

LEFT BLANK
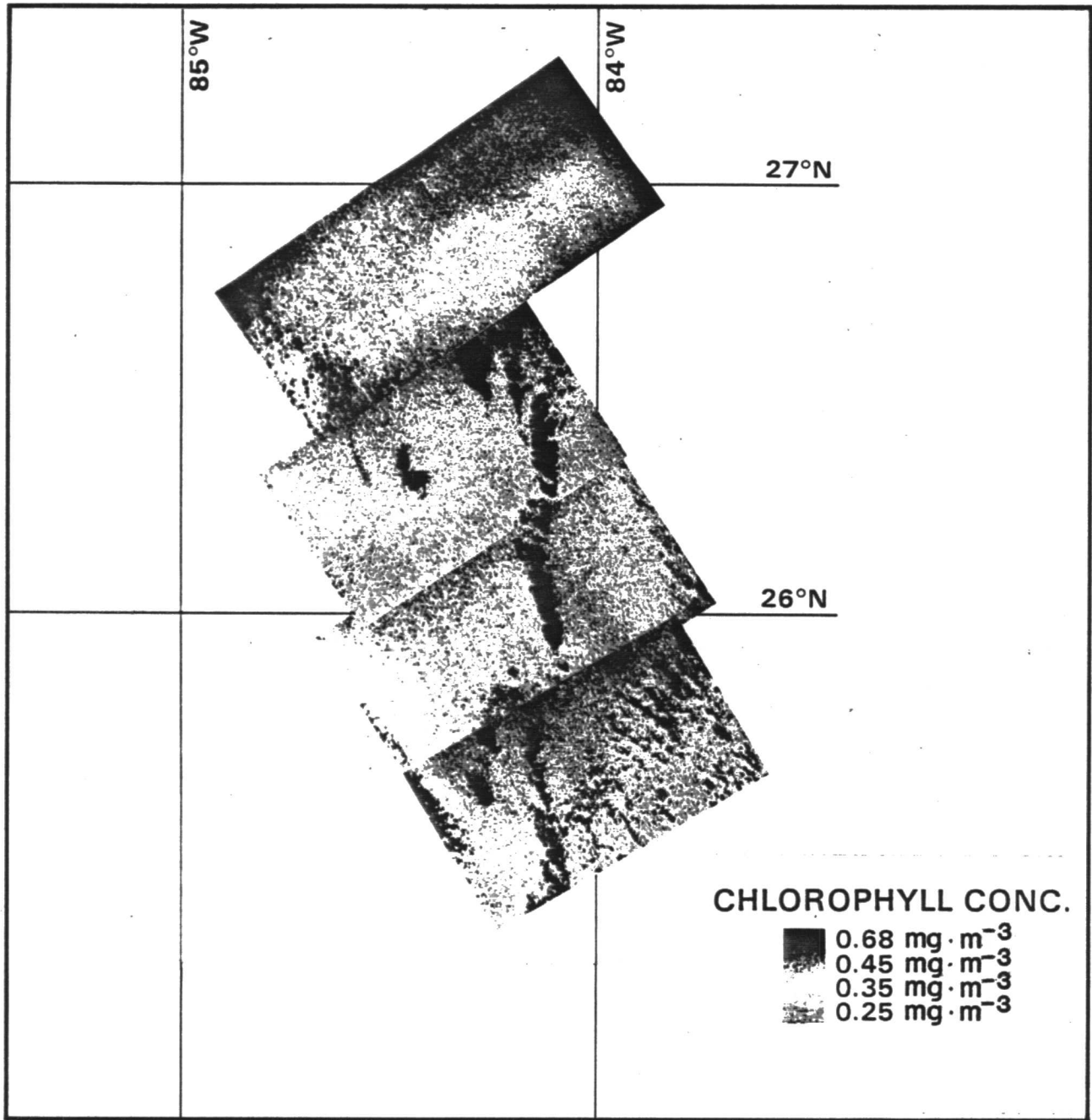
Figure 7-7.   OCS chlorophyll mapping results for April 2, 1982.

7.4. Discussion

One of the more obvious features of the two OCS mappings is the generally low background levels of chlorophyll recorded over the relatively large surface area. In the second day's mapping (Figure 7-7), due allowance must be made for what appears to be cloud bands in the northernmost section and along the center of the composite; however, the background level of about 0.25 $mg \cdot m^{-3}$ is still evident over most of the mapped area. Using a similar technique from the NIMBUS-7 Coastal Zone Color Scanner (CZCS), Gordon et al. (1980) have also reported similar chlorophyll concentrations in generally the same area in a November 1979 experiment. This lack of plant nutrients, or oligotrophic condition, agrees with previously reported values for on-shelf and central Gulf waters and suggests no real distinction between outer continental shelf and open Gulf of Mexico surface waters in this regard. These surface values are also in basic agreement with the values reported in Sections 5.0 and 6.0.

Near-surface chlorophyll concentrations in October/November 1980 and April/May 1981 in the 50 to 100 m depth range on the shelf generally did not exceed 0.5 $mg \cdot m^{-3}$ (WCC/CSA, 1982) in spite of the fact that studies to date indicate spring is one* of the most productive seasons in the eastern Gulf of Mexico (Steidinger, 1973). Steidinger's data give no comparative seasonal estimates for biomass or organic carbon content. Additionally, El-Sayed's (1972) data indicate an average standing crop for Gulf surface waters to be about 0.2 $mg \cdot m^{-3}$ with lowest values occurring at open Gulf stations and highest values in the northeastern Yucatan Peninsula and in parts of the Loop Current.

---

* The other season is summer.

A notable exception to the general uniformity is evident at the extreme northern edge of the April 1 mapping. If Figure 7-5 (thermal distribution) is compared to Figure 7-6 (OCS chlorophyll distribution), it can be seen that the 22°C isotherm near 27°N corresponds roughly to the edge of the chlorophyll maximum protruding into the survey area from the north. Referring back to Figure 3-27, it appears quite likely that this feature is a surface manifestation of the eddy that was measured by the GYRE on April 6 as it sampled northward while the eddy propagated southward. In other words, the OCS mapping area which was established to map the surface features of the southern eddy had just enough of a northward extent to sample part of the northern eddy as it progressed southward on April 1.

Additional features worth noting in the OCS mapping can be seen by comparing the Chl a + Ph a shipboard measurements of April 2 and 3 to the April 1 OCS results along the cruise track. A similar comparison has been presented by Gordon et al. (1980) for their CZCS/RV ATHENA II Gulf of Mexico data set. The values recorded in the upper 2 to 3 m are graphed at a scale comparable to Figure 7-6 in Figure 7-8. Both chlorophyll-a and phaeopigments (i.e., predominantly phaeophytin and phaeophorbide) are considered in this comparison because they absorb light in the same region of the spectrum as Chl a and have comparable effects on $I^{water}_{\lambda i}$.

Factors to consider in this comparison are:

1. Superficially, it appears as if the OCS chlorophyll concentrations are consistently about double that of the shipboard value. Part of this discrepancy arises from the depth integrating effect that forms $I^{water}_{\lambda i}$.

THIS PAGE IS INTENTIONALLY

LEFT BLANK
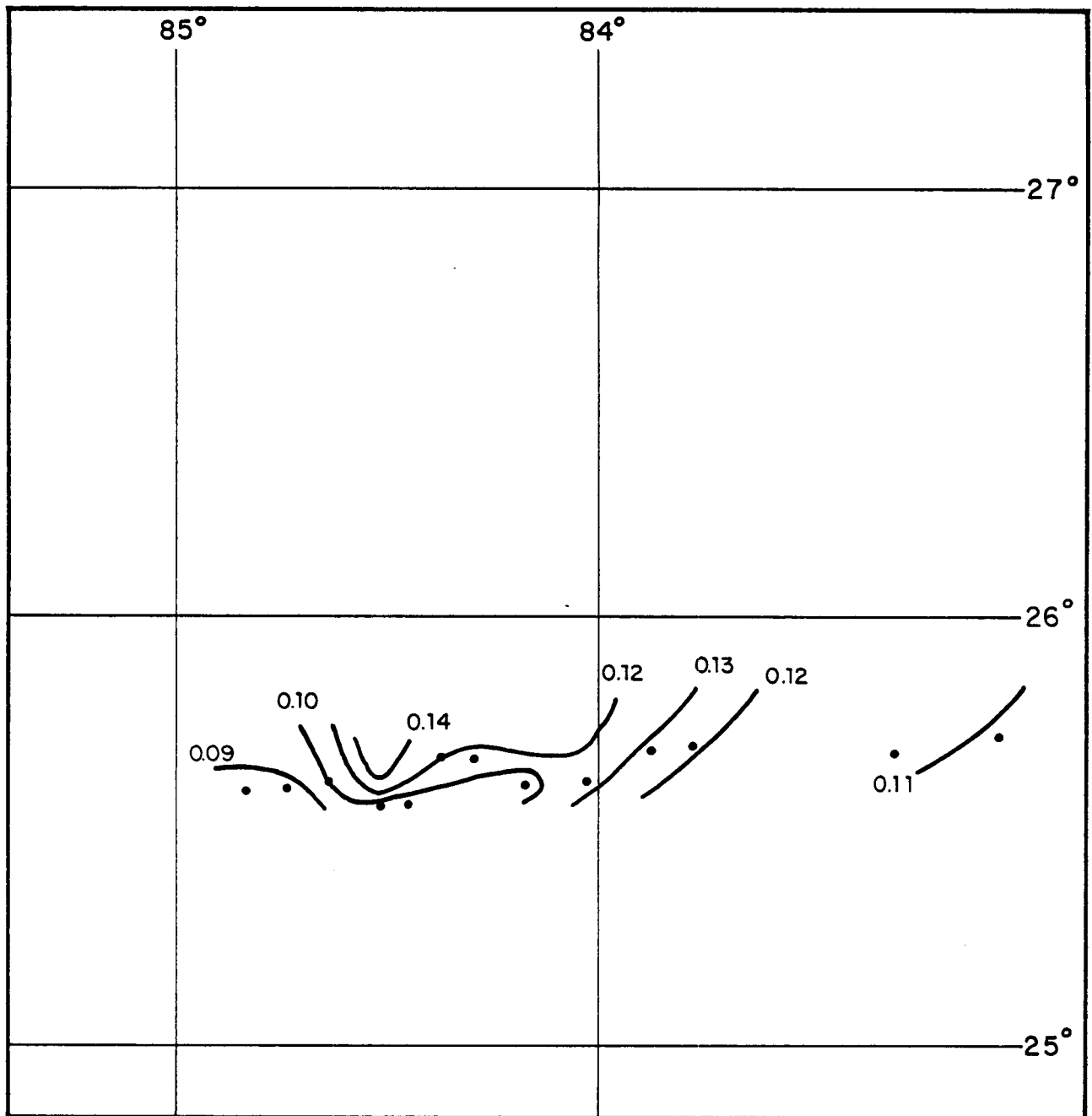
Figure 7-8. Near-surface Chl _a_ + Ph _a_ isopleths (mg·m^{-3}) across transect 1.

That is, although the station chlorophyll profiles indicate a generally constant value in the upper, say 20 m, the depth of upwelling light carrying the OCS chlorophyll signature is more than likely formed over a series of depths before leaving the sea surface. For the wavelengths being considered, this layer is probably on the order of 10 m thick.

2. A second point to consider is the logarithmic fashion in which the OCS concentrations are calculated. Thus small differences at low concentrations can result in rather large errors when reconverted. The OCS reduction algorithm appears to work best under rapidly changing dynamic conditions where large gradients are more evident.

3. Although the absolute concentrations appear to disagree, the relative gradient patterns appear to be similar. For instance, the maximum shipboard value (0.14 $mg \cdot m^{-3}$) at 25°40'N, 84°30'W roughly coincides with the higher OCS value (0.45 $mg \cdot m^{-3}$) in the same region. Similarly, the higher concentration values situated just north of 27°N coincide with the next propagating eddy as discussed earlier.

7.5 <u>Recommendations and Conclusions</u>

Even though work in relating the intensity of backscattered light from the sea surface to chlorophyll concentrations has been under active development since 1969, the idea of applying these techniques to managing development activities on the outer continental shelf or formulating inputs for ecosystem productivity modeling is still rather novel. The information gained from this particular study may therefore serve as a series of guidelines for future

354

studies along these lines. In particular, two recommendations should be considered:

1. Since ocean color detection techniques permit measurement at different altitudes, the horizontal scale of the phenomenon under investigation should be allowed to determine which system will be used. For instance, in this particular study, if appropriate logistic arrangements could have been completed, the space shuttle OCS or NIMBUS-7 CZCS imagery with a $(826 \text{ m})^2$ footprint may have been able to track both the northern and southern eddies as they developed and moved between March 24 and April 2. This would have removed the ambiguity concerning which eddy the U-2 flight pattern was to use as a target.

2. Future chlorophyll studies should utilize ocean color statistics with other aircraft or satellite derived data of comparable scales to develop additional insight about dominant distributions. As an example, studies such as that of Vukovich et al. (1979) which characterized the statistical positions of the Loop Current front in the eastern Gulf of Mexico might be augmented with statistical distributions of phytoplankton to infer either transport patterns or fisheries potential with respect to a major surface current.

An underlying objective of a number of ocean color studies to date (e.g., Hovis et al., 1980; Kim et al., 1980; and Gordon and Clark, 1980) has been to improve our understanding of the state of the standing crop of phytoplankton not only on the continental shelves of the U.S. but across the world's oceans. This new information may then, in turn, lead to improved methods of

managing and exploiting near-surface fisheries, early detection of phytoplankton blooms, or even oil spill tracking and discharge mud plume definition on the continental shelves. This new technology should now be applied to investigation of the wide variety of continental shelf processes visible at the surface.

Conclusions drawn from this study are as follows:

1. The U-2/OCS can be used effectively to map chlorophyll gradients in the upper 10 m of the eastern Gulf of Mexico. In terms of areal coverage, the U-2/OCS was able to map four times the area of a ship in one-sixth the time.

2. The surface layers in the vicinity of the shelf break are basically oligotrophic in nature with background chlorophyll concentrations on the order of 0.1 to 0.2 $mg \cdot m^{-3}$. Higher concentrations occur in patches.

3. Although absolute values (at low chlorophyll concentrations) from OCS and shipboard sources appear to disagree, the gradients derived from both sources are similar.

4. Since visible light cannot penetrate clouds, an OCS mapping procedure cannot be used in cloudy or even partially cloudy areas. Preferably all four conditions for an overflight should be met for best data results.

5. Continental shelf ocean color changes on scales larger than about 70 m can be effectively mapped using OCS techniques.

7.6 References

El-Sayed, S.Z. 1972. Primary productivity and standing crop of phytoplankton. In "Chemistry, Primary Productivity, and Benthic Marine Algae of the Gulf of Mexico. Serial Atlas of the Marine Environment," Folio 22, Amer. Geograph. Soc.

Gordon, H.R., D.K. Clark, J.L. Mueller and W.A. Hovis 1980. Phytoplankton pigments from the Nimbus-7 Coastal Zone Color Scanner: Comparisons with surface measurements. Science, 210 (4465): 63-66.

Hovis, W.A., D.K. Clark, F. Anderson, R.W. Austin, W.H. Wilson, E.T. Baker, D. Ball, H.R. Gordon, J.L. Mueller, S.Z. El-Sayed, B. Sturm, R.C. Wrigley and C.S. Yentsch 1980. Nimbus-7 Coastal Zone Color Scanner: System description and initial imagery. Science, 210 (4465): 60-63.

Kim, H.H., C.R. McClain, L.R. Blaine, W.D. Hart 1979. Chlorophyll gradient map from high-altitude ocean-color-scanner data. Applied Optics, 18 (22): 3715-3716.

Kim, H.H., C.R. McClain, L.R. Blaine, W.D. Hart, L.P. Atkinson and J.A. Yoder 1980. Ocean chlorophyll studies from a U-2 aircraft platform, J. Geophys. Res., 85 ((C7): 3982-3990.

Kim, H.H., R.S. Fraser, L. Thompson, and O.P. Bahethi 1980a. A system study of an advanced ocean color scanner. Boundary Layer Meteor, 18: 343-355.

Kim, H.H., W.D. Hart, H. Van der Piepen 1982. Initial Analysis of OSTA-1
Ocean Color Experiment Imagery. Science, 218 (4576): 1027-1032.

Steidinger, K.A. 1973. Phytoplankton. In "A Summary of Knowledge of the
Eastern Gulf of Mexico," coordinated by the State University System of
Florida Institute of Oceanography. III E-1 through III E-18.

Vukovich, F.M., B.W. Crissman, M. Bushnell and W.J. King 1979. Some aspects
of the oceanography of the Gulf of Mexico using satellite and in-situ data.
V. J. Geophys. Res., 84 (C12): 7749-7768.

Woodward-Clyde Consultants/ Continental Shelf Associates 1982. Southwest
Florida shelf ecosystems study - Year 1. Prepared for Minerals Management
Service under Contract No. AA851-CTO-50 (in review).

8.0 CONCLUSIONS AND RECOMMENDATIONS

HONG CHIN*
WOODWARD-CLYDE CONSULTANTS

8.1 <u>Phase III Study Conclusions</u>

Within the results of the three measurement techniques (<u>in-situ</u> sampling, interpretation of measured optical properties, and remote sensing of surface characteristics), the data concur in their description of overall Loop Current intrusion features. An obvious study conclusion, therefore, is that primary production on the outer southwest Florida continental shelf is enhanced by the transport of offshore waters and nutrients onto the shelf. These Loop Current upwellings may, in fact, control the observed variability in primary production of the outer shelf. Between the spring and summer data sets, summer productivity values associated with a subsurface Chl $\underline{a}$ maximum were generally higher than comparable spring values. Productivity in waters affected by a Loop Current eddy showed increases by a factor of six over uneffected waters.

Surface Chl $\underline{a}$ values in the study area were generally less than 0.25 mg$\cdot$m^{-3} with most values below 0.10 mg$\cdot$m^{-3}. Higher surface chlorophyll values usually occurred in patches. Subsurface maxima in Chl $\underline{a}$ ranged from 0.2 to 1.2 mg$\cdot$m^{-3}. Average primary productivity during the spring cruise was 0.5 gC$\cdot$m^{-2} day^{-1} with the nitracline remaining about 40 to 50 m below the surface. Summer productivity values were higher but showed a greater variability with depth. About 70% of the observed variability in daily primary productivity could be explained by changes in Chl $\underline{a}$ concentration and irradiance.

---

* Present affiliation: Oceanology Associates, San Diego, CA 92120

359

One of the highest productivity regions observed in these data was in the summer, near-surface, low salinity lens of 10 to 30 m in thickness. Productivity values of 10 $gC \cdot m^{-3} \cdot day^{-1}$ were noted near the surface with a sharp decline with depth. A single Diatom species, _Rhizosolenia_ _alata_ comprised more than 80% of the total Diatom population measured within this low salinity lens.

The dominant species of Coccolithophorid during both cruises was _Coccolithus_ _huxleyi_ (Lohman) Kamptner. Approximately 40 to 50% of all phytoplankton species were common to selected station pairs used for comparison. Cell counts at shallow stations were generally low with little variation with depth; around upwelling regions, counts were higher with greater variability with depth.

Finescale mixing and interleaving were evident between different water masses. Lateral mixing lengths were on the order of 30 to 40 km. Estimates for the effective lateral diffusion coefficient ranged from 0.15 to 4.0 x 10^7 $cm^2 \cdot sec^{-1}$.

The surface length scale of a frontal eddy was on the order of 200 km. At depth, the length scale was inferred to be at least 100 km. Upwelling within the frontal eddy system occurred beneath the cold core (CEW) between the main body of LCW and the warm LCW filament. Effects of an eddy intrusion were evident to the 60 m isobath on the shelf.

Between September 13 and 18, 1982, a 28 km movement of the Loop Current towards the east was documented near the outer shelf. This movement caused an

increase in isopycnal doming, an increase in subsurface salinity, warmer subthermocline temperatures, and a decrease in the volume of the lower salinity lens near the surface. The tracking of this five day progression and the noting that significant thermal changes were evident over periods as short as 24 hours suggests that the seasonal depictions presented in the "hydrographic atlas" (Section 2.3) actually represent a composite of several different regimes occurring over the 13 to 29 days of data collection. Only general features (such as those discussed in the text) should be sought from these composites.

Loop Current frontal eddies occurring off the southwest Florida shelf are basically similar to Gulf Stream frontal eddies observed off the southeastern U.S. shelf in terms of characteristic length scales and speeds. The relatively lower rates of primary production and phytoplankton biomass in the former appear to be coupled with the greater depth maintained by the nitracline during an intrusion event. In turn, the deeper nitracline appears to be related to differences in topographic relief between the two slope areas.

Remote (infrared) sensing of boundary current features gave a reliable spatial depiction (within ± 15 km) of the same features measured from onboard ship. Processed ocean color images reproduced relative surface chlorophyll gradients well and supported the oligotrophic nature of the upper 10 m. The use of remote color scanners (i.e., either the CZCS or OCS) as a management tool for mapping surface features larger than about 70 m appears to be a viable alternative to shipboard sampling --- especially in light of their ability to cover large areas in relatively short time periods. The use of color scanners for primary productivity studies, however, may lead to misleading results

because of the importance of subsurface (below 10 m) chlorophyll maxima to the productivity processes.

Simultaneous optical oceanographic studies have demonstrated the applicability of color index algorithms to the southwest Florida shelf study area as well as the present dearth of particulate matter in the water column.

The overall results of this study phase have identified a shelf break mechanism for enhancing the production of food elements at the most basic levels of the "food chain". The importance of such a mechanism for estimating recovery rates in the event of potential area contamination due to oil and gas development activities is quite apparent. In light of anticipated increases in leasing activity in the subject area, it is anticipated that an even greater understanding of the processes associated with this mechanism must be gained before MMS decision-makers have sufficient information for planning future developments in federal outer continental shelf waters, or effective fate and effects models can be formulated. The following are a number of project recommendations for the directions that these future studies should take. Most of these recommendations were developed in joint session at the University of South Florida project workshop.

8.2 Southwest Florida Shelf Ecosystems Study Workshop

On November 16, 1982, the results of this study were presented in open forum at the University of South Florida in St. Petersburg, Florida. The day-long discussions covered as many details and points of view as time permitted. Table 8-1 presents a list of the workshop participants.

362

A critical review was requested from the four panel members and workshop participants. Written comments pertaining to four specific points were solicited from the panel members. The discussion points were;

1. significant processes and/or factors relating to outer continental shelf primary productivity, either illustrated by the collected data or directly assessable from them,

2. assessment of the present state of knowledge of productivity effects in this study area,

3. recommendations for incorporation of such features into either numerical or conceptual models of Fates and Effects of outer continental shelf resource development, and

4. recommendations for further work.

Table 8-1. Southwest Florida Shelf Ecosystems

Study Workshop Participants

Workshop Chairman

Dr. Hong Chin
(Woodward-Clyde Consultants)

Review Panel

Prof. William M. Dunstan
(Old Dominion University)
Prof. Richard L. Iverson
(Florida State University)
Prof. Thomas N. Lee
(MPO/RSMAS, University of Miami)
Prof. Gabriel A. Vargo
(University of South Florida)

Principal Investigators

Hydrography	Prof. Larry P. Atkinson (Skidaway Institute of Oceanography) Ms. Theresa Paluszkiewicz (Skidaway Institute of Oceanography)
Primary Productivity	Prof. James A. Yoder (Skidaway Institute of Oceanography)
Mixing Processes	Prof. Eric S. Posmentier (Long Island University, Southampton College)
Optical Oceanography	Dr. Niels K. Hojerslev (University of Copenhagen, Institute of Physical Oceanography)
Ocean Color Scanner	Dr. Hongsuk H. Kim (National Aeronautics and Space Administration)
Workshop Participants	Dr. William W. Behrens, Jr. (Florida Institute for Oceanography) Dr. Murray Brown (Minerals Management Service) Dr. Ken Carder (University of South Florida) Dr. David Gettleson (Continental Shelf Associates) Dr. Ken Haddad (Bureau of Marine Science and Technology) Prof. A. D. Kirwan, Jr. (University of South Florida) Mr. William Lyons (State of Florida, Department of Natural Resources) Dr. Keith Macdonald (Woodward-Clyde Consultants) Mr. Dean Milliken (Florida Institute for Oceanography) Dr. Sandra Vargo (Florida Institute for Oceanography).

The panel members' responses were as follows.

8.2.1 Workshop Comments (Prof. W. M. Dunstan, Old Dominion University)

1. A host of physical and biological processes were identified at the
    Workshop which should be considered within the context of oil and gas
    development on the Southwest Florida shelf. Some of these processes have
    been addressed in earlier studies (distribution and diversity of benthic
    fauna, etc.); others are being studied within the present program (Loop

Current movement, the potential influence of intruded nitrogen on water column productivity and optical characteristics of shelf water); still others were identified at the meeting as being necessary for future consideration (macrobenthic and microalgal primary productivity, light and its influence on benthic production, the nitrogen cycle other than nitrate, etc.).

2. Models of Fates and Effects

It is clear that the biological system on the southwest Florida shelf is driven by the physics, especially on the outer shelf. Further, it is clear that the most important component of the physics is the movement of the Loop Current near the shelf break. There is simply not enough data on water mass movement to do much more than draw the broadest of conceptual models at this time. As indicated in the data presented, filaments of the Loop Current may move as much as 50 kilometers per day. The state of our knowledge is exemplified but the fact that we really don't understand the origin of the filament structures that seem to be so characteristic of the study area. Physical oceanographers are in the early hypothesis stage as illustrated by the interesting presentation by Dr. Eric Posmentier. He suggested a southerly origin for the Loop Current filament found in the study area of the shelf. The Ocean Color Scanner data could be interpreted in another way and the hydrographic data base adds another perspective. It is important that the existing data be worked up and then analyzed and interpreted prior to any modeling efforts. Primary production cannot really be modeled without more information on the temporal and spatial extent of the intruded deep nitrate rich water. From

the data presented on the first cruise by Dr. Jim Yoder, it would seem that the area (water column) as expected, is quite oligotrophic and there were only a few indications of enhanced productivity at the shelf break. It must be noted that studies on the South Atlantic Bight have been proceeding for almost 10 years and workers are still gaining new insights into the patterns of productivity.

3. Present Knowledge of Primary Productivity

The present state of knowledge of productivity on the Southwest Florida shelf is quite incomplete. There is not enough data to determine how much nitrate is brought to the shelf by intrusion processes and what percent of primary production is supported by this "new" nitrogen. We do now know whether intruded nitrate is utilized primarily in water column production or in benthic production. Initial studies suggests that vast areas of benthic macro-algae exist on the outer shelf and the Florida system may be quite different from that found along the Gulf Stream on the south Atlantic coast. Furthermore, we do not know how close the benthic macro-algae are to the light limit for photosynthesis (critical depth).

4. Further Studies

In addition to completing the data bases initiated, (e.g., standard hydrographic stations coupled with primary production, nutrients, remote sensing and optical characteristics), it was clear from the discussions at the Workshop that three major studies needed to be initiated:

a)   current meter arrays,

b)   biological work on the rates and distribution of benthic algal production,

c)   studies of the nitrogen cycle to include dissolved organic nitrogen (DON), ammonia and nitrogen fixation.

The following questions need to be addressed:

- What percentage of the nitrogen utilized for productivity on the shelf comes from Loop Current intrusion?

- What percentage of primary production on the shelf is provided by benthic macro or micro algae?

- How important is intruded nitrate to the benthic algae?

- What about the rest of the nitrogen cycle (only nitrate and nitrite data was reported)? How important is regenerated nitrogen?

- Does the benthic macro-algae support a commercially or ecologically important food chain?

- How significant is the data concerning the transmission of UV-B 310nm to the inhibition of photosynthesis?

- Is there any connection between the Everglades and Loop Current intrusion?

- Are the newly found pleistocene molluscs dependent upon the benthic macro-algae?

- What is the temporal and special distribution of the Loop Current induced water masses on the southwest Florida shelf?

- What are the origins of the freshwater masses found on the shelf?

Other Comments

I suggest that the data so far accumulated be worked up with a more complete analysis phase and that further interaction between the component groups be planned so that a joint interpretive effort can be made.

I commend the use of the workers from the South East Bight who have a large data base and extensive experience in shelf-oceanic interaction. This should provide an enhanced scientific contribution from the work as well as the more timely interpretation of the mission oriented questions.

8.2.2 Workshop Comments (Prof. R. L. Iverson, Florida State University)

1. Significant processes relating to outer shelf primary productivity.

   a) The southwest Florida outer continental shelf waters were very oligotrophic during the periods sampled. Nitrate concentrations were low as were chlorophyll concentrations within the top 40 to 60 meters of the water column. The nutrient and chlorophyll concentrations were similar to those reported for the oligotrophic central waters of the Gulf of Mexico, suggesting that there is no real distinction between outer continental shelf and open Gulf of Mexico surface waters. This situation contrasts with that of other continental shelves where there is a distinct difference in nutrient and chlorophyll properties compared with offshore waters.

   b) Most of the primary productivity within the water column was associated with a mid-depth chlorophyll maximum layer which ranged

from 40 m to 60 m in depth. This pattern is similar to that reported for the open Gulf of Mexico by Hobson and Lorenzen.

c)   There is strong support for the applicability of the enrichment model proposed by Riley to explain the occurrence of water containing high nutrient concentrations near the bottom along continental shelf edges. Salinity, temperature, density, and nitrate isopleths suggest an advective upwelling of nutrient-rich water along the shelf edge in southwest Florida waters.

2.   Present state of knowledge of productivity effects in this study area.

The literature concerning phytoplankton productivity in the Gulf of Mexico was summarized by Iverson and Hopkins in a NOAA publication published in 1981. The data collected under the auspices of the Southwest Florida Shelf Ecosystem Study are the first data collected in an organized fashion which characterize the phytoplankton productivity of that area. We had assumed that the area would be oligotrophic, based on satellite imagery of the southwest Florida continental shelf, but this is the first data set which substantiates that hypothesis.

3.   Incorporation of features into a conceptual model of fates and effects of outer continental shelf resource development.

The existence of a subsurface chlorophyll maximum layer with its associated phytoplankton productivity suggests that accidental input of hydrocarbons to the sea surface may not primarily affect phytoplankton productivity through toxic effects. The primary effect would be through

reduction of light energy if enough material were to accumulate on the sea surface. It should be possible to prepare a numerical model of the phytoplankton and nutrient dynamics on the southwest Florida shelf since the physical factors which drive nutrients onto the shelf appear to be understood.

4. Recommendations for further work.

Measurements of nitrate and ammonium uptake by phytoplankton in the subsurface chlorophyll maximum would be valuable as would measurement of the response of benthic algae to the nutrient enrichment phenomenon described by Riley and supported by data collected during this study.

8.2.3 Workshop Comments (Prof. T. N. Lee, Rosenstiel School of Marine and Atmospheric Science

Introduction

Woodward-Clyde Consultants and their contracted Principal Investigators have been conducting a study on the S.W. Florida shelf for Minerals Management Service to obtain environmental data for use in evaluating potential impacts of petroleum exploration and production activities on the outer shelf. The purpose of this review is to evaluate the work to date and make recommendations concerning future efforts. The opinions expressed derive from written materials provided by Woodward-Clyde and participation in the S.W. Florida Shelf Study Workshop on November 16, 1982 in St. Petersburg, Florida.

General Comments
_____

The S.W. Florida Shelf Study was conducted in three phases. The first phase
began July 1980 and involved shelf-scale geophysical mapping and water column
characterization during fall and spring seasons. The second phase obtained
water column data during summer and winter seasons giving a four-season data
base for the period from July 1980 to February 1982 and covering the shelf
area from the 20 to 200 m isobaths between Cape Charlotte to the north and Dry
Tortugas to the south. The third phase involved investigation of Loop
Current-shelf interaction during the spring and fall of 1982.

The sampling strategy appears to have been well-conceived from MMS purposes.
First obtain general environmental background data spanning the total shelf
area of interest and all four seasons and then to study in more detail one of
the more important mechanisms affecting physical, chemical and biological
distributions on the outer shelf, i.e., Loop Current-shelf interaction.

The combination of Phase I and II background data with historical data from
the region should be sufficient to characterize the shelf spatial
distributions and seasonal variations of the important physical, chemical and
biological parameters. This data base could then serve as the first order or
ambient state for: 1) input into numerical models; 2) EIS evaluation of
future oil exploration and production impacts; 3) identification of
ecologically sensitive areas.

The Phase III study of Loop Current intrusions over the outer shelf is the
first of its kind for the S.W. Florida shelf and clearly demonstrates the

importance of this offshore current to outer-shelf physical, chemical biological processes. The finding of Loop Current frontal eddies over the outer shelf similar to those observed along the southeast U.S. outer shelf (Gulf Stream frontal eddies have been found to be the primary mechanism controlling current, temperature, nutrient and primary production variability over the outer-shelf of the southeast U.S.) strongly dictates the need for continued studies of this process. Special emphasis should be placed on analyzing historical data (current meter, hydrographic and satellite IR, in addition to the Phase III data), to estimate the frequency of occurrence, modes of interaction, and area of influence of Loop Current intrusions.

Specific Comments

Biology

1) The finding of new species or previously undiscovered relics is an important discovery and should attract considerable attention. More consideration could be given to the significance of these results, especially as they relate to MMS interests.

2) The benthic biota was found to be distributed in four zones: inner-shelf 0-20 m; inner mid-shelf 40-80 m; outer mid-shelf 80-100 m; and outer-shelf 100-200 m. With the data in hand you may be able to determine the cause of the zonation (sediment type, physical parameters in the water column, distance from shore or Loop Current).

3) The finding of extensive areas of bottom attached algae appears to be another new and significant discovery for the area. Many questions arise regarding these algae. How important are they to shelf biomass, nutrient

cycles and primary production? How would they be impacted by future oil related activities.

Water Column Distributions (Phase I and II)

1) Three stations were made across the shelf at each section. These data are useful in characterizing inner, mid and outer shelf distributions by seasons but should be treated cautiously due to the limited number of stations and lack of synopticity. It may be more useful to plot vertical profiles and T-S relationships rather than contoured sections which can be misleading given the station spacing.

2) These data could be combined with historical hydrographic, wind, run-off and satellite IR data sets to determine the characteristic seasonal cycles and distributions of water mass properties on the shelf, and to enlarge the historic data base for modeling efforts.

Loop Current Intrusions (Phase III)

1) The comparison of detailed hydrographic sampling with satellite IR imagery clearly identifies a Loop Current frontal eddy over the outer shelf and demonstrates the power of the combination of these measuring techniques.

2) Gulf Stream frontal eddies are known to play a major role in the physical, chemical and biological processes along the outer southeast U.S. shelf. The finding of similar features in the Loop Current front over the S.W. Florida outer shelf suggests that these eddies may play an analogous role there.

3) It is unfortunate that there were no current meters present in the outer shelf during the shipboard sampling for they can be a useful tool in determining the frequency of eddy/Loop Current occurrence, as well as fluxes of momentum, heat and nutrients.

4) Historical satellite IR, hydrographic and current meter data from the region could be used to make a first attempt at estimating the frequency of occurrence of the Loop Current adjacent to the outer shelf, and the frequency of eddies propagating along the Loop Current front.

5) Low-salinity water was observed within the upper layer of the frontal eddy cold-core during April 1982. Two possible sources of low salinity water were discussed: a) upwelling of deeper Loop Current waters; and b) entrainment of low salinity shelf water. This point needs further clarification, possibly with the use of Phases I-III hydrographic and satellite IR data and historical data.

Color Zone Coastal Scanner/Chlorophyll

1) The results of the CZCS analyses, calibration, and in-situ verification are showing a great deal of promise. Studies of this type are of considerable importance for this developing science. The convergence of calibration/correction algorithms is a significant advancement that will aid the reliability of future studies.

2) Shipboard chlorophyll a measurements were shown to be a useful means of making rapid assessments of phytoplankton distributions.

3) Observed chlorophyll a/phytoplankton distributions in the subsurface waters of the outer shelf were shown to be casually related to the Loop Current frontal eddy dynamics. It is also possible that surface distribution of chlorophyll a may show extrema in the cold-core of frontal eddies during periods when upwelling in the core influences the surface waters.

Recommendations

1) Phase I, II and III hydrographic data sets need to be combined with historic hydrographic, current meter, wind and river run-off data to

characterize the seasonal cycle of shelf water mass properties. These combined data sets could also be useful for numerical model studies.

2. Phase III data could be analyzed with available satellite IR images, historic current meter and hydrographic data to estimate the frequency of Loop Current intrusions along the outer shelf and then the frequency of Loop Current frontal eddies that actually affect the outer shelf region.

3) An effort should be made to assess the significance of the discovery of new species and of large areas of bottom attached algae as they relate to MMS leasing of shelf areas for oil exploration and production.

4) The Phase III investigation represents the first concentrated study of Loop Current/shelf interactions. Additional studies of this type are needed in combination with moored current meter arrays and remote sensing of surface temperature and ocean color/chlorophyll $\underline{a}$ in order to properly evaluate the significance of Loop Current intrusions on shelf processes.

8.2.4 <u>Workshop Comments (Prof. G. A. Vargo, University of South Florida)</u>

Point 1: Significant processes/factors relating to primary productivity

A. Loop Current intrusions with a subsequent upwelling and, therefore, input of "new" nitrogen (as nitrate) and presumably other nutrients to the water column along the west Florida shelf.

The nearshore and along shore penetration of the oceanic intrusion could imply that the upwelled nitrate is a principal source of nitrogen for both water column phytoplankton and benthic macro-algae in an area regarded to be nutrient depleted, i.e., oligotrophic. Since the Loop Current has a

375

southerly direction the intrusion may also have a southward as well as
eastward component. Therefore, carbon produced and/or entrained within an
intrusion would be transported south contributing to the organic loading
(organic nutrient component) of the Florida Current. Earlier drift-bottle
work by the Florida Department of Natural Resources (reported in the
Memoirs of the Hourglass Cruises) and the transport of the west coast
red-tide species to the east coast (Murphy, et al., 1975) further support
this possibility. Such intrusions have also been implicated by Haddad and
Carder (1979) as a mechanism for initiating red-tide (Ptychodiscus brevis)
blooms. Since these blooms appear to originate north of Tampa Bay, then
intrusions may also occur north of the SWFSES area. Eastward penetration
of the current could also be implicated as a concentrating mechanism for
these blooms yielding a shoreward transport of high populations which are
responsible for subsequent fish kills.

B. Presence of what may prove to be extensive benthic macrolgae beds in 80 m
to 100 m of water, at low light levels (21% I_o) within the area of Loop
Current intrusion.

Since very little is known about the seasonal production and loss rates of
the species present or their areal extent, the contribution to the
productivity of the region cannot be evaluated. An initial hypothesis
would be that upwelled nitrate is an important factor for determining the
extent and productivity of this deep living macroalgal community.

C. Although not a direct process or factor, the finding of relict populations

of several species and the finding of geographically distinct populations

of South American species.

This finding points to the entire Caribbean-Yucatan Straits-Loop Current

system as a potentially important feature in the zoogeographic

distribution of vertebrates and invertebrates within the Gulf and

Caribbean region. Conditions along the west Florida Shelf which account

for the survival of such relict populations could be useful in

ascertaining the reasons for their demise elsewhere.

Point 2: Recommendations for incorporating such processes into conceptual

and/or numerical models.

The data which was presented at the workshop represents an initial

interpretation of the cruise results and a preliminary effort to correlate

such features as phytoplankton biomass and productivity, and benthic algal

biomass to the episodic intrusions of nutrient rich Loop Current water onto

the west Florida shelf. As such the data represent a starting point for a

conceptual model of production on the shelf. Obviously, additional

information on the extent and duration of intrusions, the relative

contribution of upwelled "new" nitrogen to other sources (regenerated

nitrogen, N_2 fixation, benthic fluxes and organic nitrogen), the relative

contribution of phytoplankton compared to macroalgal production, and loss

rates is required before an expanded (or more precise) conceptual model of

production is attempted.

There is, however, an extensive literature on light-photosynthesis and nutrient-production models for both phytoplankton and macroalgae. Both cruises by the Skidaway group incorporated the measurements required for such models (i.e., light-photosynthesis curves, water column extinction coefficients, pigment concentration, incident irradiance etc.). The data is, therefore, amenable for such an effort and this should be attempted. This effort should be used to evaluate and elucidate other aspects of the shelf ecosystem and the features which represent driving forces, which might otherwise not be noted.

Incorporation of the data from this phase of the study into a Fates and Effects model, other than in a general way, should be avoided. Most of the biological impact for conceptual Fates and Effects models comes from studies undertaken in temperate and/or more northern environments. There has been essentially no work done on the effects of petroleum hydrocarbons on phytoplankton or macroalgal production and community dynamics in tropical or subtropical environments (to the best of my knowledge). Effects of low, chronic input of a petroleum hydrocarbon on the phytoplankton community composition, the zooplanton physiological and behavioral responses and, in particular, the epontic microalgal, macroalgal, and microfouling community done at the Marine Ecosystems Research Laboratory (MERL) are relevant (MERL final report Yr. 2 and 3; Elmgren et al., 1980; Vargo et al., 1982; Vargo, 1981). These reports point out that obvious but seemingly minor initial effects of a hydrocarbon can lead to dramatic secondary effects which result in a complete change in the community composition and, in turn, in the interactive pathways within the community. Steele and Hanisak (1979) found that growth of macroalgal reproductive stages can be completely repressed at

petroleum hydrocarbon levels of 10 ppb. The MERL reports and these additional results should be seriously considered. Obviously if production by the deep living macroalgal populations along the west Florida shelf contributes significantly to the entire shelf dynamics, then any disruption of this ecosystem could have serious consequences.

The previous statements fit into the category of a "general" application of data into conceptual Fates and Effects models. We unfortunately do not have the data available to be able to make more precise statements.

Point 3: Assessment of the present state of knowledge of productivity effects
in this area and the Gulf of Mexico.

I am not quite sure what you are requesting with this point. If it is a consideration of the effects of the physical-chemical environment on water column and/or benthic production within the West Florida shelf system then, to the best of my knowledge, there is little data available other than the study we are discussing. Several theses by students of R. Iverson at FSU and a model described in Wroblewski (1973) and Wroblewski and O'Brien (1976) are pertinent to the northeastern Gulf and, of course, the recent studies in the western Gulf as part of the Gulf Circulation Studies (as presented at the February, 1982 ASLO conference in San Antonio, Session on "Relations between Biology and Circulation in the Gulf of Mexico") are also relevant to the Gulf as a whole. To my knowledge little else is available for the Southwest Florida Shelf.

379

If you wish a consideration of potential OCS drilling effects, such as petroleum hydrocarbons, for example, on Southwest Florida Shelf productivity then my comments would be the same as above. The statements and references to the MERL results are relevant but a look at the forthcoming update of Petroleum in the Marine Environment, to be published by the National Academy of Sciences, will reveal essentially no literature <u>directly</u> related to an environment such as the sub-tropical -tropical oligotrophic habitats of the Southwest Florida Shelf.

Point 4: Recommendations for further studies.

A. Assess the extent to which primary production on the west Florida shelf is partitioned between the water column phytoplankton and the deep-living benthic macroalgal populations. Which is the major source of carbon into the ecosystem?

B. Determine to what extent primary production within the region directly affected by Loop Current intrusions is dependent upon such intrusions for upwelled or "new" nitrogen. A subset would include extending the survey northward and southward (into the Florida Straits) to determine the extent of upwelling along the western boundary of the Loop and Florida Currents.

C. A subset of A and B above is to determine the relative contribution of "new" nitrate versus regenerated nitrogen within the study area.

D. Initiate a study to directly evaluate the effects of OCS exploratory activities (drilling) and petroleum hydrocarbons (both acute and low-level

chronic responses) on primary production by microalgae and macroalgae in subtropical and tropical oligotrophic regions, especially shelf area.

8.3 Recommendations for Further Studies

In a very simple sense, a noticeable effect of the upwelling might be expected in areas where the Loop Current front is statistically more frequent. As a test of this hypothesis, the epibotal boundaries reported by WCC/CSA (1982) (in their Figure 11-20) were compared to the corresponding monthly frequency positions reported by Vukovich et al. (1979). The comparisons were largely inconclusive because several frequency bands crossed each dendogram grouping. They were, however, indictive of the general complexity of area processes and the general requirement for further study. A number of these study recommendations such as the need to determine the frequency of Loop Current upwelling events and coupling these types of data with current meter data have been mentioned in different parts of the text. These recommendations can now be formalized as a series of questions requiring study, followed by suggested analyses to answer them.

Because of the important nutrient constraints inherent in this process, most of the recommendations have been developed around the nitrogen dynamics of shelf processes.

8.3.1 Nitrogen Dynamics

There are three basic questions to study in this category.

1. Are phytoplankton or benthic macroalgae the principal source of carbon in the west Florida shelf ecosystem?

2. To what degree does "new" (upwelled) nitrate contribute to the observed primary production relative to other nitrogen sources (e.g., regenerated nitrogen)?

3. What fraction of the total available nitrogen is contributed by the upwelling mechanism?

Studies recommended to address these three questions have been divided into six categories.

1. Phytoplankton studies.

   a. Conduct phytoplankton production studies using ^{14}C uptake procedures on a seasonal basis to estimate annual totals and nitrogen demands, and on a before, during, and after basis through a Loop Current intrusion event. The latter is an extension of the time series transect technique used during the summer cruise to a season where infrared imagery would be applicable for delineating surface features. This would provide a measure of the overall effect of one of these events. This time, an estimate for the productivity of Trichodesmium (Oscillatoria) erytherium, a nitrogen blue-green alga, should be included.

   b. Provide an assessment of a nitrogen preference index. This will be helpful in establishing the source of nitrogen being used (nitrate versus ammonia; "new" versus regenerated). A methodology for

conducting these studies is the ^{15}N labeled nitrate and ammonia technique.

c. Nitrate reductase assays should be conducted to substantiate the assimilation of nitrate by phytoplankton populations.

d. Proximate analyses can be used as an indicator of physiological state; i.e., the C/N ratio, protein/carbohydrate ratio combined with C/Chl can be used to estimate the total standing crop of phytoplankton (with an estimated detrital correction) and, to some extent, whether the population is nitrogen stressed.

2. Macroalgal distribution and production.

a. Using the Phase I and II benthic results to establish appropriate sampling sites, conduct seasonal samplings of productivity rates (determined by either O_2 evolution or ^{14}C uptake).

b. Complete proximate analyses including C/N protein/carbohydrate, and pigment ratios of chlorophyll: phycoerytherin and/or other phycobilins. These tests can determine the degree of nitrogen stress and the type of nitrogen resource being used.

c. For these benthic studies, compare macroalgal populations within an area of nitrate intrusion to populations growing in similar light fields but are not subject to the high nitrate flux. The area off Cay Sal Banks in the Florida Straits should have the same species

present. Since it would be on the eastern edge of the Florida Current, it would not be expected to have western boundary current type upwelling.

3. Nitrogen fixation and microbiological component.

   a. Using water bottle samples, net tows, counts, trichome size and a carbon/trichome or chlorophyll/trichome method, develop seasonal distribution and biomass estimates for _Trichodesmium erytherium_.

   b. Establish nitrogen fixation rates of _Trichodesmium_ based on the acetylene reduction method.

   c. Assess production and biomass of _Azoterbacter_ populations (a nitrogen fixing bacteria found in association with _Trichodesmium_ trichomes). Bacterial production and biomass will permit estimation of nitrate utilization and/or regeneration potential at this trophic level. Recommended methods are tritiated thymidine uptake for production and DNA fluorescence for biomass.

4. Water column nutrient and benthic flux measurements of pore water inorganic and organic nitrogenous compounds.

   a. Another important component of primary productivity are the benthic fluxes of ammonia, nitrite, and nitrate. Measurements of this factor should coupled with the phytoplankton and macroalgal components discussed above.

b. Estimates for benthic fluxes of ammonia, nitrate, and DON from sediments can be developed by measuring interstitial profiles of these nutrients in cores. Flux rates can be calculated from pore water profiles, established diffusion constants, and an estimate of bioturbation and sediment resuspension based on Radium-226 and Radon-222 measurements of near-bottom shelf water.

5. Total dissolved organic nitrogen.

a. Present data suggest that total DON concentrations are 2.5 to 5 times greater than the sum of inorganic nitrogen. At the present time, it is not known what fraction of this DON pool is utilized or its relation to the upwelling input of nitrates.

b. The following measurements are therefore recommended.

- Establish the seasonal standing stock of total DON by UV oxidation methods (Auto Analyzer).

- Establish the potential useable amino nitrogen as a fraction of the total DON pool using the fluorescamine method.

- If a significant fraction of the DON is useable nitrogen, then establish which compounds are important and their concentration by High Pressure Liquid Chromatography, Gas Chromatography, or amino acids.

6. Macrozooplankton (copepods) and microzooplankton excretion of nitrogenous compounds.

a. Zooplankton excretion of ammonia can account for 30 to 50% of the nitrogen required for primary production. Regenerated ammonia has been identified as a principle nitrogen source for phytoplankton production in oligotrophic waters. Thus some estimate of regenerated nitrogen is needed to put the role of upwelled nitrate into perspective.

b. Excretion rates of zooplankton can be measured either by bottle incubations using initial and final ammonia concentrations corrected for phytoplankton uptake after nitrogen loading or by ^{15}N isotope dilution techniques; the latter method is recommended.

8.3.2. Reef Studies

In a recent paper by Andrews and Gentien (1982), the Great Barrier Reefs of the Coral Sea were characterized as an "ecological response to tropical upwelling". They concluded that a large part of the heterogeneity observed in the coral reef ecosystems was supported by tropical upwellings from the East Australian Current.

The obvious, analogous question to ask is if the reef areas in southern Florida waters are either formed or supported by the upwellings associated with the Loop Current.

The recommended study to address this question would be a combined field and laboratory effort. Establish a transect of current meter/thermograph moorings from the Keys - coral reef area seaward to the Loop Current or Florida Current

front. At three to six week intervals, conduct hydrographic/servicing cruises along the transect for instrument refurbishment and sampling for temperature, salinity, sigma-t, plankton, light attenuation, productivity, and water origins (i.e., isotope analyses). Near the coral region side, establish closely spaced stations to establish fine scale mixing gradients. Provide sufficient flexibility in the sampling schedule to allow for data collection during "special events" as determined by satellite imagery. Establish the frequency of intrusion from the thermograph and current records and the mode of nitrogen supply to the reefs (i.e., as inorganic ammonium, nitrite, and nitrate ions or bound in particulates - phytoplankton). Conduct benthic surveys to establish contributions from macroalgae (as described above).

8.3.3 Frequency and Fluxes

As noted in earlier discussions (e.g., Section 3.2.1.6), the formation mode and frequency of shelf intrusions are presently not understood sufficiently. Likewise, nitrate fluxes across the shelf need to be evaluated.

It is believed that satellite imagery and current meter data along 26°N are presently being collected as part of the MMS Gulf of Mexico Physical Oceanography Program; each of these data sources can be instrumental in resolving much of the ambiguity in each of the questioned areas. A final recommendation, therefore, is that these data be made available for such analyses via the methods of Vukovich et al. (1979) for the former point and Lee et al. (1981) for the latter.

8.4 <u>References</u>

Andrews, J.C. and P. Gentien 1982. Upwelling as a source of nutrients for the Great Barrier Reef ecosystems: A solution to Darwin's question? Mar. Ecol. - Prog. Series, 8: 257-269.

Elmgren, R., J.F. Grassle J.P. Grassle, D.R. Heinle, G. Langlois, S.L. Vargo, and G.A. Vargo, 1980. Trophic interactions in experimental marine ecosystems perturbed by oil. In: John P. Giesy, ed., Microcosms in Ecological Research. DOE Symposium Series, Augusta, GA, Nov. 8-10, 1978, CONF 781101, NTIS, pp. 779-800.

Haddad, K.D. and K.L. Carder 1979. Oceanic intrusions: One possible initiation mechanism of red tide blooms. In: Toxic Dinoflagellate Blooms, pp. 269-274, Taylor and Selinger, eds1; Elsevier, New York.

Lee, T.N., L.P. Atkinson, and R. Legeckis 1981. Observations of a Gulf Stream frontal eddy on the Georgia continental shelf, April 1977, Deep-Sea Res., 28A(4): 347-378.

Murphy, E.B., K.A. Steidinger, B.S. Roberts, J. Williams, and J.W. Jolley, Jr. 1975. An explanation for the Florida east coast Gymnodinium breve red tide of November 1972. Limnol. Oceanogr. 20: 481-486.

Steele, R.L. nd M.D. Hanisak. 1979 Sensitivity of some brown algal reproductive stages to oil pollution. Proc. Int. Seaweeds Symp. 9: 181-190.

Vargo, G.A., M. Hutchins, and G. Almquist 1982. The effect of low, chronic
levels of No. 2 fuel oil on natural phytoplankton assemblages in
microcosms: 1. Species composition and seasonal succession. Mar.
Environ. Red. 6: 245-264.

Vargo, S.L. 1981. The effects of chronic low concentration of No. 2 fuel oil
on the physiology of a temperate estuarine zooplankton community in the
MERL microcosms. In: F.J. Vernberg, A. Calabrese, F.P. Thurberg, and
W.B. Vernberg, eds., Biological Monitoring of Marine Pollutants, Academic
Press, N.Y., 295-322.

Vukovich, F.M., B.W. Crissman, M. Bushnell, and W.J. King 1979. Some aspects
of the oceanography of the Gulf of Mexico using satellite and in-situ
data. J. Geophy. Res. 84(C12): 7749-7768.

Woodward-Clyde Consultants/Continental Shelf Associates 1982. Southwest
Florida shelf ecosystems study - Year 1. 4 vols. plus marine habitat
atlas, prepared under BLM Contract No. AA851-CTD-50, in review.

Wroblewski, J.S. 1973. A simulation of the mesoscale distribution of the
lower marine trophic levels off West Florida. Invest. Pesquera 37(2):
193-244.

Wroblewski, J.S. and J.J. O'Brien 1976. A spatial model of phytoplankton
patchiness. Mar. Biol. 35: 161-175.

9.0 ACKNOWLEDGEMENTS

HONG CHIN*
WOODWARD-CLYDE CONSULTANTS

The project team is a geographically diverse group who have studied similar oceanographic features on an individual basis in the past but have now combined their talents to address this Loop Current problem from a unified, multi-disciplinary point of view. The program manager was Dr. Hong Chin, formerly of Woodward-Clyde Consultants (San Diego, California). Dr. Chin wrote Sections 1.0, 2.0, 7.0, 8.0 and 9.0 and served as technical editor for both volumes of this final report.

Primary productivity aspects of the study and the development of Section 5 were handled by Dr. James A. Yoder (Principal Investigator) of the Skidaway Institute of Oceanography (Savannah, Georgia). Dr. Yoder was assisted by his very capable staff at the Skidaway Institute of Oceanography.

Phytoplankton identification, enumeration and discussions in Sections 5.3.1.3 and 5.3.2.3 were completed by Mr. Albert Mahood (San Rafael, California). Dr. Greta Fryxell of Texas A&M University assisted with the identification of some of the species.

Hydrographic analyses in Section 3.0 were handled by Ms. Theresa Paluszkiewicz (Research Coordinator with the Skidaway Institute of Oceanography) under the direction of Dr. Larry P. Atkinson (Principal Investigator) of the Skidaway

---

* Present affiliation: Oceanology Associates, San Diego, CA 92120

391

Institute of Oceanography. Management of both spring and summer cruise data sets were the responsibility of Mr. William S. Chandler (also of the Skidaway Institute of Oceanography).

The mixing processes analyses in Section 4.0 were completed by Dr. Eric Posmentier (Principal Investigator), Southampton College of Long Island University.

Optical oceanographic data collection, processing, and analyses in Section 6.0 were developed by Dr. Niels K. Hojerslev (Principal Investigator) of the Institute of Physical Oceanography, University of Copenhagen. A special note of thanks is extended to the Institute for their no-cost loan of personnel and specialized optical sensors during the spring cruise. The expert assistance of Mr. H. Hundahl (Institute of Physical Oceanography, University of Copenhagen) during the spring cruise is also gratefully acknowledged.

The April Ocean Color Scanner mappings were managed by Dr. Hongsuk H. Kim of the National Aeronautics and Space Administration (GSFC) under separate inter-agency agreement. Dr. Kim reviewed and approved Section 7.0 of this report.

The reviews, critique, and general support provided by the project workshop review panel (Drs. W.M. Dunstan, R.L. Iverson, T.N. Lee, and G.A. Vargo) are also gratefully acknowledged along with the helpful comments supplied by all workshop participants (Table 8-1).

The Department of the Interior Mission

As the Nation's principal conservation agency, the Department of the Interior has responsibility for most of our nationally owned public lands and natural resources. This includes fostering sound use of our land and water resources; protecting our fish, wildlife, and biological diversity; preserving the environmental and cultural values of our national parks and historical places; and providing for the enjoyment of life through outdoor recreation. The Department assesses our energy and mineral resources and works to ensure that their development is in the best interests of all our people by encouraging stewardship and citizen participation in their care. The Department also has a major responsibility for American Indian reservation communities and for people who live in island territories under U.S. administration.

The Minerals Management Service Mission

As a bureau of the Department of the Interior, the Minerals Management Service's (MMS) primary responsibilities are to manage the mineral resources located on the Nation's Outer Continental Shelf (OCS), collect revenue from the Federal OCS and onshore Federal and Indian lands, and distribute those revenues.

Moreover, in working to meet its responsibilities, the **Offshore Minerals Management Program** administers the OCS competitive leasing program and oversees the safe and environmentally sound exploration and production of our Nation's offshore natural gas, oil and other mineral resources. The MMS **Minerals Revenue Management** meets its responsibilities by ensuring the efficient, timely and accurate collection and disbursement of revenue from mineral leasing and production due to Indian tribes and allottees, States and the U.S. Treasury.

The MMS strives to fulfill its responsibilities through the general guiding principles of: (1) being responsive to the public's concerns and interests by maintaining a dialogue with all potentially affected parties and (2) carrying out its programs with an emphasis on working to enhance the quality of life for all Americans by lending MMS assistance and expertise to economic development and environmental protection.